

NEI DK 3090

# RESUME 95

Rapid

Environmental

Surveying

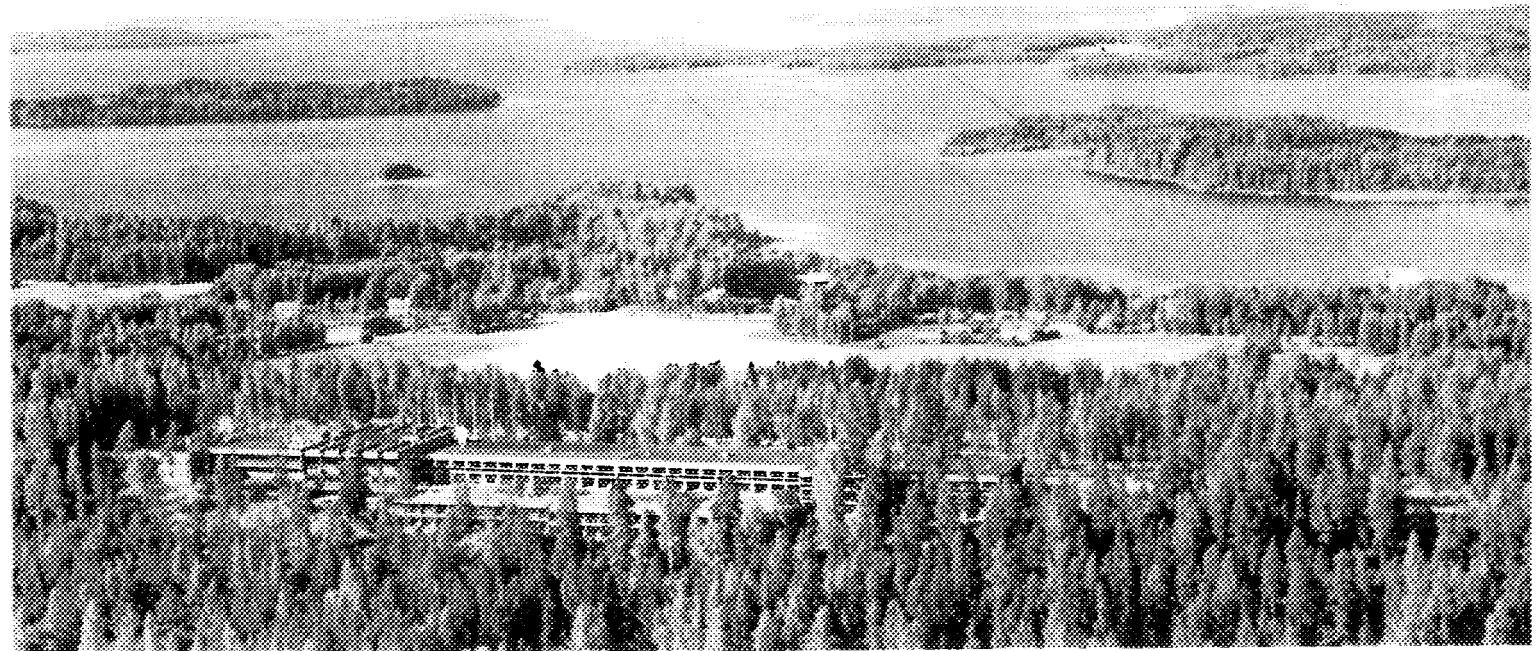
Using

Mobile

Equipment



DK9800024



Nordic Nuclear Safety Research

*L*

*2000*

mks

# RESUME 95

**Rapid  
Environmental  
Surveying  
Using  
Mobile  
Equipment**

RESUME-95:Rapid Environmental Surveying Using Mobile Equipment  
Copenhagen: NKS, 1997  
ISBN 87-7893-014-6

Cover photography: Hotel Talluka, the base of exercise RESUME-95.  
Photographer Christian Bourgeois

Published by  
NKS-secretariat            Phone: +45 46 77 40 45  
FRIT, Building 101        Fax     +45 46 35 92 73  
Postbox 49                E-mail  annette.lemmens@risoe.dk  
DK-4000 Roskilde  
Denmark

Printed by Frederiksberg Bogtrykkeri a/s

Printed in Denmark

## FOREWORD

This report has been prepared under the EKO-3 project *Preparedness Strategy and Procedures* within the framework of the Nordic Nuclear Safety Research (NKS) program 1994-1997. NKS is a cooperative body in nuclear safety, radiation protection and emergency preparedness. Its purpose is to support Nordic research projects, organize exercises, provide information and make recommendations to decision makers and other concerned staff members in organizations within the nuclear industry.

Early in the NKS program, mobile measuring techniques were identified as an important field for research and cooperation within the Nordic countries. The field exercise RESUME95 (*Rapid Environmental Surveying Using Mobile Equipment*) conducted in Finland in 1995 is expected to be the first of a number of such exercises. This report is a comprehensive documentation of this first exercise. The individual papers presented in this publication are reports made by the different participating monitoring teams describing their own results, interpretation, and experiences. In addition, selected papers are included which provide a general description of the exercise from the original planning documents to a final summary of the results.

For such a large exercise, many people must be involved. Special thanks are due to the Exercise Planning Committee for their efforts in planning the RESUME95 exercise, to all the participating teams and to all the authors for their contributions to this publication. Ms. Kirsten Juul who coordinated the compilation and preparation of this publication also deserves special recognition.

Jens Hovgaard  
Exercise Planning Chair

## **The Exercise Planning Committee:**

**Jens Hovgaard,**  
Exercise Planning Chair,  
Danish Emergency Management Agency,

**Harri Toivonen,**  
coordinator of the carborne measurements and source search,  
Finnish Centre for Radiation and Nuclear Safety,

**Jukka Multala,**  
coordinator of the airborne measurements,  
Geological Survey of Finland

**Hans Mellander,**  
coordinator of the in-situ measurements,  
Swedish Radiation Protection Institute,

**Johs Jensen,**  
coordinator of the directing staff,  
Jensen Consult, Denmark,

**Janne Koivukoski,**  
representative from the Finnish Rescue Department,  
Finnish Ministry of the Interior.

# CONTENTS

INTRODUCTION.....	7
GAMMA RAY SPECTROMETRY RESULTS FROM CORE SAMPLES COLLECTED FOR RÉSUMÉ 95 .....	9
CHARACTERISTICS AND LOCATIONS OF SOURCES.....	41
DETERMINING THE ACTIVITY AND LOCATION OF HIDDEN POINT SOURCES ON THE GROUND BY MEASUREMENTS AT DISTANCE.....	59
OPERATIONAL STAFF DURING EXERCISE RESUME95 .....	63
<b>CANADA</b>	
Exploranium: “A Carborne Gamma-ray Spectrometer System for Natural Radioactivity Mapping and Environmental Monitoring”.....	71
<b>DENMARK</b>	
Danish Emergency Management Agency: “The Danish Airborne Gamma Ray Surveying Results” .....	91
<b>FINLAND</b>	
Finnish Defence Force Research Centre: “Airborne Fallout Mapping of <sup>137</sup> Cs” .....	101
Geological Survey of Finland: “Exercise Results and Experience” .....	107
Finnish Centre for Radiation and Nuclear Safety: “In-Situ Measurements in Vesivehmaa Air Field” .....	117
Finnish Centre for Radiation and Nuclear Safety / Helsinki University of Technology: “Airborne Fallout Mapping of <sup>137</sup> Cs” .....	127
“Carborne Fallout Mapping”.....	133
“Detecting Hidden Sources”.....	143
“Source Passing Test in Vesivehmaa Air Field” .....	151
<b>FRANCE</b>	
Commissariat à L’Energie Atomique - Hélinuc: “RESUME95 Nordic Field Test of Mobile Equipment for Nuclear Fallout Monitoring” .....	169
<b>GERMANY</b>	
Bundesamt für Strahlenschutz: “Aerial Measurements in Finland” .....	195
<b>NORWAY</b>	
Geological Survey of Norway: “Airborne Mapping of Radioactive Contamination” .....	205
Norwegian Institute for Air Research: “Exercise Résumé95” .....	225
Norwegian Radiation Protection Authority: “Car-borne Survey Measurements with a 3x3” NaI Detector” .....	229
<b>SCOTLAND</b>	
Scottish Universities Research & Reactor Centre: “Airborne Gamma Ray Measurements Conducted During an International Trial in Finland”.....	235
<b>SWEDEN</b>	
Department of Radiation Physics, Lund University, Lund: “Applying Statistical Methods to Carborne NaI(Tl) Spectrometry Results” .....	255

"Carborne Measurements in Area II by the Jubileum Institute" .....	261
Department of Radiation Physics, Lund University, Malmö:	
"In-Situ Gamma Spectrometry performed at Vesivehmaa Airport" .....	265
National Defence Research Establishment - FOA Stockholm:	
"Total Deposition of <sup>137</sup> Cs Measured in Finland during the Exercise RESUME95" .....	281
National Defence Research Establishment - Division of Ionising Radiation and Fallout - FOA Umeå:	
"Measurements with Mobile Equipment" .....	291
Geological Survey of Sweden:	
"RESUME95" .....	307
<b>COMPARISON OF RESULTS</b>	
"Detection of Hidden Sources - Prompt Reports by Airborne Teams in RESUME95" .....	323
"Comparison of Results at Area I and Area II between different Swedish In-situ Teams" .....	341
"Comparison of the Results of the RESUME-95 Exercise" .....	369
<b>APPENDIX 1 "The Exercise Plan" .....</b>	<b>387</b>
<b>APPENDIX 2 "List of Participants in RESUME95 and Contributors to the Publication" .....</b>	<b>411</b>
<b>COLOUR APPENDIX .....</b>	<b>415</b>

## INTRODUCTION

The RESUME95 exercise - Rapid Environmental Surveying Using Mobile Equipment, took place in Finland in August 1995. The objectives of the RESUME exercise were to compare different monitoring systems when used under the same conditions as well as to compare results from similar systems with different data analysis and presentation software. Another objective was to acquire some basic knowledge to standardize and cross calibrate the European airborne gamma-ray surveying capability so that the results from different systems could be directly comparable. Finally, one of the objectives was to test potential mutual co-operation and assistance in the event of a nuclear emergency.

In previous NKS research projects and similar programs elsewhere, it is common to evaluate a single specific measuring technique. However, in an emergency situation, after a major release of radioactive material, many different kinds of measuring systems will be used. These systems may have different principles for measuring the gamma radiation field. The systems could include NaI spectrometers, HpGe detectors, ionization chambers, simple GM counters or total count scintillometers. Consequently, the results from such a wide variety of systems may not be directly comparable. In addition the individual detector systems could be mounted in a mobile vehicle such as a helicopter, fixed wing aircraft or a car. In-situ gamma-ray measurements would also be made. With this wide variety of configurations, the field of view of the detector can vary from a few square meters to several thousands of square meters.

The exercise involved 10 airborne monitoring teams, 7 teams with vehicle monitoring systems as well as ground survey teams from 8 countries. Most systems incorporated GPS satellite navigational aids and computers for real time display of the data which was also recorded for post flight analysis. Most of the car- and airborne systems were based on NaI detectors whereas most of the In-situ systems and a few airborne systems were based on HpGe detectors.

The exercise took place in an area near Asikkala and Padasjoki, 25 - 50 km north of Lahti (Plate 1a).

Three different areas were surveyed. These were

1) An airfield near Vesivehmaa, which was intended as a calibration site (Area I). Soil samples had been taken previously and used to establish the  $^{137}\text{Cs}$  activity of the soil as well as the activity of the natural radioactivity elements  $^{40}\text{K}$ ,  $^{214}\text{Bi}$  and  $^{208}\text{Tl}$ .

2) An area contaminated by the Chernobyl nuclear accident, Area II (Plate 1b). This area was intended to test the capabilities of the car- and airborne teams for mapping  $^{137}\text{Cs}$ . A number of predefined points in the area were used by In-situ teams.

3) An area with a variety of hidden radioactive sources, Area III (Plate 1b). These sources of  $^{60}\text{Co}$ ,  $^{137}\text{Cs}$ ,  $^{192}\text{Ir}$  and  $^{99}\text{Tc}$  ranged in activity from 0.6 mCi to 15 Ci and was used to test the capability of the different airborne teams for locating lost radioactive sources.

Immediately after all the three areas were surveyed, it was a requirement that the results of the search for the hidden radioactive sources should be delivered to the organizers. During the week of the exercise, more detailed analyses were carried out. Maps of the cesium distribution of Area II were also produced and presented on a common bulletin board during the course of the exercise. On the last day, each participating team presented their results at a seminar. In January 1996, the final results were presented at an international conference in Copenhagen.

The results from the exercise demonstrated the excellent capability of the airborne teams. Eight of the ten airborne teams were able to deliver  $^{137}\text{Cs}$  maps very soon after the surveys were completed, in some cases within a few hours. In general, the  $^{137}\text{Cs}$  deposition maps from the airborne and carborne teams showed the same spatial features but with some variation in absolute levels. Most of the observed differences can be attributed to differences in the calibration methodology and the spatial attributes of the different measuring techniques. It was found that accurate flight path navigation and presentation and analysis software played an important role in the search for the hidden sources.

The lessons learned from RESUME95 indicate a need for further operational exercises in which a number of specific problems should be addressed. These include the calibration and repeatability of the equipment as well as the field of view of the different systems. Influence of positional errors is also an important aspect when comparing the results from a variety of systems. Problems such as these should be considered in the design of the exercise and the choice of the areas to be surveyed.



# Scottish Universities Research and Reactor Centre - Finnish Centre for Radiation and Nuclear Safety

## Gamma Ray Spectrometry Results from Core Samples Collected for RÉSUMÉ95

SUMMARY .....	12
ACKNOWLEDGEMENTS .....	13
1. INTRODUCTION .....	14
2. SAMPLING .....	15
2.1. Vesivehmaa Airfield (Area I) .....	15
Fig. 2.1 Area I calibration site .....	15
Fig. 2.2. Hexagon pattern orientation .....	16
Tab. 2.1. Labelling system .....	16
Tab. 2.2. Samples taken at Area I .....	17
2.2. Other Samples .....	19
2.3. Sample Treatment and Allocation .....	19
Tab. 2.3. Sampling in Area II .....	19
3. ANALYTICAL DETAILS .....	21
3.1. Analyses at SURRC .....	21
3.2. Analyses at STUK .....	22
3.3. Quality Assurance Checks .....	22
4. RESULTS .....	23
4.1. Reference Materials .....	23
Tab. 4.1. Reference materials .....	23
4.2. Common Samples .....	23
Tab. 4.2a. Common samples .....	24
Tab. 4.2b. Ratio of STUK/SURRC common samples .....	24
4.3. Results from Vesivehmaa Airfield (Area I) .....	25
4.3.1. Summary of Results from Each Shell and Position .....	25
Tab. 4.3. Vesivehmaa Airfield (Area I): $^{137}\text{Cs}$ activity 0-16cm/kBq $\text{m}^{-2}$ .....	25
Tab. 4.4. Vesivehmaa Airfield (Area I): $^{40}\text{K}$ activity 0-16cm/Bq per kg (wet) .....	26
Tab. 4.5. Vesivehmaa Airfield (Area I): $^{214}\text{Bi}$ activity 0-16cm/Bq per kg (wet) .....	26
Tab. 4.6. Vesivehmaa Airfield (Area I): $^{208}\text{Tl}$ activity 0-16cm/Bq per kg (wet) .....	27
4.3.2. Weighted Activity Estimates .....	28
Tab. 4.7. Shell weighting factors .....	28
Tab. 4.8. Effective radionuclide concentrations at Area I .....	28
4.3.3. Depth Distributions .....	29
4.3.3.1. $^{137}\text{Cs}$ .....	29
Tab. 4.9. ....	29
4.3.3.2. Natural radionuclides .....	29
Fig. 4.1. Measured activity concentrations in wet soil verse mass depth .....	30
Fig. 4.2. Measured activity concentrations verse mass depth .....	31
Fig. 4.3. $^{40}\text{K}$ distribution with depth .....	32
Fig. 4.4. $^{214}\text{Bi}$ distribution with depth .....	33
Fig. 4.5. $^{208}\text{Tl}$ distribution with depth .....	34

4.4. Results from Area II.....	35
4.4.1. Summary of results from each point.....	35
Tab. 4.10. Analysis of samples taken from Area II .....	35
4.4.2. <sup>137</sup> Cs Depth distributions .....	35
Tab. 4.11. Distribution coefficients in Area II .....	35
Fig. 4.6. Measured activity concentrations in wet soil verse mass depth .....	36
5. CONCLUSIONS .....	37
REFERENCES .....	38

**GAMMA RAY SPECTROMETRY RESULTS FROM  
CORE SAMPLES COLLECTED FOR RÉSUMÉ 95**

**SEPTEMBER 1995**

**D.C.W. SANDERSON<sup>1</sup>, J.D. ALLYSON<sup>1</sup>, H. TOIVONEN<sup>2</sup>, T. HONKAMAA<sup>2</sup>**

**1. SURRC, East Kilbride, Scotland**

**2. STUK, Helsinki, Finland**

## SUMMARY

Field sampling of an airfield at Vesivehmaa, near Vääksy, Finland (Area I) was carried out between 26-29 May 1995, to establish the radionuclide deposition and inventory of Chernobyl derived  $^{137}\text{Cs}$ , and natural radionuclides. The objective was to establish a common calibration site for in-situ and airborne gamma spectrometers, for Exercise RÉSUMÉ 95 conducted in August 1995.

The report presents the sampling details, handling and treatment. The analyses are discussed with particular emphasis given to  $^{137}\text{Cs}$ ,  $^{134}\text{Cs}$ ,  $^{40}\text{K}$ ,  $^{214}\text{Bi}$  and  $^{208}\text{Tl}$  radionuclides, and the quantification of their respective deposition and inventories.

The calibration site was based upon a hexagonal sampling pattern developed by The Scottish Universities Research and Reactor Centre (SURRC). This sampling scheme enables ground level deposition to be related to gamma-ray spectrometers at different heights, taking account of differences in fields of view.

More than 50 soil cores were collected in May, split vertically, and taken to Säteilyturvakeskus (STUK) for drying prior to gamma spectrometry. Some 160 individual samples were counted between SURRC and STUK, with 5 samples measured in both laboratories and two IAEA reference materials. Results from common samples and reference materials confirm both compatibility between the two laboratories and traceability to recognised standards.

The results have been used to estimate the effective concentrations of nuclides at the calibration site for in-situ and airborne gamma spectrometry, and the depth distribution. For  $^{137}\text{Cs}$  the weighted mean activity per unit area takes on values of  $50.7 \pm 5.2 \text{ kBq m}^{-2}$  at 1 m ground clearance,  $51.1 \pm 6.9 \text{ kBq m}^{-2}$  at 50 m height and  $47.9 \pm 8.5 \text{ kBq m}^{-2}$  at 100m. The similarity of these values confirms the suitability of the Vesivehmaa site for comparison of in-situ and airborne results despite variations of a factor of two between results from individual cores. The mean  $\alpha/\rho$  value for  $^{137}\text{Cs}$  in Area I is  $0.77 \pm 0.10 \text{ cm}^2\text{g}^{-1}$  (relaxation mass per unit area,  $\beta = 1.31 \pm 0.15 \text{ gcm}^{-2}$ ).

Additional soil sampling across parts of Area II (a 6x3 km area selected for mapping Chernobyl deposition) was carried out. The mean level of  $^{137}\text{Cs}$  activity from these samples was  $92.4 \pm 63 \text{ kBq m}^{-2}$ , a sample taken near Laihansuo showing the largest value obtained at  $172 \text{ kBq m}^{-2}$ . The dose rate measured at this last location was  $0.5 \mu\text{Sv hr}^{-1}$  taken with a hand held instrument at ground level. The mean  $\alpha/\rho$  value for  $^{137}\text{Cs}$  in Area II is  $0.44 \pm 0.21 \text{ cm}^2\text{g}^{-1}$  ( $\beta = 2.43 \pm 0.66 \text{ gcm}^{-2}$ ), and therefore deeper activity than that found in Area I.

This work was supported by NKS and the Danish Emergency Management Agency.

## **ACKNOWLEDGEMENTS**

We would like to thank STUK for hospitality and assistance during the sampling period. The assistance of Ahti Kansanaho, Jens Hovgaard, Hans Mellander and all personnel from STUK who participated in the field sampling is gratefully acknowledged. We are also grateful to the Tallukka Hotel, Vääksy, for putting up with an unusual party of guests. The work was partially funded by NKS through the Danish Emergency Management Agency as a supporting measure to the RÉSUMÉ 95 exercise.

## 1. INTRODUCTION

This report presents an account of work conducted in preparation for the RÉSUMÉ 95 exercise to establish a calibration site at Vesivehmaa airfield, designated Area I, based on soil samples analysed in the laboratory for  $^{137}\text{Cs}$ ,  $^{134}\text{Cs}$ ,  $^{40}\text{K}$ ,  $^{214}\text{Bi}$  and  $^{208}\text{Tl}$ , and traceable to international reference materials. An additional series of cores was collected from Area II, the area used for deposition mapping in the RÉSUMÉ study to enable "spot" comparisons to be made between airborne and ground based results.

For natural radioelement mapping it has become conventional to perform ground to air comparisons using in-situ spectrometry systems calibrated with the same concrete calibration pads as used to characterise airborne gamma spectrometers, thus providing a means of projecting the response of the small scale pads onto larger calibration ranges [1-7]. Whilst this provides a means of determining system sensitivities for airborne spectrometers relative to pads [8], it does not lead directly to absolute concentrations, and does not in general take account of variations in soil density, and the heterogeneity of source distribution both in the spatial vertical and horizontal planes. Calibration of systems for mapping anthropogenic radionuclides, can be approached on theoretical grounds [9], or more conventionally by ground to air comparison using in-situ measurements or soil samples [10]. Since the primary photon fluence rates for anthropogenic nuclides are strongly influenced by source distribution the use of soil samples to make traceable estimates of activity per unit area, and to investigate the vertical source distribution is the preferred approach.

However with environmental  $^{137}\text{Cs}$  concentrations corresponding to typically  $10^{-15}$  and  $10^{-12}$  parts by weight deposited in a heterogeneous matrix, and subject to small scale spatial variability it is unsurprising that individual core samples are of limited value in representing the fields of view of in-situ and airborne measurements, of spatial dimensions which are some  $10^5$  -  $10^7$  times greater than typical soil cores. Matching soil samples to in-situ and aerial spectrometric measurements should take account of spatial variability of environmental radioactivity and *field of view* of the detector. Calibration sites therefore must be selected and sampled to: i) represent the field of view of airborne detectors for various altitudes, ii) account for within site variability, and iii) examine source depth characteristics.

The calibration procedures adopted here utilises methods developed by the Scottish Universities Research and Reactor Centre (SURRC), based on an expanding hexagonal sampling pattern [16,17]. Core samples analysed by high resolution spectrometry provide traceability to international reference materials. The sampling plan consists of a series of concentric hexagons, spaced apart by a partial geometric progression. This provides an efficient sampling scheme for determining activity concentrations and their spatial variability over dimensions of several hundred metres for calibrating airborne detectors. It is possible to compensate for spatial variability within the site by evaluating weighted expectation values for radiometric variables, taking account of observation height, energy, detector angular response and the source distribution.

## 2. SAMPLING

### 2.1 Vesivehmaa Airfield (Area I)

The calibration site was based upon the expanding hexagon pattern shown in figure 2.1. Core samples were collected at the centre of the site and at the apexes of each hexagonal shell the radial dimensions of which expand out in a progressive interval (eg. x2 or x4). Thus sample spacing increased for each successive shell. In this instance samples were collected at 2, 8, 32, 128 and 256 metres from the central point. The site was flat, and at least 500 m across.

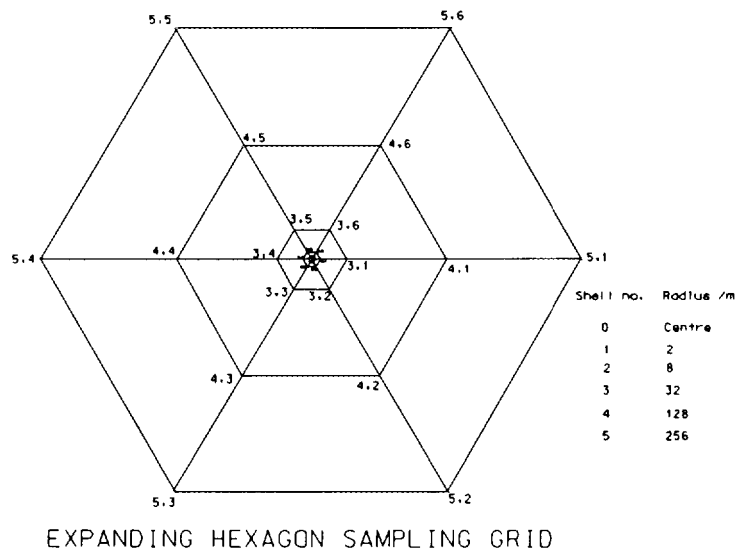


**Figure 2.1** Area I calibration site.

The sampling pattern was laid out on the 26 May 1995. Subsequent soil cores were taken over the next 3 days. The pattern was constructed with the reference axis parallel with a grass runway towards direction  $126^\circ$  (figure 2.2). It was felt that this would facilitate easy identification, especially observed from the air by fixed wing aircraft. Shell apexes were found by measurements from the central position and sighting compass. Wooden pegs were placed at these positions, together with labels. STUK provided DGPS measurements at each position for future reference.

Two soil coring tools were used. The central position was sampled by both tools (SURRC tool "A", diameter 10 cm; STUK tool "B", diameter 7 cm). The STUK tool consisted of a smooth steel bore tube, with soils removed by applying internal pressure. The SURRC coring tool consisted of an adapted golf-course hole cutter, fitted with extended blades. The twin blades can be easily removed to enable a soil core to be taken relatively intact and whole. Both tools were driven to a depth of about 16 cm. It became increasingly difficult to core beyond this depth due to hard stone fragments between the B1-B2 subsoil layer.

### Vesivehmaa Airfield

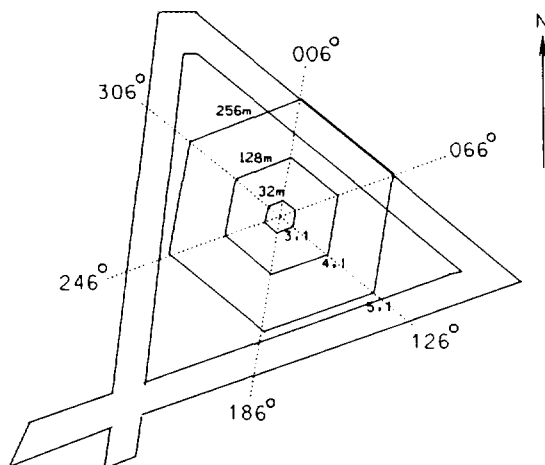


**Figure 2.2** Hexagon pattern orientation.

### Orientation of Hexagonal Sampling Pattern

The labelling convention used is shown in table 2.1. A summary of the cores taken at Area I is shown in table 2.2.

In-situ measurements were taken by STUK across the entire site of Area I at the time of the sampling, including parallel tracks along the main axis at 128 m spacing, and reported that the airfield appeared to have relatively uniform  $^{137}\text{Cs}$  activity.

**Table 2.1** Labelling system.

Radius /m	Tool, shell number, clockwise orientation					
0	Centre position: A0, B0					
2	B1,1	B1,2	B1,3	B1,4	B1,5	B1,6
8	A2,1	A2,2	A2,3	A2,4	A2,5	A2,6
32	A3,1	A3,2	A3,3	A3,4	A3,5	A3,6
128	A4,1	A4,2	A4,3	A4,4	A4,5	A4,6
256	A5,1	A5,2	A5,3	A5,4	A5,5	A5,6

**Table 2.2** Samples taken at Area I.

<b>Label</b>	<b>Core taken</b>	<b>WGS84</b>	<b>KKJ 3</b>
B0	3 cores taken: 2 in box marked I, 1 in box marked II 0-2, 2-4, 4-6, 6-16cm	61.148°N 25.696°E (non-DGPS)	3429858 6782710
A0	2 complete cores taken from centre point	61.148°N 25.696°E (non-DGPS)	3429858 6782710
B1,1	2 cores taken 0-2, 2-4, 4-6, 6-16cm	-	3429862 6782709
B1,2	2 cores taken 0-2, 2-4, 4-6, 6-17cm	-	3429862 6782708
B1,3	2 cores taken 0-2, 2-4, 4-6, 6-16cm	-	3429856 6782709
B1,4	2 cores taken 0-2, 2-4, 4-6, 6-16cm	-	3428856 6782711
B1,5	2 cores taken 0-2, 2-4, 4-6, 6-16cm	-	3428858 6782712
B1,6	2 cores taken 0-2, 2-4, 4-6, 6-16cm	-	3428860 6782711
A2,1	1 core taken 0-2, 2-4, 4-6, 6-11cm	-	3429866 6782707
A2,2	1 core taken 0-2, 2-4, 4-6, 6-11, 11-16cm	-	3429866 6782706
A2,3	1 core taken 0-2, 2-4, 4-6, 6-11, 11-16cm	-	3429852 6782707
A2,4	1 core taken 0-2, 2-4, 4-6, 6-11, 11-16cm	-	3428852 6782708
A2,5	1 core taken 0-2, 2-4, 4-6, 6-11, 11-16cm	-	3428856 6782709
A2,6	1 core taken 0-2, 2-4, 4-6, 6-11, 11-16cm	-	3428856 6782708

**Table 2.2** continued.

<b>Label</b>	<b>Core taken</b>	<b>WGS84</b>	<b>KKJ 3</b>
A3,1	1 core taken 0-2, 2-4, 4-6, 6-11, 11-16 cm	61.14681°N 25.69486°E	3429882.2 6782687.1
A3,2	1 core taken 0-2, 2-4, 4-6, 6-11, 11-16cm	61.14672°N 25.69431°E	3429852.4 6782677.7
A3,3	1 core taken 0-2, 2-4, 4-6, 6-11, 11-16cm	61.14693°N 25.69383°E	3429826.9 6782701.5
A3,4	1 core taken 0-2, 2-4, 4-6, 6-11, 11-16cm	61.1472°N 25.69392°E	3429832.4 6782731.5
A3,5	1 core taken 0-2, 2-4, 4-6, 6-11, 11-16cm	61.1473°N 25.69453°E	3429865.2 6782741.2
A3,6	1 core taken 0-2, 2-4, 4-6, 6-11, 11-16cm	61.14709°N 25.69497°E	3429888.8 6782718.0
A4,1	1 core taken 0-2, 2-4, 4-6, 6-11, 11-16cm	61.14626°N 25.69620°E	3429953.1 6782624.4
A4,2	1 core taken 0-2, 2-4, 4-6, 6-11, 11-16cm	61.14588°N 25.69400°E	3429833.8 6782584.3
A4,3	1 core taken 0-2, 2-4, 4-6, 6-11, 11-16cm	61.14671°N 25.69211°E	3429733.7 6782678.0
A4,4	1 core taken 0-2, 2-4, 4-6, 6-11, 11-16cm	61.14775°N 25.69258°E	3429761.4 6782794.1
A4,5	1 core taken 0-2, 2-4, 4-6, 6-11, 11-16cm	61.14811°N 25.69494°E	3429889.4 6782831.9
A4,6	1 core taken 0-2, 2-4, 4-6, 6-11, 11-16cm	61.14737°N 25.69663°E	3429978.7 6782747.6
A5,1	1 core taken 0-2, 2-4, 4-6, 6-11, 11-16cm	61.14551°N 25.69800°E	3430048.4 6782538.9
A5,2	1 core taken 0-2, 2-4, 4-6, 6-11, 11-16cm	61.14474°N 25.69349°E	3429803.8 6782457.9
A5,3	1 core taken 0-2, 2-4, 4-6, 6-11, 11-16cm	61.14641°N 25.68975°E	3429606.1 6782647.0
A5,4	1 core taken 0-2, 2-4, 4-6, 6-11, 11-16cm	61.1485°N 25.69079°E	3429666.7 6782879.8
A5,5	1 core taken 0-2, 2-4, 4-6, 6-11, 11-16cm	61.14927°N 25.69548°E	3429920.6 6782959.9
A5,6	1 core taken 0-2, 2-4, 4-6, 6-11, 11-16cm	61.14772°N 25.69895°E	3430104.4 6782783.6

## 2.2 Other Samples

The Exercise region Area II was also sampled to allow direct comparisons to be made at selected points. Area II comprised an area 3x6 km to the north-west of Area I and contained a mixture of forestation, cultivation, lakes, limited grassland, marsh and exposed bedrock. Differences between gamma spectrometry estimates of deposition established from calibration of Area I, may be attributable to the presence of each of these. Table 2.3 shows the locations of the sampling conducted in Area II, with approximate GPS position (non-differential available). One notable location near Laihansuo (between a stream and parking area) provided  $0.5 \mu\text{Sv hr}^{-1}$  at ground level.

## 2.3 Sample Treatment and Allocation

The ground based soil sampling program resulted in a set of at least 50 cores taken from Areas I and II, forming 160 individual samples for high resolution gamma spectrometry. The cores were sectioned in the field at intervals of 2 cm for the upper 6 cm layers. It was impractical to separate a core with less than this, due to the friability of the soil. From 6 cm, the cores were sectioned at intervals of mostly 5 cm. Each section of core was placed into an air-tight container to retain moisture. The samples were taken back to STUK and dried (at  $105^{\circ}\text{C}$  for 2-3 days) to constant weight to assess moisture content. The dried samples were then allocated to each laboratory approximately 50:50, with STUK also analysing the additional cores taken from Area II.

Some complete cores were collected from Areas I and II, and packed using plastic film to retain moisture. These were taken back to STUK and Statens Strålskyddsinstitut (SSI) for analysis.

**Table 2.3** Sampling in Area II.

Sampling Site	Nearest named location	Lat/Long. (non DGPS)	Core(s) taken
1	Auttoinen (Football field)	61°17.92N 25°04.56E	1 core: 0-2, 2-4, 4-6, 6-11, 11-16cm  + 1 complete core  Tool: A
2	Near Lake Sepänsuonjarvi	61°19.19N 25°05.98E	1 core: 0-2, 2-4, 4-6, 6-8, 8-13, 13-18cm  Tool: A
3	Near Viitastenniittu	61°19.54N 25°04.65E	1 core: 0-2, 2-4, 4-6, 6-11, 11-16cm  Tool: A

**Table 2.3** continued.

<b>Sampling Site</b>	<b>Nearest named location</b>	<b>Lat/Long. (non DGPS)</b>	<b>Core(s) taken</b>
4	Peltomtausta	61°21.00N 25°05.55E	1 core: 0-2, 2-4, 4-6, 6-11, 11-16cm  + 1 complete core  Tool: A
5	Near Laihansuo (next to stream)	61°20.06N 25°05.36E	1 core: 0-2, 2-4, 4-6, 6-8, 8-13 13-18cm  Tool: A
6	Near Laihansuo (midway between stream and parking area: 0.5μSv hr <sup>-1</sup> )	61°20.06N 25°05.36E	1 core: 0-2, 2-4, 4-6, 6-11 11-16cm  + 1 complete core  Tool: A
7	Near Lake Ehojärvi	61°19.12N 25°03.30E	1 core: 0-2, 2-4, 4-6, 6-11 11-16cm  Tool: A
8	Near Lake Särkijärvi	61°18.33N 25.03.03E	1 core: 0-2, 2-4, 4-6, 6-11 11-16cm  Tool: A
9	Near Lake Valkea Hirsjärvi	61°20.59N 25°06.38E	1 core: 0-2, 2-4, 4-6, 6-11, 11-16cm  +1 complete core  Tool: A

### 3. ANALYTICAL DETAILS

#### 3.1 Analyses at SURRC

Approximately 80 samples were received at SURRC after drying at STUK. A 1 kg capacity mixer-mill was used to homogenise the samples and reduce the particle size to below about 50 microns. Weighed subsamples were then dispensed into standard containers (50, 75, 100 and 150 cm<sup>3</sup>) and sealed prior to gamma spectrometry. The containers were agitated to allow samples to settle, and were fully packed without compressing the material. Although the container lids were sealed with gas sealing tape, it is likely that some radon leakage may still have occurred. Samples of two IAEA reference materials (Soil-6 and IAEA-375) together with an internal reference sample (SURRC CAER Standard spike) were dispensed in an identical manner.

The internal standard was prepared from a larger quantity of marine saline gley from a site near the Irish sea, containing <sup>241</sup>Am, <sup>137</sup>Cs, <sup>134</sup>Cs, with additional quantities of potassium, uranium and thorium derived from IAEA RG-K, RG-U and RG-Th reference materials [13]. The working values for the internal standard had been previously determined relative to a series of soils labelled with NPL multinuclide reference solutions, and Amersham calibrated spikes [10].

Gamma spectra from samples and standards were measured for 50000-80000 seconds using three hyperpure Ge spectrometers (one GMX and two LOAX detectors), housed within low background lead shields. The samples were presented to the detector in an identical manner to the reference materials. Full gamma ray spectra from 30 keV to 3 MeV were stored and analysed using Ortec software to estimate full-energy peak count rates for the following radionuclides:

anthropogenic nuclides -

<sup>137</sup>Cs (662 keV), <sup>134</sup>Cs (796 keV)

natural nuclides -

<sup>40</sup>K (1461 keV), <sup>214</sup>Pb (609 keV), <sup>208</sup>Tl (583 keV).

Dry activity concentrations were calculated relative to standards after subtraction of background count rates for each gamma-ray line. Counting data from samples and standards were corrected for density variations using data derived from a series of spiked soils of different densities [10].

For Cs nuclides the activities per unit area (Bq m<sup>-2</sup>) for each depth layer were calculated using the dry bulk weight of the original sample layer, and the core area. These were then summed vertically to obtain the total inventory down to the sampling depth (16 cm). For the natural nuclides the wet activity concentrations of each layer, and the weighted mean activity concentrations were calculated taking the mass fractions and moisture contents of each core layer into account.

Since the counting programme has finished, it has been recognised that the geometrical precision of the LOAX measurements may be limited to some  $\pm 5\%$  and that the results from

the IAEA Chernobyl soil when measured in 150 cm<sup>3</sup> geometry with a 50% relative efficiency GMX detector showed some unexpected instrumental dead time losses. Corrections for dead time were applied to the data from the IAEA-375 standard, based on inverse square experiments. Dead time losses from the other samples or standards were negligible.

### 3.2 Analyses at STUK

After drying, the soil samples were crushed and homogenised carefully. Subsamples were packed in the measuring beaker. Plastic beakers 42mm in diameter, 25 mm in height were used. The mass of measured subsample varied from 9.6 g to 62 g. The beaker was not radon-tight, so the radon emanation from the sample couldn't be taken into account. This will cause a small (5-15%) systematic error on <sup>214</sup>Bi results.

The samples were measured in gammalaboratory of STUK. Altogether five different detectors were used. Relative efficiencies of the detectors varied from 20% to 100% and they were housed within low background lead shields. Some samples were measured on all five detectors to check the cross-calibration of the equipment. As a result, no significant discrepancy were found between the detectors. The detectors are calibrated using solutions made from commercial standards and the calibration is confirmed in international intercomparisons and checked continuously. The measurements were done in a quite rapid schedule. The measuring times varied from 54.22 to 5385 minutes. Typically, the samples from the depth of 0 to 2 were measured 2 hours, samples from the depth of 2 to 6 were measured 3 to 5 hours and samples below the depth of 6 were measured 8 to 16 hours. The measurements were continued at least so long that the statistical accuracy of 661.6 keV peak was better than 20%. The gamma analysis program GAMMA-83 performs the following tasks: peak searching, peak identification, activity calculation and report printing. It can make the density correction automatically. The printout of the analysis program is in Appendix 3.

The nuclides reported here are <sup>137</sup>Cs (662 keV), <sup>134</sup>Cs (604 keV), <sup>40</sup>K (1461 keV), <sup>214</sup>Bi (all detected transitions) and <sup>208</sup>Tl (all detected transitions).

### 3.3 Quality Assurance Checks

The reference materials used for the calibration are traceable to IAEA Soil-6 and IAEA-375. Soil-6 is certified by the IAEA for the calibration of <sup>137</sup>Cs although the specific activity is low in comparison with most of the soil samples collected and much less than reference material IAEA-375.

Five common samples from a single core were measured by STUK and SURRC for inter laboratory comparison.

## 4. RESULTS

The results from IAEA reference materials and common samples analysed in both SURRC and STUK laboratories are presented first in sections 4.1 and 4.2 to demonstrate the traceability and compatibility of the data sets from field samples. Section 4.3 presents results from Area I (Vesivehmaa airfield), including Cs depth distribution parameters and densities, and section 4.4 shows similar results of cores taken from Area II.

### 4.1 Reference Materials

For the purpose of this study, common reference materials have been used to serve as a means of tracing the calibration soil samples to recognised standards. Two reference materials were chosen, and acquired from IAEA (Analytical Quality Control Services) Vienna. Both STUK and SURRC have analysed these standards and a comparison is shown in table 4.1. The densities of Soil-6 and IAEA-375 were about 1.06 and 1.47 gcm<sup>-3</sup>. For <sup>137</sup>Cs the mean values obtained by both laboratories is highly consistent, and within the range of IAEA values. The results from <sup>134</sup>Cs and from natural nuclides are more variable reflecting in part the limited counting time available for the laboratory analysis.

**Table 4.1** Reference materials.

Radionuclide	IAEA Value / Bq per kg		Mean STUK Value / Bq per kg		Mean SURRC Value / Bq per kg	
	SOIL-6	IAEA-375	SOIL-6	IAEA-375	SOIL-6	IAEA-375
<sup>137</sup> Cs	40.28 (38.6- 43.47)	4870.1 ±73.8	40.96 ±0.82	4884.05 ±73.26	40.00 ±0.20	4877.45 ±24.52
<sup>134</sup> Cs	-	142.76 ±2.77	-	156.07 ±2.18	-	73.97 ±17.2
<sup>40</sup> K	-	424.0 ±8.0	367.03 ±8.07	412.78 ±8.25	378.21 ±25.72	375.92 ±29.19
<sup>214</sup> Bi	-	22.6 ±2.0	69.72 ±0.98	17.10 ±0.87	77.61 ±8.15	44.48 ±8.52
<sup>208</sup> Tl	-	7.45 ±0.22	10.31 ±0.38	8.76 ±0.48	18.56 ±1.92	11.35 ±2.28

### 4.2 Common Samples

Five common soil samples, comprising a single core were analysed by STUK and SURRC. The results of this analysis are shown below in table 4.2a and 4.2b. Table 4.2a shows the activity concentrations determined in Bq kg<sup>-1</sup> (dry) in both laboratories, and Table 4.2b shows the ratios of results from STUK to those from SURRC. For <sup>137</sup>Cs the agreement is within ±5% for activity concentrations above 20 Bq kg<sup>-1</sup>. The agreement for <sup>40</sup>K is satisfactory. Results from <sup>214</sup>Bi may indicate differences in radon retention between the two laboratories,

while those from  $^{208}\text{Tl}$  suggest the possibility of systematic differences. Overall the agreement between laboratories is acceptable, especially for  $^{137}\text{Cs}$  and  $^{40}\text{K}$  analyses.

**Table 4.2a** Common samples (Bq kg<sup>-1</sup> dry)

Core	$^{137}\text{Cs}$		$^{40}\text{K}$		$^{214}\text{Bi}$		$^{208}\text{Tl}$	
	SURRC	STUK	SURRC	STUK	SURRC	STUK	SURRC	STUK
A2.6 0-2cm	5707.6 ±382.4	5735 ±172	367.8 ±58.8	392.7 ±27	45.7 ±9.3	34.4 ±3.44	7.8 ±3.4	9.4 ±2.3
A2.6 2-4cm	252.4 ±17.7	238.8 ±7.2	852.8 ±51.2	727.8 ±29.1	35.1 ±5.9	38.9 ±1.9	12.8 ±3.2	11.3 ±1.0
A2.6 4-6cm	27.5 ±3.3	26.2 ±1.8	969.4 ±126.0	931.1 ±46.6	61.9 ±26.6	36.6 ±2.6	20.3 ±12.9	13.9 ±1.4
A2.6 6-11cm	10.9 ±1.4	13.3 ±0.5	821.3 ±57.5	835.0 ±25.0	70.4 ±23.9	44.1 ±0.9	9.5 ±1.8	12.7 ±0.5
A2.6 11-16cm	9.49 ±1.3	10.96 ±0.4	767.7 ±53.7	769.9 ±23.1	82.2 ±27.8	37.2 ±0.7	11.2 ±2.0	13.1 ±0.5

**Table 4.2b** Ratio of STUK/SURRC common samples

Core	$^{137}\text{Cs}$	$^{40}\text{K}$	$^{214}\text{Bi}$	$^{208}\text{Tl}$
A2,6 0-2cm	1.00 ±0.07	1.07 ±0.20	0.75 ±0.17	1.2 ±0.6
A2,6 2-4cm	0.95 ±0.07	0.85 ±0.06	1.1 ±0.19	0.88 ±0.23
A2,6 4-6cm	0.95 ±0.13	0.96 ±0.13	0.59 ±0.26	0.68 ±0.44
A2,6 6-11cm	1.22 ±0.16	1.02 ±0.08	0.63 ±0.21	1.34 ±0.26
A2,6 11-16cm	1.15 ±0.16	1.00 ±0.08	0.45 ±0.15	1.17 ±0.21

### 4.3 Results from Vesivehmaa Airfield (Area I)

Results for the calibration site at Vesivehmaa airfield are presented in three parts. The results from each position are considered first. Thereafter weighted mean estimates are evaluated for the effective activities observed with detectors at 1m, 50m and 100m are presented. Finally the depth distribution is discussed in section 4.3.3. Primary data are presented in Appendices.

#### 4.3.1 Summary of Results from Each Shell and Position

In the tables 4.3-4.6 are listed the radionuclide deposition and inventories for  $^{137}\text{Cs}$ ,  $^{40}\text{K}$ ,  $^{214}\text{Bi}$  and  $^{208}\text{Tl}$ . Each shell number represents increasing distance from the centre point. Each hexagonal apex is listed as a clockwise orientation from the main reference axis along the direction  $126^\circ$ . Mean values are shown for each shell and are incorporated into the weighted activity estimates shown in 4.3.2.

Sampling date: 26-29 May 1995

Gamma spectrometry STUK/SURRC June-July 1995

Reference date: 1 June 1995

Traceable to IAEA Soil-6 and IAEA-375

**Table 4.3** Vesivehmaa Airfield (Area I):  $^{137}\text{Cs}$  activity 0-16cm / kBq m<sup>-2</sup>

Shell	Radius /m	Clockwise Orientation						Mean ±Std dev
		1 STUK	2 SURRC	3 STUK	4 SURRC	5 STUK	6 SURRC	
0	0	40.83±2.55 (SURRC), 63.3±2.5 (STUK)						52.1 ±15.9
1	2	48.0 ±2.0	43.2 ±2.3	58.9 ±2.5	48.9 ±2.8	50.9 ±2.5	59.1 ±3.6	51.5 ±6.3
2	8	34.7 ±4.0	46.2 ±2.0	59.2 ±4.0	45.9 ±2.0	47.3 ±3.0	49.2 ±2.8	47.1 ±7.8
3	32	48.3 ±2.0	41.7 ±1.9	36.4 ±2.0	53.6 ±2.6	55.7 ±2.0	59.5 ±2.6	49.2 ±8.8
4	128	57.9 ±2.0	53.2 ±2.8	40.7 ±2.0	55.0 ±2.6	96.0 ±4.0	60.8 ±2.8	60.6 ±18.7
5	256	3.7 ±0.3 *	51.7 ±2.7	119.0 ±5.0	11.7 ±0.7 *	44.0 ±2.0	51.8 ±2.3	46.9 ±40.9

\* These samples comprised mainly sand and gravels.

**Table 4.4** Vesivehmaa Airfield (Area I): <sup>40</sup>K activity 0-16cm / Bq per kg (wet)

Clockwise Orientation								
Shell	Radius /m	1	2	3	4	5	6	Mean ±Std dev
		STUK	SURRC	STUK	SURRC	STUK	SURRC	
0	0	725.6±156.3 (SURRC), 560.8±113.6 (STUK)						643.2 ±116.5
1	2	523.5 ±81.3	583.4 ±98.5	575.0 ±108.6	622.6 ±94.8	478.0 ±78.0	607.5 ±82.1	565.0 ±54.5
2	8	579.5 ±135.8	648.0 ±140.3	636.7 ±120.2	725.6 ±142.9	481.4 ±73.0	691.6 ±131.3	627.1 ±87.0
3	32	498.8 ±87.9	725.0 ±134.1	570.5 ±91.0	666.6 ±112.8	577.5 ±97.2	773.7 ±101.1	635.4 ±104.3
4	128	724.0 ±42.6	889.9 ±181.7	652.0 ±96.3	762.4 ±134.7	521.1 ±34.9	592.9 ±116.6	690.4 ±130.9
5	256	782.4 ±56.6 *	843.1 ±92.0	617.1 ±107.3	769.8 ±21.4 *	621.5 ±86.1	641.9 ±192.5	712.6 ±97.6

\* These samples comprised mainly sand and gravels.

**Table 4.5** Vesivehmaa Airfield (Area I): <sup>214</sup>Bi activity 0-16cm / Bq per kg (wet)

Clockwise Orientation								
Shell	Radius /m	1	2	3	4	5	6	Mean ±Std dev
		STUK	SURRC	STUK	SURRC	STUK	SURRC	
0	0	41.4±9.9 (SURRC), 29.3±2.9 (STUK)						35.4 ±8.6
1	2	29.4 ±5.6	46.3 ±11.8	49.1 ±9.1	49.1 ±12.5	24.1 ±3.0	39.7 ±8.7	39.6 ±10.7
2	8	34.1 ±3.4	54.6 ±12.9	39.2 ±6.5	60.9 ±14.2	26.9 ±2.6	59.0 ±12.4	45.8 ±14.3
3	32	27.0 ±1.6	62.9 ±13.5	38.6 ±4.8	62.5 ±12.5	32.0 ±0.7	63.7 ±10.9	47.8 ±17.1
4	128	35.1 ±1.8	104.5 ±38.7	36.2 ±6.0	59.8 ±11.8	30.2 ±1.0	59.3 ±11.9	54.2 ±27.8
5	256	32.9 ±2.2 *	82.3 ±17.9	36.9 ±4.8	60.4 ±5.3 *	27.5 ±1.4	50.7 ±14.6	48.5 ±20.5

\* These samples comprised mainly sand and gravels.

**Table 4.6** Vesivehmaa Airfield (Area I):  $^{208}\text{Tl}$  activity 0-16cm / Bq per kg (wet)

Clockwise Orientation								
Shell	Radius /m	1	2	3	4	5	6	Mean $\pm$ Std dev
		STUK	SURRC	STUK	SURRC	STUK	SURRC	
0	0	10.0 $\pm$ 2.4 (SURRC), 9.6 $\pm$ 0.6 (STUK)						9.8 $\pm$ 0.3
1	2	9.2 $\pm$ 0.4	10.2 $\pm$ 3.0	11.3 $\pm$ 1.7	8.9 $\pm$ 1.3	8.7 $\pm$ 1.8	8.4 $\pm$ 1.5	9.5 $\pm$ 1.1
2	8	10.3 $\pm$ 2.9	13.8 $\pm$ 2.3	10.4 $\pm$ 1.3	9.3 $\pm$ 1.1	7.1 $\pm$ 0.9	10.3 $\pm$ 2.4	10.2 $\pm$ 2.2
3	32	7.6 $\pm$ 0.3	11.6 $\pm$ 1.8	10.7 $\pm$ 0.5	9.9 $\pm$ 1.7	10.0 $\pm$ 1.0	16.2 $\pm$ 3.6	11.0 $\pm$ 2.9
4	128	9.7 $\pm$ 0.6	10.6 $\pm$ 1.7	9.5 $\pm$ 1.7	9.9 $\pm$ 1.7	10.1 $\pm$ 0.8	9.4 $\pm$ 2.1	9.9 $\pm$ 0.4
5	256	9.8 $\pm$ 0.9 *	11.8 $\pm$ 2.3	10.0 $\pm$ 0.8	13.2 $\pm$ 1.9 *	9.8 $\pm$ 1.2	11.8 $\pm$ 2.5	11.1 $\pm$ 1.4

\* These samples comprised mainly sand and gravels.

### 4.3.2 Weighted Activity Estimates

The mean inventory estimates from each shell were weighted to match the spatial averaging of a detector at 1, 50 and 100 m altitude [10]. The source depth tends to narrow the field of view of the detector, but the effect on the shell weighting factors is small given the unrefined nature of the field sampling. The weighting factors are given below in table 4.7 and the effective radionuclide concentrations at different detector heights given in table 4.8.

**Table 4.7** Shell weighting factors

Shell	Detector Height /metres		
	1	50	100
1	0.80	0.02	0.01
2	0.17	0.13	0.04
3	0.03	0.60	0.40
4	0	0.20	0.35
5	0	0.05	0.10

**Table 4.8** Effective radionuclide concentrations at Area I

Detector Height /m	Mean $^{137}\text{Cs}$ / kBq m <sup>-2</sup>	Mean $^{40}\text{K}$ / Bq per kg	Mean $^{214}\text{Bi}$ / Bq per kg	Mean $^{208}\text{Tl}$ / Bq per kg
1	50.7±5.2	577.7±46.1	40.9±8.9	9.7±1.0
50	51.1±6.9	647.8±68.9	53.1±11.9	10.7±1.8
100	47.9±8.5	597.8±62.8	45.2±12.1	9.5±1.2

### 4.3.3 Depth Distributions

#### 4.3.3.1 <sup>137</sup>Cs

The most common approximation of radiocaesium concentration profile in soil is the exponential distribution:

$$S(z) = s(0) \exp^{-(\alpha/\rho)(\rho z)}$$

where  $\alpha/\rho$  is the exponential mass activity distribution coefficient,  $\rho$  is the density of the soil and  $S(z)$  is the activity concentration [Bq/kg] in soil at the depth  $z$ . The inverse of  $\alpha/\rho$  is the relaxation mass per unit area,  $\beta$  [15].

In the figures 4.1-4.2 some <sup>137</sup>Cs activity concentration profiles measured from Vesivehmaa airfield are plotted in semi-logarithmic scale. The distribution coefficient  $\alpha/\rho$  was determined by using LOGEST function of Microsoft Excel (Microsoft corp., USA) spreadsheet program. It returns the parameters for logarithmic fitting. Only three uppermost layers (0-2 cm, 2-4 cm and 4-6 cm) were used in the fitting, since they contained about 95 % of <sup>137</sup>Cs activity. If the whole data had been used, the lower tails of the distribution profiles would have had too strong influence on the calculated values. The values for the distribution coefficient  $\alpha/\rho$  are shown in table 4.9. The mean  $\alpha/\rho$  value is  $0.77 \pm 0.10 \text{ cm}^2\text{g}^{-1}$  (mean  $\beta = 1.31 \pm 0.15 \text{ gcm}^{-2}$ ).

The mean wet soil density (0-16 cm depth) was  $1.29 \pm 0.49 \text{ gcm}^{-3}$  ( $\pm$ sd,  $n=151$ ) in May. At the 0-2 cm layer, the wet density was found to be  $0.74 \pm 0.36 \text{ gcm}^{-3}$ ; increased to  $1.37 \pm 0.50 \text{ gcm}^{-3}$  at the 2-4 cm layer;  $1.67 \pm 0.43 \text{ gcm}^{-3}$  for 4-6 cm; and remained constant for the 6-11 cm and 11-16 cm layers of  $1.42 \pm 0.23 \text{ gcm}^{-3}$  respectively.

**Table 4.9**

Shell	0	1	2	3	4	5
$\alpha/\rho$	0.79 $\pm 0.14$	0.69 $\pm 0.06$	0.71 $\pm 0.08$	0.70 $\pm 0.19$	0.79 $\pm 0.43$	0.96 $\pm 0.56$
$\beta$	1.27 $\pm 0.23$	1.45 $\pm 0.13$	1.41 $\pm 0.16$	1.43 $\pm 0.39$	1.27 $\pm 0.69$	1.04 $\pm 0.61$

#### 4.3.3.2 Natural radionuclides

The <sup>40</sup>K, <sup>214</sup>Bi and <sup>208</sup>Tl activity concentration distribution profiles are in figures 4.3, 4.4 and 4.5 respectively. The assumption of homogeneous activity distribution seems to be reasonable.

**Figure 4.1**

Measured activity concentrations in wet soil verse mass depth at the points 2.1, 2.3, 2.5 and 2.6. The activity distributions shown are typical for all the points at the shells 0, 1, 2 and 3. The distribution is not an exponential, but it has a long lower tail. The tail contains, however, a very little amount of  $^{137}\text{Cs}$ .

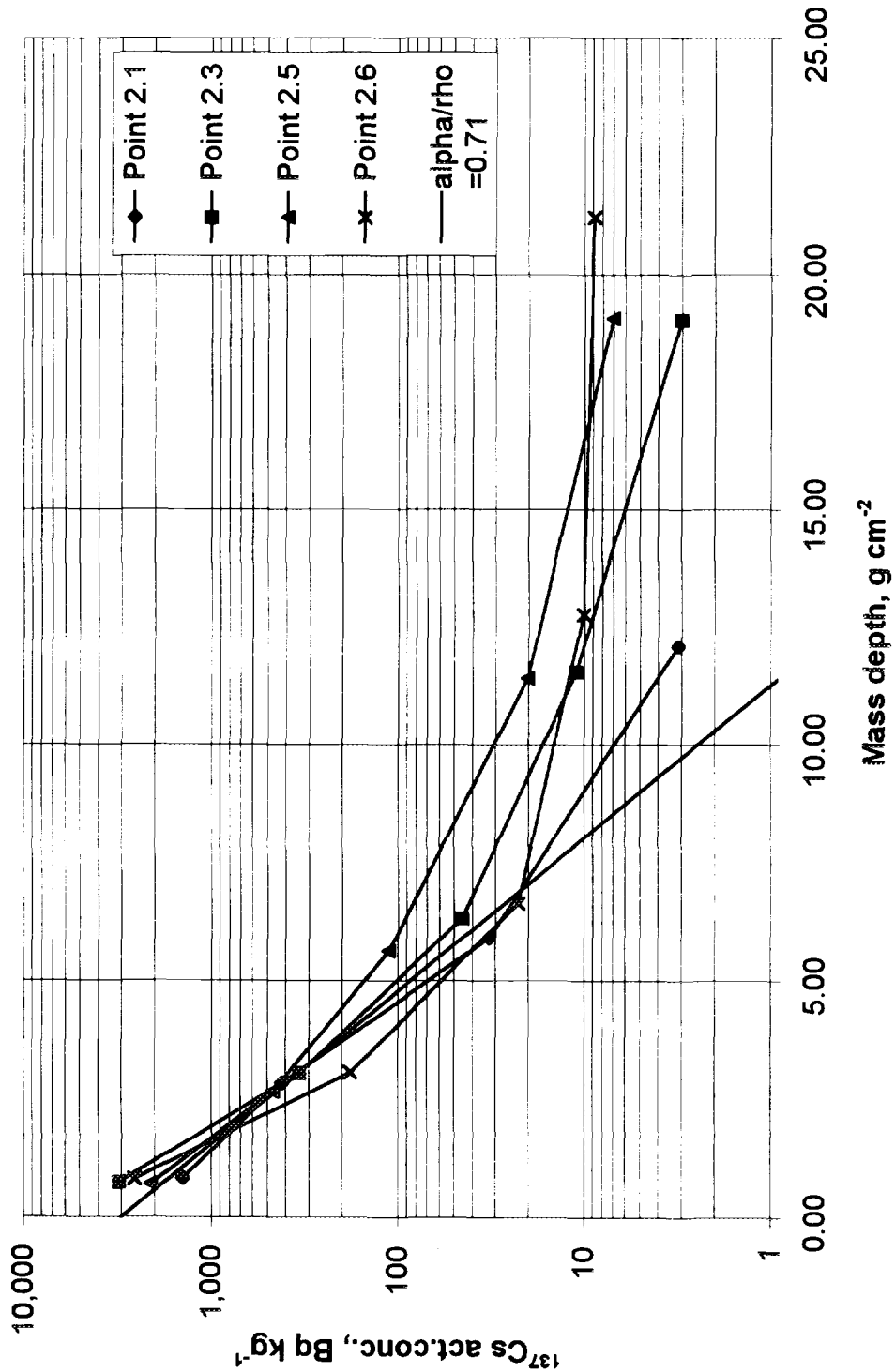


Figure 4.2

Measured activity concentrations versus mass depth at the points 4.1, 4.5 and 5.1. At the outer shells the depth distribution profiles show much more variability. The distribution in depth at the point 4.5 is similar to those at the inner shells 0, 1, 2 and 3. At the point 5.1 the soil comprised sand and gravels and the  $^{137}\text{Cs}$  has penetrated deeper. The distribution profile is quite even. At the point 4.1 the distribution profile is also quite even. However, the total surface activity at this point is  $58 \text{ kBq m}^{-2}$ , which is slightly higher than the average value on the airfield. Possibly, the different layers were mixed, when the core was taken.

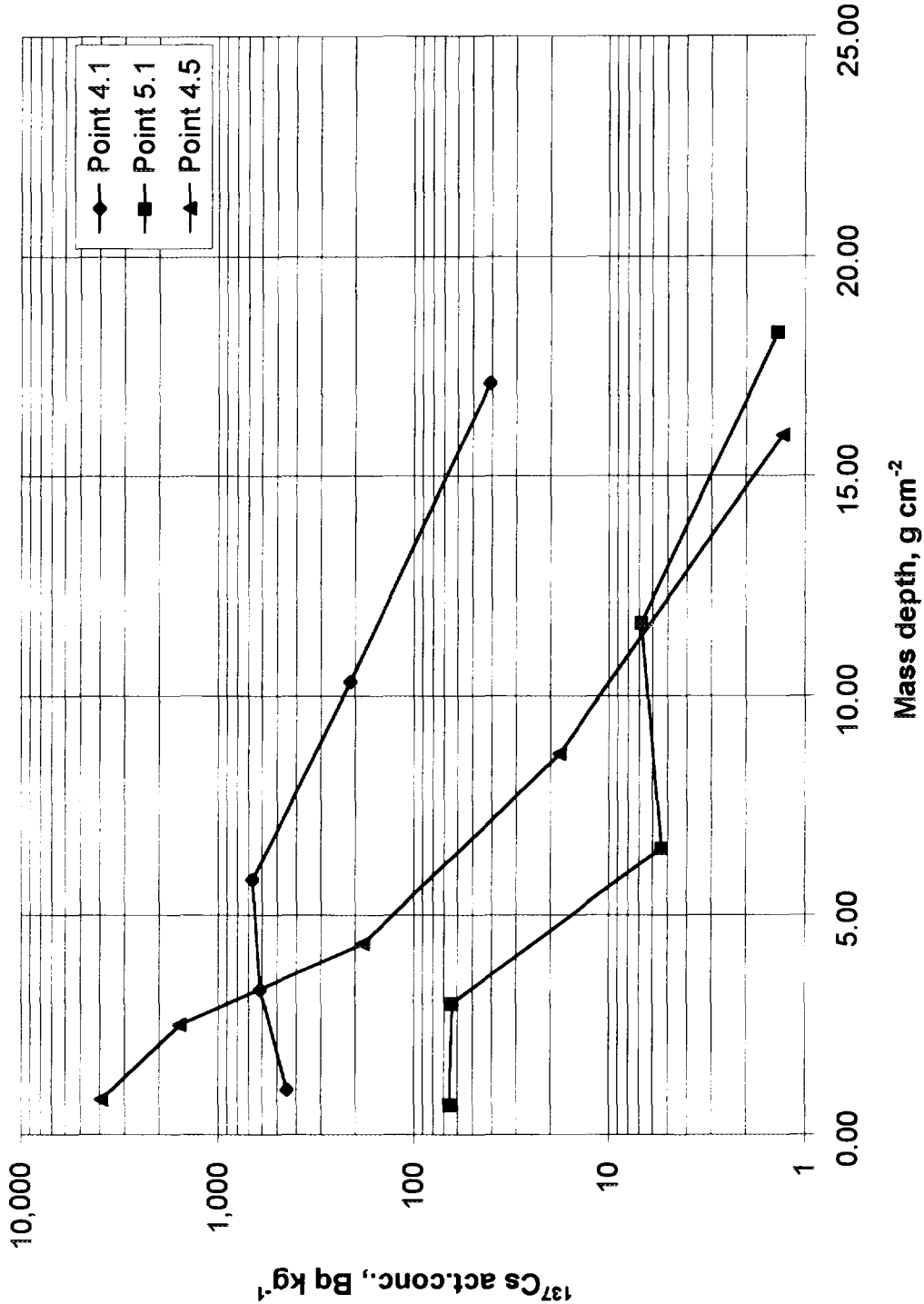


Figure 4.3

$^{40}\text{K}$  distribution with depth. All the measured subsamples are plotted in the graph. Activity concentration in the topmost layers is smaller than in the lower parts of the core.

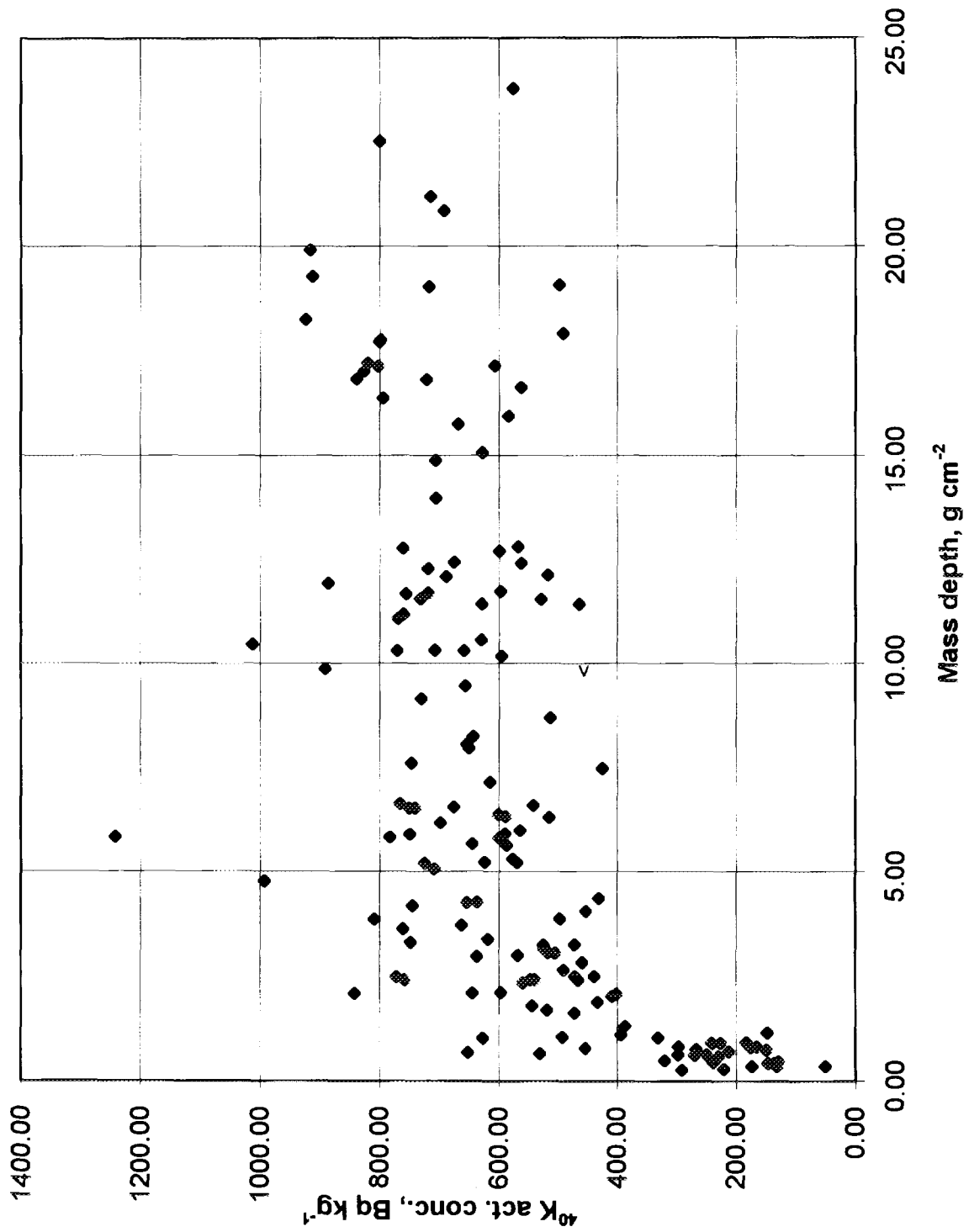
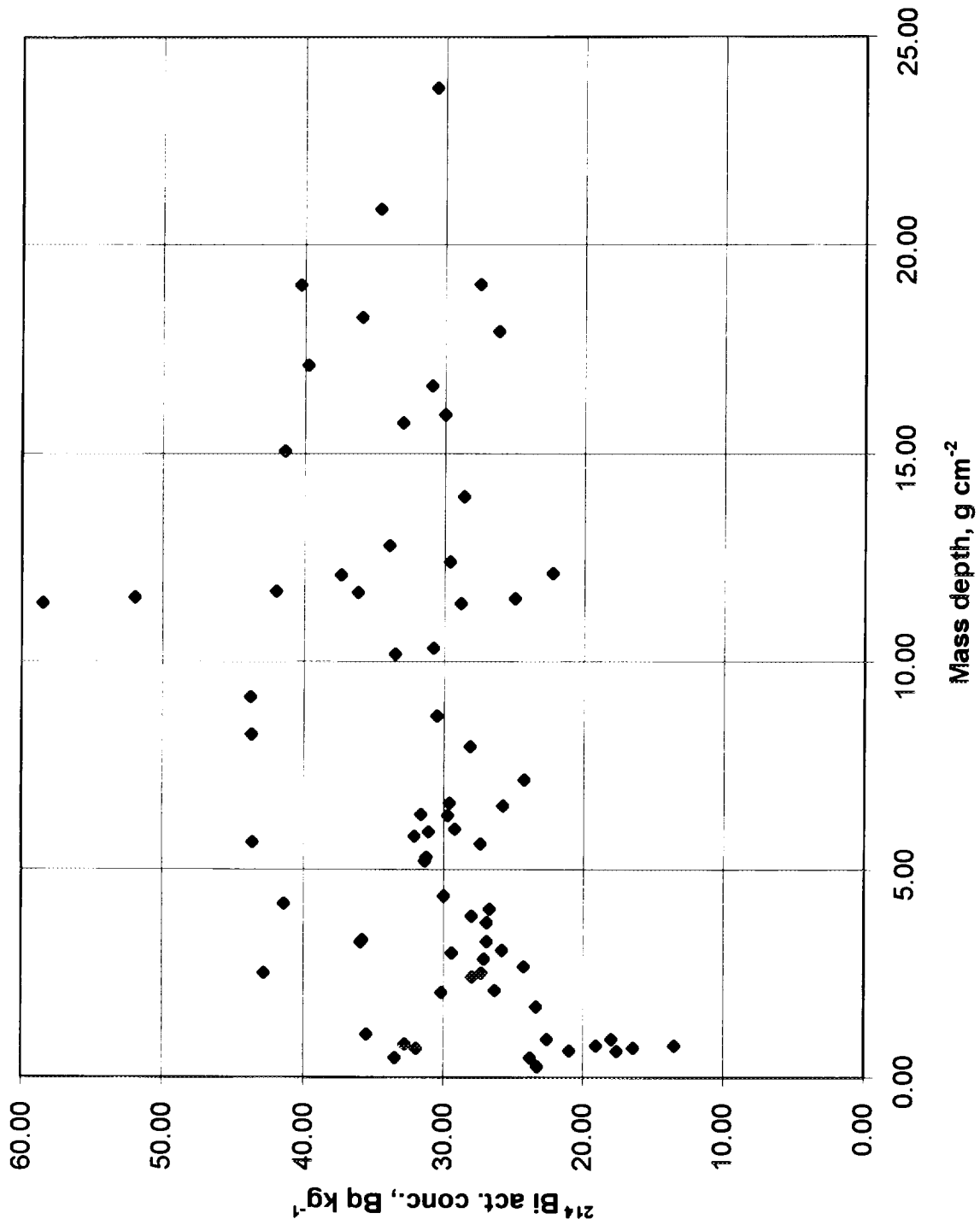


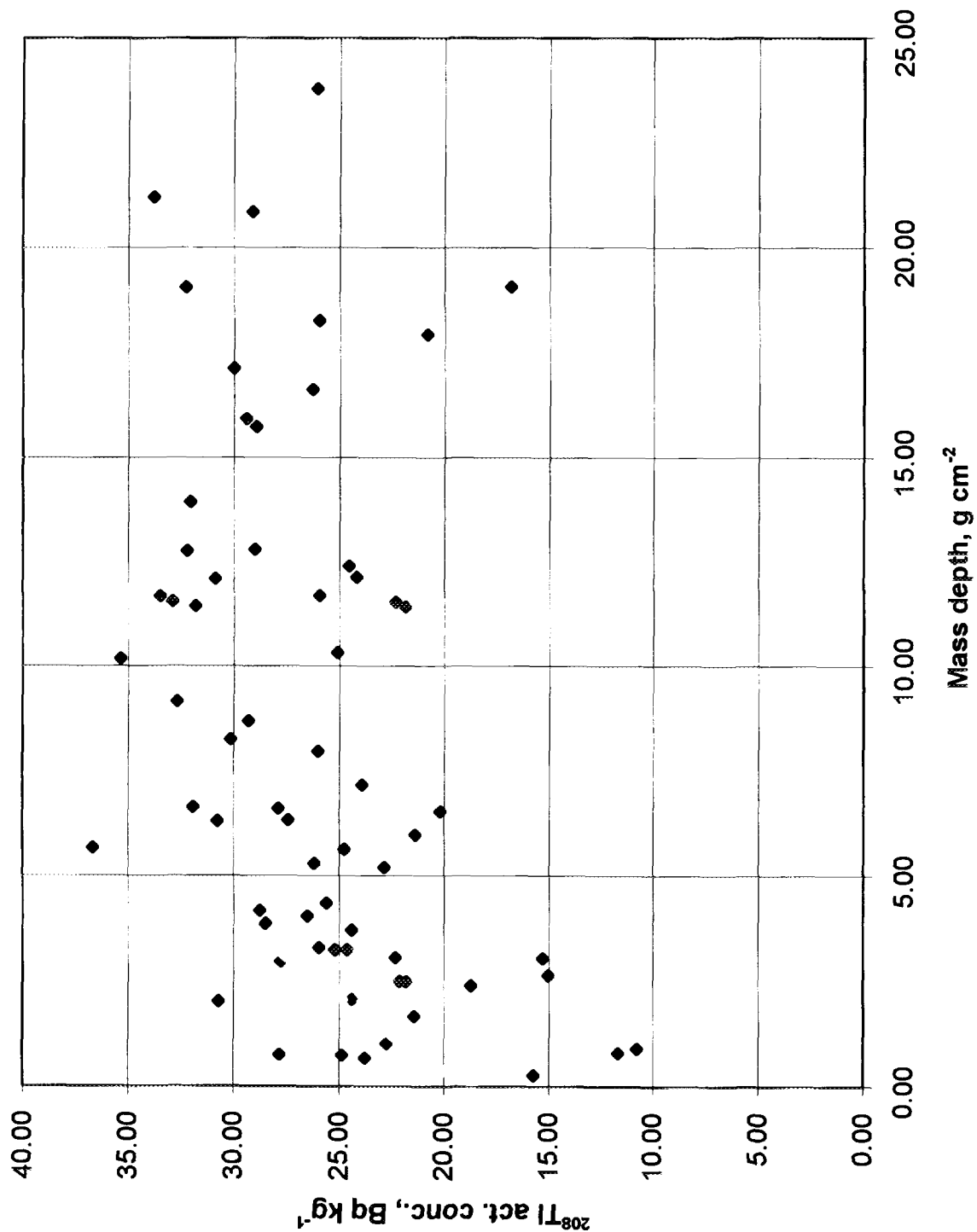
Figure 4.4

$^{214}\text{Bi}$  distribution with depth. Only the subsamples measured in STUK are plotted in the graph. Assumption of homogenous activity concentration is good.



**Figure 4.5**

$^{208}\text{Tl}$  distribution with depth. Only the subsamples measured in STUK are plotted in the graph. The values are given as  $^{232}\text{Th}$  equilibrium activity. Thus, the numerical values should be multiplied by the branching ratio of  $^{208}\text{Tl}$  (0.3593) to obtain the actual  $^{208}\text{Tl}$  activity concentration. Assumption of homogenous activity concentration is good.



## 4.4 Results from Area II

### 4.4.1 Summary of results from each point

Sampling time 27-28 May 1995

Gamma spectrometry STUK July/August 1995

Reference date 1 June 1995

Traceable to IAEA Soil-6 and IAEA-375

**Table 4.10** Analysis of samples taken from Area II

Site	$^{137}\text{Cs}$ / kBq m <sup>-2</sup>	$^{40}\text{K}$ / Bq kg <sup>-1</sup>	$^{214}\text{Bi}$ / Bq kg <sup>-1</sup>	$^{208}\text{Tl}$ / Bq kg <sup>-1</sup>
1	141.0±4.3	719±13	37.9±2.5	9.6±0.7
2	146.0±5.6	444±137	11.5±3.1	3.5±0.1
3	1.29±0.14	442±15	29.6±1.7	11.8±0.8
4	43.1±1.3	500±21	17.4±1.9	5.8±0.4
5	103±4	bdl	2.5±3.0	bdl
6	172±7	526±107	20.1±1.5	4.9±0.3
7	40.0±1.6	443±55	23.1±3.5	7.1±0.7
8	150±6	451±40	18.3±1.6	6.7±0.6
9	35.1±1.3	bdl	bdl	3.9±1.0

### 4.4.2 $^{137}\text{Cs}$ Depth distributions

In figure 4.6 the depth distribution profiles are drawn in semi-logarithmic scale. Again, the distribution coefficient  $\alpha/\rho$  is determined using LOGEST function of Microsoft Excel (see chapter 4.3.3). Here only four uppermost layers were used, since the most of the activity was in the topmost layers, and most profiles seem to have long lower tails. Distribution coefficients are calculated in the table 4.11.

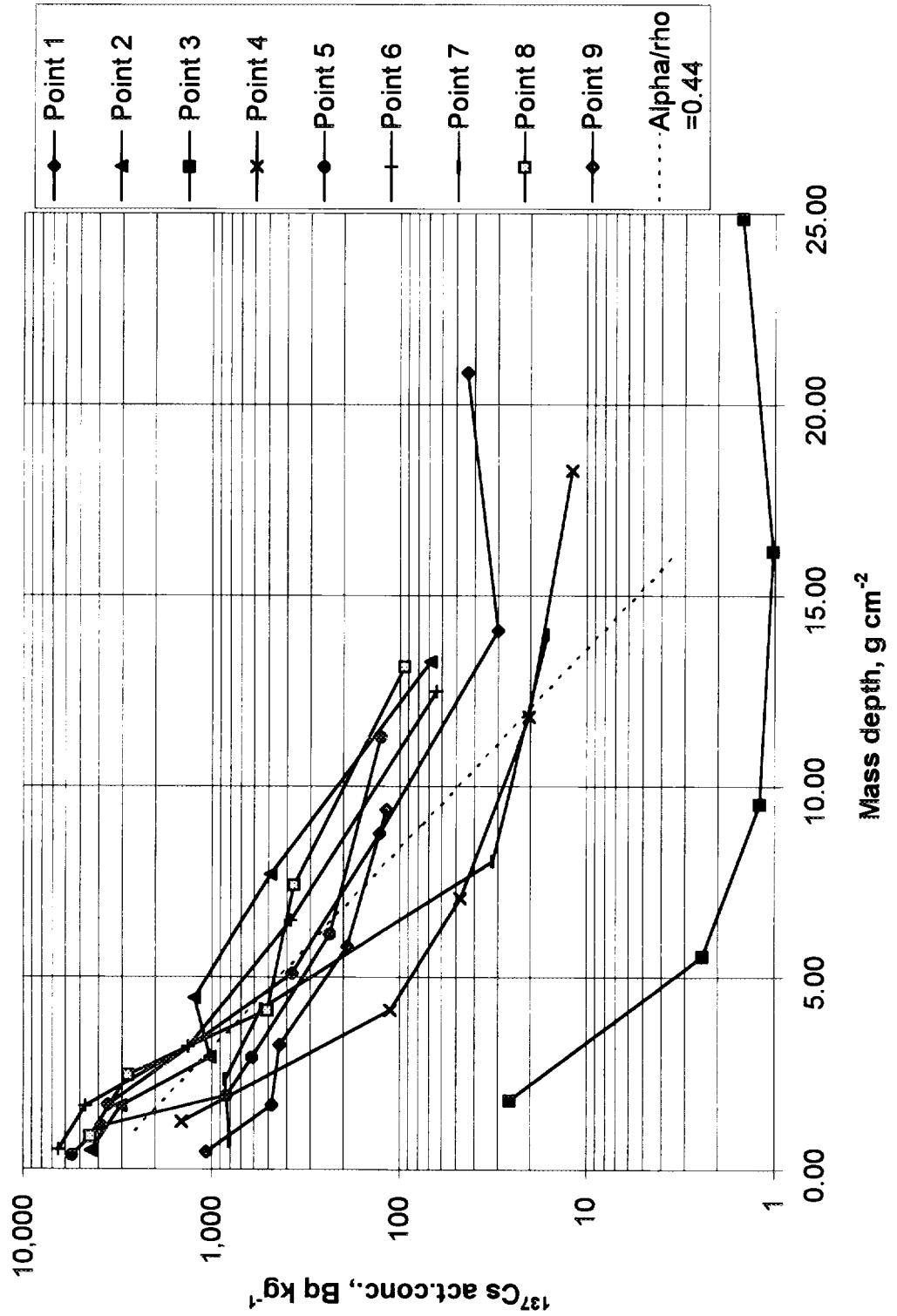
**Table 4.11** Distribution coefficients in Area II.

Site	1	2	3	4	5	6	7	8	9	Mean ±sd
$\alpha/\rho$	0.37	0.36	0.39	0.38	0.95	0.49	0.47	0.40	0.29	0.44 ±0.21
$\beta$	2.70	2.78	2.56	2.63	1.05	2.04	2.13	2.5	3.45	2.43 ±0.66

The mean  $\alpha/\rho$  value for  $^{137}\text{Cs}$  deposition across Area II was found to be  $0.44 \pm 0.21 \text{ cm}^2\text{g}^{-1}$ , ie. the activity is deeper than Area I. The mean wet soil density (0-16 cm depth) in May was  $1.07 \pm 0.46 \text{ gcm}^{-3}$  ( $\pm\text{sd}$ ,  $n=47$ ).

Figure 4.6

Measured activity concentrations in wet soil versus mass depth at the sampling sites in Area II. Most profiles seem to have long lower tails, but some profiles, like at point 2 and point 8 are almost exponential. Generally, exponential distribution is applicable.



## 5. CONCLUSIONS

The results in this report provide a means of establishing a traceable calibration for the RÉSUMÉ study. The sampling plans and methodology are well established and provide a means for compensating for spatial variability in the environment of the calibration site, and for estimating the effective activities observed with different fields of view. This provides a means of comparison between the results of in-situ, carborne and airborne gamma spectrometry and traceable absolute laboratory analysis.

The results for  $^{137}\text{Cs}$  from reference materials and samples counted in both laboratories are highly consistent. Individual core results from the calibration site varied by more than a factor of two, with a mean value close to  $50 \text{ kBq m}^{-2}$ . There was evidence of greatest variability towards the edges. For example at point A4,5 (128 m from centre)  $96 \text{ kBq m}^{-2}$  was found, and A5,3 (256 m radius)  $119 \text{ kBq m}^{-2}$ , while the lower reading at point A5,1 (256 m from centre) of  $3.7 \text{ kBq m}^{-2}$  was associated with an anomalous sand/gravel mixture completely lacking in humus. The weighted mean activity per unit area on the calibration site takes on values of  $50.7 \pm 5.2 \text{ kBq m}^{-2}$  at 1 m ground clearance,  $51.1 \pm 6.9 \text{ kBq m}^{-2}$  at 50 m height and  $47.9 \pm 8.5 \text{ kBq m}^{-2}$  at 100 m. The similarity of these values confirms the suitability of the Vesivehmaa site for comparison of in-situ and airborne results despite the variations in individual results.

The mean  $\alpha/\rho$  value for  $^{137}\text{Cs}$  deposition across Area I was found to be  $0.77 \pm 0.10 \text{ cm}^2\text{g}^{-1}$  ( $\beta = 1.31 \text{ gcm}^{-2}$ ). The mean wet soil density (0-16 cm depth) in May was  $1.29 \pm 0.49 \text{ gcm}^{-3}$ . The SURRC 16 litre NaI detector array at 100 m above the centre point yielded a calibration factor of  $0.10 \pm 0.02 \text{ kBq m}^{-2}/\text{cps}$  during the Exercise period in August. This compares favourably with theoretical calculations of  $0.116 \text{ kBq m}^{-2}/\text{cps}$  for the above parameters [9].

The analysis by STUK of samples taken in Area II showed wide variability of  $^{137}\text{Cs}$ . The mean is  $92.4 \pm 63 \text{ kBq m}^{-2}$ , with a sample collected at site number 6 showing the largest deposition of  $172 \pm 7 \text{ kBq m}^{-2}$ . The sample was collected near Laihansuo, about half way between the parking area at the end of the road, and the stream. A handheld dosimeter recorded a reading of  $0.5 \mu\text{Sv hr}^{-1}$  at ground level. Site number 3 (near Viitastenniittu) showed the least radiocaesium ( $1.29 \pm 0.14 \text{ kBq m}^{-2}$ ) from an area with little humus, and large quantities of rock overburden, sand and gravels. The mean  $\alpha/\rho$  value for  $^{137}\text{Cs}$  deposition across Area II was found to be  $0.44 \pm 0.21 \text{ cm}^2\text{g}^{-1}$  ( $\beta = 2.43 \pm 0.66 \text{ gcm}^{-2}$ ) and therefore deeper than activity found in Area I. The mean wet soil density (0-16 cm depth) in May was  $1.07 \pm 0.46 \text{ gcm}^{-3}$ .

In-situ measurements were performed at the airfield using the STUK emergency vehicle at the time of sampling and during the exercise to examine changes due to moisture content variations. Unfortunately although the count-rate observed at 661.6 keV in August was 40% higher than in May it was not possible to exclude potential changes in the vehicle background or counting efficiency between these two dates. Although a lower moisture content in August is quite likely, the  $^{137}\text{Cs}$  activity is quite close to the surface, and thus would not be expected to be highly influenced by moisture content. The effect on natural nuclides would have been more pronounced, however it has not been possible to quantify this accurately using existing data. For future studies it is suggested that changes between the time of sampling and use should be monitored using ground based in-situ spectrometry, rather than vehicular systems.

## 6. REFERENCES

- [1] IAEA, 1974, Recommended instrumentation for Uranium and Thorium exploration, Technical Report Series 158, IAEA, Vienna
- [2] GRASTY R.L., 1975, Uranium measurement by airborne gamma-ray spectrometry, *Geophysics* **40**, 503-519
- [3] IAEA, 1976, Radiometric reporting methods and calibration in uranium exploration, Technical Report Series 174, IAEA, Vienna
- [4] IAEA, 1979, Gamma ray surveys in uranium exploration, Technical Report Series 186, IAEA Vienna
- [5] IAEA, 1989, Construction and use of calibration facilities for radiometric field equipment, Technical report series 309, IAEA Vienna
- [6] ALEXANDER, P., Kosanke, K., 1978, The Quality of Airborne Radiometric data. Nevada Section - American Nuclear Soc. Aerial Techniques for Environmental Monitoring, Top. symp. proc.
- [7] LØVBORG, L., Grasty, R.L., Kirkegaard, P., 1978. A Guide to the Calibration Constants for Aerial Gamma-ray Surveys in Geoexploration. Top. Symp. Proc. Nevada Section - American Nuclear Soc. Aerial Techniques for Environmental Monitoring.
- [8] LØVBORG, L., 1982. Error Analysis of Calibration and Field Trials with Spectrometers and Counters. Symp. on Uranium Exploration Methods. OECD Nuclear Energy Agency in collaboration with IAEA, Paris 1-4th June.
- [9] ALLYSON, J.D., 1994. Environmental Gamma-ray Spectrometry: Simulation of Absolute Calibration of In-Situ and Airborne Spectrometers for Natural and Anthropogenic Sources. The University of Glasgow.
- [10] TYLER, A.N., 1994. Environmental Influences on Radionuclide Inventories and Activity Estimations through Laboratory Based, In-situ and Aerial Gamma Spectrometry. The University of Glasgow.
- [11] SANDERSON, D.C.W, Allyson J.D., Tyler A.N., 1992, An aerial gamma ray survey of Chapelcross and it's surroundings in February 1992, *SURRC Aerial Survey Report*, to BNF, 36p.
- [12] SANDERSON, D.C.W, Allyson J.D., Tyler A.N., Murphy S., 1993, An aerial gamma ray survey of Springfields and the Ribble Estuary in September 1992, *SURRC Aerial Survey Report*, to BNF, 46p.
- [13] SANDERSON, D.C.W, Allyson J.D., Tyler A.N., Ni Riain S., Murphy S., 1993, An airborne gamma ray survey of parts of SW Scotland in February 1993, *SURRC Aerial Survey Report*, to the Scottish Office, 26p.

[14] FINCK R. R., 1992. Field Gamma-Ray Spectrometry, Theory of Calibration and Measurement Using a Germanium Spectrometer. FOA Report C20900-4.3, 49p

[15] ICRU REPORT 53, 1994. Gamma-Ray Spectrometry in the Environment. International Commission on Radiation Units and Measurements.

[16] SANDERSON, D.C.W., ALLYSON, J.D., TYLER, A.N., SCOTT, E.M., 1993. Environmental Applications of Airborne Gamma Spectrometry. *Technical Committee Meeting on the Use of Uranium Exploration Data and Techniques in Environmental Studies, Vienna, Austria. 9-12 November 1993.* IAEA Report.

[17] SANDERSON, D.C.W., ALLYSON, J.D., TYLER, A.N., 1993. Rapid Quantification and Mapping of Radiometric Data for Anthropogenic and Technically Enhanced Natural Nuclides. *Technical Committee Meeting on the Use of Uranium Exploration Data and Techniques in Environmental Studies, Vienna, Austria. 9-12 November 1993.* IAEA Report.

**NEXT PAGE(S)  
left BLANK**



# Finnish Centre for Radiation and Nuclear Safety

## Characteristics and Location of Sources

ABSTRACT .....	43
1. INTRODUCTION .....	45
2. RADIONUCLIDE SOURCES IN AREA III .....	46
2.1. Terrain and population characteristic of the area .....	46
2.2. Sources .....	46
Tab. 1. Radionuclide sources hidden in Area III .....	47
2.3. Location of sources .....	48
Fig. 1. Locations of radioactive sources .....	49
Fig. 2. Collimated $^{137}\text{Cs}$ source (Cs2) (see Appendix 1) .....	50
Fig. 3. $^{99\text{m}}\text{Tc}$ source (Tc) activity as a function of time .....	51
2.4. Source placement and radioation protection .....	51
2.4.1. Caesium, cobalt and technetium sources .....	52
2.4.2. Iridium source .....	52
3. RADIONUCLIDE SOURCES USED IN THE AIRFIELD .....	54
4. CONCLUSIVE REMARKS .....	55
APPENDIX 1 .....	56
Fig. A1. Details of the supporting structure of the $^{137}\text{Cs}$ source (Cs2) .....	56
Fig. A2. Collimation of the primary photons .....	58

**NEXT PAGE(S)**  
**left BLANK**

## Characteristics and Locations of Sources

**J. Lahtinen, R. Pöllänen, H. Toivonen**  
Finnish Centre for Radiation and Nuclear Safety

### ABSTRACT

Ten artificial radiation sources were placed in the terrain in order to test the capability of airborne measuring teams to detect them. One of the sources was a line source, others were point sources (three of them collimated). The radionuclides used in the sources were  $^{60}\text{Co}$ ,  $^{137}\text{Cs}$ ,  $^{99\text{m}}\text{Tc}$  and  $^{192}\text{Ir}$ . The source activities ranged from about 26 MBq (one of the cobalt sources) to 0.56 TBq (iridium).

FINNISH CENTRE FOR RADIATION  
AND NUCLEAR SAFETY  
P.O.BOX 14 FIN-00881 HELSINKI  
Finland  
Tel. +358 0 759881

**NEXT PAGE(S)  
left BLANK**

# 1 INTRODUCTION

An exercise was arranged to test the performance of airborne teams to locate radiation sources. For this purpose, several artificial sources were placed (or “hidden”) in the terrain within a well-defined area (Area III) in the Padasjoki region. Also, some measurements with cars were performed in Area III but above all at the Vesivehmaa airfield.

The present report gives an account of the characteristics and locations of all artificial sources used in the exercise. The arrangements for radiation protection are also described.

## 2. RADIONUCLIDE SOURCES IN AREA III

### 2.1 Terrain and population characteristics of the area

The topography of Area III (see Fig. 1), 1 km by 5 km in size, and its immediate surroundings is characterized by low hills. The landscape is mainly covered by coniferous trees, although there are some patches of leaf trees (birches and aspens). Here and there are bogs or swampy areas, as well as boulders and rocky areas of various dimensions. There are also a couple of cutting areas in the northern half of the area. The northeastern corner of the area is formed by a small bay of the lake Vesijako.

There is a small village of Palsa in the northern-most part of the area, situated near the lake Vesijako, but otherwise the population is very scarce. However, in the south there are a few summer cottages, as well as dwelling houses with permanent residents. Two major secondary roads cross the area, one in the north (from Area II) through the village of Palsa and the other in the south. In addition, there are some unpaved private roads and forest lorry roads accessible by passenger cars.

The most evident landmark in the region in question is a cellular phone mast (nmt), located at the top of the hill Tervavuori, just outside the northeastern border of Area III.

### 2.2 Sources

The sources hidden in Area III and nearby were of various origins (see Table 1 for codes). The caesium source Cs2 is normally used by STUK for different calibration and alarm-level checking purposes, while the 15 Ci iridium source (Ir) is actually an industrial gamma radiography device (used, for example, for inspection of welded seams). A few of the cobalt and caesium sources were detached in STUK from aged industrial sources (e.g. liquid-level gauges). Also, some small cobalt sources were borrowed from the Defence Forces.

The technetium source (Tc) consisted of two ampoules that were fetched (15th and 16th of August) from the central hospital in the town of Lahti, some fifty kilometres southwards from Area III. The initial activity (at nine o'clock in the morning) of both ampoules was about 1.1 GBq (30 mCi).

The sources were different with respect to their portability and handling in the woods. For example, the heaviest cobalt source - i.e., one of those disassembled industrial sources - weighed in total some 70 kilograms. This was so because the source was kept in its original shield which was designed for a much higher activity; in addition, the old gamma radiography instrument, intended for industrial use, is very robust by nature. On the other hand, most of the other gamma sources were very easy to handle.

**Table I.** *Radionuclide sources hidden in Area III. The sources Ir, Co2 and Cs2 were collimated.*

	Source code	Nuclide	Activity (Bq)	Activity (mCi)	
1	Co1	<sup>60</sup> Co	2.6*10 <sup>8</sup>	7.0	
2	Co2	<sup>60</sup> Co	3.3*10 <sup>8</sup>	9.0	
3	Co3	<sup>60</sup> Co	2.6*10 <sup>7</sup>	0.7	
4	Co4 <sup>a</sup>	a	<sup>60</sup> Co	6.7*10 <sup>7</sup>	1.8
		b	<sup>60</sup> Co	6.7*10 <sup>7</sup>	1.8
		c <sup>b</sup>	<sup>60</sup> Co	3.7*10 <sup>7</sup>	1.0
		d	<sup>60</sup> Co	6.2*10 <sup>7</sup>	1.7
		e	<sup>60</sup> Co	6.4*10 <sup>7</sup>	1.7
		f	<sup>60</sup> Co	5.3*10 <sup>7</sup>	1.4
5	Cs1	<sup>137</sup> Cs	2.8*10 <sup>9</sup>	77	
6	Cs2	<sup>137</sup> Cs	1.3...1.7*10 <sup>9c</sup>	36...45 <sup>c</sup>	
7	Cs3	<sup>137</sup> Cs	2.8*10 <sup>8</sup>	7.5	
8	Cs4	<sup>137</sup> Cs	5.4*10 <sup>8</sup>	15	
9	Ir	<sup>192</sup> Ir	5.6*10 <sup>11</sup>	15000	
10	Tc	<sup>99m</sup> Tc	1.1*10 <sup>9</sup> + 1.1*10 <sup>9</sup>	30+30	

- <sup>a)</sup> A line source consisting of six 'point' sources (a,...,f) located 20...30 metres from each other. Each point source was composed of one to four single sources.
- <sup>b)</sup> Intended activity of this point was 6.5\*10<sup>7</sup> Bq (1.76 mCi) but one of the component sources failed to open (i.e. its top cover was stuck).
- <sup>c)</sup> Exact information on activity not available.

## 2.3 Location of sources

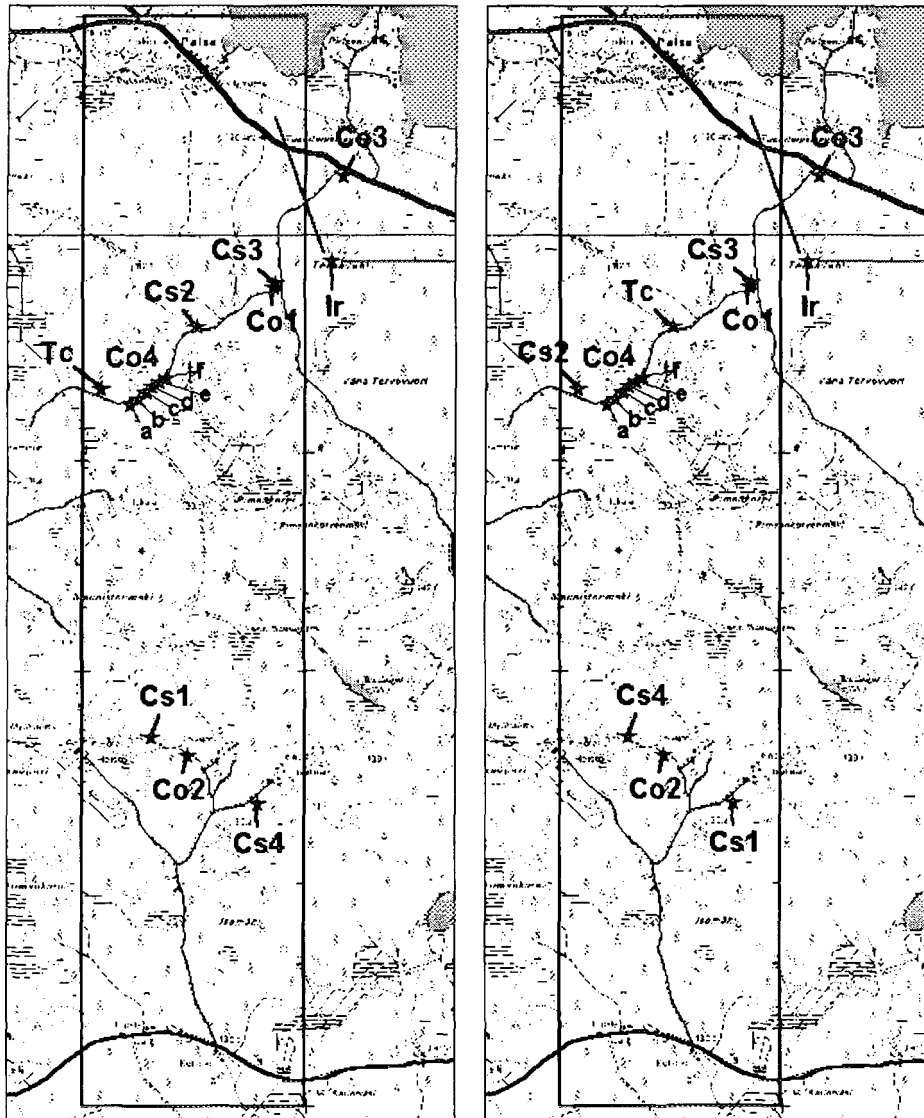
Area III was mapped in May and June several times in order to find suitable locations for the sources. However, the final decision on the exact places was made during the last mapping survey carried out in the evening of August 14th, the day before the beginning of the airborne measurements. Due to the restrictions imposed by the poor portability of some of the sources and the manpower (only five person) available for guarding them, the sources had to be hidden in places relatively close to the roads in the area.

The locations of the ten sources (see Table 1), both on Tuesday 15th and Wednesday 16th, are shown in Fig. 1. All sources apart from the iridium source and one of the cobalt sources were located within the boundaries of Area III. The placement of the sources was on Wednesday slightly different from that on Tuesday. The locations of Tc and Cs2 sources were interchanged, as well as those of Cs1 and Cs4.

The iridium source (Ir) was placed on the top (near the foot of the nmt mast ) of the 20-metres-high hill Tervavuori, some 50 metres from the border of Area III. The collimated beam was directed towards the road leading from Area II to Area III in such a way that only scattered photons could be detected in Area III. In the transverse direction the collimation angle (opening angle) of the beam was  $\sim 130^\circ$ . In the vertical direction, the angle above the horizontal level was some  $50\text{--}60^\circ$ . However, the total vertical opening angle was  $90^\circ$ , so that part of the beam was directed to the ground, thus giving a strong contribution to the scattered radiation. Altogether, the geometry was such that the primary photons emitted by the source could not be observed on the road at the bottom of the hill but secondary radiation was thought to reach the roads nearby.

The sources Co1 and Cs3 were point sources situated at the same location side by side. The cobalt source Co3 was a point source, located at the foot of the hill some fifty metres from the road. This small source was intended to be detected also from cars driving along the road. The source Co4 was a 'line source' composed of six separate point sources, each of which in turn consisted of one to four single sources. The distance between successive line points was 20...30 metres depending on the specific small-scale terrain features. The caesium sources in the southern part of Area III, Cs1 and Cs4, were point sources.

The caesium source Cs2 in the north was collimated (Fig. 2), as was the cobalt source Co2 in the south. The exact dimensions of the latter source are not available but the beam was altogether rather narrow.



a)

b)

**Figure 1.** Locations of radioactive sources.  
 a) Tuesday, 15th of August. b) Wednesday, 16th of August.

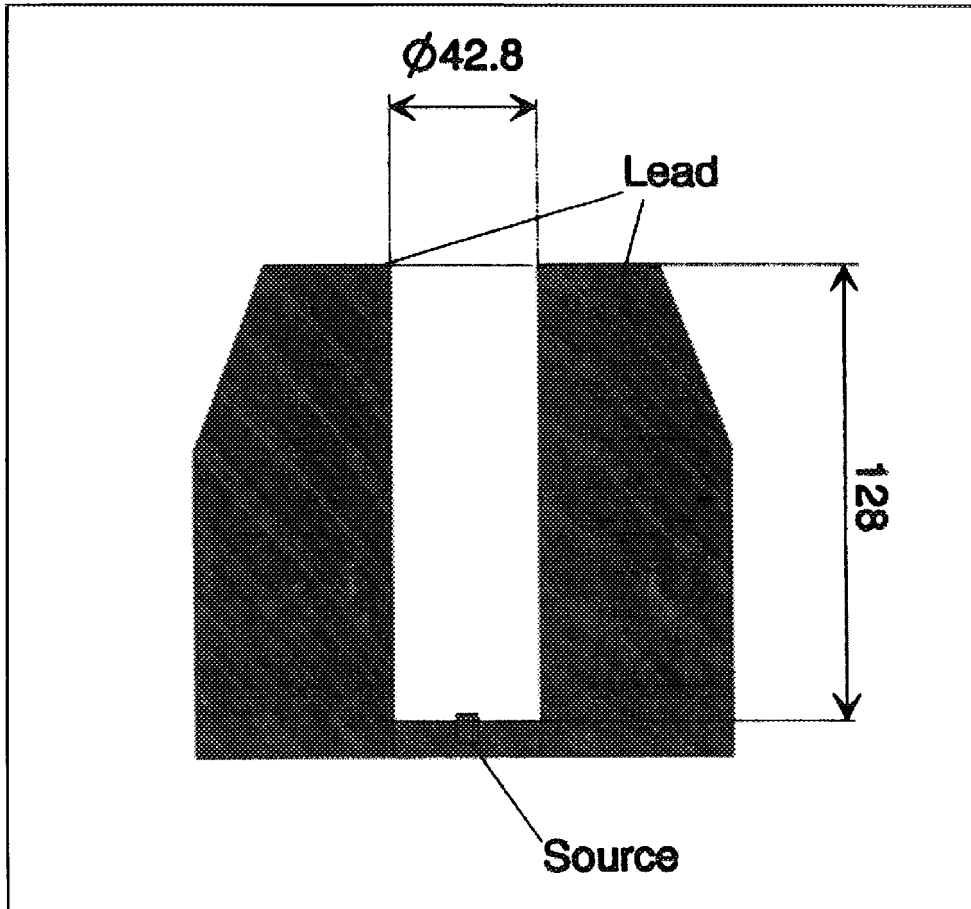


**Figure 2.** Collimated  $^{137}\text{Cs}$  source (Cs2) (see Appendix 1). Dimensions are given in millimetres. The collimation angle is about  $19^\circ$  (at the height of 60 m the diameter of the beam is some 20 m).

The technetium source consisted of two separate ampoules. One of the ampoules was taken out of the shield-container immediately at nine o'clock - which was the dead-line for placing sources - while the other remained in the shield until three o'clock in the afternoon when it, too, was taken off from the shield. This kind of arrangement was considered necessary because of the relatively short half-life (six hours) of  $^{99\text{m}}\text{Tc}$ . Figure 3 shows the time dependence of the technetium-source activity.

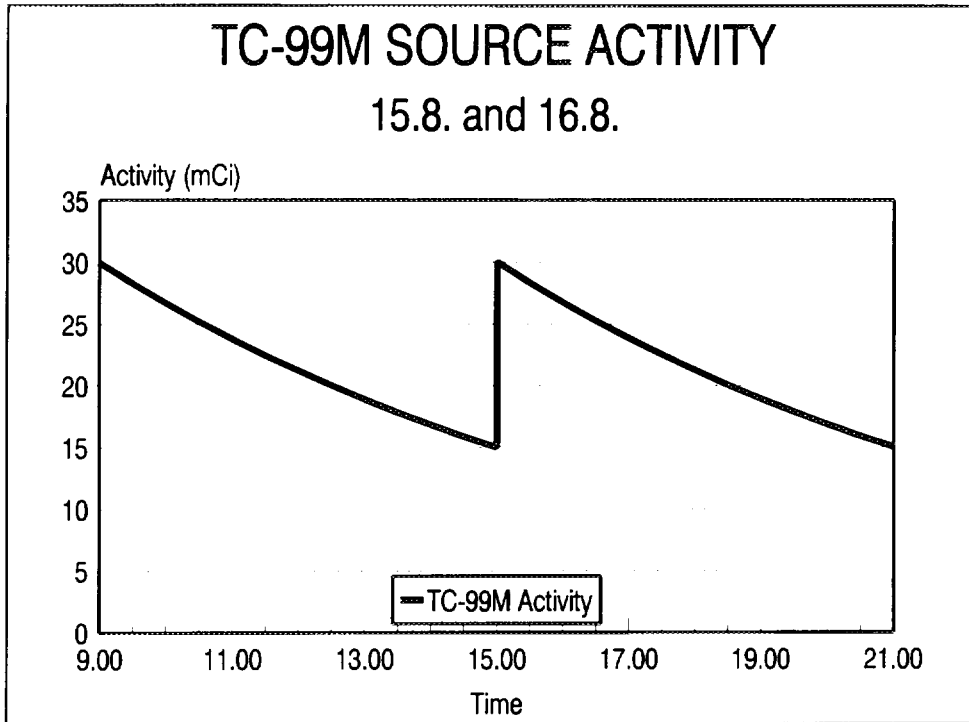


**Figure 3.**  $^{99m}\text{Tc}$  source (Tc) activity as a function of time.

## 2.4 Source placement and radiation protection

The team responsible for the management of sources had at its disposal four cars (two private ones), three walkie-talkie radios, five nmt telephones (two of which were in the cars) and a special radio device for listening the communication between aircrafts and the control tower at the Vesivehmaa airfield.

In the morning of August 15 and 16, one of the team members fetched the technetium ampoules from Lahti while the others went directly into Area III to put the other sources in their proper places. Since there were ten distinct source locations (the line source Co4 is considered to form one source) in Area III and only a five-people team, it was impossible to keep all sources under continuous surveillance. Instead, it was decided that only the iridium source - which by far constituted the most severe potential danger to the public - would be guarded all the time (as the radiation protection stipulations require). Other sources would more or less be looked after on a patrolling-tour basis. A complete tour in the northern part

of area III (with some radiation measurements near the sources) took on foot almost an hour.

There were always at least one person in the southern area and two in the north, one of which was a patrol man and the other guarded the Ir source. The patrols checked the sources either once or twice in every two hours.

In the nights, the radioactive sources were stored in locked cars which, in turn, were kept in a locked garage of a petrol station in Vääksy, close to the accommodation localities. The cars were marked with appropriate radiation warning signals. Personal radiation protection equipment consisted of dose rate meters and dosimeters. In addition, there were two special (they could not be turned off) alarming dose rate meters that were carried by those staying close to the Ir source.

The overall radiation protection arrangements were surveyed in-situ by an expert from the Radiation Safety Department of STUK. Considering the circumstances and allocated resources, the arrangements were found to be satisfactory.

#### **2.4.1 Caesium, cobalt and technetium sources**

The sources were surrounded by red-yellow signal ribbons placed at a distance of 1.5...10 metres, depending on the strength of the source and on the minor-scale terrain features. At each source location there was also at least one official radiation warning signboard tied on a tree trunk or on a separate wooden stick in the vicinity of the source. In addition, in the southern area a bulletin describing the RESUME exercise was put on a prominent, easy-to-be-seen place near each source (attached to the signal ribbon or to a nearby tree).

The highest radiation levels measured just outside the signal ribbons were about 15...20  $\mu\text{Sv h}^{-1}$  both in the north (Co1 + Cs3) and in the south (Cs1).

#### **2.4.2 Iridium source**

The iridium source was the only source guarded continuously; that is, there was always at least one person on the top of the hill near the source. The Ir source was surrounded by a twofold signal ribbon. However, the radius of the access-controlled area was now some 30 metres down the hill slope in the 'direction' of the beam and about ten metres in the opposite direction. There were also four radiation warning signs attached to the ribbon. In addition, the hill slope facing the road in the northeast (i.e., the direction of the beam) was checked in order to warn people

possibly moving there. No one was ever encountered during these patrolling tours but this was not surprising because the terrain near the source is very difficult to walk (lots of small bushes and trees, very high grass etc.). However, at the bottom of the hill, some 150...200 metres from the source, the terrain was rather open. In retrospect it is considered that there could have been more signboards available, so that a few warning signs could have been placed beside the road leading from Area III to the major secondary road in the northeast, and also at the bottom of the hill farther from the source.

The maximum dose rate at the signal ribbon (on the hill slope) was of the order of 100...150  $\mu\text{Sv h}^{-1}$ .

### 3. RADIONUCLIDE SOURCES USED IN THE AIRFIELD

On Thursday, 17th of August, airborne radiation measurements were performed in the Vesivehmaa airfield. The primary source was Cs1 (see Table 1), which was quite easy to handle. First it was moved to a predetermined distance (from ten to 200 metres) from the “runway”, placed on top of a small stand and turned over on its side. Then the top shield cover was opened and the source was carefully pushed to its uppermost position (the beam was still slightly collimated) from behind with a special tool. When necessary, the source container was rotated so as to direct the beam properly. After measurements at a specific distance, the source was closed in a reverse order and moved to another position.

Originally, it was intended to use also the 1.8 mCi cobalt source Co4 a (or Co4 b). However, during the first measurements in the airfield it became evident that recurrent opening and closing of these sources was too labourious (pulling the source out and pushing it back into its container was difficult, especially when the container apparatus was lying on its side) and time-consuming. Therefore, the 1.8 mCi source was replaced by one of the easy-to-use (but weaker) cobalt sources borrowed from the Defence Forces. Its activity was about  $2.3 \cdot 10^7$  Bq (0.62 mCi).

## 4. CONCLUSIVE REMARKS

From the point of view of the source-management-team, the RESUME exercise gave valuable experience regarding the handling of different radioactive sources in the field. The difficulties encountered, i.e. long working days, busy mornings spent on placing the sources and a few minor shortcomings in radiation protection arrangements, originated chiefly from the fact that the number of people in the team was too small. However, the weather was fine and the spirit among “the Bushmen” was most of the time very high.

## Appendix 1 Details of the collimated $^{137}\text{Cs}$ source used in the carborne test measurements

Mika Nikkinen

The activity of the  $^{137}\text{Cs}$  source (Cs2) used in the pass-driving test on 17 August 1995 was not very well defined causing some inaccuracy to the results. In addition, an unintended collimation of the source caused extra attenuation at wide angles.

The collimation was due to a special source capsule and a lead shield surrounding it. The source capsule and the shield are shown in Fig. A1. The source is a 3 mm diameter bean inside a cylindrical steel capsule having a dual steel cap. The capsule is put in a 8 mm deep and 6 mm diameter well in a cylindrical lead shield (see Fig. 2, p 8).

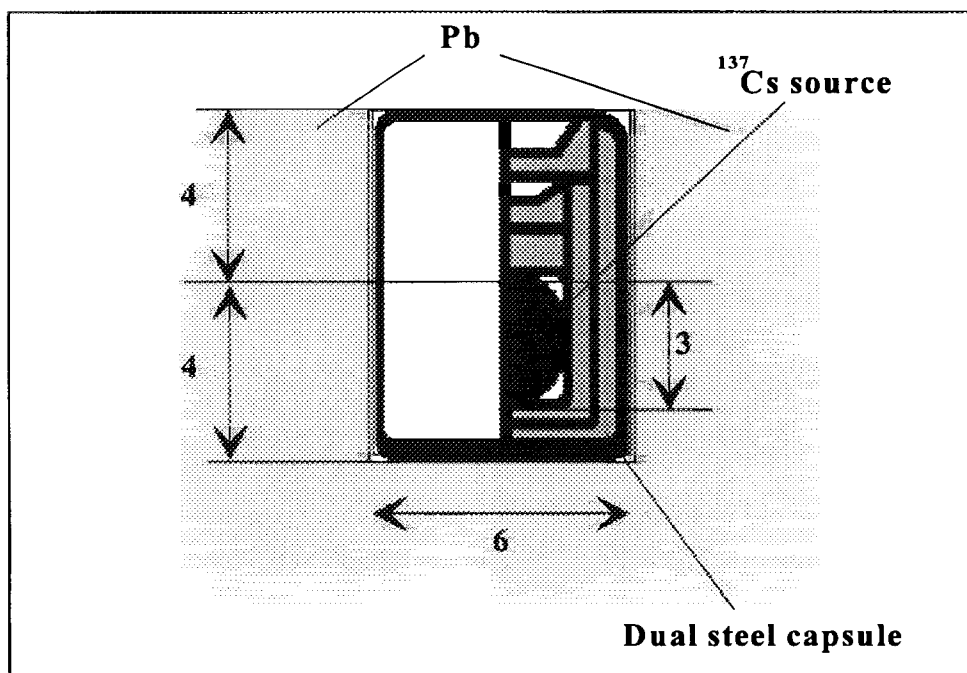


Figure A1. Details of the supporting structure of the  $^{137}\text{Cs}$  source (Cs2).

The collimation geometry is shown in Fig. A2. The primary gamma flux has an opening angle of 40°. This flux is attenuated by the 3 mm thick dual steel cap of the source. When moving further out of the axis the 2 mm thick steel walls of the capsule start to have an additional effect giving a total thickness of about 4 mm. The capsule walls are dominating at opening angles between 40° and 80°. At even larger angles the attenuation in the lead shield starts to dominate.

The manufacturer of the source, Amersham, reports the 'equivalent activity' of the Cs-137 source to be 50 mCi (-0 mCi, +12.5 mCi) in autumn 1981. When decay correction is performed we get an 'equivalent activity' of 36.5 mCi (-0 mCi, +9 mCi) in August 1995.

Amersham defines the 'equivalent activity' as:

The equivalent activity is equal to the activity of a point source of the same radionuclide which would give the same exposure rate at same distance from the centre of the source.

Exposure rate should be measured under conditions of minimum scatter. In this case it means measuring in the radial direction, where the capsule is thinnest. Due to the collimation, however, the primary flux was measured in the axial direction giving rise to an extra attenuation of

$$G_{extra} = 1 - e^{-\mu\Delta} = 0.06 ,$$

where  $\Delta = 3 \text{ mm} - 2 \text{ mm} = 1 \text{ mm}$  and  $\mu = 0.574 \text{ cm}^{-1}$  (661.6 keV in steel). The build-up is negligible and has been ignored. The result means that in the primary beam one should use the value of 34 mCi (-0 mCi, +8.5 mCi) for the nominal activity.

At opening sector between 40° and 80° the effective attenuator thickness is 4 mm which again gives rise to an additional attenuation of 0.06 (Fig. A2). At larger angles the photons must pass the lead shielding. The attenuation coefficient for 661.6 keV gammas in lead is  $1.143 \text{ cm}^{-1}$ .

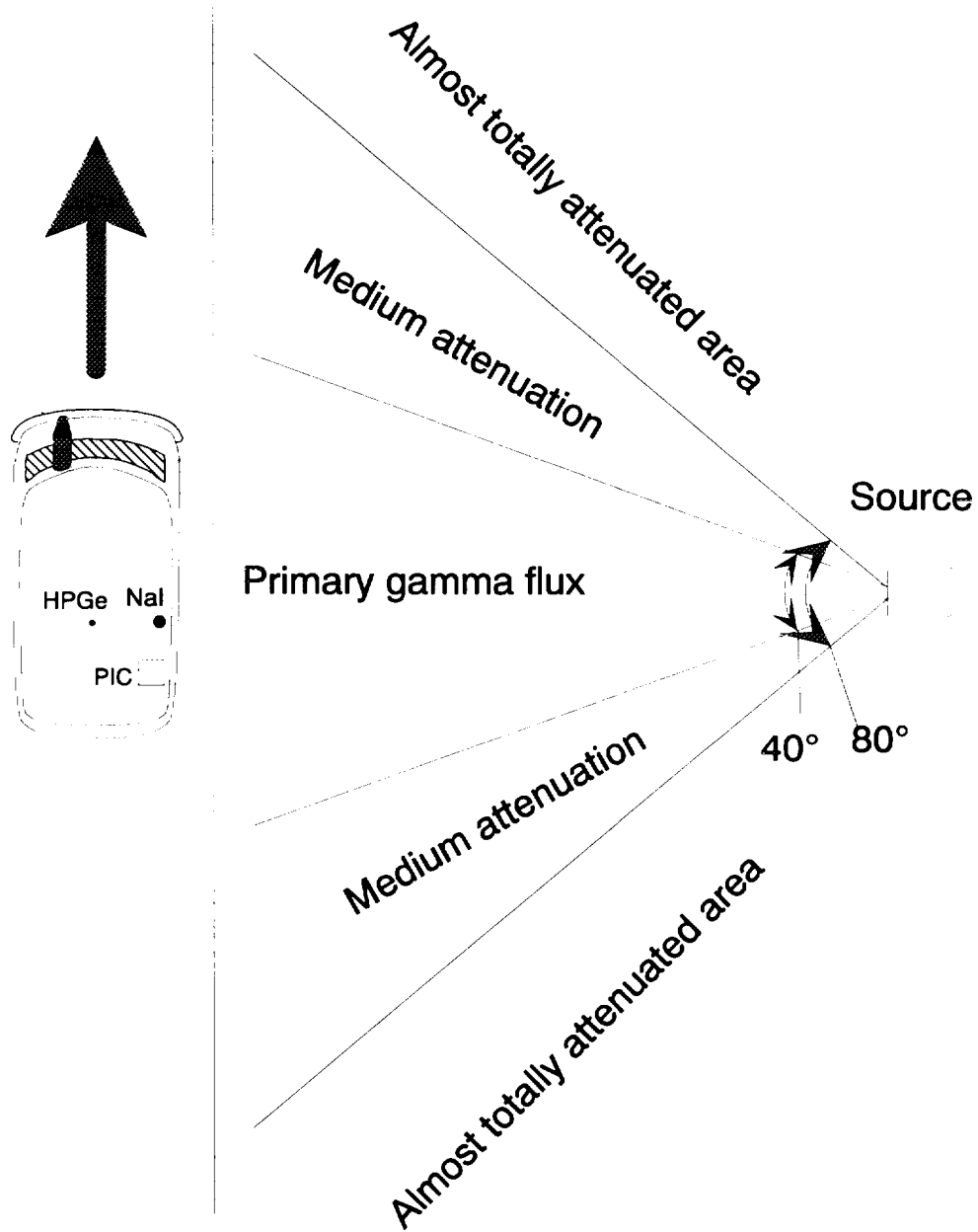


**Figure A2.** Collimation of the primary photons. A sudden drop in the count rates is expected at the angles of 40° and 80° (c.f. results of the STUK/HUT team).



DK9800027

## **Swedish Radiation Protection Institute**

Determining the activity and location of hidden point sources on the ground by measurements at distance

**NEXT PAGE(S)  
left BLANK**

# Determining the activity and location of hidden point sources on the ground by measurements at distance.

## An exercise

Robert Finck and Hans Mellander, SSI

As a part of the RESUME95 exercise a small exercise of detecting simulated lost radiation sources was arranged for the *in situ* teams at the Vesivehmaa airfield. The intent was to simulate measurement procedures suitable to locate and determine the activity of one or more lost point sources. The activities were thought of as being so high that the sources could not be approached and visually identified. In the exercise the geometry and activity was scaled down. As in the real situation, however, the teams were not allowed to get close to the sources

The exercise took place in the north-east part of the Vesivehmaa airfield in an area with relatively long grass. Two squares of 10 x 10 m<sup>2</sup> were fenced off. Each corner of the 10 x 10 m<sup>2</sup> squares was marked by a pole. Within these squares the sources were hidden in high grass so that they could not be seen. The teams were not allowed inside the squares. The task was to identify the number of point sources in each square and the location, radionuclide and activity of each source. All measurements had to be performed outside the fenced off area.

In the first square, two Co-60 sources with activity of 20 and 70 MBq ( $\pm 10\%$  overall uncertainty) were placed on the ground as shown in Fig 1. In the second square a single Cs-137 source with activity 300 MBq ( $\pm 10\%$ ) was placed as shown in Fig 2.

The ambient dose rate  $H^*(10)$  for each source was measured separately by the organizers with a GM-based instrument. The instrument (RNI 10/S) was calibrated for 662 keV photons from Cs-137 with a systematic uncertainty of about 2%. The instrument was not calibrated for Co-60. After correction for instrument response and the natural background, the ambient dose rate was measured to 30.2  $\mu\text{Sv/h}$  for the Cs-137 source 1 m above the source on the ground (overall uncertainty about 10%). For the Co-60 sources the ambient dose rate was measured to 34.5 and 11.3  $\mu\text{Sv/h}$  respectively at 1 m above the sources (overall uncertainty about 30%) The measured values include scattered radiation from the ground.

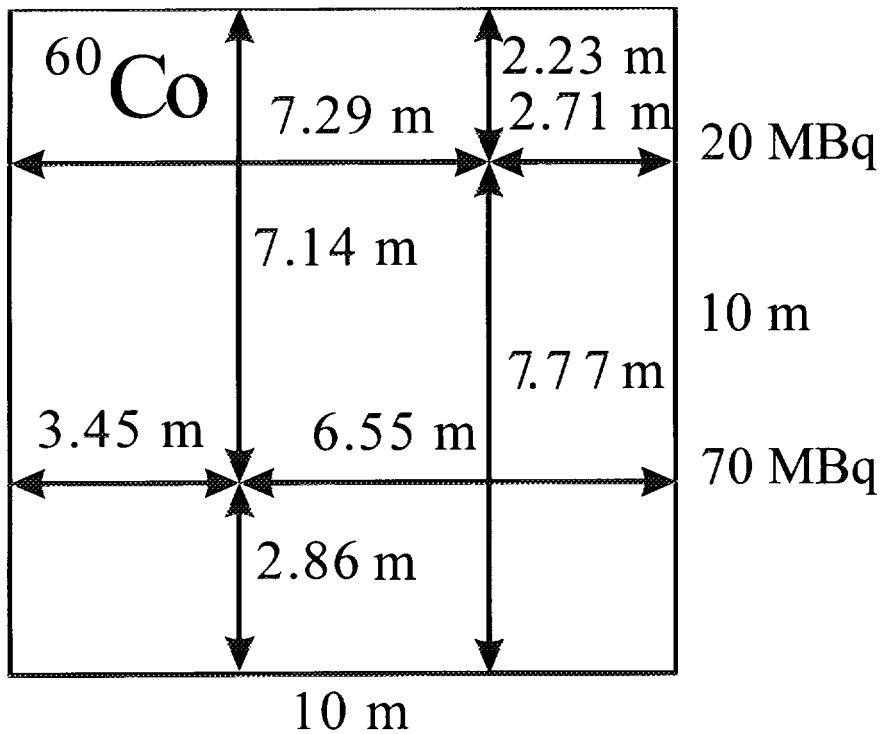


Fig 1. Position of the two Co-60 point sources within the  $10 \times 10 \text{ m}^2$  square. The activity of the sources are 70 MBq and 20 MBq respectively with a systematic uncertainty of about  $\pm 30 \%$ .

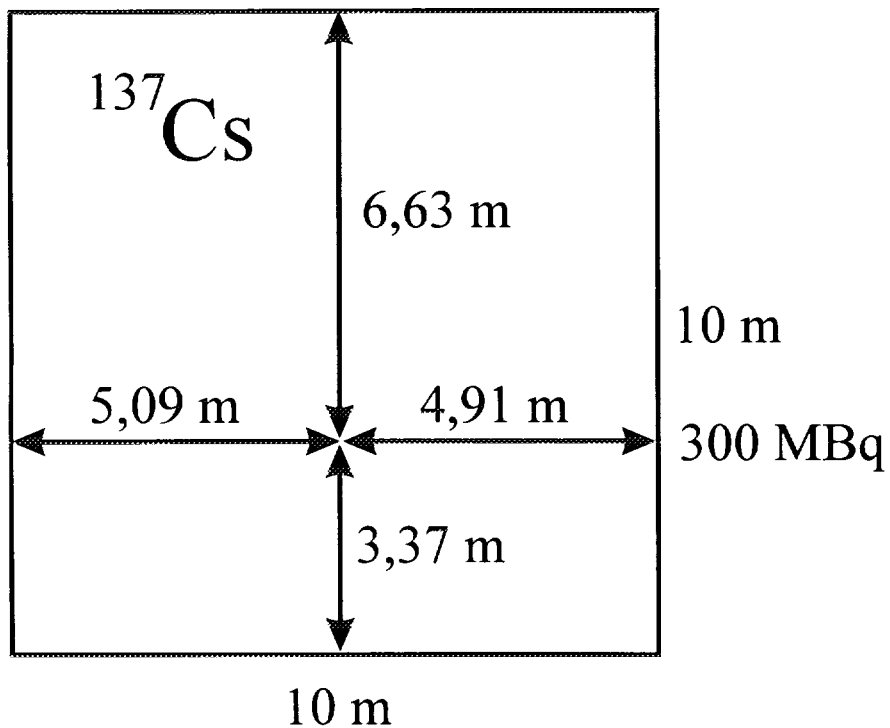


Fig 2. Position of the Cs-137 point source within the  $10 \times 10 \text{ m}^2$  square. The activity of the source is 300 MBq with a systematic uncertainty of about  $\pm 10 \%$ .



# Johs Jensen

## The Operational Staff during Exercise RESUME95

- INTRODUCTION ..... 65
- 1. EXPERIENCES OF DISTAFF FROM EXERCISE RESUME95 ..... 65
  - 1.1. Implementation of DISTAFF ..... 65
    - 1.1.1. Duties ..... 66
    - 1.1.2. Composition and size of staff ..... 66
    - 1.1.3. Location of staff ..... 67
    - 1.1.4. Communication ..... 67
    - 1.1.5. Equipment ..... 68
    - 1.1.6. Maps ..... 68
    - 1.1.7. Other logistic problems ..... 68
  - 1.2. Registration ..... 68
  - 1.3. Briefings ..... 69
    - 1.3.1. General orientation of the participants ..... 69
    - 1.3.2. Morning briefing ..... 69
    - 1.3.3. Last day seminar ..... 69
    - 1.3.4. Daily work ..... 69
- 2. CONCLUSIONS ..... 69
- RECOMMENDATIONS ..... 69

**NEXT PAGE(S)  
left BLANK**

# The operational staff during exercise RESUME-95

Johs Jensen  
Jensen Consult  
Virum, Denmark

## Introduction

An operational staff is an element of an independent unit, which assists in various kinds of tasks and problems arising during special situations. However an operational staff can also be used in exercises, and throughout many years operational staffs have been used for assisting and coordinating tasks in a lot of military and civil defence exercises.

With more than 100 participants entering the exercise RESUME-95 the Exercise Planning Committee decided to establish an operational staff named Directing Staff (DISTAFF) to ensure that the exercise plan was followed, the planned activities were carried out and to intervene if anything went wrong.

In general the duties of the operational staff involve tasks such as secretarial assistance, keeping log of the progress of the situation and gathering, updating and distributing information on all aspects of the situation. Throughout the entire event it is the staff's responsibility to keep a general view of the current situation and to make the necessary plans for the progress of the situation based on the available information. Furthermore the staff should ensure necessary contact to the public and to the media.

In the planning phase of the RESUME-95 exercise the following points concerning the DISTAFF were addressed:

- Duties
- Composition and size of staff
- Location of staff
- Communication
- Equipment
- Information

## 1. Experiences of DISTAFF from Exercise RESUME-95

### 1.1. Implementation of DISTAFF

The Danish personnel arrived on August 10<sup>th</sup>, 3 days before the start of the exercise and prepared the DISTAFF in two conference rooms in hotel TALLUKKA. The DISTAFF was ready to operate on the evening of August 13<sup>th</sup>. The Finnish personnel arrived on August 14<sup>th</sup>, when the exercise started.

### **1.1.1. Duties**

The duties of the DISTAFF were to ensure that the participants in the exercise were able to devote themselves to their main job, i.e. measure, calculate and display their findings according to the very detailed plan for their activities made before the exercise.

In the plan for the exercise the tasks of the DISTAFF in relation to the measuring teams were described as follows:

- prepare checklists for all the planned activities,
- keep a log for all incoming information from the measuring teams,
- give starting signals to the measuring teams, when they are ready to start their tasks,
- delay a team if a previous team has not finished its task and updating the schedules,
- call for assistance from rescue service in case of accidents.

One of the most important factors that could influence the progress of the exercise was the weather. Therefore the DISTAFF had to ensure that weather prognoses were made available to the participants at any time.

In order to ascertain that all teams fulfilled their planned tasks, it was necessary that all teams reported to the DISTAFF regularly, so that they could be supervised as closely as possible.

Minor delays primarily in the airborne measuring program was expected and it was the task of the DISTAFF to make the necessary adjustment of the flight schedule and to redirect the carborne teams with short notice. The carborne measuring teams were not expected to have the same problems although many of the roads in the area were only very narrow dirt tracks.

Accidents of any kind in the air or on the ground, fires in the dry vegetation in the exercise area etc. were to be reported to the DISTAFF who then would take care of the immediately request of rescue services and information to next of kin and the media.

In case the media wanted to see or follow the exercise in detail, they were able to get the necessary information at the DISTAFF and finally it was the task of the DISTAFF to arrange press conferences.

### **1.1.2. Composition and size of staff**

It was estimated that the DISTAFF should be manned with at least one duty officer and 2 - 3 secretaries in order to follow the measuring teams and their activities in field, for the necessary paperwork, certain logistic functions. arranging of press conferences and a few social events. It was necessary to have secretaries that could speak English and Finnish and preferably understand the other Nordic languages.

The personnel in the DISTAFF consisted of one duty officer and two secretaries. Later on two calculators were present periodically to assist the teams in preparing plots of results. Besides these the DISTAFF had a permanent representative in the tower at Vesivehmaa airfield to communicate with the airborne teams and report back to the DISTAFF.

After the daily program all the members of the exercise planning committee took part in the DISTAFF work in order to discuss the progress of the exercise and adjusting the following days program.

To address information questions a press officer from Danish Emergency Management Agency was available periodically from the beginning of the exercise.

### **1.1.3. Location of staff**

In the planning period before the exercise a Fire Fighting School was considered as Headquarters and quarters for the exercise participants. However the buildings were rather primitive and far too small to accommodate all the participants in the exercise. In stead hotel TALLUKKA with rooms for the DISTAFF activities and enough rooms for all participants was examined and chosen.

The DISTAFF needed a working room of about 100 m<sup>2</sup> with 5 - 6 working places for secretaries and a number of calculators. Another room of about 200 m<sup>2</sup> with seats for all participants and the media, i.e. about 120 persons, was needed as briefing room. Easy access to communication means was also needed.

The working room for the DISTAFF was about 70 m<sup>2</sup> and equipped with chairs and tables and a bulletin board. It took some time to find the right places for the office equipment and the working places.

The briefing room was about 120 m<sup>2</sup> - too small for more than 100 persons. It was equipped with chairs and tables, overhead projector, loud speaker and a bulletin board.

The problem of having close connections between the DISTAFF and the airfield, where the aircrafts were operated from, was considered, and it was decided to place a permanent representative in the tower at the Vesivehmaa airfield.

### **1.1.4. Communication**

In order to run the DISTAFF activities properly it was foreseen that telephones (permanent and mobile) and telefax would be the main communication means. It would be necessary to have switchboard facilities for both permanent telephone and telefax traffic.

The communication between the DISTAFF and the airborne teams went via the tower at the Vesivehmaa airfield with telephone from the DISTAFF to the tower and VHF radio from the tower to aircrafts. A VHF receiver in the DISTAFF was considered and made available, but it was impossible to follow the radio traffic between tower and aircrafts. Most of the telephone traffic went by mobile telephones, but the coverage for GSM telephones were not too good.

From the switchboard in the hotel two lines went permanently to the working room. Three extra lines were established and the staff was then able to use three telephone lines and one telefax line. A telephone directory was established from the beginning of the exercise and updated every day.

### **1.1.5. Equipment**

It was necessary to have office machines for the DISTAFF in form of computers, printer, copy machines, telefax, paper and all other office equipment.

Four computers (one for telefax communication), one printer and office equipment, except from paper, were brought from Denmark. It turned out to be necessary to purchase plugs, cable, sockets and adapters, as the Finnish electric standards are different from the Danish standards.

Copying proved to be a problem. The hotel administration gave access to their copymachine, but it was not available all the time and it was very expensive to use it. A copymachine with limited capacity and copypaper were brought from STUK, but it should have been available earlier due to the paperwork before the exercise started.

### **1.1.6. Maps**

In order for the measuring teams to navigate without problems in the air and on the ground it was necessary to have adequate maps over the areas where the measuring should take place, in scales of 1:50000 or better. Special maps were needed for the airborne measuring. Maps in other scales, such as tourist maps (1:250000) were necessary for the road transport to the exercise area.

Maps were made available by STUK in several scales. STUK and the Danish Emergency Management Agency produced special maps for the airborne teams.

### **1.1.7. Other logistic problems**

A number of transport vehicles for the DISTAFF personnel and equipment had to be made available (rented) or brought from the respective countries.

Two transport vehicles for the Danish DISTAFF personnel and equipment were brought from Denmark.

It was supposed from the beginning of the exercise planning, that fuel for aircrafts and vehicles would be available in Finland, where and whenever wanted.

It was foreseen that users of fluid nitrogen for cooling purposes would need an unspecified quantity of fluid nitrogen to be delivered on request by the DISTAFF.

The nitrogen was furnished by STUK and the delivery was organised so that the users preferably at the morning briefing requested their nitrogen and it was delivered when they wanted it. A delivery place for liquid nitrogen was set-up in a hotel garage

## **1.2. Registration**

The exercise participants started arriving at the hotel on August 11<sup>th</sup> and had all arrived about noon on August 14., according to the regulations for the exercise.

### **1.3. Briefings**

#### **1.3.1 General orientation of the participants**

After welcome, roll call and presentation of the participants the first briefing began with practical remarks. Then the plans for the exercise and the daily routine were gone through. The weather forecast for the next days was given and there was a short question period.

#### **1.3.2. Morning briefing**

The morning briefing was given at 0645 including the weather forecast, changes concerning the plan for the day and other things of common interest. It was only necessary to change few of the planned activities. The briefings were given this early because teams starting first should have the opportunity to begin their job on time. Not all teams were represented at the morning briefings, but the important information about the weather was available any time.

#### **1.3.3. Last day seminar**

On the last day of the exercise, August 18<sup>th</sup>, a seminar was scheduled where the participants described their findings and problems during the exercise. The results of all the efforts were shown on the bulletin board for comparison and discussion. However it was agreed, that some of the findings would need further study in other surroundings.

#### **1.3.4. Daily work (opening hours)**

The DISTAFF was manned from 0630 to 1900 and after that time the duty officer could be called whenever needed.

### **2. Conclusions**

The DISTAFF benefited much from the very meticulous planning before the exercise and also from the daily meetings with the planning staff after working hours.

The daily work did not present any unforeseen events, mainly because the weather was fine all the time and the participants were good to follow their instructions. Also there were no accidents and the safety regulations for the airborne teams were followed correctly.

It is the opinion that the DISTAFF worked satisfactorily internally. The set-up with the permanent representative at Vesivehmaa airfield worked also satisfactorily, though it probably was a lonesome job and it would have been better to have two persons at the job.

### **3. Recommendations**

Among the things that were essential were all the office equipment, that made the relative fast installation of the DISTAFF in hotel Tallukka possible.

The standards for electric and electronic connections differ from country to country and it is necessary to know the host country's standards and order the relevant material before you install your equipment. It might be possible to request descriptions of the standards in future host countries.

**NEXT PAGE(S)  
left BLANK**



# Exploranium

## A Carborne Gamma-ray Spectrometer System for Natural Radioactivity Mapping and Environmental Monitoring

ABSTRACT .....	73
THE CARBORNE GAMMA-RAY SPECTROMETER SYSTEM .....	73
Fig. 1. A screen display of the vehicle track showing the location where the uranium concentration exceeds 8 ppm .....	74
Fig. 2. A screen display of the gamma-ray spectrum from a contaminated area in Finland showing a prominent <sup>137</sup> Cs peak .....	75
Fig. 3. A screen display showing a chart record of the potassium, uranium and thorium count rates and a window ratio .....	76
CALIBRATION OF THE CARBORNE SYSTEM .....	76
Calibration for natural radioactivity mapping .....	76
Fig. 4. The energy calibration procedure for the carborne system showing the linear relationship between channel and energy .....	77
Tab. 1. Stripping Ratios for a 10.2 x 10.2 x 40.6 cm detector .....	78
Fig. 5. The field of view of a detector at a height of 2 meter above the ground .....	78
Fig. 6. A schematic diagram showing a typical sampling scheme for the calibration of a carborne gamma-ray spectrometer system .....	79
Calibration for <sup>137</sup> Cs using soil analyses .....	80
Fig. 7. A gamma-ray spectrum from the carborne system on the Vesivehmaa airfield .....	80
Tab. 2. Ground concentrations of four calibration sites at Vesivehmaa airfield .....	80
Tab. 3. Sensitivities of the carborne system to <sup>137</sup> Cs, potassium, uranium and thorium .....	81
Calibration for <sup>137</sup> Cs using a point source .....	81
Fig. 8. The sampling scheme used for calibrating a carborne system using small sources of <sup>137</sup> Cs .....	82
Fig. 9. A map showing the variation in detector efficiency with source position .....	82
APPLICATIONS OF THE GR-650 CARBORNE SYSTEM .....	83
Natural Radioactivity Measurements .....	83
Fig. 10. A profile measured in the Philippines showing the increase in potassium concentration near the Antamok gold mine .....	84
Fig. 11. A profile measured in Venezuela showing uranium anomalies probably related to phosphate deposits .....	84
Fig. 12. A stacked profile showing the activity of <sup>137</sup> Cs and the concentrations of potassium, uranium and thorium measured in area II .....	85
<sup>137</sup> Cs measurements in Finland .....	86
Searching for radioactive sources .....	86
Fig. 14. A profile of the low/high energy ratio from an area in Finland contaminated with <sup>137</sup> Cs .....	87
Fig. 15. A profile of the low energy (35 to 350 keV) to high energy (350 to 2810 keV) ratio showing the location of the hidden radioactive source .....	88
Fig. 16. A profile of the low energy back-scattered component from 35 to 350 keV showing the location of the hidden radioactive source .....	88
CONCLUSIONS .....	89
ACKNOWLEDGEMENTS .....	89
REFERENCES .....	89

# **A CARBORNE GAMMA-RAY SPECTROMETER SYSTEM FOR NATURAL RADIOACTIVITY MAPPING AND ENVIRONMENTAL MONITORING**

**R.L. GRASTY AND J.R. COX**

Exploranium Ltd. 264 Watline Rd. Mississauga, Ontario, L4Z 1P4, Canada

---

**Presented at the Seminar "Exercise Résumé95"  
Copenhagen, Denmark, 17-19th January, 1996**

---

## **ABSTRACT**

This paper summarizes the experience gained in the use of a carborne gamma-ray spectrometer system for mapping both natural and man-made radiation. Particular emphasis is placed on the calibration of the system for converting the gamma-ray measurements to ground concentrations of potassium, uranium and thorium and the activity of  $^{137}\text{Cs}$ . During the Finnish Emergency Response Exercise (Résumé95), the carborne system was shown to be effective in mapping both natural and man-made radiation from  $^{137}\text{Cs}$  fallout and in locating radioactive sources. The application of the carborne system for mineral exploration is also demonstrated.

## **THE CARBORNE GAMMA-RAY SPECTROMETER SYSTEM**

The International Atomic Energy Agency (IAEA) recently supported the development of a carborne gamma-ray spectrometer system. This system, intended both for natural radioactivity mapping and environmental monitoring, was first tested in Portugal in 1994. Since that time, three additional systems have been installed and tested through IAEA technical assistance programs in Malaysia, Venezuela and the Philippines.

The original systems were based on an Exploranium GR-256 portable gamma-ray spectrometer which records 256 channels of gamma-ray spectral data and can be controlled by computer. This spectrometer has been shown to be effective in monitoring man-made radiation from Chernobyl (Grasty et al, 1992). The detector for the carborne system is a large volume sodium iodide crystal with dimensions of 10.2 x 10.2 x 40.6 cm (4 x 4 x 16 inches) which is normally mounted on the roof of a vehicle. The more recent version used during Résumé95 is based on Exploranium's GR-320 portable spectrometer. The system also incorporates a Global Positioning System (GPS) for reliable navigation and to aid in map production.

The software for controlling the GR-256 or GR-320 spectrometer and for displaying the results has the following main features:

- a) The selection of up to 8 windows of gamma-ray data which would typically include windows for monitoring natural radiation from potassium, uranium and thorium as well as man-made radiation such as  $^{137}\text{Cs}$ .
- b) The capability to convert the window count rates to ground concentrations of  $^{137}\text{Cs}$ , potassium, uranium and thorium as well as exposure or dose rate.
- c) The selection of up to 174 co-ordinate systems in order that the GPS co-ordinates can be converted to local co-ordinates.
- d) A screen display of the vehicle track with a superimposed grid of longitude and latitude or local co-ordinates. The vehicle track shows the location where any preselected parameter exceeds a certain threshold (Fig.1).

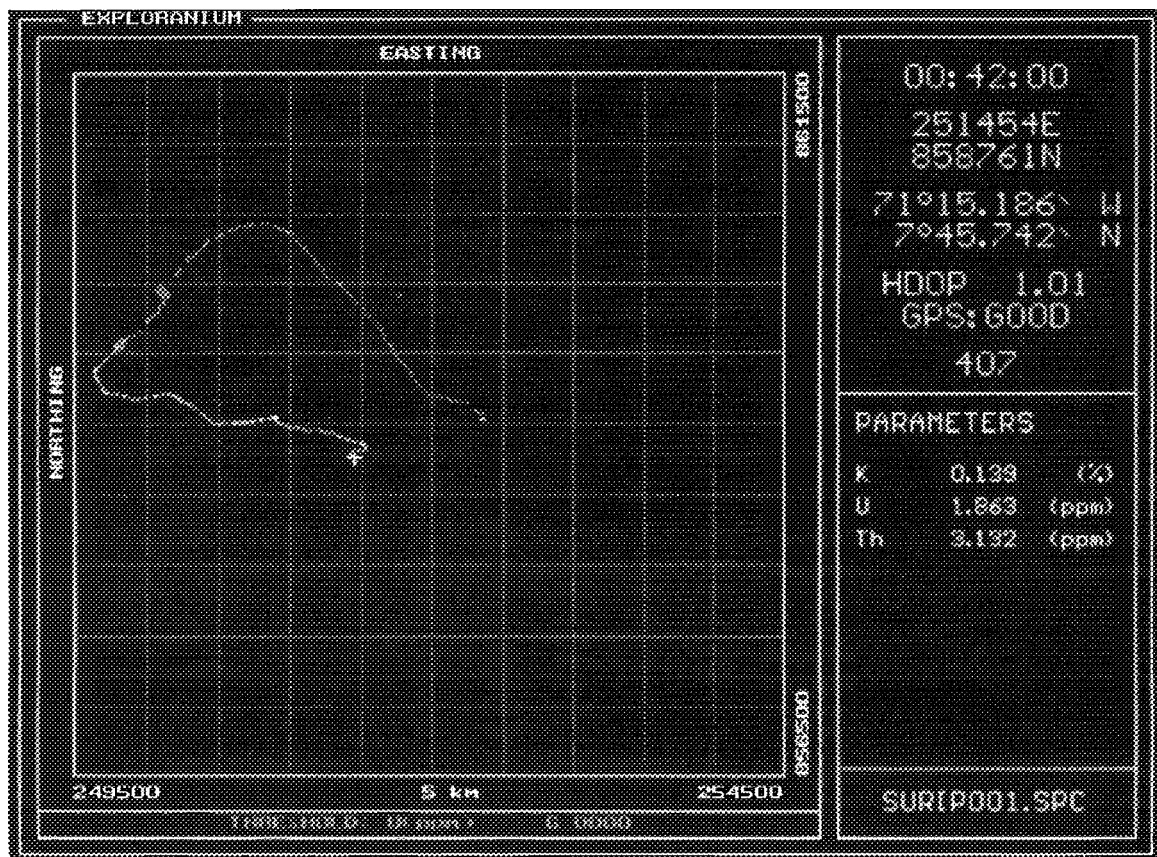


Figure 1. A screen display of the vehicle track showing the location where the uranium concentration exceeds 8 ppm.

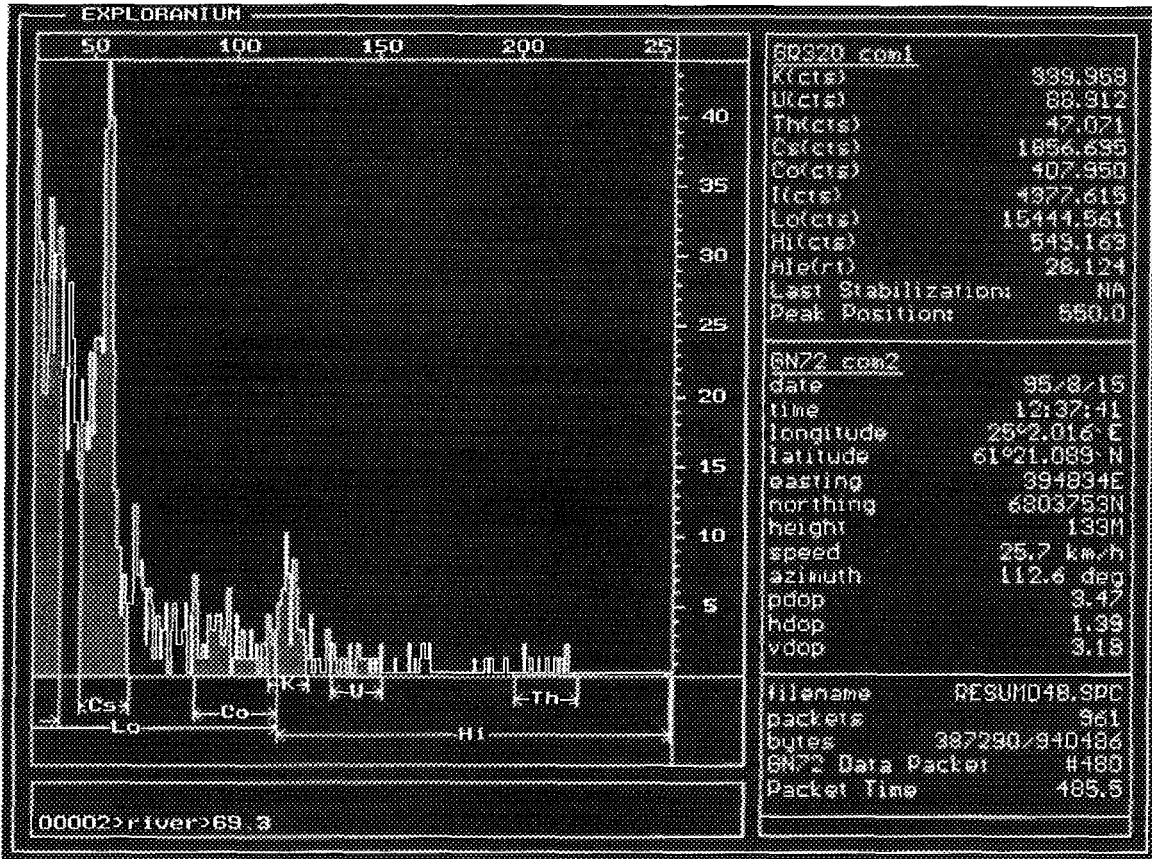


Figure 2. A screen display of the gamma-ray spectrum from a contaminated area in Finland showing a prominent  $^{137}\text{Cs}$  peak.

- e) A screen display of the gamma-ray spectrum over a preselected energy range (Fig. 2).
- f) A screen display showing a chart record with up to 4 parameters of processed window data with automatic chart scaling (Fig. 3. )
- g) A playback mode which allows each survey to be replayed as if the survey was being repeated.

One of the main problems in carrying out surveys with a carborne system is that the road is a significant contributor to the gamma-ray measurements. This can be a problem, particularly when the road material is not representative of the surrounding ground. There are several ways this problem can be minimized. The detector should be mounted as high as possible, to increase its field of view, preferably on the roof of the vehicle. The detector should also be orientated with its long axis along the length of the vehicle. In addition, it is good practice to mount the detector on the passenger's side of the vehicle, so that the

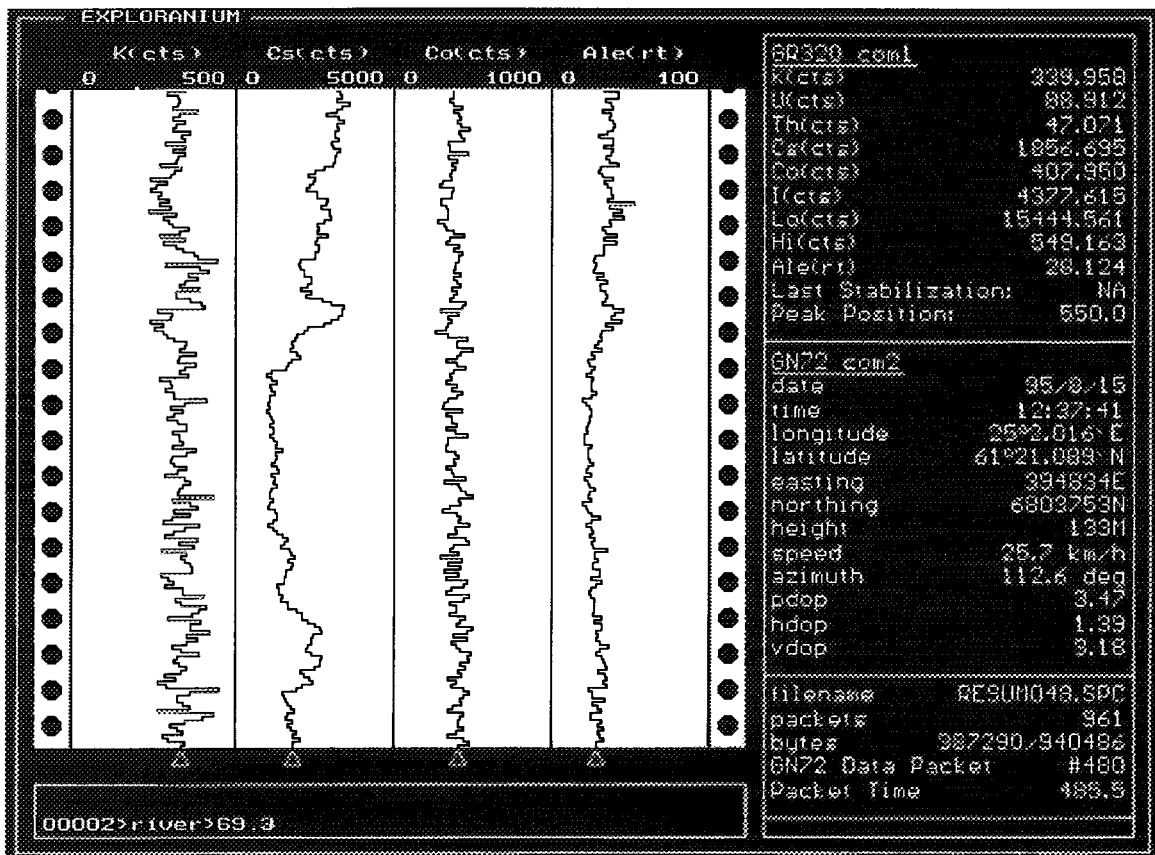


Figure 3. A screen display showing a chart record of the potassium, uranium and thorium count rates and a window ratio.

detector is as close as possible to the shoulder of the road. It has also been found that people in the vehicle can reduce the gamma-ray signal from the ground. To minimize this effect, it is probably best to mount the detector to the rear of the roof.

## CALIBRATION OF THE CARBORNE SYSTEM

### Calibration for natural radioactivity mapping

The basic calibration procedure for the GR-650 is to compare the potassium, uranium and thorium count rates of the carborne system with the ground concentrations of potassium, uranium and thorium as measured with a calibrated portable gamma-ray spectrometer. The calibration of the portable spectrometer is achieved from measurements on concrete blocks with known concentrations of potassium, uranium and thorium as described by Grasty et al (1991). Calibration using the results of soil analyses is not recommended due to possible differences in soil gas  $^{222}\text{Rn}$  concentration between the field and laboratory measurements (Grasty and Minty, 1995)

In order to convert the count rates recorded by the carborne system to ground concentrations of potassium, uranium and thorium, the stripping ratios and backgrounds of the system must be determined. With the appropriate corrections, the count rates that originate solely from potassium, uranium and thorium can then be calculated.

The stripping ratios for the carborne system are normally determined from measurements with the detector removed from the vehicle and placed on concrete calibration pads. The first stage in the calibration process is to energy calibrate the spectrum. This is achieved by determining the channel position of several prominent gamma-ray peaks. Suitable peaks would be the 609, 1120 and 1760 keV peaks from  $^{214}\text{Bi}$  on the uranium pad, the 2615 keV peak from  $^{208}\text{Tl}$  on the thorium pad and the 1460 keV peak  $^{40}\text{K}$  on the potassium pad. If the 662 keV peak from  $^{137}\text{Cs}$  is being used for stabilization, this peak, which is normally centered on channel 55 can also be used.

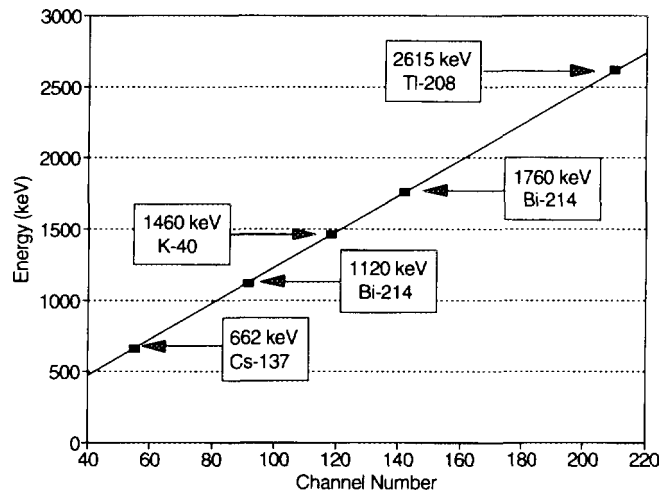


Figure 4. The energy calibration procedure for the carborne system showing the linear relationship between channel and energy.

For all practical purposes, it has been found that in the energy range from 600 to 2600 keV, there is a linear relationship between channel position and energy (Fig 4). From this linear relationship, the count rates in the recommended IAEA windows can be determined and the stripping ratios calculated using the program PADWIN (Lovborg et al, 1981). The stripping ratios for the carborne system used in Résumé95 are shown in Table 1 together with the contributions of potassium, uranium and thorium to a  $^{137}\text{Cs}$  window. This 150 keV window, centered on the  $^{137}\text{Cs}$  photopeak at 662 keV, was selected on the basis of a spectrum measured in Finland.

Table 1. Stripping Ratios for a 10.2 x 10.2 x 40.6 cm detector

Stripping Ratio	Value
Alpha	0.303
Beta	0.421
Gamma	0.847
a	0.056
Cs/K	0.367
Cs/U	3.41
Cs/Th	2.19

Any calibration requires a knowledge of the background count rates in the three radioelement windows, both for the portable spectrometer and the carborne system. These backgrounds originate from cosmic radiation, radon decay products in the air and any radioactivity due to the equipment itself. They are normally obtained from measurements in a metal or fiberglass boat on a large body of water, such as a river or a lake. In the case of the carborne system, the detector would normally be removed from the vehicle and connected to a portable spectrometer.

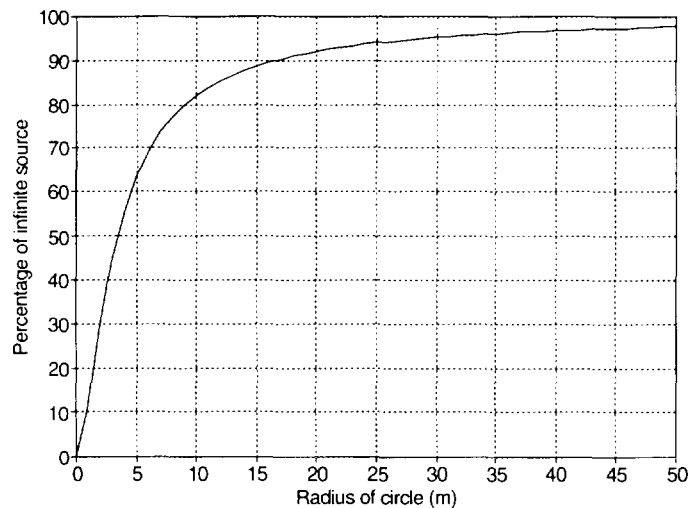


Figure 5. The field of view of a detector at a height of 2 meters above the ground

Due to their small size, calibration pads cannot be used for the determination of the system sensitivities. The calibration is normally carried out using a specially selected site with elevated levels of potassium, uranium and thorium. The site should be relatively flat as well as being uniformly radioactive. Since the carborne

detector is normally mounted on the roof of the vehicle, about 2m above the ground, it has a much larger field of view than a ground spectrometer. As shown in figure 5, ten percent of the detected gamma radiation originates from sources in the ground which are more than 15 m from the detector. The calibration sites must therefore be at least this size. Suitable calibration sites have been found to be school playing fields, asphalt parking areas and airport parking ramps.

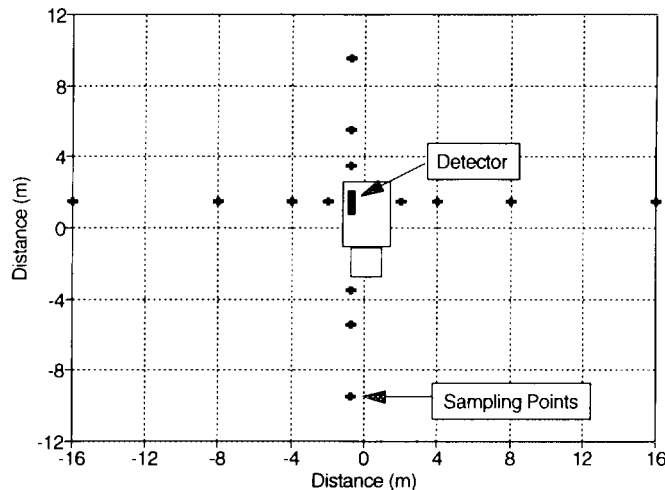


Figure 6. A schematic diagram showing a typical sampling scheme for the calibration of a carborne gamma-ray spectrometer system.

Because of the shape of the detector, ground measurements with the calibrated spectrometer have normally been made in two directions, along the long axis of the detector and at right angles to it. Since the detector has a much smaller cross-section in the long axis direction (10.2 x 10.2 cm) than it does in the direction at right angles ( 10.2 x 40.6 cm), fewer measurements would normally be made in the long axis direction. Figure 6 shows a typical sampling scheme in which a total of fourteen 100 second measurements are made. From these measurements, the average ground concentrations of the calibration site can be determined.

While the ground measurements are being performed, the carborne system would normally be accumulating data. The sensitivities of the system can then be determined by dividing the average background corrected and stripped potassium, uranium and thorium window count rates by the corresponding ground concentration.

Calibration for  $^{137}\text{Cs}$  using soil analyses.

During Résumé95, the carborne system was calibrated at Vesivehmaa airfield so that the carborne counts could be converted to  $^{137}\text{Cs}$  activity in  $\text{kBq/m}^2$ . This was achieved by comparing the background corrected and stripped count rates in the cesium window to the measured  $^{137}\text{Cs}$  ground concentration of  $50 \text{ kBq/m}^2$  as reported by the coordinators of the project.

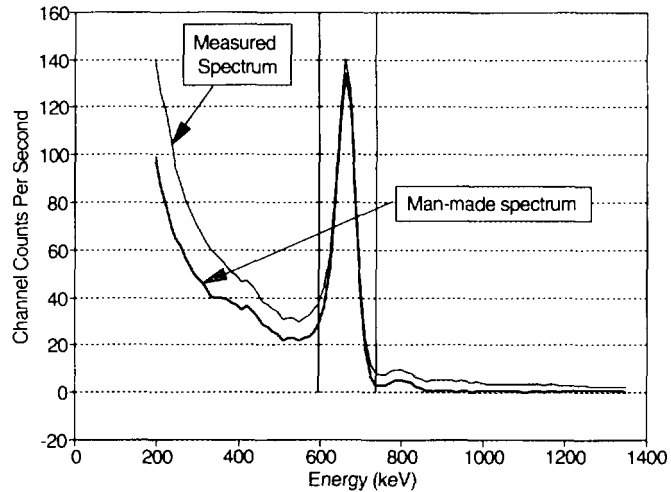


Figure 7. A gamma-ray spectrum from the carborne system on the Vesivehmaa airfield. The man-made spectrum from  $^{137}\text{Cs}$  and  $^{134}\text{Cs}$  is also shown.

Figure 7 shows the average spectrum from approximately 200 seconds of data from the carborne system at the central point of the airfield (ORIGO). The figure also shows the man-made spectrum from  $^{137}\text{Cs}$  and  $^{134}\text{Cs}$  which was obtained by removing the natural components due to potassium, uranium and thorium as described by Grasty et al, (1992). Calibration measurements were also performed at 3 additional sites, designated 2.4, 3.4 and 4.4.

Table 2. Ground concentrations of four calibration sites at Vesivehmaa airfield

Site	Potassium (pct)	Uranium (ppm)	Thorium (ppm)
ORIGO	2.10	2.32	7.77
2.4	2.07	2.57	8.63
3.4	2.20	2.09	7.68
4.4	2.08	2.16	8.4
Average	2.22 +/- 0.03	2.28 +/- 0.11	8.11 +/- 0.27

\* The errors indicated are the standard deviations of the mean.

The carborne system was also calibrated for potassium, uranium and thorium from measurements at the four sites following the procedure described in the previous section. A GR.-320 portable spectrometer, previously calibrated on concrete pads at Explorandum's plant in Toronto, Canada was used to measure the ground concentrations of potassium, uranium and thorium at the four sites. These results are shown in Table 2.

Table 3 shows the calculated sensitivities of the carborne system for  $^{137}\text{Cs}$ , potassium, uranium and thorium at the four sites. The errors quoted are the errors on the mean values assuming that four independent sensitivities were made.

Table 3. Sensitivities of the carborne system to  $^{137}\text{Cs}$ , potassium, uranium and thorium

Site	$^{137}\text{Cs}$ (cps/kBq/m <sup>2</sup> )	Potassium (cps/pct)	Uranium (cps/ppm)	Thorium (cps/ppm)
ORIGO	14.25	27.13	3.70	1.40
2.4	13.89	27.29	3.61	1.20
3.4	14.33	25.48	3.90	1.48
4.4	15.79	27.77	3.84	1.31
Average*	14.57 +/- 0.84	26.92 +/- 1.00	3.76 +/- 0.13	1.35 +/- 0.12

\* The errors indicated are standard deviations of the mean.

#### Calibration for $^{137}\text{Cs}$ using a point source

In areas where there is little or no  $^{137}\text{Cs}$  fallout, the calibration of a carborne system cannot be carried out by comparing the carborne measurements with the activity of soil samples.

For a carborne system, a significant fraction of the gamma-ray flux emitted from a uniform distribution of  $^{137}\text{Cs}$  on the surface of the ground will be attenuated by the materials of the vehicle. This attenuation will depend on the path of the radiation from the ground to the detector. For instance, there are locations on the ground where no radiation reaches the detector because of the engine block. These inhomogeneities in the distribution of material in the vehicle make it difficult to calculate the response of the entire system. In this situation, the calibration can best be performed from measurements of the detector response using small calibrated sources of  $^{137}\text{Cs}$ .

Figure 8 illustrates the procedure that has been used to measure the sensitivity of a carborne from a series of point source measurements. The measurement site

selected was an aircraft parking ramp which was flat, relatively homogeneous and low in radioactivity to minimize possible sources of error. 10  $\mu\text{Ci}$  of  $^{137}\text{Cs}$  were placed on the ground on a 1 m grid at 144 separate locations. The grid covered an area of 12 x 12 m centered on the detector. Background measurements without the cesium sources were also recorded.

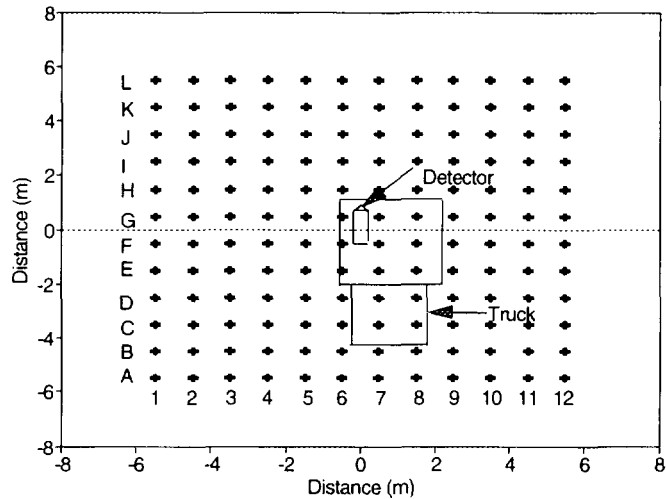


Figure 8. The sampling scheme used for calibrating a carborne system using small sources of  $^{137}\text{Cs}$ .

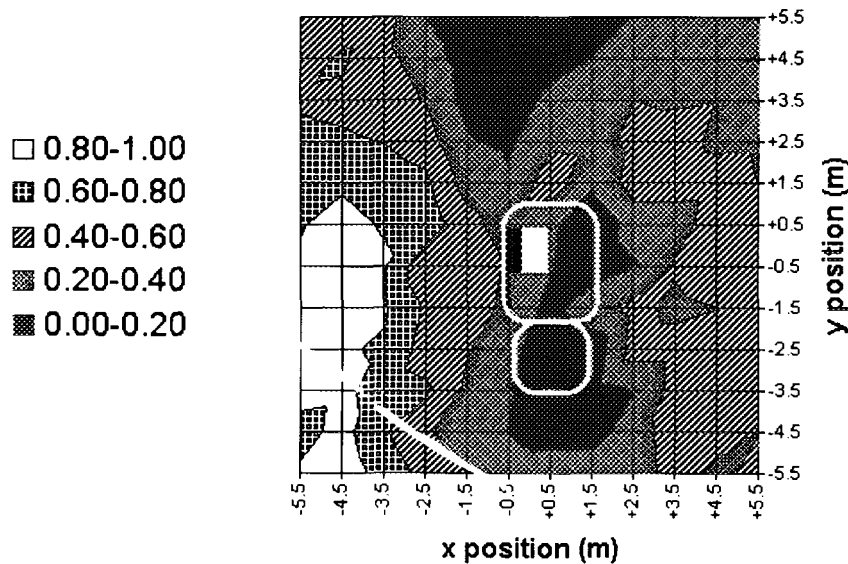


Figure 9. A map showing the variation in detector efficiency with source position

The measured gamma-ray count rates will depend not only on the detector efficiency, but also on the distance of the source from the detector. In order to compare the detector efficiency for different positions of the source, the background corrected measurements were normalized to a constant distance from the detector.

Figure 7 shows a map of the normalized  $^{137}\text{Cs}$  measurements for all 144 grid points together with the position of the vehicle and detector. This map effectively shows how the detector efficiency varies with the position of the source. As expected, the figure shows that the measured count rates are higher with the source facing the large side area of the detector compared to the measurements along the axis of the detector. Due to partial shielding of the sources by the vehicle roof, the measurements are higher on the detector side of the vehicle compared to the measurements on the opposite side of the vehicle. In addition, the count rates are significantly lower with the source facing the photomultiplier tube end of the detector compared to the measurements at the opposite end. This reflects the absorption of the gamma-radiation by the photomultiplier and its associated electronics.

In order to compute the sensitivity of the system, it is necessary to predict the count rate for points outside the measured area. This was achieved using data from the unshielded side of the vehicle. These predicted count rates were then combined with the measured values to give the count rate from an infinite homogeneous source of known activity.

## **APPLICATIONS OF THE GR-650 CARBORNE SYSTEM**

### **Natural Radioactivity Measurements**

Prior to Résumé95, the GR650 carborne system has been used primarily for the measurement of natural radioactivity to aid geological mapping and mineral exploration. The system has also been used in Portugal to provide information for a natural background radioactivity map of the entire country (Torres and Grasty, 1993). With a calibrated system, this can be achieved by converting the measured potassium, uranium and thorium concentrations to air absorbed dose rate using the following conversions:

1 percent potassium	= 13.1 nGh <sup>-1</sup>
1 part per million of uranium	= 5.42 nGh <sup>-1</sup>
1 part per million of thorium	= 2.69 nGh <sup>-1</sup>

In the Philippines, the system was also intended to map potassium, uranium and thorium concentrations for the production of natural background radioactivity maps. During system calibration and testing, a small survey was carried out in a gold mining district to assess the potential of the system for gold exploration. Increases of potassium are frequently associated with gold mineralization. Figure

10 clearly shows a significant increase in potassium concentration near the entrance to the Antamok gold mine which could well be related to hydrothermal alteration associated with the gold.

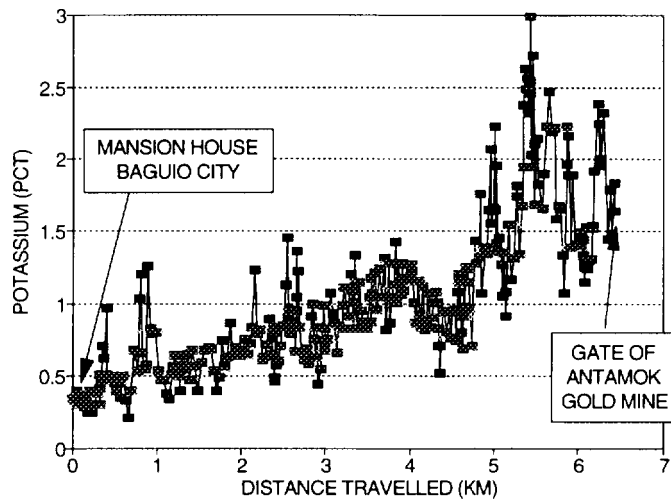


Figure 10. A profile measured in the Philippines showing the increase in potassium concentration near the Antamok gold mine.

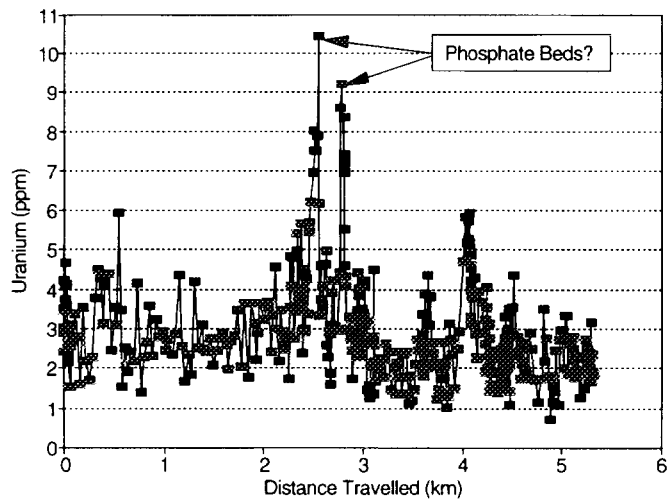


Figure 11. A profile measured in Venezuela showing uranium anomalies probably related to phosphate deposits.

In Venezuela, the system was initially tested in a phosphate mining district to identify possible areas for future exploration. Phosphate deposits invariably have a significantly increased uranium concentration which is readily identifiable by gamma-ray spectrometry. Figure 11 shows a profile from one particular vehicle track with two significant uranium anomalies believed to relate to phosphate beds. These two anomalies are also shown in Figure 2 which is a screen dump of the vehicle track.

During Résumé95, it was intended to compare the measurements from the different carborne systems along a few selected roads. Figure 12 shows a stacked profile of the potassium, uranium and thorium concentration as well as  $^{137}\text{Cs}$ . Profiles such as these were produced by the program SURVIEW developed at the Geological Survey of Canada (Grant, 1993). The GR650 software provides files which are directly compatible with SURVIEW.

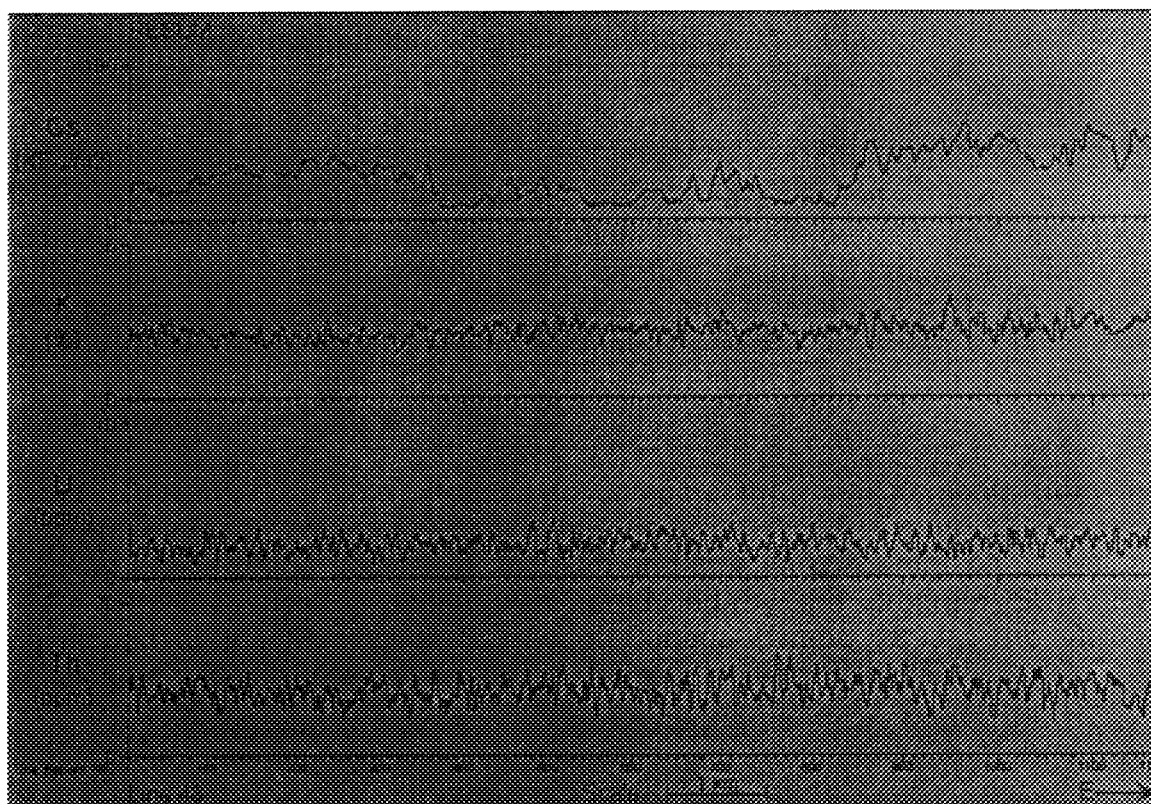


Figure 12. A stacked profile showing the activity of  $^{137}\text{Cs}$  and the concentrations of potassium, uranium and thorium measured in area II. The profile was produced using the program "SURVIEW".

The potassium uranium and thorium concentrations on the profiles can be converted to activity per gram of  $^{40}\text{K}$ ,  $^{214}\text{Bi}$  and  $^{208}\text{Tl}$  using the following relationships (IAEA, 1989) :

$$\begin{aligned}
 1 \%K &= 313 \text{ Bq kg}^{-1} \text{ of } ^{40}\text{K} \\
 1 \text{ ppm eU} &= 12.35 \text{ Bq kg}^{-1} \text{ of } ^{238}\text{U} \\
 1 \text{ ppm eTh} &= 1.42 \text{ Bq kg}^{-1} \text{ of } ^{232}\text{Th}
 \end{aligned}$$

The small “e” signifies “equivalent”, since  $^{214}\text{Bi}$  and  $^{208}\text{Tl}$  may not be in equilibrium with their parents  $^{238}\text{U}$  and  $^{232}\text{Th}$ . It should also be noted that the conversion from equivalent thorium concentration to activity per gram of  $^{232}\text{Th}$  is given by :

$$1 \text{ ppm eTh} = 4.06 \text{ Bq kg}^{-1} \text{ of } ^{232}\text{Th}$$

The difference between the activities of  $^{232}\text{Th}$  and  $^{208}\text{Tl}$  arises because only 36 percent of  $^{212}\text{Bi}$  atoms decay into  $^{208}\text{Tl}$ .

### $^{137}\text{Cs}$ measurements in Finland

As described previously, the carborne system was calibrated for  $^{137}\text{Cs}$  at four sites on the Vesivehmaa airfield. Based on the stripping ratios (Table 1) and sensitivities (Table 3), a 4 x 4 matrix was calculated to convert the recorded count rates to concentrations of potassium, uranium and thorium as well as the activity of  $^{137}\text{Cs}$ . This 4 x 4 matrix serves as a calibration file for processing and reviewing the recorded data using the system software. The processed data were then combined with the GPS co-ordinate position information to produce a grid which could be imported into SURVIEW and displayed on a screen or printed on a colour plotter. Figure 13 shows a coloured map of the cesium distribution for area II together with the route taken by the vehicle and the major lakes in the area. The map shows that the  $^{137}\text{Cs}$  concentrations vary from around 10 kBq m<sup>-2</sup> to as high as 80 kBq m<sup>-2</sup>.

### Searching for radioactive sources

As part of the Emergency Response Exercise in Finland, the carborne teams were directed to drive along a particular road and locate a hidden radioactive source. No information was given as to the nature of the source, which was a collimated 15 Ci source of  $^{192}\text{Ir}$  located approximately 400 m from the road with its beam of radiation directed vertically upwards.  $^{192}\text{Ir}$  emits gamma-rays of various energies, of which the most abundant are at 468, 316, 308 and 295 keV. Since the source is collimated, the only gamma-rays that can be detected at ground level will be low energy back-scattered skyshine radiation which will have a broad range of energies from 0 to around 300 keV.

It is a characteristic of most artificial radioactive sources that they emit a higher proportion of low energy gamma rays compared to those emitted by naturally occurring radioactive elements. Based on this fact, one procedure for detecting man-made radiation from an unknown gamma-ray source is to monitor the ratio of a low and high region of the gamma-ray spectrum. This procedure was

successfully utilized in the search for radioactive debris from the Russian nuclear powered satellite COSMOS 954 which crashed in northern Canada in 1978 (Bristow, 1978; Grasty, 1980). In the search operation, the low energy region covered a range from 300 to 1400 keV and the high energy region from 1400 to 2800 keV. The ratio of these two energy regions was found to remain relatively constant irrespective of the concentrations of the naturally occurring radioactive elements, even when flying over water.

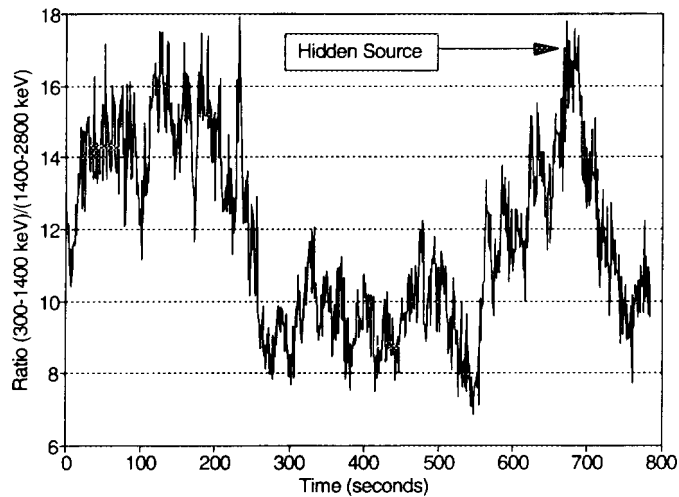


Figure 14. A profile of the low/high energy ratio from an area in Finland contaminated with  $^{137}\text{Cs}$ . The energy regions are the same used to locate radioactive debris from COSMOS-954.

The GR650 airborne system software was designed so that any two window ratios could be monitored in real-time. Initially, the same two regions of the spectrum that were used during the COSMOS incident were also used in the search for the hidden radioactive source. However, in Finland, the analysis of the results is complicated due to the high and variable concentration of  $^{137}\text{Cs}$  from the Chernobyl nuclear accident. This variation in  $^{137}\text{Cs}$  results in large fluctuations in the low to high energy ratio. Figure 14 shows the variation in this ratio along the road where the source was located.

When no obvious discrete man-made radiation source was identified using the standard low and high energy regions of the spectrum, some alternative procedures were investigated. One particular procedure involved ratioing two different parts of the spectrum to reduce the effects of varying  $^{137}\text{Cs}$ . Figure 15 shows a ratio profile along the same road using a low energy window from 35 to 350 keV and a high energy window from 350 to 2800 keV. A distinct high ratio region is indicated on this profile which relates to back-scattered radiation from the hidden  $^{192}\text{Ir}$  source.

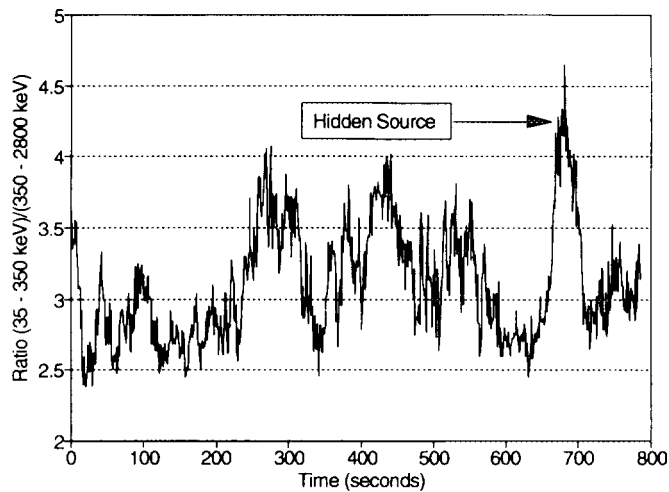


Figure 15. A profile of the low energy (35 to 350 keV) to high energy (350 to 2810 keV) ratio showing the location of the hidden radioactive source.

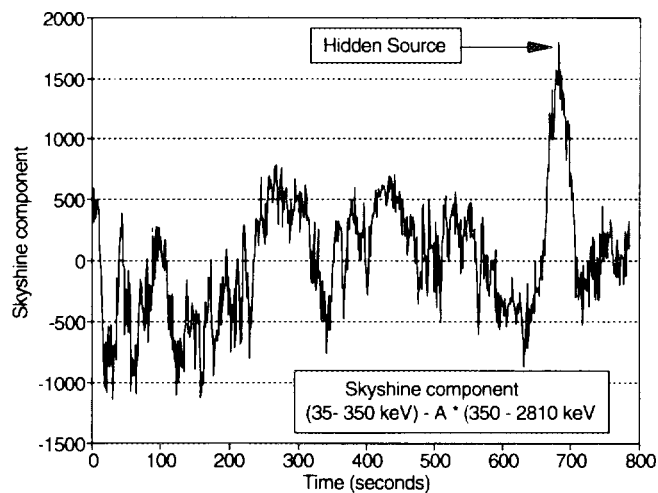


Figure 16. A profile of the low energy back-scattered component from 35 to 350 keV showing the location of the hidden radioactive source.

An alternative technique to locate man-made sources of radiation that has been successfully utilized is to remove the natural component from the low energy part of the spectrum using a simple stripping procedure (EG&G ,1995). The man-made component (M) is calculated using the expression:

$$M = L - A * H$$

where,

L is the low energy window count rate,  
H is the high energy window count rate and,  
A is the low to high energy ratio for natural radiation.

Figure 16 shows a profile of the skyshine component along the road with the hidden source. The skyshine component corresponds to the man-made count rate in the above equation where the value of A was determined from the low and high energy windows for the entire line. This profile also identifies the hidden radioactive source and can be seen to be similar in character to the ratio profile of Figure 15. Theoretically, it can be shown that provided the low/high energy ratio remains constant for all sources of natural radiation, the ratio technique and the stripping procedure are equally effective in identifying man-made sources or radiation.

### **CONCLUSIONS**

Exploranium's GR650 carborne gamma-ray spectrometer system has been shown to be effective in mapping both natural and man-made sources of radiation. With appropriate calibration procedures, the software allows the raw count rate data to be converted to standardized units of potassium, uranium, thorium and  $^{137}\text{Cs}$ . During the Finnish Emergency Response Exercise, the flexibility of the system allowed a variety of processing procedures to be used to map an area contaminated with  $^{137}\text{Cs}$  and to locate a hidden radioactive source.

### **ACKNOWLEDGEMENTS**

We are grateful to the Ministerio de Energia Y Minas, Venezuela, the Servicio de Fomento, Portugal and the Philippine Nuclear Research Institute, the Republic of the Philippines for permission to publish results obtained during IAEA technical assistance programs.

### **REFERENCES**

- Bristow, Q., 1978, The Application of Airborne Gamma-Ray Spectrometry in the Search for Radioactive Debris from the Russian Satellite Cosmos-954 ("Operation Morning Light"): Geol. Surv. Can. Paper 78-1B, p. 151-162.
- EG&G., 1995, T.J. Hendricks, private communication.
- Grant, J.A., 1993, SURVIEW - a Microsoft Windows 3.1 application to view geophysical survey data (line, grid, contour and stacked profiles). Geol. Surv. Can. Open File 2661.

- Grasty, R.L., 1980, The Search for COSMOS-954: Proceedings of the NATO Conference on Search Theory and Applications, Portugal 1979, Plenum Press, New York and London, p. 211-220.
- Grasty, R.L., Holman, P. B. and Blanchard, Y., 1991, Transportable calibration pads for ground and airborne gamma-ray spectrometers: Geol. Surv. Can., Paper 90-23, 26 p.
- Grasty, R.L., Multala, J. and Lemmela, H., 1992, Monitoring man-made radiation using a 256 channel portable gamma-ray spectrometer: Proceedings of the 8th International Congress of the International Radiation Protection Association, Montreal, Canada; p. 273-276.
- Grasty, R.L. and Minty B. R., 1995, A guide to the technical specifications for airborne gamma-ray surveys: Australian Geological Survey Organization, Record 1995/60, p. 89.
- International Atomic Energy Agency, 1989, Construction and use of calibration facilities for radiometric field equipment: Technical Report Series no. 309 (International Atomic Energy Agency, Vienna), 86 p.
- Løvborg, L., Christiansen, E. M., Bøtter-Jensen, L. and Kirkegaard, P., 1981, Pad facility for the calibration of gamma-ray measurements on rocks: Riso Report R-454, 43 p.
- Torres, L. M. and Grasty, R. L., 1993, The natural radioactivity map of Portugal. Applications of uranium exploration data and techniques in environmental studies. International Atomic Energy Agency TECDOC-827, Vienna, Austria, p. 127-133.



# Danish Emergency Management Agency The Danish Gamma Ray Surveying Results

ABSTRACT ..... 93

1. INTRODUCTION ..... 93

2. EQUIPMENT AND STAFF ..... 94

3. SURVEY ..... 94

4. RESULTS ..... 94

    Fig. 1. Actual and planned flight lines in Area II ..... 95

4.1. Results fro AREA I & II ..... 95

    Fig. 2a. First and second spectral component ..... 96

    Fig. 2b. Third and fourth spectral component ..... 96

    Fig. 3a. First and second cesium spectral component ..... 96

    Fig. 3b. First and second natural spectral component ..... 96

4.2. Results from AREA III ..... 97

    Fig. 6. Screen dump from graphical display showing the signature of an uncollimated <sup>137</sup>Cs source ..... 98

    Fig. 7. Screen dump from graphical display showing the signature of a narrow collimated <sup>137</sup>Cs source ..... 98

    Fig. 8. Screen dump from graphical display showing the signature of a collimated <sup>60</sup>Co source ..... 98

    Fig. 9. Screen dump from graphical display showing the signature of sky-shine from an <sup>99</sup>Ir source ..... 98

    Fig. 10a. First and second spectral component ..... 99

    Fig. 10b. Third and fourth spectral component ..... 99

    Fig. 10c. Fifth spectral component ..... 99

    Fig. 11a. A low energy spectral component and a cesium spectral component ..... 100

    Fig. 11b. A cobalt spectral component and a natural element spectral component ..... 100

    Fig. 11c. A combined scattered cesium and natural spectral component ..... 100

5. CONCLUSION ..... 100

REFERENCES ..... 100

Figures in Colour Appendix (C.A.)

Fig. 4. Cesium deposition in AREA II ..... C.A. plate 2

Fig. 5. Estimated cesium deposition depth in AREA II ..... C.A. plate 2

Fig. 12. Maps showing the source search result from AREA III ..... C.A. plate 3

**NEXT PAGE(S)  
left BLANK**

# THE DANISH AIRBORNE GAMMA-RAY SURVEYING RESULTS

Jens Hovgaard  
Danish Emergency Management Agency  
Datavej 16  
DK-3460 Birkerød, Denmark,

## Abstract

The Danish Emergency Management Agency (DEMA) in co-operation with the Technical University of Denmark (TUD), Department of Automation, participated in the international exercise RESUME-95 arranged in Finland in August 1995. DEMA performed measurement with their airborne gamma-ray surveying system. Surveys were done in the three areas known as AREA I, II, III. Results from AREA II (3 km x 6 km) show that the apparent  $^{137}\text{Cs}$  deposition assuming a deposition profile equal to the profile in AREA I based on soil samples varies from a few 10th  $\text{kBqm}^{-2}$  up to  $110 \text{kBqm}^{-2}$ . However, a detailed analysis using a new method, Noise Adjusted Singular Value Decomposition (NASVD), shows that the true variations probably are smaller and that the observed differences to some extent are due to major variations in the depth distribution of the cesium. For example agricultural areas appears to have cesium much deeper deposit than the undisturbed areas. Another interesting result is that the NASVD analysis shows that the ration of  $^{134}\text{Cs}$  to  $^{137}\text{Cs}$  is fixed and approximately 0.03 (August 1995) a number in good agreement with the expected ratio from the Chernobyl accident. No true real-time software for source detection is yet integrated in the Danish system. Results from AREA III, however, show that the implemented software for rapid post processing of data worked excellent for detection of radioactive sources. Post analysis using NASVD demonstrates that all sources except for a small  $^{137}\text{Cs}$  source can be localized.

## 1. Introduction

The RESUME-95 exercise took place in Finland in August 1995. Three different areas were surveyed by the Danish airborne team; Vesivehmaa airfield calibration site (AREA I), a 6 km times 3 km area near Padasjoki/Auttoinen contaminated with up to  $100 \text{kBqm}^{-2}$   $^{137}\text{Cs}$  from the Chernobyl accident (AREA II), and a source survey area (AREA III).

## **2. Equipment and staff**

Staff involved in operation of DEMA's airborne gamma-ray surveying system:

Jens Hovgaard	DEMA
Frank Andersen	Technical University of Denmark (TUD)
Kim Bargholz	TUD
Dorthe Eide Paulsen	TUD
Pilots	Finnish Frontier Guard

The Danish airborne gamma ray spectrometer system was developed from 1992 to 1994. The system is intended to be used in the case of nuclear fallout on Danish territory. The system is based on a standard surveying  $^{161}\text{NaI(Tl)}$  detector and multichannel spectrometer system, a Global Positioning System (GPS) based navigation system, and a industrial personal computer (PC) for controlling data acquisition and navigation. During surveys, a 512 channel gamma ray spectrum is collected every second and stored on disk together with positional information.

In the RESUME-95 exercise the system was installed in an Augusta Bell helicopter provided by the Finnish Frontier Guard. One of the aims with the exercise was to demonstrate how easy or difficult it is to aid a foreign country in case of an emergency situation. Prior to the exercise it was tested how the Danish system could be integrated in the Finnish helicopter and it was decided how the different electrical interfaces between the Danish system and the helicopter should be carried out.

## **3. Survey**

At 10.30AM on Tuesday the 15 August 1995 the Danish team took off from Vesivehmaa airfield. The take off was scheduled to 10AM, but a delay in the flight of the team prior to our flight followed by a failure in a ground power supply just before take-off all together gave a delay of half an hour. All waypoints of the flights in AREA II and AREA III respectively were stored in files on the PC before the survey. In area II the survey was planned to be at 80 m ground clearance along lines separated 150 m apart, pre-defined by the organizers. In AREA III, however, it was up to each individual team to decide on flight strategy, the only limitation was that only 1 hour of flight in the area was permitted. The Danish team decided to use a close line spacing of 50 m combined with a relative high air speed of 90-100 knots.

Unfortunately an error in both of the waypoint files had to be corrected during the flight. As a result the part of the survey along road 100 leading from AREA II to AREA III was not performed.

## **4. Results**

Immediately after the survey a report of the source search results had to be submitted to the organizers. Another, more detailed, report could be submitted within 24 hours after landing. Later on more detailed analysis of the data from all three areas was carried out.

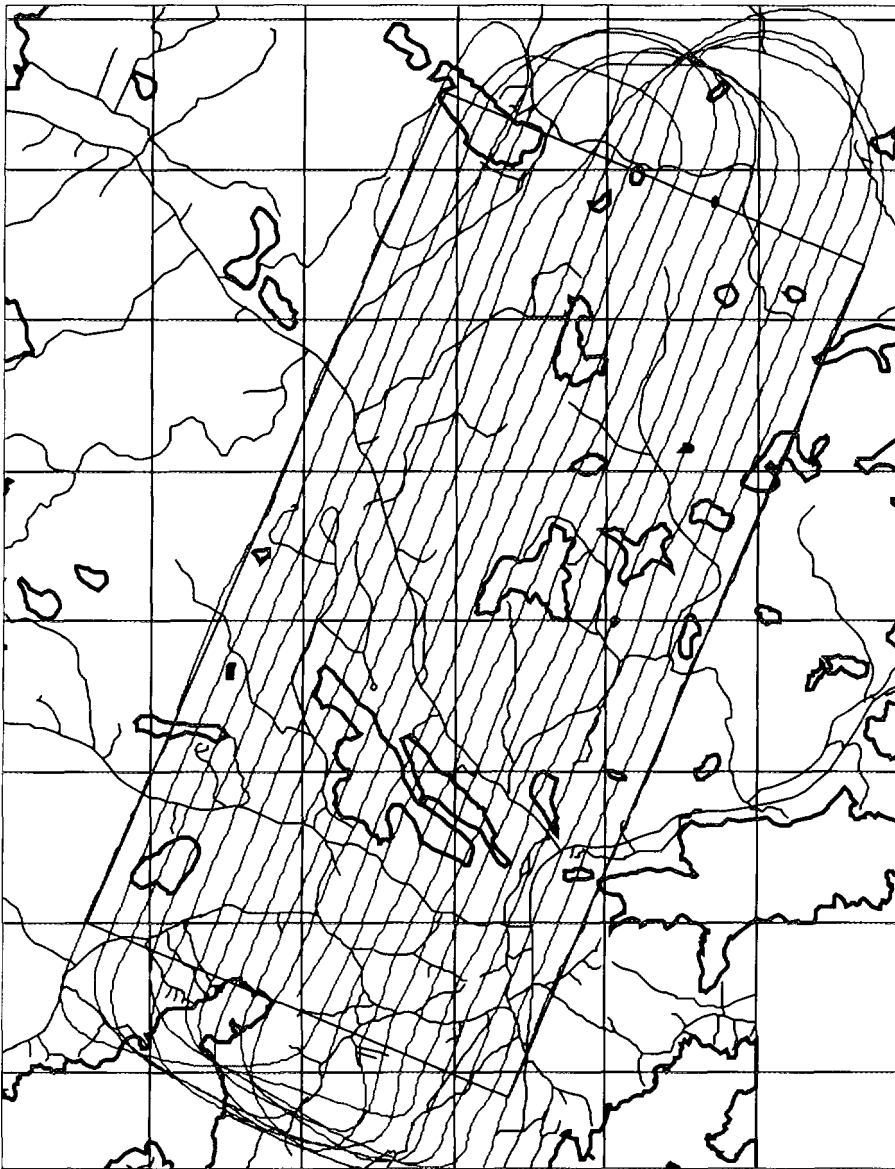


**Figure 1** Actual and planned flight lines in Area II. Scale 1:50,000

#### 4.1 Results from AREA I & II

A quick look at the data from AREA II showed that  $^{137}\text{Cs}$  was very dominant in the lower part of the spectrum. A crude deposition map was produced a few hours after landing based on the uncorrected  $^{137}\text{Cs}$  raw window count rates and a fixed  $\text{Bqm}^{-2}/\text{cps}$  calibration constant. The map was thus neither corrected for the influence of the natural background or height differences. The calibration constant was found using information from AREA I where the  $^{137}\text{Cs}$  deposition was known to be approximately  $50 \text{ kBqm}^{-2}$  according to soil samples.<sup>1</sup> Later on more detailed analysis of the deposition in AREA II was carried out.

A new method, NASVD<sup>2</sup>, has become the standard way to analyze airborne gamma-ray spectra

at DEMA. NASVD is a method where a statistical evaluation of all observed spectra from a survey is carried out. The idea is that all the observed spectra can be constructed of a linear combinations of a number of different basic spectra or spectral components. Initially both the number of spectral components and the spectral components themselves are unknown. The NASVD analysis constructs an ordered list of orthonormal spectral components ordered in accordance with their overall importance. The hypothesis that linear combinations of only the first  $k$  spectral components are sufficient to explain all the observed spectra is then tested. Often, even with complex spectra it turns out that less than eight spectral components are sufficient to explain all the observations. Figure 2 shows the first four spectral components from AREA II. As seen in the figure each individual spectral component is a mixture of natural elements and  $^{137}\text{Cs}$  and thus not identical to respectively a "clean" potassium, uranium, thorium, or cesium spectrum. The four spectral components define an orthonormal basis of a four-dimensional spectral subspace. A new non-orthogonal basis of this four-dimensional subspace can be defined in such a way that two spectral directions are "clean" cesium spectra and two additional spectral directions contain no cesium at all. Figure 3a shows the two cesium spectral components and Figure 3b shows the two spectral components with no cesium.

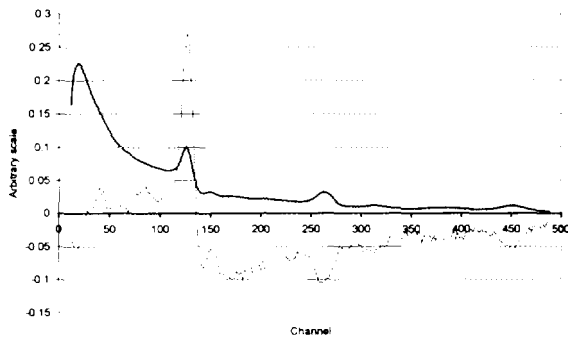


**Figure 2a** First (bold) and second spectral component.

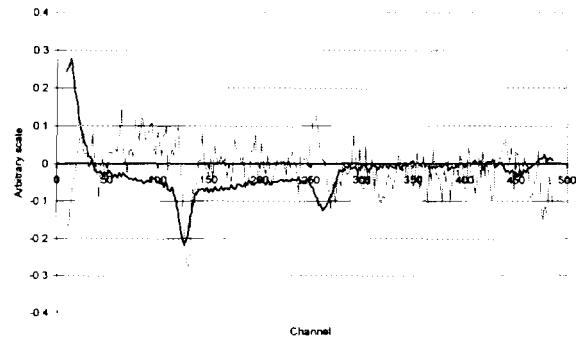


**Figure 2b** Third (bold) and fourth spectral component.

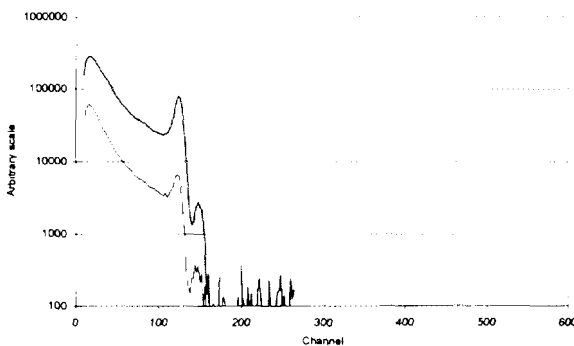


**Figure 3a** First (bold) and second cesium spectral component.

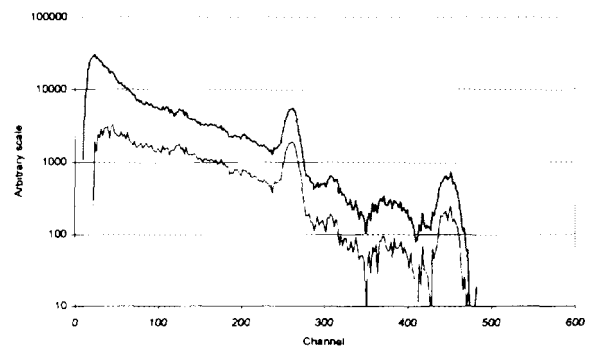


**Figure 3b** First (bold) and second natural spectral component.

A least square fit of the transformed spectral component to the original data is carried out resulting in the concentrations of each of the transformed components. The concentrations of

the two cesium components can be converted to equivalent  $^{137}\text{Cs}$  windows count rates and then into ground deposition. Figure 4 shows the  $^{137}\text{Cs}$  deposition map using this approach.

The spectral component method is more informative than the traditional window method. Examination of the primary cesium component in Figure 2a shows the presents of  $^{134}\text{Cs}$ . It is possible to determine the relative amount of  $^{134}\text{Cs}$  and  $^{137}\text{Cs}$  in the spectrum by a simple two-window analysis using two windows at 600 keV - 720 keV and 730 keV - 900 keV respectively. The analysis shows that the relative amount of  $^{134}\text{Cs}$  in the primary cesium component is approximately 0.03, a number in good agreement with the expected ratio in the Chernobyl fall-out (1995). Information from the cesium components can also be used to estimate the deposition depth. It is seen that the two cesium components differ in the relative amount of primary and secondary radiation. There exist a close to linear relationship between the mass depth and the ration between the secondary radiation and the primary radiation for infinite planar source. It is thus possible to estimate the mass depth using the two cesium components. The estimated mass depth is the sum of the soil mass depth and the equivalent mass depth of the air column between ground and aircraft. A correction for the latter can be applied using the information of the ground clearance. Figure 5 shows a map of the estimated deposition depth in AREA II. It is seen that the cesium appears to be much deeper distributed in especially the lower right corner of the map and to some extend along a east-west going stripe in lower part of the map. These areas turn out to be agricultural areas where plowing is expected to bring the deposited cesium deeper down in the soil. The map is not expected to be very accurate rather it is intended to give a rough estimate of zones with different cesium depth profiles.

#### 4.2 Results from AREA III

The display program for rapid post processing of data in the Danish airborne gamma-ray surveying system proved to be excellent for localization and identification of lost sources. Figure 6-9 show screen dumps from the program, each display shows two image windows and two information windows. The upper image window shows a sequence of gamma-ray spectra, each spectrum is displayed as single vertical line of colored pixels reflecting the intensity of individual spectrum channels. The lower image window displays a selected gamma-ray spectrum. The lower information window shows additional information of the selected spectrum, measurement number, time, co-ordinates, line number, live time, and count rate in a marked energy window. The upper information window shows similar information but for the last measurement.

Sources are often easily identified using this display technique. Figure 7 shows the fingerprint of a narrow collimated  $^{137}\text{Cs}$  source. A collimated sources is characteristic because it shows up very sharp on only a few measurements with a relative high proportion of primary photons. The contrary is seen in Figure 6 which shows the signal from an unshielded  $^{137}\text{Cs}$  source. It is seen that the signal is much wider and a substantial amount of the signal comes from Compton scattered photons. Figure 8 shows the signal from a collimated  $^{60}\text{Co}$  source and Figure 9 shows sky-shine radiation from an  $^{192}\text{Ir}$  source.

An NASVD analysis of the data from AREA III came out with five significant spectral components. The five components are shown in Figure 10.

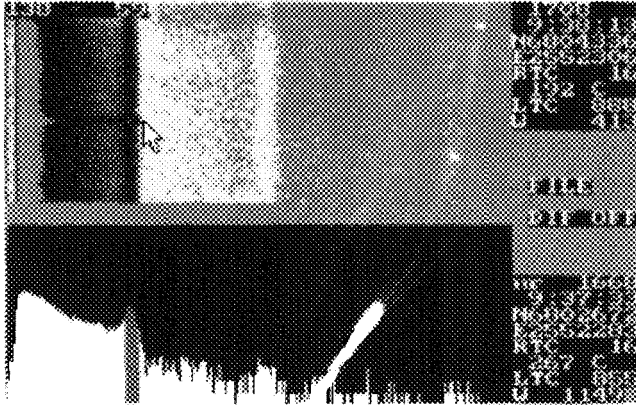


**Figure 6** Screen dump from graphical display program showing the signature of an uncollimated  $^{137}\text{Cs}$  source (source Cs1)

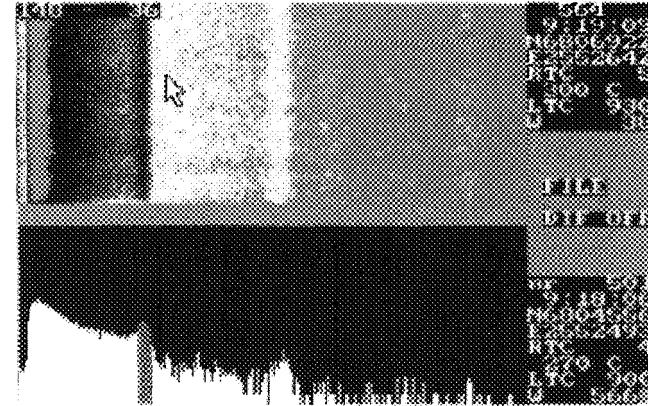


**Figure 7** Screen dump from graphical display program showing the signature of a narrow collimated  $^{137}\text{Cs}$  source (source Cs2)

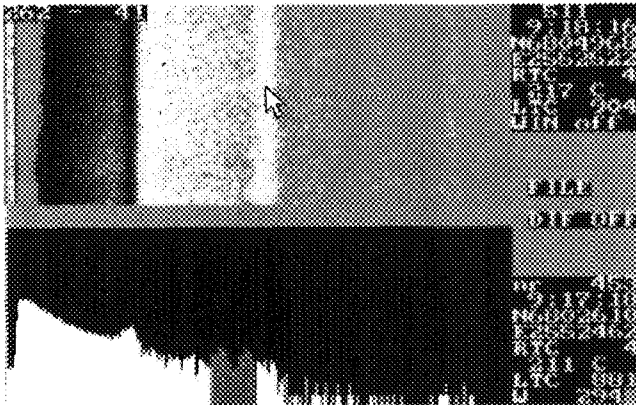


**Figure 8** Screen dump from graphical display program showing the signature of a collimated  $^{60}\text{Co}$  source (source Co1)

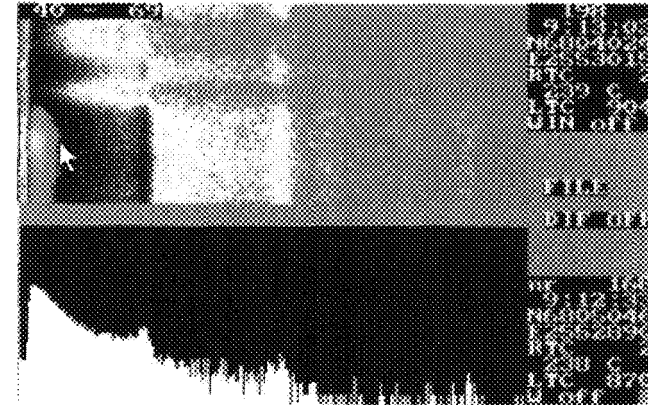


**Figure 9** Screen dump from graphical display program showing the signature of sky-shine from an  $^{99}\text{Ir}$  source (source Ir).

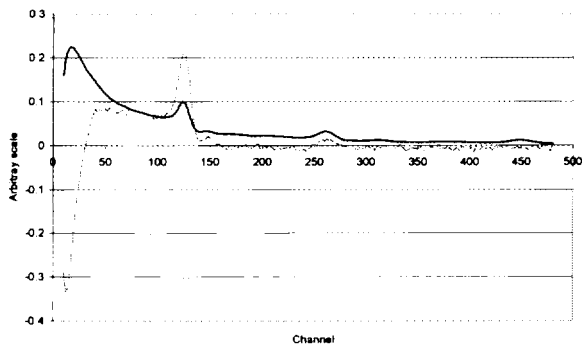


**Figure 10a** First (bold) and second spectral component.

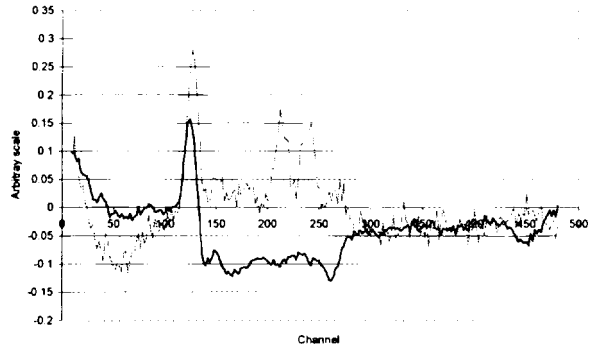


**Figure 10b** Third (bold) and fourth spectral components.

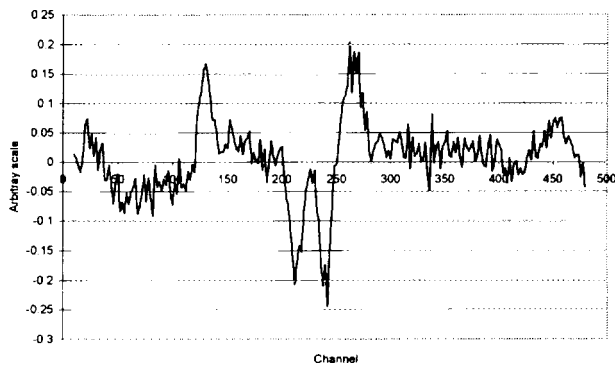


**Figure 10c** Fifth spectral component.

Different source responses can be identified in the figures. Cesium can be seen in all the spectral components and cobalt is seen in spectral component 4 and 5 and a strong negative low energy continuum can be seen in spectral component two. As described in section 4.1 a new basis, based on spectral component 1 to 5, can be defined in such a way that new basic spectra are easier to quantify in terms of specific nuclides. The new spectral basis is shown in Figure 11. Figure 11a shows a low energy spectral component and a cesium spectral component, Figure 11b shows a cobalt spectral component and a natural element spectral component, and finally Figure 11c shows a combined scattered cesium and natural spectral component. A map of the concentration of the cesium spectral component is shown in Figure 12a. Three of the four cesium sources can be identified on the map. The lower left cesium source, however, is not more significant than the “natural” cesium feature just below it, only the clean circular shape indicates that it is a point source. The narrow collimated cesium source in the middle of upper part of the map is almost invisible but significant. The source is only detected in two measurements and the feature is blurred out in the contouring. The three cobalt sources are easily identified in Figure 12b. On Figure 12c is the dominating feature the sky-shine from the  $^{192}\text{Ir}$  source. The  $^{99\text{m}}\text{Tc}$  source can be seen on the map but it is not significant.

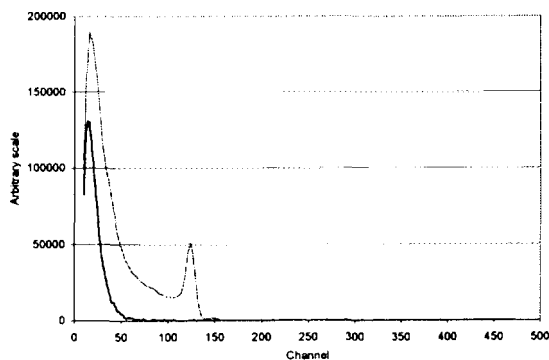


**Figure 11a** A low energy spectral component (bold) and a cesium spectral component.

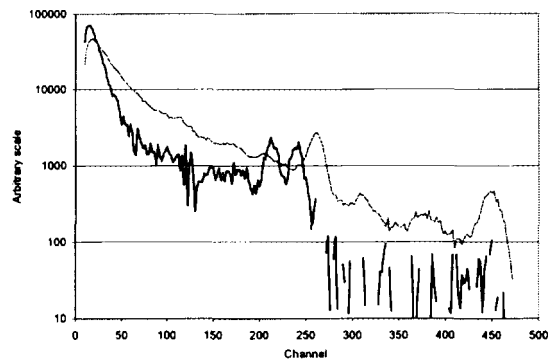


**Figure 11b** A cobalt spectral component (bold) and a natural element spectral component.

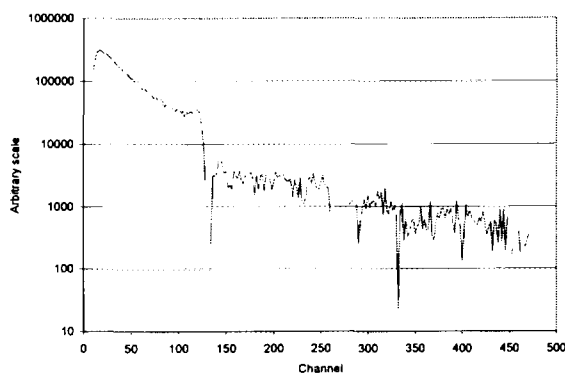


**Figure 11c** A combined scattered cesium and natural spectral component.

## 5. Conclusion

The overall performance of the Danish airborne gamma-ray surveying system in the RESUME-95 exercise was very satisfactory. The results of the  $^{137}\text{Cs}$  deposition mapping is in good agreement with the majority of the airborne surveying deposition results. Based on the experiences gained from the exercise further development in real-time analysis and in further development of the NASVD approach has been initiated.

## References

1. D.C.W.Sanderson et al, "Gamma ray spectrometry results from core samples collected for RESUME 95", *report, Scottish University Research & Reactor Centre*, September 1995.
2. J. Hovgaard, "A new processing technique for airborne gamma-ray spectrometer data", *Proceedings, ANS Sixth topical meeting on emergency preparedness and response*, San Francisco, April 1997.



# Finnish Defence Forces Research Centre

## Airborne Fallout Mapping of <sup>137</sup>Cs

ABSTRACT .....	103
1. INTRODUCTION .....	104
2. EQUIPMENTS .....	104
3. CALIBRATION .....	104
4. FLIGHT LINES .....	105
Fig. 1. Planned and actual flight lines on area II on August 1995 .....	105
5. RESULTS .....	106
6. DISCUSSION .....	106

Figures in Colour Appendix (C.A.):

Fig. 2. Fallout map of area II measured with HPGe on 16 <sup>th</sup> August 1995 .....	C.A. plate 4
---	--------------

**NEXT PAGE(S)**  
**left BLANK**

# Airborne Fallout Mapping of $^{137}\text{Cs}$ Finnish Defence Forces Team

**M Kettunen,<sup>1</sup> T Heininen,<sup>1</sup> M Pulakka<sup>2</sup>**

1 Finnish Defence Forces Research Centre  
P.O. Box 5  
FIN-34111, Lakiala  
Finland

2 Finnish Air Force Depot  
P.O. Box 210  
FIN-33101, Tampere  
Finland

## **Abstract**

The main task of the team was to create a fallout map of  $^{137}\text{Cs}$  in a specified area in Padasjoki Auttoinen village. The team used an MI-8 helicopter of the Finnish Air Force. The team had an HPGe system (relative efficiency 70%) to measure nuclide specific ground contamination level. For navigation the team took advantage of the DGPS service provided by Finnish Broadcasting company utilizing the RDS-channel to get position accuracy within 2 meters. The correction signal is reachable nationwide on the FM transmitter network. The system produced a distribution map for  $^{40}\text{K}$  and fallout maps for  $^{134,137}\text{Cs}$  using a Micro Station Program with TerraModeler application. The maximum measured  $^{137}\text{Cs}$  ground contamination exceeded 130-140 kBq $\text{m}^{-2}$ .

## 1 INTRODUCTION

The Finnish Defence Forces Research Centre is developing operational airborne equipment based on the HPGe detector. At the exercise navigation technique was based on a differential corrected GPS system (DGPS). The position was shown to the pilots in real time on a digital map on the computer screen and to the operator of the radiation measurement system. The Finnish Air Force provided an MI-8 helicopter for the exercise. For larger scale fallout mapping the system has been installed in a jet plane. The used measurement system has also been tested in cold winter conditions and stability was good.

## 2 EQUIPMENTS

The measuring instrument consist of the following components: an HP germanium detector, resolution 1.9 keV @1.33 MeV and relative efficiency 70.3%. The detector was mounted on a stand to eliminate shock and vibration. The spectroscopy system (which requires a high voltage power supply, linear amplifier and multichannel analyzer) was thermally isolated from the environment to allow good stability. The computer is a ruggedized industrial PC-computer with a 66 MHz 486-processor and a color active matrix VGA display. The computer has 16 Mb RAM and 1.1 Gb hard disk. The GPS-receiver's manufacturer is Trimble and it's type is TANS II. The RDS-receiver is Differential Corrections Inc. type RDS-3000.

## 3 CALIBRATION

Calibrations were confirmed at the Vesivehmaa airfield over the origo selected by the organizers. The detector was mounted over the open bottom hatch of the cabin. The only medium between the detector and the ground was air. Altitudes 60, 100 and 150 meters were used for the HPGe detector. Basic calibrations were based on the earlier calibration measurements and theoretical calculations combined with laboratory measurements. The altitude was checked by radar altimeter during the flight. It was possible to keep the defined altitude very accurately.

The soil samples taken from area II and the airfield showed that caesium had penetrated deeper in area II. The values of  $^{137}\text{Cs}$  distribution coefficients were  $\alpha / \rho = 0.77$  in the airfield and  $\alpha / \rho = 0.44$  in area II (Sanderson et al. 1996). This would indicate a 12% higher soil attenuation at the flying altitude over area II than over the airfield for 662 keV primary gamma flux.

Our own soil sample laboratory measurements confirmed that caesium had penetrated deeper in area II than in the area of the airfield. The rough values (based on five samples from airfield and ten samples from area II) for  $^{137}\text{Cs}$  distribution coefficients were  $\alpha / \rho = 0.7$  in the airfield and  $\alpha / \rho = 0.4$  in area II.

The resulting calibration coefficient for area II at 60 meters altitude, to convert the count rate at  $^{137}\text{Cs}$  peak to fallout, was  $6.1 \text{ kBqm}^{-2} \text{ cps}$  for HPGe spectra.

#### 4 FLIGHT LINES

For navigation the team took advantage of the DGPS service provided by the Finnish Broadcasting company by utilizing RDS-channel to get position accuracy to within 2 meters. The position was shown in real time on a digital map on the computer screen. The planned and actual flight lines are shown in Figure 1.



Figure1. Planned and actual flight lines on area II on August 1995.

## 5 RESULTS

The fallout map based on the HPGe spectra is shown in Figure 2. The highest fallout values exceeded 130-140 kBqm<sup>-2</sup>.

## 6 DISCUSSION

The fresh fallout may contain tens of fission products with several hundred gamma lines. The energy resolution of the used HPGe detector is good enough to resolve that kind of complex spectra and it is possible to get a quantitative deposition estimation. The <sup>137</sup>Cs detection limit of 2 kBqm<sup>-2</sup> (with 15 seconds integration time) is low enough for purposes of operational emergency preparedness. The use of shorter integration time makes it possible to get better position accuracy to map sharply varying deposition, when the level of radioactivity is higher than a few kBqm<sup>-2</sup>. Of course the coverage and direction of the flight lines over the measured area have a great influence to the results. For small scale mapping near a nuclear power station and when the system is used to locate lost point sources, the accurate position of the activity is of special interest. In such a case the team can take advantage of the DGPS service provided by the Finnish Broadcasting company utilizing RDS-channel to get position accuracy within 2 meters. The correction signal is reachable nationwide on the FM transmitter network.

For the reasons mentioned above, the HPGe detector based systems are of primary value compared to NaI systems for rapid fresh fallout mapping and reconnaissance of radioactive cloud.



# Geological Survey of Finland Exercise Results and Experience

ABSTRACT .....	109
1. INTRODUCTION .....	110
2. THE AIRBORNE EQUIPMENT/SYSTEM OF GSF .....	111
2.1. Aircraft .....	111
2.2. Equipment .....	111
3. MEASUREMENT FLIGHT ON JUNE 9 <sup>TH</sup> , 1995 .....	112
4. DATA PROCESSING AND RESULTS .....	113
4.1. Area III, hidden sources .....	113
4.2. Area I, calibration at Vesivehmaa airfield .....	113
4.3. Area II, mapping of Cesium fallout .....	114
5. EXPERIENCES .....	114

Figures in Colour Appendix (C.A.):

Fig. 1. The Cs window kBq/m <sup>2</sup> and Co count rate maps showing the location of two hidden sources on Area III on June 9 <sup>th</sup> 1995 .....	C.A. plate 5
Fig. 2. Cs-137 map from Area II on 9 <sup>th</sup> of June 1995 .....	C.A. plate 6

**NEXT PAGE(S)  
left BLANK**

# **Exercise Results and Experience of GSF**

**J. Multala, H. Hautaniemi**  
Geological Survey of Finland

## **ABSTRACT**

Geological Survey of Finland carried out its airborne gamma ray measurement flight for RESUME95 exercise at the planning stage of the exercise; actually 9 weeks beforehand. Although some of the flight parameters (line spacing 100 metres and altitude 30 - 40 metres) differ from those used by the other teams during RESUME95, the results obtained by GSF are in line with the others. Mapping Cs-137 fallout at Area II gave mean value of 83.8 kBq/m<sup>2</sup> and maximum of 137 kBq/m<sup>2</sup>.

**GEOLOGICAL SURVEY OF FINLAND**  
Betonimiehenkuja 4  
FIN-02150 ESPOO  
Finland  
Tel. +358 0 46931  
Fax. +358 0 4693 2197

## 1. INTRODUCTION

For the Geological Survey of Finland (GSF) the main purpose to carry out airborne measurements is to complete the second national aerogeophysical mapping project. During the last 10 years several applications have been "developed" for airborne geophysics. One of those is mapping of man made fallout and hunting of lost sources based on gamma ray measurements using large NaI detector packages and spectrometers.

GSF took part in the RESUME95 exercise at its early planning stage. Measurement flight was done on 9th of June 1995, about 9 weeks before the actual exercise. The experience received from this flight was used for the final adjustment of the flight patterns, schedules, flight line spacing etc.

One important aspect of the exercise was to locate and to identify as many hidden sources as possible. It should be noticed that for this test flight of GSF there were only two radioactive sources hidden in Area III: one Cs-137 and one Co source. Therefore, the results by GSF from Area III are not comparable to the results by the other teams.

## **2. THE AIRBORNE EQUIPMENT/SYSTEM OF GSF**

### **2.1 Aircraft**

Twin engine DHC-6/300 Twin Otter (OH-KOG) owned by Karair Co. During the measurement flight in Finland the ground speed is about 50 m/s. This aircraft has been used since 1980. Twin Otter was selected for the measuring platform as the most suitable fixed wing aircraft for low level STOL (short takeoff and landing) operations.

The aircraft offers several major advantages in terms of utility and cost, including excellent performance reserves, low-speed handling characteristics and operational flexibility to operate from unpaved strips without any ground equipment. During the manufacturing of the Twin Otter several modifications were made to its electrical systems to reduce the electrical noise level.

### **2.2 Equipment**

The measurement units installed in the aircraft are connected to each other by local area network (LAN). This makes it easy to install just the right measurement units for each running project.

In 1995 the following equipment were used:

- \* Two Cesium magnetometers at wing tips and automatic compensating unit (Scintrex MAC-3 with CS-2 sensors and MEP-2111 processor module)
  - sensitivity 0.001 nT
  - registration rate normally 4 times/sec, max 10 samples/sec
  - transverse horizontal gradiometer, sensor distance 21.36 m,
  - expected FOM 1 nT
  
- \* Electromagnetic unit, Model GSF-80, vertical coplanar coil configuration, coil distance 21.36 m,
  - frequency 3113 Hz,
  - sensitivity 1 ppm,
  - average noise level: 7 ppm in quadrature component and 14 ppm in in-phase component,
  - measurement range +- 12 000 ppm,
  - registration 4 times/sec (12.5 meters),

- \* VLF-unit
  - measures 3 orthogonal magnetic components,
  - frequency range 10 - 25 kHz
  - registration twice/sec (25 m)
  
- \* Gamma-ray spectrometer modified McPhar,
  - 6 NaI crystals, total volume 25 litres,
  - registered energy range 0.2 - 3.0 MeV, 120 channels, each 24 keV,
  - registration once/sec (50 m),
  - 2 NaI upward looking crystals (total volume 8.3 litres) for monitoring background radiation.
  
- \* Navigation system
  - GPS system / Real time DGPS if differential signal is available (anyway DGPS correction is done after flight using own GPS base station)
  - visual navigation with maps,
  - radar altimeter (Collins),
  
- \* Others
  - barometer, thermometer, accelerometer, spherics monitor, etc.
  
- \* Recording
  - the measurement data is recorded to PC compatible cassette,
  - the flight path is recorded to normal VHS video (modified Panasonic 6200),
  - analog display for monitoring the geophysical instruments operation during the flights.
  
- \* Magnetic reference station and GPS receiver at the measurement area.
  - Geometrics G803, registration every fifth second,
  - Geometrics G811, registration normally every fifth second, max. once/sec, registration accuracy 0.01 nT
  - Ashtec Ranger GPS receiver.

### **3. MEASUREMENT FLIGHT ON JUNE 9TH, 1995**

As already mentioned, the flight was carried out about 9 weeks before the actual exercise RESUME95 in order to get more information to plan the final details of the exercise. Changes in soil moisture between 9th of June and 15th of August certainly have some influence on the results and makes detailed comparison of the measurement values more complicated.

Unlike all the other teams GSF flew Area II using 100 meters line spacing and 100 feet nominal altitude. For Area III every team decided themselves what kind of flight pattern to use. GSF used 100 meters flight line spacing and 100 feet nominal altitude. During the measurement flight the ground speed was kept as sharply as possible at 50 m/s. Areas I, II and III were covered with one flight. The complete flight took 2h 20m, Area II was covered in 1h 12m and Area III in 42 minutes.

## **4. DATA PROCESSING AND RESULTS**

### **4.1 Area III, hidden sources**

In the first hand the task was to find and to identify as many hidden sources as possible and even as quickly as possible. The spectra from Area III was viewed with the graphical program received from J. Hovgaard. At the first run the Cs-137 source was identified and located. The Co source could not be seen with this program due to large channel width used in GSF's spectrometer (24 keV).

At the second stage the man made gamma radiation was separated after the background correction. Cs and Co window count rates were calculated and after altitude correction the count rates were plotted with the differential corrected GPS-coordinates. The Cs and Co maps in Figure 1 clearly show the location of both the Cs and the Co sources.

### **4.2 Area I, calibration at Vesivehmaa airfield**

The previous calibration of GSF instruments was done in 1990. Although that calibration was based on several sites of different Cs activity the error was considerable large. In 1990 the flight path recovery was based on doppler system and fix points on videotape. Nowadays differential GPS system allows a positional accuracy better than 10 meters for every single measurement from aircraft.

Using the old calibration coefficients to the airborne data from the Vesivehmaa airfield a result of 47.4 kBq/m<sup>2</sup> was obtained. New sensitivity coefficient was calculated based on the value of 51.1 kBq/m<sup>2</sup> of Cs-137 presented by SURRC and STUK. The new sensitivity coefficient was found to be 28.7 counts/(kBq/m<sup>2</sup>).

### 4.3 Area II, mapping of Cesium fallout

After the background correction man made gamma radiation was separated from the measured spectral data from Area II. Cesium window count rates were calculated and altitude corrections were applied. Also traditional K, U and Th maps were processed using background, stripping, altitude and temperature corrections.

Processing the data from Area II with new sensitivity coefficients gave following statistics for Cs-137 activity: maximum 135 kBq/m<sup>2</sup>, mean 83.8 kBq/m<sup>2</sup>, standard deviation 20.95, variance = 439. Figure 2 shows the Cs-137 map.

At least NILU and SGU teams have reported their results from Area II based on their earlier calibrations. It is interesting to notice that their values are quite the same as our Cs-137 values that are calculated using old calibration constant (mean 73 kBq/m<sup>2</sup>, max 114 kBq/m<sup>2</sup>, std. dev. 17 kBq/m<sup>2</sup> and variance 289 kBq/m<sup>2</sup>).

## 5. EXPERIENCES

Exercises like RESUME95 give experiences at least in two respects. Teams taking part in the exercise learn much by comparing their results, programs and equipments with other teams and the distaff people have a great opportunity to learn how things could or should be done during the next exercise.

The Cs-map from Area III based on GSF's preflight gave valuable information about the remarkable variation of the Cs in the area. It might have been possible to hide some of the low activity Cs sources into areas of high Cs fallout and thus make the detection of them very difficult.

Before the exercise, the airborne teams sent information about the operation time of their aircraft (or helicopter) as well as how they would prefer to operate. It came evident that there were teams needing more than one flight in order to measure both areas II and III. On the other hand there were teams using the one and same helicopter so they required some time to install their equipments. These kind of facts caused certain problems in the RESUME95 flight schedules. It was really a challenge to work in the planning group.

One of those problems was the very limited budget for the exercise. That is why the number of distaff persons had to be minimized. Communication lines within the distaff as well as between distaff and team leaders is of high importance.

There were this time only ten teams doing airborne measurements. If the number of the teams will increase it will mean that the number of unexpected events, like troubles with instruments, installing the instruments etc will grow. In order to keep the exercise running as effectively as possible every team leader should be reached by phone during 24 hours.

The exercise was a success in many ways. It showed that an effective group of (airborne as well as ground borne) specialists from different countries can be called together very quickly. Although the instrumentation might vary considerably between the teams, the results are in line and can be calibrated. RESUME95 proved that airborne installations mainly used for geophysical and geological applications can be successfully used in fall-out mapping and in detecting point sources.

RESUME95 exercise was the first of this kind and everybody who was involved learned a lot. For those who did not take part in the exercise, these NKS publications are the best way to get familiar with the topic before the next exercise, which we hope, will be arranged within the next five years.

**NEXT PAGE(S)  
left BLANK**



# Finnish Centre for Radiation and Nuclear Safety

## In-Situ Measurements in Vesivehmaa Air Field

ABSTRACT .....	119
1. IN-SITU MEASUREMENTS .....	120
2. EQUIPMENT AND CALIBRATIONS .....	120
3. EVALUATION OF RESULTS .....	120
Tab. 1. <sup>137</sup> Cs activity assuming plane, uniform and real source distribution .....	122
Tab. 2. <sup>134</sup> Cs activity assuming plane, uniform and real source distribution .....	123
Tab. 3. Activity concentrations of natural radionuclides .....	124
Tab. 4. Derived external gamma dose rates and measurements performed with a pressurized ionization chamber .....	125
4. DISCUSSION .....	126
REFERENCES .....	126

**NEXT PAGE(S)  
left BLANK**

*In-Situ* Measurements in Vesivehmaa  
Air Field  
-STUK team

**M. Markkanen, T. Honkamaa, P. Niskala**

Finnish Centre for Radiation and Nuclear Safety  
P. O. Box 14  
FIN-00881, Helsinki  
Finland

**Abstract**

Nineteen *in-situ* gamma-ray spectrometric measurements were performed in Vesivehmaa air field on 17th August 1995. The results for  $^{137}\text{Cs}$  and natural radionuclides are in good agreement with the results from soil sampling and laboratory analyses.

## 1. *IN SITU* MEASUREMENTS

The *in-situ* measurements were performed in Vesivehmaa air field on 17th August. Total number of measurements was seventeen on the marked points. The team carried out no measurements on area II.

## 2. EQUIPMENT AND CALIBRATIONS

The team used a 18% HPGe detector with an Ortec Nomad gamma-ray spectroscopy unit. The HPGe detector was calibrated using point sources  $^{241}\text{Am}$ ,  $^{133}\text{Ba}$ ,  $^{137}\text{Cs}$  and  $^{60}\text{Co}$  and the well-known theory by Beck et al. (1972). Calibration factors were calculated for plane distribution ( $^{137}\text{Cs}$  and  $^{134}\text{Cs}$ ), uniform distribution (natural radionuclides and  $^{137}\text{Cs}$ ) and exponential distribution ( $^{137}\text{Cs}$ ). The measurements were carried out on a tripod at the height of 90 cm. For real fallout an  $\alpha/\rho$  value of  $0.66 \text{ cm}^2 \text{ g}^{-1}$  was used (Sanderson et al, 1996). The calibration factors are given in Tables I-III.

Dose-rate measurements were accomplished using RS-111 pressurized ionization chamber (PIC). The calibration of PIC is guaranteed by the manufacturer, and it was checked by STUK using a  $^{137}\text{Cs}$  source.

## 3. EVALUATION OF RESULTS

Each *in-situ* gamma measurement lasted at least 300 seconds. The statistical accuracies of peak areas were 3.1 - 3.3 % for 661.6 keV peak, 4.9 - 9.4 % for 604.8 keV peak, 4.9 - 7.2 % for 1461 keV peak and 10-21 % for 352 and 911 keV peaks. Calibration factors include a systematic uncertainty of 10%.

The derived  $^{137}\text{Cs}$  and  $^{134}\text{Cs}$  activities based on the *in-situ* gamma measurements are presented in Tables I and II, respectively. In the postulated case of a uniform source, the results are given in becquerels per wet weight. Soil sample results were not available at all the points, so the corresponding results cannot be given. The derived activity concentrations of natural radionuclides are given in Table III.

The external gamma dose rate was derived in each point based on the activity concentrations in soil. The following conversion coefficients were used:

Uranium:	0.431 nGy h <sup>-1</sup> per Bq kg <sup>-1</sup>
Thorium:	0.668 nGy h <sup>-1</sup> per Bq kg <sup>-1</sup>
Potassium:	0.0423 nGy h <sup>-1</sup> per Bq kg <sup>-1</sup>
Cesium-137:	0.00147 nGy h <sup>-1</sup> per Bq m <sup>-2</sup> (for a soil distribution with $\alpha/\rho = 0.6 \text{ cm}^2/\text{g}$ )

The derived gamma dose rates are given in Table IV with the measured results of a pressurized ionization chamber. An average response 32 nGy h<sup>-1</sup> of the ionization chamber to cosmic radiation has been subtracted from the results.

**Table I.** <sup>137</sup>Cs activity assuming plane, uniform and real source distribution.

<sup>137</sup> Cs		Source distribution			
		Soil samples	Real $\alpha/\rho = 0.7$ cm <sup>2</sup>	Plane $\alpha/\rho = \infty$	Uniform $\alpha/\rho = 0$
Calibration factor			0.0161 cpm per Bq/m <sup>2</sup>	0.0228 cpm per Bq/m <sup>2</sup>	1.06 cpm per Bq/kg
Circle	Point	Bq/m <sup>2</sup>	Bq/m <sup>2</sup>	Bq/m <sup>2</sup>	Bq/kg
0	0	52100	61500	44900	930
1	1	48000	60900	44400	920
1	2	43200	61600	45000	930
1	3	58900	60600	44300	920
1	4	48900	63600	46400	960
1	5	50900	65700	48000	1000
1	6	59100	63100	46100	960
2	1	34700	61700	45100	940
2	2	46200	65200	47600	990
2	3	59200	61400	44800	930
2	4	45900	58200	42500	880
2	5	47300	56100	40900	850
2	6	49200	61500	44900	930
3	2	41700	62800	45800	950
3	4	53600	65500	47800	990
3	6	59500	65900	48100	1000
4	1	57900	74500	54400	1130
4	3	40700	68400	49900	1040
4	5	96000	71800	52400	1090
Average		52300	63700	46500	965

Table II.  $^{134}\text{Cs}$  activity assuming plane, uniform and real source distribution.

$^{134}\text{Cs}$		Source distribution			
		Soil samples	Real $\alpha/\rho = 0.7$ $\text{cm}^2$	Plane $\alpha/\rho = \infty$	Uniform $\alpha/\rho = 0$
Calibration factor			0.0200 cpm per $\text{Bq/m}^2$	0.0286 cpm per $\text{Bq/m}^2$	1.28 cpm per $\text{Bq/kg}$
Circle	Point	$\text{Bq/m}^2$	$\text{Bq/m}^2$	$\text{Bq/m}^2$	$\text{Bq/kg}$
0	0	2140	2000	1430	31
1	1	1680	1940	1380	30
1	2		2090	1490	33
1	3	2030	2020	1440	32
1	4		1930	1380	30
1	5	2170	2180	1560	34
1	6		1980	1410	31
2	1	2120	1680	1200	26
2	2		1980	1410	31
2	3	1910	1870	1340	29
2	4		1960	1400	31
2	5	1600	1820	1300	28
2	6	1430	2000	1430	31
3	2		1870	1340	29
3	4		2100	1500	33
3	6		2010	1440	31
4	1	1990	2200	1570	34
4	3	1360	1990	1420	31
5	5	3260	1990	1420	31
Average		1880	2000	1770	39

Table III. Activity concentrations of natural radionuclides.

Homogenous source		Uranium ( $^{238}\text{U}$ )		Thorium ( $^{232}\text{Th}$ )		Potassium ( $^{40}\text{K}$ )	
Peak energy		352 keV ( $^{214}\text{Pb}$ )		911 keV ( $^{228}\text{Ac}$ )		1462 keV	
<i>In-situ</i> calibration factor		0.64 cpm per Bq/kg		0.28 cpm per Bq/kg		0.094 cpm per Bq/kg	
		<i>In-situ</i>	Soil samples	<i>In-situ</i>	Soil samples	<i>In-situ</i>	Soil samples
Circle	Point	Bq/kg	Bq/kg	Bq/kg	Bq/kg	Bq/kg	Bq/kg
0	0	33	39	25	32	750	643
1	1	39	39	33	32	580	523
1	2	29		44		730	583
1	3	37	64	32	40	620	575
1	4	36		24		700	623
1	5	39	38	31	32	620	478
1	6	27		33		690	608
2	1	30	41		37	620	580
2	2	35		32		570	648
2	3	29	49	31	35	690	637
2	4	32		32		660	726
2	5	34	39	29	28	530	481
2	6	33	41	25	36	750	692
3	2	32		36		680	725
3	4	28		27		650	667
3	6					680	774
4	1	37	41	33	30	830	724
4	3	43	46	29	31	670	652
4	5	30	38	36	35	640	521
Average		32	43	30	32	670	624

**Table IV.** Derived external gamma dose rates and measurements performed with a pressurized ionization chamber.

		Derived from <i>in-situ</i> results	Derived from soil sample results	Measured dose rate <sup>1</sup>
Circle	Point	nGy h <sup>-1</sup>	nGy h <sup>-1</sup>	nGy h <sup>-1</sup>
0	0	153	158	144
1	1	154	141	146
1	2	163		146
1	3	153	168	146
1	4	156		145
1	5	160	142	143
1	6	153		142
2	1		124	146
2	2	156		151
2	3	151	161	141
2	4	149		138
2	5	139	130	140
2	6	153	147	152
3	2	156		144
3	4	152		146
3	6			155
4	1	183	156	161
4	3	167	132	157
5	5	170		156
Average		157	145	147

<sup>1</sup> Estimated dose rate due to cosmic radiation, 32 nGy h<sup>-1</sup> has been subtracted from all results.

#### 4. DISCUSSION

All the *in-situ* results are reasonably close to the values obtained from soil sampling (Sanderson et al, 1996). The discrepancies are tolerable compared to the possible errors that might exist e.g, in sampling.

#### REFERENCES:

**Beck HL, DeCampo J, Gogolak C.** *In-situ* Ge(Li) and NaI(Tl) Gamma-Ray Spectrometry. US Atomic Energy Commission, New York, Report HASL-258, 1972.

**Sanderson CDW, Allyson JD, Toivonen H, Honkamaa T.** Gamma-Ray Spectrometry Results from Core Samples Collected for Resume95, *ibid*.



# Finnish Centre for Radiation and Nuclear Safety/ Helsinki University of Technology

## Airborne Fallout Mapping of <sup>137</sup>Cs

ABSTRACT .....	129
1. INTRODUCTION.....	130
2. CALIBRATION .....	130
3. FLIGHT LINES .....	131
Fig. 1. Fligth lines on the area II.....	131
4. RESULTS .....	132
5. DISCUSSION .....	132
REFERENCES.....	132

Figures in Colour Appendix (C.A.):

Fig. 2. Fallout map of area II measured with NaI on 16<sup>th</sup> August 1996 ..... C.A. plate 7

**NEXT PAGE(S)  
left BLANK**

# Airborne Fallout Mapping of $^{137}\text{Cs}$ -STUK/HUT Team

**M Nikkinen<sup>1,2</sup>, P. Aarnio<sup>2</sup>, T. Honkamaa<sup>1</sup>, H. Tiilikainen<sup>1</sup>**

1 Finnish Centre for Radiation and Nuclear Safety

P. O. Box 14  
FIN-00881, Helsinki  
Finland

2 Helsinki University of Technology

FIN-02150, Espoo  
Finland

## **Abstract**

The task of the team was to create a fallout map of  $^{137}\text{Cs}$  on a specified area in Padasjoki Auttoinen village. The team used AB-420 helicopter of the Finnish Frontier Guard. The team had two measuring systems: HPGe system (relative efficiency 18%) and NaI system (5"x5"). Both systems produced similar maps. The average  $^{137}\text{Cs}$  fallout within the area (lakes and ponds included) was  $88 \text{ kBq m}^{-2}$ ; the maximum value being  $161 \text{ kBq m}^{-2}$ . In an emergency the HPGe is superior to NaI because of its better energy resolution, giving possibility to obtain nuclide-specific results.

## 1 INTRODUCTION

The Finnish Centre for Radiation and Nuclear Safety, STUK has no operational airborne equipment. However, for the purposes of RESUME95, STUK and HUT (Helsinki University of Technology) together compiled a system mainly from existing laboratory instruments that were tested for the first time a week before the exercise. Two types of detectors were used (HPGe and NaI). The hardware is described by Nikkinen et. al (1996). The first flight was performed at Malmi airfield in Helsinki (HPGe only). The Finnish Frontier Guard provided the helicopter (Agusta Bell 420) for the exercise.

## 2 CALIBRATION

The calibrations were carried out at the Vesivehmaa airfield over the origo selected by the organizers. Altitudes of 100, 200 and 300 feet were used. Only the NaI detector collected the data. The calibration of the HPGe detector was calculated by comparing the average count rates at area II to the NaI calibration spectra.

The continuum, and the  $^{134}\text{Cs}$  and  $^{214}\text{Bi}$  peaks at 604 and 609 keV, were subtracted from the  $^{137}\text{Cs}$  peak area. The continuum was estimated from the long term signal to noise ratio for the  $^{137}\text{Cs}$  peak. The same procedure was applied both to calibration and fallout measurement spectra.

The soil sample taken from the area II and airfield show that caesium has penetrated deeper in area II. The values of  $^{137}\text{Cs}$  distribution coefficients were  $\alpha/\rho = 0.77 \text{ cm}^2/\text{g}$  in the airfield and  $\alpha/\rho = 0.44 \text{ cm}^2/\text{g}$  in area II (Sanderson et al. 1996). This would indicate 12% higher soil attenuation at the flying altitude over the area II than over the airfield for 661.6 keV primary gamma flux. This effect was included in the calibration.

The resulting calibration coefficients for area II at 200 feet altitude, to convert the count rate at the  $^{137}\text{Cs}$  peak to fallout, were  $1.23 \text{ kBq m}^{-2} \text{ cps}^{-1}$  for the NaI spectra and  $34.4 \text{ kBq m}^{-2} \text{ cps}^{-1}$  for the HPGe spectra.

The altitude was not recorded during the fallout mapping. Thus, the nominal altitude of 200 feet was assumed for the whole area.

### 3 FLIGHT LINES

The pilots used only visual navigation. No extra navigation devices were used. Flight lines covered the area II quite well, because there were many landmarks to help the navigation. The actual flight lines are shown in the Figure 1.

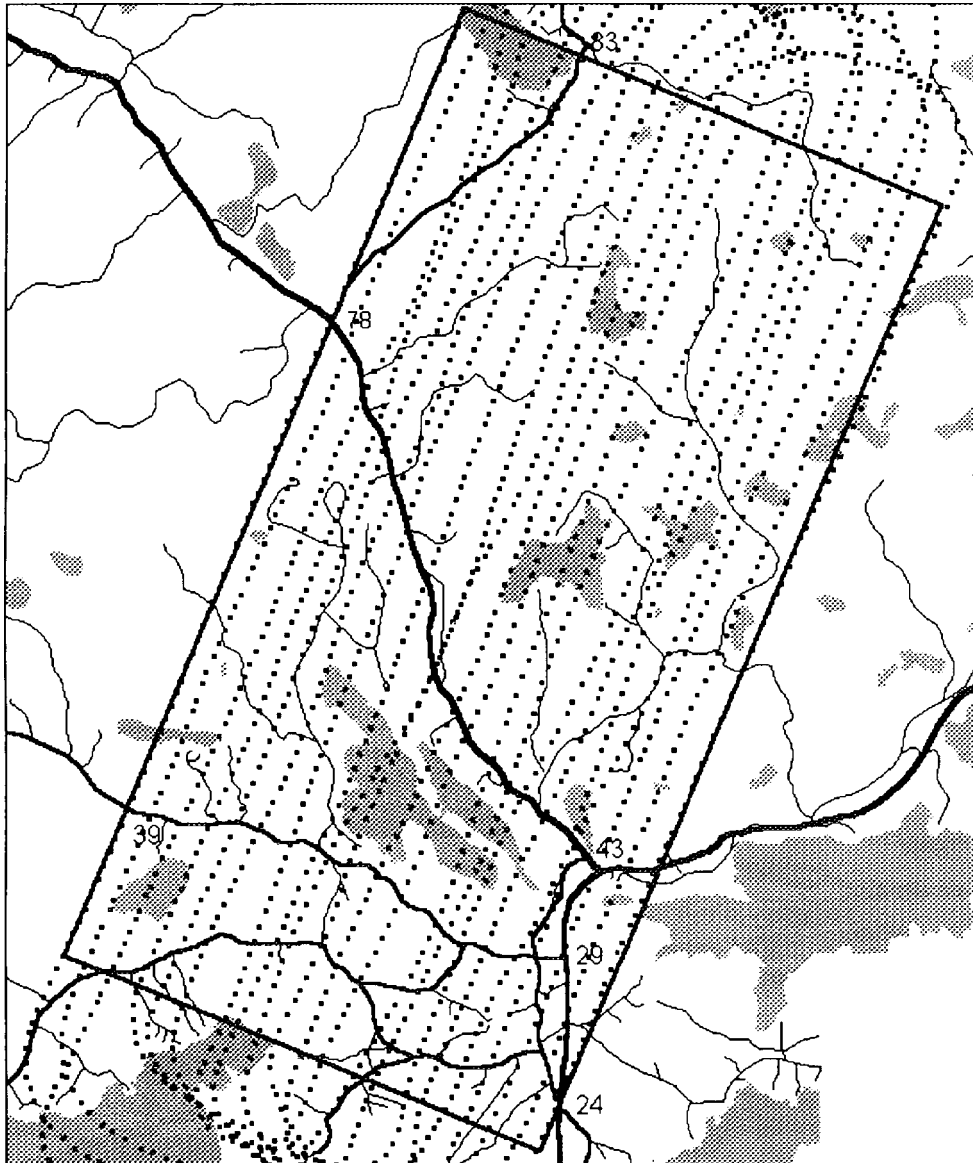


**Figure 1.** *Flight lines on the area II.*

## 4 RESULTS

The fallout map based on the NaI spectra is shown in the Figure 2. A similar map was produced with the HPGe detector. The highest fallout values exceeded  $160 \text{ kBq m}^{-2}$ , shown by both measuring systems. The data shown in Figure 2 are smoothed, decreasing slightly the highest values. The average fallout within the area, when also the lakes and ponds are included, was  $88 \text{ kBq m}^{-2}$  ( $N=1397$ ,  $SD=26 \text{ kBq m}^{-2}$ ).

## 5 DISCUSSION

The measuring systems NaI and HPGe produced similar fallout maps. However, nuclide identification and quantitative deposition estimation are extremely difficult for NaI spectrometers in fresh fallout that may contain tens of fission products with several hundred gamma lines. Thus, for operational emergency preparedness, HPGe detectors are of primary value. NaI systems can be used to fallout mapping after 10-30 days when the short-lived nuclides have decayed off.

## REFERENCES

**Nikkinen M, Aarnio P, Honkamaa T, Tiilikainen H.** Detecting Hidden Sources-STUK/HUT Team. *Ibid.*

**Sanderson CDW, Allyson JD, Toivonen H, Honkamaa T.** Gamma-Ray Spectrometry Results from Core Samples Collected for Resume95, *ibid.*



# Finnish Centre for Radiation and Nuclear Safety/ Helsinki University of Technology Carborne Fallout Mapping

ABSTRACT .....	135
1. EQUIPMENT .....	136
2. MEASUREMENTS ON AREA II AND ON ROAD FROM AREA II TO AREA III .....	136
Tab. 1. The measuring systems in the emergency vehicle .....	137
Tab. 2. Measurements on area II and on area III.....	138
3. RESULTS OF THE <sup>137</sup> Cs FALLOUT AND DOSERATE MEASUREMENTS .....	138
Fig. 2. HPGe measurements performed on different days .....	139
Fig. 3. Count rates in the <sup>137</sup> Cs window versus dose rate on road 1.....	139
Fig. 4. Estimated <sup>137</sup> Cs fallout along the road 1 measured from the helicopter and from the car .....	140
4. SEARCHING AND LOCATING THE HIDDEN SOURCES .....	141
Fig. 5. Finding the <sup>192</sup> Ir source .....	141
5. DISCUSSION .....	142
REFERENCE .....	142

Figures in Colour Appendix (C.A.):

Fig. 1. (a) Fallout map measured using HPGe. (b) Dose rate measured using PIC..... C.A. plate 8

# Carborne Fallout Mapping -STUK/HUT Team

T. Honkamaa<sup>1</sup>, P. Aarnio<sup>2</sup>, M. Nikkinen<sup>1,2</sup>, H. Tiilikainen<sup>1</sup>

1 Finnish Centre for Radiation and Nuclear Safety  
P. O. Box 14  
FIN-00881, Helsinki  
Finland

2 Helsinki University of Technology  
FIN-02150, Espoo  
Finland

## ABSTRACT:

During the summer 1995 altogether 8,625 spectrometric and 3,108 dose-rate measurements were performed in Padasjoki Auttoinen village using carborne measuring devices. As a result <sup>137</sup>Cs fallout and dose-rate maps were produced. The highest measured values in the test area II were 160 kBq m<sup>-2</sup> for fallout and 0.22 μSv h<sup>-1</sup> for dose-rate. One hot spot was found beside the test area (dose rate 0.31 μSv h<sup>-1</sup>). On the cultivated areas the measured count rates in <sup>137</sup>Cs-window are three to four times lower than in the forest areas in average, indicating an altered depth profile of caesium.

# 1 EQUIPMENT

The team used STUK's emergency vehicle (VW Transporter van), which is modified to a moving laboratory. Radiation surveys can be carried out in the field using the measuring systems in the vehicle and the measuring data can be sent in real time to headquarters via mobile phones (Honkamaa et al., 1996). The car was equipped with three different measuring systems (Table I).

## 2 MEASUREMENTS ON AREA II AND ON ROAD FROM AREA II TO AREA III

The purpose of the measurements was:

- a) to create fallout and dose-rate maps on area II and on five specified roads.
- b) to locate and identify a hidden source beside the road from area II to area III. This exercise took place on 15th August.

The measurements were performed during three days: on 20th June (dose-rate measurements and HPGe-spectroscopy), on 13th August (dose-rate measurements and HPGe-spectroscopy) and on 15th August (HPGe spectroscopy and NaI spectroscopy). Most roads on area II were driven. Description about performed measurements is in the Table II. Altogether 8,625 spectra were acquired and over 3108 dose-rate measurements were performed.

Three kinds of technical problems occurred during the surveys:

- 1) A data collection PC failed due to hardware problems. The hot weather during the exercise made the computers to overheat. This caused a short break in measurements, typically a few minutes.
- 2) The HPGe-system was not stable. The energy calibration drifted many keV at the peak of 661.6 keV, which made postprocessing of the data more labourious. A serious disruption occurred, when FWHM of the peaks suddenly increased several hundreds of percents. Fortunately, the detector recovered in a few minutes and the survey could be continued.
- 3) The DGPS navigation system did not work due to weak signal or software failure. If the DGPS data was not available less accurate raw GPS data were used. During some short periods both GPS signals were lost and the measuring point was estimated by interpolation.

*Table I. The measuring systems in the emergency vehicle*

	HPGe-spectroscopy system	NaI-spectroscopy system	Dose-rate measuring system
Detector	Ortec <sup>1</sup> POP-TOP, relative efficiency 36.9 %	NaI-detector <sup>2</sup> 5x5"	RS-111 <sup>3</sup> Pressurized ionisation chamber
HV-supply, amplifier & MCA unit	Ortec Nomad 92X	Ortec Nomad 92XP	-
Calibration	Point source calibration for <sup>137</sup> Cs, measurements against known fallout	None. (Comparison with the HPGe)	Guaranteed by the manufacturer, checked by STUK using a <sup>137</sup> Cs point source
Data collection PC	Compaq <sup>4</sup> Elite 4/40	Compaq Elite 4/75	Compaq Contura 4/25
GPS-integration	Trimble <sup>5</sup> PCMCIA-card in the computer	-	External DGPS TRIMBLE unit connected to the computer
Software	SAMPO 90+ <sup>6</sup>	SAMPO 90+	SAKU <sup>7</sup>

<sup>1</sup>EG&G Ortec, Oak Ridge, USA

<sup>2</sup>Teledyne Brown Engineering, USA

<sup>3</sup>Reuter-Stokes, USA

<sup>4</sup>Compaq Computers Corporation

<sup>5</sup>Trimble Navigations, Sunnyvale, USA

<sup>6</sup>Logion OY, Helsinki, Finland

<sup>7</sup>STUK, Helsinki, Finland

*Table II. Measurements on area II and on area III.*

Date	HPGe	NaI	PIC
20th June	928 spectra, collection time 12 s	-	10-15 s intervals 2,883 readings
13th August	888 spectra, collection time 2.7 s	-	10-15 s intervals 225 readings
15th August	2,299 spectra, collection time 4 s	4,510 spectra, collection time 2 s	-

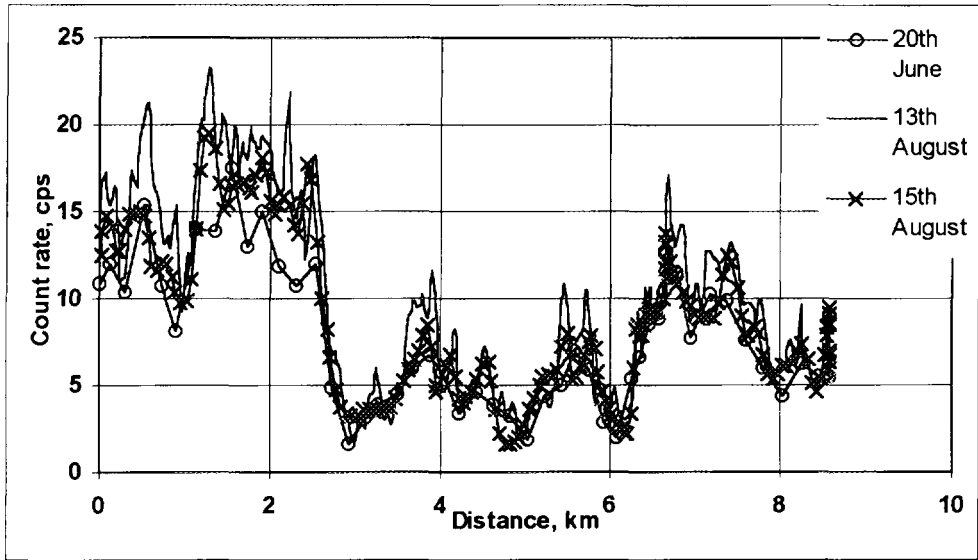
After the survey, the analyses of the vast number of spectra were quite labourious. It transpired that DOS and Windows operating systems are not created to manage datasets of this size.

### 3 RESULTS OF THE <sup>137</sup>CS FALLOUT AND DOSE-RATE MEASUREMENTS

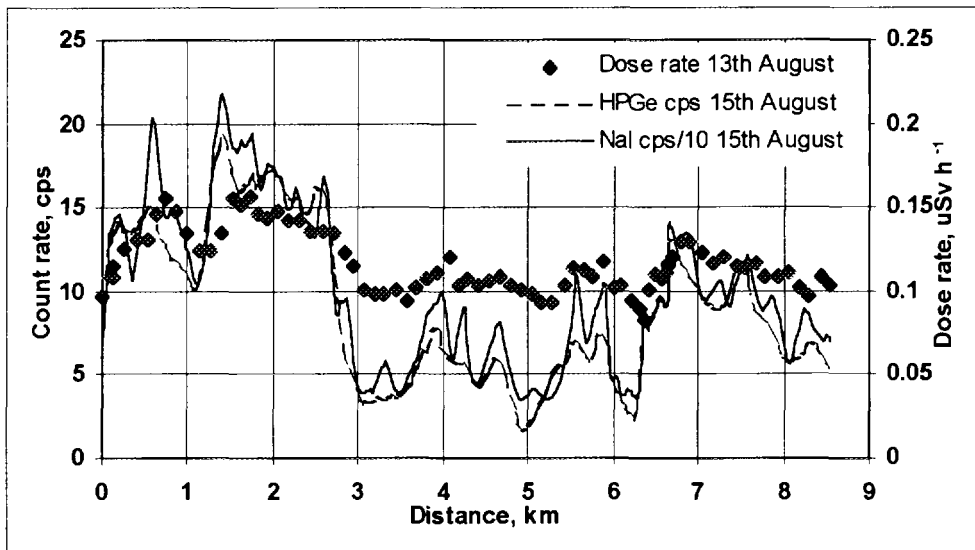
The fallout and dose-rate maps are colour-coded in Figures 1a and 1b. For fallout,  $\alpha/\rho$  value of 0.44 cm<sup>2</sup>/g was used. The body of the car attenuates the gamma-rays coming from horizontal direction much less than those coming through the vehicle floor, i.e. the fallout measurement is performed in anticollimated geometry. Converting the measured surface activities to equivalent surface deposition is not possible without knowing the actual depth distribution. If a value of  $\infty$  is used for  $\alpha/\rho$  the results should be multiplied by 0.45. On the cultivated areas caesium has penetrated deeper and the calculated values are too low. Those areas can clearly be distinguished from the maps.

Figure 2 reveals the bias between HPGe measurements performed on different days. The reasons for the bias between the measurements are changes in soil and air moisture, air temperature and attenuation around the detector. The contamination of the vehicle cannot be the reason, since the baseline of the count rates is the same. The results are equal if the count rates measured in 20th June are multiplied by 1.29 and count rates measured in 15th August are multiplied by 1.14. Figure 3 compares the dynamics of different measuring devices.

The count-rate and dose-rate profiles along the specified roads show variation typical of this area and they are not presented here. In Figure 4 the measurements from the helicopter over the road 1 and from the car are compared.



**Figure 2.** HPGe measurements performed on different days. The distance is measured from a point (43) defined by the organizers along the major road from area II to area III. The data is smoothed. Areas with low count rates are cultivated.



**Figure 3.** Count rates in the  $^{137}\text{Cs}$  window (36.9% HPGe, 5x5" NaI) versus dose rate on the road 1. For definition of distance, see Figure 2. The spectrometric data is smoothed. The spectrometers and the PIC show the same kind of behaviour, but the dynamics of the spectrometric measurements are much larger.

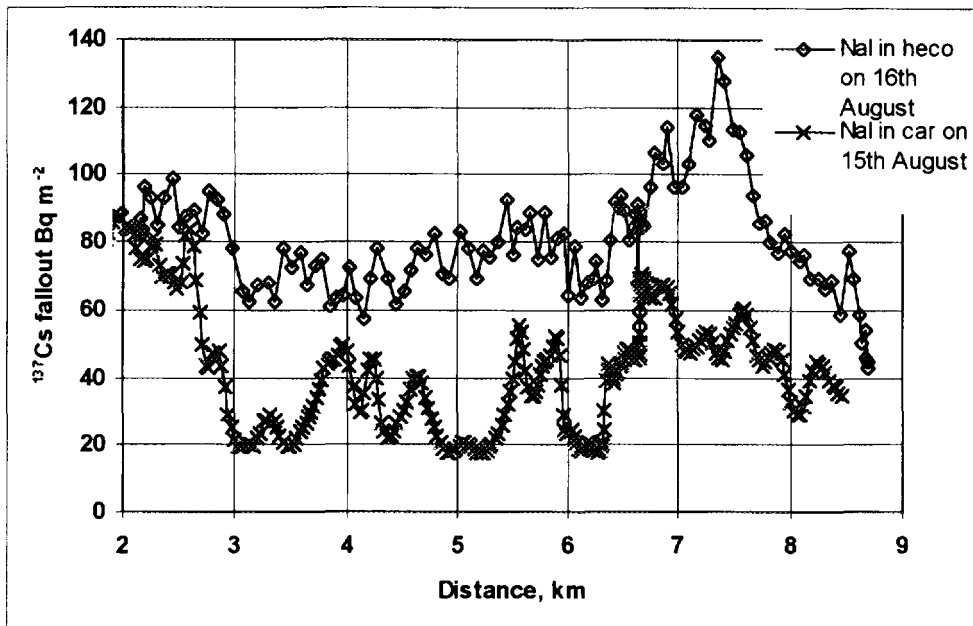


**Figure 4.** Estimated  $^{137}\text{Cs}$  fallout along the road 1 measured from the helicopter and from the car. For definition of distance, see Figure 2. The detector in the helicopter sees a much wider area than the detector in the car and the fallout estimate is more even. The peak in the measurements between 7 and 8 km is due to the  $^{192}\text{Ir}$  source.

## 4. SEARCHING AND LOCATING THE HIDDEN SOURCES

On 15th August the road from area II to area III was driven twice, first at the speed of 50 km h<sup>-1</sup> and then at the speed of 30 km h<sup>-1</sup>. The count-rate profiles along the road at the energy range below 615 keV are shown in Figure 5. At the marked point unusual radiation at lower energies was observed. The observation was visually clear from the spectra and it was immediately reported to the leader of the exercise. Later analysis revealed that the source was covered because no primary gamma lines were found. Thus, the source couldn't be identified. <sup>137</sup>Cs was suggested by the crew, because the scattered radiation was below 661 keV. Actually, the source was a 15 Ci <sup>192</sup>Ir source about 350 m from the road. The detected radiation was mainly sky-shine.

The second hidden source beside the road was 0.6 mCi <sup>60</sup>Co, but it was too far from the road (about 30 - 40 m) to be seen with the detectors. The activity of the source was approximately one decade below the detection limit.

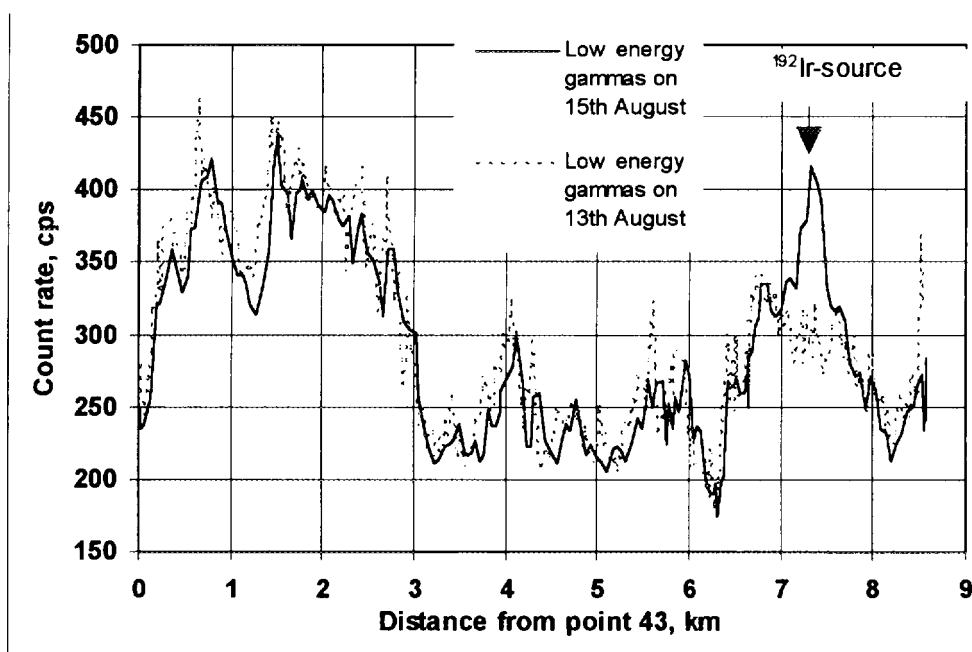


**Figure 5.** Finding the <sup>192</sup>Ir source. Strong increase in the count-rate at lower energies were observed at the marked point. The measurements were performed with the HPGe detector. The increase was detected immediately on the real-time display of the acquisition program.

## 5. DISCUSSION

The following conclusions can be drawn:

(1) The fallout in the test area has a complex structure. The maximum fallout and dose rate on area II are  $127 \text{ kBq m}^{-2}$  and  $0.22 \text{ } \mu\text{Sv h}^{-1}$ , respectively. The average fallout in the area II, calculated from 539 observations, is  $48 \text{ kBq m}^{-2}$  ( $\text{SD}=21 \text{ kBq m}^{-2}$ ). The fallout is calculated using  $\alpha/\rho$  value of  $0.44 \text{ cm}^2/\text{g}$ . One hot spot was found just outside the area II (dose rate  $0.31 \text{ } \mu\text{Sv h}^{-1}$ ).

(2) The count rate in 661.6 keV energy window varies. In the cultivated areas the count rate is four times lower than in badly contaminated forest areas along the same road. Also, the road type affects the count rate; on the small forest roads the count rate is higher.

(3) The system installed in the STUK emergency vehicle is suitable for searching point sources as well as monitoring fallout and dose rate in the environment. The use of sophisticated software (rapid time cycle) makes it possible to detect small local changes and point sources. However, the postprocessing of the data is labourious if the number of collected spectra is high. Therefore, very short time cycles should be avoided.

(4) Some hardware components in our system did not work properly. The Notebook PC (Compaq Elite) caused most of the problems. A more suitable computer would be a rugged industrial PC (installed in autumn 1995!). Also the HPGe detector is not specially designed for a moving laboratory, and that may be a reason for unreliability.

(5) Performing accurate reproducible *in-situ* measurements inside a car is not very easy. The attenuation around the detector is complex and varying. The system is prone to changes in air density and soil moisture.

(6) Software worked fine during the surveys. The online display shown by SAMPO 90+ was good for NaI spectra, but for HPGe spectra it could be improved. The exercise gave valuable information for the work in future.

### REFERENCE:

**Honkamaa T, Toivonen H, Nikkinen M.** Monitoring of Airborne Contamination Using Mobile Equipment. STUK A-130. Helsinki: Finnish Centre for Radiation and Nuclear Safety, 1996.



# Finnish Centre for Radiation and Nuclear Safety/ Helsinki University of Technology Detecting Hidden Sources

ABSTRACT .....	145
1. STUK/HUT AIRBORNE MEASUREMENTS .....	146
Tab. 1. Measuring equipment .....	146
2. RESULTS .....	147
2.1. Analysis during flight, report immediately after landing .....	147
2.2. Analysis report 24h after landing .....	147
2.3. Sources found after the announcement of their positions .....	147
2.4. Radiation sources not seen .....	148
3. SUGGESTION FOR IMPROVEMENT .....	148
Measuring equipment .....	148
Navigation .....	149
Software .....	149
4. REFERENCE .....	149
Fig. 2. Fligh lines at area III.....	150

Figures in Colour Appendix (C.A.):

Fig. 1. Maps of area III .....	C.A. plate 9
--------------------------------	--------------

**NEXT PAGE(S)**  
**left BLANK**

# Detecting Hidden Sources-STUK/HUT Team

**M Nikkinen<sup>1,2</sup>, P. Aarnio<sup>2</sup>, T. Honkamaa<sup>1</sup>, H. Tiilikainen<sup>1</sup>**

1) Finnish Centre for Radiation and Nuclear Safety

P. O. Box 14  
FIN-00881, Helsinki  
Finland

2) Helsinki University of Technology

FIN-02150, Espoo  
Finland

## **Abstract**

The task of the team was to locate and to identify hidden sources in a specified area in Padasjoki Auttoinen village. The team used AB-420 helicopter of the Finnish Frontier Guard. The team had two measuring systems: HPGe system (relative efficiency 18%) and 5"x5" NaI system. The team found two sources in real-time and additional two sources after 24 h analysis time. After the locations and characteristics of the sources were announced it was found out that altogether six sources would have been possible to find using the measured data. The total number of sources was ten. The NaI detector was good at detecting and locating the sources and HPGe was most useful in identification and calculation of the activity estimates. The following development should be made: (1) larger detectors are needed. (2) the software has to be improved. (this has been performed after the exercise) and (3) the navigation must be based on DGPS. Visual navigation causes easily gaps between the flight lines and some sources may not be detected.

# 1 STUK/HUT AIRBORNE MEASUREMENTS

The measurements were performed on 16th August 1995. They were carried out using two separate systems: 5"x5" NaI scintillation crystal and 18 % HPGe detector. Both systems were using Ortec Nomad portable MCA's and Compaq LTE Elite computers. Both systems were mounted on the same chassis. External power feed (28V DC from the helicopter) was essential because the computers were able to run only 2 hours with internal battery. The battery of Nomad lasts 4 to 8 hours.

The measuring software was SAMPO 90, version 3.5. Some online analysis during the flight was carried out. Integration time of 4 s was used for HPGe spectra and 2 s for NaI spectra. SAMPO can measure spectra with a minimum integration time down to 0.6 s using this hardware (0.3 s, if there are less than some 500-1000 spectrum files stored (MS-DOS limitation)). The 2 and 4 second integration times were chosen to decrease the amount of data.

Technically, everything worked during the flight. Because AC power was not used and the measuring day was relatively cool compared to other days during the exercise, also Compaq computers worked fine. The  $^{137}\text{Cs}$  peak of the HPGe system floated about 1 keV during the measurement, even with stabilizer enabled.

The activity calculations are based on using an efficiency calibration measured through the helicopter floor using calibration sources. Efficiency calibration was further corrected for the attenuation in air.

**Table I.** *Measuring equipment:*

Type of detector	HPGe (18%)	NaI (5"x 5")
Sampling time	4s	2s
Navigation	Visual	
Recording of coordinates:	DGPS	
Flight line spacing	100 m	
Flight altitude	60 m	
Speed	60 knots	
Analysis software	SAMPO 90 + real time toolkit	
Mapping software	MapInfo	

## 2 RESULTS

In the following text the sources are referred using source codes given in Lahtinen et al. (1996).

### 2.1 Analysis during flight, report immediately after landing

\* Ir (15,000 mCi) was clearly visible on the real-time display of both HPGe and NaI systems. The source remained unidentified with no specific gammapeak energy estimates. The source was declared as a strong low-energy emitter.

\* Cs1 (77 mCi) was clearly visible on the real-time display of both HPGe and NaI systems. The source was identified as  $^{137}\text{Cs}$ .

### 2.2 Analysis reports 24h after landing

\* Ir (15,000 mCi) was reported as unidentified, strong low-energy radiation source. There were no primary energy lines available. Strong scattering spectrum was seen below 400 keV. Shielded source was suspected (both NaI and HPGe).

\* Cs1 (77 mCi) was identified as  $^{137}\text{Cs}$ , with activity of 50 mCi. The reported position was a little shifted because the source was seen on many flight lines. (both NaI and HPGe)

\* Cs4 (15 mCi) was identified as  $^{137}\text{Cs}$ , with activity of 20 mCi. The position is exactly correct. (both NaI and HPGe)

\* Co1 (7 mCi) was identified as  $^{60}\text{Co}$ , with activity of 8 mCi. The position was shifted because several spectra were summed to get more statistics and accidentally an incorrect spectrum was interpreted to be in the centre of gravity of the spectra. Our offline software was not able to interpolate the position when the DGPS had been blank for a while and this caused further error (interpolation is now possible).

### 2.3 Sources found after the announcement of their positions

Every source except the collimated Cs2 and Co3 sources showed some traces in the data. However, only the following sources could have been detected using our data:

\* Co4 (line of the 1-2 mCi sources) can be seen on the summed NaI spectra.

\* Co2 (9 mCi, collimated) can be seen on the summed NaI spectra; this data is very close to the detection limit.

After the source announcement six of the sources were seen on spectra. See Figure 1 for a smoothed picture of some of the sources. The two extra sources were found on summed NaI spectra. Some traces were found also on HPGe spectra, but they were definitely below the detection limit.

NaI spectra gave poor real-time analysis results. That was due to the large variation of the gain during the measurement which made our preset analysis parameters useless.

## 2.4 Radiation sources not seen

\* Cs2 (50 mCi, actually 32-40 mCi) was a collimated source and it was not seen, because it was too far (50 m) from the flying line. The radius of the primary gamma flux of the collimated 50 mCi <sup>137</sup>Cs source is approximately 10 m at 60 m altitude. Some luck is needed to hit the primary radiation cone with 100 m flying line separation.

\* Cs3 (7.5 mCi) was located near a cobalt source (Co1). Some traces can be seen, but they must be considered as normal variations of the caesium fallout.

\* Co3 (0.7 mCi) shows no sign; it is definitely below the detection limit.

\* Tc (30+30 mCi) shows an extremely light signal. It is below the detection limit. The attenuation in the air was too much for our equipment.

## 3 SUGGESTION FOR IMPROVEMENT

### *Measuring equipment*

\* *More efficient detectors.* An 18 % HPGe detector is suitable for fallout mapping, but in a real-time airborne radiation source location it is too insensitive to find sources below about 8-10 mCi.

\* *More stable MCA.* Ortec Nomad suffered from gain shifts and some crashes due to cable malfunctions between the computer and MCA. A cable malfunction is naturally fatal for spectrum refresh, but the MCA should be able to restart immediately after the cable is fixed.

\* *More stable computers.* Compaq LTE Elite's (75 and 40 MHz 486's) were unstable due to temperature problems. Especially the external AC-power caused frequent crashes because the temperature of the computer rose too high.

\* *Continuous altitude measurement* is essential to the activity calculation.

### ***Navigation***

\* *Differential GPS aided navigation.* Visual navigation causes easily gaps between flying lines. (See Figure 2).

### ***Software***

Several improvements has been performed after the exercise and the development is still going on. For example, the shape of the rise and fall of the peak intensity, when passing the source, will be used to get better real-time estimates for the activity, distance and collimation angles of the source in question.

## **REFERENCE**

**Lahtinen J, Pöllänen R, Toivonen H.** Characteristics and Locations of Sources. *ibid.*

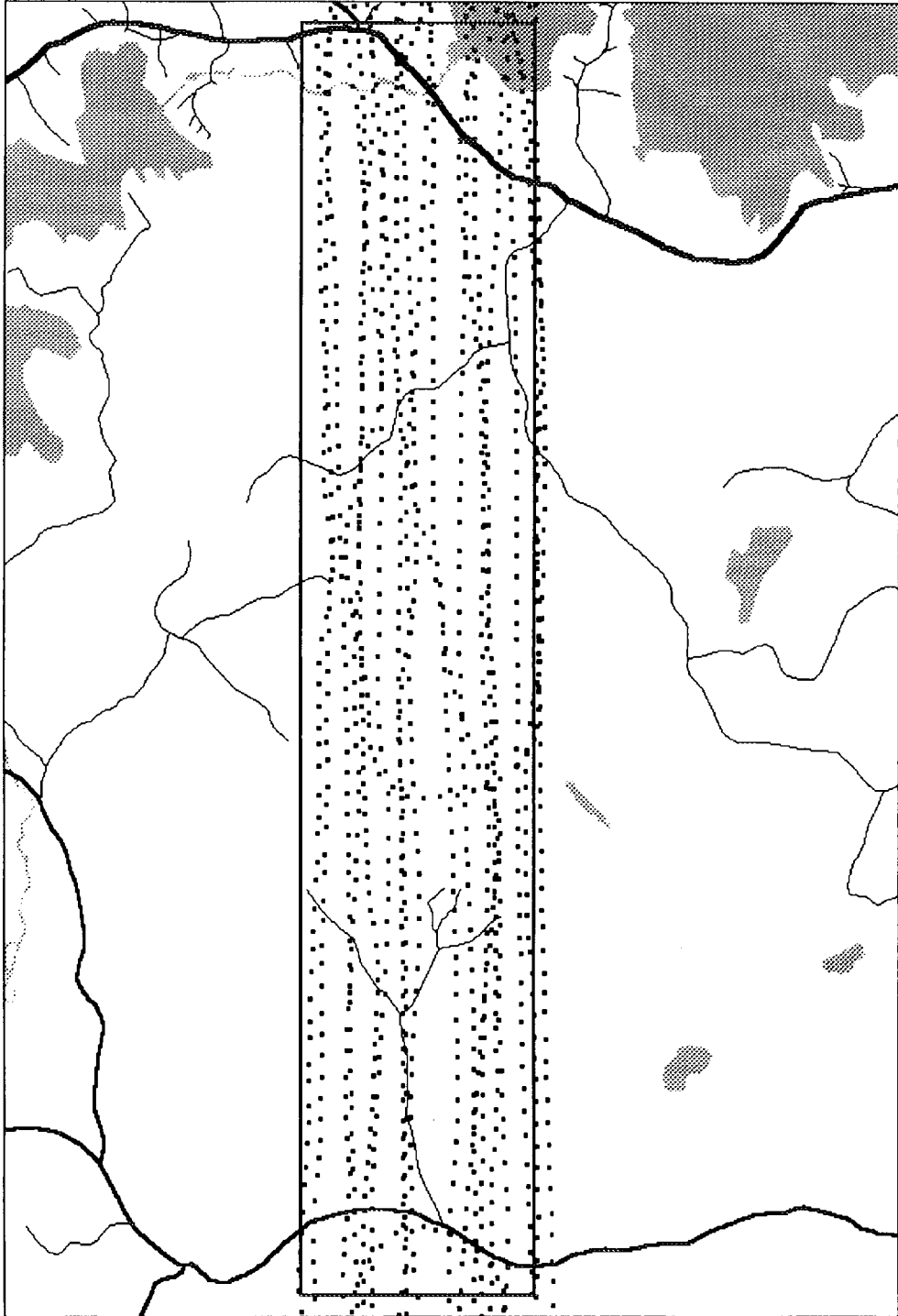


**Figure 2.** *Flight lines at the area III on 16th August 1995 (visual navigation).*



# Finnish Centre for Radiation and Nuclear Safety/ Helsinki University of Technology

## Source Passing Test in Vesivehmaa Air Field

ABSTRACT .....	153
1. INTRODUCTION .....	154
Fig. 1. Position of the detectors inside the vehicle .....	154
Tab. 1. The passing measurements .....	155
2. MEASUREMENTS .....	156
3. RESULTS .....	156
3.1. Background .....	156
3.2. Passing tests .....	156
Fig. 2. Background count rate at seven points on the driving line in $^{137}\text{Cs}$ window .....	157
4. DETECTION LIMIT ANALYSES .....	158
4.1. Dose rate .....	158
4.2. Spectrometric measurements .....	158
Fig. 3. Passing at 10 m, speed 20 km h <sup>-1</sup> .....	159
Fig. 4. Passing at 10 m, speed 50 km h <sup>-1</sup> .....	159
Fig. 5. Passing at 20 m, speed 20 km h <sup>-1</sup> .....	160
Fig. 6. Passing at 20 m, speed 50 km h <sup>-1</sup> .....	160
Fig. 7. Passing at 50 m, speed 20 km h <sup>-1</sup> .....	161
Fig. 8. Passing at 50 m, speed 50 km h <sup>-1</sup> .....	161
Fig. 9. Passing at 100 m, speed 20 km h <sup>-1</sup> .....	162
Fig. 10. Passing at 100 m, speed 50 km h <sup>-1</sup> .....	162
Fig. 11. Passing at 150 m, speed 20 km h <sup>-1</sup> .....	163
Fig. 12. Passing at 150 m, speed 50 km h <sup>-1</sup> .....	163
Fig. 13. Passing at 200 m, speed 20 km h <sup>-1</sup> .....	164
Fig. 14. Passing at 200 m, speed 50 km h <sup>-1</sup> .....	164
Fig. 15. Passing at 20 m, speed 2.1 m s <sup>-1</sup> .....	165
Fig. 16. Passing at 20 m, speed 2.1 m s <sup>-1</sup> .....	165
Tab. 2. Summary of the passing tests .....	166
5. DISCUSSION .....	168
6. REFERENCES .....	168

# Source Passing Test in Vesivehmaa Air Field - STUK/HUT Team

**T. Honkamaa<sup>1</sup>, P. Aarnio<sup>2</sup>, M Nikkinen<sup>1,2</sup>, H. Tiilikainen<sup>1</sup>**

1 Finnish Centre for Radiation and Nuclear Safety  
P. O. Box 14  
FIN-00881, Helsinki  
Finland

2 Helsinki University of Technology  
FIN-02150, Espoo  
Finland

## **Abstract:**

Carborne radiation monitors were tested for point source responses at distances 10 m, 20 m, 50 m, 100 m, 150 m, and 200 m using speed of 20 km h<sup>-1</sup> and 50 km h<sup>-1</sup>. A large pressurised ionisation chamber (PIC), an HPGe detector (relative efficiency 36.9%) and a NaI(Tl) scintillator detector (size 5"x5") were used. The sources had a nominal activity of 22 MBq (<sup>60</sup>Co) and 1.85GBq (<sup>137</sup>Cs). The <sup>60</sup>Co source strength was under the detection limit in all measurements. The detection of the <sup>137</sup>Cs source is visually clear up to 50 m for the spectrometers and up to 20 m for PIC. A statistical analysis shows that <sup>137</sup>Cs source could be detected up to 100 m with the spectrometers and up to 50 m with PIC if the background is well known.

# 1 INTRODUCTION

The pass-driving test took place in Vesivehmaa air field on 17th August 1995. The purpose of the test was to measure the responses of radiation detector systems mounted in the car, when a radionuclide source was passed. A  $^{137}\text{Cs}$  (nominal activity 50 mCi) and a  $^{60}\text{Co}$  (nominal activity 0.6 mCi) source were used in the test.

The team used the STUK's emergency vehicle (VW Transporter van), which is modified to a moving laboratory. Radiation survey can be carried out in the field using the measuring systems in the vehicle and the results can be sent in real time to headquarters via mobile phones (Honkamaa et al., 1996). In the test the vehicle was equipped with an HPGe detector (relative efficiency 36.9%), a large pressurized ionisation chamber (PIC) and a NaI(Tl) scintillation detector (size 5x5"). The positions of the detectors inside the car are shown in Figure 1.

A computer (Compaq Elite) suffered from the excessive heat in the airfield causing some breaks in the measurements.

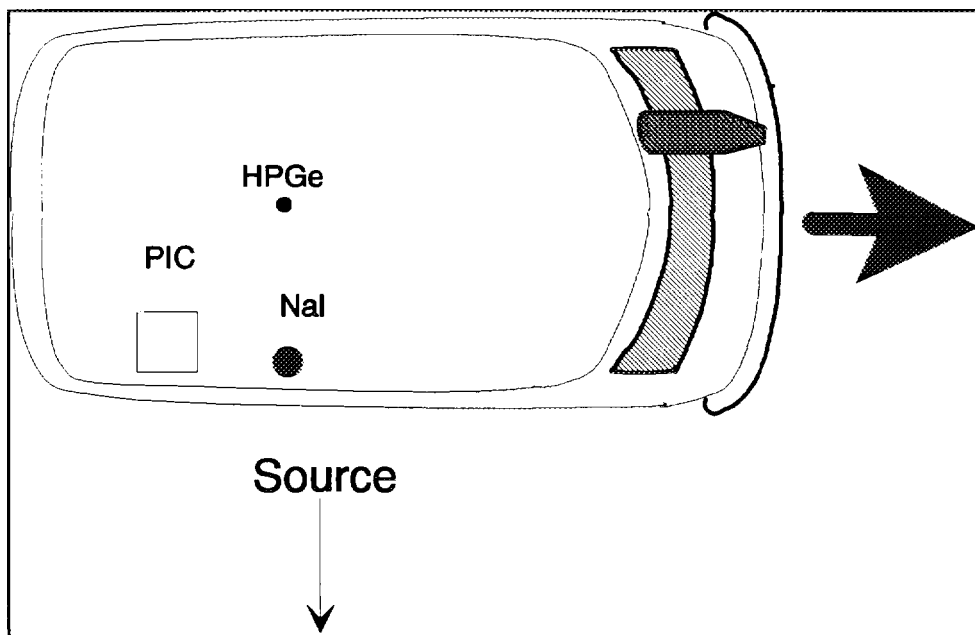


*Figure 1. The positions of the detectors inside the vehicle. In principle the HPGe detector is in a poorer position than the other detectors. This difference is insignificant for large distances.*

*Table I. The passing measurements. Values in brackets are given by the DGPS. Distances measured with DGPS may contain systematic errors.*

Passing time (UTC)	Passing speed	Passing distance	HPGe time cycle	NaI time cycle	PIC time cycle
6:31:50	20 km h <sup>-1</sup>	10 m (10.4 m)	missing	0.32 s	13 s
6:42:37	50 km h <sup>-1</sup>	10 m (10.2 m)	0.92 s	0.50 s	missing
6:52:10	20 km h <sup>-1</sup>	20 m (18.2 m)	missing	0.63 s	13 s
7:04:23	50 km h <sup>-1</sup>	20 m (20.7 m)	0.66 s	0.80 s	13 s
7:07:47	20 km h <sup>-1</sup>	50 m (50.1 m)	2.7 s	0.87 s	13 s
7:13:01	50 km h <sup>-1</sup>	50 m (50.1 m)	2.9 s	0.90 s	13 s
7:20:44	20 km h <sup>-1</sup>	100 m	0.67 s	1.0 s	13 s
7:32:04	50 km h <sup>-1</sup>	100 m	0.85 s	1.1 s	14 s
7:44:43	20 km h <sup>-1</sup>	150 m	0.67 s	0.30 s	13 s
7:50:14	50 km h <sup>-1</sup>	150 m	0.65 s	0.33 s	13 s
7:58:37	20 km h <sup>-1</sup>	200 m	0.67 s	0.35 s	13 s
8:05:06	50 km h <sup>-1</sup>	200 m	0.67 s	0.37 s	13 s
8:22:48	(2.1 m s <sup>-1</sup> )	20 m (20.9 m)	missing	0.46 s	13 s
8:29:14	(2.1 m s <sup>-1</sup> )	20 m (20.9 m)	0.66 s	missing	13 s

## 2 MEASUREMENTS

Detector responses were measured at the distances of 10 m, 20 m, 50 m, 100 m, 150 m and 200 m using  $^{137}\text{Cs}$  and  $^{60}\text{Co}$  sources. At each distance, speeds of 20 km h<sup>-1</sup> and 50 km h<sup>-1</sup> were used. The position of the car was measured with a DGPS navigator once a second. Background count rates were measured at seven points on the driving line.

The passings are listed in Table I. Due to technical problems some measurement rounds are missing. Time cycles of the different measuring systems are also presented. Time cycles were not constant, because saving one spectrum in a hard disk of a computer takes longer time, if the number of files in the saving directory is large. This feature of DOS lengthened gradually the time cycles of the measurements, until another saving directory was chosen. The missing measurements are due to computer malfunctions (overheating). The high data acquisition rate (=27 kB/s) surprised the crew a few times and caused some "disk full" errors.

## 3 RESULTS

### 3.1 Background

The background count-rate profile measured with the NaI detector is presented in Figure 2. The changes in background on the driving line were not taken into account in the detection limit analysis; only an average background was used. The average count-rates in the  $^{137}\text{Cs}$  window measured with the HPGe and the NaI detectors were 5.9 (0.2) cps and 60.1(0.3), respectively. Also the dose rate decreased along the driving line from 0.106 to 0.101  $\mu\text{Sv h}^{-1}$ .

### 3.2 Passing tests

The  $^{60}\text{Co}$  source was too weak to be properly detected. A total of 3 counts (approximately 3 cps) at the 1172 and 1333 keV peaks were seen in an HPGe spectrum when passing the source at the distance of 10 m. However, those few counts could be used for source location and identification, because the background continuum at those energies was practically zero. When the source was moved farther off, no counts were detected.

The dose rates and count rates during the passings are presented in Figures 3 to 16. The theoretical count rates,  $T$ , in the figures are calculated as

$$T = \Phi \text{ Eff} + B = A\gamma \frac{1}{4\pi r^2} \exp(-\mu r) \text{ Eff} + B$$

where  $\Phi$  is the primary photon fluence rate from the source,  $r$  is the distance from the source,  $\gamma$  is the gamma yield of  $^{137}\text{Cs}$  (0.85),  $\mu$  is the attenuation coefficient of air,  $A$  is the activity of the source,  $\text{Eff}$  is the intrinsic efficiency of the detector ( $0.00075 \text{ m}^2$ ) measured at the angle of incidence and  $B$  is the background count rate in 661.6 keV photopeak. Attenuation caused by the shielding of the source or the body of the vehicle is not taken into account. The activity of the source,  $A$ , can be calculated (Figure 15) from the photopeak count rate ( $142 \text{ s}^{-1}$ ) at 20m. The calculation gives 0.92 GBq (25 mCi) for activity of the  $^{137}\text{Cs}$  source. The uncertainty in the distance is 2 m, which creates 20% uncertainty in the activity. The corresponding uncertainties in count rate and in detector efficiency are 10% and 5%, respectively.

The time is synchronised between the spectrometers and PIC according to the time labels in data logging files. The time resolution of the PIC and DGPS systems is 1 s.

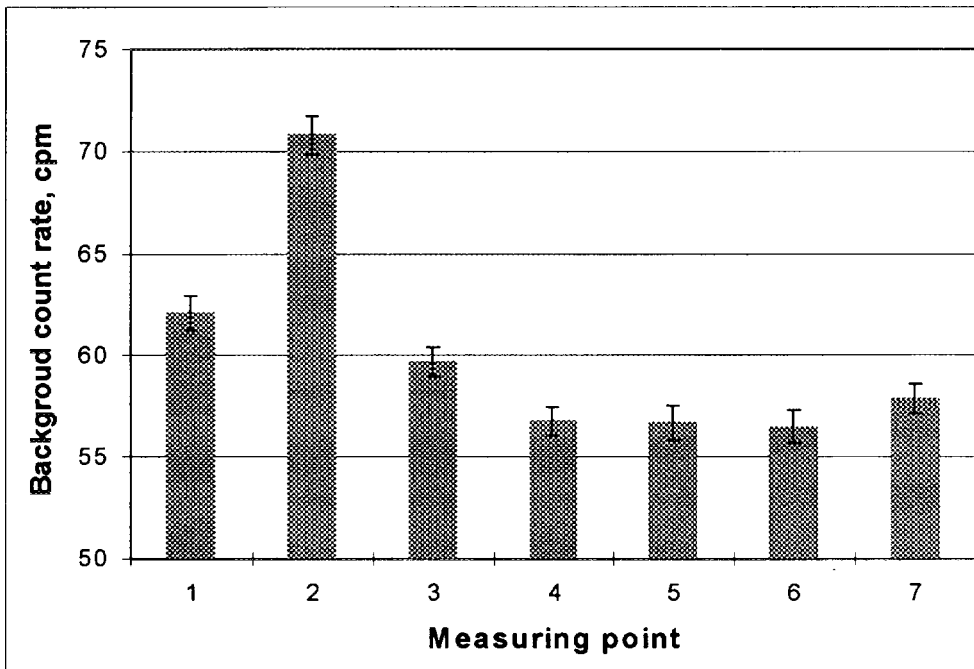


**Figure 2.** Background count rate at seven points on the driving line in  $^{137}\text{Cs}$  window. The count rates are measured with the NaI detector. The point 4 is the midpoint of the line, where the distance from the source is the shortest. At point 2 the count rate is much higher than at other points.

## 4 DETECTION LIMIT ANALYSES

### 4. 1 Dose rates

A relative increase of the dose rate is calculated for each time slice. An increase of 10% is considered significant compared with the average of three previous measurements.

### 4. 2 Spectrometric Measurements

An optimal collection time can be estimated for each distance and velocity giving the lowest minimum detectable activity. Its precise calculation is not trivial, because the source is slightly collimated (Lahtinen et al, 1996). Therefore, the collection period was determined visually from the theoretical and actual shape of the fluence rate. The length of this collection time is individual for each passing. The spectra collected during the selected periods were summed together. For each period, the number of net counts and background counts were also calculated. Background counts were estimated multiplying the average measured background count rate by the length of the selected time period. The decision, whether a source was detected or not, was based on the standard deviation of the number of counts in the background (B):

$$\sigma = \sqrt{B}$$

If the signal was less than  $4 \sigma$  the source was considered as not detected. If the signal, on the other hand, was above  $4 \sigma$  the source was considered as detected. The adopted significance levels are subject to further discussion. The calculated sigma levels are presented in Table II.

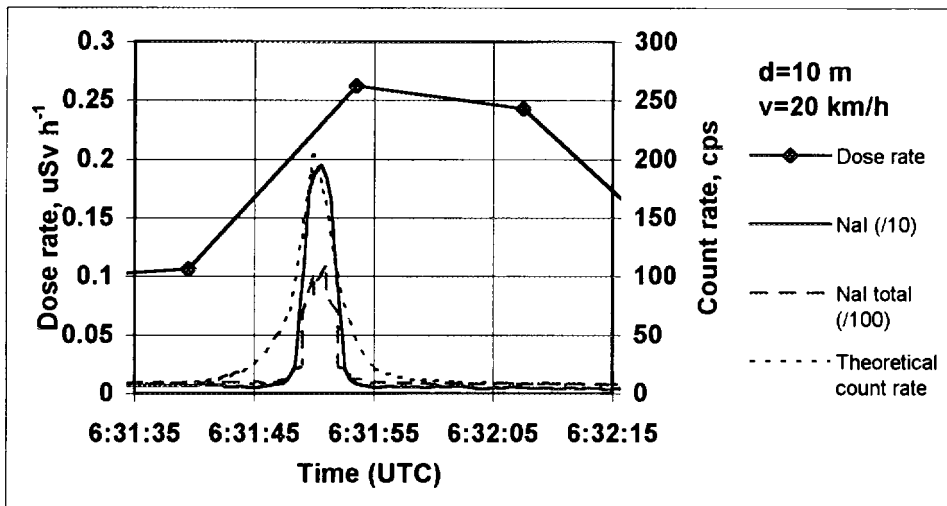


**Figure 3.** Passing at 10 m, speed 20 km h<sup>-1</sup>. The HPGe detector was not functioning. The peak in NaI spectra is very sharp. The effect of the smooth response of the PIC can be seen. Small inaccuracies (around 1 s) in time and position data cause slight changes in the position and shape of the curves. Nevertheless, the collimation of the source can be clearly seen. The peak of scattered gamma flux is not wider than the peak of primary gamma flux.

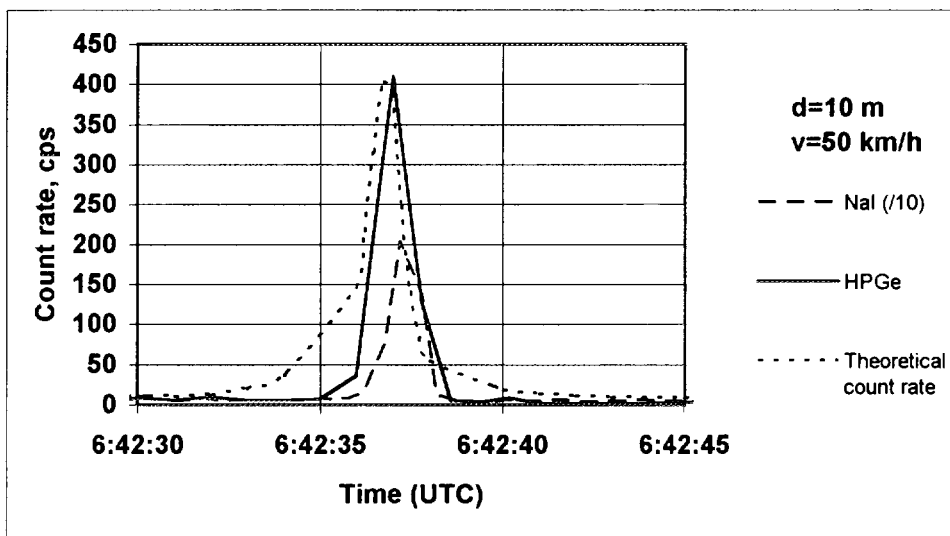


**Figure 4.** Passing at 10 m, speed 50 km h<sup>-1</sup>. The PIC detector was not functioning. The NaI and HPGe detectors gave clear signals. The measuring time cycles are too long (0.92 s, 0.50 s) and the shape of the peaks is distorted. The logging inaccuracy gives incorrect peak positions.

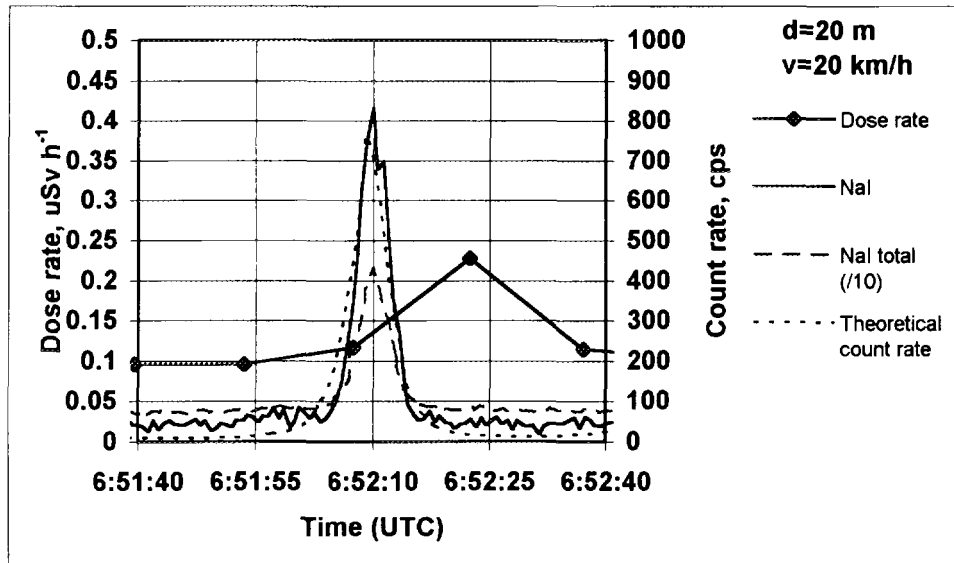


**Figure 5.** Passing at 20 m, speed 20 km h<sup>-1</sup>. The HPGe detector was not functioning. The NaI and PIC detectors gave clear signals. The PIC would have given an alarm before the source was passed at 6:52:08 (20% increase), but the maximum value came in the following time cycle.

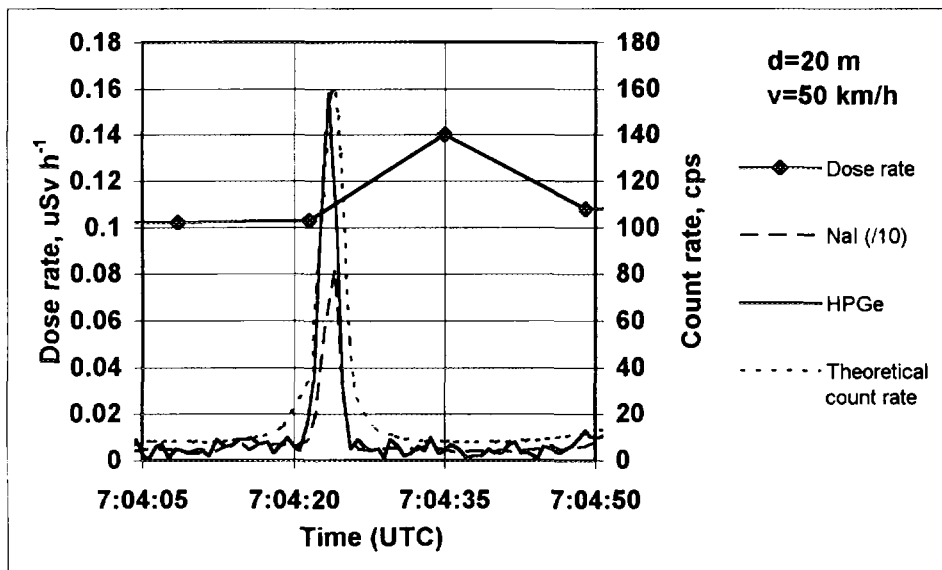


**Figure 6.** Passing at 20 m, speed 50 km h<sup>-1</sup>. All the detectors gave clear signals. For the PIC the timing was most unfortunate. The source was not detected until 11 seconds after passing, which equals 150 m in distance.

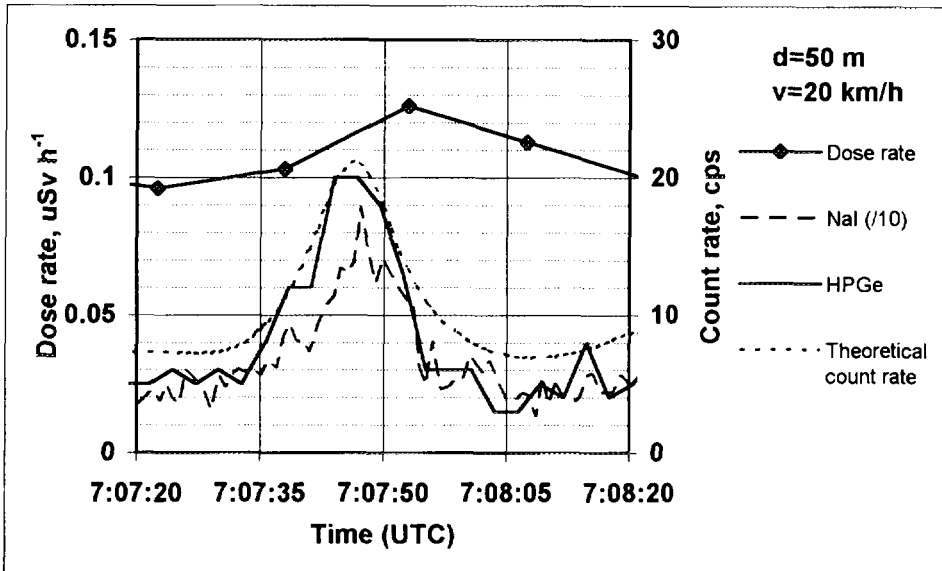


Figure 7. Passing at 50 m, speed 20 km h<sup>-1</sup>. All the detectors gave clear signals.

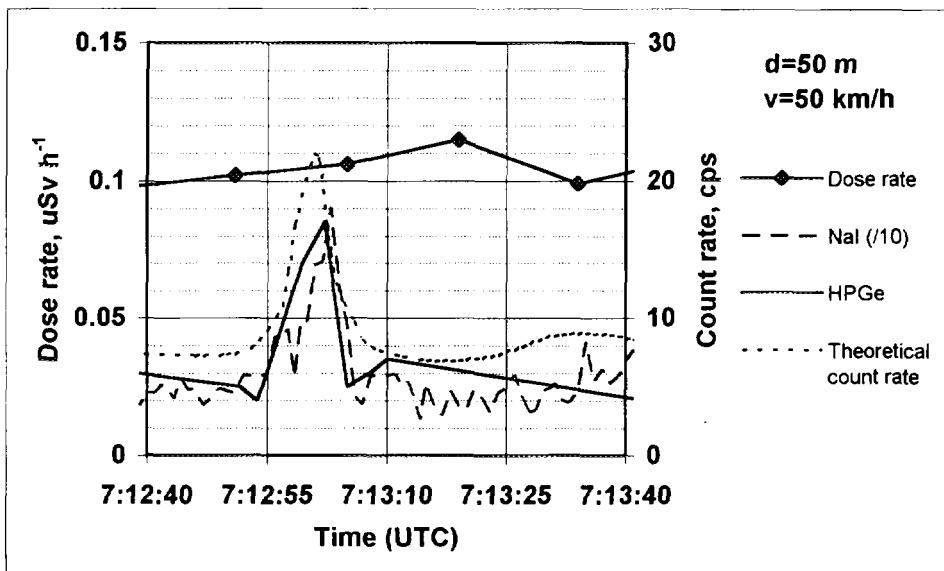
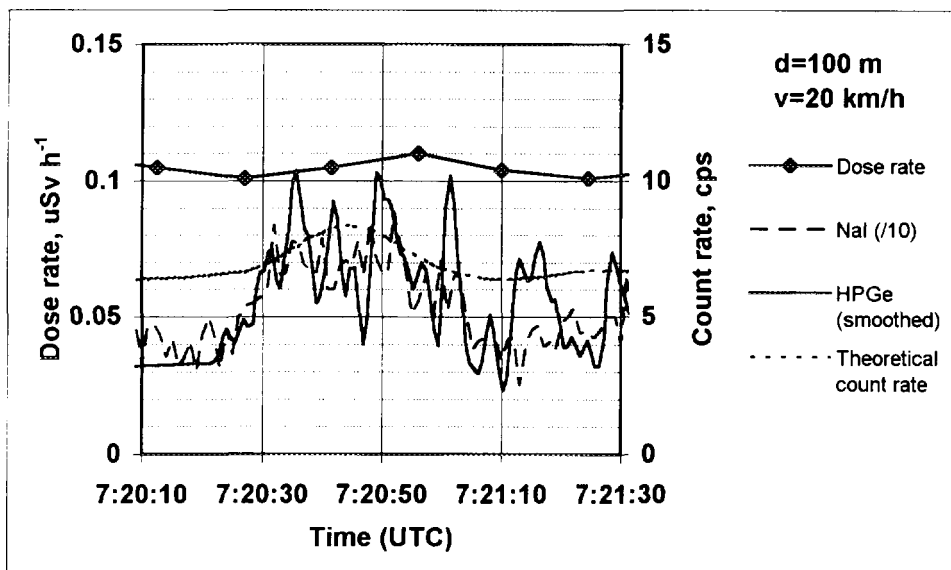
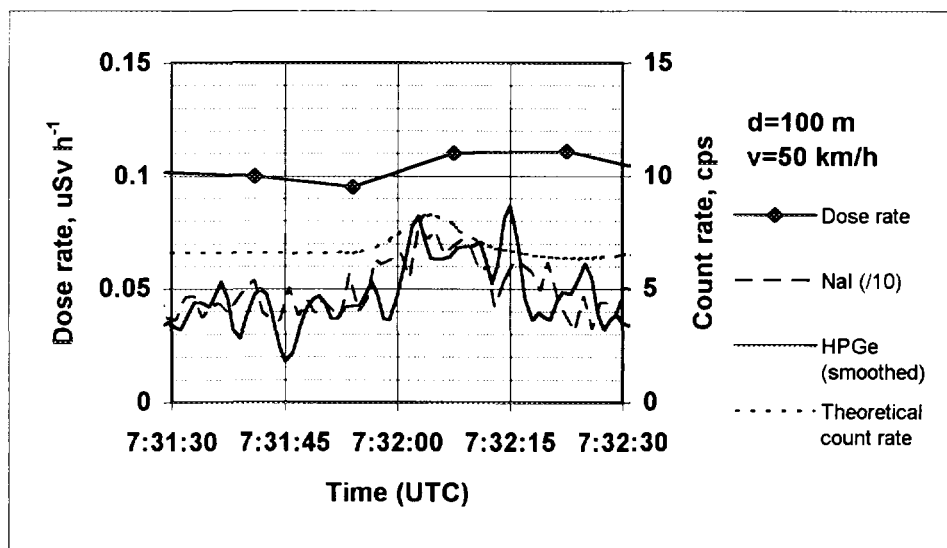


Figure 8. Passing at 50 m, speed 50 km h<sup>-1</sup>. The PIC signal is just on the detection limit. For the spectrometers the signals are clear.



**Figure 9.** Passing at 100 m, speed 20 km h<sup>-1</sup>. The presence of the source can be detected from the curves, but not very well. However, for the spectrometers, there is a significant increase in the count rate. The HPGe data are smoothed over five points using a 6-4-1 filter. The source cannot be detected with the PIC.



**Figure 10.** Passing at 100 m, speed 50 km h<sup>-1</sup>. The PIC gave an alarm signal (11% increase), but it was partly due to exceptionally low values of the preceding measurements. The source cannot be detected with the spectrometers. The HPGe data are smoothed over five points using a 6-4-1 filter.

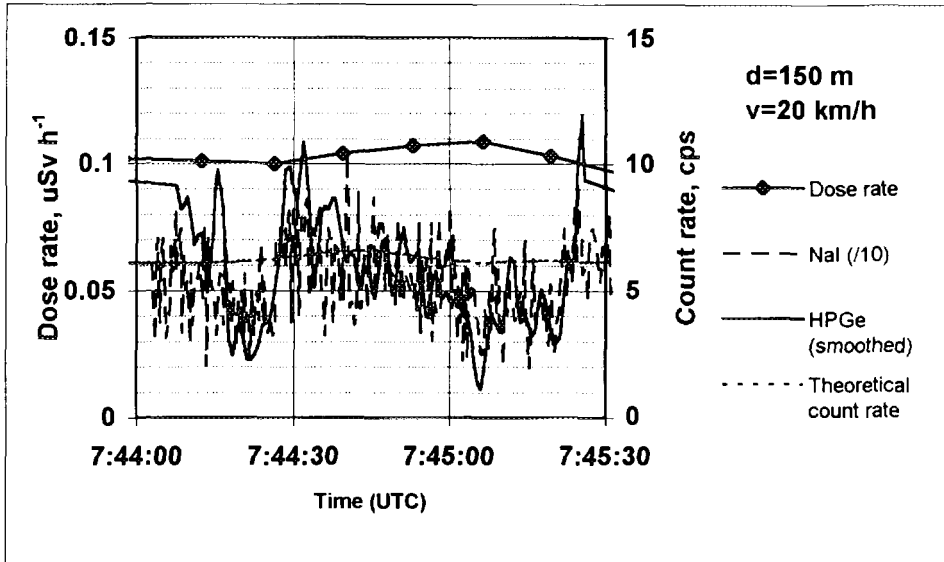


**Figure 11.** Passing at 150 m, speed  $20 \text{ km h}^{-1}$ . The curve for the NaI detector seems really noisy. However, the noise is not completely due to counting statistics. The low resolution in the measurement of counting times makes the measured live times to fluctuate. The detection with the HPGe is over 3 sigma level. The source is not detected with the NaI detector and PIC. The HPGe data are smoothed over five points using a 6-4-1 filter.

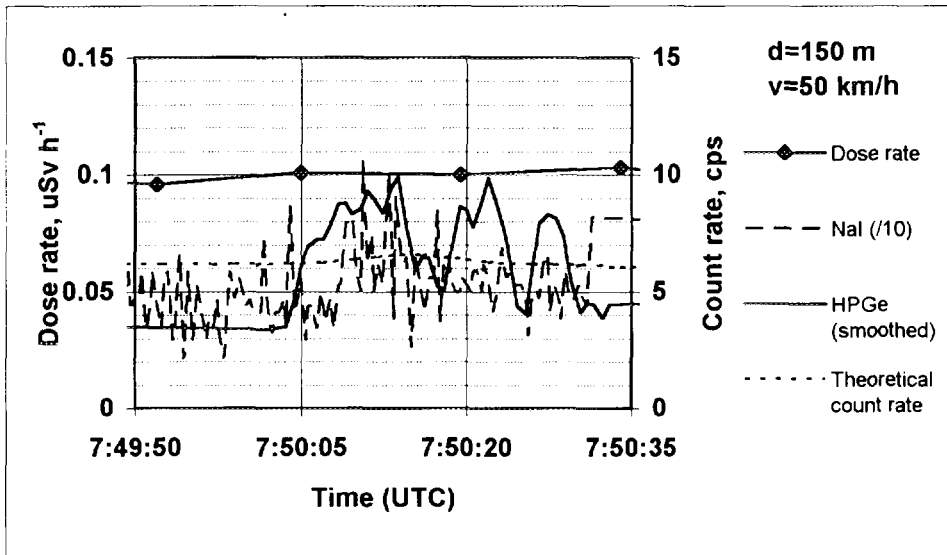


**Figure 12.** Passing at 150 m, speed  $50 \text{ km h}^{-1}$ . The source is not detected with any of the detectors. The HPGe data are smoothed over five points using a 6-4-1 filter.

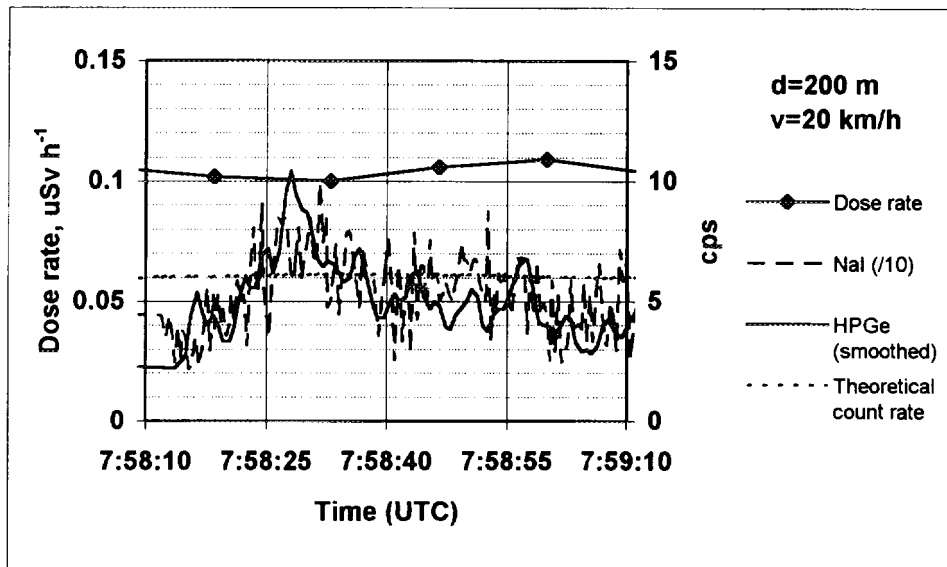


**Figure 13.** Passing at 200 m, speed 20 km h<sup>-1</sup>. The source cannot be seen with any of the detectors. The HPGe data are smoothed over five points using a 6-4-1 filter. The measured count rates reflect mostly the background of the airfield (see Figure 2).

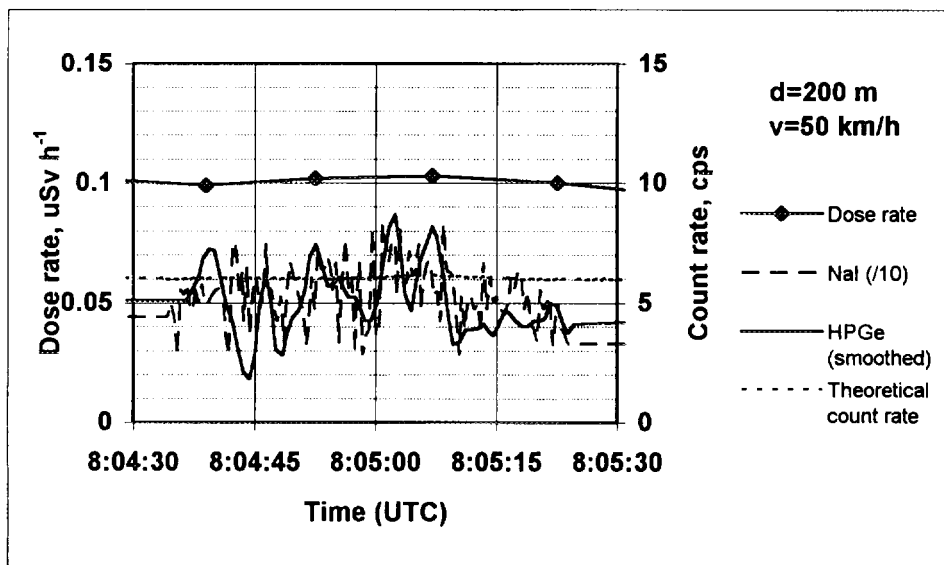


**Figure 14.** Passing at 200 m, speed 50 km h<sup>-1</sup>. The source cannot be detected with any of the detectors. The HPGe data are smoothed over five points using a 6-4-1 filter.

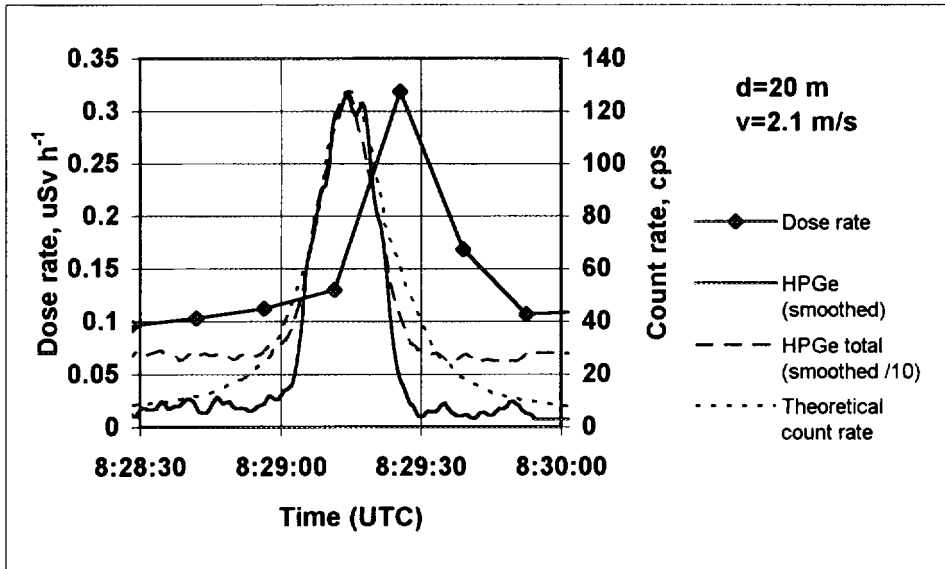


**Figure 15.** Passing at 20 m, speed  $2.1 \text{ m s}^{-1}$ . The NaI detector was not functioning. The collimation effect can be seen (Lahtinen et al., 1996).

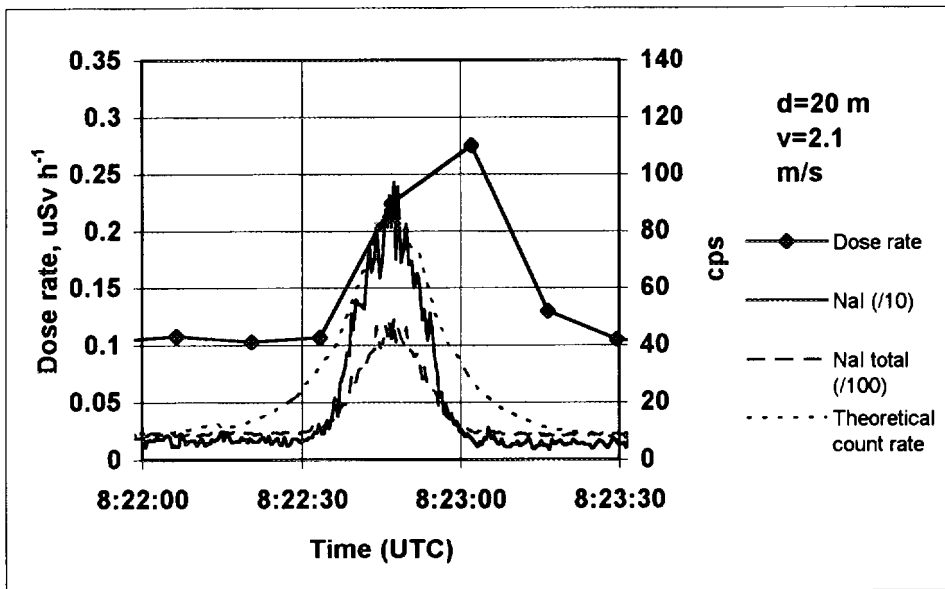


**Figure 16.** Passing at 20 m, speed  $2.1 \text{ m s}^{-1}$ . The HPGe detector was not functioning. The fluctuation in the NaI data is due to the low resolution of the live time clock. The collimation effect can be seen (Lahtinen et al., 1996).

*Table II. Summary of the passing tests*

Collection period (UTC)	Passing speed and distance	HPGe signal, background and significance	NaI signal, background and significance	PIC signal, background and relative increase
6:31:46-6:31:52	20 km h <sup>-1</sup> 10 m	missing	5855 cnts 517 cnts 240σ	0.262 μSvh <sup>-1</sup> 0.100 μSvh <sup>-1</sup> 260%
6:42:36-6:42:38	50 km h <sup>-1</sup> 10 m	285 cnts 12 cnts 79σ	1792 cnts 120 cnts 150σ	missing
6:52:04-6:52:15	20 km h <sup>-1</sup> 20 m	missing	4084 cnts 685 cnts 130σ	0.228 μSvh <sup>-1</sup> * 0.100 μSvh <sup>-1</sup> 230%
7:04:21-7:04:26	50 km h <sup>-1</sup> 20 m	268 cnts 25 cnts 49 σ	1526 cnts 301 cnts 71 σ	0.140 μSvh <sup>-1</sup> 0.102 μSvh <sup>-1</sup> 38%
7:07:35-7:07:54	20 km h <sup>-1</sup> 50 m	263 cnts 102 cnts 16 σ	1874 cnts 997 cnts 28 σ	0.126 μSvh <sup>-1</sup> 0.100 μSvh <sup>-1</sup> 25.6%
7:12:59-7:12:05	50 km h <sup>-1</sup> 50 m	62 cnts 29 cnts 6.1 σ	727 cnts 349 cnts 20 σ	0.115 μSvh <sup>-1</sup> 0.102 μSvh <sup>-1</sup> 12.7%
7:20:30-7:21:00	20 km h <sup>-1</sup> 100 m	219 cnts 158 cnts 4.9 σ	2135 cnts 1886 cnts 5.7 σ	0.110 μSvh <sup>-1</sup> 0.104 μSvh <sup>-1</sup> 6.1%
7:31:59-7:32:11	50 km h <sup>-1</sup> 100 m	78 cnts 62 cnts 2.0 σ	796 cnts 710 cnts 2.2 σ	0.110 μSvh <sup>-1</sup> 0.099 μSvh <sup>-1</sup> 11.1%
7:44:25-7:44:58	20 km h <sup>-1</sup> 150 m	205 cnts 177 cnts 2.1 σ	1907 cnts 1911 cnts 2.2 σ	0.109 μSvh <sup>-1</sup> 0.104 μSvh <sup>-1</sup> 4.8%

\*) The maximum value during the passing, but the source could already be detected in the preceding time cycle.

Table II. *Continued.*

Collection period (UTC)	Passing speed and distance	HPGe signal, background and significance	NaI signal, background and significance	PIC signal, background and relative increase
7:50:09-7:50:24	50 km h <sup>-1</sup> 150 m	120 cnts 89 cnts 3.3 $\sigma$	936 cnts 924 cnts 0.37 $\sigma$	0.100 $\mu\text{Svh}^{-1}$ 0.098 $\mu\text{Svh}^{-1}$ 2.0%
7:58:20-7:58:58	20 km h <sup>-1</sup> 200 m	225 cnts 201 cnts 1.7 $\sigma$	2340 cnts 2343 cnts 0.1 $\sigma$	0.106 $\mu\text{Svh}^{-1}$ 0.103 $\mu\text{Svh}^{-1}$ 2.9%
8:04:55-8:05:17	50 km h <sup>-1</sup> 200 m	122 cnts 135 cnts -1.1 $\sigma$	1597 cnts 1719 cnts -2.9 $\sigma$	0.103 $\mu\text{Svh}^{-1}$ 0.101 $\mu\text{Svh}^{-1}$ 2.0%
8:22:33-8:23:01	2.1 m s <sup>-1</sup> 20 m	missing	12622 cnts 1719 cnts 263 $\sigma$	0.275 $\mu\text{Svh}^{-1(*)}$ 0.106 $\mu\text{Svh}^{-1}$ 260%
8:29:00-8:29:27	2.1 m s <sup>-1</sup> 20 m	1953 cnts 141 cnts 152 $\sigma$	missing	0.319 $\mu\text{Svh}^{-1(*)}$ 0.104 $\mu\text{Svh}^{-1}$ 310%

## 4 DISCUSSION

In these measurements the 5x5" NaI scintillator and 36.9% HPGe detectors were almost as sensitive for the  $^{137}\text{Cs}$  source. It could be detected from the distance of 100 m at the speed of  $20 \text{ km h}^{-1}$  when the background was well known. Signal to background ratio is typically higher for the HPGe detector than for the NaI detector. However, the statistical accuracy for the HPGe is poorer.

The high caesium background of  $50 \text{ kBq m}^{-2}$  increases uncertainties of the measurements. The measuring results at 150 and 200 m reflect mostly changes in background radiation field rather than the location of the source. Another strong source than  $^{137}\text{Cs}$  should have been used to get more accurate results. Unfortunately, the  $^{60}\text{Co}$  source was too weak to be properly detected.

The PIC is at its detection limit at ( $50\text{m}, 50 \text{ km h}^{-1}$ ). At that distance the spectrometers gave visually clear signals. The results of PIC are affected by the driving speed and timing, since it takes about 15 to 30 s to adopt to the new dose rate level completely. These tests should be repeated many times to obtain good MDA estimates for the PIC.

The optimum collection time for the spectrometers, which reduces the detection limit, depends on source collimation, background count rate, driving speed and the distance of the source from the road. When a lost source is searched, some of these parameters are not known. This means, that all practical collection times must be tried. This makes the analysis elaborate and requires advanced software. Here we have only compared the total number of counts in the energy window with an estimated background in the same window. More sophisticated methods would perhaps utilize peak fitting algorithms.

In practical situations, the background count rate is not known prior to analysis. This means, that the background must be estimated from the background present around the suspected place. If  $^{137}\text{Cs}$  fallout is large, fluctuations in 661.6 keV photon fluence rate make it impossible to use strict thresholds for the peak count rate. For a good example, see the results of a road profile near Padasjoki (Honkamaa et al., 1996). When the measuring vehicle moved from a cultivated area into a forest the count rate in the  $^{137}\text{Cs}$  window increased fivefold. Also, the dose rate increased 20%. For less contaminated areas and for nuclides not present in the environment, the situation is much easier.

## REFERENCES:

**Honkamaa T, Toivonen H, Nikkinen M.** Monitoring of Airborne Contamination Using Mobile Equipment. STUK A-130. Helsinki: Finnish Centre for Radiation and Nuclear Safety, 1996.

**Lahtinen J, Pöllänen R, Toivonen H.** Characteristics and Locations of Sources. *ibid.*

**Honkamaa T, Aarnio PA, Nikkinen M, Tiilikainen H.** Carborne Fallout Mapping-STUK/HUT Team. *ibid.*



# Commissariat à L'Energie Atomique - Hélinuc

## RESUME 95 Nordic field test of mobile equipment for nuclear fall-out monitoring

1.	INTRODUCTION.....	171
2.	AIRBORNE MEASUREMENTS .....	172
2.1.	Operational conditions.....	172
2.1.1.	Principle of measurements .....	172
	Fig. 1. Airborne scanning principle .....	172
2.1.2.	Equipment.....	173
	Fig. 2. Helicopte starting for mesurements .....	173
	Fig. 3. Recording rack.....	173
2.1.3.	Measurements performed during R.E.S.U.M.E. 95 .....	174
2.2.	Hidden sources detection .....	174
	Tab. Detection results for each source .....	174
	Fig. 4. $^{192}\text{Ir}$ source detection during survey of the road between area 2 and 3 .....	175
	Fig. 5. $^{192}\text{Ir}$ source detection during survey of the road between area 2 and 3 .....	175
	Fig. 6. $^{99}\text{Tc}_m$ source detection during survey of area 3 .....	176
	Fig. 7. Cs3 and Co1 detection during survey of area 3 .....	177
	Conclusion .....	177
2.3.	Isoactivity maps.....	178
2.3.1.	Spectral analysis .....	178
	Fig. 8. Calculation of full absorption picks(B) by processing of a raw spectrum(A) .....	178
	Tab. 1. Synthesis of nuclides detection over area n° 2 .....	179
	Tab. 2. Synthesis of nuclides detection over area n° 3 .....	179
2.3.2.	Calibration.....	180
	Laboratory calibration .....	180
	Fig. 9. Laboratory calibration set-up .....	180
	Flight calibration.....	180
	Tab. 3. Area n° 1 concentrations (Airfield) .....	180
	Comparison of results .....	181
	Fig. 10. Variation of detection response with altitude for $^{137}\text{Cs}$ , $^{40}\text{K}$ and $^{232}\text{Th}$ .....	182
2.3.3.	Isoactivity maps .....	182
	Radioactive fall-out .....	182
	Natural activity .....	182
2.4.	Conclusion.....	183
3.	GROUND MEASUREMENTS .....	184
3.1.	Experimental conditions .....	184
3.1.1.	Measurement points .....	184
3.1.2.	Timing .....	184
3.1.3.	Experimental device .....	184
	Fig. 11. In situ gamma measurements.....	185
3.2.	Calibration .....	185
3.2.1.	Superficial avtivity .....	185
3.2.2.	Dose rate .....	185
3.3.	Results.....	186
3.3.1.	Superficial activity .....	186
	Area n° 1 .....	186

Tab. 4. Major natural nuclides activity (in kBq/m <sup>2</sup> ) .....	186
Tab. 5. Comparison of caesium and natural activities (in kBq/m <sup>2</sup> ) .....	187
Area n° 2 .....	187
Tab. 6. Major natural nuclides activities (in kBq/m <sup>2</sup> ) .....	187
Tab. 7. Comparison of caesium and natural activities (in kBq/m <sup>2</sup> ) .....	188
3.3.2. Dose rate .....	188
Area 1 .....	188
Tab. 8. Natural nuclide dose rates (in Gy/h) .....	188
Tab. 9. Comparison of caesium and natural dose rates (in Gy/h) .....	189
Tab. 10. Comparison of dose rate measurements performed with different apparatus.....	189
Area 2 .....	190
Tab. 11. Natural nuclide dose rates (in Gy/h) .....	190
Tab. 12. Comparison of caesium and natural dose rates (in nGy/h) .....	190
Tab. 13. Comparison of dose rate measurements performed with different apparatus.....	191
3.4. Conclusion.....	191
3.4.1. Superficial concentrations .....	191
3.4.2. Dose rate .....	191
4. CONCLUSION.....	192
APPENDIX:	
A1-3-1.Spectrum.....	193
A2-C-0.Spectrum .....	194

Figures in Colour Appendix (C.A.):

Map Area 2 - <sup>137</sup> Cs Activity .....	C.A. plate 10
Map Area 2 - <sup>40</sup> K Activity .....	C.A. plate 11
Map Area 3 - <sup>137</sup> Cs Activity .....	C. A. plate 12

## RESUME 95

### Nordic field test of mobile equipment for nuclear fall-out monitoring

C. Bourgeois, J. Bresson, T. Chiffot, L. Guillot

Commissariat à L'Energie Atomique  
Direction des Applications Militaires  
Centre d'Etudes de Valduc  
120 Is/Tille

### *1. Introduction*

Nordic Safety Research (NKS) organised in august 1995 a field test of various techniques and instrumentation for monitoring radioactive fall-out.

In an emergency situation, after a major release of radioactive material, many different measuring systems are going to be used, ranging from small hand hold intensitometer to complex spectrometer systems. In this test the following type of equipment were tested :

- Airborne spectrometers,
- Carborne spectrometers and dose rate meters,
- In situ spectrometers and intensitometers.

Helinuc team was equipped of an airborne system and of a germanium device for in situ measurements.

Different tasks were specified for each team :

- Mapping caesium fall-out and natural activity over two areas of 18 and 5 km<sup>2</sup>.
- Research of hidden sources.

For measurements and data processing the respect of time allowed was strictly controlled for testing the ability of each team.

## 2. Airborne measurements

### 2.1 Operational conditions

#### 2.1.1 Principle of measurements

In order to analyse in details a chosen area, the helicopter carrying the equipment sweeps back and forth over the area to be mapped according to predetermined parameters : length of profiles, distance between profiles, altitude, speed and sample time (figure 1). The detector used consists of four sodium iodide crystals (16 liters). The spectrometer amplifies and codes pulses in a 512 channels spectrum representing an energy scale from 40 to 2800 keV. At the end of sample time (1 to 3 seconds), a computer records the spectrum plus the average helicopter position (X, Y, Z) during the measurement.

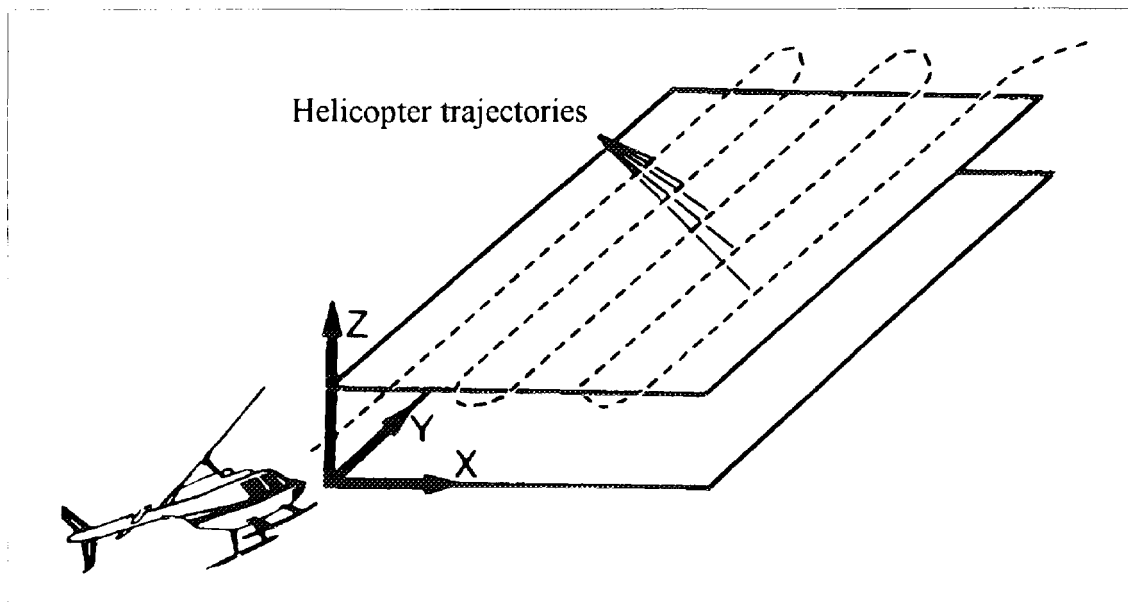


Figure 1 : Airborne scanning principle.

The helicopter's position is computed by a Trident system, constituted of :

- an interrogator on board the helicopter,
- ground beacons accurately localised.

Remark : Since January 1996, the positioning achieved by a differential GPS constituted of :

- a GPS on board the helicopter,
- a reference GPS on the ground which sends in real time corrections to mobile GPS.

### 2.1.2 Equipment

#### Helicopter:

The helicopter (AS-350-B1), belonging to the French company « HELIFRANCE » came in Finland specially for the exercise.



**Figure 2 : Helicopter starting for measurements.**

#### Measurements device:

The on board equipment is constituted of:

a recording rack (figure 2)

- an Exploranium 512 channels spectrometer
- a computer for recording spectra, helicopter positions and giving navigation information to the pilot.
- a Bernoulli disk for data storage,
- a positioning device (Trident).

a fly box carried under the helicopter

- a 16 liters NaI detector,
- a radio-altimeter.



**Figure 3 : Recording rack**

#### Processing equipment:

The processing device, integrated in a transportable box is constituted of the following equipment :

- a calculator,
- a scanner,
- a colour printer,
- a Bernoulli disk.

### 2.1.3 Measurements performed during R.E.S.U.M.E. 95

Following tasks were specified by organisers :

- Mapping of area 2 (6km per 3km), localised between two villages :f Vesijako and Auttoinen : This area should be covered by 21 profiles of 6 kilometres, spacing of 150 meters.
- Mapping of area 3 (5km per 1km) and real time detection of hidden point sources.

Both areas had to be flown in a flight. A calibration area on Vesivehmaa airfield was defined.

### 2.2 Hidden sources detection

During the survey of area 3, 15 point sources were hidden, of different natures and activities. Fly conditions were free but the time over the area restricted to one hour.

The following table shows the detection results for each source:

Nuclide	Code	Activity (mCi)	Results half an hour after landing	Results after detailed data processing	Point number	Co-ordinates
<sup>60</sup> Co	Co1	7	yes	yes	1838	(552783, 804734)
					2013	(552848, 804751)
<sup>60</sup> Co	Co2	9 collimated	no	traces	1136	(552299, 802610)
<sup>60</sup> Co	Co3	0.7	no	traces ?	846	?
<sup>60</sup> Co	Co 4 à 9	1 à 2 mCi linear source (~200 meters)	no	yes, detection of linearity	1020	(552224, 804197)
					1104	(552291, 804249)
					1276	(552388, 804304)
<sup>137</sup> Cs	Cs1	77	yes	yes	982	(552229, 802617)
					1136	(552299, 802610)
<sup>137</sup> Cs	Cs2	50 collimated	no	no		
<sup>137</sup> Cs	Cs3	7.5	no	traces ?	2013	(552848, 804751)
<sup>137</sup> Cs	Cs4	14.6	no	traces	1970	(552849, 802540)
<sup>192</sup> Ir	I	15000	yes	yes	2050	(552955, 804945)
					335	?
<sup>99</sup> Tc	T	30	no	yes	764	(552061, 804244)

The detection of « traces » averages that sources have been detected, but their contributions are too weak to conclude about their attendance.  
 Sources which have been detected on the road between areas 2 and 3 haven't any co-ordinate because Trident positioning wasn't running at this time.

The following figures presents some screen hard copies showing the detection of some sources.

The iridium source has been detected the first time during the survey of the road between both areas. The helicopter was approximately at 300 meters from the source (figure 4).

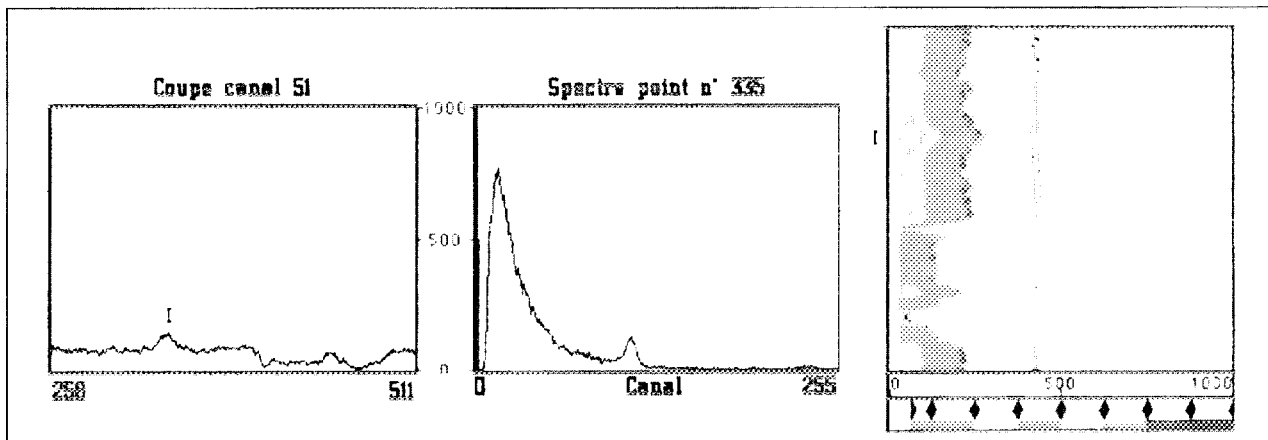


**Figure 4 :  $^{192}\text{Ir}$  source detection during survey of the road between areas 2 and 3.**

During the survey of area 3 the iridium has been again detected by scattering photons, for example on channel 14 on figure 5. Any direct photon has been detected because the angular direction of emission was tangential to the area. The decreasing slope of the spectrum 335 between channels 15 and 50 is less stiff than the slope of spectrum 2050, it shows the attendance of full absorption picks (295, 308, 316, and 468 keV) in spectrum 335.

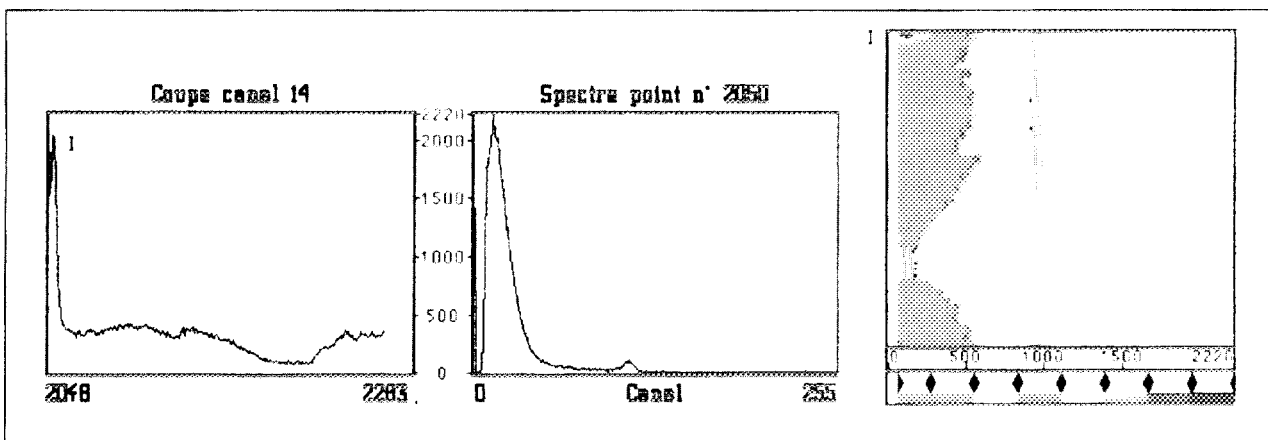


**Figure 5 :  $^{192}\text{Ir}$  source detection during survey of the road between areas 2 and 3.**

The  $^{99}\text{Tc}_m$  source has been clearly detected on spectrum 764 by the 140 keV emission ray (channel 25, figure 6).

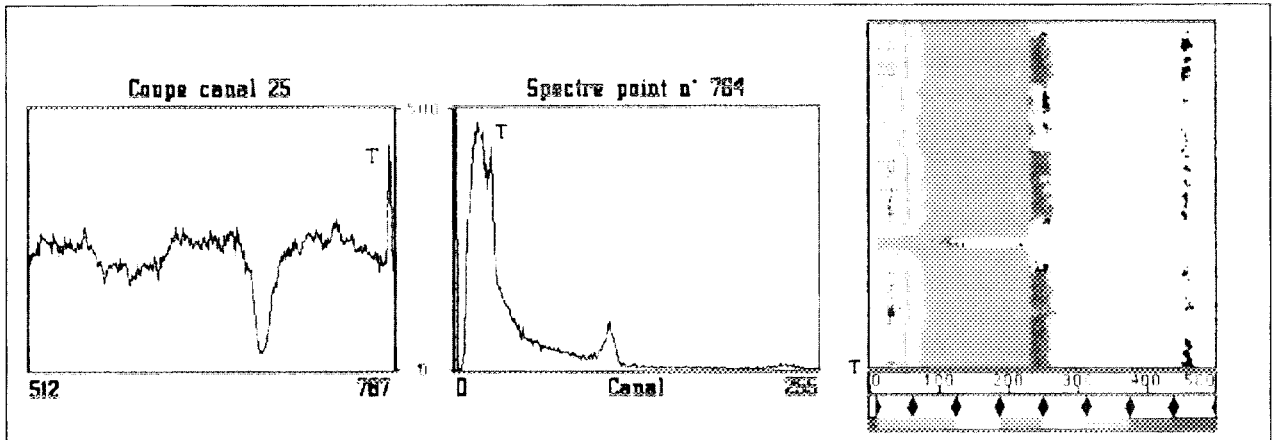


Figure 6 :  $^{99}\text{Tc}_m$  source detection during survey of area 3.

The Cs3 and Co1 sources of close activities (7,5 and 7 mCi) were localised at the same place (figure 7). The evolution of channel 190 (1173 keV) shows clearly the cobalt source. The attendance of an anomaly can be seen at channel 110 (662 keV), but it's impossible to conclude about the attendance of a caesium source because these photons should have been emitted by the cobalt source and scattered by the atmosphere.

The detection limit is function of the natural background of the spot. For a caesium source the detection threshold was about 10 mCi on area 3, for a superficial concentration about 50 kBq/m<sup>2</sup>. Therefore the Cs3 source was too little active for being detected with reliability. In France the  $^{137}\text{Cs}$  background is about 1 to 2 kBq/m<sup>2</sup> and the detection threshold for a source is about 1 mCi.

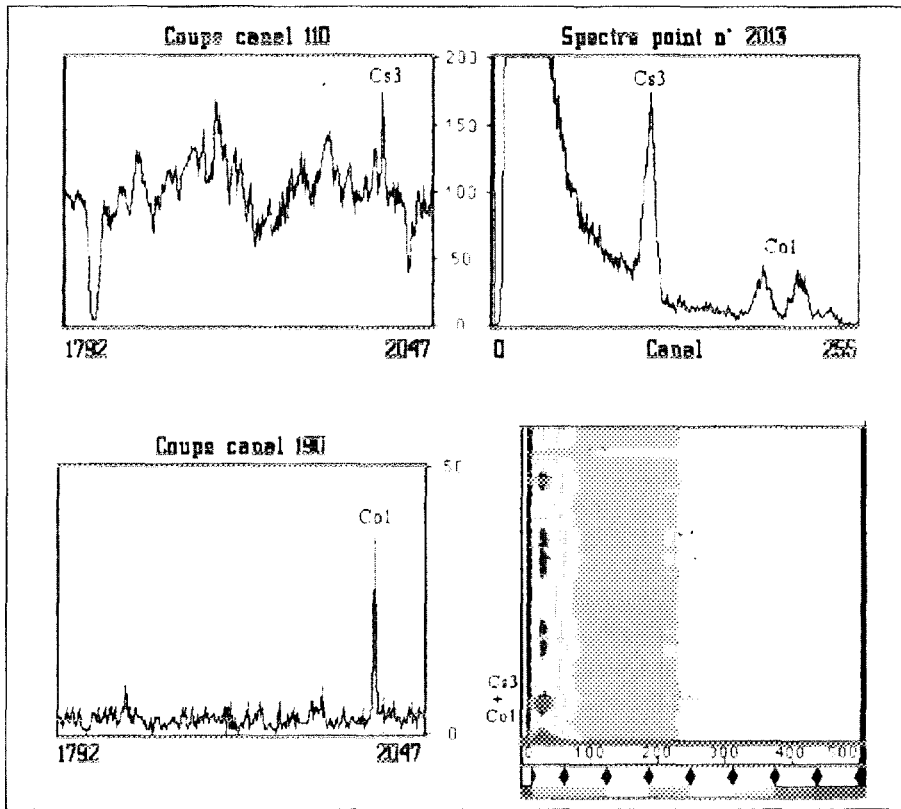


Figure 7 : Cs3 and Co1 detection during survey of area 3.

**Conclusion :**

After a detailed processing of measurements, ten sources have been clearly pointed out. The other sources were collimated or their activities were close or lower than the system detection threshold because of the high level caesium background.

The trace of four other sources has also been detected with the knowledge of their positions but their contributions are too weak to conclude about their attendance.

## 2.3 *Isoactivity maps*

### 2.3.1 Spectral analysis

Data processing is achieved by a new algorithm for spectral analysis, suitable AGRS operational conditions. This algorithm can detect and calculate full absorption picks area associated to ground nuclides. The short sample time (2s. in Finland) and the detection altitude (about 50m.) generate a poor counting statistic and a low signal/noise ratio.

Classical processing software are unusable in these conditions, and a specific algorithm has been developed. The counting fluctuations are removed by the use of numerical filters which take into account picks characteristics (gaussian shape, variation of FWHM with energy...)

After filtering, pick detection is done by the study of first and second derivatives.

Full absorption picks area is computed after calculation and subtraction of the background (figure 7).

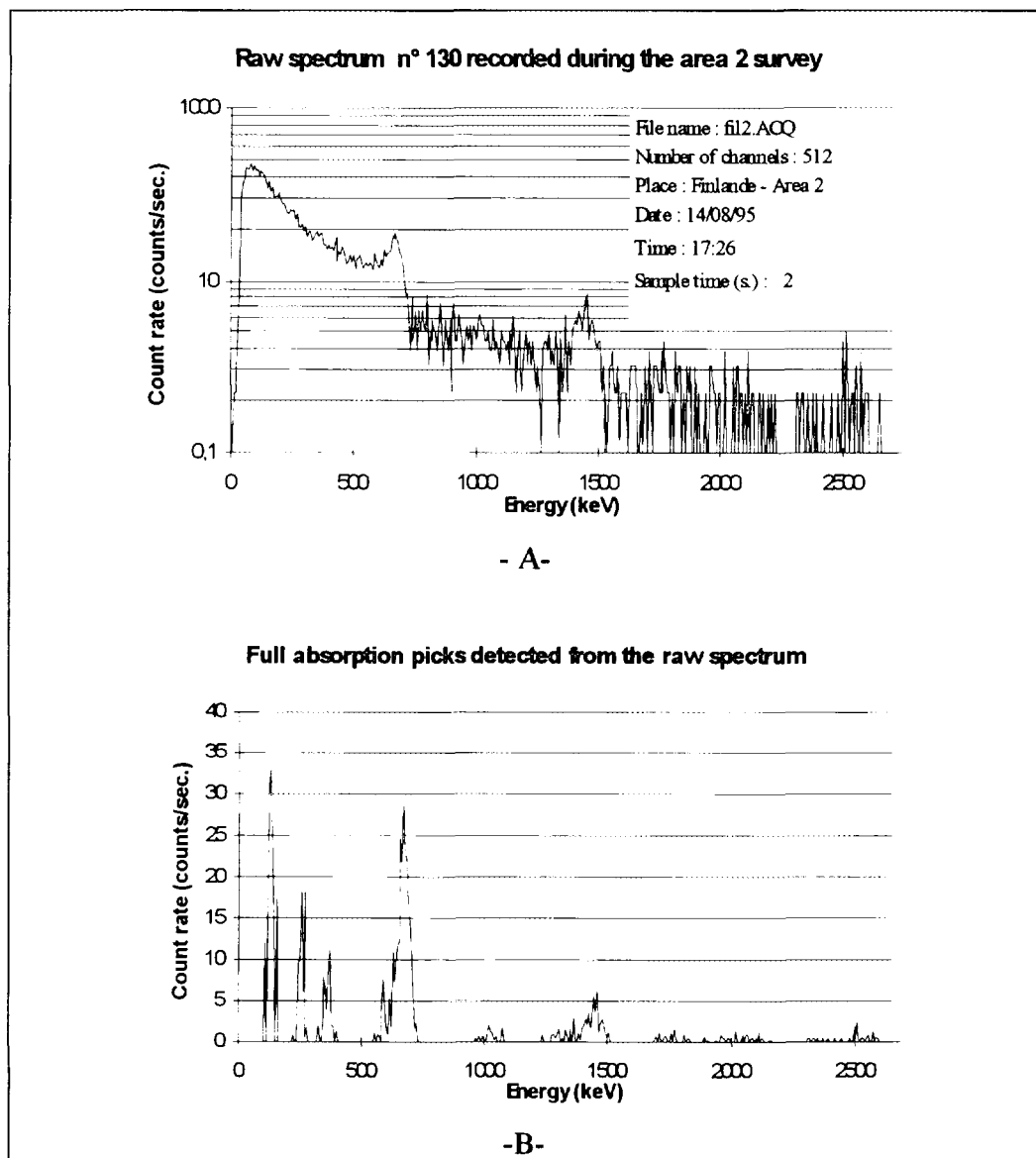


Figure 8 : Calculation of full absorption picks (B) by processing of a raw spectrum(A).

Nuclides are identified in a reference table. This list also contains variation laws of the detector response with altitude, and energy to calculate activities to calculate ground contaminations.

Data processing of the records produces the following results :

**Area n°2 :**

Source file : FIL2.ACQ

Sample time : 2 seconds

Number of measurements : 3100

Nuclides	Energy (keV)	Number of detections	Average activity	Experimental precision (%)	Statistical precision (%)	Average detection threshold
<sup>212</sup> Pb	238	290		35	19	
<sup>214</sup> Pb	295	482		34	27	
<sup>228</sup> Ac	338	11		32	29	
<sup>214</sup> Pb	352	515		36	28	
<sup>137</sup> Cs	662	3091	64.3 kBq/m <sup>2</sup>	38	3	1.6 kBq/m <sup>2</sup>
<sup>134</sup> Cs	795	2210	4.0 kBq/m <sup>2</sup>	36	17	0.5 kBq/m <sup>2</sup>
<sup>228</sup> Ac	911	2147	12.0 kBq/m <sup>2</sup>	37	25	2.7 kBq/m <sup>2</sup>
<sup>40</sup> K	1461	3096	380.1 Bq/kg	37	9	16.3 Bq/kg
<sup>214</sup> Bi	1764	2826	24.9 Bq/kg	32	22	3.5 Bq/kg
<sup>232</sup> Th	2615	3100	23.1 Bq/kg	33	17	1.4 Bq/kg

**Table 1 : Synthesis of nuclides detection over area n°2.**

**Area n°3 :**

Source file : FIL3.ACQ

Sample time : 2 seconds

Number of measurements : 2600

Nuclides	Energy (keV)	Number of detections	Average activity	Experimental precision (%)	Statistical precision (%)	Average detection threshold
<sup>212</sup> Pb	238	149		47	16	
<sup>214</sup> Pb	295	461		42	25	
<sup>228</sup> Ac	338	187		42	26	
<sup>214</sup> Pb	352	441		39	26	
<sup>137</sup> Cs	662	2562	51.5 kBq/m <sup>2</sup>	39	2	1.5 kBq/m <sup>2</sup>
<sup>134</sup> Cs	795	1907	3.4 kBq/m <sup>2</sup>	38	14	0.6 kBq/m <sup>2</sup>
<sup>228</sup> Ac	911	1956	8.7 kBq/m <sup>2</sup>	41	22	2.3 kBq/m <sup>2</sup>
<sup>40</sup> K	1461	2584	365.5 Bq/kg	41	7	19.2 Bq/kg
<sup>214</sup> Bi	1764	2388	21.3 Bq/kg	34	22	3.7 Bq/kg
<sup>232</sup> Th	2615	2590	25.4 Bq/kg	36	15	1.6 Bq/kg

**Table 2 : Synthesis of nuclides detection over area n°3.**

Only nuclides which have peaks of energies higher than 662 keV are detected in a great proportion of measurements. The high caesium concentration creates an important background at low energies and the detection at these energies is disturbed.

The experimental precision of activities represents :

- Spatial variations of nuclides concentration on the area,
- Statistical fluctuations of counting (which depends on concentration).

The statistical precision represents the uncertainty associated with the calculation of peak area. The detection threshold is computed for each nuclide and depends essentially on the scattering background intensity.

### 2.3.2 Calibration

The evaluation of activities requires the knowledge of variation laws of the detector response with the flying altitude and the energy of incident photons.

#### Laboratory calibration :

The design of an experimental set-up to simulate fly conditions in laboratory has been done to perform calibration measurements. The active surface is reproduced by point sources or active carpets. The surface dimensions are finite (about 2 meters per 2 meters) and the response calculation to an infinite contamination requires the correction of these measurements. Correction factors are function of the absorber thickness and of the energy and the position of the sources.

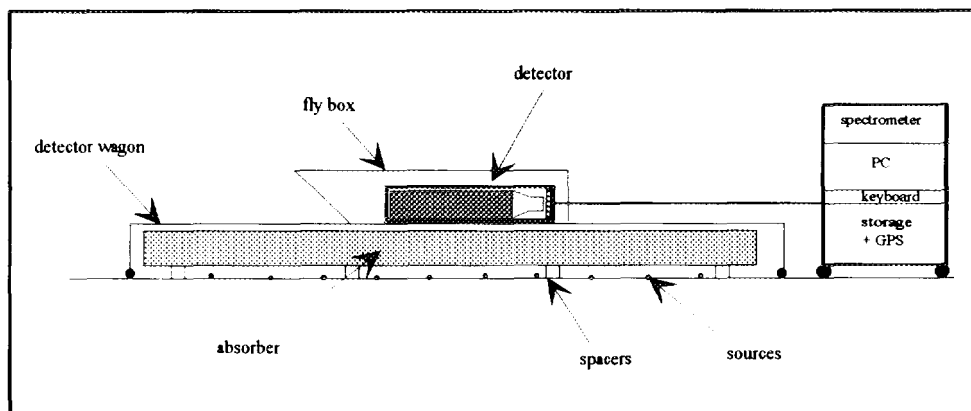


**Figure 9 : Laboratory calibration set-up.**

With this set-up, detector response measurements can be achieved in standard conditions (293°K, 1 bar). Only superficial distributions of contaminations are reproduced, so response to volume distribution should be deduced from superficial response by numerical calculations.

#### Flight calibration :

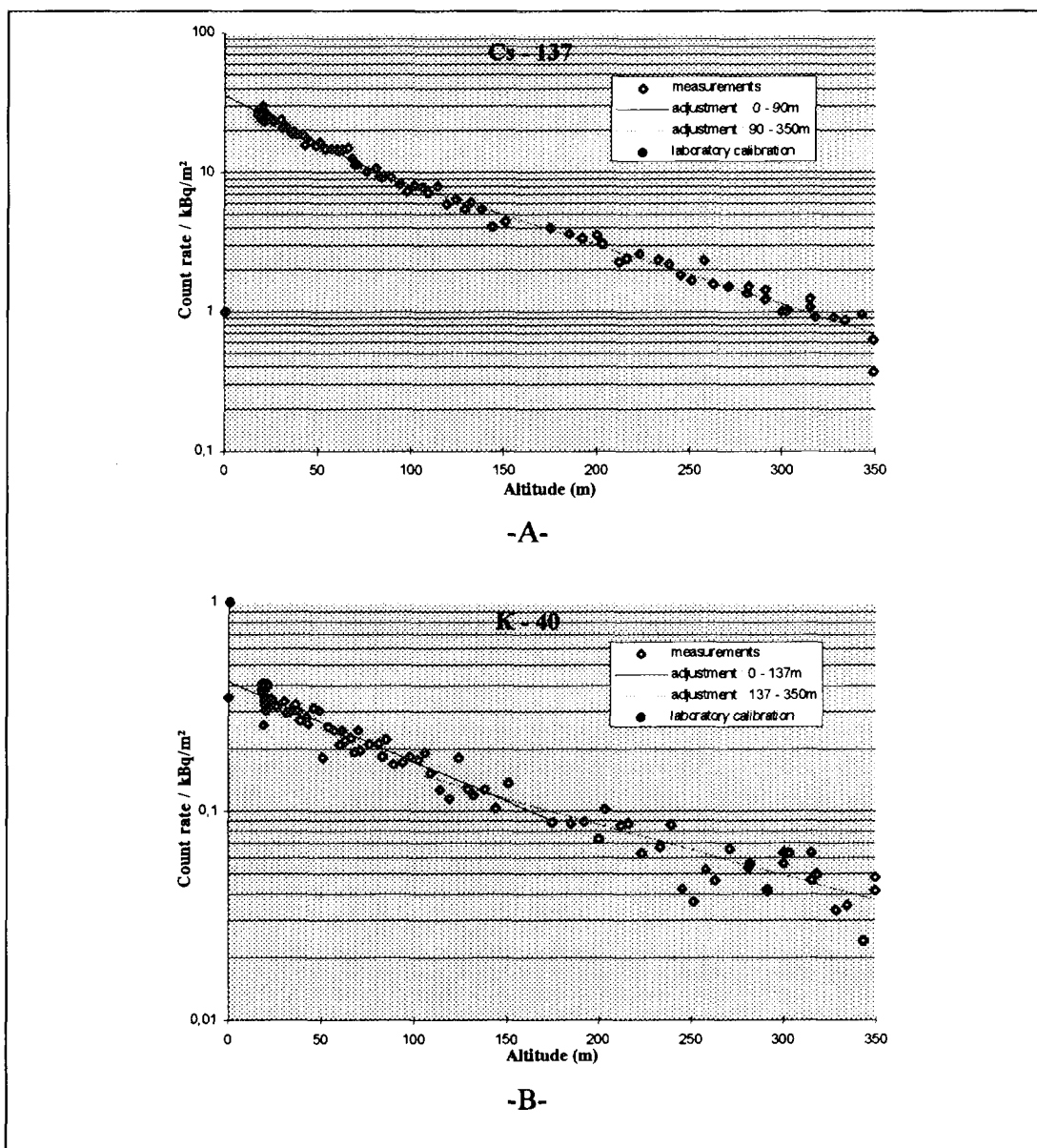
Usually, calibration factors are calculated in laboratory and corrected for experimental conditions (temperature, pressure, hygrometry). During RESUME 95, we also recorded response in flight over the calibration area at Vesihvema airfield.

Nuclides	Concentration
<sup>137</sup> Cs	50 ± 7 kBq/m <sup>2</sup>
<sup>40</sup> K	600 ± 60 Bq/kg
<sup>214</sup> Bi	50 ± 11 Bq/kg
<sup>232</sup> Th	36 ± 4 Bq/kg

**Table 3 : Area n°1 concentrations (Airfield).**

### Comparison of results :

Laboratory and flight responses have been compared (figure 3). The three pictures shows full absorption picks area per unit of ground concentration (kBq/m<sup>2</sup> or Bq/kg). The variations laws of caesium response are in good agreement. In return, potassium and thorium responses recorded in laboratory are lower of about 20%. This difference probably comes from the ground composition assumption (used to calculate volume response from laboratory superficial response) which is probably different from real soil of Finland. Reference concentrations on the airfield have been calculated with incertitudes of about 10 to 20%, so the difference between fly and laboratory response isn't significant.



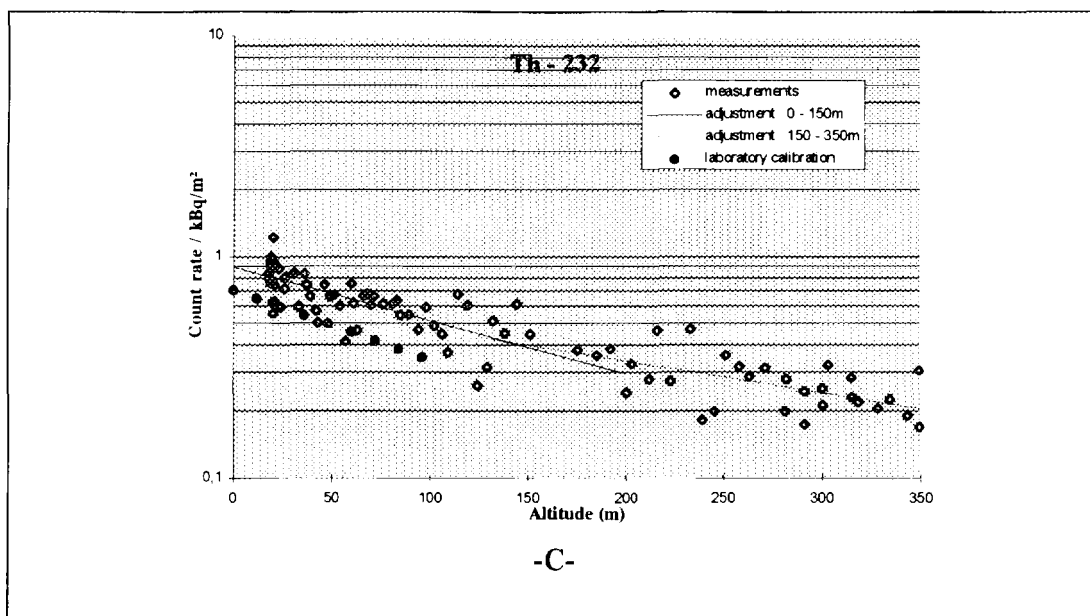


Figure 10 : Variation of detector response with altitude for  $^{137}\text{Cs}$ ,  $^{40}\text{K}$  and  $^{232}\text{Th}$ .

### 2.3.3 Isoactivity maps

The isoactivity maps of caesium fall-out and natural background ( $^{40}\text{K}$ ,  $^{214}\text{Bi}$  and  $^{232}\text{Th}$ ) have been achieved on both areas. All maps are compressed in « JPEG » format and added to this report. Here are presented only three maps of  $^{137}\text{Cs}$  and  $^{40}\text{K}$  concentrations.

#### Radioactive fall-out :

Caesium fall-out is always very active today. On area n°2,  $^{137}\text{Cs}$  average concentration is about 65 kBq/m<sup>2</sup>, with some forest parts reaching 110 kBq/m<sup>2</sup>. For cultures areas or villages (Auttoinen for example, at south-east of area n°2),  $^{137}\text{Cs}$  contamination is between 30 et 40 kBq/m<sup>2</sup>. The activity is approximately twice weaker in villages where the fall-out has been washed or in cultivated areas where the soil has been turned over.

The area n°3 can be divided into two parts of different concentrations. At south-east  $^{137}\text{Cs}$  concentration is comparable with area 2 (about 60 kBq/m<sup>2</sup>) and at north-west the concentration is between 40 et 50 kBq/m<sup>2</sup>.

$^{134}\text{Cs}$  concentration on both areas is proportional to  $^{137}\text{Cs}$  concentration with a ratio of about thirty, in accordance with today's proportions of Tchernobyl fall-out.  $^{134}\text{Cs}$  maps show great variations because of the great count rate fluctuations at these concentrations (1 à 8 kBq/m<sup>2</sup>). These fluctuations aren't significant.

#### Natural activity :

The isoactivity maps of  $^{40}\text{K}$ ,  $^{214}\text{Bi}$  et  $^{232}\text{Th}$  show activity levels which are comparable with measurements recorded in France. Concentrations are rather homogeneous with some local increasing on villages or cultures probably because there is an important attenuation by trees above forest areas.

## 2.4 Conclusion

New developments concerning spectral analysis and calibration of airborne measurements have been tested during this exercise for mapping caesium fall-out and natural activity. The results have showed a detection limit weaker than concentrations of major natural nuclides ( $^{40}\text{K}$ ,  $^{214}\text{Bi}$  et  $^{208}\text{Tl}$ ) and have confirmed the good performances of these new processing methods.

Our results are in good agreement with other teams results but some differences between each team results show the necessity of an harmonisation of processing methods.

## ***3. Ground measurements***

### **3.1 Experimental conditions**

#### **3.1.1 Measurement points**

The measurements were performed at specified points on area n° 1 (airfield) and n° 2.

On area n° 1, 21 measurements were recorded at specified grid points with a sample time of 900 seconds (with an average dead time about 23%) :

- 6 points on circles n° 2, 4 et 5.
- 2 points on circle n° 3 (n° 1 et 4)
- The central point.

On area n° 2, the measurements were performed at six different places :

- 3 points (A, B, C) defined by organisers, with a sample time of 600 seconds for points (A0, B0, C0), 300 seconds at one meter at north (A1, B1, C1) and 300 seconds at one meter at south (A2, B2, C2).
- 3 points (N, M, S) chosen respectively in the north, in the middle and in the south of area n°2 (with a sample time of 600 seconds).

All spectra and doses rates measurements were recorded at one meter above the ground.

#### **3.1.2 Timing**

The measurements on places defined by organisers were achieved on Tuesday, and the three additional points on area 2 recorded on Wednesday after airborne survey. Spectral analysis was achieved on Wednesday.

#### **3.1.3 Experimental device**

##### **In situ gamma spectrometry:**

The Ge detector dedicated to these measurements (with an efficiency of 15%) broke down the day before the beginning of measurements, and was replaced by one lent by the German team. The spectrometer is factured by Eurisys company and records spectra on 4096 channels.

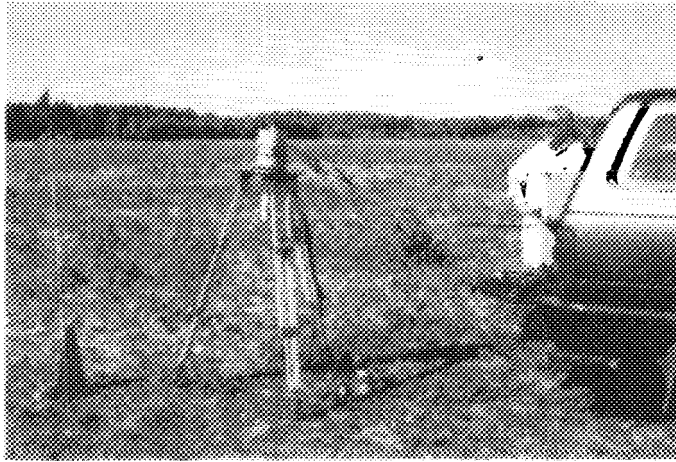


**Figure 11 : In situ gamma measurements.**

**Extra measurements:**

The dose rate measurements were performed with a Scintomat 6134A (Béfic).  
 Some total count rate measurements were done with a hand hold gamma detector called DG5 (Novelec).  
 These measurements are presented to compare with germanium measurements.

3.2 Calibration

**3.2.1 Superficial activity**

The 15% Ge detector that should be used was calibrated for superficial concentrations and point sources. The calibration of German detector was done with the same point sources used for the calibration of our detector.

For the natural activity, only the major nuclides have been considered :

- Thorium series :  $^{208}\text{Tl}$ ,  $^{228}\text{Ac}$ ,  $^{212}\text{Pb}$
- Uranium series :  $^{214}\text{Pb}$ ,  $^{214}\text{Bi}$
- Potassium :  $^{40}\text{K}$

Concentrations have been calculated from one pick for all nuclides, except for  $^{134}\text{Cs}$  : picks at 604 and 795 keV have been considered and the average activity calculated.

**3.2.2 Dose rate**

One meter above a uniform and superficial contamination, the dose rate calculations have been performed from the following formula <sup>1</sup>:

$$I(R/h) = 14. A.E.F$$

---

<sup>1</sup> : H. Joffre, « Génie atomique », part 1.

with  $A$  : activity in Ci/m<sup>2</sup>,  
 $E$  : energy in MeV,  
 $\Gamma$  : emission rate.

Calculations have been done for all major spectrum lines and added to obtain the total dose rate of the nuclide.

### 3.3 Results

#### 3.3.1 Superficial activity

##### Area n°1 :

The table 4 shows activities of major natural nuclides.

The table 5 compares these values, summed per series, with man-made activity (caesium fall-out).

Point	<sup>214</sup> Bi	<sup>214</sup> Pb	<sup>208</sup> Tl	<sup>228</sup> Ac	<sup>213</sup> Pb	<sup>40</sup> K
A1-0-0	2.63	1.3	1.27	1.80	0.76	57.4
A1-2-1	2.71	1.22	1.22	1.65	1.13	58.4
A1-2-2	2.85	1.23	1.23	1.79	0.63	58.1
A1-2-3	2.89	1.47	1.09	1.63	1.20	57.7
A1-2-4	2.95	0.87	1.16	1.88	1.18	60.2
A1-2-5	3.01	1.70	1.02	1.67	1.21	52.9
A1-2-6	2.77	1.19	1.33	1.54	0.38	56.4
A1-3-1	2.81	1.26	1.10	1.54	1.39	57.6
A1-3-4	3.25	1.66	1.31	2.14	1.97	55.9
A1-4-1	3.43	1.58	1.30	1.91	0.73	71.3
A1-4-2	3.07	1.29	1.09	1.66	1.37	62.9
A1-4-3	2.99	1.72	1.30	1.68	0.45	62.6
A1-4-4	3.16	1.32	1.12	1.38	0.82	57.5
A1-4-5	2.88	1.35	1.25	1.98	1.10	60.3
A1-4-6	2.70	1.49	1.08	1.61	1.05	58.7
A1-5-1	2.67	1.25	1.04	1.57	1.38	65.9
A1-5-2	3.11	1.39	1.32	1.69	1.47	62.6
A1-5-3	3.89	2.02	1.47	2.12	1.63	70.0
A1-5-4	3.71	1.75	1.26	2.08	1.03	62.2
A1-5-5	3.57	2.05	1.45	1.66	0.88	61.7
A1-5-6	2.63	1.67	1.39	1.92	1.67	61.4

**Table 4 : Major natural nuclides activities (in kBq/m<sup>2</sup>).**

Point	<sup>134</sup> Cs	<sup>137</sup> Cs	Th series	U series	K	Total Natural	Total Cs	Cs/Nat ratio
A1-0-0	2.01	56.7	3.83	3.93	57.4	65.2	58.7	0.90
A1-2-1	1.78	58.3	4.00	3.93	58.4	66.3	60.1	0.91
A1-2-2	1.78	58.7	3.65	4.08	58.1	65.8	60.5	0.92
A1-2-3	1.70	56.3	3.92	4.36	57.7	66.0	58.0	0.87
A1-2-4	1.46	54.4	4.22	3.82	60.2	68.2	55.9	0.82
A1-2-5	1.62	54.7	3.90	4.71	52.9	61.5	56.3	0.92
A1-2-6	1.73	56.6	3.25	3.96	56.4	63.6	58.3	0.92
A1-3-1	1.95	58.9	4.03	4.07	57.6	65.7	60.9	0.93
A1-3-4	1.89	56.5	5.42	4.91	55.9	66.2	58.5	0.88
A1-4-1	2.23	67.3	3.94	4.01	71.3	79.2	69.5	0.88
A1-4-2	2.10	65.2	4.12	4.36	62.9	71.4	67.3	0.94
A1-4-3	2.07	66.1	3.43	4.71	62.6	70.7	68.2	0.96
A1-4-4	2.11	63.2	3.32	4.48	57.5	65.3	65.3	1
A1-4-5	2.13	63.8	4.33	4.23	60.3	68.9	65.9	0.96
A1-4-6	1.89	61.7	3.74	4.19	58.7	66.6	63.6	0.95
A1-5-1	0.90	30.9	3.99	3.92	65.9	73.8	31.8	0.43
A1-5-2	1.72	62.2	4.48	4.50	62.6	71.6	63.9	0.89
A1-5-3	2.12	62.6	5.22	5.91	70.0	81.1	64.7	0.80
A1-5-4	1.80	55.1	4.37	5.46	62.2	72.0	56.9	0.79
A1-5-5	1.35	44.6	3.99	5.58	61.7	71.3	45.9	0.64
A1-5-6	1.11	41.4	4.98	4.30	61.4	70.7	42.5	0.60

Table 5 : Comparison of caesium and natural activities (in kBq/m<sup>2</sup>).

Area n° 2 :

The tables 6 and 7 are similar to tables 4 and 5 but for area n°2. For each point A, B and C three measurements have been performed and the average value calculated.

Point	<sup>214</sup> Bi	<sup>214</sup> Pb	<sup>208</sup> Tl	<sup>228</sup> Ac	<sup>212</sup> Pb	<sup>40</sup> K
A2-A-0	3.10	1.18	1.36	1.44	1.05	64.0
A2-A-1	3.53	1.68	1.23	1.40	1.46	61.6
A2-A-2	3.11	1.72	1.28	1.19	0.55	66.1
Average A	3.25	1.53	1.29	1.34	1.02	63.9
A2-B-0	1.56	1.08	1.02	1.29	0.73	55.9
A2-B-1	1.53	0.63	1.07	0.99	1.12	47.1
A2-B-2	1.87	1.17	0.92	1.70	0.61	51.9
Average B	1.65	0.96	1.00	1.33	0.82	51.6
A2-C-0	2.97	0.92	1.00	1.39	1.71	69.0
A2-C-1	2.12	1.73	1.03	0.77	0.99	64.7
A2-C-2	2.45	2.09	0.80	1.38	0.94	68.7
Average C	2.51	1.58	0.94	1.18	1.21	67.5
A2-N	3.10	1.77	1.41	2.04	2.16	71.2
A2-M	2.47	1.81	1.17	1.57	0.99	63.5
A2-S	2.72	1.45	1.07	1.37	0.87	59.5

Table 6 : Major natural nuclides activities (in kBq/m<sup>2</sup>).

Point	<sup>134</sup> Cs	<sup>137</sup> Cs	Th series	U series	K	Total Natural	Total Cs	Cs/Nat ratio
A2-A-0	2.87	94.2	3.85	4.28	64.0	72.3	97.0	1.35
A2-A-1	2.74	89.1	4.09	5.21	61.6	75.4	91.8	1.22
A2-A-2	2.80	94.8	3.02	4.83	66.1	73.9	97.6	1.32
Average A	2.80	92.7	3.65	4.77	63.9	73.9	95.5	1.30
A2-B-0	2.06	66.1	3.04	2.64	55.9	61.6	68.2	1.11
A2-B-1	1.88	66.7	3.18	2.16	47.1	50.3	68.6	1.37
A2-B-2	1.81	66.5	3.23	3.04	51.9	58.2	68.3	1.18
Average B	1.92	66.4	3.15	2.61	51.6	56.7	68.3	1.20
A2-C-0	2.99	100.3	4.10	3.89	69.0	77.0	103.3	1.35
A2-C-1	2.86	99.9	2.79	3.85	64.7	71.3	102.8	1.45
A2-C-2	3.83	101.2	3.12	4.54	68.7	76.3	105.0	1.37
Average C	3.22	100.5	3.34	4.09	67.5	74.8	103.7	1.39
A2-N	1.95	76.5	5.61	4.87	71.2	81.7	78.6	0.96
A2-M	2.50	83.7	3.73	4.28	63.5	71.5	86.1	1.20
A2-S	2.74	101.7	3.31	4.17	59.5	67.0	104.8	1.61

Table 7 : Comparison of caesium and natural activities (in kBq/m<sup>2</sup>).

### 3.3.2 Dose rate

The table 8 shows dose rate contribution of major natural nuclides.

The table 9 compares these values, added per series, with man-made dose rate (caesium fallout).

#### Area 1 :

Point	<sup>214</sup> Bi	<sup>214</sup> Pb	<sup>208</sup> Tl	<sup>228</sup> Ac	<sup>212</sup> Pb	<sup>40</sup> K
A1-0-0	7.20	0.89	15.5	3.20	0.30	33.8
A1-2-1	7.40	0.84	14.9	2.90	0.44	34.4
A1-2-2	7.80	0.84	15.0	3.10	0.25	34.2
A1-2-3	7.90	1.00	13.3	2.90	0.47	34.0
A1-2-4	8.10	0.60	14.1	3.30	0.46	35.5
A1-2-5	8.20	1.16	12.4	2.90	0.48	31.2
A1-2-6	7.60	0.82	16.2	2.70	0.15	33.3
A1-3-1	7.70	0.86	13.4	2.70	0.55	33.9
A1-3-4	8.90	1.14	16.0	3.80	0.77	32.9
A1-4-1	9.40	1.08	15.8	3.40	0.29	42.0
A1-4-2	8.40	0.88	13.3	2.90	0.54	37.1
A1-4-3	8.20	1.18	15.8	3.00	0.18	36.9
A1-4-4	8.70	0.90	13.6	2.40	0.32	33.9
A1-4-5	7.90	0.92	15.2	3.50	0.43	35.6
A1-4-6	7.40	1.02	13.2	2.80	0.41	34.6
A1-5-1	7.30	0.85	12.7	2.80	0.50	38.8
A1-5-2	8.50	0.95	16.1	3.00	0.58	36.8
A1-5-3	10.60	1.38	17.9	3.70	0.64	41.3
A1-5-4	10.10	1.20	15.3	3.70	0.40	36.7
A1-5-5	9.80	1.38	17.7	2.90	0.35	36.4
A1-5-6	7.20	1.14	16.9	3.40	0.65	36.2

Table 8 : Natural nuclide dose rates (in Gy/h).

Point	<sup>134</sup> Cs	<sup>137</sup> Cs	Th series	U series	K	Total Natural	Total Cs	Cs/Nat ratio
A1-0-0	10.3	121.0	19.0	8.1	33.8	60.9	131.3	2.17
A1-2-1	8.5	124.4	18.2	8.2	34.4	60.8	132.9	2.17
A1-2-2	8.6	125.2	18.3	8.6	34.2	61.1	133.8	2.17
A1-2-3	8.1	120.1	16.7	8.9	34.0	59.6	128.2	2.17
A1-2-4	7.0	116.1	17.9	8.6	35.5	62.0	123.1	2.00
A1-2-5	7.7	116.7	15.8	9.4	31.2	56.4	124.4	2.22
A1-2-6	8.3	120.8	19.0	8.4	33.3	60.7	129.1	2.13
A1-3-1	9.4	125.7	16.7	8.6	33.9	59.2	135.1	2.27
A1-3-4	9.2	120.6	20.6	10.0	32.9	63.5	129.8	2.04
A1-4-1	10.7	143.6	19.5	10.5	42.0	72.0	154.3	2.13
A1-4-2	10.1	139.1	16.7	9.3	37.1	63.1	149.2	2.38
A1-4-3	10.0	141.1	19.0	9.4	36.9	65.3	151.1	2.32
A1-4-4	10.4	134.9	16.3	9.6	33.9	59.8	145.3	2.44
A1-4-5	10.4	136.1	19.1	8.8	35.6	63.5	146.5	2.32
A1-4-6	9.1	131.7	16.5	8.4	34.6	59.5	140.8	2.38
A1-5-1	4.3	65.9	16.0	8.1	38.8	62.9	70.2	1.11
A1-5-2	8.2	132.7	19.7	9.4	36.8	65.9	140.9	2.12
A1-5-3	10.3	133.6	22.2	12.0	41.3	75.5	143.9	1.92
A1-5-4	8.7	117.6	19.4	11.3	36.7	67.4	126.3	1.88
A1-5-5	6.5	95.2	20.9	11.2	36.4	68.5	101.7	1.49
A1-5-6	5.3	88.3	20.9	8.3	36.2	65.4	93.6	1.43

Table 9 : Comparison of caesium and natural dose rates (in nGy/h).

The following table shows the comparison of dose rate measurements with three different apparatus. The DG5 only performs a total count measurement but we can appreciate the proportionality with Ge and scintomat results.

Point	Spectre nGy/h	Scintomat nGy/h	DG5 c/s	Point	Spectre nGy/h	Scintomat nGy/h	DG5 c/s
A1-0-0	192	180	195	A1-4-1	226	190	225
A1-2-1	194	200	210	A1-4-2	212	200	225
A1-2-2	195	180	220	A1-4-3	216	250	215
A1-2-3	188	230	220	A1-4-4	205	220	215
A1-2-4	185	170	210	A1-4-5	210	250	220
A1-2-5	181	180	205	A1-4-6	200	210	220
A1-2-6	190	170	210	A1-5-1	133	140	150
A1-3-1	194	170	210	A1-5-2	207	250	200
A1-3-4	193	220	215	A1-5-3	219	200	220
				A1-5-4	194	170	215
				A1-5-5	170	170	190
				A1-5-6	159	220	175

Tableau 10 : Comparison of dose rate measurements performed with different apparatus.

**Area 2 :**

The three following tables presents dose rates measurements on area 2.

Point	<sup>214</sup> Bi	<sup>214</sup> Pb	<sup>208</sup> Tl	<sup>228</sup> Ac	<sup>212</sup> Pb	<sup>40</sup> K
A2-A-0	8.50	0.81	16.6	2.50	0.41	37.7
A2-A-1	9.70	1.15	15.0	2.50	0.57	36.3
A2-A-2	8.50	1.18	15.6	2.10	0.22	38.9
Average A	8.90	1.05	15.7	2.37	0.40	37.6
A2-B-0	4.30	0.74	12.4	2.30	0.29	33.0
A2-B-1	4.20	0.43	13.0	1.70	0.44	27.8
A2-B-2	5.10	0.80	11.2	3.00	0.24	30.6
Average B	4.53	0.66	12.2	2.33	0.32	30.5
A2-C-0	8.10	0.63	12.2	2.40	0.67	40.7
A2-C-1	5.80	1.19	12.5	1.40	0.39	38.1
A2-C-2	6.70	0.55	9.8	2.40	0.37	40.5
Average C	6.90	0.79	11.5	2.06	0.48	39.8
A2-N	8.50	1.21	17.2	3.60	0.85	42.0
A2-M	6.80	1.24	14.3	2.80	0.39	37.4
A2-S	7.50	0.99	13.0	2.40	0.34	35.1

**Table 11 : Natural nuclide dose rates (in Gy/h).**

Point	<sup>134</sup> Cs	<sup>137</sup> Cs	Th series	U series	K	Total Natural	Total Cs	Cs/Nat ratio
A2-A-0	13.60	201.0	19.51	9.31	37.7	66.5	214.6	3.22
A2-A-1	13.30	190.0	18.07	10.85	36.3	65.7	203.3	3.12
A2-A-2	13.50	202.3	17.92	9.68	38.9	66.5	215.8	3.33
Average A	13.47	197.8	18.5	9.94	37.6	66.2	211.2	3.22
A2-B-0	10.30	141.1	14.99	5.04	33.0	53.0	151.4	2.85
A2-B-1	9.00	142.3	15.14	4.63	27.8	47.6	151.3	3.22
A2-B-2	8.70	139.7	14.44	5.90	30.6	50.9	148.4	2.94
Average B	9.33	141.0	14.85	5.019	30.5	50.5	150.4	3.03
A2-C-0	14.70	214.0	15.27	8.73	40.7	64.7	228.7	3.57
A2-C-1	13.80	213.3	14.29	6.99	38.1	59.4	227.1	3.84
A2-C-2	18.70	216.1	12.57	7.25	40.5	60.3	234.8	3.84
Average C	15.73	214.7	14.04	7.66	39.8	61.5	230.2	3.70
A2-N	10.00	163.3	21.65	9.71	42.0	73.4	173.3	2.38
A2-M	11.60	178.6	17.49	8.04	37.4	62.9	190.2	3.03
A2-S	15.00	217.0	15.74	8.49	35.1	59.3	232.0	3.85

**Table 12 : Comparison of caesium and natural dose rates (in nGy/h).**

Point	Spectre nGy/h	Scintomat nGy/h	DG5 c/s	Point	Spectre nGy/h	Scintomat nGy/h	DG5 c/s
A2-A-0	280			A2-C-0	293		
A2-A-1	268			A2-C-1	287		
A2-A-2	282			A2-C-2	295		
Average A	277	250	285	Average C	292	290	340
A2-B-0	227			A2-N	247	250	290
A2-B-1	199			A2-M	253	260	290
A2-B-2	199			A2-S	291	300	345
Average B	208	200	225				

Tableau 13 : Comparison of dose rate measurements performed with different apparatus.

### 3.4 Conclusion

Measurements specified by organisers were achieved in respect of time allowed. In spite of the exchange of detector just before the beginning and a relative calibration, results from germanium measurements are in good agreement with Scintomat dose rate measurements.

#### 3.4.1 Superficial concentrations

On area 1, natural activity is rather uniform with a average value about 70 kBq/m<sup>2</sup>. Potassium contribution represents approximately 85% of the activity. <sup>137</sup>Cs concentration is about 60 kBq/m<sup>2</sup>, but with more important variations depending on point location.

Measurements performed on circle 5 are very different for caesium fall-out. The lower values have been recorded under the trees (points 5-1 and 5-6) with a ratio of about two with the average value on the airfield.

On area 2, natural activity is similar to area 1, but caesium values are greater of 40%, in particular in the south of the area. The maximum <sup>137</sup>Cs concentration recorded on this area reaches 100 kBq/m<sup>2</sup>.

#### 3.4.2 Dose rate

Dose rate variations are proportional to activity variations. The caesium fall-out dose rate is approximately twice bigger than the natural dose rate.

On area 1, caesium dose rate is about 140 nGy/h and natural dose rate about 65 nGy/h. The average total dose rate is about 205 nGy/h.

On area 2, caesium dose rate is more important and reaches 215 nGy/h. The natural contribution is similar to area one and the average total dose rate is about 280 nGy/h. Caesium contribution represents about 75% of the total dose rate.

## ***4. conclusion***

This exercise has confirmed the ability of airborne gamma spectrometry to evaluate quickly man-made and natural activity, and to perform lost sources searching.

In spite of restricting conditions (distance, reduce team, respect of time allowed), Hélinuc team have achieved all tasks defined by the organisers. This exercise, very close to an accidental situation, has been a good test for equipment and has shown the ability of the team to operate in this conditions.

The new developments concerning spectral analysis and calibration of airborne measurements were tested during this exercise for mapping caesium fall-out and natural activity. Airborne results are in good agreement with in situ measurements and confirms the performances of new airborne data processing methods. For  $^{137}\text{Cs}$  fall-out, the maximum concentration recorded reaches 100 to 110 kBq/m<sup>2</sup> on area 2, for both airborne and in situ measurements.

The detection of a great part of the hidden sources has confirmed the sensibility of our device.

Our results are in good agreement with other teams results but some differences show the necessity of an harmonisation of processing methods.

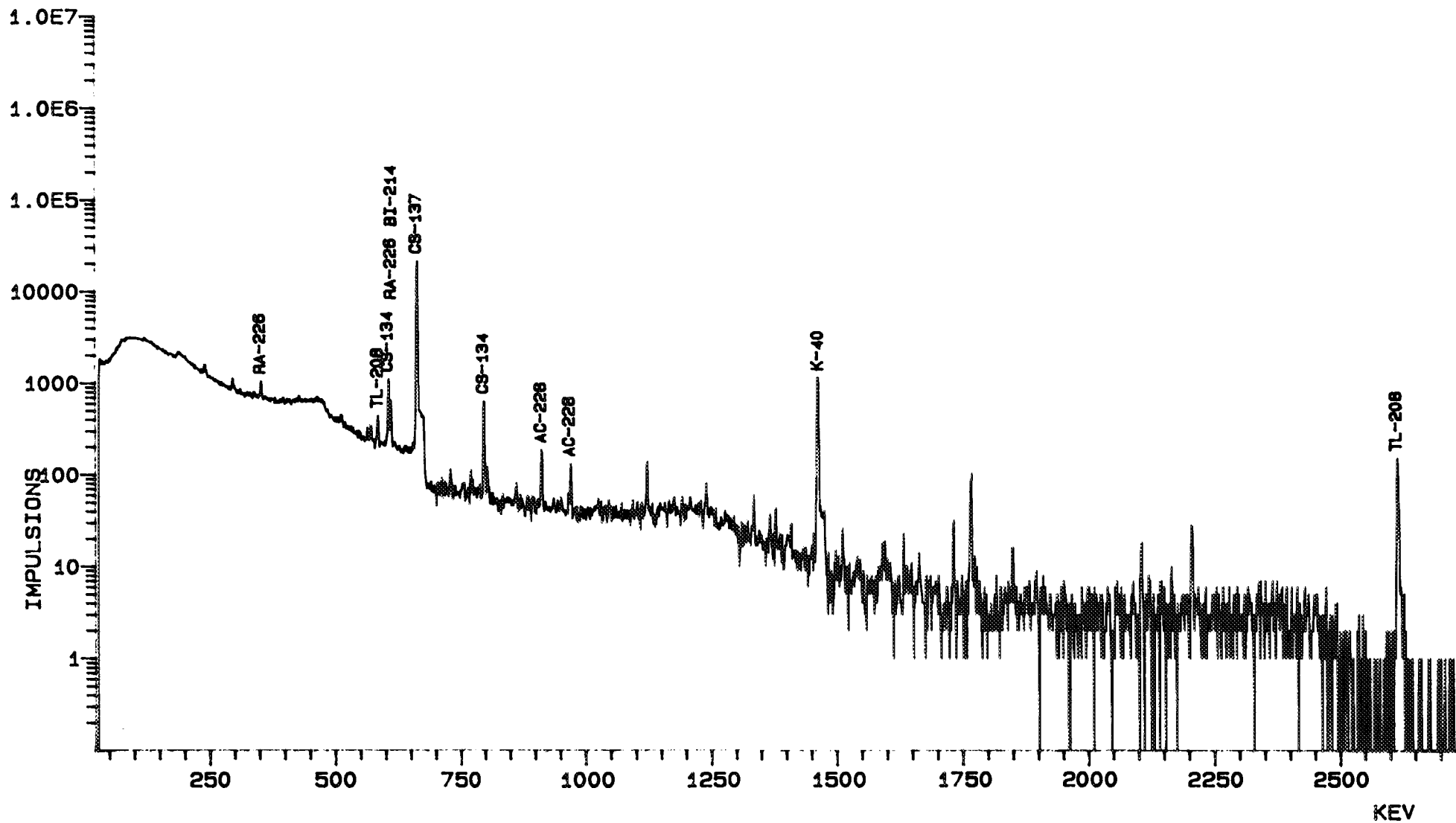
We want to congratulate and to thank all the organisers for the remarkable arranging and development of this exercise which has been a real evaluation of mobile radiological control means.

HELINUC  
FRANCE

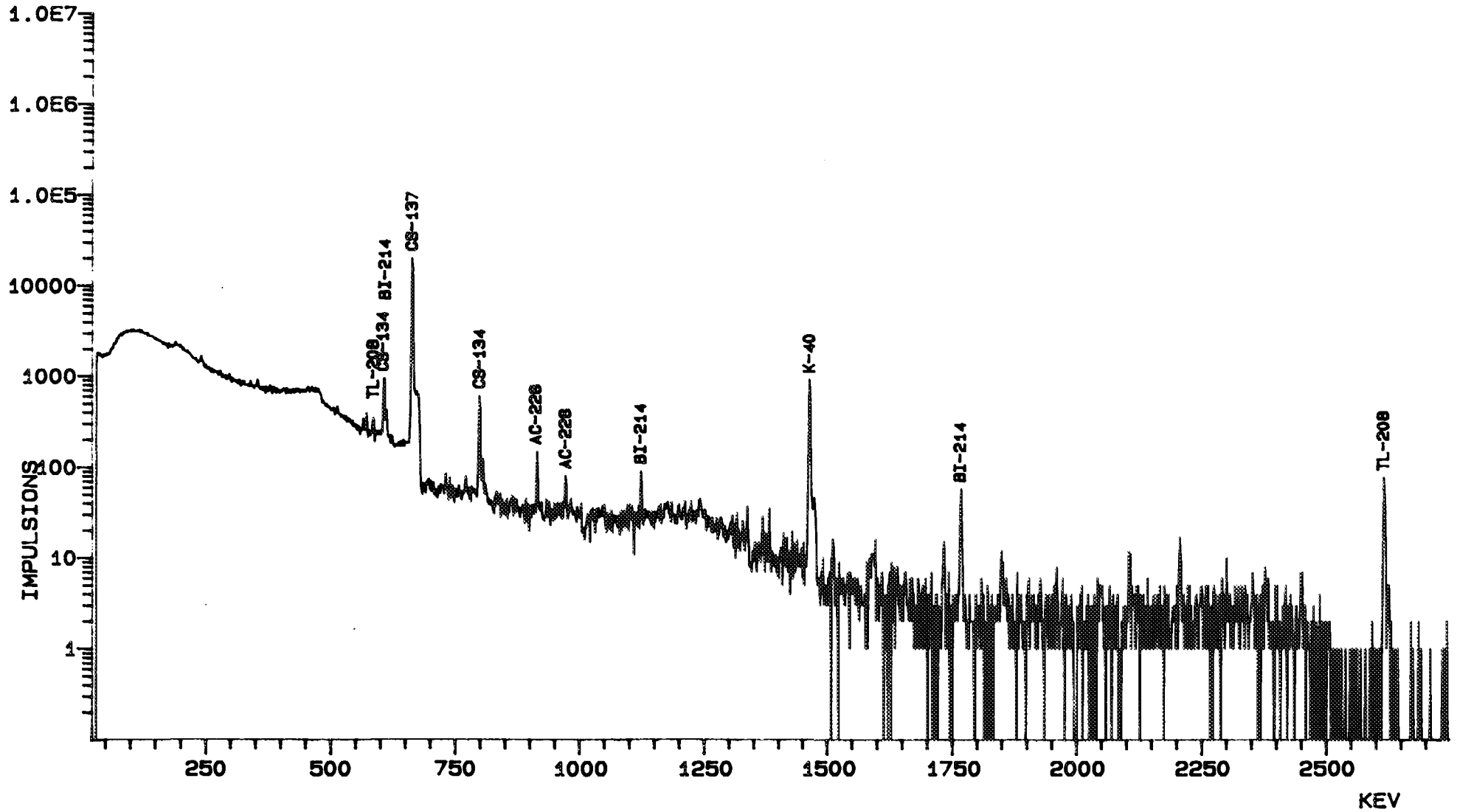
FINLANDE  
RESUME 95

DATE  
16.08.95

NOM SPECTRE...: A1-3-1.SPE  
DATE MESURE...: 16.08.95 08: 21: 36  
EFFICACITE...: EU-152.AUS  
MASSE/VOLUME...: 1.000 m<sup>2</sup>



HELINUC FRANCE	FINLANDE RESUME 95	DATE 16.08.95	NOM SPECTRE...: A2-C-0.SPE DATE MESURE...: 15.08.95 18: 34: 20 EFFICACITE...: EU-152.AUS MASSE/VOLUME.: 1.000 m <sup>2</sup>
-------------------	-----------------------	------------------	---





# Bundesamt für Strahlenschutz

## Aerial measurements in Finland

ABSTRACT .....	197
1. INTRODUCTION .....	197
2. MEASURING SYSTEM .....	198
3. MEASUREMENTS .....	198
3.1. Measurement flights over area I .....	198
3.2. Measurement flights over area II .....	199
Fig. 2. <sup>137</sup> Cs soil contamination along the 21 flight routes covering area II .....	200
3.3. Measurement flights over area III .....	200
3.3.1. Introductory remark .....	200
3.3.2. NaI(Tl)-detector measurements .....	201
Tab. 1. Detected sources and estimated activity .....	202
3.3.3. HPGe-detector measurements .....	202
Fig. 4. Scattered radiation from the shielded <sup>192</sup> Ir source, measured by HPGe-detector ....	203
Fig. 5. Typical spectrum measured by HPGe-detector over area III .....	203
4. CONCLUDING REMARK .....	204
5. REFERENCES .....	204

Figures in Colour Appendix (C.A.):

- Fig. 1. <sup>137</sup>Cs soil contamination measured by NaI(Tl)-detector in the cesium window during the flight over area II ..... C.A. plate 13
- Fig. 3. <sup>137</sup>Cs soil contamination measured by HPGe-detector during the flight over area II ..... C.A. plate 14

**NEXT PAGE(S)**  
**left BLANK**

## Aerial measurements in Finland

I. Winkelmann, M. Thomas, H. Buchröder, Ch. Brummer, G. Carloff\*

Federal Office for Radiation Protection,  
Köpenicker Allee 120 - 130, D-10318 Berlin, Germany

### Abstract

Aerial measurements were performed to determine the  $^{137}\text{Cs}$  soil contamination in a given region to detect unknown radiation sources and to assess their activity. For these measurements a computerized gamma ray spectrometer, equipped with a high purity Ge-semiconductor detector and a 12 l volume NaI(Tl)-detector was used. HPGe-detector measurements from different altitudes over area I were done to test and re-calibrate the aerial measuring system. The known  $^{137}\text{Cs}$  contamination of  $(50.7 \pm 5.2) \text{ kBq m}^{-2}$  could be confirmed by the measured value of  $(57 \pm 10) \text{ kBq m}^{-2}$ . The NaI(Tl)-detector was re-calibrated at that site for further  $^{137}\text{Cs}$  measurements over area II. The area II was surveyed from an altitude of about 70 m and at a parallel line distance of 150 m at an flying speed of  $100 \text{ km h}^{-1}$  to determine the  $^{137}\text{Cs}$  soil contamination. The measuring time was two seconds for the NaI(Tl)-detector. For the spectra measured with the HPGe-detector, a measuring time of 30 s each was chosen. From the NaI(Tl)-measurements, a mean  $^{137}\text{Cs}$  value of  $(60 \pm 20) \text{ kBq m}^{-2}$  was determined with a maximum value of  $90 \text{ kBq m}^{-2}$ . The corresponding values measured by HPGe-detector were  $(70 \pm 20) \text{ kBq m}^{-2}$  and  $120 \text{ kBq m}^{-2}$ , respectively. For the evaluation of the HPGe-spectra a depth distribution parameter  $\alpha/\rho = (0.44 \pm 0.21) \text{ cm}^2 \text{ g}^{-1}$  for  $^{137}\text{Cs}$  was used measured from soil samples. From data measured with the NaI(Tl)-detector during flights over area III, three  $^{60}\text{Co}$ -sources and one  $^{137}\text{Cs}$  source could be detected, localized and their activity assessed. By HPGe-detector measurements, only scattered  $^{192}\text{Ir}$  radiation was registered.

### 1 Introduction

Between the time from August 14 - 18, 1995, the Finish Geological Service had scheduled radioactivity measurements to be performed via aerial measuring systems in helicopters and fixed wing aircrafts over selected areas in Finland. As a participant in this exercise, Germany was represented by the Federal Office for Radiation Protection (BfS). The measuring flights started from a small airport in Vesivehmaa near Vääksy in the vicinity of Lahti, about 150 km north-east of Helsinki. The intent was to conduct measurements from helicopters or fixed-wing airplanes over three different areas.

---

\* German Federal Border Police, Grenzschutz-Fliegergruppe, Bundesgrenzschutz-  
straße 100, 53757 Sankt Augustin, Germany

## 2 Measuring system

The aerial measuring system consists of several components able to be separately installed in an Alouette II Astazou type helicopter operated by the German Federal Border Police (BGS). The central unit consists of a computerized gamma ray spectrometer with a high purity Ge-semiconductor detector of 50 % relative efficiency. In addition, a NaI(Tl)-scintillation detector array with a volume of 12 l is used to detect sources of radioactivity. The altitude is continuously measured by radar altimeter. The indicator gauge is fitted into the instrument panel to be easily read by the pilot. The position of the helicopter is set by a GPS satellite navigation system. The GPS system employed for these measurements achieved only a accuracy of approximately  $\pm 100$  m. In addition, the flight path is recorded by a video system. The German Federal Aviation Agency approved the operation of this system in an Alouette II Astazou type helicopter.

## 3 Measurements

### 3.1 Measurement flights over area I

The task of measurement flights over this area was to provide the individual participants with an opportunity to examine and, if necessary, re-calibrate their measuring systems by way of comparison measurements of a marked area with known contamination. The organizer determined the mean  $^{137}\text{Cs}$  soil contamination to be  $(50.7 \pm 5.2)$  kBq m<sup>-2</sup> by prior soil sample measurements and in-situ gamma ray spectrometric measurements [1]. These values were confirmed by our own in-situ gamma ray spectrometric measurements.

Measurements were performed while hovering at altitudes of 14 m, 25 m, 50 m and 75 m, respectively. For calibrating the NaI(Tl)-detector, the count rates in the cesium window (530 - 720 keV) were measured from these altitudes. Thus, the  $^{137}\text{Cs}$  soil contamination of area II could easily be measured to produce a fallout map. For determining  $^{137}\text{Cs}$  deposition, gamma ray spectra were taken by HPGe-detector spectrometer from these altitudes. This detector was calibrated using point sources. For evaluating measured spectra to determine  $^{137}\text{Cs}$  soil contamination, an exponential decrease in activity concentration with increasing soil depth was assumed. For that calibration a depth distribution parameter  $\alpha/\rho = (0.77 \pm 0.10)$  cm<sup>2</sup> g<sup>-1</sup>, was used [1]. This value was reported by the organizer and confirmed by own results from soil sample measurements. The measured weighted mean  $^{137}\text{Cs}$  value of  $(57 \pm 10)$  kBq m<sup>-2</sup> is in good agreement with the soil contamination of  $(50,7 \pm 5.2)$  kBq m<sup>-2</sup> reported by the organizer [1]. The individual values measured from an altitude of 14 m, 25 m, 50 m and 75 m are  $(58 \pm 12)$  kBq m<sup>-2</sup>,  $(50 \pm 10)$  kBq m<sup>-2</sup>,  $(53 \pm 13)$  kBq m<sup>-2</sup> and  $(81 \pm 25)$  kBq m<sup>-2</sup>. The measurement uncertainty was calculated according to the error propagation law.

### 3.2 Measurement flights over area II

The task was to determine the soil contamination in area II, a rectangular area measuring 6 km in length and 3 km in width. The terrain has gentle hills, it is rocky, densely forested and has numerous small lakes.

The NaI(Tl)-detector and the HPGe-detector were used for measuring  $^{137}\text{Cs}$  soil contamination. Flights were performed at an altitude of 70 m at a flying speed of about 100 km h<sup>-1</sup>. Figure 1 shows the  $^{137}\text{Cs}$  soil contamination calculated from count rates measured by NaI(Tl)-detector in the cesium window. The measuring time was two seconds each. The mean  $^{137}\text{Cs}$  value was calculated to be  $(60 \pm 20)$  kBq m<sup>-2</sup> with a maximum value of about 90 kBq m<sup>-2</sup>. For this calculation, the calibration factor determined from area I measurements was used. The background count rate of 50 s<sup>-1</sup> measured during flights over a lake was taken into account. The contributions to the cesium window count rates from gamma rays with higher energies were not included in the calculation. No corrections were made for gamma ray absorption by trees.

For determining  $^{137}\text{Cs}$  soil contamination from spectra measured by HPGe-detector (measuring time 30 s), the 662 keV gamma line was used. On account of a relatively high  $^{137}\text{Cs}$  contamination of some 10 kBq m<sup>-2</sup>, a measuring time of 30 s was sufficient for HPGe-detector measurements to achieve a statistically significant peak at 662 keV. For evaluating the measured spectra, a depth distribution parameter  $\alpha/\rho = (0.44 \pm 0.25)$  cm<sup>2</sup> g<sup>-1</sup> was used [1]. Deviations in altitude were corrected (standardized to 70 m). No corrections were made for gamma ray absorption by trees. The measurement uncertainty was calculated according to the error propagation law.

Figure 2 shows the  $^{137}\text{Cs}$  results from nuclide specific measurements by HPGe-detector flights over area II (21 flight routes covering the measured area). Each of the measured values represents a mean contamination value over a distance of about 900 m. The  $^{137}\text{Cs}$  mean value amounts to  $(70 \pm 20)$  kBq m<sup>-2</sup> with a maximum value of about 120 kBq m<sup>-2</sup>. These data were used to produce a fallout map over area II, shown in Figure 3. Lowest values of about 60 kBq m<sup>-2</sup> for  $^{137}\text{Cs}$  were measured in the southern part of area II and in a small area near the northern boundary. The activity values show an increase from south to north; the highest values of more than 100 kBq m<sup>-2</sup> are reached in the center and in the northern part of area II.

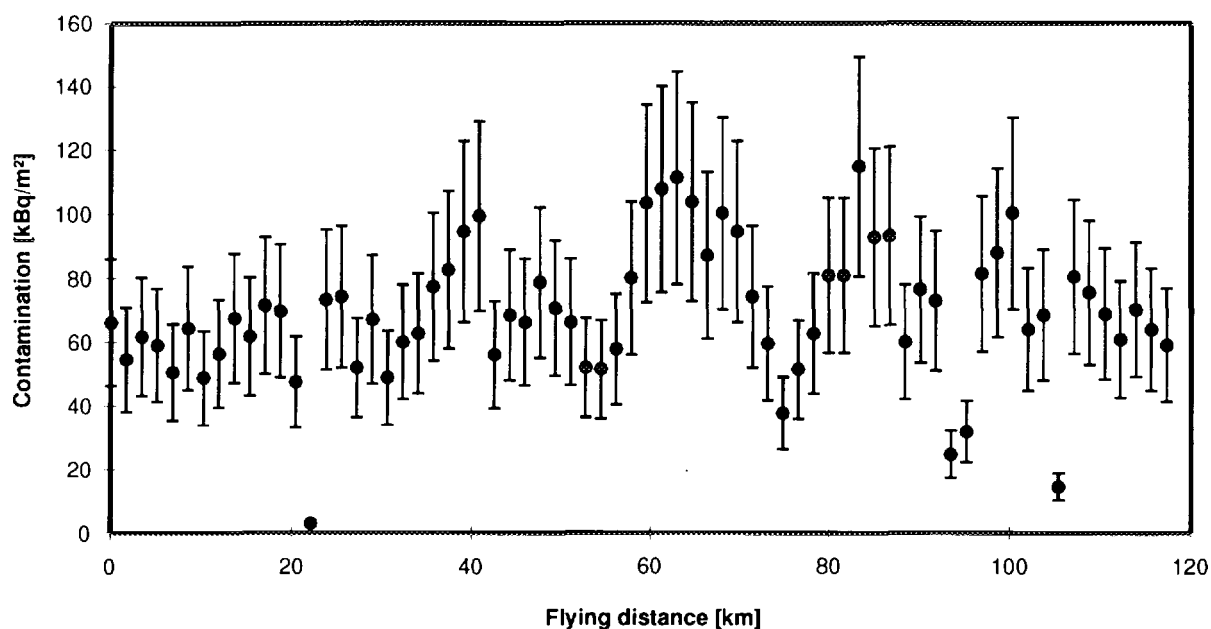


Figure 2.  $^{137}\text{Cs}$  soil contamination along the 21 flight routes covering area II (3 km x 6 km).

For determining  $^{134}\text{Cs}$  and  $^{40}\text{K}$ , the individual gamma ray spectra measured over area II were summarized. The mean  $^{134}\text{Cs}$  soil contamination was measured to be  $(3.0 \pm 0.9) \text{ kBq m}^{-2}$ . For  $^{40}\text{K}$  a mean specific activity of  $(420 \pm 130) \text{ Bq kg}^{-1}$  was determined.

### 3.3 Measurement flights over area III

#### 3.3.1 Introductory remark

The aerial measuring system the Federal Office for Radiation Protection is using for these measurements was primarily designed to perform rapid nuclide specific measurements over large areas following a nuclear accident. For that purpose, a computerized gamma ray spectrometer with HPGe-detector is employed. The 12 l volume NaI(Tl)-detector is used to detect, for example, lost or stolen sources of radioactivity. With a flight path distance of 300 m and at a flight speed of  $100 \text{ km h}^{-1}$ , an area of approximately  $30 \text{ km}^2$  can be covered per hour in which gamma radiation sources with an activity of some GBq are still detectable from an altitude of 100 m. The count rates measured by NaI(Tl)-detector have so far not been corrected to increase sensitivity (for example stripping procedures). Thus, the detection of point sources caused some problems.

The task was to detect unknown radiation sources in area III, a rectangular area measuring 5 km in length and 1 km in width. Structure and nature of the terrain were similar to those of area II. Each team was free to select its own strategy, while the time allotted for detection was strictly limited to one hour; no hovering for closer detection of a radiation source was permitted. A strict flying altitude of not less than 70 m above ground had to be kept. A distance of 100 m had to be maintained between individual flight paths, the flying speed was 80 km h<sup>-1</sup>. Immediately after landing, a map had to be handed over to the organizer marking the detected sites of radiation sources. As expected also over this terrain, it was difficult to keep a constant distance between flight paths due to the lack of characteristic points of orientation. The pilots had some navigation difficulties over this terrain in the absence of a precise navigation aid. The GPS system is currently only recording the flight path with an accuracy of  $\pm 100$  m and is not yet capable of guiding flights by given coordinates. A differential GPS system was not available. The localization of radioactive sources consequently presented some problems.

The NaI(Tl)-detector was used for detecting the sources (measuring time 2 s). The count rates were continuously measured in the cesium and cobalt windows and on-line displayed on the screen. The count rates were additionally measured in energy ranges of between 260 - 510 keV and 1670 - 1880 keV. The measured data were stored together with coordinates and altitudes for a more detailed evaluation. Additional spectra were continuously taken by HPGe-detector (measuring time 30 s).

### **3.3.2 NaI(Tl)-detector measurements**

The count rates measured in the cobalt window approximately are between 100 s<sup>-1</sup> and 150 s<sup>-1</sup> while those measured in the cesium window are between 500 s<sup>-1</sup> and 650 s<sup>-1</sup>. The lowest values with about 50 s<sup>-1</sup> in the cesium window and 30 s<sup>-1</sup> in the cobalt window were from measurement flights over lakes.

During the flights, two <sup>60</sup>Co sources could be detected but, due to the above mentioned navigation difficulties, only one location was correctly reported immediately after landing. An evaluation of the data measured by NaI(Tl)-detector shows the following:

Three <sup>60</sup>Co sources and one <sup>137</sup>Cs source were detected and localized. By taking the uncertainty in determining the location on hand of the GPS navigation system ( $\pm 100$  m) and other uncertainties into account, the range of activities of the <sup>60</sup>Co sources Co1, Co2, Co4 and the <sup>137</sup>Cs source Cs3 were estimated (see Table I). The activities reported by the organizer are within the range of estimated values [2].

Table I. Detected sources and estimated activity.

Nuclide	Source code	Given activity [2]	Estimated activity
<sup>60</sup> Co	Co1	260 MBq (7.0 mCi)	100 - 300 MBq
<sup>60</sup> Co	Co2	330 MBq (9.0 mCi) <sup>1)</sup>	200 - 500 MBq
<sup>60</sup> Co	Co4, a-f	350 MBq (9.4 mCi) <sup>2)</sup>	100 - 400 MBq
<sup>137</sup> Cs	Cs3	280 MBq (7.5 mCi)	100 - 400 MBq

1) Collimated source

2) A line source consisting of six "point" sources located 20 ... 30 m from each other.

An evaluation of the measured GPS data shows that all of the 15 concealed sources – except the shielded <sup>192</sup>Ir source with an activity of 560 GBq (15 Ci) and the <sup>60</sup>Co source Co3 with an activity of 26 MBq (0.7 mCi), located outside area III – were overflown (within a range ± 100 m). The <sup>137</sup>Cs sources Cs1 with an activity of 2.8 GBq (77 mCi) was overflown once (within a range of ± 100 m). One should expect a significant increase in the count rate measured in the <sup>137</sup>Cs window, even when passing over this strong source at a distance of about 100 m (this value corresponds to the measurement uncertainty of the GPS navigation system), but the increase in count rate we measured was relatively insignificant compared to the background count rate of about 600 s<sup>-1</sup>. Therefore it was difficult to identify this source on the basis of measured data. From other measurements in 1994, a count rate of more than 1000 s<sup>-1</sup> should have been measured. There is no explanation why this relatively strong <sup>137</sup>Cs source was not detected. The – collimated – <sup>137</sup>Cs source Cs2 with an activity of about 1.5 GBq could in principle be localized by the NaI(Tl)-detector measurements; its activity, however, could not be confirmed.

### 3.3.3 HPGe-detector measurements

No source could be detected by HPGe-detector measurements. Nevertheless, the scattered low energy radiation of the shielded <sup>192</sup>Ir source with an activity of 560 GBq (15 Ci), located outside area III, could be measured. Figure 4 shows the contribution to the low energy portion in the spectrum from scattered <sup>192</sup>Ir radiation. There is a significant increase in the low energy portion. This spectrum was taken about 200 m west of the shielded <sup>192</sup>Ir source, close to the location where sources Co1 and Cs3 were located. Due to shielding, the radionuclide could not be identified. Figure 5 in comparison shows a HPGe-spectrum representative of the spectra measured over area II at identical conditions.

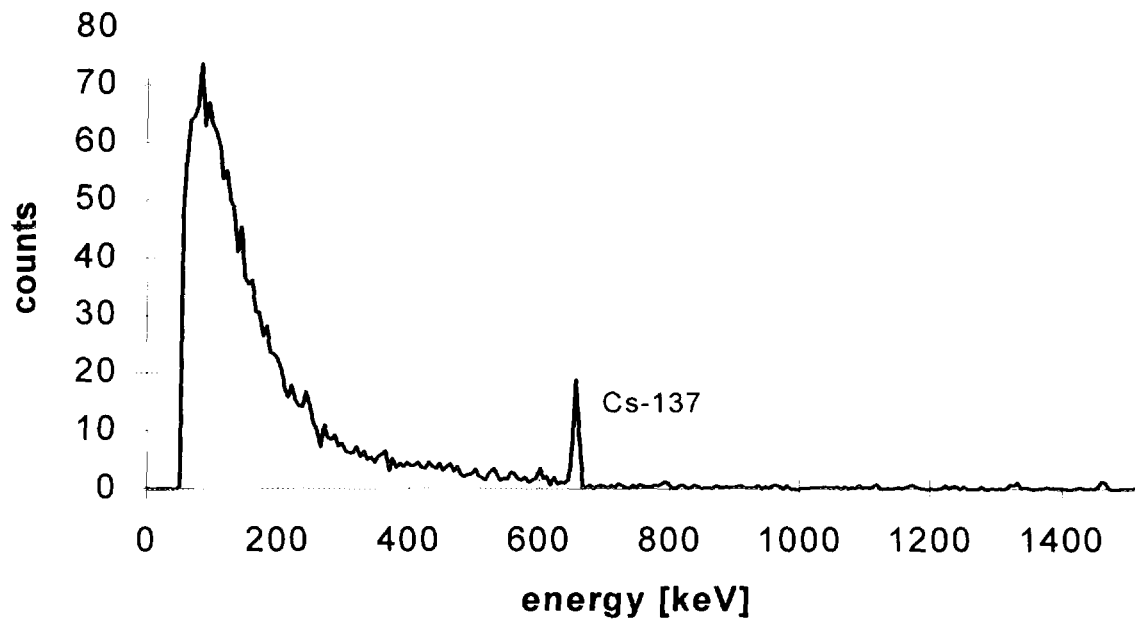


Figure 4. Scattered radiation from the shielded  $^{192}\text{Ir}$  source, measured by HPGe-detector (flight altitude 70 m, measurement time 30 s).

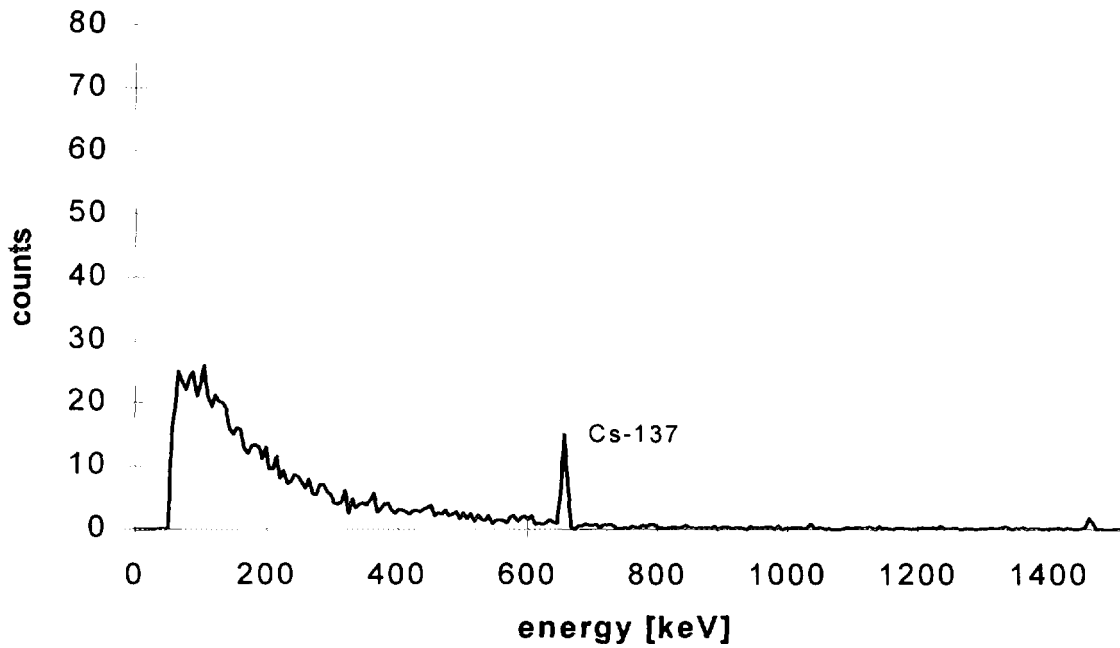


Figure 5. Typical spectrum measured by HPGe-detector over area III (flight altitude 70 m, measurement time 60 s).

#### **4 Concluding remark**

The measurements have shown that there could be two major improvements for the system to search for radioactive sources:

First an improved navigation system such as a differential GPS (**G**lobal **P**ositioning **S**ystem) could redefine the localisation of radioactive sources. Furthermore additional mathematical analysis of the measured data could improve the detection of radioactive sources with lower activity.

#### **References**

- [1] D.C.W. Sanderson, J.D. Allyson, H. Toivonen, T. Honkamaa  
Gamma ray spectrometry results from core samples collected for RÉSUMÉ '95  
Scottish Universities Research & Reactor Centre, East Kilbride, Glasgow,  
September 1995
  
- [2] J. Lahtinen, R. Pöllänen, H. Toivonen  
Characteristics and locations of sources  
Internal report, Finnish Centre for Radiation and Nuclear Safety, Helsinki,  
Januar 1996



# Geological Survey of Norway

## Airborne mapping of radioactive contamination

SUMMARY .....	207
1. INTRODUCTION .....	208
2. FIELD OPERATIONS .....	208
2.1. Discription of test areas .....	208
Tab. 1. Radiation sources area III .....	209
2.2. Description of equipment .....	209
2.3. General .....	210
3. MAPPING OF CESIUM GROUND CONCENTRATION .....	210
3.1. Processing of Cs maps .....	210
3.2. Calibration .....	211
3.2.1. Stripping ratios for Cesium window .....	211
Tab. 2. Measurements over calibration pads in unit counts per second .....	211
3.2.2. Ground concentration .....	212
Tab. 3. Counts in the Cesium window over known ground concentration .....	212
Fig. 1. Counts as a function of altitude over calibration area (area I) .....	213
Tab. 4. Counts at ground level calculated from measurements at different altitudes .....	214
3.3. Results .....	214
4. DETECTION OF POINT SOURCES .....	215
4.1. Software for rapid detection of point sources .....	215
Fig. 2 Application for examining spectra: main window .....	216
4.2. Example of spectra from hidden point sources .....	216
Fig. 3. The signal produced by the Technetium source .....	217
Fig. 4. The signal produced by the Iridium source .....	218
Fig. 5. Location of the Iridium source .....	218
Fig. 6. Gamma ray spectra over Cobalt-60 source Co2 .....	219
Fig. 7. Spectra obtained above source Cs1 .....	220
Fig. 8. Spectra obtained in the vicinity of the Iridium source are dominated by it .....	220
Fig. 9. When the low energy parts of the spectra in Fig. 8 are excluded view the signals cause by Cs3 and Co1 become clear .....	221
4.3. Results as map presentation .....	222
5. CONCLUSION .....	222
6. REFERENCES .....	223

Figures in Colour Appendix (C.A.):

MAP 1 Cesium Ground Concentraiton .....	C.A. plate 15
MAP 2 Point Source Detection Area III .....	C.A. plate 16

**NEXT PAGE(S)  
left BLANK**

# **Airborne mapping of radioactive contamination. Results from a test in Finland, RESUME95**

**Stig Rønning, Mark A. Smethurst**  
Geological Survey of Norway

## **SUMMARY**

The Geological Survey of Norway participated in the exercise RESUME95 (Rapid Environmental Surveying Using Mobile Equipment 95) in Finland, during August 1995. The purpose of the exercise was to (1) test preparedness in the Nordic countries for accidents involving the release and dispersal of radioactive material, (2) compare results from the different teams participating in the exercise, (3) establish routines for the exchange of data and (4) investigate the possibility of international assistance in the event of nuclear accidents.

The Geological Survey of Norway carried out a survey over three test areas (area I, II and III). All three areas were contaminated with man made radionuclides in the days following the Chernobyl nuclear reactor accident. The Cesium-137 contamination level was reported to be about 50 kBq/m<sup>2</sup> in area I, and this area was used for calibration. In area II mapping of Cesium-137 ground concentration was carried out. Detection of hidden artificial radiation sources were the main purpose in area III.

This report describes the exercise - RESUME95, field operations, calibration, mapping of Cesium-137 ground concentration and detection of hidden point sources. Results are presented as colour maps.

## 1. INTRODUCTION

The Geological Survey of Norway participated in the exercise RESUME95 (Rapid Environmental Surveying Using Mobile Equipment 95) in Finland, August 1995. Organiser of the exercise was NKS (Nordisk kjernesikkerhetsforskning). Teams from the Nordic and other countries carried out airborne gamma ray surveys over three test areas (I, II and III) to (1) test their preparedness for accidents involving the release and dispersal of radioactive material, (2) compare results from the different teams (3) establish routines for the exchange of data and (4) investigate the possibility of international assistance in the event of nuclear accidents. All three test areas had traces of Chernobyl fallout. Ten artificial radiation sources unknown to the participants were placed in the terrain in area III. Results from the exercise include (1) mapping of  $^{137}\text{Cs}$  ground concentration in area II and III and (2) location of hidden point sources in area III.

In order to obtain further standards of reference, measuring systems from Canada, France, Germany and Scotland participated in the exercise.

## 2. FIELD OPERATIONS

### 2.1 Description of test areas

Measurements took place in three different areas, known as areas I, II and III. All areas were contaminated with man made radionuclides in the days following the Chernobyl nuclear reactor accident. A number of radioactive sources were hidden in area III.

**Measurements area I:** Area I was a part of the Vesivehmaa airfield and was used for calibration of the radiometric system. Measurements were carried out for a few minutes at different altitudes (10, 25, 50 and 75 metres) over a part of the airfield where the  $^{137}\text{Cs}$  contamination level was reported to be  $50 \text{ kBq/m}^2$  (Multala & Erkinheimo 1995). Data from the calibration were used to find the function converting counts at height  $h$  to ground concentration of  $^{137}\text{Cs}$ .

**Measurements area II:** Area II was rectangular in shape with side lengths of 3 km and 6 km. Radiometric data were collected in this area to map Cs falldown from the Chernobyl accident. Parallel survey lines were flown with a line spacing of 150 metres. Flying altitude was nominally 60 metres. Total flying distance in this area was approximately 200 km.

**Measurements area III:** Area III was rectangular and measured 1 km by 5 km. Ten artificial radiation sources were placed in area III (Lahtinen et al 1996). One of the sources was a line source, the others were point sources (three of them colimated). The radionuclides used in the sources were  $^{60}\text{Co}$  (Cobalt),  $^{137}\text{Cs}$  (Cesium),  $^{99\text{m}}\text{Tc}$  (Technetium) and  $^{192}\text{Ir}$  (Iridium). Table 1 gives information on the radiation sources in area III. Line spacing in this area was approximately 100 metres and same flying altitude as area II was used. The total flying distance in this area was 55 km.

**Table 1 Radiation sources area III**

	Code name	Nuclide	Activity (Bq)
1	Co1	<sup>60</sup> Co	2.6x10 <sup>8</sup>
2	Co2 (Columated)	<sup>60</sup> Co	3.3x10 <sup>8</sup>
3	Co3	<sup>60</sup> Co	2.6x10 <sup>7</sup>
4	Co4 (A 'line' of 6 point sources)	<sup>60</sup> Co	3.7-6.7x10 <sup>7</sup>
5	Cs1	<sup>137</sup> Cs	2.8x10 <sup>9</sup>
6	Cs2 (Columated)	<sup>137</sup> Cs	*1.3-1.7x10 <sup>9</sup>
7	Cs3	<sup>137</sup> Cs	2.8x10 <sup>8</sup>
8	Cs4	<sup>137</sup> Cs	5.4x10 <sup>8</sup>
9	Ir (Columated)	<sup>192</sup> Ir	5.6x10 <sup>11</sup>
10	Tc	<sup>99m</sup> Tc	2(1.1x10 <sup>9</sup> )

\*Exact information on activity not available.

## 2.2 Description of equipment

**Aircraft:** The survey was flown using an Aerospatiale Ecureuil, Twin Star AS 355F.

**Radiometrics:** Radiometrics were recorded with a 1024 cubic inch crystal volume detector which was coupled to a Exploranium GR820 gamma-ray spectrometer system. The crystal was mounted under the helicopter. Accumulation time for the spectrometer was one second during the measurements. With flying speed 100 km/hour and altitude 60 meter the radiation from approx. 120 meter X 150 meter ground area is recorded every second.

**Data Acquisition:** Data were recorded digitally with a DAS-8 data acquisition system manufactured by RMS Instruments Ltd. An integrated part of the data acquisition system is a thermal graphic printer, which allows output of the system to be monitored in real time.

**Navigation:** The survey was flown with satellite navigation (GPS). Differential corrections were applied to the navigation data during processing, giving an accuracy of ±15 m in the positioning.

**Radar altimeter:** A King KRA-10A radar altimeter was mounted in the helicopter to provide ground clearance information to an accuracy of 5% of flying height. The primary use of the radar altimeter data is an aid for maintaining constant ground clearance, but the data were also used in the processing of the measured radiometric data.

### 2.3 General

Data were collected over all three areas in one flight during the 16th of August 1995. The weather conditions during the flight were good. Operators from the Geological Survey of Norway were Henrik Håbrekke and John Olav Mogaard.

## 3 MAPPING OF CESIUM GROUND CONCENTRATION

### 3.1 Processing of Cs maps

Software from Aerodat Ltd (Canada) and Geosoft (Canada) were used in the processing of collected data. Mapping of the Total Count, Potassium, Uranium and Thorium window is the normal procedure during geophysical helicopterborne measurements at the Geological Survey of Norway. The processing sequence normally used was modified to include mapping of Cesium ground concentration. The processing tasks for the Total Count, Potassium, Uranium and Thorium (TC, K, U and Th) window are divided into these logical steps:

- Importing data to the software system (database)
- Correcting data for instrument deadtime
- Removing background contributions from cosmic radiation and aircraft
- Correcting spectral overlapping (Compton scattering) and height attenuation effects

Output from these processing steps are required in the processing of the Cesium window ( $^{137}\text{Cs}$ ). Spectrometer data are normally measured in counts per second. The spectrometer requires some time each second to process the incoming data, and during this time period (deadtime) no counts are measured. The Exploranium GR820 gamma-ray spectrometer system records the time during which the crystal is actually measuring. This resulting value is referred to as livetime (measuring period minus the deadtime). In this case the processing software applies a livetime (in sec) correction:

$$C = c / \text{lifetime}$$

C - corrected count in each second

c - uncorrected data

Background radiation is caused by high energy cosmic ray particle interaction with the atmosphere and radiation from the radioactivity of the aircraft and equipment. Correction for background radiation were made by subtracting average background values from the data at each data point. The average background values were determined from measurements over water (e.g. lakes).

Stripping was carried out to remove effects of spectral overlap. This is prerequisite in radiometric data processing to give the counts in the potassium, uranium and thorium windows that are uniquely from potassium, uranium and thorium. Usually the Total Count, Potassium, Uranium and Thorium window are presented as counts per second in flying altitude (250 feet) maps. This is done by normalising data to a height of 250 feet using data from the radar altimeter. Processing of the Cesium ( $^{137}\text{Cs}$ ) window requires stripped, but not height corrected, data in the Potassium, Uranium and Thorium window.

Livetime correction was also applied to the data in the Cesium window ( $^{137}\text{Cs}$ ) to normalise data to counts per second. The next step was to remove background radiation (cosmic radiation and radiation from aircraft). The background radiation measured over water was removed by subtracting the background from the data at each data point in the Cesium window. Due to spectral overlap Potassium, Uranium and Thorium was stripped out of the Cesium window to give the counts in the Cesium window that are uniquely from Cesium. The stripping ratios (Cs/U, Cs/K and Cs/Th) were experimentally determined by a procedure over calibration pads. Results from the calibration area (area I at Vesivehmaa airfield) were used to convert stripped data in the Cesium window from 'counts at flying altitude' to ground  $^{137}\text{Cs}$  concentration ( $\text{kBq/m}^2$ ).

## 3.2 Calibration

### 3.2.1 Stripping ratios for the Cesium window

Stripping ratios for the Cesium window were experimentally determined by a procedure over calibration pads. Three pads with pure Potassium, Uranium and Thorium spectra were used to determine interfering effects of Potassium, Uranium and Thorium in the Cesium window. A fourth low radioactivity pad (background pad) was used to remove effects of the background radiation from the surrounding ground, the equipment, cosmic radiation and radon decay products in the air. Measurements were carried out over the different pads for a period of 2-3 minutes. Data in the Potassium, Uranium, Thorium and Cesium window were recorded for the determination of the stripping ratios. Table 2 shows the average counts per second in each window over the four different pads.

**Table 2 Measurements over calibration pads in unit counts per second.**

PAD	Potassium	Uranium	Thorium	Cesium
Background	245.27	28.39	27.74	353.80
Potassium	1013.97	22.83	24.66	784.00
Background	244.56	28.63	27.61	363.31
Uranium	635.29	516.85	67.48	2736.64
Thorium	472.54	204.40	545.95	2540.36
Background	244.05	28.56	27.51	363.18

Stripping ratios are given by:

Potassium pad:  $Cs/K = (Cs - Cs \text{ background}) / (K - K \text{ background})$

Uranium pad:  $Cs/U = (Cs - Cs \text{ background}) / (U - U \text{ background})$

Thorium pad:  $Cs/Th = (Cs - Cs \text{ background}) / (Th - Th \text{ background})$

Cs - counts per second in cesium window

K - counts per second in potassium window

U - counts per second in uranium window

Th - counts per second in thorium window

Background values of Cs, U, K and Th are measured over the background pad.

Determined stripping ratios:

$$Cs/K = (784.00 - 353.80) / (1013.97 - 245.27) = 0.56$$

$$Cs/U = (2736.04 - 363.31) / (516.85 - 28.63) = 4.87$$

$$Cs/Th = (2540.36 - 363.18) / (545.95 - 27.51) = 4.20$$

From this we can find counts in the Cesium window using:

$$Cs^* = Cs - (Cs/K)K^* - (Cs/U)U^* - (Cs/Th)Th^*$$

Where X\* represents counts uniquely from the element.

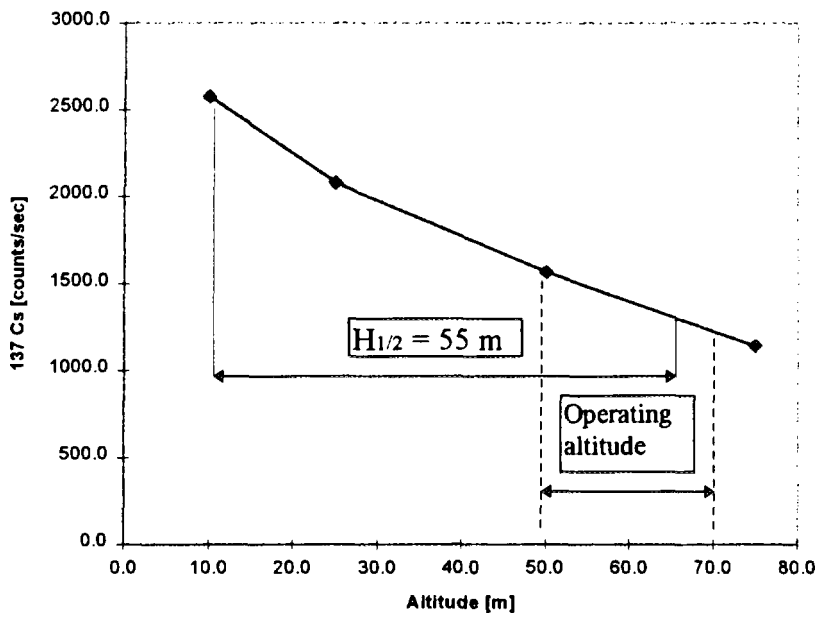
### 3.2.2 Ground concentration

During the exercise in Finland calibration measurements were carried out at Vesivehmaa airfield over an area with known contamination level ( $^{137}\text{Cs}$ ). Measurements were taken in different altitude (10, 25, 50 and 75 metres) for a time interval of 1- 2 minutes. Table 3 shows data (average values) recorded for the Cesium-137 window in unit counts per second.

**Table 3** Counts in the Cesium window ( $^{137}\text{Cs}$ ) over known ground concentration - approx. 50 kBq/m<sup>2</sup>

Altitude [m]	$^{137}\text{Cs}$ [counts per second]
10	2569
25	2074
50	1560
75	1135

**Fig. 1** Counts as a function of altitude over calibration area (area D).



The counts at ground level are calculated from counts at height h using the formula:

$$\text{Counts}_{(\text{ground level})} = \text{Counts}_{(\text{flying altitude})} * e^{-\lambda h}$$

$$\lambda = (\log 2) / H_{1/2}$$

Where H<sub>1/2</sub> is the height where counts are halved. From Fig. 1 we have H<sub>1/2</sub> = 55m which gives:

$$\lambda = 0.0126$$

Counts at height h to ground level is then given by:

$$\text{Counts}_{(\text{ground level})} = \text{Counts}_{(\text{flying altitude})} * e^{-0.0126h}$$

Table 4 shows calculated counts/sec at ground level for the different altitudes.

**Table 4** Counts at ground level calculated from measurements at different altitudes.

Altitude [m]	<sup>137</sup> Cs - ground level [counts/sec]
10	2914
25	2841
50	2929
75	2920

Counts normalised to ground level from altitude 25 m are anomalously low compared to the other three. This may be due to inaccurate radar altimetry or inhomogenous contamination in the calibration area. The value calculated at altitude 25 m is only 2-3% lower than the other values. The average value for counts at ground level using all four values is 2899 counts/sec. The contamination level in the calibration area was known to be approx. 50 kBq/m<sup>2</sup> (Multala & Erkinheimo 1995). Counts at height h are then converted to ground concentration using :

$$\text{Concentration}_{(\text{ground})} = \text{Counts}_{(\text{height } h)} * e^{0.0126h} * (50 / 2899)$$

$$\text{Concentration}_{(\text{ground})} = \text{Counts}_{(\text{height } h)} * e^{0.0126h} * 0.0172$$

### 3.3 Results

Map 1 shows calculated Cs-137 ground concentrations in area II and III. In this map we have used the Finnish coordinate system.

The average ground concentration of <sup>137</sup>Cs in area II at the time of the exercise (August 95) was found to be approximately 60 kBq/m<sup>2</sup> (<sup>137</sup>Cs). Standard deviation was found to be 16.0 (variance 16.0<sup>2</sup>). The peak concentration of <sup>137</sup>Cs in area II was approx. 90 kBq/m<sup>2</sup> (around coordinates 2558600,6802800).

The peak concentration of (Chernobyl) <sup>137</sup>Cs in area III was approx. 70 kBq/m<sup>2</sup> (around coordinates 255300, 6801700). Note that the highest value in the Cesium window is from a artificial source (around coordinates 2552800, 6802400).

## 4 DETECTION OF POINT SOURCES

### 4.1 Software for rapid detection of point sources

One purpose of the exercise was the detection of hidden sources in area III. The Geological Survey of Norway was only capable of detecting sources leading to the production of gamma rays with energies in the Potassium, Uranium, Thorium and Cesium-137 windows at the time of the exercise. Detection of man made point sources (with unknown compositions) requires inspection the full gamma ray spectrum, and software was developed for this task after the exercise.

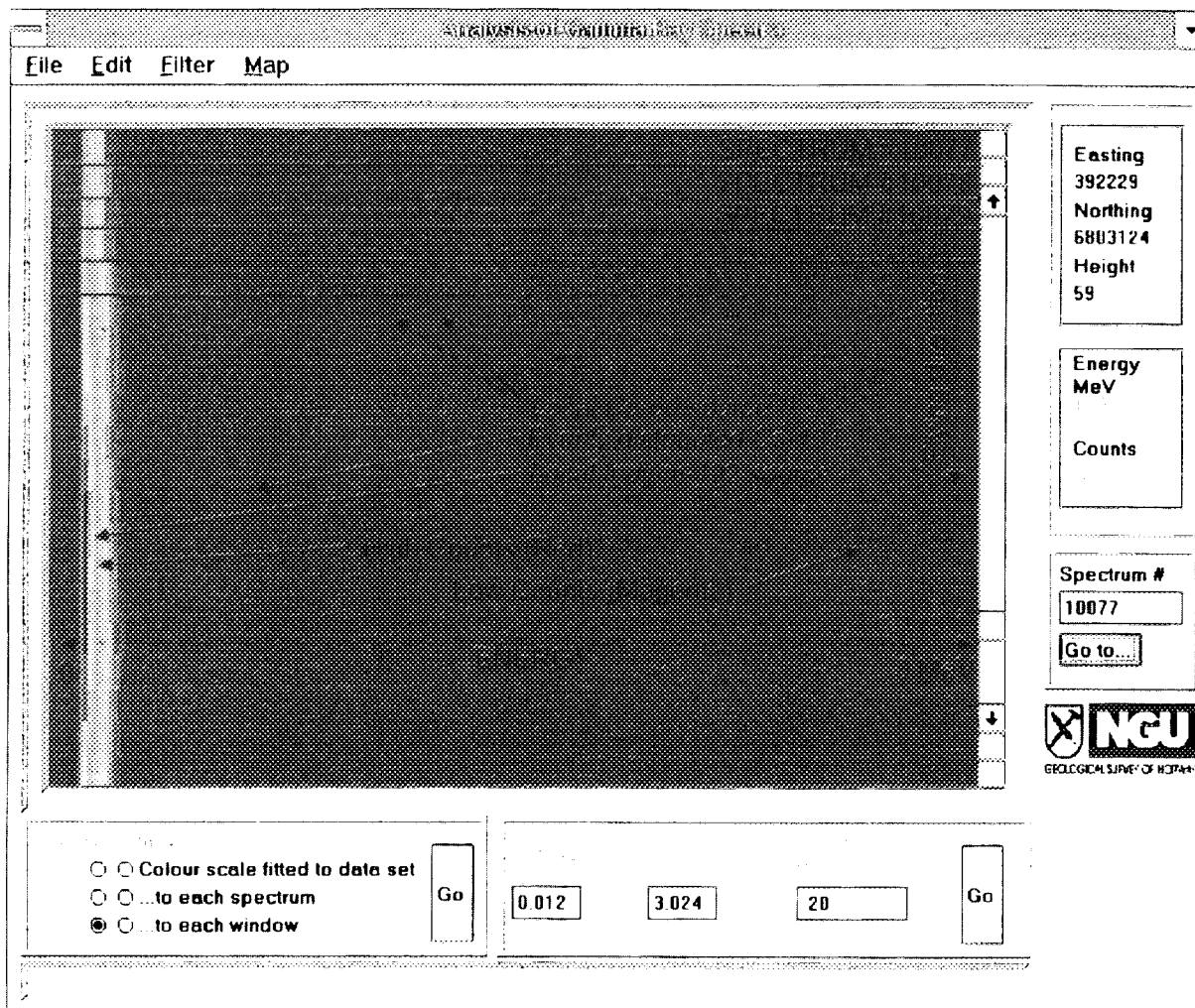
During helicopterborne surveying one (255 channel) spectrum is acquired per second. Over 12500 full spectra were recorded during NGU's survey of areas II and III. The new computer application graphically displays a single spectrum as a horizontal strip. The start (left) of the strip represents low energy gamma rays and the end (right) represents high energy. The changing colour of the strip along its length indicates changing numbers of gamma rays detected. Increasing numbers of gamma rays are represented by the colours Magenta, Blue, Green, Yellow and Red respectively. Many spectra can be displayed simultaneously as strips arranged in a graphical window one below the other. Fig. 2 shows the computer application's main window displaying 20 spectra from the Finland test. In the figure, 20 adjacent spectra are displayed in a vertical stack where the first is at the top and the last at the bottom. In this case spectrum number 10077 is the first and 10096 the last. There is a scroll bar to the right of the graphical window which can be used to scroll all 12500 spectra through the window, thereby revealing previously hidden portions of the data. It is possible to use a map of the flight plan (accessed via menu item 'Map') to jump to a part of the data set at a specific geographic location. Conversely, the map can be used to show the geographic location of the spectra in the graphical window.

As the computer mouse is moved over the strips representing gamma ray spectra the following information is displayed:

- The number of the spectrum displayed under the mouse (#10077 in Figure 2)
- The geographic location and height for the spectrum under the mouse (East=392229, North=6803124, Height=59m, WGS 84)
- The energy range being displayed (0.012 MeV to 3.024 MeV in Figure 2)
- The Energy of the channel positioned under the mouse (0.693 MeV in Figure 2)
- The number of spectra displayed in the window (20 in Figure 2)
- The state of filtering of data displayed in the window (not filtered in Figure 2, with a colour scale adjusted to fit only the spectra displayed in the window)

Fairly evenly distributed nuclides produce spectral peaks which appear in all measured spectra and therefore appear in the graphical window (Fig. 2) as vertical lines - peaks present in all 20 spectra on display (e.g.  $^{137}\text{Cs}$ ). Gamma rays due to point sources are only detected in a few spectra as the aircraft quickly passes them. In figure 2 a few adjacent spectra have high counts (red colour) at low energies caused by a nearby point Iridium-192 source.

**Fig. 2 Application for examining spectra: main window (see text for explanation)**



#### 4.2 Example of spectra from hidden point sources

We detected all but one of the point sources hidden in area III (Cs2). The analysis of individual gamma ray spectra with the computer program described in section 4.1 took approximately 3 hours. Two sources (Technetium and Iridium) were easy to find (Fig. 3 and Fig. 4), although we were unable to identify the nuclides responsible for the detected radiation. It was clear from our data that the Iridium source was located to the east of the survey area (Fig. 5). The Cobalt sources were not easy to observe in the total spectrum, but looking at a window from 0.708 MeV to 1.560 MeV they were comparatively easy to find (Fig. 6). All Cobalt sources created two clear peaks in nearby gamma ray spectra at 1.17 and 1.33 MeV.

The Cesium sources were difficult to find, not least because of varying amounts of Chernobyl Cesium in the region. We identified 3 of the four Cesium sources placed in the survey area. Cs1 (Fig. 7) and Cs4 were found first, while examining spectra from the survey. Cs3 was found only because attention was being paid to the nearby Co1 source. Initially, the proximity

of the source Ir made the Co1 and Cs3 sources difficult to see (Fig.8). This is because much of the colour scale used to display the spectra was used on the large anomaly caused by Ir. When the lower energy channels were removed from the display both Co1 and Cs3 became clear (Fig. 9).

**Fig. 3** The signal produced by the Technetium source. Gamma radiation caused by the presence of the source is visible on only three spectra, obtained over a horizontal distance of approx. 100 m.

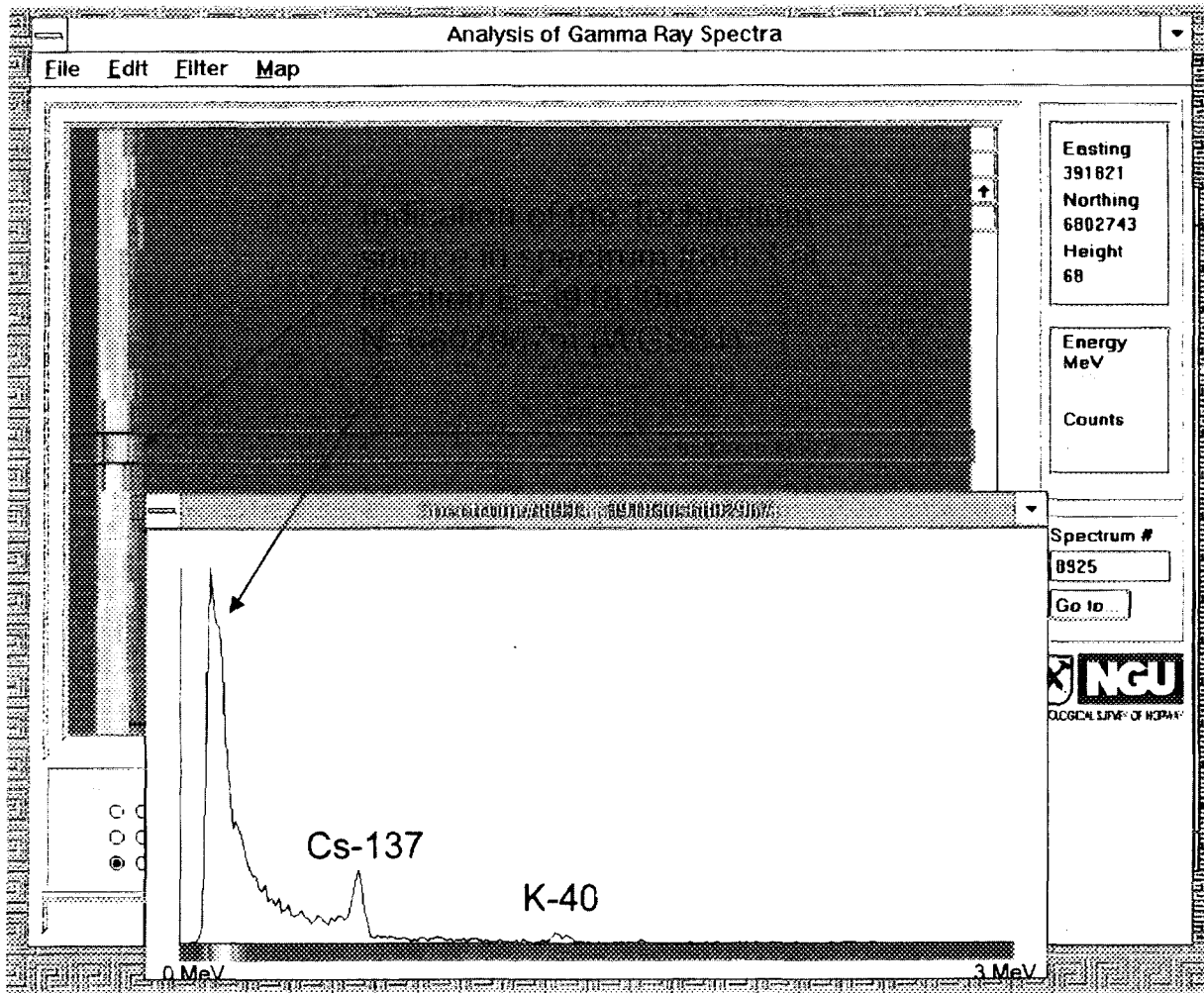


Fig. 4 The signal produced by the Iridium source.

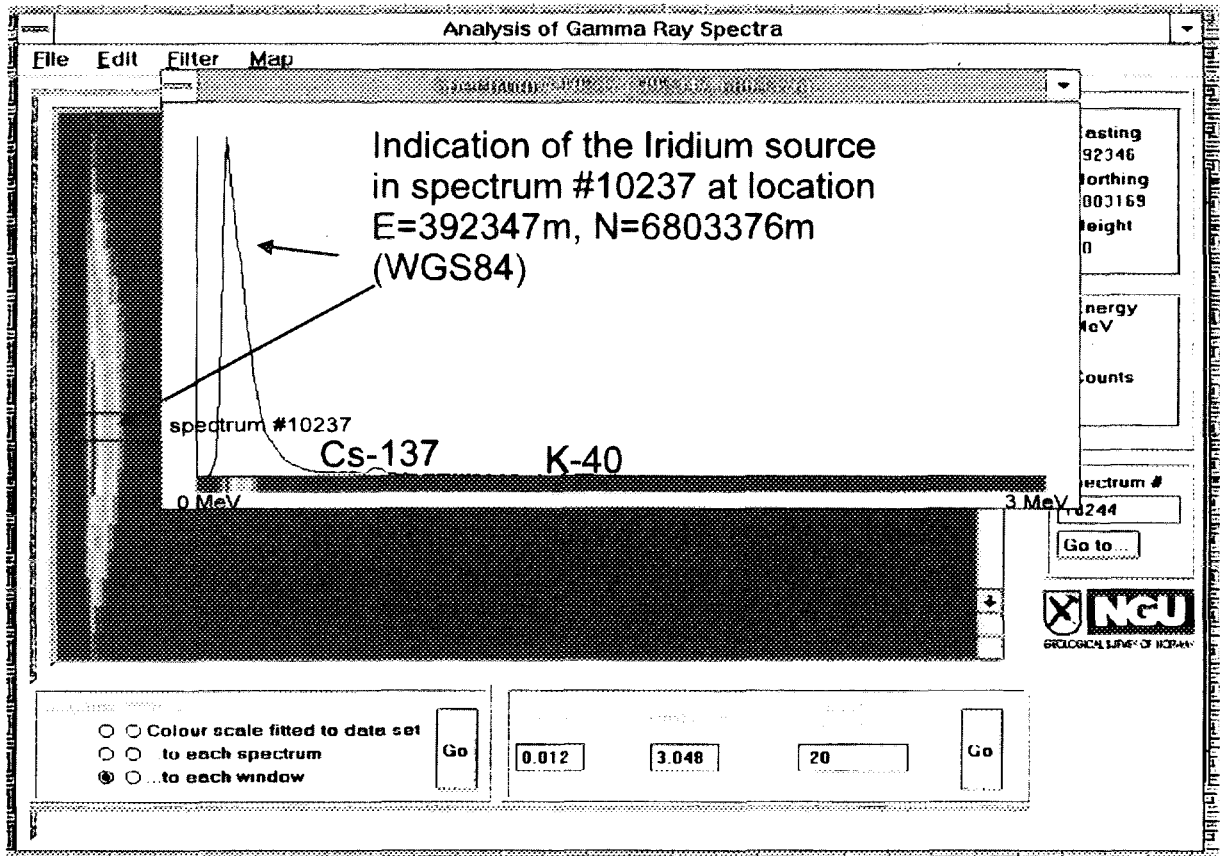


Fig. 5 Location of the Iridium source

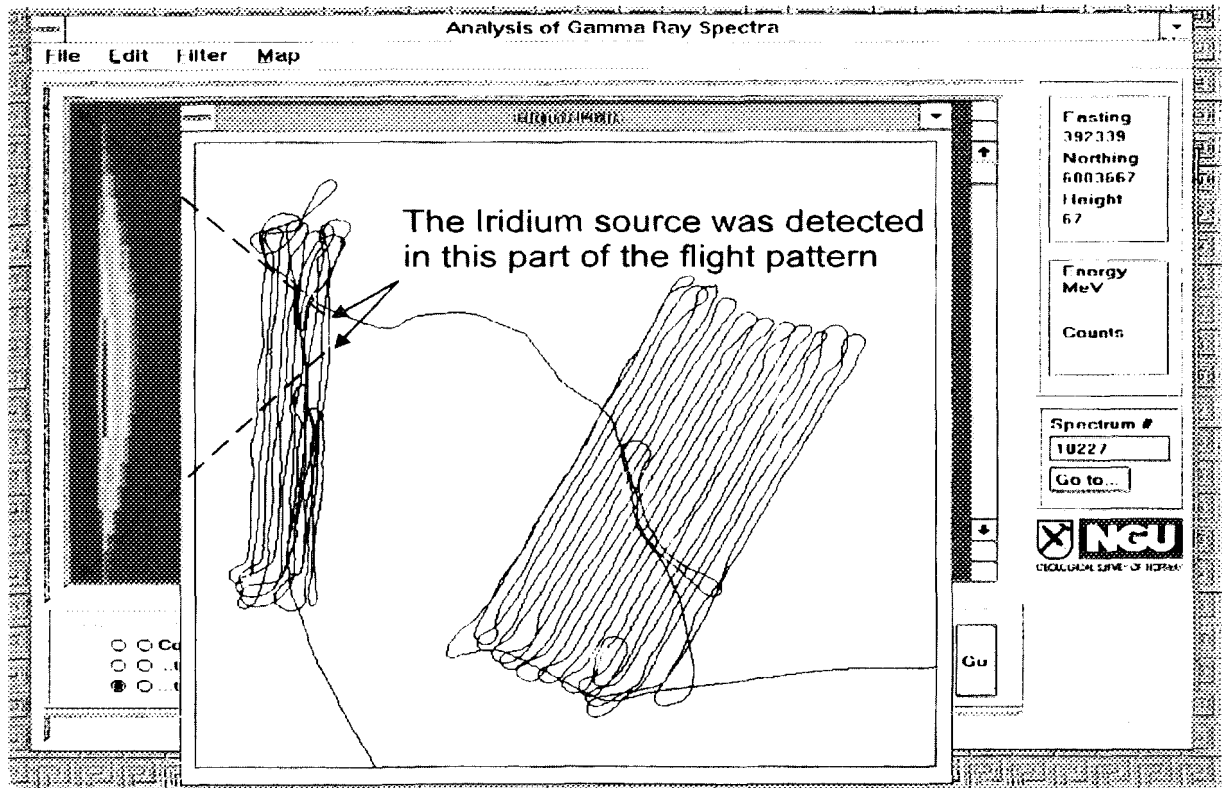
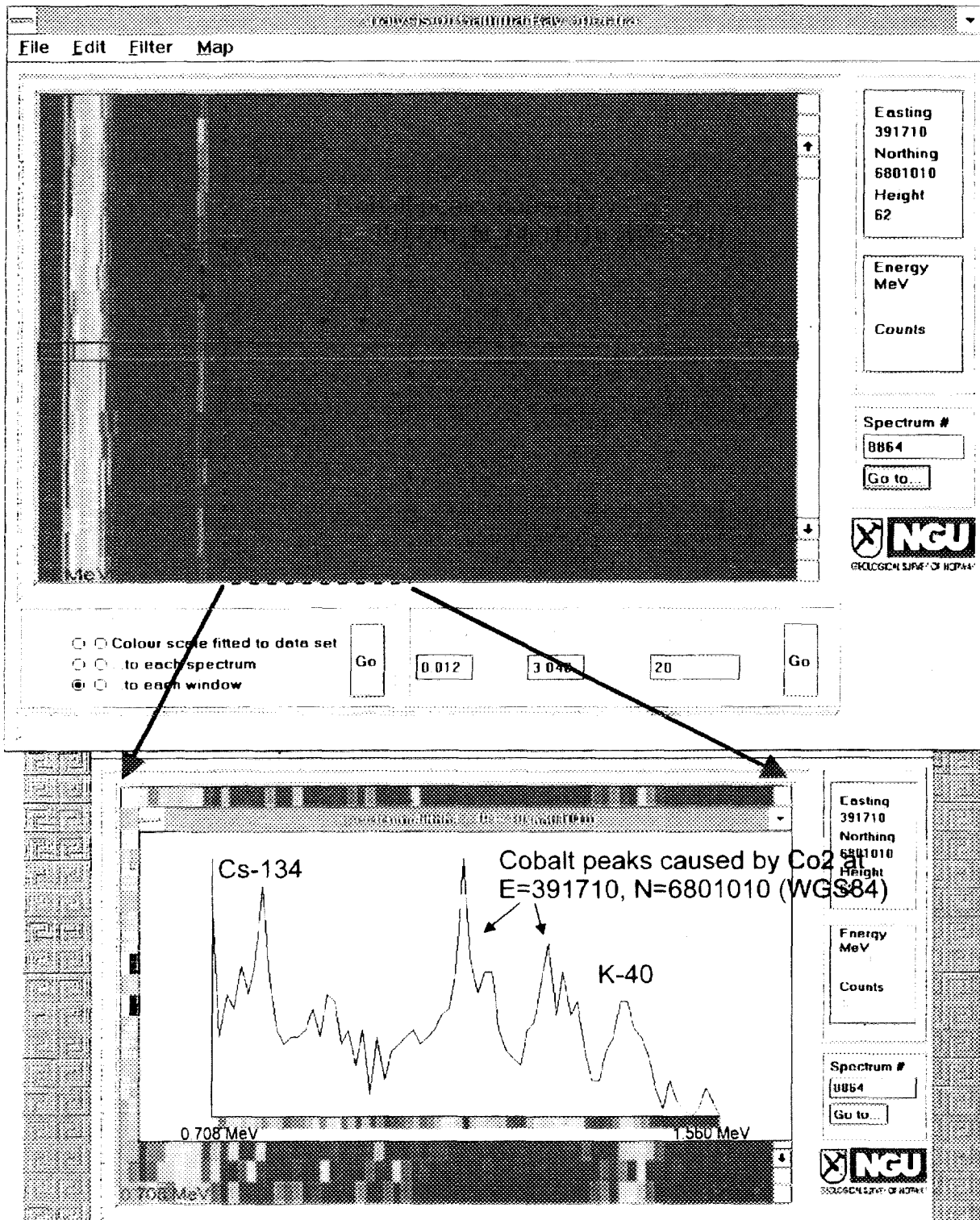
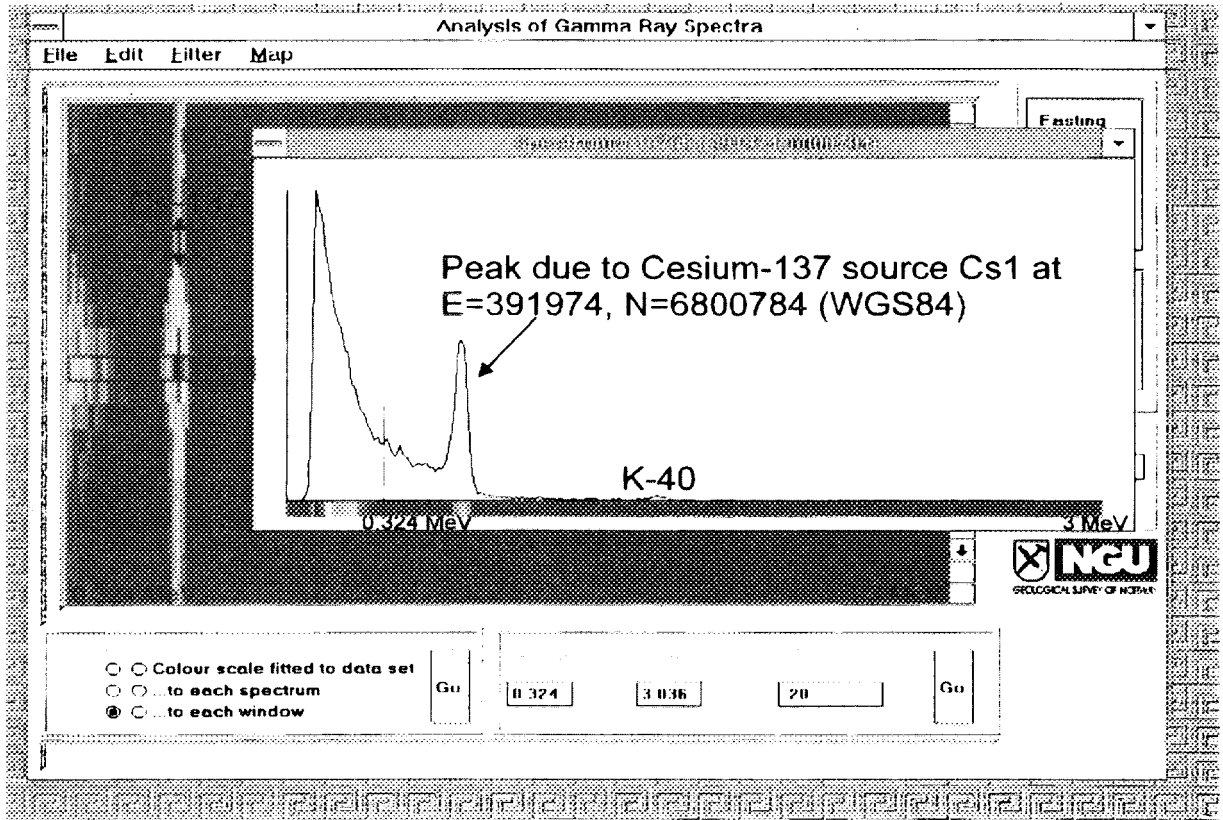


Fig. 6 Gamma ray spectra over Cobalt-60 source Co2. Note that in the lower diagram the energy window 0.708 MeV to 1.560 MeV is used to enhance the view of the Cobalt-60 peaks. This energy window was used to 'scan' the data set for Cobalt-60 sources.



**Fig. 7 Spectra obtained above source Cs1. Low energy channels (<0.324 MeV) are not shown.**



**Fig. 8 Spectra obtained in the vicinity of the Iridium source are dominated by it.**

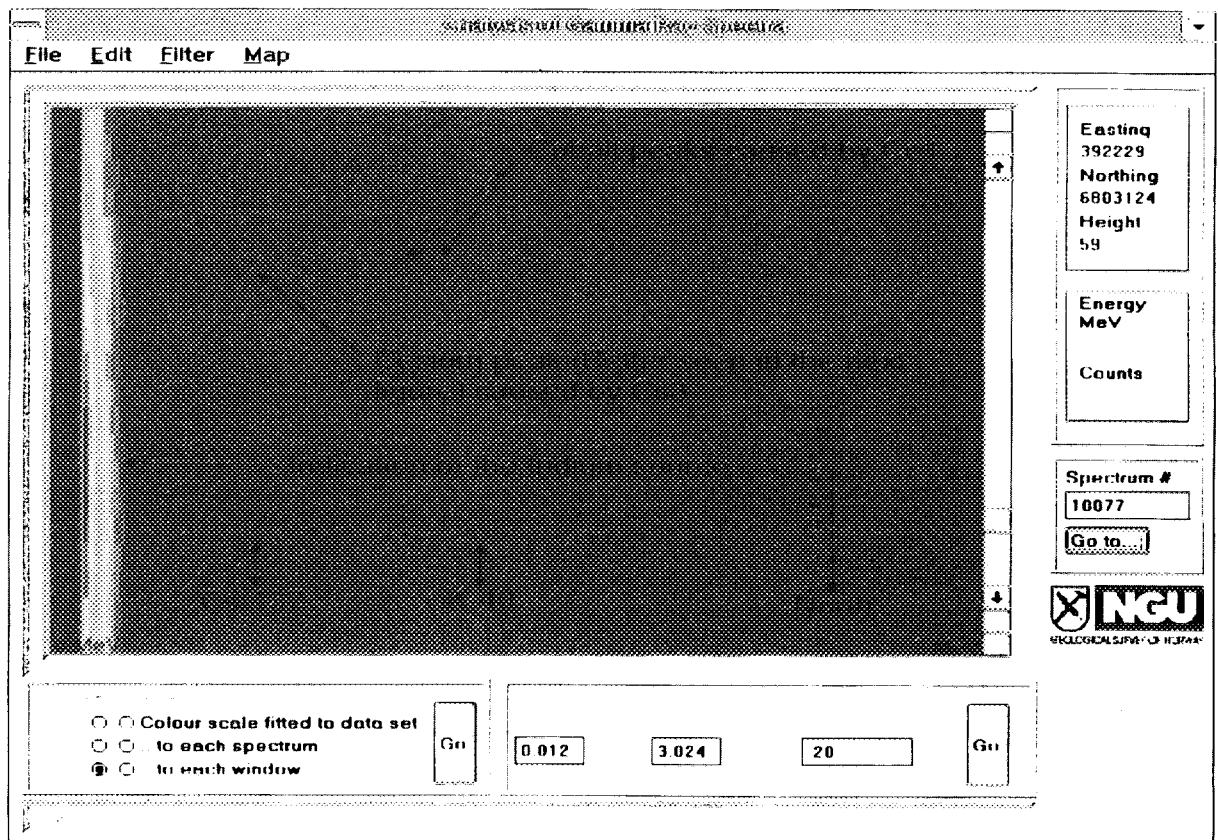
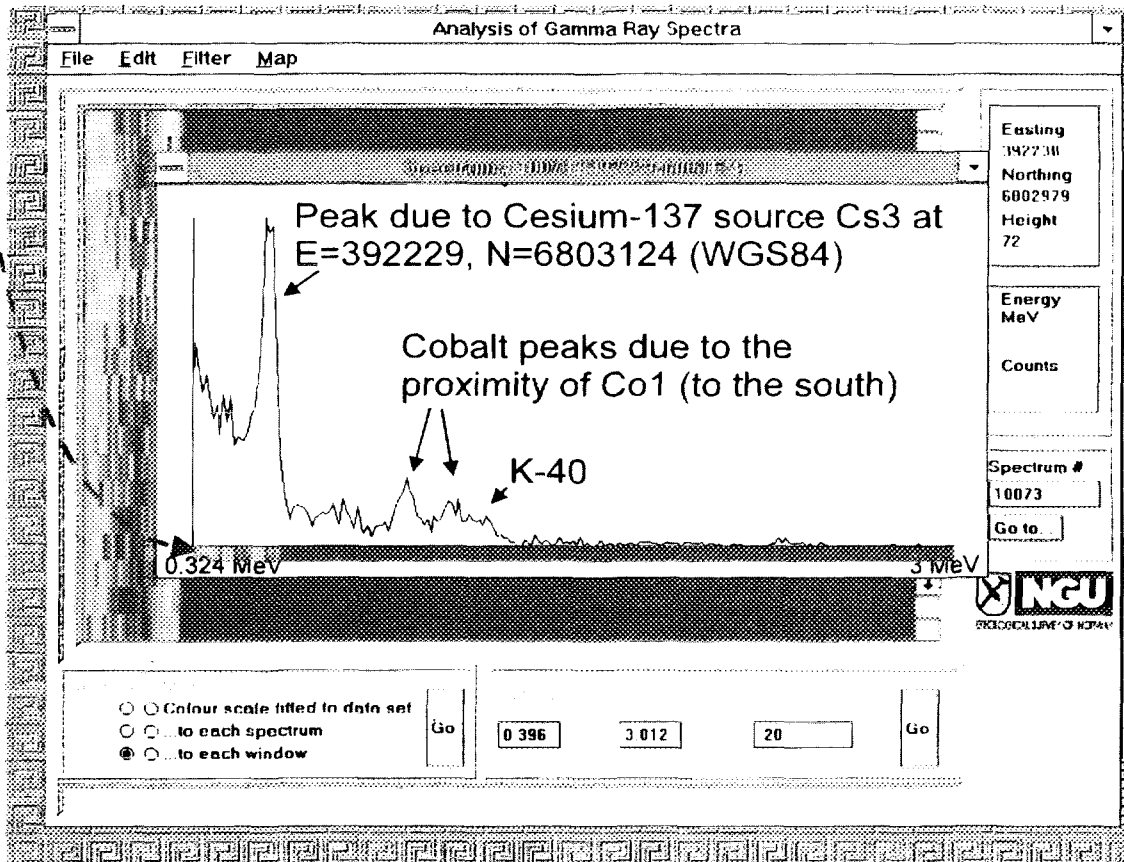
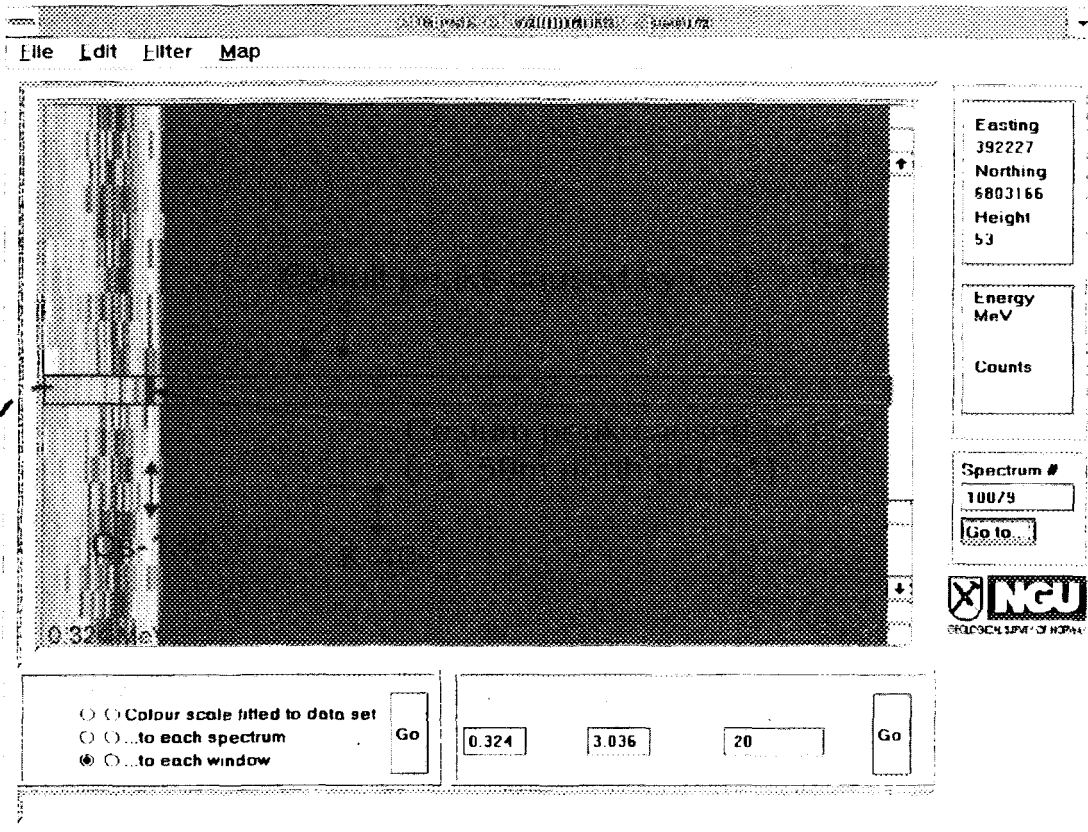


Fig. 9 When the low energy (< 0.324 MeV) parts of the spectra in Fig. 8 are excluded view the signals cause by Cs3 and Co1 become clear.



### 4.3 Results as map presentations

A hard copy Cesium source map was produced in approximately 20 minutes (Map 2b, WGS84 coordinates). In this case we created a Cesium-137 map extracting counts in the cesium energy window, and performed two-dimensional high-pass filtering to retain just the sharp detailed spatial features of the cesium-137 distribution. Filtering was carried out in the frequency domain using a Gaussian cut-off with a standard deviation of 0.004 cycles per metre (which has the effect of eliminating Cesium anomalies with wavelengths much in excess of 500 m). The Cesium source map (Map 2b) clearly indicates the positions and relative activities of Cs1 and Cs4. Although Cs3 was identified during examination of the spectra, it does not appear on the map. One anomaly appears on the map which does not correspond in position to any of the cesium sources. This feature is caused by high-pass filtering of the gamma radiation from a small island or peninsula. The high-pass filtering procedure hides low radiation areas such as lakes (which are easy to see in the original Cesium map). Conversely, the sharp increase in Cesium on an island will be retained in the high-pass filtered data set. We returned to the original spectra to check this Cesium anomaly and immediately noticed that all spectra peaks (Cs-137, U, Th and K) fell to zero on either side of the Cesium anomaly, as would happen over water. This anomaly could therefore be discounted as a source without ground follow-up work. Another feature was found of the Cesium map approximately 1 km north of Cs1. There was no Cesium source placed at that position and it is therefore of unknown significance. There is wet ground in the vicinity of the feature which might enclose a small dry region - a pattern which could result in a sharp local Cesium anomaly. This feature is crossed by two flight lines. The colimated Cs2 source was not detected by NGU, probably due to the line spacing.

Once the Cobalt sources were recognised it took approximately 20 minutes to extract counts in the two energy windows (for Co-60) and make and print a Cobalt map (see map 2c). All three of the Cobalt sources placed within the survey area are clearly represented on the map, along with an indication of their relative activities. The shape of the line-source Co4 is reproduced well in the map. The fourth is located outside the survey area to the east.

## 5 CONCLUSION

The purpose of the exercise in Finland was to obtain standards of reference and detection of hidden sources in area III. A reference for calculation of Cesium-137 ground concentration was obtained through the calibration test over area I. This reference can be used when mapping Cesium-137 contamination level after a fall out. The average ground concentration of <sup>137</sup>Cs in area II was found to be 60 kBq/m<sup>2</sup> with a peak value of 90 kBq/m<sup>2</sup>.

The software application developed at the Geological Survey of Norway detected all but one hidden source in area III. The application allows analysis of gamma ray spectra almost immediately after a flight.

## 6 REFERENCES

International Atomic Energy Agency, Vienna 1991: Airborne gamma ray spectrometer surveying, technical reports series No 323, ISBN 92-0-125291-9

Lahtinen J., Pollanen R. and Toivonen H. 1996: Characteristics and locations of sources RESUME95, Finnish Centre for Radiation and Nuclear safety.

Multala J. & Erkinheimo N., Finland 1995: Airborne measurements RESUME95(appendix air), Geological Survey of Finland.

**NEXT PAGE(S)  
left BLANK**

# Norwegian Institute for Air Research

## Exercise Résumé95. Report from the NILU team.

Figures in Colour Appendix (C.A.):

Fig. 1. Cesium Ground Concentration..... C.A. plate 17

**NEXT PAGE(S)  
left BLANK**

## **Exercise Résumé '95**

Report from the NILU team  
by  
Thor Chr. Berg

Norwegian Institute for Air Research (NILU) participated in the Résumé '95 exercise in Finland 14-18 August, 1995 with the institute aircraft and a research team.

- Team leader : Thor Chr. Berg
- Flight crew : Ole Henriksen, pilot  
Svein Larsen, navigator/co-pilot  
Harald Willoch, system operator
- Aircraft : Twin engine, fixed wing Piper Navajo PA-31
- Detector : 4x4 litres Exploranium Sodium Iodine
- System : Canberra Analog to digital converter model 1510.  
Canberra multichannel analyzer model S100 installed in a PC
- Measuring rate : 3 spectra per second
- Navigation : Trimble GPS receiver model TNL 2100  
King radar altimeter

The NILU team was scheduled to fly in the afternoon on 15 August and the areas II, III and the calibration strip in Area I was measured in about 90 minutes.

Area II was overflown from north to south and vice versa where an east-west spacing of 150 meter between the tracks was tried to obtain. This was rather difficult, because a fixed wing aircraft is quite different from a helicopter in respect of manoeuvrability. A fixed wing aircraft must use higher speed and needs a lot more space for the turn in each end of the field. The speed is also a limiting factor for minimum safe altitude over the area.

However, a successful measuring flight was performed and the result is shown in figure 1.

Area III was measured in the same way as Area II, but the preliminary results are not good suited for pointing out the hidden sources. To be able to do such surveys with a fixed wing aircraft, more sophisticated methods concerning the data handling must be developed. Result from this area is therefore not reported.

The calibration strip on the Vesivehma airport, Area I, was overflown 4 times at different altitudes. The center point was picked out from the data stream and based on STUK data for the point, a correction factor for Area II was calculated. This factor was determined to be 1.9 compared to the calibration NILU had performed in the forehand by overflying a point source. This opens a discussion of what is a correct measurement. A point source calibration can perhaps be used when measuring a fresh fallout while an integrated soil value could be used at old fallout. The difficulties will obviously be in the cases between.



# Norwegian Radiation Protection Authority

## Car-borne survey measurements with a 3x3" NaI detector

SUMMARY ..... 231

INTRODUCTION ..... 231

INSTRUMENTATION ..... 231

    Fig. 1. Car-borne measuring system ..... 232

CALIBRATION ..... 232

FIELD MEASUREMENTS ..... 232

ANALYSIS ..... 232

SURVEY RESULTS ..... 232

ESTIMATION OF DETECTION LIMIT ..... 233

DISCUSSIONS ..... 233

CONCLUSIONS ..... 233

    Fig. 2. Variations in dose rate and in count rate in ROI on route 1 ..... 234

Figures in Colour Appendix (C.A.):

Fig. 3. Fallout maps area II and III ..... C.A. plate 18

**NEXT PAGE(S)**  
**left BLANK**

# Car-borne survey measurements with a 3x3" NaI detector.

**E.Larsen, F.Ugletveit, L.Flø & O. Mikkelsen**  
Norwegian Radiation Protection Authority,  
P.O. Box 55, N-1345 Østerås.

## Summary

The Norwegian Radiation Protection Authority (NRPA) took part in the international survey measurement exercise RÈSUMÈ95 that was arranged in Finland in August 1995. NRPA performed measurements with a simple car-borne measuring system based on standard equipment, a 3x3" NaI detector, an MCA and a GPS connected to a portable PC.

The results show substantial variations in dose rate inside areas of a few square kilometres. Spectrum analysis shows that a major part of these differences are caused by variations in deposition of  $^{137}\text{Cs}$ .

Our results show that even standard 3x3" NaI detectors can be used for car based survey measurements in fall out situations and search for sources. The detection limits are higher than for larger detectors, but the main limiting factor seem to be the timing capabilities of the acquisition system.

## Introduction

In august 1995 the exercise RÈSUMÈ95 was arranged in Vesivehmaa in Finland by the Nordic Nuclear Safety Project, EKO-3. The main objective of the exercise was to compare results from survey measurements from air-borne, car-borne and in-situ measurements on the ground. Different areas and routes had been defined for survey purposes and artificial sources had been hidden.

In Norway there are about 100 sets of equipment with a 3x3" NaI detector connected to an MCA. This standardised system is basically intended for food control, but the equipment could very well serve other purposes during an emergency. The Norwegian Radiation Protection Authority, NRPA, was therefore interested in investigating the use of this standard equipment for survey purposes. This exercise was a good opportunity to test whether this equipment was suitable for this kind of measurements or not and to identify the limiting factors.

## Instrumentation

A prototype for car-born measurements was assembled from standard equipment based on a 3x3" NaI(Tl) detector connected to a Canberra Serie 10+ multi channel analyser (MCA). A 9600 baud serial communication was established between a portable PC and the MCA (Figure 1). In addition a GPS unit for determination of geographical position was connected to the PC through a serial communication port. A computer programme was written to run the MCA and the GPS and store the results on disc during the survey.

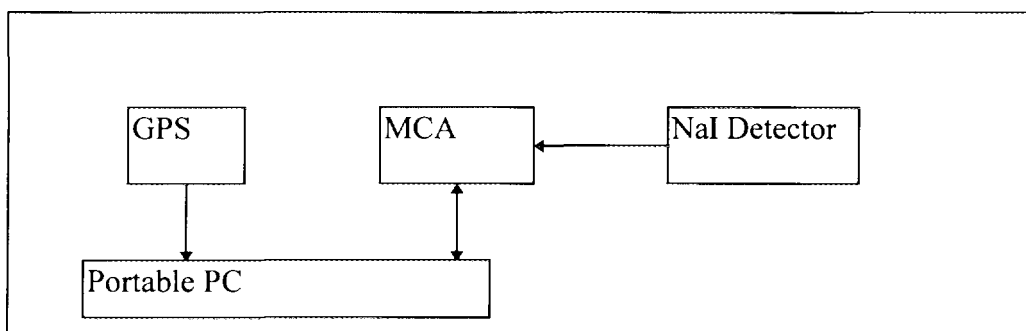


**Figure 1. Car-borne measuring system**

### Calibration

The detector was calibrated in terms of dose rate against a standard  $^{60}\text{Co}$  source in our laboratory. A relationship between dose rate and total spectrum integral was established. This way the dose rate could be determined from the total integral of the NaI spectra. No correction was made for the energy dependence of the detector.

### Field measurements

The NaI detector was placed vertically in the middle of the car facing downwards. Spectra were accumulated in 512 channels spectra over the energy interval 50 - 2000 keV. The data accumulation time was set to 10 seconds per spectrum for all our measurements.

### Analysis

The analysis was not performed «in flight» but just after the measurements had been completed. The dose rate was calculated from the integrated spectra. The position was read from the GPS just before and after each collection period of 10 seconds. The mean value of these two positions was taken as the position associated with the mean dose rate over the collection period.

To investigate the variations of  $^{137}\text{Cs}$  in the in the different areas, analysis was performed with respect to the number of counts in the energy interval 570 - 750 keV.

### Survey results.

On the basis of the field measurements a map was produced (figure 3). This map showed that significant differences in gamma dose rate within the area could be observed.

Along route 1 a small area with high dose rate could be identified. It was assumed that this increased dose rate was caused by a radioactive source in this area. To verify this, a plot of dose rate (proportional to total number of counts in spectrum) and the number of counts in the  $^{137}\text{Cs}$  was made (figure 2). From this plot it can be seen that there is an area just outside area III where the dose rate increased at the same time as the integral of the  $^{137}\text{Cs}$  region decreased. This indicated that one (or more) hidden source were present, presumably with lower energy than  $^{137}\text{Cs}$ . A more thorough spectrum analysis was not carried out.

### **Estimation of detection limit.**

A test for determination of detection limits was carried out. A 2 GBq  $^{137}\text{Cs}$  (50mCi) source and a 20 MBq  $^{60}\text{Co}$  (0.6 mCi) source were placed at distances 10, 20,50, 100 and 200 metres from the road where the cars passed at a speed of 20 and 50 km/h.

During our measurements it was observed that the variation of dose rate was significantly higher than expected from counting statistics alone. The observed variation of dose rate with a fixed detector indicated an additional uncertainty contribution of approx. 5% from the data acquisition system. With this uncertainty it was still possible with a standard 3x3" NaI detector to detect a significant increase in the dose rate from these sources at distances of 100m and 50 m driving at 20 km/h and 50 km/h respectively.

### **Discussions**

The purpose of car-borne survey measurements in Norway would be to identify areas to be further investigated by other means, e.g. well equipped teams on foot. This implies that complete analysis with respect to sources and their exact positions would not be within the scope of our car-borne measurements. For our purpose, recording of dose rate seem to be sufficient. In the early phase of an emergency situation with fresh fallout, it is believed that it is impossible to take advantage of the spectroscopic capabilities of NaI detectors.

The main limiting factor for our system proved to be the data acquisition system rather than the size of the detector. Our use of a standard multi channel analyser for time critical measurements was not quite successful. The communication over the serial port at 9600 baud was too slow and resulted in an enhanced dead time and reduced geographical resolution for the results. For short acquisition periods the system did not offer sufficient accuracy for determination of acquisition time. This resulted in a considerable increase in uncertainty for our measurements. In our search for hidden point sources it would have been an advantage to have better geographical resolution and smaller variations. This can of course be compensated for by making the survey at lower speed.

One major difference between our measuring system and the measuring systems used by other participants at the exercise was the size of the detector. Some participants used detectors more than 40 times the volume of our 3x3" NaI detector. Our detector gave a count rate of about 500 counts per second at normal background resulting in a statistical uncertainty of approx. 2% in the calculated dose rate. Large detectors will give better results at low dose rates but there is a possibility that the acquisition system during an emergency will be overloaded due to high count rates.

### **Conclusions**

Our conclusion from the exercise is that the most important part of the system is the data acquisition unit rather than the size of the detector. With a better acquisition system we think that our car-borne 3x3" NaI detector offers quite good enough data for calculating dose rate with sufficient accuracy. At a dose rate of 100 nSv/h corresponding to natural background, the statistical uncertainty in the calculated average dose rate would typically be 2%. This we consider quite sufficient for this purpose.

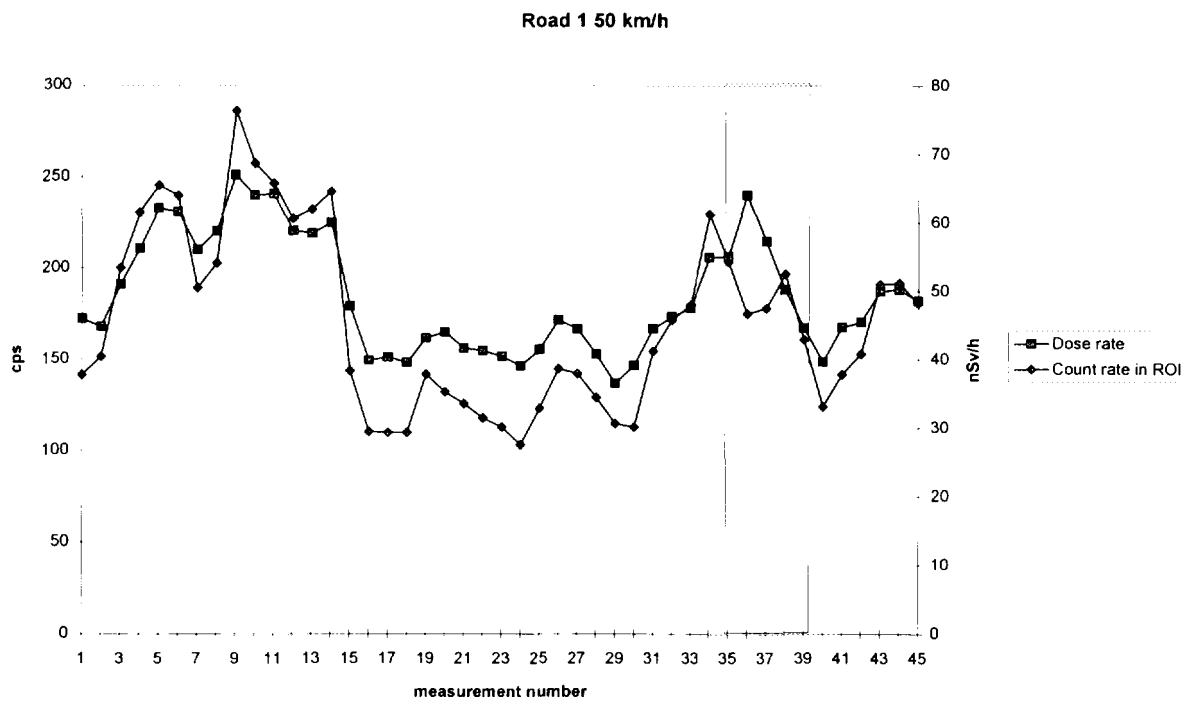


**Figure2. Variations in dose rate and in count rate in ROI on route 1 (50 km/h). Marked area indicates location of hidden source**

**Figure 3. Fallout map of area II and III**



# Scottish Universities Research and Reactor Centre

## Airborne Gamma Ray Measurements Conducted During an International Trial in Finland

ABSTRACT .....	237
1. INTRODUCTION .....	238
2. PREPARATION AND DEPLOYMENT .....	239
3. DATA COLLECTION .....	241
4. RESULTS AND DISCUSSION .....	242
4.1. Area I: Vesivehmaa Airfield Calibration Site .....	242
Tab. 4.1. Effective radionuclide concentrations at Area I .....	242
Tab. 4.2. Comparison of 16 litre NaI calibrations at 100 m height (soil radionuclide analysis and theoretically based).....	243
4.2. Area II: Fallout Mapping .....	243
Fig. 4.1. Flight lines in Area II .....	244
Tab. 4.3. Mean levels across area II (n=1880) .....	244
4.3. Area III: Mapping and Location of Point Sources .....	245
Fig. 4.3. Area III flight lines .....	246
Fig. 4.5. Area III Source Search .....	247
Fig. 4.6. GMX Spectra .....	249
5. DISCUSSION AND CONCLUSIONS .....	250
ACKNOWLEDGEMENTS .....	251
REFERENCES .....	252

### Figures in Colour Appendix (C.A.):

Fig. 4.2. <sup>137</sup> Cs deposition map .....	C.A. plate 19
Fig. 4.4. Mapped data for four of the channels examined .....	C.A. plate 20

**NEXT PAGE(S)  
left BLANK**

## **Airborne Gamma Ray Measurements Conducted During an International Trial in Finland**

D.C.W Sanderson, J.D. Allyson, P. McConville, S. Murphy, J. Smith  
Scottish Universities Research and Reactor Centre  
East Kilbride, Glasgow G75 0QF, Scotland

### **ABSTRACT**

The Scottish Universities Research and Reactor Centre (SURRC) contributed to the Resume 95 exercise by developing the calibration site at Vesivehmaa, and by participating in the airborne gamma spectrometry (AGS) part of the study. This paper summarises the airborne survey results from the SURRC team. The AGS tasks included fallout mapping of a 6x3 km area in central Finland with nominal 150 m line spacing, and a time constrained search for an undisclosed number of hidden radioactive sources. Measurements at the calibration site were also taken to provide a basis for traceable cross comparison between each teams' quantification procedures at a single, well characterised, location.

A decision was taken to transport the SURRC AGS system by land and sea, and to utilise a Finnish Twin Star Helicopter chartered from Helijet OY from Rovaniemi and flown by a UK pilot. Prior to departure the SURRC spectrometer, comprising a 16 l. NaI detector and a 50% GMX detector, was checked, and NaI stripping ratios measured using pads, absorbers and active sheets. Installation and CAA approval details were forwarded to Finland, together with the CV of the proposed pilot, to obtain clearances for the operation. Maps of the study area were digitised to form geographical backdrops for the AGS results. The equipment was transported in a single Landrover, via Harwich, north Germany, and Helsinki; a journey taking 2 days and involving 3 overland stages and two ferries. The system was installed at tested in the Helijet aircraft immediately prior to the study.

The SURRC team was the first to fly starting at 8.00 am on the day of study. Fallout mapping in Area II was accomplished within the allotted 2 hour period, and the source search conducted in Area III within the allotted hour. Immediately on landing the positions of 3 hidden sources were reported to the organisers, with paper copies of tabular data available within a few minutes of landing, and initial mapping taking place within 30 minutes. Fallout maps were prepared later that day, and digital summary data for the flights delivered to DISTAFF that evening. A full set of calibrated maps of Chernobyl deposition and natural radionuclides, together with overlays corresponding to topography, roads, rivers and lakes were finished during the survey and displayed at the end of the exercise. The main survey area (Area II) was found to have a mean  $^{137}\text{Cs}$  deposition of  $64.4 \pm 24.4 \text{ kBq m}^{-2}$ , based on the calibration appropriate to the Vesivehmaa site.

The major point sources in Area III were discovered, although the collimated  $^{137}\text{Cs}$  and  $^{60}\text{Co}$  sources were not. Retrospective analysis has shown that sources Cs3 and Cs4 were not significantly above local environmental levels in our data set; whereas the low activity  $^{60}\text{Co}$  source Co3 was detected. This confirms the improved sensitivity of AGS source searches to nuclides which are not already present as environmental contaminants. The collimated  $^{192}\text{I}$  was found both using scattered radiation and from full energy lines detected with a Ge detector. The  $^{99\text{m}}\text{Tc}$  was located using a ratio of low energy integrals from the NaI spectra.

The exercise provided valuable experience of overseas deployment, confirming the feasibility of transporting a full system for use in local aircraft. The fallout mapping tasks were readily accomplished, producing results which show interesting correlations with land use. The source search provided a valuable demonstration of the importance of rapid spectral analysis under exercise conditions. The experience has also served the valuable purpose of identifying areas for further system development.

## 1. INTRODUCTION

Airborne and in-situ measurement techniques allow rapid measurement and assessment of  $\gamma$ -ray emitting radionuclides in environmental contexts. Fallout deposition, following a major nuclear accident, does not respect national boundaries, as was clearly shown after the Chernobyl accident. The importance of reliable deposition estimates for public information, and to provide a level basis for counter-measures such as food intervention, in turn raises questions of transnational standardisation of radioactivity measurement. The **RÉSUMÉ 95** (Rapid Environmental Surveying Using Mobile Equipment) exercise, originally planned by NKS as a Nordic study, but with enlarged participation from German, French, Canadian and UK teams, represents the first attempt to cross compare airborne gamma spectrometry and other mobile monitoring techniques in the context of an international study.

The study was located in central Finland, based on a small military airfield at Vesivehmaa, some 150 km north of Helsinki. This area received deposition of some 100 kBq $m^{-2}$  or more, set in a geological context of mainly acidic rocks and therefore provide a setting of generally elevated levels of both anthropogenic and natural radionuclides. A calibration site was established at the airfield (Area I) based on the SURRC expanding hexagon design. A series of core samples was collected in May 1995, and analysed by high resolution gamma spectrometry at SURRC, STUK and SSI, relative to international reference materials to establish a basis for traceable calibration of mobile equipment. Each team was asked to make airborne measurements above this site as the first part of their survey task.

The other two AGS tasks were to perform  $^{137}\text{Cs}$  deposition mapping in a 6x3 km area 37 km to the NW of Vesivehmaa, designated Area II, with nominal flight line spacing of 150 m, within a 2 hour period, and to search for an undisclosed set of point sources within a 5 x 1 km area (Area III) 3 km to the west of Area II, within a maximum search time of one hour. Both of these tasks required a combination of accurate navigation and short sampling times, thus favouring AGS systems based on high volume scintillation spectrometers. The exercise was organised by NKS, and managed by a DISTAFF drawn from the Danish Emergency Management Agency, STUK, the Geological Survey of Finland, and SSI.

Areas II and III contained mostly forestation (coniferous and birch trees) of variable density, lakes, marsh ground, rocky terrain and some open spaces associated with agriculture. The topography was relatively flat, with higher ground seldom exceeding 50 m in height. Some of the lake-sides were quite steep. Both Areas II and III were pre-selected for their known high  $^{137}\text{Cs}$  deposition based on airborne survey results collected by the Geological Survey of Finland (GSF). GSF facilitated aircraft operations before and during the exercise.

SURRC has conducted a series of developmental airborne gamma ray surveys deposition mapping, definition of natural background, source searches, studies of nuclear sites and emergency exercise since 1988<sup>1-17</sup>. In parallel system development and research into calibration methodology has taken place<sup>18-25</sup>. Two systems are maintained in a state of readiness for use in the laboratory. This paper presents a summary of the SURRC airborne survey participation in the RÉSUMÉ 95 exercise, giving details of preparatory work, deployment and operational details, together with results and a discussion of the main conclusions from the experience. A full technical report, giving further details of the other nuclides mapped is available from SURRC.

## 2. PREPARATION AND DEPLOYMENT

Preparatory activities included preparation of the calibration site, identification of the mode of deployment, selection and preparation of the spectrometer, transportation and deployment in Finland.

Prior to the exercise the suggestion of implementing a traceable calibration site based on the sampling schemes developed in previous SURRC work<sup>4,5,12,13,23-25</sup> was put to NKS, and a sampling trip organised in May 1995 to the study area. A standard hexagonal calibration pattern was constructed across the grass airfield during May, and approximately 50 soil cores taken for gamma spectrometry at SURRC and STUK. The results showed effective <sup>137</sup>Cs deposition values in Area I were  $50.7 \pm 5.2$  kBq m<sup>-2</sup> observed from 1 m detector height,  $51.1 \pm 6.9$  kBq m<sup>-2</sup> at 50 m and  $47.9 \pm 8.5$  kBq m<sup>-2</sup> at 100 m height. The depth distribution of activity could be loosely described by an exponential profile down to 6 cm, with a relaxation mass per unit area<sup>27</sup> ( $\beta$ ) of  $1.31 \pm 0.15$  g cm<sup>-2</sup>. The majority of activity on the calibration site is thus within the first 2 cm of soil depth, a superficial distribution compared with other areas where such sites have been established. Tyler et al<sup>24</sup> have shown a quantitative empirical relationship between mean mass depth and calibration constant, which is consistent with that expected<sup>22</sup> on the basis of theoretical simulation of the detector response.

During the sampling visit the opportunity was taken to investigate options for obtaining a local aircraft. Back in East Kilbride the options of fitting a local aircraft and transportation to Finland, sharing an aircraft with the Helinuc team, or using a Finnish aircraft were considered. The costs of each option were surprisingly similar, each possibility presenting a slightly different range of technical risks. A key factor in deciding to use a chartered Twin Star helicopter obtained from Helijet OY in Rovaniemi was that it was possible to agree for Paul Heathcote alias Hector, a pilot who had worked extensively with the SURRC team, to operate the aircraft, during a short period of leave from his usual duties. This entailed forwarding details of the spectrometer installation and pilots' CV to Finland. A temporary licence for Hector was obtained. We are both impressed and grateful to both the Finnish authorities and to Helijet for permitting an unknown, overseas, pilot to fly the aircraft for the international study.

The detector configuration selected for the study comprised a combined NaI/Ge spectrometer, with a 16 litre NaI detector array and a single 50% GMX detector, both mounted internally to the aircraft. The navigational system was a complementary pair of NavStar XR4 DGPS receivers, with a telemetry beacon system hired from CM&T to facilitate differential GPS location. The SURRC instrumentation rack provides power supplies and data logging for up to 2 independent NaI spectrometers, and up to 4 summed Ge detectors. The configuration used for this study thus leaves some instrumental redundancy. Prior to the survey the system was tested in East Kilbride. NaI stripping ratios were measured using a set of small scale Grasty pads for U,Th, K together with a 1 m<sup>-2</sup> <sup>137</sup>Cs source, a point <sup>60</sup>Co source and a set of 20 full area perspex absorbers.

Maps of the local topography, geology, rivers, lakes, land-use, urban areas and roads were obtained from the Geological Survey of Finland and digitised using Intergraph Microstation V 4.0 to form a series of thematic maps for Areas II and III. These data were transferred into CorelDraw as layered backdrops to be used for presentation of mapping results and radiometric data sets. The solid geology of Area II is predominantly granodiorite, with a small granite intrusion in the SW part of the area, and a veined gneiss in the southern and eastern parts. Drift deposits are mainly of glacial origin, and include an esker running from the SE to Western parts of the area. The topographic relief is mainly dominated by the esker, being limited to some 50 m variation. The area includes more than 20 lakes of varying size. As stated in the introduction the majority of the area is coniferous forest, however small cleared areas of cultivated also occur, and were identified in the thematic maps prepared. Other geographical preparation included development of subroutines within the SURRC AGS data processing software suite to transform GPS latitude and longitude into local KJ metric coordinates. Jane Drummond from the Topographic Sciences Department in Glasgow University very kindly prepared a stand-alone Fortran programme to perform this transformation to 1 m or better precision. The algorithms from this programme were incorporated into SURRC AGS software and verified using both the FORTRAN code, and the edge coordinates for Area II which were supplied by the geological survey of Finland.

The flight plans were determined before hand using software developed by SURRC, that provides a sequential series of way-points in latitude/longitude such that the start and end points of each flight line can be defined.

The flight line separation was fixed by the NKS exercise coordinators (150 m). The waypoint tables were loaded into the Navstar XR4 GPS system to assist with navigation.

Having completed these preparatory tasks the system, together with a spare spectrometer and crystal pack, two ground mapping computers and a colour printer was packed into a Landrover Defender for shipment to Finland. The vehicle was chosen to represent the finest traditions of British fieldwork, but also with the possibility of participating in off-road carborne measurements if desired during the survey. The route taken involved overland transit from East Kilbride to Harwich, a ferry to Hamburg, a 50 km drive to Lubeck, and then an overnight ferry to Helsinki, followed by the drive to the Tallukka hotel in Vääksy. The system arrive late on the evening of 11th August, ready for a rendezvous with Helijet on the morning of the 12th August.

The Twin Star aircraft arrived at Vesivehmaa late in the morning of 12th August. After stripping carpets and rear seats the SURRC baseplates, racks, and detectors were installed ready for a short flight trial at the end of the afternoon. The detectors and spectrometer functioned well on the 12th; minor problems with generator noise being overcome by introducing an additional power line filter. However the radar altimeter fitted to the aircraft produced erratic performance, and problems were encountered with the DGPS telemetry link. Helijet succeeded in locating a replacement radar altimeter which arrived on the 14th August, and was installed in time for a late evening orientation flight to the start of Area II. The radar altimeter height conversion constants were checked briefly on the calibration site during this flight. The telemetry link was not functioning at this stage, and therefore the decision was made to use autonomous GPS navigation for the flights.

### 3. DATA COLLECTION

The RÉSUMÉ 95 exercise was formally launched with a DISTAFF briefing in the afternoon of 14th August. Flights were scheduled from 8:00 am the following morning, with start times at 2 hour intervals, through the following 3 days. Initially it appeared that the operational plan allowed very little time for delays for operational reasons, or as a result of difficulties with equipment. The Vesivehmaa airfield was not in direct radio contact with aircraft at all times during the flights, and therefore air safety rules were imposed whereby only one aircraft was permitted in each of Areas II and III at any time, and transfer routes between Vesivehmaa were controlled to avoid the possibility of aircraft collision. An observer with a receiving radio was placed between areas II and III, and pilots were instructed to radio their departure from Area II to this observer, for telephone confirmation to Vesivehmaa prior to the take off of the next team.

SURRC was given the unenviable task of flying first with a start time of 8.00 am on 15th Tuesday, and the heavy burden of responsibility to avoid introducing delays to the study at the outset. Having completed flight trials the previous evening after the briefing session, the survey team arrived at Vesivehmaa before 7.30 am, and conducted spectrometer pre-flight checks. Composite energy resolution of the detector was measured using a 50x50 cm board coated with 10 kBq of  $^{137}\text{Cs}$ . The aircraft was prepared for flight, and engines started shortly before 8:00am. At precisely 8:00 am the aircraft lifted off, flying a track across the calibration site en-route to Area II. Background data were collected over lakes en-route, and Area II was reached at 08:15.

As noted in the introductory sections the study protocol had been designed to favour short integration times and DGPS navigation. The spectrometer system used is capable of interleaving scintillation and Ge spectra with a higher sampling rate for the scintillation spectra; however the highest sampling rates are limited by the data storage timescales for Ge data. For this reason a decision was taken to run the main surveys with 2s integration on the NaI detector only, and to use both the detectors with 3s integration on the NaI detector and 6 second integration on the Ge detector, to collect supplementary data after the main mapping objectives had been met. GPS positional data were recorded between every pair of spectra, and interpolated to the estimated midpoints of each acquisition. Ground clearance for each observation was recorded using time-averaged radar altimetry. Scintillation spectra were recorded in 500 channels, and Ge spectra in 2000 channels, together with real time integrated count rates from a set of 8 pre-defined energy regions - which were displayed continuously to the detector operators. The Navstar-XR4 GPS system was used for flight guidance, with steering information being relayed to the pilot over the intercom. Survey data were collected with a ground clearance of 50-75 m and ground speed of 65 knots.

The main 150 m nominal flight lines were completed by 09:45, one line having been repeated to improve positioning, and supplementary data with Ge spectra were collected between 09:45 and 10:02 within Area II and en-route to Area III. The arrival time in Area III was 10:06. Between this time and the departure time of 11:06 from Area III the source search was conducted, again mainly with the NaI detector, arranging N-S flight lines with a nominal 75 m spacing, with the last few minutes devoted to free flying with both NaI and Ge detectors operating. The aircraft returned the Vesivehmaa, spending 6 minutes collecting data at a series of heights on the calibration site, and landing at 11:36. The positions of three sources in Area III were reported verbally to H. Toivonen at 11:36, plus other anomalies to be investigated later. The first colour maps of  $^{137}\text{Cs}$  and  $^{60}\text{Co}$  were displayed in the control tower at 11:48, and tabular summaries of the integrated count rates for each observation were printed out by 11:50.

It was with a sense of relief that the data acquisition tasks were completed successfully and within time targets, setting a target for other teams to emulate. The weather conditions were superb during the exercise, and the few technical delays which were incurred by later AGS teams did not prevent completion of their main survey tasks within the study period.

## 4. RESULTS AND DISCUSSION

The data collected were used to prepare maps of  $^{137}\text{Cs}$ ,  $^{40}\text{K}$ ,  $^{214}\text{Bi}$ ,  $^{208}\text{Tl}$  and gamma dose rate for area II, using standard procedures, and for further analysis of the source search data set. This last analysis took place during the survey, without knowledge of the source positions, and also after the study period once the locations of sources which had not been identified during the study had been disclosed. The following sections discuss results from the calibration site - used to verify system sensitivities for mapping, mapping results from Area II, and results from the source search.

### 4.1 Area I: Vesivehmaa Airfield Calibration Site

As explained previously and elsewhere the calibration site at Vesivehmaa ( $61^{\circ} 08.63' \text{N}$ ,  $25^{\circ} 41.783' \text{E}$ ) had been sampled in May to define environmental radionuclide levels, and their spatial variability<sup>26</sup>. Table 4.1 shows the effective mean inventory and deposition estimates appropriate to observations for airborne survey heights. The values for natural nuclides refer to the wet activity concentrations at the time of sampling, which may not be fully representative of conditions during the exercise, since moisture content probably changed. Although this will not affect  $^{137}\text{Cs}$  measured deposition to any great extent since it has a near surface distribution, it may influence calibration factors for the natural radionuclides, particularly  $^{214}\text{Bi}$ , a daughter product of  $^{222}\text{Rn}$ . Unfortunately the intended use of in-situ gamma spectrometry from the STUK vehicle to record such changes was not successful due to system changes between May and August. The mean relaxation mass per unit area ( $\beta$ ) of  $^{137}\text{Cs}$  in Area I was found to be  $1.31 \pm 0.15 \text{ g cm}^{-2}$ . The mean wet density (in May) was  $1.29 \pm 0.49 \text{ g cm}^{-3}$  (0-16 cm).

**Table 4.1** Effective radionuclide concentrations at Area I.

Detector Height /m	Mean $^{137}\text{Cs}$ / kBq m <sup>-2</sup>	Mean $^{40}\text{K}$ / Bq per kg	Mean $^{214}\text{Bi}$ / Bq per kg	Mean $^{208}\text{Tl}$ / Bq per kg
1	$50.7 \pm 5.2$	$577.7 \pm 46.1$	$40.9 \pm 8.9$	$9.7 \pm 1.0$
50	$51.1 \pm 6.9$	$647.8 \pm 68.9$	$53.1 \pm 11.9$	$10.7 \pm 1.8$
100	$47.9 \pm 8.5$	$597.8 \pm 62.8$	$45.2 \pm 12.1$	$9.5 \pm 1.2$

The AGS results at the calibration site were used to measure height correction coefficients; the values obtained being used to standardise data, as well as to check for system sensitivities relative to working values, or those derived on a theoretical basis. In this way absolute errors due to radar altimeter calibration, or to attenuation of gamma radiation in the aircraft hull do not lead to systematic errors in quantification. The height correction coefficients are tabulated in the SURRC technical report.

The quantification procedures used for rapid deposition mapping<sup>20,27</sup> follow a sequence of integration of full energy count rates for each nuclide, subtraction of background, stripping of interferences, standardisation to constant ground clearance, and scaling to calibrated deposition or activity concentration units using a linear calibration function. The slope of the calibration function represents system sensitivity, while the intercept can be used to compensate for any systematic uncertainties in stripping. In practice the intercept values are close to zero. At Vesivehmaa the measured count rates for nuclides corresponding to ground truth results were used to estimate empirical calibration constants. These were compared with theoretical sensitivity estimates based on a combination of Monte Carlo calculations of  $\gamma$ -ray transport, 16 litre detector response and numerical integrations of exponential and uniformly distributed sources<sup>22</sup>. Table 4.2 shows both sets of results with a very acceptable agreement between both sets of values. The differences can be attributed to changes from the assumed radionuclide depth profile. For  $^{40}\text{K}$  in particular, a depletion of activity per unit mass was observed in the first few centimetres of the soil depth. This led to a significantly higher calibration factor owing to the

count-rate being less than expected when assuming a uniform distribution with depth. This was similarly observed, but to a lesser extent with  $^{214}\text{Bi}$  and  $^{208}\text{Tl}$  radionuclides. In particular it is notable that experimental and theoretical Cs calibration factors are in agreement within  $\pm 10\%$ .

**Table 4.2** Comparison of 16 litre NaI calibrations at 100 m height (soil radionuclide analysis and theoretically based).

Radionuclide	Fieldwork	Theoretical
$^{137}\text{Cs}$	$0.099 \pm 0.02 \text{ kBq m}^{-2}/\text{cps}$	$0.11 \text{ kBq m}^{-2}/\text{cps}$
$^{40}\text{K}$	$6.77 \pm 0.71 \text{ Bq kg}^{-1}/\text{cps}$	$5.23 \text{ Bq kg}^{-1}/\text{cps}$
$^{214}\text{Bi}$	$3.77 \pm 1.00 \text{ Bq kg}^{-1}/\text{cps}$	$3.16 \text{ Bq kg}^{-1}/\text{cps}$
$^{208}\text{Tl}$	$0.42 \pm 0.05 \text{ Bq kg}^{-1}/\text{cps}$	$0.47 \text{ Bq kg}^{-1}/\text{cps}$

## 4.2 Area II: Fallout Mapping

Area II, a 3x6 km region, was contaminated during the first few days after the release from Chernobyl in 1986 and although not extensively investigated was known to have deposition of some 50-100  $\text{kBq m}^{-2}$   $^{137}\text{Cs}$ . Flight lines for the survey conducted on 15th August are shown in figure 4.1. The data were used to prepare radiometric maps for  $^{137}\text{Cs}$  (in  $\text{kBq m}^{-2}$ ),  $^{40}\text{K}$ ,  $^{214}\text{Bi}$ ,  $^{208}\text{Tl}$  (in  $\text{Bq kg}^{-1}$ ) and gamma dose rate (in  $\text{mGy a}^{-1}$ ), using the quantification procedures described above, together with colour mapping routines, and juxtaposition with the transparent thematic map layers prepared prior to the survey. All these maps were prepared during the study period, and are presented in the full technical report.

Mean values of all radiometric variables are shown below in table 4.3.

The  $^{137}\text{Cs}$  deposition map is presented here as figure 4.2. The mean value of Cs inferred from these data is  $64.4 \pm 24 \text{ kBq m}^{-2}$ , with peak values above  $100 \text{ kBq m}^{-2}$ . The highest levels of  $^{137}\text{Cs}$  occur on the central and northern parts of the area, which were noted to be mainly forested areas. It is notable that lower levels are observed in those areas identified on thematic maps as being associated with cultivation. The reasons for this could be a combination of the original deposition pattern and subsequent natural and anthropogenically influenced re-distribution. The possibility that the forested areas have a significant proportion of activity in tree canopies should be considered, as well as burial effects in cultivated areas.

The absolute status of the deposition maps clearly depends on whether the source distribution at Vesivehmaa is representative of Area II. During the soil sampling conducted in May, nine soil cores were collected at different locations within Area II and provided some information about the depth distribution of  $^{137}\text{Cs}$  in this region. The mean  $\beta$  for  $^{137}\text{Cs}$  in Area II ( $n=9$ ) was found to be  $1.31 \pm 0.15 \text{ g cm}^{-2}$  (mean density in May  $1.07 \pm 0.46 \text{ g cm}^{-3}$ ), and therefore represents a slightly deeper activity distribution than that found in Area I. It may mean that some under estimation of absolute radiocaesium levels will be produced in Area II (or at least at the nine locations sampled), however the extent to which the 9 samples are representative of Area II cannot be established.

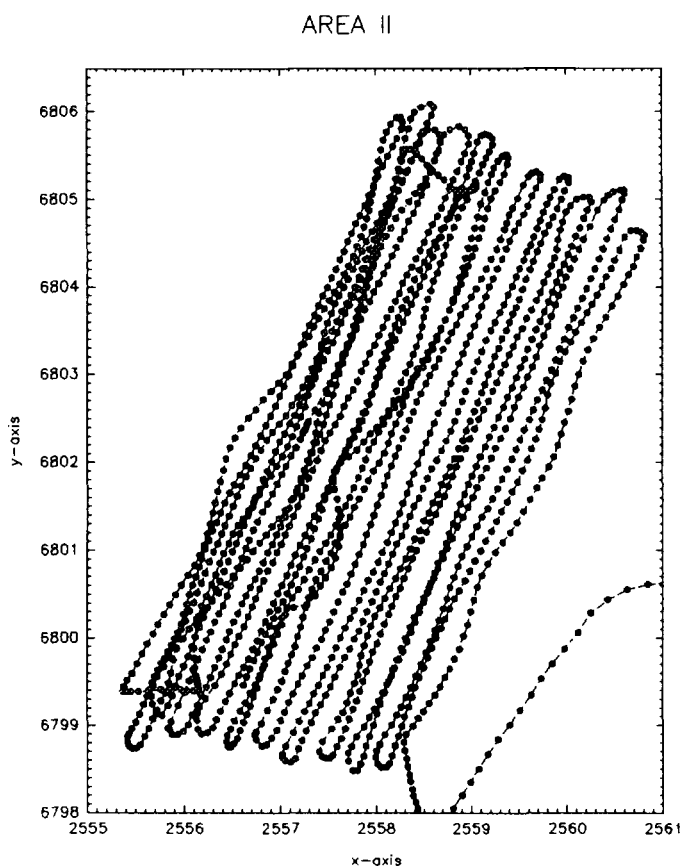


**Figure 4.1** Flight lines in Area II.

**Table 4.3** Mean levels across Area II (n=1880).

Radionuclide	Mean Value
$^{137}\text{Cs}$	$64.0 \pm 24.4 (\pm 0.6) \text{ kBq m}^{-2}$
$^{60}\text{Co}$	$18.67 \pm 13.3 (\pm 0.3) \text{ cps @ 100 m}$
$^{40}\text{K}$	$369.9 \pm 172.4 (\pm 3.9) \text{ Bq kg}^{-1}$
$^{214}\text{Bi}$	$29.1 \pm 18.1 (\pm 0.4) \text{ Bq kg}^{-1}$
$^{208}\text{Tl}$	$5.52 \pm 3.12 (\pm 0.07) \text{ Bq kg}^{-1}$
Gamma	$0.99 \pm 0.33 (\pm 0.008) \text{ mGy a}^{-1}$

Concentrated forestation has a shielding and collimating effect. A 15% attenuation has been reported in dense tree cover in tropical environments<sup>27</sup>. Whilst no field experiments were conducted during the exercise, some systematic effects may exist in the calibration of the data sets of Area's II and III. There was no tree cover on the calibration pad of Area I. The other maps for natural nuclides show far less spatial variability, although there is evidence of the esker in K, Bi and Tl maps. The gamma dose rate map shows a significant spatial correlation with the <sup>137</sup>Cs deposition pattern; consistent with inferred levels of Cs, which in near surface distributions would represent a significant proportion of the external radiation field.

#### 4.3 Area III: Mapping and Location of Point Sources

Fifteen discrete sources of activity were hidden on 15th August within the confines of Area III, in the Padasjoki region. The topography was similar to Area II, with a small bay of Lake Vesijako to the NE corner of the 1 km x 5 km rectangular box. Of the nine <sup>60</sup>Co sources Co1, Co2 and Co3 were 7, 9 and 0.7 mCi activity respectively. Co3 was placed along the road joining Area's II and III, at an intersection. The remaining six (Co4-Co9) were 1.8, 1.8, 1.0, 1.68, 1.74 and 1.44 mCi, and arranged closely together along 300 m of road (about 20-30 m spacing). Four <sup>137</sup>Cs sources were hidden (Cs1-Cs4) of activity 77, 50, 7.5 and 14.6 mCi. Cs2 was a collimated source. In addition, a single source of <sup>192</sup>Ir (15 000 mCi, an industrial gamma radiography device) was placed just outside of Area III. A single source of <sup>99m</sup>Tc (30+30 mCi; two ampoules) was placed midway between the last in the line of Co sources and the western boundary.

The flight conditions were described in section 3, based on N-S flights with a nominal line spacing of 75 m. The precision of navigation in this part of the study was limited by the absence of DGPS, and by terrain which did not lend itself to visual navigation under time constrained conditions, for those not familiar with the landscape.

The flight lines for the main part of the source search, based on NaI spectrometry are shown in figure 4.3.

In-flight data processing included real-time integration of 8 pre-defined spectral windows, the first 6 of which, corresponding to <sup>137</sup>Cs, <sup>60</sup>Co, the natural nuclides and gamma dose rate were tabulated in the form of a summary file at the end of the survey. Initial source identifications were based on numerical examination and profile plotting of the flight records for these channels. Back at the Tallukka hotel, the full spectral data set was re-integrated to provide a second set of regions of interest including further low energy components, and individual spectra were also analysed. One benefit of the exercise is the recognition that software which had been optimised for rapid mapping, and which was capable of recovery of individual spectra from identified features, was not efficient at conducting generalised spectral searches without any knowledge of the identities of individual sources. However the majority of sources which had been detected in the SURRC flight could be identified using a combination of integrated spectral regions.

Figure 4.4 shows mapped data for four of the channels examined; <sup>137</sup>Cs, <sup>60</sup>Co, a low energy integral from 180-270 keV, and a low energy ratio, together with the stated locations of relevant sources. Figure 4.5 presents selected profile plots for the data set, again indicating the closest positions for each source, and the associated anomalies.

The <sup>137</sup>Cs map in figure 4.4, together with the associated profile of figure 4.5 shows clearly the combined effects of the radionuclide deposition within Area III, and its variations, together with localised signals from some of the point sources. The calibration in kBq m<sup>-2</sup> of <sup>137</sup>Cs does not of course apply to those positions where point sources are located. Source Cs1 was clearly located, and had been successfully identified in the initial report.

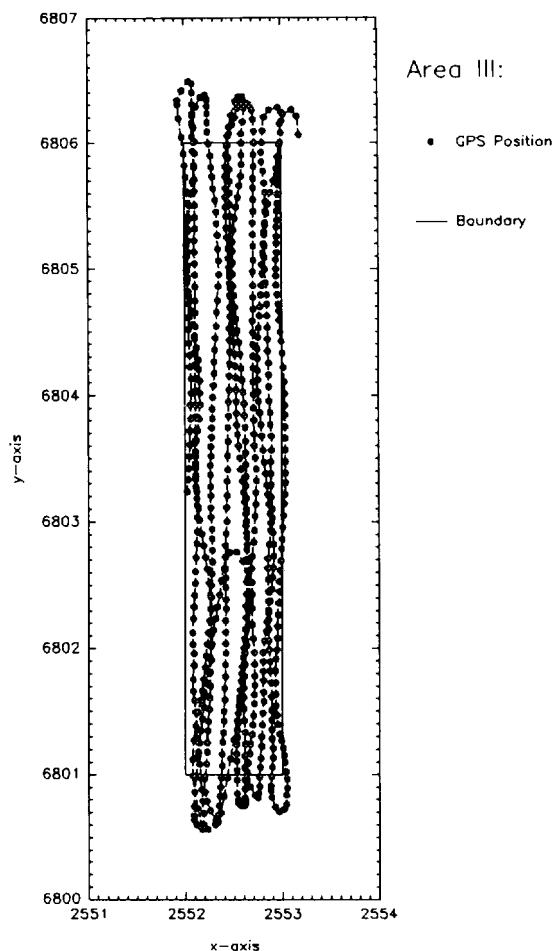


**Figure 4.3** Area III flight lines.

The collimated source Cs2 could not have been located without an almost a direct fly over, which was not achieved during this flight; and there is no evidence of its presence in the data set. Sources Cs3 and Cs4 could not be positively identified above local environmental levels in the maps, although Cs3 was observed in the stripped data, and was part of the component reported in the vicinity of Co1 during the survey. Cs4 did not produce significantly different results in this data set compared with local environmental variations.

The  $^{60}\text{Co}$  results, also shown in figures 4.4 and 4.5 demonstrate the clear advantages when nuclides are not present in the ambient surroundings. Three of the four source locations can be identified corresponding to sources Co1, Co3 (along the road) and the line source Co4-9, the last one being recovered from retrospective analysis. It is believed that we may have been the only team to have positively identified the low activity source Co3. The collimated source Co2 was not found during the survey. Examination of the stripped count rate profile shows that there is a very small local anomaly at the appropriate position; however the presence of a several (up to 4) slightly larger anomalies in stripped data at locations where no source was located undermines the significance of this single observation. In a true source search, of course there would be opportunities to conduct confirmatory flights, in which case a list of low significance events, including some false positive locations could be investigated with longer counting times. However it is evident that the collimated source was not a prominent feature in our data set from the exercise.

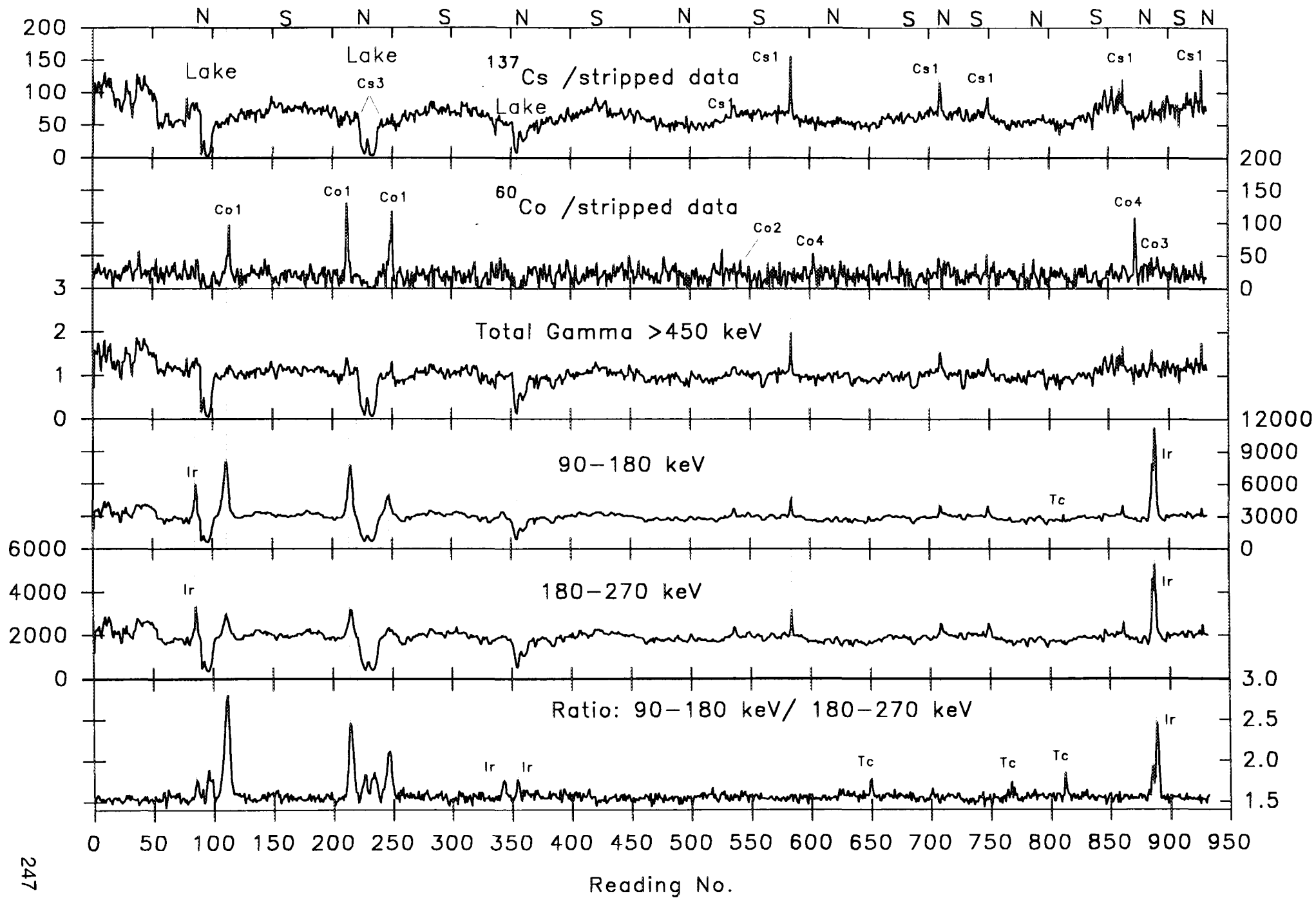


Figure 4.5 Area III Source Search.

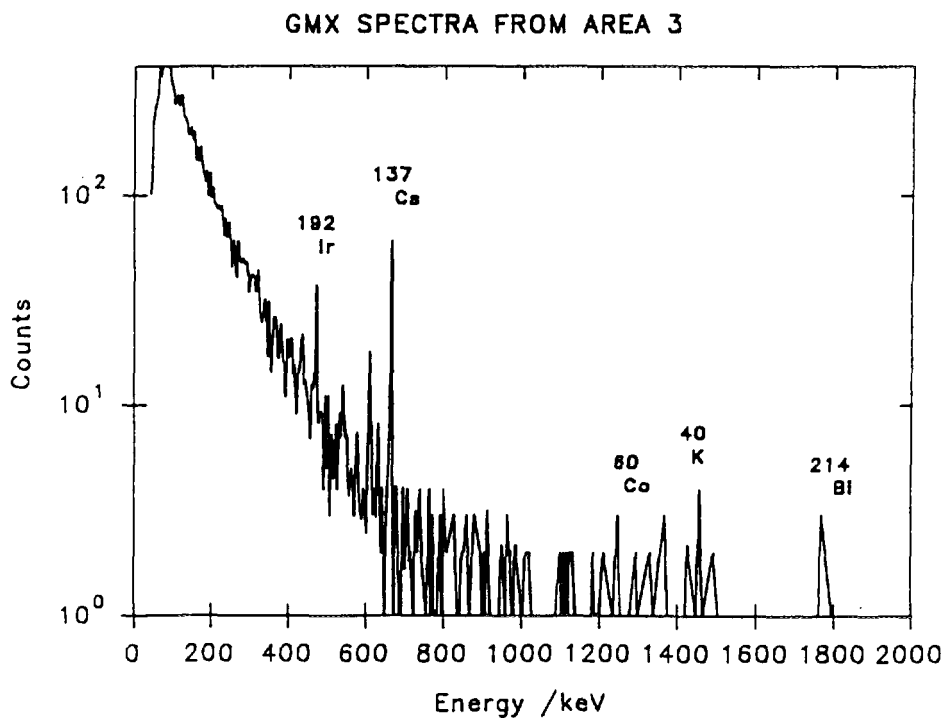
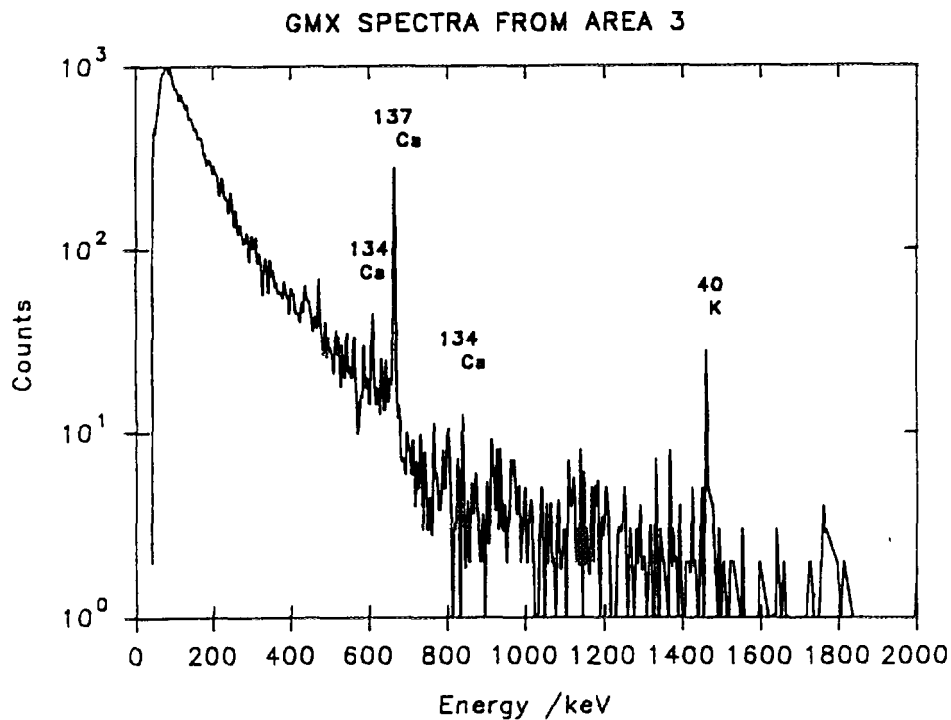
Low energy scatter and Pb x-rays were observed during the survey and within the first 24 hours and attributed to a shielded source. Also a series of line energies from the GMX detector was tabulated, but not successfully identified during the survey. These features can be related to the 10 Ci shielded  $^{192}\text{Ir}$  source which was collimated in such a way that only scattered photons could be detected in Area III, with the exception of a narrow beam projected at a low angle towards the lake in the north. However, full energy lines (320 and 470 keV) and scatter were subsequently shown to be due to the  $^{192}\text{Ir}$  source, located outside Area II. Both low energy plots in figure 4.4 identify the Ir source; the ratio of (90-180 keV/180-270 keV) plot also shows the position of the  $^{99\text{m}}\text{Tc}$  source, which again was retrospectively identified. Two examples of GMX spectra from the source search area are shown in figure 4.6. The first shows the generally elevated levels of  $^{137}\text{Cs}$  and  $^{40}\text{K}$  in this area. In the second spectrum, recorded for 6 seconds,  $^{192}\text{Ir}$  lines, and a very small number of events from the low activity source Co3 can be seen.

The results of the survey conducted in Area III demonstrate that in searches for collimated sources, closely spaced flight lines are required to ensure that the radiation beam is intercepted. For this differential GPS technology is essential. In addition, the greater number of flight lines required necessitates a higher survey speed in order to complete the operation within the same time period. This has the effect of reducing the number of events per unit integration period and worsen statistical uncertainty, but may be tolerable.

A reduction in altitude has a compensating effect and increases count rate, but also reduces the beneficial factor of detector field of view especially applied to observing non-collimated sources. The results show very clearly that detection limits for low activity point sources depend critically on the presence or absence of the individual nuclide in the ambient environment; the successful identification of Co3 with 0.7 mCi contrasting with the failure to observe Cs4 (14.6 mCi), which could certainly have been detected in a low Cs environment.

The exercise conditions presented a stimulating and challenging scenario, in that the time constraint, number of sources within a small area, unknown spectra, and use of collimation presented a combination of factors which reveal the limitations of most systems. The scenario differs from situations where we have previously conducted source searches<sup>8,9</sup> where the target sources were known, and it was possible to design flight patterns to match their characteristics. The experience of the RÉSUMÉ 95 conditions, albeit introducing somewhat artificial circumstances was most valuable in identifying areas for further system improvement, some of which have been implemented since the study.

Figure 4.6 GMX Spectra.



## 5. DISCUSSION AND CONCLUSIONS

SURRC completed an airborne survey of three areas in Finland during 15th August 1995, within a specified time period. This included a calibration site at the airfield, an area with varied Chernobyl deposition and topography, and an area containing point radioactive sources. The printed tabular results were displayed within minutes of arrival at the landing airfield and mapping of the source search area within 30 minutes. The calibrated maps of Chernobyl deposition and natural radionuclides, together with overlays corresponding to topography, roads, rivers and lakes were printed later the same day.

The calibration site (Area I) was sampled in detail during May, and in a strategy used by SURRC for previous airborne surveys conducted in the UK. Laboratory analyses on the soil cores were performed by SURRC and STUK. This enabled a ground to air comparison to be made with the different spectrometer types used by each of the European airborne teams. It was found that calibration factors for  $^{137}\text{Cs}$  determined by weighted soil analyses and by theoretical estimates of detector response to be in very good agreement. Those differences which were observed for the natural radionuclides being largely attributed to the distribution of activity, which showed non-uniform depth profiles in core samples.

It was gratifying to be able to produce quantitative deposition maps rapidly in a deployment so far from our home base. The ability to quantify a new installation depends on rapid determination and prior knowledge detector background, stripping ratios, altitude correction coefficients and sensitivity factors. The standard of the operating procedures developed over many previous surveys worked well in this regard, as shown by the good agreement between measured sensitivity on the calibration site and theoretical values for the appropriate depth distribution. The calibration site served the dual purpose of providing traceability between airborne results and other methods, and defining the depth distribution used in this study. In the absence of a calibration site, working calibration factors corresponding to stated depth profiles, would have been used. This would not have affected the timescale for production of deposition maps. With hindsight it appears that the values determined would also have been very similar for the SURRC team.

The main survey area (Area II) was found to have a mean  $^{137}\text{Cs}$  deposition of  $64.4 \pm 24.4 \text{ kBq m}^{-2}$ . From the limited soil sampling (nine cores were taken from Area II)  $^{137}\text{Cs}$  was found to be distributed deeper than in Area I. This may have led to a slight underestimation of radiocaesium, if these burial characteristics were common throughout Area II.

The major point sources in Area III were discovered, although the collimated  $^{137}\text{Cs}$  and  $^{60}\text{Co}$  sources were not. Sources Cs3 and Cs4 were not significantly above local environmental levels. The  $^{192}\text{Ir}$  was found by virtue of using low energy windows with the NaI detector. The  $^{99\text{m}}\text{Tc}$  source was located later after reintegration of the full spectral data. High resolution data were able to confirm the identities of the line element of the shielded Ir source, and the low activity Co3 source.

Participation in RÉSUMÉ 95 gave the SURRC team valuable experience to supplement previous overseas surveys. It also confirmed the feasibility of adapting AGS operations to overseas aircraft and producing quantitative data, using standard procedures, in a temporary installation with rapid quantification and mapping. These findings have important implications for transnational assistance in the event of a major accident. As noted above there is no reason why emergency response data could not be produced on an equivalent timescale to that demonstrated during the exercise. While the calibration conditions of this exercise do not fully reflect procedures which would be appropriate to emergency response, it would be possible to conduct rapid ground to air comparisons to verify working calibration factors.

The exercise, in addition to demonstrating the mobilisation and mapping capabilities of several AGS teams, has provided an opportunity to compare results from different teams under controlled conditions. The results from other teams, observed during the exercise, suggest that deposition mapping produced very similar spatial patterns in Area II, but that there were calibration differences; particularly evident during the survey, and to a lesser extent following retrospective analysis, which require further clarification in later international studies. It is to be hoped that the exercise can be repeated, with a formal protocol which can be used for quantitative validation of dose rate and deposition mapping.

## ACKNOWLEDGEMENTS

We would like to thank our pilot Captain Paul Heathcote who provided exemplary flying skills as usual. We are also grateful to the engineers of Helijet Oy (Rovaniemi, Finland) who met our instrumental requirements in time for our flight trials. In addition, we acknowledge all assistance provided by NKS, STUK, DISTAFF and the staff of the Tallukka Hotel, Vääksy. Jane Drummond from the Topographic Sciences Department of Glasgow University kindly advised on transformation between latitude and longitude and the Finnish KKJ coordinate system.

This work was partially funded by British Nuclear Fuels plc, whose sponsorship allowed SURRC to participate in the airborne trials, and is gratefully acknowledged. NKS and the Danish Emergency Management Agency also contributed to SURRC costs associated with preparation of the calibration site.

## REFERENCES

1. Sanderson, D.C.W.; Scott, E.M.; Baxter, M.S.; Preston, T. (1988): A feasibility study of airborne radiometric survey for UK fallout. SURRC, East Kilbride. 10p.
2. Sanderson, D.C.W.; Scott, E.M. (1989): Aerial Radiometric Survey in West Cumbria in 1988. MAFF Report N611 and Technical Annex. 125p.
3. Sanderson, D.C.W.; East, B.W.; Scott, E.M. (1989): Aerial Radiometric Survey of Parts of North Wales in July 1989. SURRC, East Kilbride. 10p
4. Sanderson, D.C.W.; Allyson, J.D.; Martin, E.; Tyler, A.N.; Scott, E.M. (1990): An Aerial Gamma Ray Survey of Three Ayrshire Districts, Commissioned by the District Councils of Cunninghame, Kilmarnock & Loudon, and Kyle and Carrick. SURRC, East Kilbride.
5. Sanderson, D.C.W.; Allyson, J.D.; Tyler, N.; Ni Riain, S.; Murphy, S. (1994): An airborne gamma ray survey of parts of SW Scotland in February 1993. Final Report. SURRC, East Kilbride. 118p
6. Sanderson, D.C.W.; Scott, E.M.; Baxter, M.S.; Martin, E.; Ni Riain, S. (1993): The use of aerial radiometrics for epidemiological studies of leukaemia: A preliminary investigation in SW England. SURRC, East Kilbride. 165p.
7. Sanderson, D.C.W. et al (1996): Survey for the 10th Anniversary of the Chernobyl Accident. SURRC, East Kilbride. 1p.
8. Sanderson, D.C.W.; Allyson, J.D. (1991): An Aerial Gamma Ray Search for a missing  $^{137}\text{Cs}$  source in the Niger Delta, May 1991. SURRC, East Kilbride. 29p.
9. Sanderson, D.C.W.; East, B.W.; Robertson, I.; Scott, E.M.; (1988): The use of aerial radiometrics in the search for a lost  $^{137}\text{Cs}$  source - Feasibility study and Preliminary Survey of the Forth Estuary at Grangemouth on 16/12/88. SURRC, East Kilbride. 5p.
10. Sanderson, D.C.W.; Tyler, A.N.; Cairns, K.J; (1991): Radiometric Flight Trials in the Forth Estuary on 7/8/91. SURRC, East Kilbride. 5p.
11. Sanderson, D.C.W.; Allyson, J.D.; Cairns, K.J.; MacDonald, P.A. (1991): A Brief Aerial Survey in the Vicinity of Sellafield in September 1990. SURRC, East Kilbride. 34p.
12. Sanderson, D.C.W.; Allyson, J.D.; Tyler A.N. (1992): An aerial gamma ray survey of Chapelcross and its surroundings in February 1992. SURRC, East Kilbride. 36p.
13. Sanderson, D.C.W.; Allyson, J.D.; Tyler, A.N.; Murphy, S. (1993): An aerial gamma ray survey of Springfields and the Ribble Estuary in September 1992. SURRC, East Kilbride. 46p.
14. Sanderson, D.C.W.; Allyson, J.D.; Gordon, G.; Murphy, S.; Tyler, A.N.; Fisk, S. (1995): An Aerial Gamma Ray Survey of Hunterston Nuclear Power Station 14th-15th April and 5th May 1994. SURRC, East Kilbride. 23.
15. Sanderson, D.C.W.; Allyson, J.D.; Ni Riain, S.; Gordon, G.; Murphy, S.; Fisk, S. (1995): An Aerial Gamma Ray Survey of Torness Nuclear Power Station 27th-30th March 1994. SURRC, East Kilbride. 24p.
16. Sanderson, D.C.W.; Allyson, J.D.; Tyler, A.N.; Teasdale, I. (1993): An Airborne Gamma Ray Survey of the Duddon Estuary in February 1993. 6.
17. Sanderson, D.C.W.; Allyson, J.D. (1994): Aerial Survey Response to Scottish Nuclear Exercise Katrine 17-18 November 1994. SURRC, East Kilbride. 17p.

18. Sanderson, D.C.W.; Scott, E.M.; Baxter, M.S. (1990): The use and potential of aerial radiometrics for monitoring environmental radioactivity. In: Nuclear Contamination of Water Resources. Proceedings of, Institute of Civil Engineers meeting held in Glasgow, 7-8 September 1989. Thomas Telford, London. 99-106.
19. Sanderson, D.C.W.; Scott, E.M.; Baxter, M.S. (1990): Use of airborne radiometric measurements for monitoring environmental radioactive contamination. In: Environmental contamination following a major nuclear accident. Proceedings of an international symposium held in Vienna, 16-20 October 1989. Vol. 1. IAEA-SM-306/138, 411-421.
20. Sanderson, D.C.W.; Allyson, J.D.; Tyler, A.N. (1995): Rapid quantification and mapping of radiometric data for anthropogenic and technologically enhanced natural nuclides. In: Application of uranium exploration data and techniques in environmental studies. IAEA -TECDOC-827, 197-216, IAEA, Vienna.
21. Sanderson, D.C.W.; Allyson, J.D.; Tyler, A.N.; Scott, E.M. (1995): Environmental Applications of Airborne Gamma Spectrometry. In: Application of uranium exploration data and techniques in environmental studies. Vol. IAEA-TECDOC-827, 71-92. IAEA, Vienna.
22. Allyson, J.D. (1994): Environmental Gamma Ray Spectrometry : Simulations of absolute calibration of in-situ and airborne spectrometry for natural and anthropogenic sources. PhD thesis, University of Glasgow.
23. Tyler A.N. (1994) : Environmental Influences on Gamma Ray Spectrometry, PhD thesis, University of Glasgow.
24. Tyler, A.N.; Sanderson, D.C.W.; Scott, E.M. (1996): Estimating and Accounting for  $^{137}\text{Cs}$  source burial through in-situ gamma spectrometry in salt marsh environments. J. Environ. Radioactivity 33(3), 195-212.
25. Tyler, A.N.; Sanderson, D.C.W.; Scott, E.M.; Allyson, J.D. (1996): Accounting for spatial variability and fields of view in environmental gamma ray spectrometry, J. Environ. Radioactivity 33(3), 213-235.
26. Sanderson, D.C.W., Allyson, J.D., Toivonen, H., Honkamaa, T. Gamma Ray Spectrometry Results from Core Samples Collected for RÉSUMÉ 95. September 1995. Joint SURRC and STUK report.
27. ICRU (1994): Gamma ray spectrometry in the Environment. ICRU 53, International Commission on Radiation Units and Measurements, Bethesda U.S.A.
28. Richardson, K.A., 1981. High Sensitivity Airborne Radiometric Surveying over Tropical and Rain Forest Areas. IAEA-AG-162/04.

**NEXT PAGE(S)  
left BLANK**



DK9800043

**Department of Radiation Physics, Lund University**  
Applying Statistical Methods to Car-Borne NaI(Tl)  
Spectrometry Results

**NEXT PAGE(S)**  
**left BLANK**

# Applying Statistical Methods to Car-Borne NaI(Tl) Spectrometry Results

by Christer Samuelsson and Thomas Hjerpe

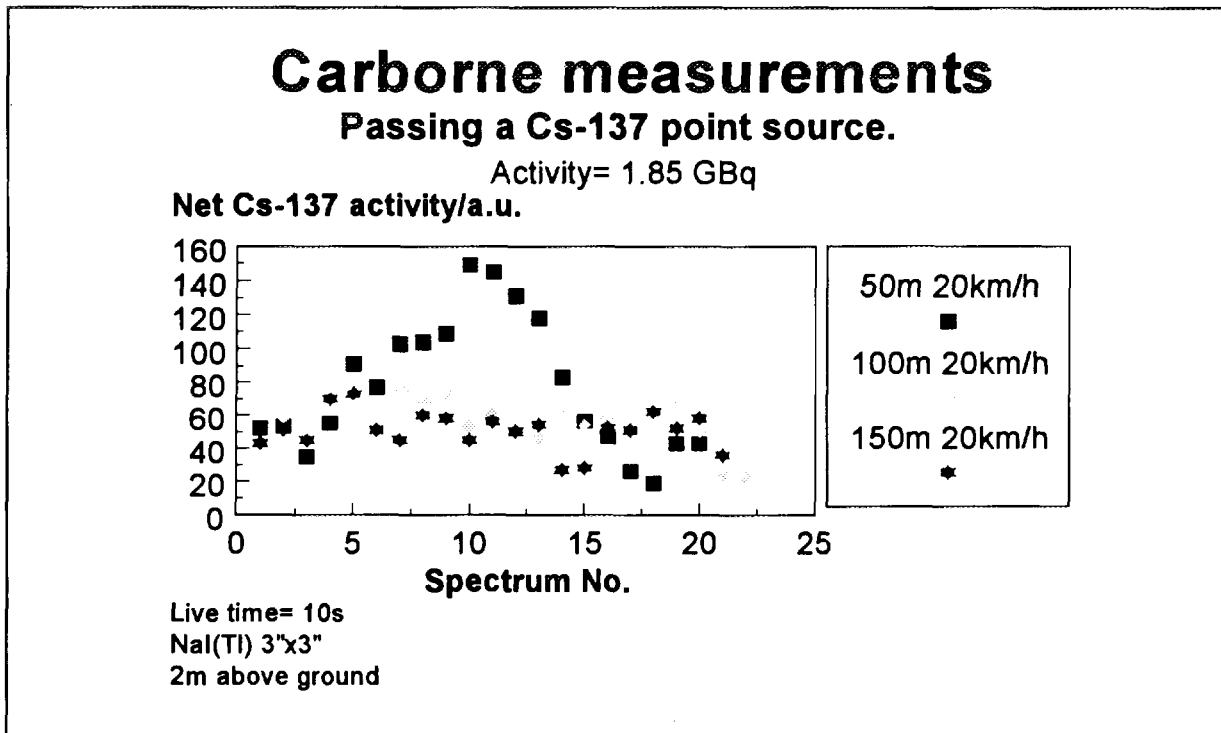
## 1. General considerations

The low energy resolution of NaI(Tl) systems limits the outdoor applicability to scenarios like finding a single, or at most few radionuclides, against the background of  $^{40}\text{K}$ , uranium and thorium series activities. In order to achieve a satisfactory spatial resolution, sampling times are typically in the order of seconds for airborne and carborne systems, indicating that only large NaI detectors will give reasonable good pulse statistics for close to natural background situations. A good strategy for rapid mobile gamma spectrometry is to have a large sensitive NaI(Tl) detector for coarse initial scan and a HPGe detector for close-up measurements in "suspected" areas.

During accidental conditions there is usually no time for too fancy statistical calculations, instead rapidness in the evaluation of data is of premier importance. The common situation of a less well known irradiation geometry also speaks in favour not overdoing the mathematical treatment of incoming data. The ideal measuring system has built-in calculation tools able to present not only derived quantities such as surface activity concentration, but also the significance of these measured and derived quantities.

It is not the objective of this contribution to present a comprehensive survey of more or less sophisticated "alarm levels", but instead to give an example of how parameter-free statistics can be applied to judge if any "extra" radioactivity is present or not.

## 2. Kolmogorov-Smirnov (K-S) statistics applied to Carborne measurements in Area I



Estimating if a sequence of experimentally obtained data differs significantly from an expected distribution can be done by several methods. In our analysis of carborne results in Area I from passing the  $^{137}\text{Cs}$  source at the different distances, we have applied the non-parametric method of Kolmogorov-Smirnov (K-S). In this case a one-tailed two sample K-S is suitable; a one-tailed K-S is chosen due to the fact that we are only interested in finding areas with increased values. Compared to the more common  $\chi^2$  analysis, the K-S statistics applies also in situations where the numbers of cases in one or several intervals are very low, even zero.

In practice a K-S analysis may be applied as an on-line method by continuously survey and calculate the cumulated frequencies of the different energy bands of the latest, say, X spectra. Once the X+1:th spectrum is at hand, the oldest value is thrown away, all distributions updated with the new values and recalculated. The resulting cumulated frequencies are compared to the expected “background” distribution and the significance level of an eventual difference can be drawn from a statistical table.

The net contents of the  $^{137}\text{Cs}$  window in a number of consecutive spectra are plotted in the figure above, as an example of the experimental results. (The activity units have been denoted as arbitrary, remembering that the detector is calibrated only for areal contaminations, not for point source geometries). If we now as an example put X equal to 20 and analyse the 22 spectra of the 100m passage (cf. figure), we have three distributions (1-20, 2-21, 3-22) of  $^{137}\text{Cs}$ -window results to compare with the reference (“background”) distribution. The cumulated frequencies of these three distributions are compared in the table below to a background distribution of 69 spectra taken along the same route without the point source in place. (The activity numbers have been grouped into 7 intervals.)

Activity interval/au (I)	Background spectrum		Cumulated frequency sequence		
	frequency	cum. Freq. ( $S_{X1}$ )	1-20 ( $S_{X2}$ )	2-21 ( $S_{X2}$ )	3-22 ( $S_{X2}$ )
$\leq 25$	0,13	0,13	0	0,05	0,10
26-40	0,17	0,30	0,10	0,10	0,15
41-45	0,20	0,50	0,10	0,10	0,15
46-50	0,07	0,57	0,30	0,30	0,35
51-55	0,17	0,74	0,50	0,50	0,55
56-70	0,16	0,90	0,85	0,85	0,85
$\geq 71$	0,10	1,00	1,00	1,00	1,00
Max difference, $D, D = \max\{S_{X1}(I)-S_{X2}(I)\}$			0,40	0,40	0,35

Table. Kolmogorov-Smirnov statistics for three sequences of spectra, spectra No. 1-20, No. 2-21, and No. 3-22, passing in a straight line a 1.85 GBq source at a closest distance of 100m.

A one-sided Kolmogorov-Smirnov test with  $D=0,40$  and  $0,35$ ,  $X_1=20$  and  $X_2=69$  returns that there is a probability of 1% and 5%, respectively, that chance is causing the differences in the cumulated frequencies. Consequently, choosing a confidence level of 95% means that the all

three sequences will alert the operator of a “suspicious”  $^{137}\text{Cs}$  activity above (in this case) Chernobyl background, but the third sequence is just on the limit of being significantly different from this background. The maximum K-S difference of the 150m passage (20 km/h, cf. figure) is 0.22 and this is not a significant difference on the 5% level. Thus the 3"x3" detector is not able to spot the source at this distance, with the driving parameters given.

**NEXT PAGE(S)  
left BLANK**

# Department of Radiation Physics, Lund University

## Carborne Measurements in Area II by the Jubileum Institute

Figures in Colour Appendix (C.A.):

- Fig. 2. Gammadata GDM 40 RPS with Ortec  $\mu$ ACE multichannel analyser card and NEC V25+ microprocessor..... C.A. plate 21
- Fig. 3. The software for extracting and treatment of spectral- and GPS-data is written by Hans Mellander..... C.A. plate 21
- Fig. 4. Cs-137 results from area II and the road between area II and III..... C.A. plate 22

**NEXT PAGE(S)  
left BLANK**

## Carborne measurements in Area II by The Jubileum Institute, Department of Radiation Physics, Lund University

*Christer Samuelsson and Jacob Eberhardt*

During the RESUMÉ carborne (Fig. 1) exercise RPDLU utilised a detector system (Fig. 2) provided by SSI, the Gammadata\_RPS (Unit No.4).

The objectives were:

- to test the RPS during field conditions
- to train our team in using the RPS system

The spectrometry unit was picked up at SSI only a few days ahead of the exercise, but thanks to a continuous support by SSI and Gammadata during RESUMÉ we were able to test and use the RPS system fairly successfully.



*Fig. 1. The Lund team used a minibus GMC during the RESUMÉ exercise. The car has an enhanced roof and a build-in 6 kW power supply and an extra air-conditioner during standstill. The NaI(Tl)-detector resided inside the car 2 meters above ground looking towards right side.*

The unit was not calibrated for point source or fall-out geometries beforehand, and as our intention to calibrate the system by means of the areas  $^{137}\text{Cs}$  contamination in Area I failed, all data presented below is only preliminary (based on calibration figures from SSI, valid for another NaI(Tl) detector of the same size). The roads covered by our car team is perceptible from the map displaying preliminary  $^{137}\text{Cs}$  levels (fig 4).

**NEXT PAGE(S)  
left BLANK**



# Department of Radiation Physics, Lund University

## In-Situ Gamma Spectrometry performed at Vesivehmaa Airport

1. INTRODUCTION .....	268
2. MODELS .....	268
2.1. Calculation algorithms .....	268
2.2. Error propagation .....	270
3. METHODS .....	271
3.1. Preparatory experiments .....	271
Fig. 1. Intrinsic Full Energy Efficiency at $\theta = 90^\circ$ .....	271
Fig. 2. Normalised intrinsic angular efficiency for the detector at three different photon energies .....	272
Fig. 3. Field Efficiency Correction Factor as a Function of Primary Photon Energy for a Number of Source Distributions .....	272
3.2. Field gamma measurements .....	273
3.3. Treatment of data .....	273
4. RESULTS .....	274
4.1. Activity values obtained from field measurement - Artificial radionuclides .....	274
Tab. 4.1. Activity of $^{137}\text{Cs}$ per Unit Area in Soil at Selected Points at Vesivehmaa Airport Obtained in the RESUME95 Exercise .....	274
Tab. 4.2. Activity of $^{134}\text{Cs}$ per Unit Area in Soil at Selected Points at Vesivehmaa Airport Obtained in the RESUME95 Exercise .....	276
4.2. Activity values obtained from field measurement - Natural radionuclides .....	276
Tab. 4.3. Activity of $^{40}\text{K}$ , total Uranium- and total Thorium-series per Unit Mass of Soil at Selected Points at Vesivehmaa Airport Obtained in the RESUME95 Exercise .....	277
4.3. Comparison with the radionuclide deposition as measured by STUK and SURRC at 1 m above ground level .....	278
Tab. 4.4. Comparison Between our Overall Mean Values with the Effective Radionuclide Concentration at 1 m Detector Height as Obtained from the STUK/SURRC Soil Sample .....	278
5. CONCLUSION .....	278
5.1. Artificial radionuclides .....	278
5.2. Natural radionuclides .....	279
5.3. Systematic and stochastic uncertainties .....	280
5.4. Miscellaneous comments regarding practical experiences from the exercise .....	280
6. REFERENCES .....	280

**NEXT PAGE(S)  
left BLANK**

**RESULTS FROM THE RESUME-95 EXERCISE**  
***IN-SITU* GAMMA SPECTROMETRY PERFORMED AT VESIVEHMAA**  
**AIRPORT, FINLAND**

**Christopher L. Rääf**

**1996 - 01 -16**

Department of Radiation Physics  
Lund University  
University Hospital MAS  
20502 MALMÖ

## 1. INTRODUCTION

The Department of Radiation Physics in Malmö has an agreement with the Swedish Radiation Protection Institute, in which we are obliged to perform instantaneous field measurements of gamma-emitting radionuclides in case of a major release of radionuclides in the environment. The department possesses a High Purity Germanium detector system (35 % @ 1.33 MeV) with a PC software spectrum analyser that was purchased and calibrated for this reason. The aim of our participation in the RESUME-95<sup>1</sup> exercise, which took place in Vääxsy, Finland, in August 1995, was both to obtain efficiency values for different source geometries (both artificial and natural radionuclides) in field and to compare our results with those of other groups. Furthermore, this exercise was an ideal opportunity to test the full equipment under field conditions.

## 2. MODELS

### 2.1 Calculation algorithms

The method used in this study to evaluate the activity concentration of gamma-emitting radionuclides by field measurements strictly follows the protocols given by Finck [1].

A field measurement will yield spectra with different peak count rates,  $N'_{in\ situ}$ , that depend on the source strength and on the detector geometry. From there to calculate the activity per unit area or unit mass in soil, the following parameters need to be known;

- I. The Intrinsic full energy peak efficiency as a function of energy,
- II. The Angular dependence of the intrinsic efficiency,
- III. The Source geometry. I.e. the depth-profile in soil of nuclear fallout radionuclides as well as naturally occurring radionuclides.

The activity concentration,  $A_{in\ situ}$ , [Bq/m<sup>2</sup>] can with similar notations as in [1] be expressed as;

$$A_{in\ situ} = \dot{N}_{in\ situ} * \left( \frac{1}{\epsilon_{field} * \left( \frac{\Phi_p}{A} \right)} \right) \quad (2.1)$$

Where;

$\dot{N}_{in\ situ}$  = the peak count rate, (s<sup>-1</sup>), at a certain full energy peak,

---

<sup>1</sup> Rapid Environmental Surveying Using Mobile Equipment, 1995.

$\frac{\Phi_p}{A}$  = the quotient between the primary photon fluence and the activity in soil per unit area ( $\text{m}^{-2}/\text{m}^{-2}$ ).

$A_{\text{in-situ}}$  depends both on the distribution of the specific radionuclide in the soil and at the surface, as well as on the primary photon energy and the detector height above the ground. In [1], values for this quotient are tabulated for several different photon energies and source distributions.

Throughout our calculations, lateral uniformity of the source geometry has been assumed, and the detector height is always 1 m above the ground.

Furthermore, the air and soil densities have been set to  $1.24 \text{ kg/m}^3$  and  $1600 \text{ kg/m}^3$  respectively. Tabulated values from [1] refer to a standard soil with a specific elemental composition originally defined by H.L. Beck (1964).

$\epsilon_{\text{field}}$  = the field efficiency, is the “overall efficiency of the detector for the *in situ* measurement of the primary photon fluence from a photon source in the environment”. This quantity depends on the intrinsic efficiency of the detector and on the angular distribution of the primary photon fluence at the point of measurement. The field efficiency is obtained as follows;

$$\epsilon_{\text{field}} = \left( \frac{\dot{N}_F}{\dot{N}_{90}} \right) * \left( \frac{\dot{N}_{90}}{\dot{\Phi}_p} \right) \quad (2.2)$$

The first term is denoted “*field efficiency correction coefficient*” [unity] and can be obtained numerically by summing the incremental contributions of the primary photon field over a certain vertical angular interval,  $\Delta\theta$ , weighted by the normalised angular efficiency of the detector. Values of the latter have been normalised with respect to a reference direction, in our case at  $\theta = 90^\circ$ .

The normalised angular efficiency is in turn dependent on the primary photon energy and must be determined experimentally. In [1], it is recommended that the angular efficiency be determined in at least 10 points between  $0^\circ$  and  $90^\circ$ , i.e. with  $\Delta\theta = 10^\circ$ .

The second term is the *intrinsic efficiency of the detector for a parallel primary photon field, with a  $90^\circ$  angle of incidence with respect to the axis of the cylindrical detector* [ $\text{s}^{-1}/(\text{m}^{-2} * \text{s}^{-1})$ ]. This quantity too is determined experimentally in the laboratory before setting up the detector equipment in the field.

The previous equations may be combined to give;

$$A_{\text{in-situ}} = \dot{N}_{\text{in-situ}} * \left( \frac{1}{\left( \frac{\dot{N}_F}{\dot{N}_{90}} \right) * \left( \frac{\dot{N}_{90}}{\dot{\Phi}_p} \right) * \left( \frac{\dot{\Phi}_p}{A} \right)} \right) \quad (2.3)$$

A special case is the Equivalent Surface Deposition,  $A_{\text{esd}}$ , where the true source geometry is unknown;

$$A_{\text{esd}} = \dot{N}_{\text{insitu}} * \left( \frac{1}{\left( \frac{\dot{N}_{\text{Surface}}}{\dot{N}_{90}} \right) * \left( \frac{\dot{N}_{90}}{\dot{\Phi}_p} \right) * \left( \frac{\dot{\Phi}_p}{A_{\text{surface}}} \right)} \right) \quad (2.4)$$

The primary photon field above ground also depends on the source geometry. Three different types of source geometries are commonly used in field gamma spectrometry to approximate the true radionuclide concentration in soil; i.) *Surface* deposition on ground (or fresh fallout where the radionuclides haven't had time to penetrate into the soil), ii.) *Exponential* distribution and iii.) *Uniform* distribution in soil. All three types can be described mathematically by an exponential expression;

$$S(z) = s(0) * e^{-((\alpha/\rho) * \rho(z) * z)} \quad (2.5)$$

where  $\alpha/\rho$  is the *exponential mass activity distribution coefficient* [ $\text{m}^2/\text{kg}$ ] and the key parameter in this expression.  $\rho(z)$  is the density of soil [ $\text{kg}/\text{m}^3$ ], which may vary with the soil depth  $z$ .  $S(z)$  is the activity concentration [ $\text{Bq}/\text{kg}$ ] in soil at depth  $z$  [m].

The extreme types of distributions can thus be described by (2.5) by setting  $\alpha/\rho = 0$  in case of superficial ground deposition (surface deposition), and  $\alpha/\rho = \infty$  for uniform distribution in soil. For cesium distributions in ground soil one often tries to fit a suitable exponential distribution coefficient, although in some cases different other expressions have proven to be more accurate. In our case, we knew on forehand that a major part of the cesium content in soil was found in the first two centimetre layer, and it was likely that the  $\alpha/\rho$  at Area I would be in the order of  $0.1 \text{ [m}^2/\text{kg}]$ .

## 2.2 Error propagation

Estimations of the uncertainties involved when obtaining the activity values may be expressed as follows by recalling (2.1);

$$\left( \frac{\Delta A_{\text{insitu}}}{A_{\text{insitu}}} \right)^2 = \left( \frac{\Delta \dot{N}_{\text{insitu}}}{\dot{N}_{\text{insitu}}} \right)^2 + \left( \frac{\Delta \left( \frac{\dot{N}_{90}}{\dot{\Phi}_p} \right)}{\left( \frac{\dot{N}_{90}}{\dot{\Phi}_p} \right)} \right)^2 + \left( \frac{\Delta \left( \frac{\dot{N}_{\text{field}}}{\dot{N}_{90}} \right)}{\left( \frac{\dot{N}_{\text{field}}}{\dot{N}_{90}} \right)} \right)^2 + \left( \frac{\Delta \left( \frac{\dot{\Phi}_p}{A_{\text{insitu}}} \right)}{\left( \frac{\dot{\Phi}_p}{A_{\text{insitu}}} \right)} \right)^2 \quad (2.6)$$

The first term is given by Poisson statistics, and the uncertainty varies with the square root of the number of counts in the full energy peak. The second term is typically within 5 % if the calibration has been successful. The same number should be applied to the third and the fourth term. In the latter term there may be systematic uncertainties regarding the soil density since we assumed a standard Beck-soil and any real deviations from its density ( $1600 \text{ kg}/\text{m}^3$ ) will effect the calibration. The total relative uncertainty should be in the order of;

$$\left(\frac{\Delta A_{\text{insitu}}}{A_{\text{insitu}}}\right) \approx \sqrt{\left(\frac{\Delta N_{\text{insitu}}}{N_{\text{insitu}}}\right)^2 + 3 * 0.05^2} \quad (2.7)$$

The above formulae apply (approximately) under ideal geometrical conditions where no ground roughness and lateral homogeneity have been taken into account. It should also be noted that the second and third term are correlated with each other and the quadratic error propagation may be a rough estimation only of the total uncertainty.

### 3. METHODS

#### 3.1 Preparatory experiments

Prior to the exercise in Finland, some preparatory detector efficiency calibrations were made. At the National Defence Research Establishment (Sweden), the normalised angular efficiency was obtained for each ten degrees between  $0^\circ$  and  $90^\circ$ , at three photon energies between 122 and 1408 keV (See fig. 2!). Additional values for 661.6 keV and 59.6 keV were obtained later at our own laboratory.

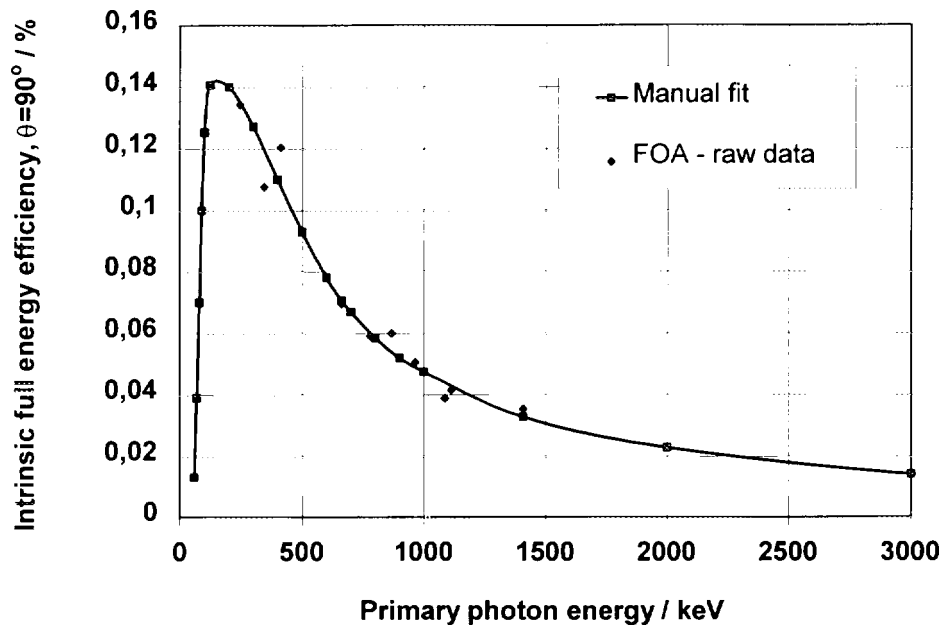


**Fig. 1.** *Intrinsic Full Energy Efficiency at  $\theta = 90^\circ$ .*

*Single markers indicate raw data obtained from initial measurement; solid curve indicates a manual curve fit to the raw data.*

Intrinsic efficiency was obtained at the reference direction,  $\theta = 90^\circ$ , for energies between 59.6 and 1408 keV.

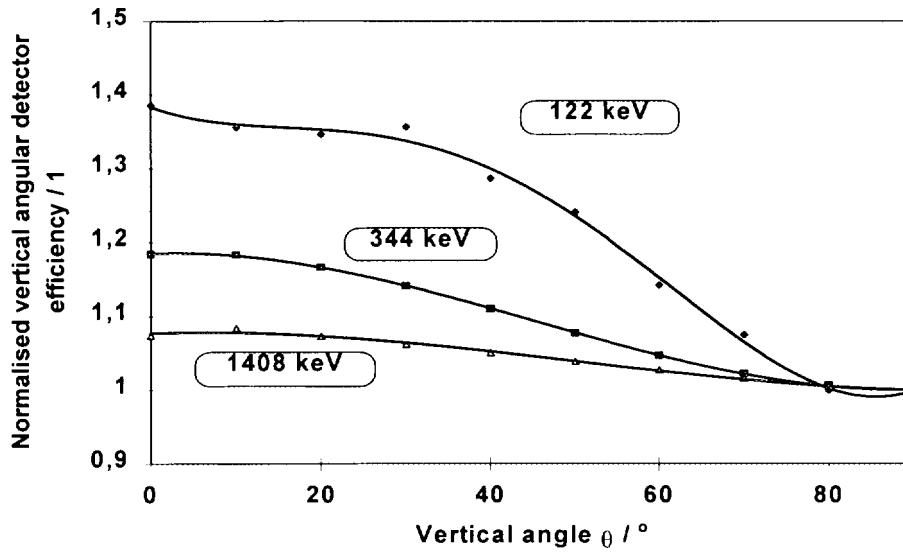


**Fig. 2.** Normalised intrinsic angular efficiency,  $(N(\theta)/N(90))$ , for the detector at three different photon energies. Solid curves indicate linear regression of data points.

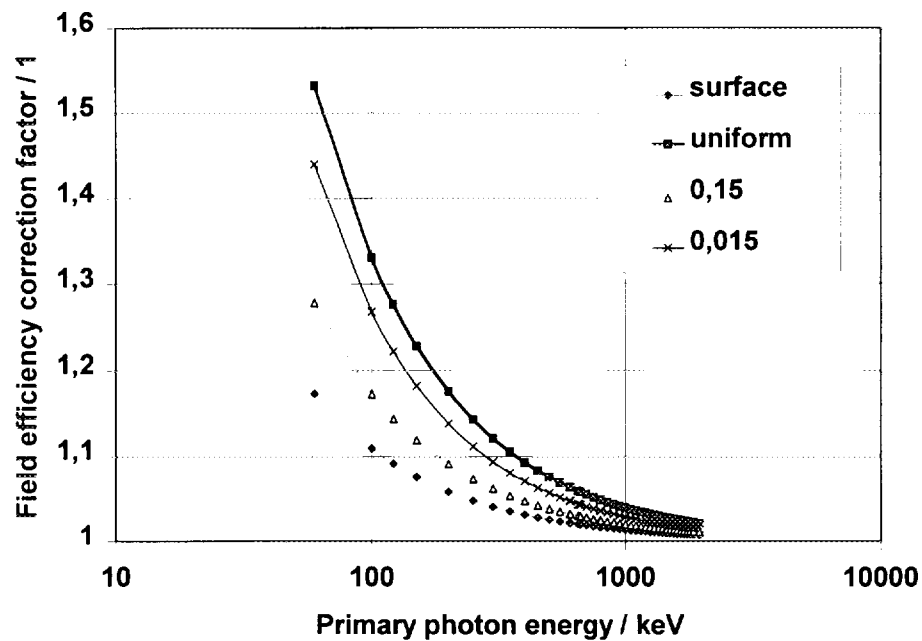


**Fig. 3.** Field Efficiency Correction Factor,  $N'_{\text{F}}/N'(90^\circ)$ , as a Function of Primary Photon Energy for a Number of Source Distributions.  
 $(\rho_{\text{soil}} = 1600 \text{ kg/m}^3, \rho_{\text{air}} = 1.24 \text{ kg/m}^3)$ .

Numerous calculations must be performed in order to translate the peak count rate of a full energy peak into activity per unit area. Since the field efficiency was required for a number of full energy peaks, a curve was fit to the important points calculated at 238, 604, 662 and 1461 keV. The curve was in turn used to easily interpolate new values of the field efficiency for photon energies above 238 keV (See Fig. 3!). For energies above 1461 keV, the field efficiency had to be extrapolated up to 2615 keV. Larger uncertainties may thus be expected at higher (>1.5 MeV) photon energies.

### 3.2 Field gamma measurements

The exercise offered two different measuring sites for the in-situ field gamma measurement groups: Area I, the Vesivehmaa airport, and Area II (forest area). Due to heavy equipment, our group managed to only partly cover the measuring points at Area I, (15 out of 25). These points were arranged in an expanding hexagonal pattern in five shells. The apex of each shell had a radius two times the one for the previous inner shell expanding from 2 to 256 m of radius. The poles at each point were labelled with a figure consisting of two numbers where the first number indicated the order of the hexagonal shell from a centre pole and the second one referred to the clockwise position in this hexagonal shell. This sampling pattern has been elaborated by the Scottish Universities Research & Reactor Centre (SURRC).

No measurements were performed at Area II.

The fallout at Area I (950815) consisted solely of Cs-137 and Cs-134 which originated from the Chernobyl-accident, the former nuclide being the most abundant. In the exercise we were asked to determine the activity per unit Area In soil for both artificial as well as natural radionuclides including K-40 and the U- and Th-series. The natural radionuclides were assumed to be distributed homogeneously in the soil throughout the measuring site. Core samples of soil had been taken at each point and analysed by SURRC and the Finnish Radiation Protection Institute, STUK.

Measurements were conducted according to procedures given in [1]. Doserate measurements could only be spuriously measured due to a relatively slow responding measuring device. All spectra (with one exception) were recorded with a preset live-time of 1000 sec and at 1 m detector height.

Calculating the field efficiency demands knowledge of the source distribution, and a fully equipped field gamma detector set-up thus requires a soil sample device in order to identify the depth profile of the present radionuclides at the site. In our case, such a device was not available, so instead we assumed some different possible depth profiles for the artificial radionuclides, Cs-137 and Cs-134, until the final results from STUK and SURRC were available. For a direct intercomparison between different groups, the equivalent surface deposition,  $A_{esd}$ , can be used instead, regardless of the assumed depth-profile.

### 3.3 Treatment of data

The peak count rates from the different gamma nuclides in the obtained spectra were manually transferred to a calculation spread-sheet. The calibration constants from [1] and experimentally determined values were applied to the peak count rates, after which the activity values and doserate values were yielded. The idea was to apply the obtained activity values from each radionuclide and their associated source geometry to the spectrum analyser software, and then creating a library consisting of a

set of different efficiency calibrations for each source geometry. Limitations of the software prevents applying two or several different source geometries to the same spectrum (calibration file). This means that different efficiency calibration files must be applied to different peaks in the same spectrum that has been recorded *in-situ*.

#### 4. RESULTS

##### 4.1 Activity values obtained from field measurement - *Artificial radionuclides*

As mentioned earlier, the only two radionuclides currently (1995) present in the fallout are Cs-137 and Cs-134. The calculated values for activity per unit soil are listed in table 4.1, assuming some different exponential distributions as well as the equivalent surface deposition,  $A_{\text{esd}}$ . The figures are compared to those obtained by STUK and SURRC from their soil samples at the site.

Note that the *overall mean* for the STUK/SURRC soil data in the tables will refer to the *effective radionuclide concentration*. This quantity is obtained by weighting the total activities (at all the measuring points altogether) in each shell (soil depth) with a so called shell weighting factor.

TABLE 4.1

Activity of Cs-137 per Unit Area In Soil at Selected Points at Vesivehmaa Airport Obtained in the RESUME-95 Exercise.

Uncertainty values refer to one standard deviation of the counting statistics for the single measuring points, and to one standard deviation of the mean for the overall-mean value.

	$A_{\text{STUK/SURRC}}$	$A_{\text{esd}}$	$A_{\text{soil}}$		
$\alpha/\rho$	0.077	$\infty$	0.15	0.0625	0
			m <sup>2</sup> /kg		
Measure-point	kBq/m <sup>2</sup>				kBq/kg
				(±1 SD)	
0	52.1	23.7	37.8	46.3±0.29	0.764
2.1	34.7	24.7	39.5	50.4±0.30	0.798
2.2	46.2	24.3	38.7	49.5±0.30	0.784
2.3	59.2	23.7	37.8	48.3±0.31	0.764
2.4	45.9	22.7	36.3	46.4±0.28	0.734
2.5	47.3	23.9	38.2	48.8±0.29	0.772
2.6	49.2	24.0	38.3	48.9±0.30	0.774
4.1	57.9	28.2	44.9	57.4±0.32	0.908
4.2	53.2	26.3	41.9	53.6±0.32	0.848

TABLE 4.1 (cont.)

	$A_{STUK/SURRC}$	$A_{esd}$	$A_{soil}$		
$\alpha/\rho$	0.077	$\infty$	0.15	0.0625	0
			m <sup>2</sup> /kg		
Measure-point	kBq/m <sup>2</sup>				kBq/kg
	(±1 SD)				
4.4	55.0	25.9	41.4	52.7±0.30	0.837
4.5	96.0	27.5	43.8	56.0±0.31	0.886
4.6	60.8	26.8	42.7	54.6±0.31	0.864
5.1	3.70	12.1	19.3	24.7±0.21	0.390
5.3	119.0	27.0	43.2	55.1±0.31	0.873
5.4	11.7	23.6	37.6	40.1±0.25	0.761
5.5	44.0	18.9	30.2	38.6±0.26	0.610
5.6	51.8	16.9	26.9	34.4±0.25	0.544
<b>Overall mean</b>	<b>51.1±19.4<sup>2</sup></b>	23.5±4.0	37.6±6.4	<b>47.4±8.4</b>	-

The overall average value for our activity values is 47.4±8.4 kBq per square meter, compared to 51.1±19.4 kBq/m<sup>2</sup> according to STUK/SURRC soil sample data. They estimate the effective radionuclide concentration at 1 m detector height to be 50.7±5.2 kBq/m<sup>2</sup>.

Some recalculations must be done in order to make the comparison between STUK and our results more compatible. If all values obtained from the calculation spreadsheet for a relaxation length of 0.0625 m<sup>2</sup>/kg are corrected for by linear interpolation to the relaxation length corresponding to the overall mean-value for STUK/SURRC data, (0.077±0.010 m<sup>2</sup>/kg), our values, including the overall mean value, should then be adjusted downwards no more than 3.6 %.

For the outer apexes there is a larger discrepancy between our values and STUK/SURRC's, whose values are in general 74 % higher (overall mean). Limitations in counting statistics (5 % uncertainty) cannot be the only explanation. It should be noted that the soil sample data are based on the count rates in the 795 keV full energy peak whereas we used the 604.7 keV peak to obtain the deposition of Cs-134.

<sup>2</sup> This value refers to the overall mean for all 26 measuring points at Area I.

TABLE 4.2  
 Activity of Cs-134 (calculated from the 604 keV peak) per Unit Area In Soil at Selected Points at Vesivehmaa Airport Obtained in the RESUME-95 Exercise.  
 Uncertainty values refer to one standard deviation of the counting statistics for the single measuring points, and to one standard deviation of the mean for the overall-mean value.

	$A_{STUK/SURRC}$	$A_{esd}$	$A_{soil}$		
$\alpha/\rho$	0.077	$\infty$	0.15	0.0625	0
			m <sup>2</sup> /kg		
Measure-point	kBq/m <sup>2</sup>				kBq/kg
	(±1 SD)				
0	1.78±0.37	0.659	0.817	1.35±0.057	0.0220
2.1	1.12	0.726	0.900	1.49±0.058	0.0243
2.2	1.36	0.588	0.729	1.21±0.055	0.0197
2.3	1.91	0.522	0.647	1.07±0.055	0.0175
2.4	1.48	0.574	0.711	1.18±0.050	0.0192
2.5	1.60	0.695	0.861	1.42±0.053	0.0232
2.6	1.43	0.696	0.863	1.43±0.053	0.0233
4.1	1.99	0.506	0.627	1.04±0.050	0.0169
4.2	1.93	0.517	0.641	1.06±0.052	0.0173
4.4	1.94	0.603	0.747	1.24±0.063	0.0202
4.5	3.26	0.580	0.719	1.19±0.065	0.0194
4.6	1.97	0.739	0.916	1.51±0.058	0.0247
5.1	0.0509	0.319	0.395	0.65±0.039	0.0107
5.3	4.03	0.419	0.519	0.86±0.050	0.0140
5.4	0.212	0.618	0.766	1.27±0.056	0.0207
5.5	1.38	0.592	0.735	1.22±0.052	0.0198
5.6	1.68	0.422	0.528	0.87±0.044	0.0142
<b>Overall mean</b>	<b>2.05±1.56</b>	0.575±0.11	0.713±0.14	<b>1.18±0.23</b>	-

#### 4.2 Activity values obtained from field measurement - *Natural radionuclides*

The natural radionuclides, including potassium-40, were assumed to be uniformly distributed in the soil. When evaluating the activity values for the total series, we used the median value of the activities obtained from all the separate radionuclides in a series. We also calculated the activity concentration from one single peak for the

Uranium- and Thorium-series each. For the Thorium-series, the 2.615 keV peak of thallium-208 was used (assuming a branching ratio  $f = 0.356$ ), and for the Uranium-series the 609 keV peak of Bi-214 was chosen.

TABLE 4.3

Activity of **K-40, total Uranium- and total Thorium-series** per Unit Mass of Soil at Selected Points at Vesivehmaa Airport Obtained in the RESUME-95 Exercise.

Values for U- and Th-series refer to the median value of data obtained from different peaks.

Uncertainty values for **total series** refer to the standard deviation of the mean-value of data obtained from different peaks. Uncertainty values for **single nuclides** refer to one standard deviation of the counting statistics for the single measuring points, and to one standard deviation of the mean for the overall-mean value.

Measuring point	K-40	Bi-214 (U) 609 keV	Tl-208 (Th) 2 615 keV	Total U	Total Th
	Bq/kg				
0	642.8±14.7	25.8±2.34	30.6±1.92	31.1±5.2	24.3±10.0
2.1	647.5±14.7	25.3±2.04	33.4±2.05	34.0±6.3	26.0±11.3
2.2	634.7±15.3	33.2±2.74	33.9±2.05	33.2±16.0	12.2±7.20
2.3	612.8±15.9	40.8±4.12	30.4±2.30	49.4±7.5	22.3±12.1
2.4	664.6±14.7	27.2±2.27	37.1±2.17	46.6±10.7	24.7±12.6
2.5	615.6±15.0	36.1±2.56	36.1±2.56	45.3±8.6	19.7±7.60
2.6	645.3±15.0	27.9±2.09	32.9±2.04	43.4±7.3	31.1±11.3
4.1	765.7±16.2	33.3±2.24	38.0±2.17	49.8±10.2	21.3±9.90
4.2	705.5±16.3	22.6±1.75	32.9±2.05	24.2±8.4	17.2±12.2
4.4	653.7±14.7	30.2±2.42	35.6±2.05	33.6±2.8	12.8±9.20
4.5	686.8±15.0	29.8±2.50	39.3±2.18	31.5±5.0	26.7±12.4
4.6	684.6±15.0	24.6±2.04	30.4±1.92	32.2±6.4	18.8±7.7
5.1	745.8±15.9	33.1±2.63	29.6±1.78	35.3±5.2	23.7±7.3
5.3	798.0±16.2	36.1±2.45	37.8±2.30	41.8±8.1	22.1±11.5
5.4	722.4±16.3	34.8±3.87	38.4±2.30	42.8±5.6	23.1±6.9
5.5	685.5±15.3	28.4±3.18	38.9±2.17	37.0±6.8	20.4±5.1
5.6	738.3±15.6	29.8±2.27	34.0±2.36	40.2±5.4	19.8±9.3
Overall mean	685.2±52.2	30.5±4.0	34.7±2.8	-	-
STUK/SURRC	<b>645.9±102.3<sup>1</sup></b>	<b>46.4±17.7<sup>3</sup></b>	<b>36.4±10.6<sup>3</sup></b>	<b>n.a.</b>	<b>n.a.</b>

<sup>3</sup> Activity values refer to wet soil weight.

The value for the total series are not valid unless equilibrium reigns between all subseries in the decay chains. The two individual radionuclides, Tl-208 and Bi-214, are both short-lived radon daughters. Their activities are not only related to the radon content in the soil but also to the exhalation rate of radon from the ground. A temporary change in the exhalation rate may create a gradient in the depth profile close to the ground surface. Data from STUK/SURRC suggest however that the assumption of a uniform distribution is valid for both of these radionuclides, and the same should then apply for the radon content in soil.

#### 4.3 Comparison with the radionuclide deposition as measured by STUK and SURRC at 1 m above ground level

STUK and SURRC presented data on the so called effective radionuclide concentration. By weighting each shell inventory for a specific radionuclide they obtained an activity concentration value that more would match the spatial averaging of a detector at 1 m altitude. Our values for Cs-137 in Table 4.4 refer to the assumed exponential depth profile  $\alpha/\rho = 0.0625 \text{ m}^2/\text{kg}$ .

TABLE 4.4  
Comparison Between our Overall Mean Values with the Effective Radionuclide Concentration at 1 m Detector Height as Obtained from the STUK/SURRC Soil Sample Data.

Radionuclide	Malmoe - data	STUK/SURRC
Mean $^{137}\text{Cs}$ / kBq $\text{m}^{-2}$	47.4±8.4	50.7±5.2
Mean $^{40}\text{K}$ / Bq per kg wet	685.2±52.2	577.7±46.1
Mean $^{214}\text{Bi}$ / Bq per kg wet	30.52±4.0	40.9±8.9
Mean $^{208}\text{Tl}$ / Bq per kg wet	34.66±2.8 (12.33±1.0)	9.7±1.0 <sup>4</sup>

## 5. CONCLUSION

### 5.1 Artificial radionuclides

The values for the Cs-137 content seem to agree well with the effective radionuclide concentration obtained by STUK and SURRC. The altogether deviation between the STUK/SURRC result and our result is no larger than 7 %. Generally, our results are somewhat lower (10 - 20 %). However, the deviations at each measuring point probably origin from the effect of *spatial averaging*. Lateral variations in deposition within the near vicinity (~ 1 m) of the point influence the soil sample data more than the gamma spectrometry data, since the “field of view” of the detector is about 20 m for a 662 keV primary photon field and at 1 m height above surface (-as interpreted from Fig. 2.17 in [1]). This is evident when comparing the average value

<sup>4</sup> Reported values refer to all detected transitions of Tl-208.

for the measuring points 2.1 - 2.6. Here, our value is in better agreement with the corresponding value for the soil sample data.

At the measuring points 5.5 and 5.6, the activity values are significantly lower than what is recorded at the other points (60 - 70 %). Both of two these points were situated at the periphery of the airport, close to boreal (pine tree) vegetation. A certain fraction of this difference can be attributed to the screening effects of the forest. However, this effect should be rather limited and the screening of the primary photon fluence should not exceed 10 %, according to rough calculations based on estimates of the pine-tree's diameter and interspacing [2]. An additional contributing effect could be that the landing area is snow ploughed annually, thereby creating walls of snow and ice which will increase the runoff of water in the springtime. In turn this could enhance vertical migration of the cesium fallout in the soil beneath the snow walls. The soil sample data contradict the latter assumption however, where no significant difference in the cesium content is found. Left is the possibility that the roughness of the ground surface is much more pronounced in the forest and consequently a decrease in photon fluence occurs at the edge of the wood.

As mentioned earlier the results are not fully compatible with each other. One reason for this is the difference between the actual soil density and the one approximated in the calculations (the "Beck-soil"). According to STUK/SURRC the average wet soil density at the measuring points in Area I varied from  $0.74 \text{ g/cm}^3$  at the top layer (first two centimetres) to about  $1.4 \text{ g/cm}^3$  at 6 cm and deeper.

## 5.2 Natural radionuclides

A comparatively large discrepancy is found between the STUK/SURRC data and our result for the K-40 content in soil when using their value for the "effective" activity concentration (18.4 % surplus for the overall mean value). A significant gradient was found in the potassium concentration in the topmost layers of soil. Detected levels were lower at surface and uniformity was not found until depths beyond approximately 3 - 4 cm. At these depths, the activity concentration amounted to 600 - 800 Bq/kg, which agrees better with our results. If applying a uniform distribution to this type of source geometry in a field measurement, the activity may be underestimated since the build-up layer acts as a shield. The magnitude of this effect is a net *decrease* of about 20 %<sup>†</sup> of the primary photon fluence rate as compared to an ideal uniform distribution which suggests that the discrepancy more could be due to the errors coming from extrapolation to higher energies of the intrinsic efficiency,  $\epsilon(\theta=90)$  (See next section!).

Depth profiles for the subseries nuclides fitted well with a uniform distribution. Accordingly the Bi-214 content was found to be in relatively well agreement with STUK/SURRC data. This was not the case for Tl-208, where a significant overestimation of the activity content (approximately 25 % surplus) in soil was found. However, this statement is not completely valid since the activity of Tl-208 for the

---

<sup>†</sup> This number is based on calculations made by Mathcad 6.0™ where an exponential potassium-40 distribution in soil has been assumed;  $S(z) = S(\infty) \cdot (1 - \exp(-(j/\rho) \cdot \rho \cdot z))$ .

soil samples taken by SURRC and STUK were measured in radon transparent plastic beakers and the equilibrium may have been altered in the soil column at the laboratory compared to the bulk soil at site. The short half live of Thoron suggests however that not too radical alterations of the equilibrium between Thoron and Tl-208 occur, making the SURRC data still somewhat compatible with the *in-situ* values.

### 5.3 Systematic and stochastic uncertainties

A great risk of uncertainties in the results are present at higher photon energies. This is due to the fact that the calibration constants for energies above 1461 keV rely on extrapolated data. At these energies (<1460 keV) the uncertainty of the intrinsic efficiency and its angular dependence can be as high as 10 % or more.

An overall estimation of the uncertainty assuming an *ideal source geometry* that is laterally homogenous and with no ground roughness present, should be about 15 - 20 % according to (2.7). Add to this the effect of ground roughness and lateral variations in source distributions, an overall uncertainty of 20 % should not be excessively high.

The systematic uncertainties greatly exceed the stochastic uncertainty in the peak count rates. For the Cs-137 values, this quantity is rarely more than 0.7 %, and for K-40 this figure does not exceed 2.5 %.

### 5.4 Miscellaneous comments regarding practical experiences from the exercise

The currently available set-up of equipment (including power generator, computer hardware and additional equipment such as dose-rate meters with fast response time, e.t.c.) is much too cumbersome to be practical in a real-time emergency situation. However, albeit its clumsiness, the detector set-up seems to yield satisfactory results. Obtained values are on the whole in good agreement with the results presented by STUK and SURRC respectively.

## 6. REFERENCES

- [1] R. Finck, High Resolution Field Gamma Spectrometry and its Applications to Problems in Environmental Radiology, Departments of Radiation Physics, Malmö and Lund, Lund University, Malmö, Sweden; 1992.
- [2] A. Raavila, Personal communication, Department of Radiation Physics in Lund, Lund University, Sweden; 1996.



# National Defence Research Establishment - FOA Stockholm

## Total Deposition of Cesium-137 in Finland during the Exercise "RESUME 95" in August 1995

EQUIPMENT AND MEASUREMENTS .....	283
Field gamma .....	283
Soil samples .....	284
RESULTS .....	284
Tab. 1. Results from measurements at the Vesivehmaa Airfield with the "BAMSE" detector .....	287
Tab. 2. Results from measurements at the Vesivehmaa Airfield with the "LILLEN" detector .....	288
Tab. 3. Comparison of the soil core results based on the NaI(Tl) annulus measurement and the germanium spectrometer profile integration for Cs <sup>137</sup> in kBq/m <sup>2</sup> .....	289

**NEXT PAGE(S)  
left BLANK**

## TOTAL DEPOSITION OF CESIUM-137 MEASURED IN FINLAND DURING THE EXERCISE "RÉSUMÉ 95" IN AUGUST 1995.

Lars-Erik De Geer, Ingemar Vintersved and Rune Arntsing  
Nuclear Detection Group  
National Defence Research Establishment, FOA480.  
S-172 90 STOCKHOLM, Sweden

In the exercise called "RÉSUMÉ 95" the Nuclear Detection Group from the National Defence Research Establishment in Stockholm participated with field gamma ray measurements combined with soil sampling and profile measurements. The results are presented in this report for the measurements of cesium-137. We considered the measurements of cesium-137 at the airfield the most important part of the in-situ exercise. Data was of course collected also for cesium-134 and natural radionuclides but time has not permitted a full analysis of these radionuclides. The methodology would, however, be the same as applied for cesium-137. Less attention was paid for area II and due to limited personnel resources the search exercise was not fully carried out.

### **Equipment and measurements:**

#### **Field gamma:**

For the field gamma ray measurements we used two setups. One of the detectors, "LILLEN", is a rugged High Purity Germanium (HPGe) detector manufactured by EG&G Ortec with a 1.6 l dewar. Its gamma efficiency for a point source at 25 cm with energy 1332.5 keV is 35 percent relative to a 3 in. diameter by 3 in. long NaI crystal. With this detector a portable multichannel analyzer, EG&G Ortec 7500, was used. Due to some electronic problems the energy resolution (FWHM) at 661 keV was about 3 keV during most measurements. The other HPGe detector used, "BAMSE", is also manufactured by EG&G Ortec and has the same dimensions as "LILLEN" but with a 3 l dewar. "BAMSE" was used with a portable multichannel analyzer, "the Inspector", from Canberra. The energy resolution at 661 keV for this detector was 1.5 keV. In the airfield (Area I) both detectors measured at all points on circle #3

and #4 and at the center point. On circle #5 "BAMSE" measured points 5.1 and 5.2 while "LILLEN" measured 5.3, 5.4, 5.5 and 5.6.

### Soil samples:

The soil samples were taken using a steel auger. The cores had a diameter of 56 mm and a length of 100 mm. In the airfield (Area I) soil samples were taken at the center (Point 0), at all points on circle #3 (3.1, 3.2 ... 3.6) and at points 4.2, 4.3, 4.4 and 4.6 on circle #4. In area II soil samples were taken at the soccer-field (Point 10) at two positions (A and D). Finally two soil samples were taken in area II at points 71 and 83. The soil samples were used for profile measurements and also to determine the total deposition.

### Results:

Preliminary results were obtained in the field, using the built-in peak search function in the portable multichannel analyzers. A more thorough analysis was later performed using our laboratory computer system.

A direct field gamma measurement 1 m above a field does not directly give a true picture of the total deposition. To do this we have to acquire information on the depth profile. People have tried to do this by comparing the main gamma peak with the low energy X-rays as respective absorption will be different and the size of the difference will depend on the average depth of the nuclide in the soil. This gives a more true value than the surface equivalent deposition, where the deposition density is calculated based on the assumption that there is no penetration at all into the soil. But obviously such a scheme can only give some kind of an averaged value as there is no way of incorporating detailed information about the profile.

Traditionally this problem is solved by carrying out cumbersome slicing of the soil samples cm by cm, which are then counted individually. The process is often difficult and there is a great risk of cross contamination.

At FOA480 we have constructed a device where the soil sample is moved untouched with its container cylinder in front of a slit in a lead shield with a germanium spectrometer behind. With the current settings it moves 5 mm, stops for counting for an hour or so and then moves 5 mm again, and so on. All along the sample rotates to make the profile measurement averaged out over the azimuthal angle. The device is totally computer

controlled, so measurements can be done continuously day and night, which makes up for the often quite long total counting times.

The Vääksy profiles were measured in 28 equidistant (5 mm) positions for 40 (Vesivehmaa Airfield) or 50 (Area II) minutes each. Then the area of the 661.6 keV peak was integrated and used as a point in the profile. There is no need for a calibration, as the profile just gives the relation between positions. Of course it is possible to make a calibration by using a standard and this was also done in this case, as shown below, to cross-check the results.

The raw profiles can be used as input to the calculations but the results will improve somewhat if we do a deconvolution of the data. This takes care of the fact that the profile is pictured with a finite resolution. A computer code, FTM, has been written (Robert Finck, SSI) that carries out this task if fed with the current profile and a profile taken with a point source. In this way the profile normally shrinks a little and one gets rid of some annoying points hovering just above the ground surface in the profile. Otherwise the effect on the calculated deposition is normally just a few percent and thus not very dramatic.

The total deposition and a number of other quantities like dose rate in air, ambient dose equivalent, angular flux densities and detector responses can now easily be calculated by Monte Carlo techniques. The adverb "easily" of course only applies when one has the code available, as well as tested and proven for the current application. In our case, we use the code MCNP, developed and maintained by the Los Alamos National Laboratory in the USA.

At the Vesivehmaa Airfield soil samples were taken at 11 points. The profiles of the center core and the 32 m ring (#3) cores were all quite similar and they were used to build a typical average core for the field. In the 64 m ring (#4) the samples were more difficult to take as they contained a lot of sand and gravel and easily decomposed.

With this average profile and with the current Chernobyl cesium isotope mixture ( $^{134}\text{Cs}/^{137}\text{Cs}$  activity ratio = 3.10 %) a Monte Carlo simulation based on 1 million events collect to the following results (all applying to a total nominal deposition of 1 kBq/m<sup>2</sup>):

Dose rate in air:	1.302	nGy/h
Ambient dose equivalent	1.622	nSv/h
Count rate of 661.6 keV peak	0.4924	cps

The latter entity depends on the individual germanium spectrometer used and calibration data in the form of directional efficiencies has to be input. For this procedure a special calibration rack has been constructed and used, where a calibration source is rotating at a constant distance and angle around the detector crystal. Like in the profile measurements the rotation averages out any azimuthal variation.

The 661.6 keV count rate given above apply to one of the detectors used, "BAMSE". For the other detector "LILLEN" the corresponding value was 0.5545 cps. The statistical error in these numbers is fairly small, of the order of 0.2 %, when 1 million histories are followed and the problem is efficiently formulated.

In area II the same procedure was used, although much less soil cores and field measurements were available.

Besides this analysis, all cores were measured individually in a well calibrated NaI(Tl) annulus. The calibration is traceable via a strong soil sample from Russia to our well calibrated (IAEA) germanium spectrometers in the laboratory. As we generally get somewhat higher total depositions at the airfield than expected by the organizers (who gave a rough value of 50 kBq/m<sup>2</sup>), we considered this a worthwhile undertaking. As can be seen in the tables the field gamma data and the soil core data are quite consistent. Naturally the cores vary more as they give the results for just 24 cm<sup>2</sup> while the field gamma detectors efficiently average the data over some 100 square meters.

At the airfield both detectors, "BAMSE" and "LILLEN", were used at the 13 innermost grid points. The ratio of the results was 1.004±0.006, which effectively shows the two detectors to be exchangeable instruments. Thus in area II only one detector was used at each point

The dose rate in air at the airfield due to the Chernobyl cesium isotopes can be calculated for each point by multiplying the total deposition of cesium-137 with the factor 1.302 nGy/h per kBq/m<sup>2</sup>. A typical value of 80

kBq/m<sup>2</sup> in this way yields 0.10 µGy/h, which is of the same order of magnitude as a normal natural background.

At the soccer-field in area II a square grid with a center point was laid out and measurements taken in these five points with both detectors working in parallel. Two soil cores were taken, which showed a total deposition of 134 and 137 (sic!) kBq/m<sup>2</sup> respectively. The field gamma results in the five points were 153, 60, 110, 112, 88 and 44 kBq/m<sup>2</sup> yielding an average value of 94±17 kBq/m<sup>2</sup>.

Point	Cps	Surface equivalent		Total	Soil
		1	2		
		kBq/m <sup>2</sup>	kBq/m <sup>2</sup>		
00	36.5367	26.3	26.4	74.2	80.0
Average				74.2	80.0
31	38.8673	27.9	27.9	78.9	79.2
32	36.5603	26.3	26.2	74.3	67.6
33	30.9366	22.2	22.3	62.8	72.6
34	38.4247	27.6	27.7	78.0	40.2
35	36.6726	26.4	26.3	74.5	97.0
36	37.0757	26.7	26.6	75.3	64.7
Average				74.0±2.4	70.2±7.6
41	44.2089	31.8	31.8	89.8	
42	40.9023	29.4	29.6	83.1	90.4
43	42.5076	30.6	30.6	86.3	65.2
44	41.7496	30.0	29.6	84.8	33.4
45	43.2285	31.1	31.1	87.8	
46	42.0034	30.2	30.3	85.3	54.5
Average				86.2±1.0	60.9±12
51	19.8571	14.3	14.2	40.3	
52	41.2982	29.7	29.8	83.9	

*Table 1. Results from measurements at the Vesivehmaa Airfield with the "BAMSE" detector: The first column indicates the point on the ground as marked by the organizers, the second column gives the count rate in the 661.6 keV peak. Next two columns give the surface equivalent deposition, calculated in the field (1) and later on in the laboratory (2). The column marked "total" gives the final results when the MCNP calculated factor has been applied. In many points a soil core sample was taken and the last column gives the result from the annulus counting of these cores.*

Point	Cps	Surface equivalent		Total	Soil
		1	2		
		kBq/m <sup>2</sup>	kBq/m <sup>2</sup>		
00	41.3222	26.5	26.5	74.5	80.0
Average				74.5	80.0
31	43.9272	28.2	28.1	79.2	79.2
32	40.8823	26.2	26.1	73.7	67.6
33	34.7957	22.3	22.3	62.7	72.6
34	43.0368	27.6	27.4	77.6	40.2
35	40.7516	26.1	25.9	73.5	97.0
36	43.6653	28.0	27.9	78.7	64,7
Average				74.2±2.5	70.2±7.6
41	50.1865	32.2	32.2	90.5	
42	47.6335	30.5	30.4	85.9	90.4
43	46.1056	29.6	29.8	83.1	65.2
44	46.9023	30.1	30.0	84.6	33.4
45	49.5762	31.8	31.6	89.4	
46	46.1888	29.6	29.5	83.3	54.5
Average				86.1±1.3	60.9±12
53	46.8220	30.0	30.0	84.4	
54	41.6949	26.7	26.6	75.2	
55	32.4941	20.8	20.7	58.6	
56	29.6544	19.0	18.9	53.5	
Average				67.9±7.2	

*Table 2. Results from measurements at the Vesivehmaa Airfield with the "LILLEN" detector. The first column indicates the point on the ground as marked by the organizers, the second column gives the count rate in the 661.6 keV peak. Next two columns give the surface equivalent deposition, calculated in the field (1) and later on in the laboratory (2). The column marked "total" gives the final results when the MCNP calculated factor has been applied. In many points a soil core sample was taken and the last column gives the result from the annulus counting of these cores.*

At the meadow near the house in area II only one field gamma measurement was made yielding a total deposition of 99 kBq/m<sup>2</sup>. Two soil cores showed 132 and 146 kBq/m<sup>2</sup> respectively.

As pointed out above our results for the airfield seems to show higher values than anticipated from the organizer's initial scanning. This tendency is clear both in the field gamma measurements and in the core measurements as can be seen in the tables above. To further check our

values the profile measurements were calibrated with an IAEA source. This is not an ideal counting setup for absolute measurements but these results were surprisingly similar to the more accurate annulus measurements as can be seen in the following table.

Point	Profile integration kBq/m <sup>2</sup>	NaI(Tl) annulus measurement kBq/m <sup>2</sup>
00	91	80.0
31	88	79.2
32	55	67.6
33	82	72.6
34	38	40.2
35	96	97.0
36	73	64.7
Average	72±9	70.2±7.6
42	102	90.4
43	58	65.2
44	35	33.4
46	47	54.5
Average	61±15	61.9±11.9

*Table 3. Comparison of the soil core results based on the NaI(Tl) annulus measurement (column 3) and the germanium spectrometer profile integration (column 2) for Cs-137 in kBq/m<sup>2</sup>. The grid point notation is given in the first column.*

All counting and analysis errors are well below the variation in the results due to the specific grid point. With an idealized field the analysis results are considered to be accurate to within just a few percent. Including the variation in the deposition field it is believed that the true average for the field is found within 10% of the average of the measurements.

To conclude, we feel fairly confident in the higher results as they are really demonstrated by three different systems, the field gamma spectrometer, the NaI(Tl) annulus and the germanium spectrometer profile integration.

This is a report of the analysis of our results from "RÉSUMÉ 95" which has very much focused on what we considered the most important part of the intercomparison, the cesium-137 fallout at the Vesivehmaa Airfield. A full report including also cesium-134 (which is in a way redundant, due to

the constant 134/137 ratio) and natural radionuclides will soon be issued as a FOA laboratory report.



# National Defence Research Establishment - Division of Ionising Radiation and Fallout - FOA Umeå

## Results from RESUME95 - Measurement with mobile equipment

1. ABSTRACT .....	294
2. INTRODUCTION .....	294
3. MATERIALS AND METHODS .....	295
3.1. Field gamma spectrometry .....	295
Fig. 1. A description of the two-slice model used in the exercise .....	296
3.2. Carborne measurements .....	296
3.3. Hidden sources .....	297
3.4. Soil samples .....	297
4. RESULTS .....	297
4.1. Area 1 .....	297
Tab. 1. Means $\pm$ one S.D. for the soil parameters, experimentally estimated in area 1 for the two-slice model .....	297
Tab. 2. The results from the In-Situ measurements in area 1 .....	298
Tab. 3. Mean $\pm$ S.D. of the field gamma measurements showed in Table 2 .....	299
Tab. 4. Mean $\pm$ S.D. for the naturally radioactive nuclides .....	300
4.2. Area 2 .....	300
Tab. 5. The soil parameters, according to Fig. 1, for the three field gamma measurements in area 2 .....	300
Tab. 6. Results from area 2 for the artificial nuclides .....	301
Tab. 7. The results for the artificial nuclides in area 2, described by a plane surface sources distribution .....	302
Fig. 2. Map over area 2, supplied by the organisers of the exercise .....	303
Tab. 8. The results of the field gamma measurements of naturally radioactive nuclides at location A, B and C in area 2. ....	304
4.3. Hidden sources .....	304
4.3.1. Site 1 .....	304
Fig. 3. The results obtained with the handheld instruments at site 1 .....	304
4.3.2. Site 2 .....	305
Fig. 4. The results from site 2 .....	305
5. DISCUSSION .....	305
6. ACKNOWLEDGEMENTS .....	306
7. REFERENCES .....	306



# Results from RÉSUMÉ 95

## Measurements with mobile equipment

Kenneth Lidström, Thomas Ulvsand and Göran Ågren

E-mail: [lidstrom@ume.foa.se](mailto:lidstrom@ume.foa.se), [ulvsand@ume.foa.se](mailto:ulvsand@ume.foa.se), [gagren@ume.foa.se](mailto:gagren@ume.foa.se)

National Defence Research Establishment  
Division of Ionising Radiation and Fallout  
Umeå 960220

## 1. Abstract

This paper presents the results obtained during the NKS, (EKO-3), Exercise Résumé-95 by a group from the Division of Ionising Radiation and Fallout, FOA, Umeå, Sweden. Field gamma measurements were performed in two areas with a HPGe-detector (p-type, 50% relative efficiency) mounted vertically 1 m above the ground or horizontally in a car. One of the areas was an airfield, *Vesivehmaa*, where 19 measurements were done. The calculated Cs-137 activity was  $52.1 \pm 4.5$  kBq/m<sup>2</sup> assuming a two slice distribution model with a homogenous density and activity distribution in each slice. The report contains also the results from a task which included the finding, classification and estimation of the activity of hidden sources within two 10\*10m-areas.

## 2. Introduction

The major purpose of the exercise RÉSUMÉ 95 ( Rapid Environmental Surveying Using Mobile Equipment ) was :

- to investigate the possibility of multilateral assistance by transferring equipment and operating staff in case of accidents involving dispersion of radioactive material,
- to test the ability of the existing measuring systems available in the Nordic countries with different airborne, carborne and in-situ (in this report called Field Gamma-ray Spectrometry) instruments to map radioactive contamination, in this case from the Chernobyl fallout,
- to test exchange of data and to establish whether comparable results can be obtained with different systems.

A number of Nordic teams participated in the exercise. Beside those there were teams from Canada, France, Germany and Scotland. The exercise was held in Finland about 150 km north of Helsinki, from the 13th to the 18th of August, 1995.

### 3. Materials and methods

#### 3.1 Field gamma spectrometry

The In situ measurements were performed with a HPGe-detector (p-type, 50% relative efficiency) mounted vertically 1 m above the ground or horizontally in a car. The detector was efficiency calibrated as a function of angle of incidence and energy of the photons, [ 1,2 ]. The detector was connected to a Nomad 92X, containing a multichannel analyser, high voltage supply and linear amplifier, manufactured by EG&G, Ortec.

The depth distribution model was based on one or more soil slices of finite thickness with homogenous density and activity. (Figure 1, [2]).

The site specific activity ( $\text{Bq/m}^2$ ) or activity concentration ( $\text{Bq/kg}$ ) was calculated assuming homogenous depth distributions in each slice. For natural radionuclides, one slice with a thickness of 1 meter was used. For Cs-134 and Cs-137, two types of distribution models were used, one containing two slices with a relative activity content in the upper slice of 90% [3], and the other, a plane surface source distribution (one slice,  $d = 0.01$  m). In all cases experimentally determined site specific densities were used.

The coordinates for the measurements in area 2 were obtained from a GPS instrument which was corrected by an RDS unit.

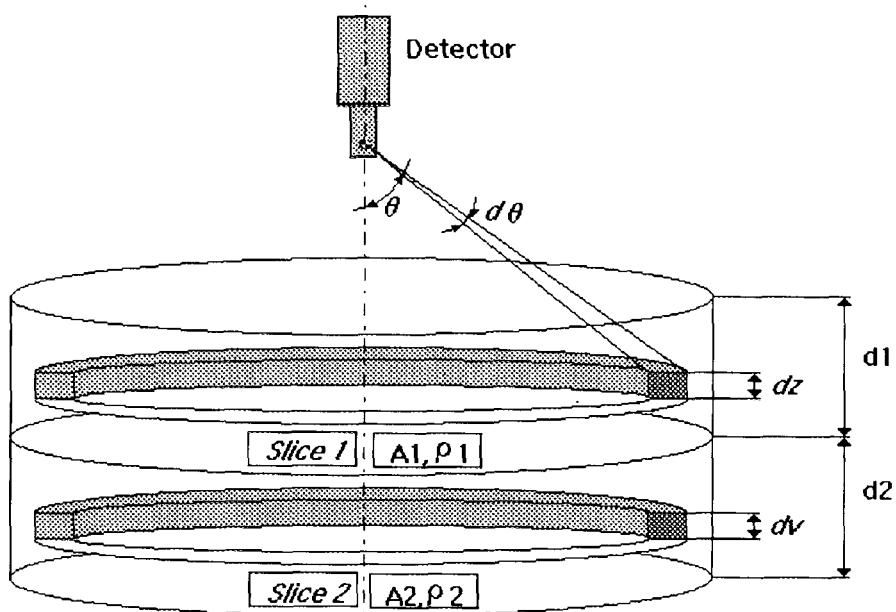


**Figure 1.** A description of the two-slice model used in the exercise. Parameters  $A_1$  and  $A_2$  represent the relative activity content in each slice.

### 3.2 Carborne measurements

Carborne measurements were carried out in eight places in area II with a measuring time of 300 s. The purpose of the measurements was to see the quality of the results that could be obtained by a simple measuring method. The idea was to perform measurements with the HPGe-detector lying in its case in the car. Corrections for the shielding of the car, were based on reference measurements at points 0.0 and 4.3 in Area I. The ratio between the number of counts in the Cs-137 photo-peak with the detector lying in the car and the counts in an ordinary in-situ measurement for the same sampling time were 0.509 and 0.469, respectively. The correction factor was chosen as the arithmetic mean of the two values, 0.49.

The number of counts in the photo peak was corrected to account for the shielding, by dividing the count rate with 0.49. The corrected values were put into the distribution model.

A ratio or shielding factor of 0.65, was obtained using a hand-held instrument SPP2 (Saphymo Stel, measuring counts per second) inside and outside the car.

The mean value of the ratio between total gamma spectrometry counts inside and outside the car at locations 0.0 and 4.3 was 0.81.

### 3.3 Hidden sources

Both field gamma spectrometry and the hand-held instrument, SPP2, were used to solve a task which included the finding, identification and estimation of the activity of hidden sources within two 10\*10m-areas. These are named site 1 and site 2 in this paper. For the purpose, one field gamma spectrometry measurement was performed in each corner of the areas and several hand-instrument measurements along each side of the sites. By means of the count rates from the hand-held instruments and the inverse square law, the locations of the sources were determined. For identification of the sources, the field gamma equipment was used. For estimation of the source activities both the handheld instrument and the results from gamma spectrometry were used.

### 3.4 Soil samples

Soil was sampled with a metal auger, diameter 0.11 m, and sectioned into soil horizons at the transition depths (vegetation, fermentation layer (F), humus (H) and/or mineral (M) soil). This was done to estimate density and thickness parameters. For this purpose, 14 samples were taken of slice 1 and 5 of slice 2 in area 1. In area two, one core of maximum depth was taken and sectioned on site at locations A, B and C, (figure 2).

## 4. Results

### 4.1 Area 1

The soil specifics, derived on site and described in Table 1, were used in the model to calculate the activity in area 1 (Table 2).

**Table 1.** Means  $\pm$  one S.D. (standard deviation) for the soil parameters, experimentally estimated in area 1 for the two-slice model.

Slice	$\rho^*$ (kg/m <sup>3</sup> )	d (cm)	Observations n
1	550 $\pm$ 325	4 $\pm$ 1.4	14
2	1260 $\pm$ 217	5	5

\* For the plane surface source distribution model, one slice with a density  $\rho = 550$  kg/m<sup>3</sup> was used.

**Table 2.** The results from the In-Situ measurements in area 1. The second column show the radius from origo to each shell in the hexagonal grid. Columns number three and four shows the Cs-134 and Cs-137 activity for the two-slice model, with an activity content of 90% in slice 1 and 10% in slice 2. Columns five and six shows the activity assuming a plane surface source distribution.

Location	Radius (m)	Cs-134 "90/10" (kBq/m <sup>2</sup> )	Cs-137 "90/10" (kBq/m <sup>2</sup> )	Cs-134 "Surface" (kBq/m <sup>2</sup> )	Cs-137 "Surface" (kBq/m <sup>2</sup> )
0	0	1.55	50.6	0.77	25.5
2:1	8	1.59	50.9	0.79	25.6
2:2	8	1.69	51.3	0.84	25.9
2:3	8	1.46	50.3	0.73	25.4
2:4	8	1.36	45.3	0.67	22.8
2:5	8	1.50	49.1	0.75	24.8
2:6	8	1.77	51.7	0.88	26.1
3:1	32	1.63	53.2	0.81	26.8
3:2	32	1.53	48.5	0.76	24.4
3:3	32	1.26	41.6	0.63	21.0
3:4	32	1.73	51.2	0.86	25.8
3:5	32	1.62	49.8	0.8	25.1
3:6	32	1.58	52.2	0.79	26.3
4:1	128	1.88	60.3	0.94	30.4
4:2	128	1.71	56.2	0.85	28.3
4:3	128	1.82	56.9	0.90	28.7
4:4	128	1.82	57.1	0.90	28.8
4:5	128	1.89	58.0	0.94	29.2
4:6	128	1.76	55.2	0.88	27.8

**Table 3.** Mean  $\pm$  S.D. of the field gamma measurements showed in Table 2.

Location	Radius (m)	Mean (S.D.) Cs-134 "90/10" (kBq/m <sup>2</sup> )	Mean (S.D.) Cs-137 "90/10" (kBq/m <sup>2</sup> )	Mean (S.D.) Cs-134 "Surface" (Bq/m <sup>2</sup> )	Mean (S.D.) Cs-137 "Surface" (Bq/m <sup>2</sup> )	Observations  n
0	0	1.55	50.6	0.77	25.5	1
2:1-2:6	8	1.56 (0.15)	49.8 (2.4)	0.78 (0.078)	25.1 (1.2)	6
3:1-3:6	32	1.56 (0.16)	49.4 (4.2)	0.78 (0.079)	24.9 (2.1)	6
4:1-4:6	128	1.81 (0.07)	57.3 (1.9)	0.90 (0.034)	28.9 (0.89)	6
Total Area 1		1.64 (0.17)	52.1 (4.5)	0.82 (0.085)	26.3 (2.3)	19

For the naturally radioactive nuclides, a one slice model with density  $\rho = 1260 \text{ kg/m}^3$  and thickness  $d = 1 \text{ m}$  was chosen. In this paper, only the means and S.D. are given for the nuclides Potassium-40, Bismuth-214 and Thallium-208 in Table 4.

**Table 4.** Mean  $\pm$  S.D. for the naturally radioactive nuclides,. The results are given for each shell and for the total area. The model described in Figure 1 was used with one slice, 1 m thick and with a density  $\rho = 1260 \text{ kg/m}^3$ .

Location Area 1	Radius (m)	Mean (S.D.) K-40 Bq/kg	Mean (S.D.) Bi-214 Bq/kg	Mean (S.D.) Tl-208 Bq/kg	Observations
0:0	0	540	32.0	8.7	1
2:1-2:6	8	522 (37)	38.6 (8.3)	7.9 (1.5)	6
3:1-3:6	32	531 (15)	39.6 (9.3)	8.5 (1.2)	6
4:1-4:6	128	564 (44)	34.9 (2.9)	8.4 (0.5)	6
Total Area 1		539 (36)	37.4 (7.2)	8.3 (1.1)	19

#### 4.2 Area 2

The soil parameters in Table 5 were derived on site and used in the model. These parameters were based on single samples, one from each location A, B and C.

**Table 5.** The soil parameters, according to Figure 1, for the three field gamma measurements in area 2.

Parameter Location	d1 (cm)	d2 (cm)	$\rho_1$ ( $\text{kg/m}^3$ )	$\rho_2$ ( $\text{kg/m}^3$ )
A	4	5	870	1110
B	4	6	660	1130
C	4.5	5	980	1120*

\* Density calculated as a mean of point A and B.

Measurements named A, B and C were field gamma measurements and the rest, carborne measurements with the detector mounted inside the car. The soil specifics used for the carborne measurements were the same as for area 1.

**Table 6.** Results from area 2 for the artificial nuclides. The model with two slices and 90% of the activity in slice 1 and 10% in slice 2 was used. In-Situ measurements were made at locations A, B and C. The other measurements were performed with the detector mounted inside a car and transformed to field gamma measurements with a correction factor. The location for each measurement point are showed in Figure 2.

Location	GPS Coordinates N (WGS 84)	GPS Coordinates E (WGS 84)	Cs-134 "90/10" (kBq/m <sup>2</sup> )	Cs-137 "90/10" (kBq/m <sup>2</sup> )
A*	61.2986	25.0757	3.2	98.7
B*	61.3494	25.0928	1.9	63.4
C*	61.3333	25.0858	3.7	122.2
77**	61.3345	25.0681	4.6	65.8
91-92**	61.3230	25.0741	9.4	116.9
92**	61.3177	25.0759	10.2	145.6
46**	61.3129	25.0866	1.5	47.5
64**	61.3192	25.1009	9.1	132.9
70**	61.3318	25.1040	6.1	101.3
39**	61.3112	25.0452	5.6	91.5
23-24**	61.2971	25.0874	8.9	136.6
Mean			5.8	102.0
S.D.			3.2	32.5

\* Represents field gamma measurements.

\*\* Represents carborne measurements.

**Table 7.** The results for the artificial nuclides in area 2, described by a plane surface source distribution. The locations are shown in Figure 2.

Location	GPS Coordinates N (WGS 84)	GPS Coordinates E (WGS 84)	Cs-134 "Surface" (kBq/m <sup>2</sup> )	Cs-137 "Surface" (kBq/m <sup>2</sup> )
A*	61.2986	25.0757	1.33	41.56
B*	61.3494	25.0928	0.87	29.82
C*	61.3333	25.0858	1.38	46.06
77**	61.3345	25.0681	2.27	33.17
91-92**	61.3230	25.0741	4.69	58.94
92**	61.3177	25.0759	5.07	73.41
46**	61.3129	25.0866	0.72	23.96
64**	61.3192	25.1009	4.51	66.99
70**	61.3318	25.1040	3.03	51.05
39**	61.3112	25.0452	2.78	46.14
23-24**	61.2971	25.0874	4.44	68.86
Mean			2.83	49.09
S.D.			1.64	16.54

\* Represents field gamma measurements.

\*\* Represents carborne measurements.

### Measurements by car - AREA II

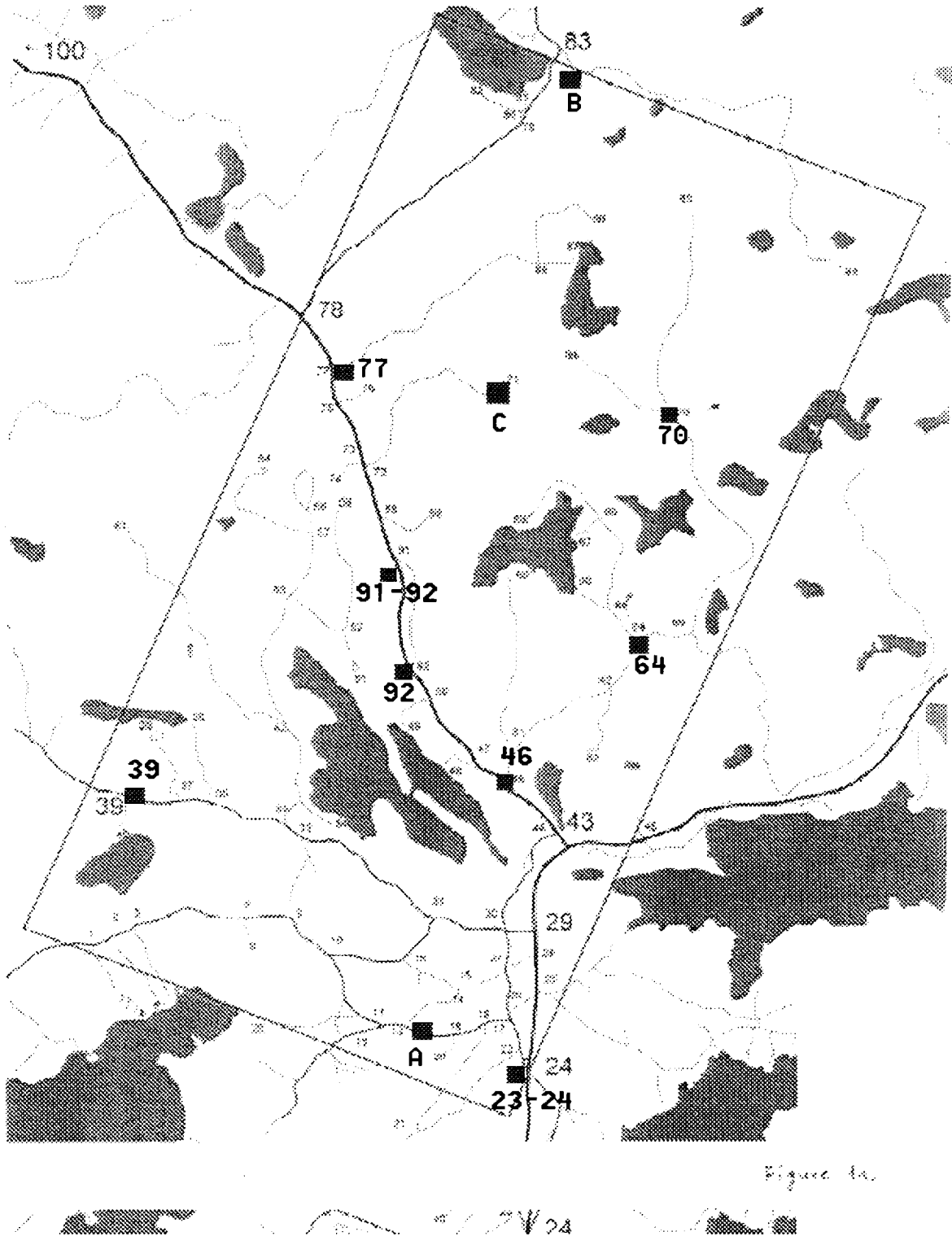


Figure 2.

**Figure 2.** Map over area 2, supplied by the organisers of the exercise. The map shows the locations for the In-Situ measurements and the measurements by car (Tables 6-8).

For the natural nuclides, the activity was calculated at the three points where field gamma measurements were performed.

**Table 8.** The results of the field gamma measurements of naturally radioactive nuclides at locations A, B and C in area 2, using the one slice model with density according to Table 5 ( $\rho_2$ ), and thickness  $d = 1$  m.

Location	K-40 (Bq/kg)	Bi-214 (Bq/kg)	Tl-208 (Bq/kg)
A	605	28	9
B	513	20	7
C	621	26	10

### 4.3 Hidden sources

#### 4.3.1 Site 1

Our conclusion was that there was more than one source in site 1. Only a probable area can be indicated and if the sources are not of the same activity, the one with the higher activity should be closer to the lower-left corner (origo) in Figure 3. Based on our gamma spectrometry measurements, the sources were classified as Co-60.

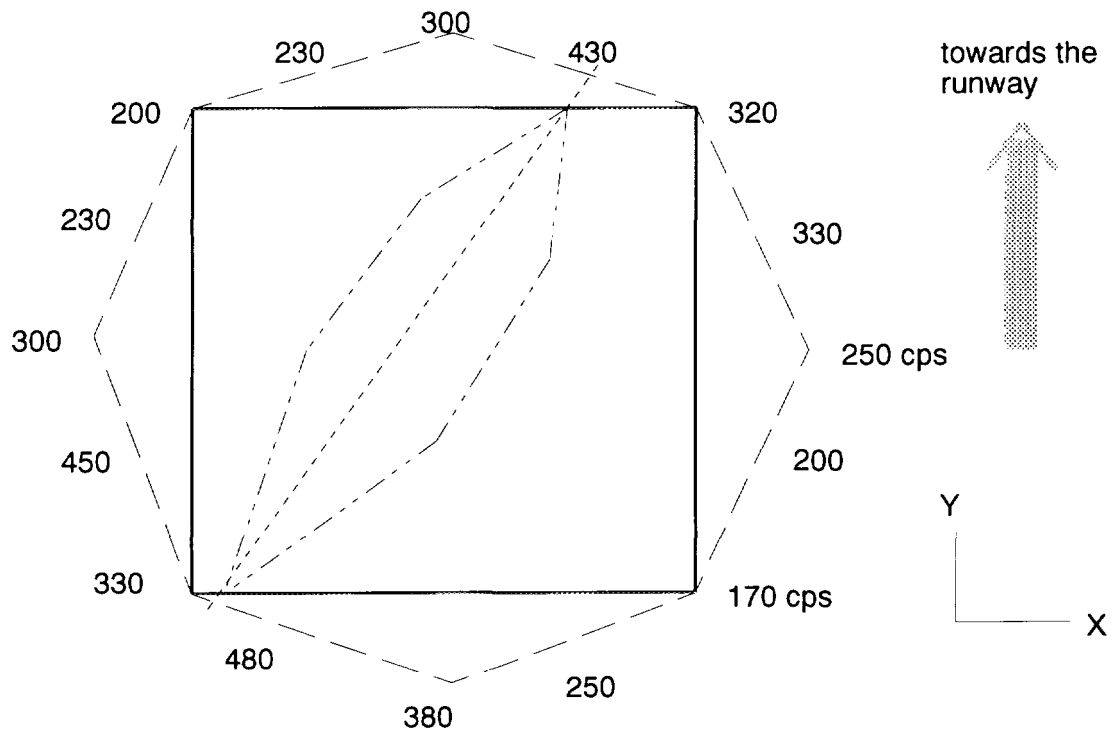


**Figure 3.** The results obtained with the handheld instrument at site 1. The values given along the dashed line ( - - - - ) are the count rates determined with the handheld instrument at that point.

### 4.3.2 Site 2

The source was identified as Cs-137 and based on the handheld instrument, the activity was calculated to somewhere between 300 and 400 MBq. The activity of the source calculated from the In-Situ measurements, one at each corner of the area, was 200 MBq. The probable position of the source, as indicated by our measurements, is given as coordinates in meters from the lower left corner of the area (Figure 4).

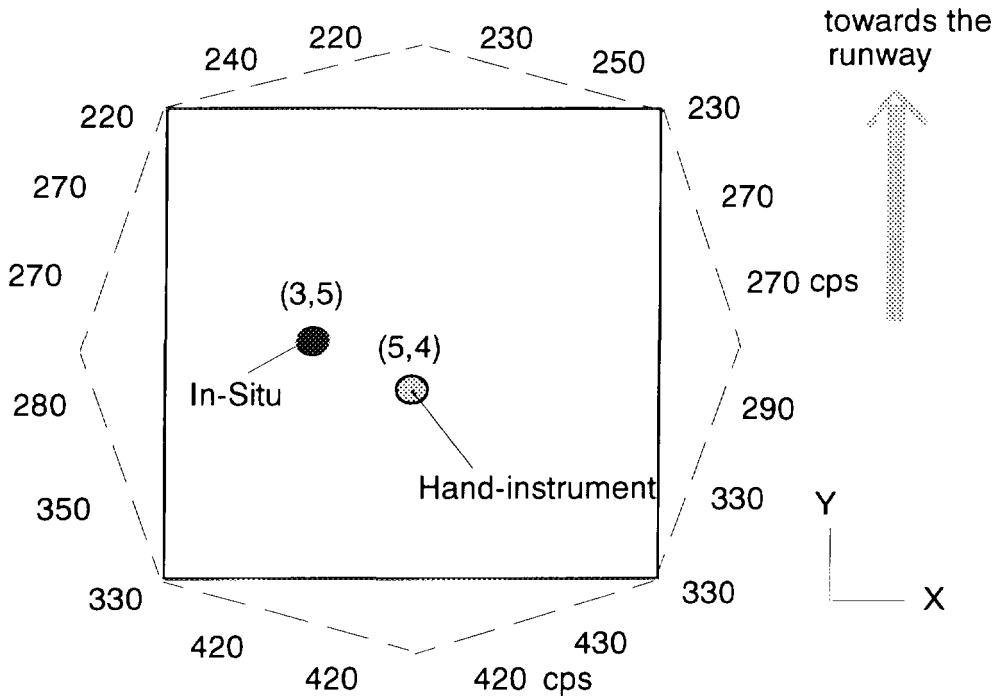


**Figure 4.** The results from site 2. The values given along the dashed line are the count rates determined with the handheld instrument at that point.

## 5. Discussion

Our assumption of the vertical depth distribution was that slice 1 contained 90% of the Cs-137 activity and slice 2, the remaining 10%. This assumption was in good agreement with calculations based on soil samples taken in area 1 by other groups [4]. They measured a Cs-137 activity content in the upper 4 cm of  $92 \pm 11\%$  ( $n=26$ ).

There were large geometrical differences between some of the sampling sites which could generate uncertainties in the field gamma measurements. Area 1 represents an almost plane surface in comparison to the measurement points in area 2. Some of these were surrounded by agricultural areas, other surrounded by woodpiles.

For the airborne measurements in area 2 a simplified method was assumed: the vertical distribution of Cs-137 was the same at the sampling sites as in the reference area. As this probably is not the case, an uncertainty will be introduced.

The shielding factor of 0.65, which was obtained using the SPP2 inside and outside the car, can be compared with the "gamma-spectrometry" inside/outside ratio of 0.49. A difference between the detectors is that SPP2 measures total counts, while the spectrometer uses the counts in the photo-peak. One explanation of the difference between the two factors could be that the interior of the car generates much scattered radiation (build-up). This is also indicated by the higher ratio, 0.81, for the total gamma spectrometry comparison.

## 6. Acknowledgements

The authors would like to thank the organisers of this exercise for a excellent work.

## 7. References

1. Arntsing R. 1993. Personal communication.
2. Lidström and Nylén. 1996. Field gamma-ray spectrometry on stratified soils. Manuscript.
3. Nylén T., Andersson T. and Lundell A. 1994. Temporal relations between Cs-137 in catchments and lakes. FOA report C 40318-4.3 (in Swedish, pictures and tables in English).
4. Sanderson.D.C.W, Allyson.J.D, Toivonen.H, Honkamaa.T *Gamma Ray Spectrometry Results From Core Samples Collected For RÉSUMÉ 95*, Scottish Universities Research & Reactor Centre 1995



# Geological Survey of Sweden RESUME95

AIRBORNE SYSTEM .....	309
Spectrometer .....	309
Navigation and Positioning .....	309
Spectrometer Calibration .....	310
Data Collection and Processing .....	310
Data Format.....	310
IN-SITU SYSTEMS .....	312
AREA I.....	313
Airborne Measurements .....	313
In-Situ Measurements.....	314
AREA II.....	316
Airborne Measurements .....	316
AREA III.....	318
Sources.....	318
Airborne Measurements .....	319

Figures in Colour Appendix (C.A.):

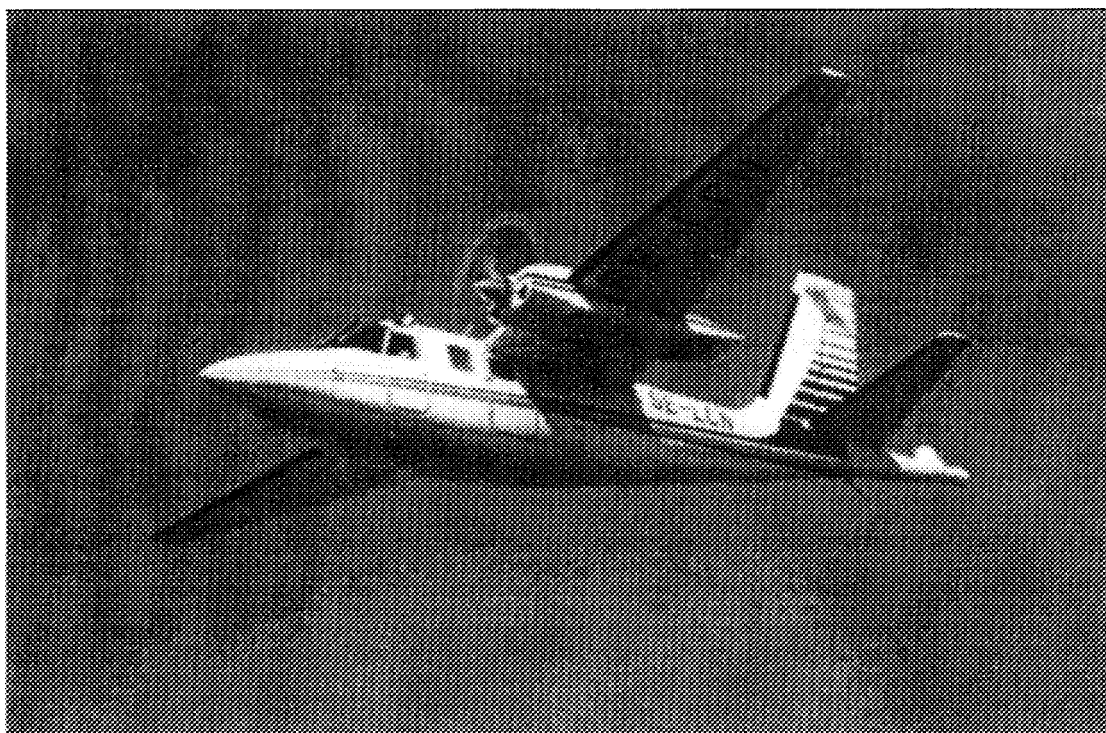
Cesium-137 AREA 2, Surface Activity .....	C.A. plate 23
AREA III, Final Map.....	C.A. plate 24

**NEXT PAGE(S)  
left BLANK**

# RÉSUMÉ 95

## SGU Airborne System

The platform for the airborne system is a **Shrike Commander 500S**. The twin-engined aircraft has a radius of action of about 5 h with a crew of two persons and a complete measuring system. Normal operation speed is 240 km/h.



### **Spectrometer**

The spectrometer employed is a 256-channel Exploranium GR-820 with a 1024 cuin downward-looking NaI(Tl) detector (4 \* 256 cuin) and a 256 cuin upward-looking detector. The detectors are mounted inside the aircraft.

The spectrometer stabilises on naturally occurring thorium, placing the 2615 keV peak from Th-232 in channel 209.

The sample rate for the NKS exercise was set to 1 Hz.

### **Navigation and Positioning**

The system uses on-line differential GPS with a Trimble Sveesix GPS receiver and a RDS differential receiver. Navigation is done using in-house built software and hardware. Altitude information is provided by a Collins ALT50. The resolution/uncertainty at an altitude of 60 m

amounts to a few meters. Altitude performance over areas covered by forest is degraded due to problems of signal penetration.

## **Spectrometer Calibration**

The spectrometer system is being calibrated on a routinely basis at the SGU calibration site at Dala Airport, Borlänge, Sweden. The site comprises four circular pads with known values of K, U and Th. The diameter of the plates is 10 m. From the measurements over the plates, normal spectra are defined which are used in the processing of the data using a spectral fitting approach.

The damping as a function of flight altitude has been determined from empirical measurements.

As for the cesium calibration, the normal spectra for Cs-134 and Cs-137 have been established within a joint project with the Swedish Defence Research Establishment ( **FOA** ) using data from the Sundbro airfield outside Uppsala and from the Gävle area, Sweden.

## **Data Collection and Processing**

The data collection system is designed and built in-house. All processing is carried out on PC platforms using software developed at SGU. Analysis of activities of naturally occurring nuclides as well as surface contaminations of Cs-134 and Cs-137 is made through spectral fitting.

Moreover, ratios of count rates in predefined energy windows to natural radiation may be output.

The output is in the form of XYZ ASCII files, adapted for further processing and map production.

In the field, maps are produced using Geosoft software, while the final map production is made using either Geosoft (PC) or Arc/Info (UNIX workstation).

## **Data Format**

The raw data is output in the form of Geosoft compatible flight line-oriented ASCII files. Each line consists of 2080 characters plus carriage return and line feed, making a total of 2082 characters per line. Each flight line is begun with a short line of the form

**Line <XXXX>**

after which each measurement follows as one line per measurement. Each measurement line is composed of 260 8-byte units (plus CR/LF) as follows:

- Byte 0001 - 0008: East coordinate
- Byte 0009 - 0016: North coordinate
- Byte 0017 - 0024: Line info (internal use only)
- Byte 0025 - 0032: Ground clearance (dm)
- Byte 0033 - 2080: Channel data (256)
- Byte 2081 - 2082: CR/LF

Coordinates are given in WGS84 in degrees and fraction of degrees.

The channel data are arranged according to the following:

- Channel 001: Internal use
- Channel 002 - 016: Upward looking detector
  - 002: 0300 - 0400 keV
  - 003: 0400 - 0500 keV
  - 004: 0500 - 0600 keV
  - 005: 0600 - 0700 keV

006: 0700 - 0800 keV  
007: 0800 - 0900 keV  
008: 0900 - 1000 keV  
009: 1000 - 1200 keV  
010: 1200 - 1400 keV  
011: 1400 - 1600 keV  
012: 1600 - 1800 keV  
013: 1800 - 2000 keV  
014: 2000 - 2400 keV  
015: 2400 - 3000 keV  
016: 3000 - 3200 keV

- Channel 017 - 255: Downward looking detector 0200 - 3187.5 keV with a channel width of 12.5 keV
- Channel 256: Downward looking detector 3187.5 - 6000 keV

Processed data is delivered in the form given by the NKS instructions.

## **Related Documents**

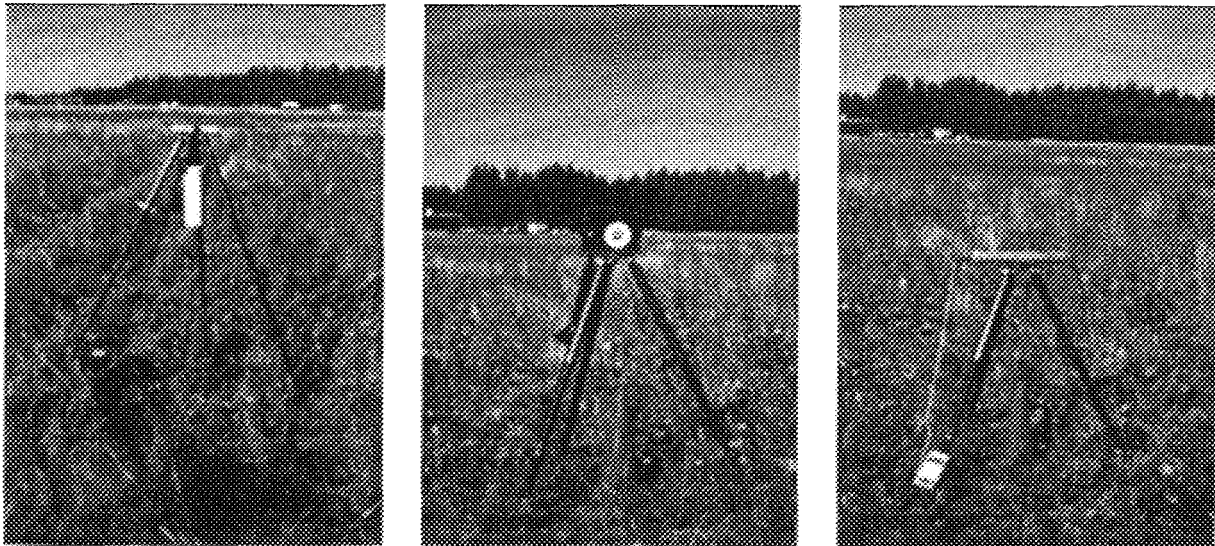
- [Results from SGU](#)
- [Home page](#)

© Geological Survey of Sweden 1995

# RÉSUMÉ 95

## SGU In-Situ Systems

The ground gamma spectrometric measurements were performed using an Exploranium GR-256 spectrometer and a 3' x 3' NaI(Tl) detector.



The measurements were taken at a level of 1 m above the ground. The cesium fallout was used to stabilize the gain of the instrument with the 662 keV barium (cesium) peak at channel 55. The spectra were analysed through spectral fitting of reference spectra for potassium, uranium and progeny, thorium and progeny and cesium. These reference spectra were modeled for the measure level by SSI, taking into account the response of the crystal.

The exposition rate were measured with a radium calibrated Exploranium GR-110 scintillometer at the same level, while the dose rate at most points was measured with a RNI 10/R (GM).

### Related Documents

- [Results from SGU](#)
- [Home page](#)

© Geological Survey of Sweden 1995

# RÉSUMÉ 95

## Area I

The area denoted **Area I** is a part of the Vesivehmaa airfield and was used for intercomparison and other controlled measurements. The contamination level at the airfield was about 50 kBq/m<sup>2</sup> Cs-137 as given by the NKS management.

The following missions were accomplished by SGU over the area:

- Airborne measurements along the calibration line at an altitude of 60 m
- Ground gamma spectrometric measurements at the predefined grid points using an Exploranium GR-256 spectrometer and a 3' x 3' NaI(Tl) detector. The measurements were taken at a level of 1 m above the ground. Furthermore, the exposition rate were measured with an Exploranium GR-110 scintillometer at the same level, while the dose rate was measured with a RNI 10/R (GM).

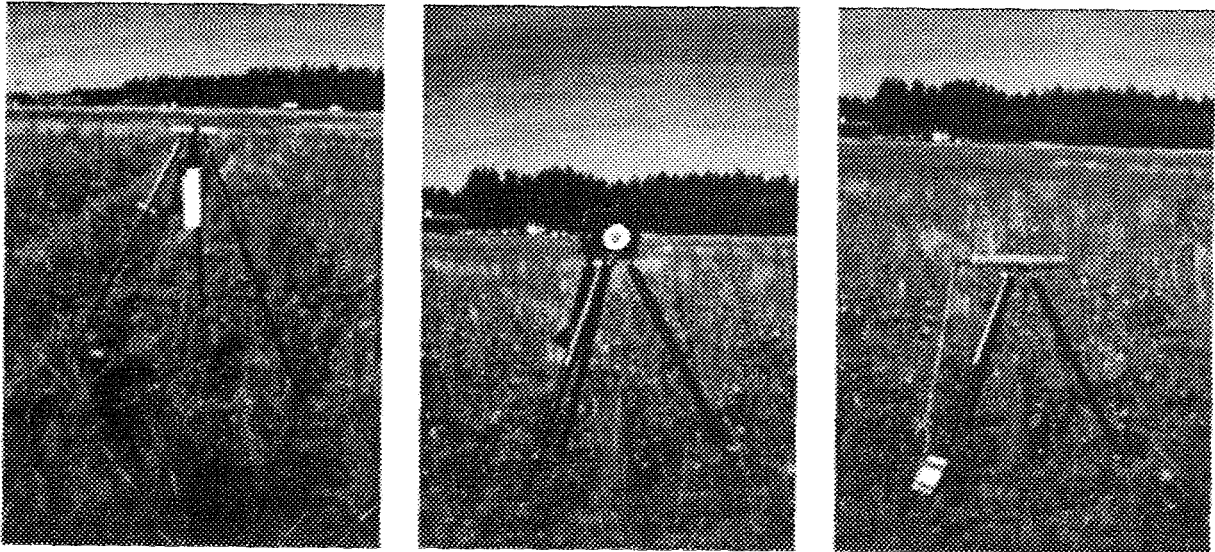
### Airborne Measurements

The airborne measurements were carried out along the predefined calibration line using instrumentation described elsewhere. A total of four overflights were performed at a nominal altitude of 60 m (true altitude 45 - 50 m). An averaging over four measurements for each of the overflights yielded equivalent surface contaminations of **35.5 kBq/m<sup>2</sup> Cs-137** and **0.7 kBq/m<sup>2</sup> Cs-134**. It should however be stressed that the Cs-134 signal did not significantly exceed the noise level.

The spectra are accessed through [Digital data](#).

## In-Situ Measurements

The ground gamma spectrometric measurements were performed using an Exploranium GR-256 spectrometer and a 3' x 3' NaI(Tl) detector.



The measurements were taken at a level of 1 m above the ground. The cesium fallout was used to stabilize the gain of the instrument with the 662 keV barium (cesium) peak at channel 55. The spectra were analysed through spectral fitting of reference spectra for potassium, uranium and progeny, thorium and progeny and cesium. These reference spectra were modeled for the measure level by SSI, taking into account the response of the crystal.

The spectra are accessed through Digital data.

The exposition rate were measured with a radium calibrated Exploranium GR-110 scintillometer at the same level, while the dose rate at most points was measured with a RNI 10/R (GM).

The table below outlines the results of the measurements.

Grid point	K (Bq/kg)	eU (Bq/kg)	eTh (Bq/kg)	Cs-137 (Bq/m <sup>2</sup> )	Exp. Rate ( $\mu$ R/h)	Dose Rate ( $\mu$ Sv/h)
0-0					13.6	
3-1					13.9	
3-2					14.2	
3-3					14.6	0.24
3-4					14.6	
3-5					15.7	0.25
3-6					14.0	
4-1					14.1	0.27
4-2					13.6	0.28
4-3					13.2	0.25
4-4					13.6	0.20
4-5					15.8	0.30
4-6					13.6	0.22

5-1	9.5	0.16
5-2	14.6	0.22
5-3	13.2	0.23
5-4	14.3	0.34
5-5	13.4	0.27
5-6	11.4	0.25

## **Related Documents**

- [Results from SGU](#)
- [Area II](#)
- [Area III](#)
- [Home page](#)

© Geological Survey of Sweden 1995

# RÉSUMÉ 95

## Area II

The area denoted **Area II** is a 3 km by 6 km contaminated by Chernobyl cesium to about the same extent as Area I.

The following mission was accomplished by SGU over the area:

- Airborne measurements at a ground clearance of 60 m and a line spacing of 150 m

### Airborne Measurements

The airborne measurements were carried out with the aim of mapping the spatial distribution of the cesium fallout as well as the activity of the natural nuclides. When processing the data, a pure surface contamination of cesium was assumed.

Nuclide	Dose Rate Volume Source (pGys <sup>-1</sup> /kBqkg <sup>-1</sup> )	Dose Rate Planar Source (pGys <sup>-1</sup> /kBqm <sup>-2</sup> )
K-40	11.8	
U-238 series total	149	
Th-232 series total	158	
Cs-134		1.97
Cs-137		0.698

Furthermore, the natural and manmade dose rates were calculated from the resulting activities using the relations outlined in the table (Finck, 1992).

### Maps

The following maps are generated in A4 format using Arc/Info software:



Potassium



Cesium-134



Uranium



Cesium-137



Thorium



Ratio Cs-137/Cs-134



Natural Dose Rate



Manmade Dose Rate

## Data

The spectra as well as the processed results are accessed through Digital data.

## Related Documents

- Results from SGU
- Airborne system description
- Area I
- Area III
- Home page

© Geological Survey of Sweden 1995

# RÉSUMÉ 95

## Area III

The area denoted **Area III** is a 1 km by 5 km area where radioactive sources were hidden during the exercise. The area is contaminated by Chernobyl cesium to about the same extent as Area I.

The following missions were accomplished by SGU over the area:

- Airborne measurements at a ground clearance of 60 m and a line spacing of 100 m
- Airborne measurements at a ground clearance of 120 m and a line spacing of 200 m

### Sources

The following sources were hidden in the area:

Source Type	Code	Activity (mCi)
Co-60	Co1	7
Co-60	Co2	9
Co-60	Co3	0.7
Co-60	Co4	1.8
Co-60	Co5	1.8
Co-60	Co6	1.00
Co-60	Co7	1.68
Co-60	Co8	1.74
Co-60	Co9	1.44
Cs-137	Cs1	77
Cs-137	Cs2	50
Cs-137	Cs3	7.5
Cs-137	Cs4	14.6
Ir-192	I	15 000
Tc-99	T	30 + 30

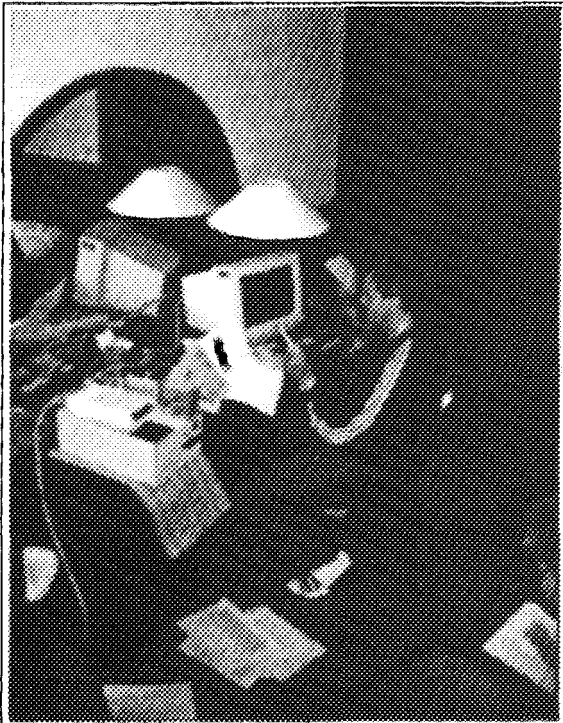
## Airborne Measurements

Since SGU is using NaI detectors there were no attempts made to analyse individual primary photon peaks. Instead, a windowing technique was employed, defining three windows covering a low, intermediate and high energy band, respectively. The energy limits were the following:

Window	Lower Limit (keV)	Upper Limit (keV)
Low	250	500
Intermediate	612	712
High	1100	1400

In each window the natural component was removed prior to analysing.

The area was flown on August 16. Since the SGU system is constructed in such a way that no monitoring of the level of radiation is displayed during the flight, no results were delivered upon landing.



During the following 24 hours the dataset was inspected with the help of software developed in-house. This process enabled visual inspection of the spectra with respect to lateral continuity and appearance of possible anomalies. The application also includes an automatic search for anomalies exceeding predefined threshold levels in the different energy windows. To demonstrate the process, a demo version is included which is accessed through the [Source search demo](#) (requires Windows 3.1 or later)

Preliminary results after 24 h of processing yielded the following result:

Point #	East	North	Possible Source	Relative Strength	Comments
3	2553050	6804940	I-131	5.3 u1	Open => N, elevated
2	2552800	6802380	Cs-137	3.8 u2	
9	2552900	6801190	Cs-137	3.2 u2	
4	2552280	6802680	Cs-137	2.3 u2	
1	2552300	6804240	Co-60	2.7 u3	Open => NE
5	2552900	6804740	Co-60	1.7 u3	Open => W?
6	2552400	6801120	Co-60	1.6 u3	
10	2552800	6801680	Co-60	1.5 u3	Strongly collimated?
7	2552500	6802600	Co-60	1.5 u3	Uncertain
8	2552100	6802520	Co-60	1.5 u3	Uncertain



Sources 1995-08-16

### Preliminary Maps

The following maps are generated in A4 format using Geosoft software based on the results after 24 h of processing without any knowledge of source composition or distribution:



Low Energy (60 m)



Low Energy (120 m)



Intermediate Energy (60 m)



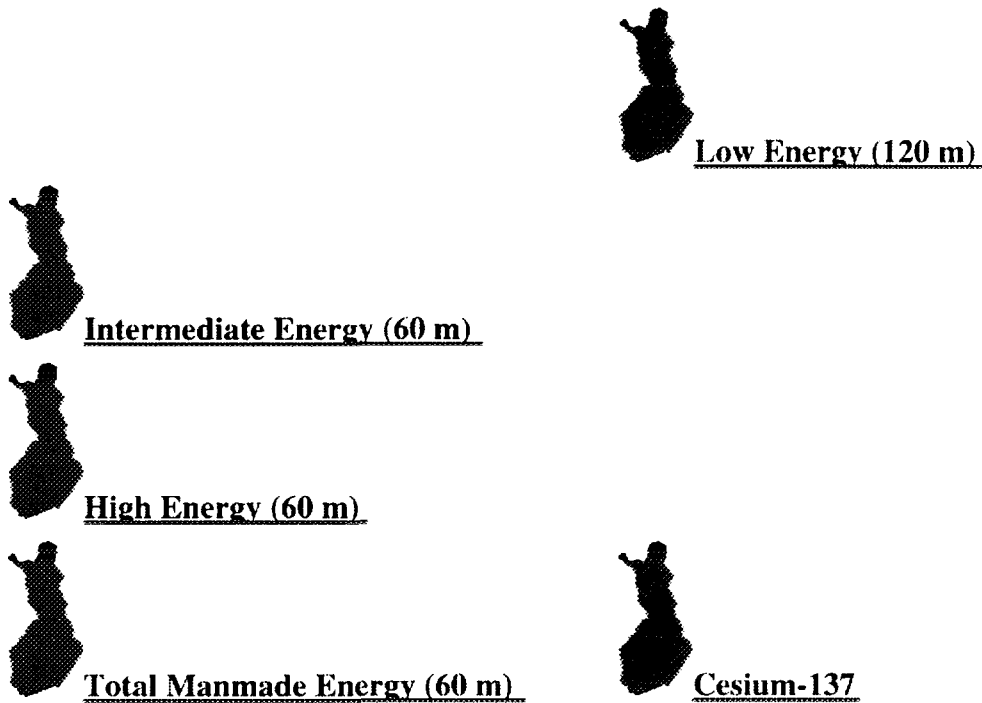
High Energy (60 m)



Total Energy Ratio (60 m)

## Final Maps

The following maps are generated in A4 format using Geosoft software based on the results after the final processing knowing the source composition and distribution. No adjustment of the energy windows has been made as compared to the preliminar maps, however, the color limits have been chosen in order to optimise the appearance of the sources.



## Data

The spectra are accessed through [Digital data](#).

## Related Documents

- [Results from SGU](#)
- [Airborne system description](#)
- [Area I](#)
- [Area II](#)
- [Home page](#)

© Geological Survey of Sweden 1995

**NEXT PAGE(S)  
left BLANK**



# Finnish Centre for Radiation and Nuclear Safety

## Detection of Hidden Sources

### Prompt Reports by Airborne Teams in RESUME95

ABSTRACT ..... 325

1. INTRODUCTION ..... 326

2. REPORTS ON THE AIRFIELD ..... 327

    Tab. 1. Reports on the airfield immediately after landing ..... 327

3. REPORTS 24 HOURS AFTER LANDING ..... 328

    Tab. 2. Summary of the observations given by teams ..... 329

    Tab. 3. The report given by SURRC 24h after the landing ..... 330

    Tab. 4. The report given by DEMA 24h after the landing ..... 331

    Tab. 5. The report given by CEA 24h after the landing ..... 332

    Tab. 6. The report given by SSI 24h after the landing ..... 333

    Tab. 7. The report given by NILU 24h after the landing ..... 334

    Tab. 8. The report given by SGU 24h after the landing ..... 335

    Tab. 9. The report given by the team of Finnish Defense Force 24h after the landing ..... 336

    Tab. 10. The report given by STUK/HUT team 24h after the landing ..... 337

    Tab. 11. The report given by BfS 24h after the landing ..... 338

    Appendix 1. Equipment and source location strategies used by the teams ..... 339

**NEXT PAGE(S)**  
**left BLANK**

# **Detection of Hidden Sources**

## **Prompt Reports by Airborne Teams in Resume95**

**H. Toivonen**

Finnish Centre for Radiation and Nuclear Safety

### **ABSTRACT**

An exercise to locate and identify lost radioactive sources was arranged near Padasjoki Auttoinen village. Ten sources, consisting of caesium, cobalt, iridium and technetium, were hidden. The teams (10) were asked to report their findings immediately after the landing and 24 h later. The teams that had a large NaI detector at their disposal could locate more sources than the teams with HPGe detectors. However, for source identification and activity calculation an HPGe detector is superior. Thus, it is highly recommended for operational purposes that both measuring systems are used simultaneously. The best location results were provided by the Danish Emergency Management Agency; the team reported four sources at landing and two other sources were found in prompt data processing after the landing.

FINNISH CENTRE FOR RADIATION  
AND NUCLEAR SAFETY  
P.O.BOX 14 FIN-00881 HELSINKI  
Finland  
Tel. +358 0 759881

# 1 INTRODUCTION

A special exercise was organized to test the ability of the teams to find lost or stolen radioactive material. On 15th and 16th of August 1995 altogether ten sources were hidden in the forest near the village of Auttoinen. Eight sources were located in 1 x 5 km exercise area, known as area III. Two of the sources were placed just outside the area.

One hour was given to the airborne teams to locate and identify the hidden sources. Other restrictions were: (1) flying altitude should not be less than 60 m (200 feet) above any obstacle (safety reasons), (2) hovering above any point on the area was forbidden and the pilots were asked to ignore suspicious visual observations (“bushmen”), (3) the helicopter or aeroplane was not allowed to enter the area east of a NMT tower. The reason for the last restriction was not given to the teams, but it is obvious when the locations and characteristics of the sources are known. Otherwise the teams were allowed to choose freely their flying pattern and line spacing.

The teams were asked to give two reports: the first just after the landing on the airfield and the second 24 h after the landing. Summary of these reports is given in this paper. Altogether ten teams took part in this exercise (Appendix 1):

- 1 SURRC Scottish Universities Reactor and Research Centre, Scotland
- 2 DEMA Danish Emergency Management Agency, Denmark
- 3 CEA Commissariat à l’Energie Atomique/Valduc, France
- 4 SSI Statens Strålskydds Institut, Sweden
- 5 NILU Norwegian Institute for Air Research, Norway
- 6 SGU Geological Survey of Sweden, Sweden
- 7 NGU Geological Survey of Norway, Norway
- 8 PV Finnish Defense Forces, Finland
- 9 STUK/  
HUT Finnish Centre for Radiation and Nuclear Safety and  
Helsinki University of Technology, Finland
- 10 BfS Bundesamt für Strahlenschutz, Germany

## 2 REPORTS ON THE AIRFIELD

The purpose of the prompt reporting was to test the existing resources for real-time data processing. This feature is very important in locating stolen sources that may be transported continuously.

**Table I.** *Reports on the airfield immediately after landing.*

<b>Team</b>	<b>Sources found</b>	<b>Spurious sources</b>
<b>SURRC</b>	3	0
<b>DEMA</b>	4 (5?)	0
<b>CEA</b>	2(3 <sup>a</sup> )	(1 <sup>a</sup> )
<b>SSI</b>	4	5
<b>NILU</b>	No report	
<b>SGU</b>	No report	
<b>PV</b>	1	0
<b>NGU</b>	3	2
<b>STUK/HUT</b>	2	2
<b>BfS</b>	1	1

<sup>a)</sup> new report 1 h after the landing

### 3 REPORTS 24 HOURS AFTER LANDING

Nine teams gave a report at 24 h. Table II shows the summary of the observations made by all teams source by source. Tables III - XI contain data team by team. In principle these tables contain only data and comments given by the team. However, in a few cases there were some ambiguous details and some conclusions had to be drawn to understand the relation between the report and actual situation.

Three sources (Co3, Cs3 and Tc) were not reported by any of the teams. Thus, they are dropped from tables III-XI.

**Table II.** Summary of the observations given by the teams. The iridium source was not identified by any team. The following suggestions were given:  $^{60}\text{Co}$  (2 suggestions),  $^{137}\text{Cs}$  (1),  $^{131}\text{I}$  (1),  $^{241}\text{Am}$  (2), low-energy emitter (2).

Source code	Nuclide	Activity (MBq)	Located <sup>b</sup>	Identified	Activity estimate <sup>c</sup> (MBq)
Co1	$^{60}\text{Co}$	260	5 (8)	8	267±53 (n=4)
Co2	$^{60}\text{Co}$	330	3 (4)	3	175±106 (n=2)
Co3	$^{60}\text{Co}$	26	0	0	-
Co4 <sup>a</sup>	$^{60}\text{Co}$	total: 350	4	4	95±7 (n=2)
Cs1	$^{137}\text{Cs}$	2,800	6	6	1,270±1,010(n=3)
Cs2	$^{137}\text{Cs}$	1,500	1	1	25 (n=1)
Cs3	$^{137}\text{Cs}$	280	0	0	-
Cs4	$^{137}\text{Cs}$	540	2	2	700 (n=1)
Ir	$^{192}\text{Ir}$	560,000	8	0	-
Tc	$^{99\text{m}}\text{Tc}$	1,100 + 1,100	0	0	-

a) Line source consisting of six 'point' sources

b) Number in the parenthesis refers to inaccurate (>100 m) locations

c) Mean, SD and number of teams

**Table III.** *The report given by SURRC 24 h after the landing.*

Source	Located	Identified	Activity estimate	Comment <sup>a</sup>
Co1	Yes <sup>b</sup>	Yes	-	
Co2	60 m to W	Yes	-	
Co4	-	-	-	
Cs1	Yes <sup>c</sup>	Yes	-	
Cs2	-	-	-	
Cs4	-	-	-	
Ir	300 m to N	as low-energy source	-	Detected from the road between area 2 and area 3
Extra sources	1 extra <sup>60</sup> Co source suspected close to the source Co1. 2 extra sources with low energy components, possibly <sup>241</sup> Am sources.			

<sup>a</sup> The report is a long essay.

<sup>b</sup> Three possible locations were reported for Co1: 40 m north, 120 m east and 160 southeast from the source. One extra cobolt source was suspected.

<sup>c</sup> Three possible locations were reported for Cs1: 80 m north 80 m west and 130 m southeast from the source.

**Table IV.** The report given by DEMA 24 h after the landing.

Source	Located	Identified	Activity estimate	Comment
Co1	100 m to E	Yes	200 MBq	may be shielded towards north
Co2	10 m to S	Yes	100 MBq	
Co4	100 m S from the centre point	Yes	100 MBq	
Cs1	50 m to S	Yes	100 MBq	
Cs2	30 m to SW	Yes	25 MBq ???	collimated
Cs4	-	-	-	
Ir	200 m to NW	low energy	-	could be Co1
Extra sources	None			

The iridium source was detected also in carborne measurements and was identified as a shielded  $^{137}\text{Cs}$  source locating 350 m from road 1 towards SW.

**Table V.** The report given by CEA 24 h after the landing.

Source	Located	Identified	Activity estimate	Comment
Co1	10 m to SE	Yes	320 MBq	
Co2	-	-	-	
Co3	-	-	-	
Co4	80 m SW from the centre point	Yes	90 MBq	
Cs1	80 m SW	Yes	1,850 MBq	
Cs2	-	-	-	
Cs3	-	-	-	
Cs4	-	-	-	
Ir	150 m to W	<sup>241</sup> Am	4,500 MBq	
Extra sources	<sup>241</sup> Am source <sup>a</sup> (activity estimate below 1500 MBq) reported also near road 1.			

<sup>a</sup> Refers to Ir source 400 m southwest.

**Table VI.** *The report given by SSI 24 h after the landing.*

Source	Located	identified	Act.estim.	Comment
Co1	25 m to E	Yes	1.7 times background	
Co2	-	-	-	
Co4	40 m to W from the centre point	Yes	1.9 times background	
Cs1	70 m to NE	Yes	1.9 times background	
Cs2	-	-	-	
Cs4	-	-	-	
Ir	130 m to NE	low-energy emitter	5.8 times background	
Extra sources	1 extra $^{134}\text{Cs}$ and 3 extra $^{60}\text{Co}$ sources reported (2 of them were "suspected" observations. One of the suspected sources was 200 m south from source Co4)			

**Table VII.** *The report given by NILU 24 h after the landing.*

Source	Located	Identified	Act.estim.	Comment
Co1	460 m to NNW	Yes	-	
Co2	-	-	-	
Co4	-	-	-	
Cs1	-	-	-	
Cs2	-	-	-	
Cs4	-	-	-	
Ir	70 m to W	as <sup>241</sup> Am	-	
Extra sources	1 extra <sup>137</sup> Cs and 1 extra <sup>60</sup> Co sources reported			

**Table VIII.** *The report given by SGU 24 h after the landing.*

Source	Located	Identified	Activity estimate <sup>a</sup>	Comment
Co1	60 m to SE	Yes	1.7 u3	Collimated open towards W
Co2	40 m to SE	Yes	1.5 u3	Uncertain
Co4	50 m to S from the centre point	Yes	2.7 u3	Collimated, open towards NE
Cs1	30 m to SE	Yes	3.8 u2	
Cs2	-	-	-	
Cs4	30 m to SW	Yes	2.3 u2	
Ir	80 m to NW	as <sup>131</sup> I	5.3 u1	Collimated, open towards north, elevated
Extra sources	1 extra <sup>137</sup> Cs and 3 extra <sup>60</sup> Co sources reported			

<sup>a</sup> Relative units u1, u2 and u3.

**Table IX.** *The report given by the team of Finnish Defense Forces 24 h after the landing.*

Source	Located	Identified	Act. estimate	Comments
Co1	-	-	-	
Co2	-	-	-	
Co4	-		-	
Cs1	-	-	-	
Cs2	-	-	-	
Cs4	-	-	-	
Ir	300 m to SSW	as <sup>137</sup> Cs		
Extra sources	No			

**Table X.** The report given by STUK/HUT team 24 h after the landing.

Source	Located	Identified	Activity estimate	Comment
Co1	300 m to N <sup>a</sup>	Yes	300 MBq	
Co2	-			
Co4	-			
Cs1	110 m to NW	Yes	1,850 MBq	
Cs2	-			
Cs4	25 m to W	Yes	740 MBq	
Ir	300 m to NW	low energy source > 400 keV	-	Covered
Extra sources	No			

The Ir source was also seen from the road between the areas 2 and 3 and reported as "low energy source below 400 keV".

- <sup>a</sup> The Co1 source was accidentally located too north. In the later analysis the position was correct.

**Table XI.** *The report given by BfS 24 h after the landing.*

Source	Located	Identified	Act. estimate	Comment
Co1	Yes <sup>a</sup>	Yes	100 - 400 MBq	
Co2	Yes <sup>a</sup>	Yes	100 - 400 MBq	
Co3	-	-	-	
Co4	See the text below <sup>a</sup>		-	
Cs1	-	-	-	
Cs2	-	-	-	
Cs4	-	-	-	
Ir	-	-	-	
Extra sources	No			

<sup>a</sup> The location is uncertain due to the problems in GPS operation. Whether these sources were really detected cannot be said for sure. The co-ordinates given by the team are ambiguous, and the observations cannot be positioned on the map. Two other suspected <sup>60</sup>Co sources were also found and Co4 seems to be among them. For some reason only <sup>60</sup>Co window results were reported.

Appendix 1. Equipment and source location strategies used by the teams.

Team	Detectors		Sampling times s	Line spacing m	Altitude (registered) m	Navigation	Coordinate recording
	NaI, litres	HPGe, %					
SURRC	16	50 <sup>x)</sup>	2+3/6		60	GPS	GPS
DEMA	16		1	150, 50	50 (yes)	DGPS+flight-indicator	DGPS
CEA	16		2	80	40 (yes)	Beacon+flight-indicator	Beacon in Finnish Coordinates
SSI	4.2		2/5	150, 100	60 (no)	Visual	DGPS
NILU	16.7		0.3	ca.150	50-200	GPS	GPS
SGU	16.7		1	150, 100	120, 60	DGPS	DGPS
NGU	16.7		1	100	60 (yes)	GPS-visual	DGPS
PV		70	13	100	60 (yes)	DGPS	DGPS
STUK	1.6	18	2/4	100	60 (no)	Visual	DGPS
BfS	12	50	2/30	150, 100	60, 70	Visual	GPS
GSF	25+8		1s	100	40 (yes)	DGPS	DGPS

<sup>x)</sup> Cmx



# Swedish In-Situ Teams

## Comparison of Results at Area I and Area II between different Swedish In-Situ Teams

OBJECTIVES .....	344
LIST OF PARTICIPANTS.....	344
MATERIAL & METHODS .....	345
Detector systems and data acquisition .....	345
Tab. 1. Overall view of different methods for estimating the Cesium depth profile in soil.....	345
Tab. 2. Overview of the measured gridpoints for each participating team in Area I .....	347
Tab. 3. Description of the three most common sampling points in Area II used by the Swedish In-Situ groups.....	347
RESULTS.....	348
<sup>137</sup> Cs at Area I .....	348
Fig. 1. Average <sup>137</sup> Cs equivalent surface deposition per hexagonal shell .....	349
Tab. 4. Equivalent surface deposition of Area I as reported by the different Swedish In-Situ teams .....	349
Fig. 2. Average <sup>137</sup> Cs content in soil per hexagonal shell .....	350
Tab. 5. Cesium content in soil at Area I as reported by the different Swedish In-Situ tema .....	350
Fig. 3. Average equivalent surface deposition of <sup>134</sup> Cs per hexagonal shell .....	351
<sup>134</sup> Cs at Area I .....	351
Tab. 6. Equivalent surface deposition of <sup>134</sup> Cs at Area I as reported by different Swedish In-Situ teams .....	352
Fig. 4. Average <sup>134</sup> Cs content in soil per hexagonal shell .....	352
Tab. 7. <sup>134</sup> Cs content in soil at Area I reported by the different Swedish In-Situ teams.....	353
<sup>40</sup> K and Natural Series at Area I .....	353
Fig. 5. Average activity of Potassium-40 in soil per hexagonal shell .....	353
Fig. 6.a. Average equilibrium activity of Thorium-series in soil per hexagonal shell .....	354
Fig. 6.b. Average equilibrium activity of Uranium-series per hexagonal shell .....	354
Tab. 8. Naturally occurring radionuclides in soil at Area I as reported by different Swedish In-Situ teams .....	355
<sup>137</sup> Cs at Ara II .....	355
Tab. 9. <sup>137</sup> Cs Equivalent surface deposition and content in soil at Area II as reported by the different Swedish In-Situ teams .....	356
Fig. 7.a. Average equivalent surface deposition of <sup>137</sup> Cs at three measuring points .....	356
Fig 7.b. Average <sup>137</sup> Cs content in soil at three measuring points at Area II .....	357
<sup>134</sup> Cs at Area II .....	357
Fig. 8.a. Average equivalent surface deposition of <sup>134</sup> Cs content in soil at three measuring points at Area II.....	357
Fig. 8.b. Average <sup>134</sup> Cs content in soil per at three measuring points at Area II .....	358
<sup>40</sup> K and Natural series at Area II .....	358
Fig. 9.a. Activity values for the Uranium-series .....	359
Fig. 9.b. Activity values for <sup>40</sup> K at Area II .....	359
Fig. 9.c. Activity values for the Thorium-series.....	360

Tab. 10. Overview of the results from the In-Situ gamma measurements from Area II for naturally occurring radionuclides .....	360
Results - An overview .....	361
Tab. 11. Average $^{137}\text{Cs}$ content in soil in $\text{kBq/m}^2$ as reported by the different In-Situ teams in Area I .....	361
Tab. 12. Spread of activity data in % of the average value of reported activity content in Area I for all reporting In-Situ teams .....	361
Tab. 13 . Deviation in % of the values reported by STUK/SURRC at Area I .....	362
Tab. 14. Deviation in % of the values reported by STUK/SURRC at Area II .....	362
CONCLUSIONS .....	362
General conclusions .....	362
$A_{\text{esd}}$ -values .....	363
$A_{\text{exp}}$ -values .....	363
Natural radionuclides .....	363
$A_{\text{soil}}$ content of naturally occurring radionuclides compared to STUK/SURRC values .....	364
Conclusions - soil sampling .....	364
DISCUSSION .....	365
Possible sources of incoherence .....	365
Possible future measures for coherence improvement .....	366
Fig. 10. ....	366

**COMPARISON OF RESULTS AT AREA I  
AND AREA II BETWEEN DIFFERENT  
SWEDISH *IN-SITU* TEAMS IN THE RESUME-  
95 EXERCISE**

Report commissioned by the Swedish Radiation Protection  
Institute  
November 1996

**Christopher L. Rääf  
Department of Radiation Physics  
Lund University  
Malmö University Hospital**

## COMPARISON OF RESULTS AT AREA I AND AREA II BETWEEN DIFFERENT SWEDISH *IN-SITU* TEAMS

### **Objectives**

In the beginning of 1996 the Department of Radiation Physics in Malmö was commissioned by the Swedish Radiation Protection Institute to perform a compilation of the results obtained by the Swedish *in-situ* teams that participated in the RESUME-95 exercise. The aim of this survey is to study the coherence in the reported activity data between the groups. It is not the purpose to see this comparison as a performance ranking of individual laboratories. Any such comparison must be made with precaution since the teams generally have collected their data with different equipment and by different methods. In this work, all *in-situ* teams have been given code-names, where each team has been labelled a number from 1 to 5. For more details, the interested reader is referred to the internal reports made by each team that (supposedly) also are to be included in the major compilation of the *in-situ* gamma spectrometry in the RESUME-95 exercise by J. Hovgaard, Danish Emergency Management Agency.

### **List of participants**

List of Swedish *in-situ* groups that participated in the RESUME-95 exercise in alphabetic order (that does not correspond to their respective code-name indices)

- Department of Radiation Physics, Gothenburg University, Sahlgren Hospital<sup>1</sup>
- Department of Radiation Physics, Malmö University Hospital, Lund University<sup>2</sup>
- National Defence Research Establishment, Stockholm, Division of Nuclear Physics<sup>3</sup>
- National Defence Research Establishment, Umeå, Division for Radiac<sup>4</sup>
- Swedish Radiation Protection Institute, S-17176 Stockholm)

A total of 4 of the 5 laboratories above have compiled internal reports on their results

---

<sup>1</sup> Mats Isaksson & Raine Vesänen; Field gamma measurements at the NKS Exercise Résumé-95.

<sup>2</sup> Christopher L. Rääf; RESULTS FROM THE RESUME-95 EXERCISE, IN-SITU GAMMA SPECTROMETRY PERFORMED AT VESIVEHMAA AIRPORT, FINLAND, October 1996

<sup>3</sup> Lars-Erik De Geer, Ingemar Vintersved and Rune Arntsing; TOTAL DEPOSITION OF CESIUM-137 MEASURED IN FINLAND DURING THE EXERCISE "RÉSUMÉ 95" IN AUGUST 1995

<sup>4</sup> Kenneth Lidström, Thomas Ulvsand and Göran Ågren; Results from RÉSUMÉ 95 Measurements with mobile equipment, February, 1996

from RESUME-95 exercise.

### Material & Methods

All five of the above Swedish *in-situ* groups participated in the exercise at Area I. Most of them report activity values for only three of the total five hexagonal shells, here denoted as shell 1, 2, 3, 4, and 5. The hexagonal pattern of measuring points is described in the SURRC's report<sup>5</sup>. In Area II, only four of the teams made any measurements and the amount of reported data varies from team to team.

#### Detector systems and data acquisition

**Team #2** has used two separate high purity germanium detector systems at Area I, and in this work these separate data series have been pooled and averaged together. All stated values from **Team #2** at Area I thus refer to the average value of these two series<sup>6</sup>.

All other teams used a single HPGe detector system, with total efficiencies typically between 10 - 50 %.

TABLE 1  
Overall View of Different Methods for Estimating the Cesium Depth Profile in Soil.  
Listed Below Are All Five Swedish *In-situ* Groups.

<i>In situ</i> group	Detector system	Method for estimating the radiocesium activity content in Area I and Area II
Team #2	2 HPGe detectors Each 35 %	<ul style="list-style-type: none"> <li>Two separate data series available on <math>A_{soil}</math>. One is based purely on activity determination from their soil core samples. The other is based on a Monte-Carlo simulated field efficiency (MNCP code) that has the average profile of the soil core, ambient dose equivalent, dose rate in air, and detector response (among other parameters) as input data to recalculate the fluence to a soil content in <math>Bq/m^2</math>. In this work only the series based on the MNCP code algorithms is used when comparing with <math>A_{soil}</math> data obtained by other <i>in-situ</i> teams. The first series from the soil sample data is instead compared directly to STUK / SURRC data.</li> </ul>

<sup>5</sup> D.C.W. Sanderson (SURRC), J.D. ALLYSON (SURRC), H. TOIVONEN (STUK), T. HONKAMAA (STUK); GAMMA RAY SPECTROMETRY RESULTS FROM CORE SAMPLES COLLECTED FOR RESUME 95, Scottish Universities Research & Reactor Centre, September 1995.

<sup>6</sup> These two data series obtained from the two separate detector systems matched each other within say 5 %. The average value of the two series then seemed a representative for the activity values reported by Team #2.

<i>In situ group</i>	<i>Detector system</i>	<i>Method for estimating the radiocesium activity content in Area I and Area II</i>
		<ul style="list-style-type: none"> <li>No data on soil content of natural radionuclides or on <math>^{134}\text{Cs}</math> were reported.</li> </ul>
Team #3	HPGe 50 %	<ul style="list-style-type: none"> <li>One slice model with layer thickness of 1 cm for obtaining <math>A_{\text{esd}}</math>. Activity data from real soil site specific samples are used as input data to account for soil density and composition.</li> <li>Two slice model for obtaining <math>A_{\text{soil}}</math>, with the two layers of soil (infinite parallel slabs) containing 90/10 % fraction of the total cesium content. Soil samples have been taken to determine the depth of the interface of these two slices.</li> <li>Single slice model is used, for obtaining the <math>A_{\text{soil}}</math> values for naturally occurring radionuclides, assuming 1 m thick soil layer.</li> </ul>
Team #4	HPGe 10 %	<ul style="list-style-type: none"> <li>Soil samples taken with a 20 cm deep soil core sampler. Only the total content in soil has been reported.</li> <li>The <math>A_{\text{soil}}</math> data obtained here are derived from assuming an exponential depth profile with <math>\alpha/\rho = 0.0625 \text{ m}^2/\text{kg}</math> following an algorithm given in [1].</li> </ul>
Team #5	HPGe	<ul style="list-style-type: none"> <li>No soil sampling data available</li> <li>Two different profiles were assumed. The first profile, which Team #5 only applied at Area II, was the one reported by STUK/SURRC and the second one is an exponential depth profile with <math>\alpha/\rho=0.0625 \text{ m}^2/\text{kg}</math>. The latter data series was used in this work for obtaining the average values for all teams.</li> </ul>
Team #1	HPGe 35 %	<ul style="list-style-type: none"> <li>No soil sampling data available</li> <li>Three different exponential depth profiles were assumed. One of them, with <math>\alpha/\rho = 0.0625 \text{ m}^2/\text{kg}</math> in Beck soil, has been used to obtain the values reported in this work</li> </ul>

Also, not all groups have measured at all the same points in the hexagonal grids at

Area I. This means that the overall mean values for the whole airfield are not completely comparable with each other.

TABLE 2  
Overview of the measured gridpoints for each participating team in Area I

Hexagonal shell	Team #4	Team #1	Team #2	Team #3	Team #5
0	x	x	x	x	x
1.1 - 1.6					
2.1 - 2.6	x	x		x	
3.1 - 3.6	x		x	x	x
4.1 - 4.6	x	x <sup>7</sup>	x	x	x
5.1 - 5.6		x <sup>8</sup>	x		x <sup>9</sup>

Four of the total five Swedish *in-situ* groups participating in the exercise performed measurements also in Area II. Most of them report activity values from only three selected measuring points within the area, here denoted as point A, B and C. In Table 3 these points are described according to the notation used in the SURRC's report.

Reported values for the cesium content in soil is expected to be less coherent between the teams since the depth profiles of each measuring point differed significantly more than in Area I. **Team #4** applied a standard depth distribution ( $\alpha/\rho = 0.0625 \text{ m}^2/\text{kg}$ ) and **Team #5** used both an assumed distribution (same as **Team #4** and as in Area I) and the distributions reported by STUK and SURRC. **Team #3** took their own soil samples at points A, B and C, and based their values of the cesium content in soil at these points on their own two slice model.

TABLE 3  
Description of the three most common sampling points in Area II used by the Swedish *in-situ* groups.

Notation used here	SURRC's report	Nearest named location
A	1	Auttoinen (Football field)
B	4	Peltomtausta
C	6	Near Laihansuo (midway between stream and parking field.)

7 All points except 4.3.

8 All points except 5.2.

9 All points except 5.5

## $A_{\text{esd},137\text{Cs}}$

Four of the Swedish in-situ teams have reported equivalent surface deposition,  $A_{\text{esd}}$ , which is a quantity that is comparable between all groups regardless of the depth profile they used. **Team #3** is a special case, since the laboratory has used a thin slice model, (layer depth 1 cm), to describe the fresh fallout of radiocesium. In this work we have chosen to pool this series together with the other reported  $A_{\text{esd}}$  values since they all in some way aim to describe the deposition in case of a fresh fallout.

## $A_{\text{soil},137\text{Cs}}$

The approach to evaluate the activity concentration of radiocesium in the soil differs somewhat between the different Swedish *in-situ* teams. The difference stems mainly from the way of estimating the depth distribution of cesium in the soil. Some groups have had soil samples taken at the vicinity of each measuring point (**Team #4**, **Team #3** and **Team #2**), but not all of them have had time to evaluate all the data (**Team #2**, **Team #4**). Other groups have not taken any soil samples at all, but have instead calculated the cesium content in soil assuming different profiles, of which three groups (**Team #4**, **Team #1** and **Team #5**) have chosen an exponential profile with  $\alpha/\rho = 0,0625 \text{ m}^2/\text{kg}$  in Beck soil ( $\rho_{\text{dry}}=1600 \text{ kg/m}^3$ ).

## Results

### 137Cs at Area I

Fig. 1 displays the equivalent surface deposition,  $A_{\text{esd}}$ , as measured by the different Swedish *in-situ* groups. Reported values refer to average values obtained for all measured gridpoints in a certain shell number.

The discrepancies that exist between the individual groups are all due to calibration characteristics of the detector in use [1]. The quantity is essentially given by Eq. 1, where  $\epsilon_f$  refers to the field efficiency for a plane surface distribution of 137Cs.

In Fig. 2 are plotted the STUK/SURRC data versus the different Swedish *in-situ* groups for the 137Cs content in soil in [ $\text{Bq/m}^2$ ]. The values have been obtained somewhat differently depending on which depth profile that has been used. Not all groups have had a soil sample device available (**Team #1**), or have had time to fully assess the soil data (**Team #4**) and instead also has assumed a suitable depth profile. Another group has used a different distribution model than the commonly employed exponential one, - a so called two slice model (**Team #3**) (See Method section!).

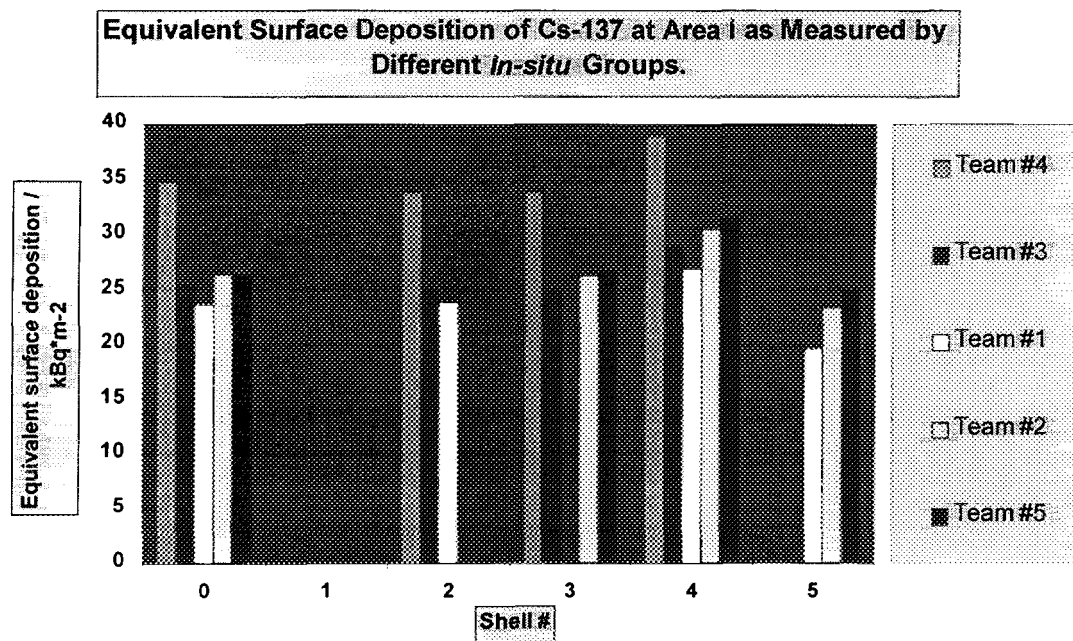


**Fig. 1.** Average <sup>137</sup>Cs equivalent surface deposition per hexagonal shell.

TABLE 4

Equivalent Surface Deposition at Area I as reported by the different Swedish *in-situ* teams.

Shell	Team #4	Team #3	Team #1	Team #2	Team #5
<b>137Cs: A<sub>esd</sub> / Bq/m<sup>2</sup></b>					
	MN ± 1 σ	MN ± 1 σ	MN ± 1 σ	MN ± 1 σ	MN ± 1 σ
0	34.8	25.5	23.7	26.35	26.4
2.1-2.6	33.9 ± 0.82	25.1 ± 1.2	23.9 ± 0.6	n.c.	n.c.
3.1-3.6	33.9 ± 2.54	24.9 ± 2.1	n.c.	26.3 ± 2.1	26.7 ± 1.88
4.1-4.6	39 ± 1.73	28.9 ± 0.89	26.94 ± 0.83	30.56 ± 0.92	31.55 ± 1.38
5.1-5.6	n.c.	n.c.	19.6 ± 5.2	23.41 ± 6.37	24.9 ± 1.68
<b>Total</b>	<b>35.6</b>	<b>26.3 ± 2.3</b>	<b>23.5 ± 4.0</b>	<b>26.7 ± 4.6</b>	<b>23.2 ± 2.9</b>

Average Cesium-137 Content in Soil in kBq per m<sup>-2</sup> at Area I for a Given Shell Number as Measured by Different *In-situ* Groups.

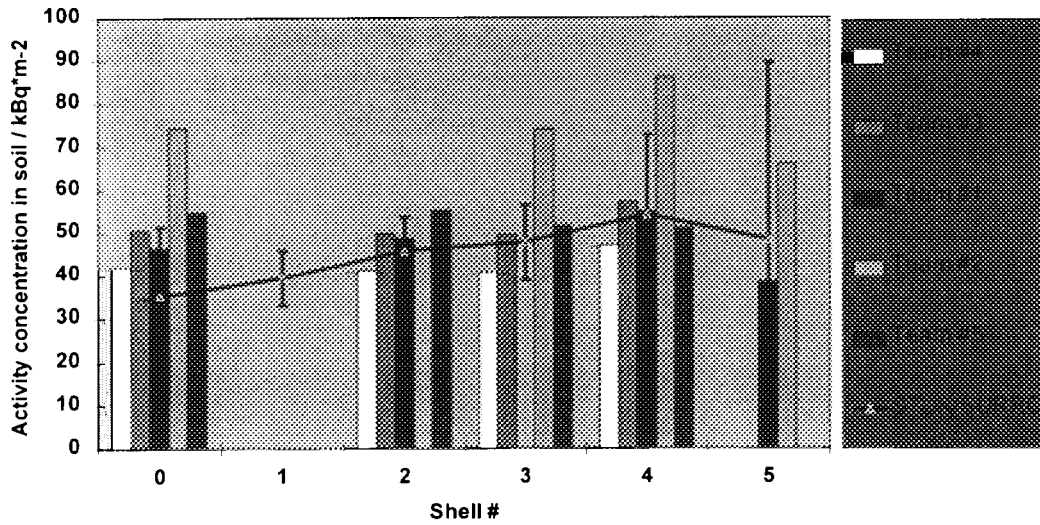


Fig. 2. Average 137Cs content in soil per hexagonal shell.

Uncertainty limit for the STUK/SURRC data refers to  $\sigma_{n-1}$  of the total mean value for all the six measuring point per shell (except shell # 0).

TABLE 5

Cesium content in soil at Area I as reported by the different Swedish *in-situ* teams.

Shell	Team #4	Team #3	Team #1	Team #2	Team #5
	<b>137Cs in soil / Bq/ m<sup>2</sup></b>				
	MN ± 1 σ	MN ± 1 σ	MN ± 1 σ	MN ± 1 σ	MN ± 1 σ
0	42	50.6	46.3 ± 0.29	74.4	54.7
2.1-2.6	41 ± 0.97	49.8 ± 2.4	48.7 ± 1.23	n.c.	n.c.
3.1-3.6	40.9 ± 3.03	49.4 ± 4.2	n.c.	74.1 ± 5.4	55.3 ± 3.8
4.1-4.6	47.1 ± 2.13	57.3 ± 1.9	54.9 ± 1.68	86.2 ± 2.3	65.3 ± 2.9
5.1-5.6	n.c.	n.c.	38.6 ± 9.85	66.0 ± 16.4	51.1 ± 16.4
<b>Total</b>	<b>43.3 ± 3.71</b>	<b>52.1 ± 4.5</b>	<b>47.4 ± 8.4</b>	<b>75.3 ± 13.0</b>	<b>57.4 ± 10.3</b>

Average value of the equivalent surface deposition of Cs-134 at Area I for a given shell number as measured by different *in-situ* groups.

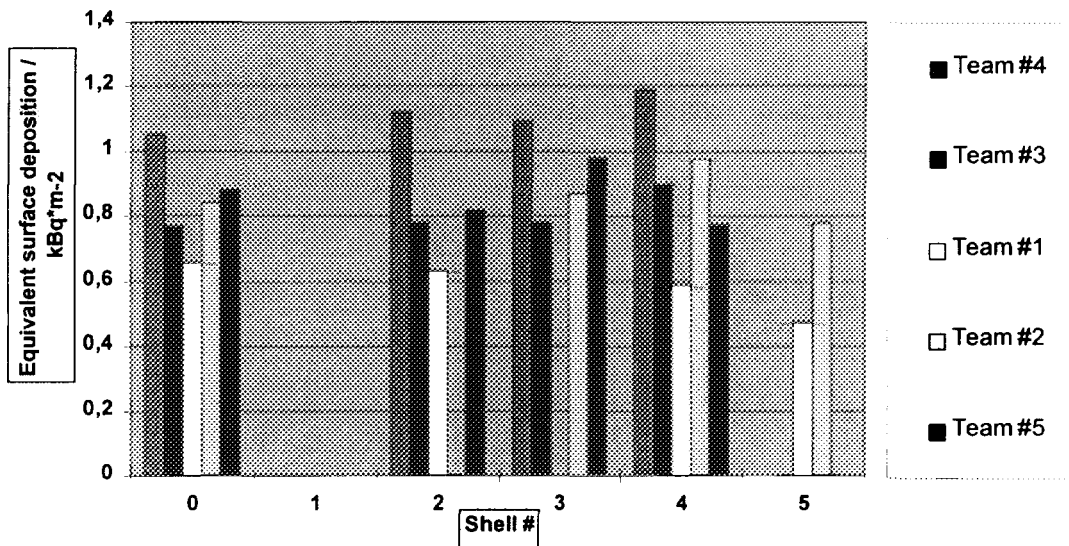


Fig. 3. Average equivalent surface deposition of <sup>134</sup>Cs per hexagonal shell.

### 134Cs at Area I

Fig. 3 displays the Equivalent surface deposition as measured by the different Swedish *in-situ* groups. The discrepancies that exist between the individual groups are all due to calibration characteristics of the detector in use [1].

In Fig. 4 are plotted the STUK/SURRC data versus the results obtained from the different Swedish *in-situ* groups for Cesium-134 content in soil. The values have been obtained somewhat differently depending on which depth profile that has been chosen. Not all groups have had a soil sample device available (**Team #1**) or have had the time to fully assess the soil data (**Team #4**) and have instead assumed a suitable depth profile. Another group has used a different distribution model than the commonly employed exponential one, - a so-called two slice model (**Team #3**).

TABLE 6  
Equivalent Surface Deposition of Cesium-134 at Area I as reported by the different Swedish in-situ teams.

Shell	Team #4	Team #3	Team #1	Team #2	Team #5
	<b><math>^{134}\text{Cs}:A_{\text{esd}} / \text{Bq}/\text{m}^2</math></b>				
	$\text{MN} \pm 1 \sigma$	$\text{MN} \pm 1 \sigma$	$\text{MN} \pm 1 \sigma$		$\text{MN} \pm 1 \sigma$
0	1.05	0.77	0.659	0.842	0.88
2.1-2.6	$1.12 \pm 0.06$	$0.78 \pm 0.08$	$0.633 \pm 0.076$	n.c.	n.c.
3.1-3.6	$1.095 \pm 0.08$	$0.78 \pm 0.08$	n.c.	$0.869 \pm 0.0728$	$0.82 \pm 0.068$
4.1-4.6	$1.19 \pm 0.05$	$0.9 \pm 0.03$	$0.589 \pm 0.083$	$0.975 \pm 0.033$	$0.977 \pm 0.064$
5.1-5.6	n.c.	n.c.	$0.474 \pm 0.11$	$0.779 \pm 0.212$	$0.774 \pm 0.22$
<b>Total</b>	<b><math>1.13 \pm 0.08</math></b>	<b><math>0.82 \pm 0.09</math></b>	<b><math>0.58 \pm 0.11</math></b>	<b><math>0.88 \pm 0.14</math></b>	<b><math>0.86 \pm 0.15</math></b>

Average value of the activity concentration of Cs-134 in soil at Area I for a given shell number as measured by different *in-situ* groups.

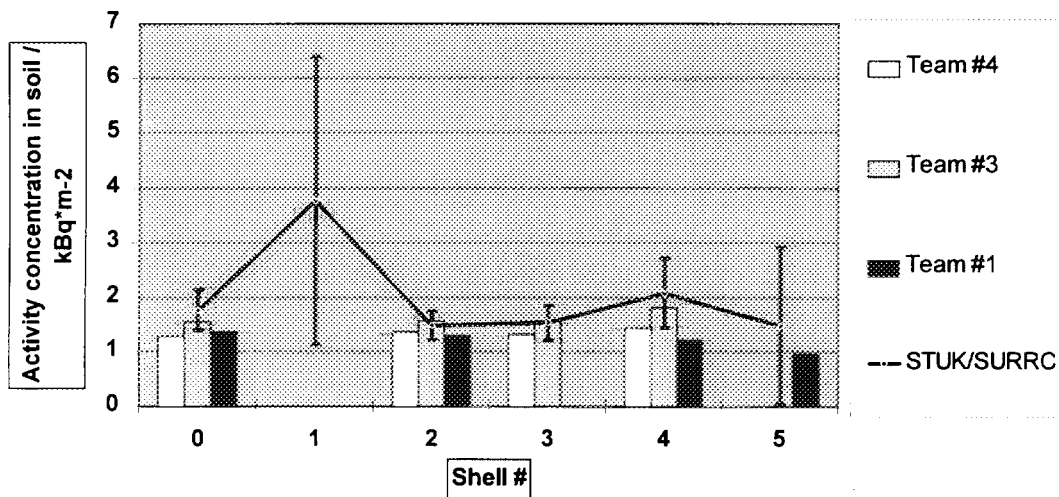


Fig. 4. Average  $^{134}\text{Cs}$  content in soil per hexagonal shell.

Uncertainty limit for the STUK/SURRC data refers to  $\sigma_{n-1}$  of the total mean value for all the six measuring point per shell (except shell # 0).

TABLE 7

*Cesium-134 content in soil at Area I as reported by the different Swedish in-situ teams.*

Shell	Team #4	Team #3	Team #1	Team #2	Team #5
	<b><math>^{134}\text{Cs}</math> in soil / <math>\text{Bq} \cdot \text{m}^{-2}</math></b>				
	$\text{MN} \pm 1 \sigma$	$\text{MN} \pm 1 \sigma$	$\text{MN} \pm 1 \sigma$	$\text{MN} \pm 1 \sigma$	$\text{MN} \pm 1 \sigma$
0	1.27	1.55	1.35	n.c.	n.c.
2.1-2.6	$1.35 \pm 0.07$	$1.56 \pm 0.15$	$1.3 \pm 0.15$	n.c.	n.c.
3.1-3.6	$1.32 \pm 0.1$	$1.56 \pm 0.16$	n.c.	n.c.	n.c.
4.1-4.6	$1.44 \pm 0.07$	$1.81 \pm 0.07$	$1.21 \pm 0.17$	n.c.	n.c.
5.1-5.6	n.c.	n.c.	$0.974 \pm 0.24$	n.c.	n.c.
<b>Total</b>	$1.36 \pm 0.09$	$1.64 \pm 0.17$	$1.18 \pm 0.23$	n.c.	n.c.

#### 40K and Natural Series at Area I

Below are given the results for the natural occurring radionuclides at Area I. IN.B. that most teams present activity values for the natural series that refers to equilibrium conditions in soil at the measuring site.

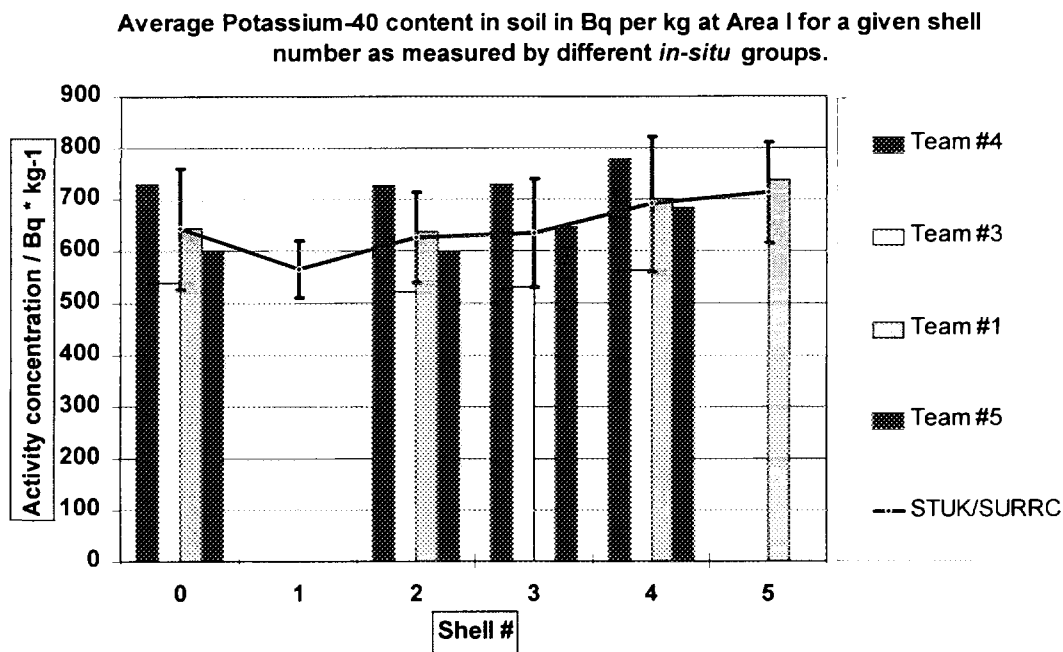


**Fig. 5.. Average activity of Potassium-40 in soil per hexagonal shell.**  
*Uncertainty limit for the STUK/SURRC data refers to  $\sigma_{n-1}$  of the total mean value for all the six measuring point per shell (except shell # 0).*

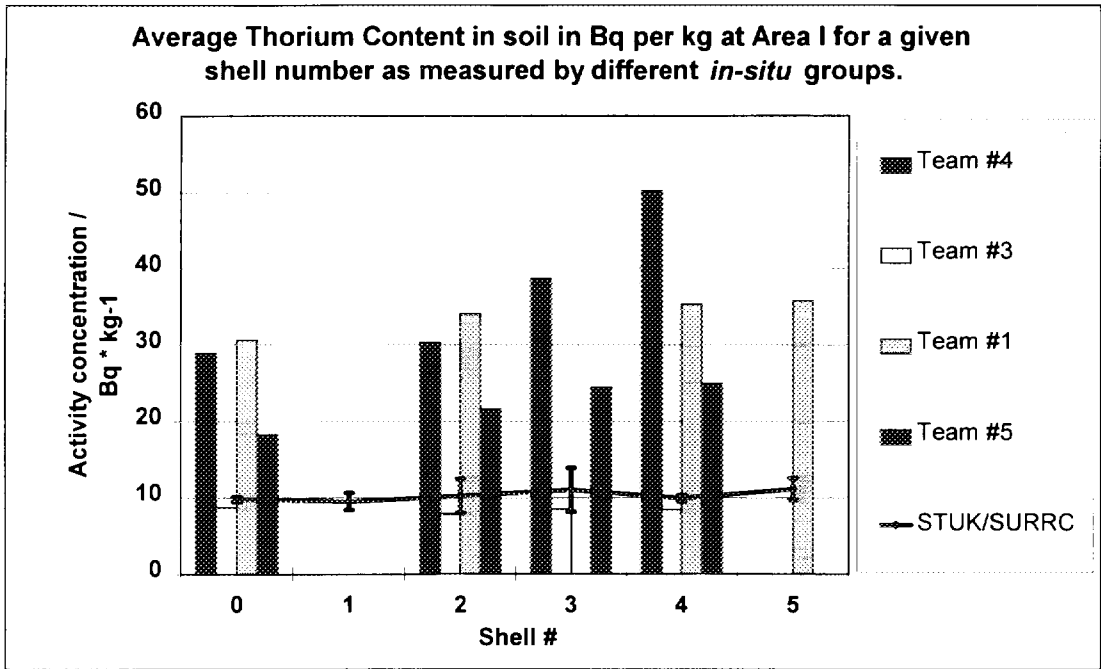


**Fig. 6.a.** Average equilibrium activity of Thorium-series in soil per hexagonal shell. Uncertainty limit for the STUK/SURRC data refers to  $\sigma_{n-1}$  of the total mean value for all the six measuring point per shell (except shell # 0).

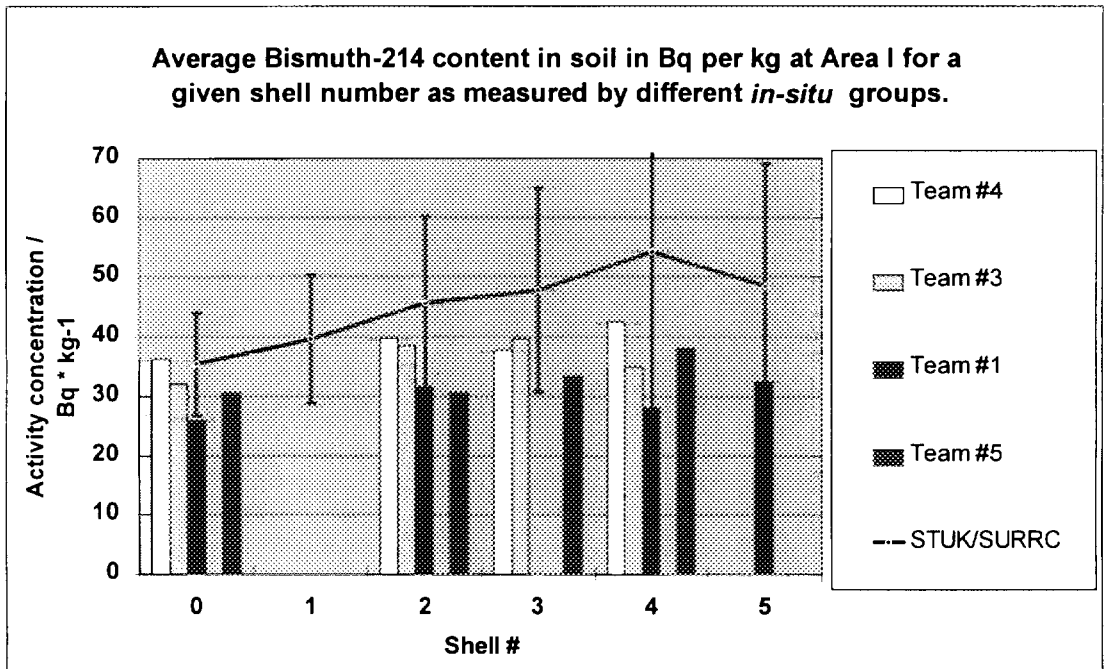


**Fig. 6.b** Average equilibrium activity of Uranium-series in soil per hexagonal shell. Uncertainty limit for the STUK/SURRC data refers to  $\sigma_{n-1}$  of the total mean value for all the six measuring point per shell (except shell # 0).

TABLE 8

Naturally occurring radionuclides in soil at Area I as reported by the different Swedish in-situ teams.

Shell	Team #4	Team #3	Team #1	Team #2	Team #5
	<b>40K:<math>a_{\text{uniform}}</math> / Bq * kg<sup>-1</sup></b>				
	MN ± 1 s	MN ± 1 s	MN ± 1 s	MN ± 1 s	MN ± 1 s
<b>0</b>	728	540	642.8 ± 14.7		601
<b>2.1-2.6</b>	727 ± 19	522 ± 37	636.75 ± 18.2	n.c.	n.c.
<b>3.1-3.6</b>	728 ± 45.6	531 ± 15	n.c.	n.c.	598 ± 23.2
<b>4.1-4.6</b>	776 ± 38.2	564 ± 44	699.3 ± 37.14	n.c.	646 ± 35.5
<b>5.1-5.6</b>	n.c.	n.c.	738 ± 36.5	n.c.	682 ± 33
<b>Total</b>	<b>743 ± 42</b>	<b>539 ± 36</b>	<b>685 ± 52</b>	-	<b>638 ± 45</b>
	<b>Uranium-series:<math>A_{\text{uniform}}</math> / Bq * kg<sup>-1</sup></b>				
	MN ± 1 s	MN ± 1 s	MN ± 1 s	n.c.	n.c.
<b>0</b>	36.3	32	25.8	n.c.	30.55
<b>2.1-2.6</b>	39.8 ± 6.03	38.6 ± 8.3	31.75 ± 5.48	n.c.	n.c.
<b>3.1-3.6</b>	37.8 ± 5.87	39.6 ± 9.3	n.c.	n.c.	30.55 ± 1.97
<b>4.1-4.6</b>	42.4 ± 6.75	34.9 ± 2.9	28.1 ± 3.92	n.c.	33.48 ± 3.17
<b>5.1-5.6</b>	n.c.	n.c.	32.4 ± 2.92	n.c.	38.16 ± 6.51
<b>Total</b>	<b>39.8 ± 6.5</b>	<b>37.4 ± 7.2</b>	<b>30.5 ± 4</b>	-	<b>33.4 ± 4.6</b>
	<b>Thorium-series:<math>A_{\text{uniform}}</math> / Bq * kg<sup>-1</sup></b>				
	MN ± 1 s	MN ± 1 s	MN ± 1 s	n.c.	n.c.
<b>0</b>	28.8	8.7	30.6	n.c.	18.2
<b>2.1-2.6</b>	30.2 ± 5.7	7.9 ± 1.5	34 ± 2.18	n.c.	n.c.
<b>3.1-3.6</b>	38.6 ± 5.7	8.5 ± 1.2	n.c.	n.c.	21.6 ± 2.2
<b>4.1-4.6</b>	50.2 ± 29.2	8.4 ± 0.5	35.2 ± 3.3	n.c.	24.4 ± 1.7
<b>5.1-5.6</b>	n.c.	n.c.	35.7 ± 3.5	n.c.	24.9 ± 1.4
<b>Total</b>	<b>39.1 ± 6.5</b>	<b>8.3 ± 1.1</b>	<b>34.7 ± 2.8</b>	-	<b>23.2 ± 2.3</b>

### 137Cs at Area II

Below are both the equivalent surface deposition of Cesium-137 and the total content in soil (Bq/m<sup>2</sup>) at the location A, B and C given.

TABLE 9  
*Cesium-137 Equivalent Surface Deposition and content in soil at Area II as reported by the different Swedish in-situ teams.*

Location	Team #4	Team #3	Team #2	Team #5	STUK/SURRC (MN ± 1 σ <sub>n-1</sub> )	
<b>137Cs:A<sub>esd</sub> / kBq/ m<sup>2</sup></b>						
A	57	41,56	44,6	46,2	n.c.	
B	39,5	29,82	17,4	31,7	n.c.	
C	60	46,06	32,25	49,9	n.c.	
<b>137Cs in soil / kBq * m<sup>2</sup></b>						
				<i>α/ρ = 0.077</i>	<i>α/ρ = 0.0625</i>	
A	68,8	98,7	153	110	95,7	<b>141 ± 4.3</b>
B	47,6	63,4	59,8	75,2	65,6	<b>43,1 ± 1.3</b>
C	72,5	122,2	111	119	103	<b>172 ± 7</b>
<b>134Cs:a<sub>esd</sub> / kBq * m<sup>2</sup></b>						
A	1,8	1,33	1,48	1,48	n.c.	n.c.
B	1,25	0,87	0,617	1,01	n.c.	n.c.
C	1,97	1,38	1,05	1,43	n.c.	n.c.
<b>134Cs in soil / kBq * m<sup>2</sup></b>						
A	2,17	3,2	n.c.	n.c.	n.c.	<b>4,6</b>
B	1,51	1,9	n.c.	n.c.	n.c.	<b>1,49</b>
C	2,37	3,7	n.c.	n.c.	n.c.	<b>5,86</b>

Equivalent Surface Deposition of Cs-137 at Area II as Measured by Different In-situ Groups.

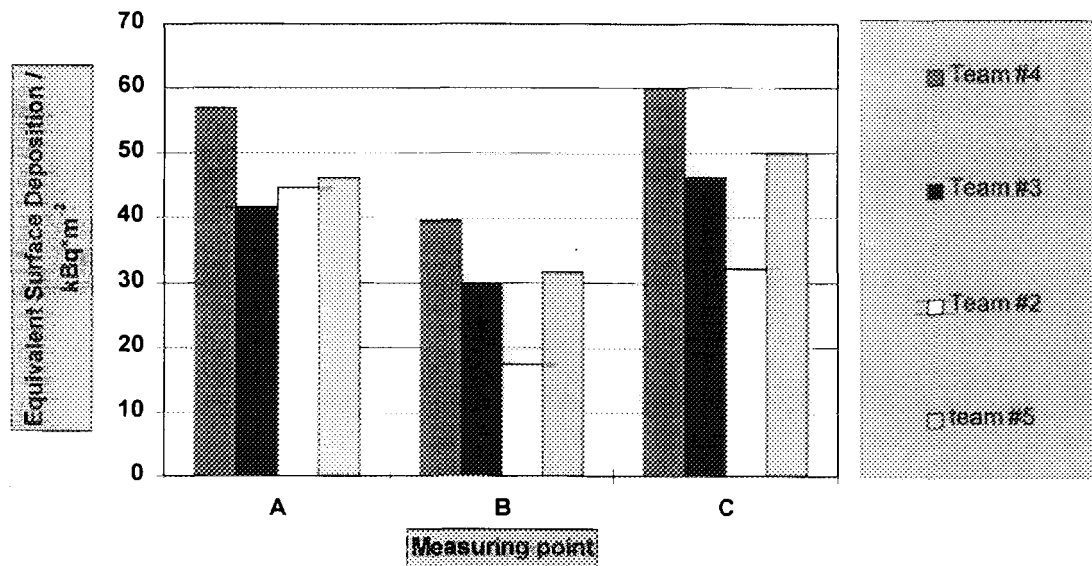
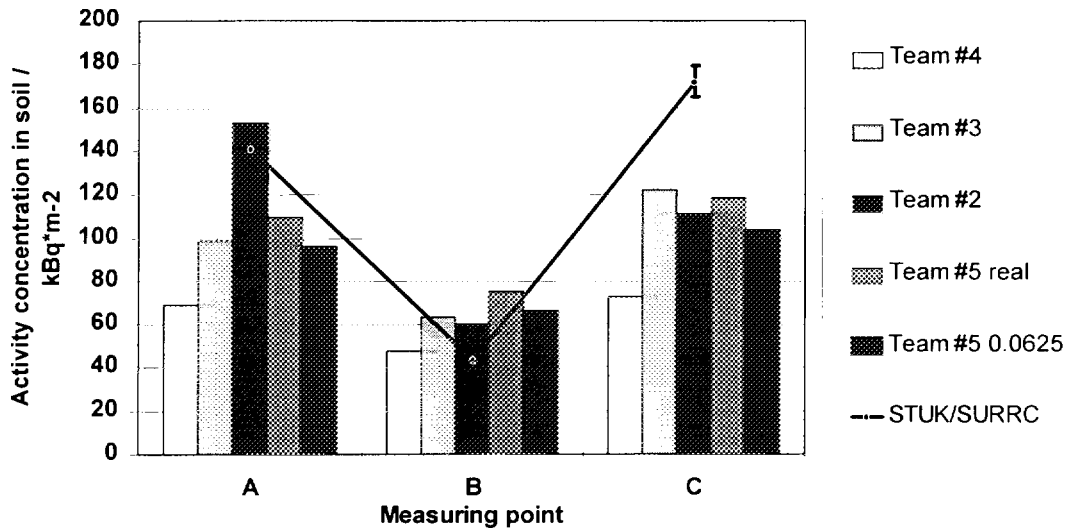


Fig. 7.a. Average Equivalent Surface Deposition of 137Cs at three measuring points

at Area II.

**Average Cesium-137 Content in Soil in kBq per m<sup>-2</sup> at Selected Points in Area II as Measured by Different *In-situ* Groups.**



**Fig. 7.b.** Average <sup>137</sup>Cs content in soil at three measuring points at Area II.

### <sup>134</sup>Cs at Area II

Below are both the equivalent surface deposition of Cesium-134 and the total content in soil (Bq/m<sup>2</sup>) at the locations A, B and C given.

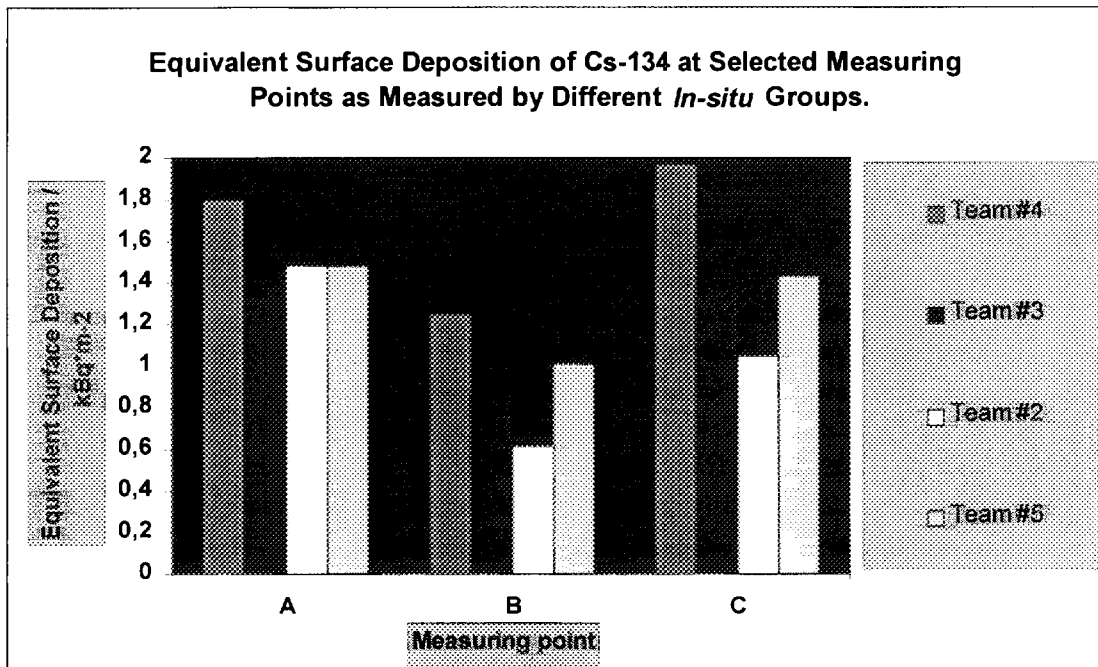


**Fig. 8.a** Average Equivalent Surface Deposition of <sup>134</sup>Cs content in soil at three measuring points at Area II.

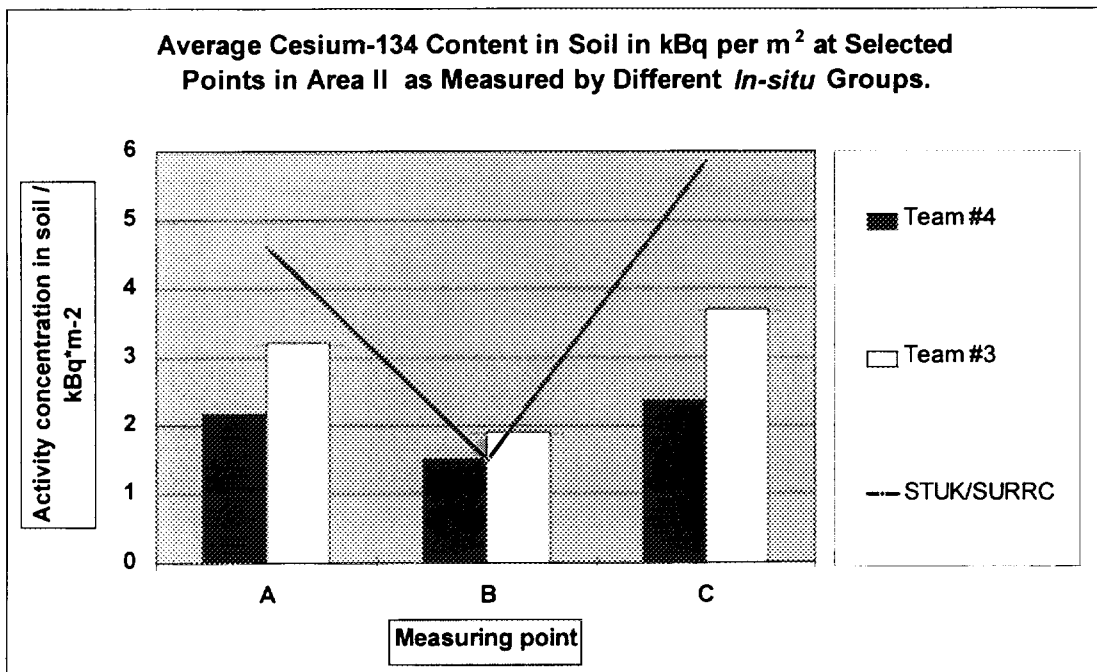


**Fig. 8.b.** Average <sup>134</sup>Cs content in soil per at three measuring points at Area II.

#### 40K and Natural series at Area II

In Table 10 is given an overview of the results from the different laboratories for the naturally occurring radionuclides. The **Team #4 *in-situ*** team tends to present somewhat larger values than do the other laboratories including the soil samples from STUK/SURRCS. Once again we see the effect of the different ways of reporting the activity values for the Thorium-series, referring to different equilibrium conditions. Scaling the **Team #3** and STUK/SURRCS results to equilibrium conditions between Bi-212 and <sup>208</sup>Tl ( $f=0.359$ ) the discrepancy is somewhat less. (Rescaling by 0.359 yields that Team #4 is on the average 80 % higher than STUK/SURRC, and the corresponding value for Team #5 team is about 30 %)

Average Bismuth-214 content in soil in Bq per kg at Selected Points in Area II as Measured by Different *In-situ* Groups.

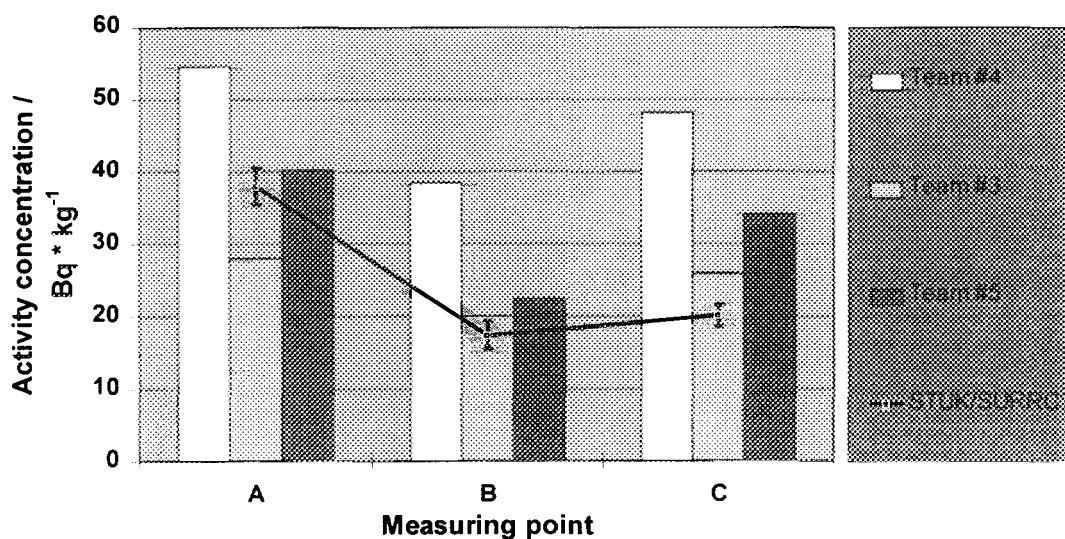


Fig. 9.a: Activity values for the Uranium-series. <sup>214</sup>Bi was chosen to represent a hypothetical equilibrium activity for the total Thorium-series in soil at Area II.

Average Potassium-40 content in Soil in Bq per kg at Selected Points in Area II as Measured by Different *In-situ* Groups.

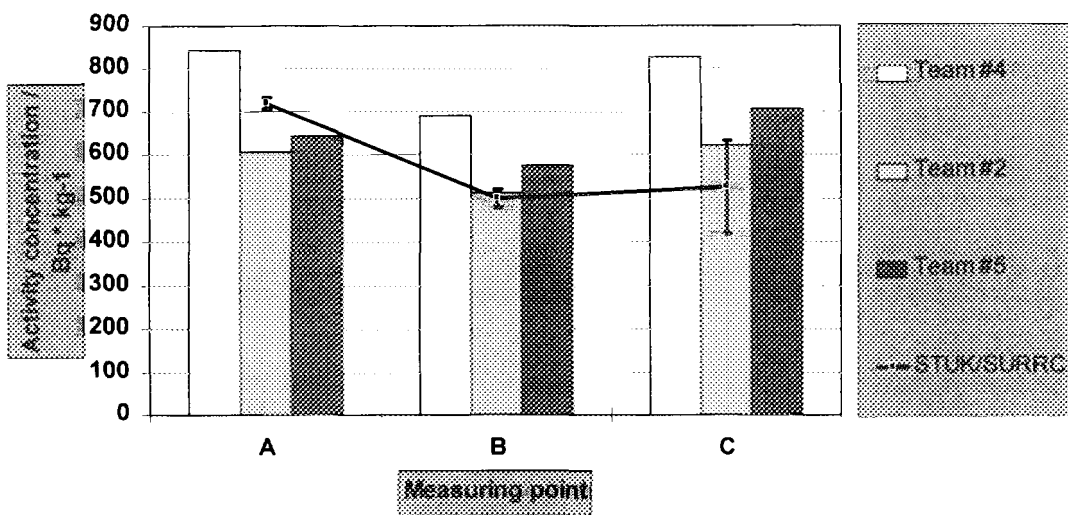


Fig. 9.b. Activity values for <sup>40</sup>K at Area II.

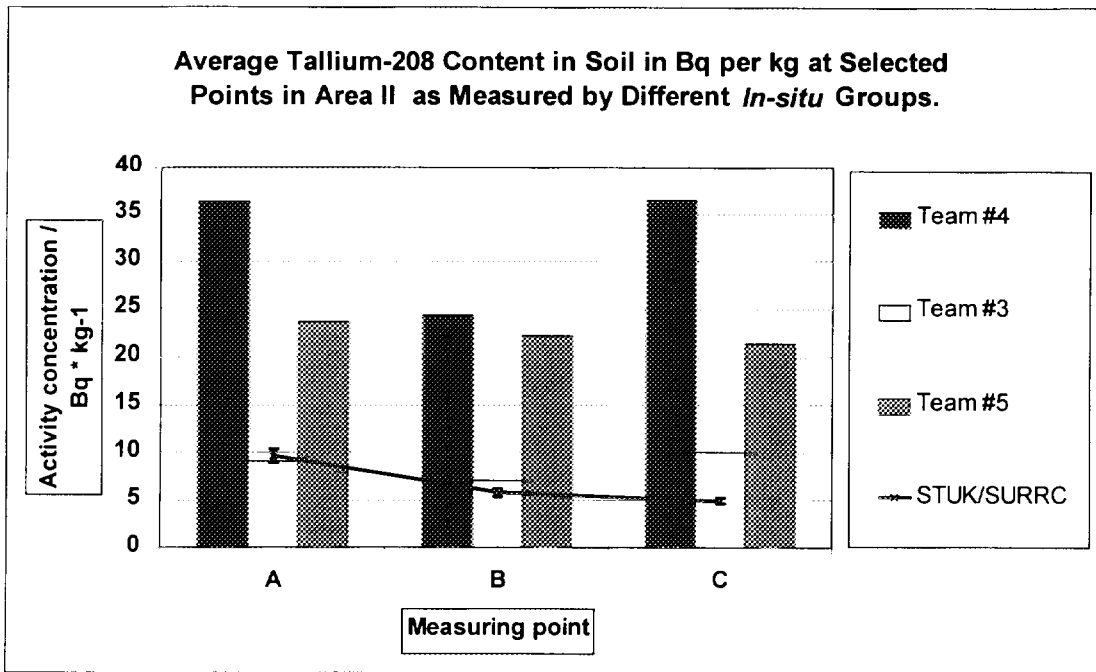


Fig. 9.c. Activity values for the Thorium-series.  
<sup>208</sup>Tl was chosen (all groups except Team #5) to represent a hypothetical equilibrium activity for the total Thorium-series in soil at Area II.

TABLE 10

*Overview of the results from the in-situ gamma measurements from Area II for the naturally occurring radionuclides*

Location	Team #2	Team #3	Team #2	Team #5	STUK/SURRC MN ± 1 σ <sub>rel</sub>
<b><sup>40</sup>K in soil / kBq * kg<sup>-1</sup></b>					
A	844	605	n.c.	643	719 ± 13
B	690	513	n.c.	576	500 ± 21
C	827	621	n.c.	705	526 ± 107
<b>Uranium-series / kBq * kg<sup>-1</sup></b>					
A	34,3	9	n.c.	23,6	9,6 ± 0,7
B	24,3	7	n.c.	22,2	5,8 ± 0,4
C	36,4	10	n.c.	21,4	4,9 ± 0,3
<b>Thorium-series / kBq * kg<sup>-1</sup></b>					
A	36,3	9	n.c.	23,6	9,6 ± 0,7
B	24,3	7	n.c.	22,2	5,8 ± 0,4
C	36,4	10	n.c.	21,4	4,9 ± 0,3

## Results - An overview

In Table 11 we find the average activity values for  $^{137}\text{Cs}$  obtained by taking the average of the activity values from all measured points at Area I. This should give an overview over the coherence in measuring  $^{137}\text{Cs}$  deposition between the different Swedish in-situ teams.

TABLE 11  
*Average  $^{137}\text{Cs}$  content in soil in kBq/m<sup>2</sup> as reported by the different in-situ teams in Area I.*

Laboratory	Team #4	STUK/ SURRC	Team #1	Team #5	Team #3 Field	Team #3 Soil	Team #2
MV	43.0	51.1	47.4	57.4	75.4	67.7	52.1
STDEV	3.7	19.8	8.6	10.3	13.0	19.5	4.5

In Table 12 we see the magnitude of the spread of data reported by the different in-situ teams relative to the mean of all reported values in Area I. The spread is expressed as the standard deviation of the mean values of all reported activity data for a given radionuclide. The spread in the reported values for the equivalent surface deposition of  $^{137}\text{Cs}$  is about 16 %, which is somewhat lower than the spread in the reported activity values for  $^{137}\text{Cs}$  content in soil. The spread values for the  $^{134}\text{Cs}$  content in Area I give a less complete picture of the coherence between the different teams since than  $^{137}\text{Cs}$  due to the smaller amount of data.

TABLE 12  
*Spread of activity data in % of the average value of reported activity content in Area I for all reporting in-situ teams.*

*N.B. that only four teams have reported values for the naturally occurring radionuclides, and only three teams have presented data on  $^{134}\text{Cs}$  content in soil*

$A_{\text{esd}}$	$A_{\text{soil}}$	$A_{\text{esd}}$	$A_{\text{soil}}$	40K	Uranium	Thorium
$^{137}\text{Cs}$		$^{134}\text{Cs}$				
16.2	22.9	22.4	16.9	12.6	11.4	27.0

In Table 13 and Table 14 we see the deviations in the reported values from the different teams relative to the values published by STUK/SURRC for Area I and Area II respectively.

TABLE 13  
Deviations in % of the values reported by STUK/SURRC at Area I

<i>Laboratory</i>	$A_{soil} - {}^{137}\text{Cs}$	$A_{soil} - {}^{134}\text{Cs}$	${}^{40}\text{K}$	<i>Uranium</i>	<i>Thorium</i>
Team #4	-15.9	-35.3	13.0	-14.9	36.4
Team #3	1.9	-20.4	-16.5	-22.1	-19.3
Team #1	-7.3	-42.7	6.2	-34.7	20.8
Team #5	12.4		-1.3	-28.6	-19.0
Team #2	47.5				
<b>AVG</b>	<b>7.7</b>	<b>-32.8</b>	<b>0.36</b>	<b>-25.1</b>	<b>4.7</b>

TABLE 14  
Deviations in % of the values reported by STUK/SURRC at Area II

<i>in-situ team</i>	${}^{137}\text{Cs}$	${}^{134}\text{Cs}$	${}^{40}\text{K}$	<i>Uranium</i>	<i>Thorium</i>
Team #4	-32.9	-37.0	37.5	101.6	108.8
Team #3	-4.0	-13.3	1.6	6.1	39.5
Team #2	3.9	n.c.	n.c.	n.c.	n.c.
Team #5 - real	7.1	n.c.	12.9	34.4	35.7
Team #5 - teo	-6.6	n.c.	n.c.	n.c.	n.c.
<b>AVG</b>	<b>-10.1</b>	<b>-25.1</b>	<b>17.3</b>	<b>47.3</b>	<b>61.3</b>

## Conclusions

### General conclusions

Good agreement is found (within 5 % for the  ${}^{137}\text{Cs}$  content in soil,  $A_{soil}$ ) between the STUK/SURRC values and the total mean values of the field gamma measurements reported by the Swedish in-situ teams at Area I. All mean values for each of the five radionuclides surveyed are within one standard deviation from the average values obtained from the STUK/SURRC soil sample data. (This is true also for  ${}^{208}\text{Tl}$  if one translates all detected transitions in the STUK/SURRC soil sample data to equilibrium conditions for the total Thorium-series).

At Area II larger discrepancies between STUK/SURRC and the Swedish in-situ teams were found, especially for the natural occurring radionuclides (more than 50 % in excess of the STUK/SURRC data).

The spread within the Swedish teams in the reported values (excluding the additional soil sample data reported by **Team #2**) was typically 15 - 30 % for artificial radionuclides and between 10 to 30 % for naturally occurring radionuclides.

### $A_{\text{esd}}$ - values

This quantity is independent of the source geometry<sup>10</sup> and thus provides a tool for determining the coherence in each team's efficiency calibration for their detector set-up. **Team #4** is above the average value for the in-situ teams (20 - 30 % for all  $A_{\text{esd}}$  values reported). **Team #1** lies below the average value for the in-situ teams, and the deviation is especially evident for  $^{134}\text{Cs}$  values in Area I where the value is 30 % lower than the average of all *in-situ* teams.

**FOA-Umeå**, **FOA-Stockholm** and **Team #5** have coherent values for all radionuclides in Area I, indicating that their efficiency calibrations agree within about 5 - 10 %.

### $A_{\text{exp}}$ - values

This quantity is both a measure of the field efficiency calibration of the set-up as well as how the depth profile of the radiocesium is either determined or estimated. In this survey all teams have use somewhat different methods for evaluating the total activity per square metre (See Materials & Method section, Table 5). Here the trend is reversed for **Team #4**, where the reported values consistently are found below the average value for all four reporting teams. **Team #2** is the other extreme whose field gamma spectrometry values (with field parameters acquired in-situ to determine the field efficiency) for  $^{137}\text{Cs}$  exceed the average by almost 35 %. **Team #1** shows again a significant deviation of 15 % below the average for  $^{134}\text{Cs}$ .

### Natural radionuclides

Since the source geometry in soil is assumed to be uniform for all naturally occurring radionuclides the soil content data will be a measure of the coherency of the efficiency calibration of the in-situ team's detector set-ups, just as the  $A_{\text{esd},^{137}\text{Cs}}$  values reported. This is the case for **Team #4**, **Team #1** and **Team #5** who have all used the same soil composition data (standard soil,  $\rho = 1600 \text{ kg/m}^3$ ). The trend is repeated here, where **Team #4** is 15 - 20 % above the average for all four reporting teams. For **Team #1** no specific trend could be seen. **Team #3** is the team who has used its own site specific

---

<sup>10</sup> This is not the case for the model used by Team #2, which uses a 1 cm soil layer model in order to describe surface deposition of radiocesium. In this work, these values have been pooled together with other  $A_{\text{esd}}$  - values when averaging over all in-situ teams was carried out.

data for the soil and reports the lowest values for the  $^{40}\text{K}$  and  $^{208}\text{Tl}$  in Area I (about 15 - 20 % less than the average). **Team #2** did not report any activity values for the naturally occurring radionuclides.

On the whole, large spread was found (27 % of average value for four reporting teams) for the values reported for  $^{208}\text{Tl}$  and it is noteworthy that all *in-situ* teams calculate the abundance of the natural series somewhat differently. For instance did **Team #1** use the 2,614 keV peak for calculating the equilibrium activity of the Thorium series whereas **Team #5** used the 911 keV photo-peak of  $^{228}\text{Ac}$  instead.

### $A_{\text{soil}}$ and Content of Naturally Occurring Radionuclides Compared to STUK/SURRC Values

**Team #4** presents values that are 15 % lower than reported STUK/SURRC values for  $A_{\text{soil}}$  in Area I, and the corresponding figure for **Team #1** is 7 %. **Team #2's** values for  $^{137}\text{Cs}$  in Area I exceed the reported STUK/SURRC data by about 50 % and the same figure for **Team #5** is 12 %. It is noteworthy that **Team #2** has soil sample data that support their field gamma spectrometry values although these data have been excluded in the total average for the Swedish *in-situ* teams<sup>11</sup>. No clear trend can be seen except that both **Team #1** and **Team #4** have lower reported values for the artificial radionuclides and that all four teams reporting the equilibrium  $^{214}\text{Bi}$  content lie significantly below the value reported by STUK/SURRC.

The results from Area II show that the Swedish *in-situ* teams on the average lie somewhat lower than the STUK/SURRC's soil sample data with respect to the radiocesium content in soil. The deviation is reversed for the naturally occurring radionuclides, where a significant deviation is found for the estimation of the  $^{208}\text{Tl}$  activity in soil.

On the whole are the  $A_{\text{soil},^{137}\text{Cs}}$  values for the Swedish *in-situ* teams in well agreement with the STUK/SURRC data (less than 10 %) for most teams except **Team #4** which on the average lie more than 30 % lower than the rest of the teams.

### Conclusions - soil sampling

The material has been too sparse to make an assessment of the soil sample preparation and the analysis of the soil samples. At the time, **1** did not have access to a soil sample device. **Team #4** sampled soil cores at Area I but have not reported their values. **Team #3** uses their soil samples in order to apply their site specific densities and layer

---

<sup>11</sup> One may object to this and claim that one laboratory (**Team #2**) has presented two independent data series on the same quantity to be determined and therefore these series should be treated equally when being averaged by the rest of the data presented from the other laboratories. In this work, however, it is the intention to compare what different laboratories report, and the figures must be unambiguous. Therefore the author of these pages has chosen to separate the soil sample data from **Team #2** from the other data, since the method of data collection of this series differs (pure soil sampling with activity determination by scanning) from the rest being reported here.

thickness of the soil into their slice models (two slice models for radiocesium and 1 m slice of uniform concentration for the natural radionuclides). The mean wet density for the mineral soil layer at Area I (slice II in the 90/10 - model) is found to be about 550 kg/m<sup>3</sup> in the top layer (0 - 4 cm) which agrees fairly poor with the values given by STUK/SURRC (700 kg/m<sup>3</sup> between 0 - 2 cm, and 1370 kg/m<sup>3</sup> between 2 - 4 cm). The average wet soil density for the mineral soil layer (beneath 4 cm according to the two slice model) is found to be 1260 kg/m<sup>3</sup> which is in better agreement with the average values of 1400 - 1670 kg/m<sup>3</sup> reported by STUK/SURRC.

The method used by **Team #3** is somewhat too different from that used by STUK and SURRC to allow for any more detailed comparisons. The latter laboratories have based their activity data on soil cores samples divided into slices of constant thickness, whereas **Team #3** slices the soil cores with the respect on the vegetational layers of the soil.

**Team #2** has presented values that can be compared directly to the STUK/SURRC's results. Both values (averaged over all measured points) lie within their respective standard deviation at Area I (67.7 kBq/m<sup>2</sup> on the average for Area I as compared to 51.7 kBq/m<sup>2</sup> according to STUK/SURRC). A second measurement series of their soil samples by a different method confirmed their results (60.9 ± 12 kBq/m<sup>2</sup> on the average for Area I). It is noteworthy that the soil sample data presented by **Team #2** are in better agreement with both the other teams as well as with STUK and SURRC than their Monte Carlo calculated activity data (Average value; 74.1 kBq/m<sup>2</sup>).

## **Discussion**

### Possible Sources of Incoherence

Part of the deviations, both between the teams and as a whole compared to STUK/SURRC, may arise from the fact that no team has measured at all marked gridpoints in Area I and the average value given for STUK/SURRC then refers to somewhat different measuring points. However, when comparing average values obtained from each hexagonal shell between the in-situ teams and STUK/SURRC, the trend seems to be consistent with the overall averages for the whole Area I. (See Fig. 2, 4, 5, 6.a, 6.b, 7.b, 8.b, 9.a - 9.c in the Result section!). A possible exception to this are the soil sample values reported by **Team #2** where shell averages differ significantly from the STUK/SURRC data although the overall mean seem to agree better with each other.

Although **Team #3** generally has the best agreement with the STUK/SURRC data, the disagreement with **Team #2** does not suggest that the use of site specific data would dramatically improve the coherence between the teams when obtaining  $A_{\text{soil}}$  data for radiocesium.

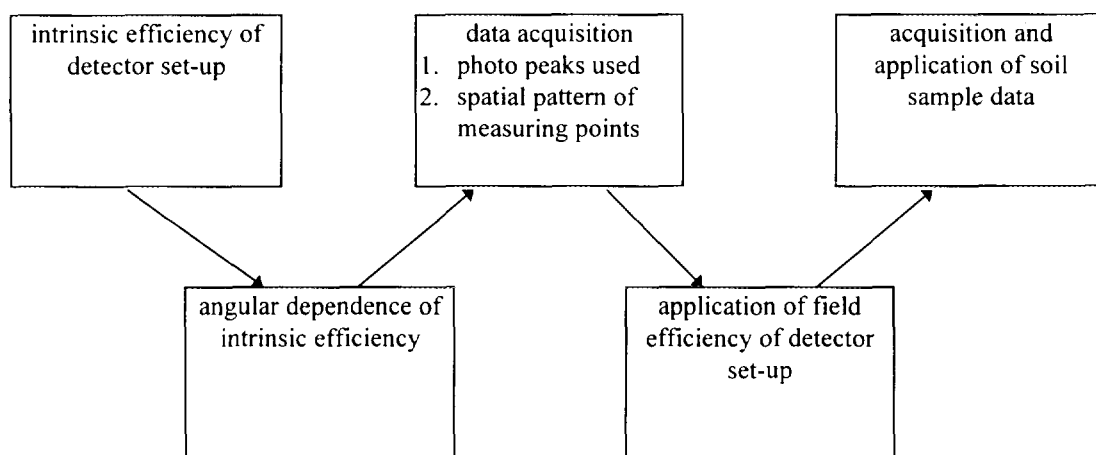
Since tables of fluence to activity ratios are easily found in the literature [1], most teams have estimated the total activity concentration of radiocesium in soil per square

metre by assuming different possible exponential profiles. The often very laborious and time consuming soil sampling and data analysis may be rationalised in an emergency situation by confining the total activity values between two reasonable extreme values (somewhere between  $A_{\text{esd}}$  and  $A_{\text{soil}}$  with a maximally reasonable depth penetration for fresh fallout of radiocesium). This procedure could compete in accuracy with field gamma measurements that include soil sampling since the deviations for the teams compared to STUK/SURRC are of the same magnitude as the difference between say  $A_{\text{esd}}$  and  $A_{\text{soil}}$  ( $\alpha/\rho = 0.150 \text{ m}^2/\text{kg}$  corresponding to a penetration depth of about half a centimetre) for  $^{137}\text{Cs}$  (See Table 12, 13 & 14 in the Result section!).

### Possible Future Measures for Coherence Improvement

The exercise has shown that the Swedish in-situ team's results on the average are in good agreement with the STUK/SURRC data, but there is a considerable variation between the teams that could be minimised. *The most obvious reason for this variation is due to difference in the intrinsic efficiency calibration of the detector set-up.* This is evident especially for **Team #1** and **Team #4**. In an emergency situation the estimations of the equivalent surface deposition are of more importance for evaluating the contamination than assuming different soil profiles. Inconsistencies in the field efficiency calibration between different in-situ teams may in the end give ambiguous results and cause confusion if the deviations between them are too large. *This is why some effort should be done in making an intercomparison of the intrinsic efficiencies of each team's field gamma detector set-up. By measuring a standard point source the spread between the laboratories could be corrected for.* A discussion about what kind of standard source to be used must be carried out in the future.

**Fig. 10**



The second reason for the spread in this exercise is due to different approaches when estimating the depth soil profiles for the artificial radionuclides. Only **FOA-Umeå** and **Team #2** have reported values for the radiocesium content in soil that origin from some kind of actual soil sampling. So far has **Team #3** exhibited a satisfactory agreement with the STUK/SURRC result by their methodology of incorporating soil

sample data as an input to their calculation of the field efficiency. A future exercise similar to RESUME-95 should also include more material on soil sampling in order to assess the impact of the different sampling methods for evaluating the total radiocesium content in soil.

An additional source of systematic deviations is the use of different calculation algorithms. It is otherwise contradictory that some teams show  $A_{\text{esd}}$  values higher than the rest but at the same time have lower  $A_{\text{soil}}$  values than on the average. A closer look on how the calculation algorithm is carried out could reveal possible source of inconsistencies between the laboratories. This study shows that these do exist.

**NEXT PAGE(S)  
left BLANK**



# Danish Emergency Management Agency - University of Glasgow, Department of Statistics Comparison of the results of the RESUME-95 Exercise

ABSTRACT ..... 371

ACKNOWLEDGEMENT ..... 371

INTRODUCTION ..... 371

DESCRIPTION OF THE DATA ..... 372

    Tab. 1. Data sets reported and measuring techniques used in RESUME95 ..... 372

    Fig. 1. Line data for three airborne data sets and nearby in-situ measurements and soil samples ..... 373

    Fig. 2. Line data for three airborne data sets and nearby in-situ measurements and soil samples ..... 373

DATA ANALYSIS ..... 374

    Fig. 3. Cumulative distribution functions ..... 374

    Fig. 4. Histograms for the 8 data sets ..... 375

    Tab. 2. Summary statistics ..... 376

SPATIAL DISTRIBUTION ..... 376

    Tab. 3. Percentiles of the distributions ..... 377

    Fig. 5. Boxplots showing distribution of results for each team ..... 377

    Fig. 6. 10 percentile ..... 378

    Fig. 7. 50 percentile ..... 378

    Fig. 8. 90 percentile ..... 378

INVESTIGATION OF THE CORRELATION IN THE RESULTS AND EXPLORATION OF THE SOURCES OF VARIATION ..... 379

    Tab. 4. Correlation coefficients ..... 379

    Fig. 9. .... 380

    Fig. 10. .... 380

    Fig. 11. .... 381

REGRESSION ANALYSIS ..... 381

    Case 1 ..... 381

    Case 2 ..... 382

    Case 3 ..... 382

SUMMARY OF THE FLIGHT LINES ..... 382

    Tab. 5. Summary of flight lines ..... 382

    Fig. 12 ..... 383

    Tab. 6. .... 383

    Tab. 7. .... 384

CONCLUSIONS AND RECOMMENDATIONS ..... 384

**NEXT PAGE(S)  
left BLANK**

## Comparison of the results of the RESUME-95 exercise.

Jens Hovgaard  
Beredskabsstyrelsen  
Datavej 16,  
DK-3460 Birkerød, Denmark

Marian Scott  
Dept of Statistics,  
University of Glasgow  
Glasgow G12 8QW, Scotland

### Abstract

Within the framework of the Nordic Nuclear Safety Research program (NKS), RESUME-95 (Rapid Environmental Surveying using Mobile equipment) took place in Finland in August 1995. Amongst the purposes of the exercise were:

- to test the ability of existing airborne, car-borne and in-situ instruments to map contaminated areas (in this case from Chernobyl) and
- to establish the comparability of results obtained with different systems.

Preliminary analysis has shown that major features of the spatial distribution of the contaminants were identified by all teams, but that significant variations in absolute figures were observed. In this paper, we describe some of the quantitative analysis undertaken to assess the comparability of the results and to explore any differences in them. We discuss future actions within a European framework of off-site emergency management to ensure comparability of results and to encourage development of standardisation techniques. Each participating team has already produced reports of their own results, and preliminary analysis has shown that major features of the spatial distribution of the contaminants were identified by all teams, but that variations in absolute figures were observed (some possible explanations for this include the calibrating procedures used and the assumptions concerning the vertical source distribution). In this paper, we describe some of the quantitative analysis undertaken to assess the comparability of the results and to explore any differences in them. In addition, from the experience gained from RESUME-95, we discuss future actions within a European framework of off-site emergency management to ensure comparability of results and to encourage standardisation techniques to be developed.

### Acknowledgement

We would like to acknowledge all participants of the RESUME exercise as well as NKS for making all the data for this analysis available. A special thanks to Dr I Anderson, Dept. of Mathematics, Glasgow University for providing the solution to a demanding combinatorial problem.

### Introduction

Within the framework of the Nordic Nuclear Safety Research (NKS) the field test RESUME-95 (Rapid Environmental Surveying Using Mobile Equipment) took place in Finland in August 1995. In the Nordic countries, there has been and continues to be development of mobile equipment for response to nuclear emergencies. However, before the RESUME-95 study a general test of such equipment had not taken place. The term *mobile equipment* is usually taken to refer to measuring devices which acquire data whilst in motion, but since these measurements often will be compared with other means for determining spatial distributions of nuclear fallout, RESUME-95 also included in-situ measurements and soil sampling. The aims of the exercise included to test the ability of the systems to map

contaminated areas and to establish the comparability of results obtained with different systems.

The exercise took place in three different areas (I,II,III) where area I (an airfield) was intended for calibration, area II was a typical Finish countryside area with a mixture of forest lakes and small villages, and finally area III was one where a number of different radioactive sources were hidden. Thus areas II and III were intended to test the capabilities of the systems for general mapping of Cs-137 and for detection of sources respectively.

### Description of the data

In this paper, the comparability of the estimated Cs-137 distributions in area II reported by the different teams is assessed. Only results reported during the exercise are considered here, reflecting the objective of comparing results under operational conditions. A total of 11 sets are thus considered and are listed in Table 1. Each data set consists of the (X,Y) co-ordinates and a measurement (Z) of Cs-137 activity at each location surveyed. No estimates of uncertainties were requested and so this has limited some of the analysis which could be carried out. From Table 1, it can be seen that not all data sets are given in the same quantities, this of course presents a scaling problem which will be further investigated. Finally, the paper will concentrate on air-borne and car-borne systems and will make only a few general comments concerning the in-situ and soil sampling results.

**Table 1: Data sets reported and measuring techniques used in RESUME 95**

Data set	Type	Reported Unit
Set 1	Airborne (NaI(Tl))	KBq/m <sup>2</sup>
Set 2	Airborne (NaI(Tl))	KBq/m <sup>2</sup>
Set 3	Car-borne (NaI(Tl))	KBq/m <sup>2</sup>
Set 4	Airborne (NaI(Tl))	KBq/m <sup>2</sup>
Set 5	Car-borne	nGy/h
Set 6	Airborne (HPGe)	KBq/m <sup>2</sup>
Set 7	Airborne (NaI(Tl))	KBq/m <sup>2</sup>
Set 8	Airborne (HPGe)	Cps
Set 9	In-Situ (HPGe)	KBq/m <sup>2</sup>
Set 10	In-Situ (HPGe)	KBq/m <sup>2</sup>
Set 11	Soil Samples	KBq/m <sup>2</sup>

Two line plots of a subset of the data sets are shown in Figures 1 and 2. Only measurements situated less than 75m from the pre-defined flight lines are considered, measurements at a greater distance are not shown. From the line plots it is quite clear that a point to point comparison of the different measuring techniques is difficult because of differences in field of view of the detectors and the different sampling times used by the different teams, both of which factors will also interact with the natural spatial heterogeneity of the <sup>137</sup>Cs deposition, for example, the two soil samples at 762100 m on Figure 1 are taken less than 10m apart and shows values of 2kBq/m<sup>2</sup> and 170kBq/m<sup>2</sup> respectively. Also a certain variation from the predefined flight lines can be observed in the missing points and also in the small shifts in position of significant features. Nevertheless, amongst the air-borne, car-borne and to a lesser extent the in-situ measurements there is still a remarkable degree of concordance. Henceforth in this analysis, we will concentrate on data sets from of airborne and car-borne measurements only; data sets 1-8 in Table 1.

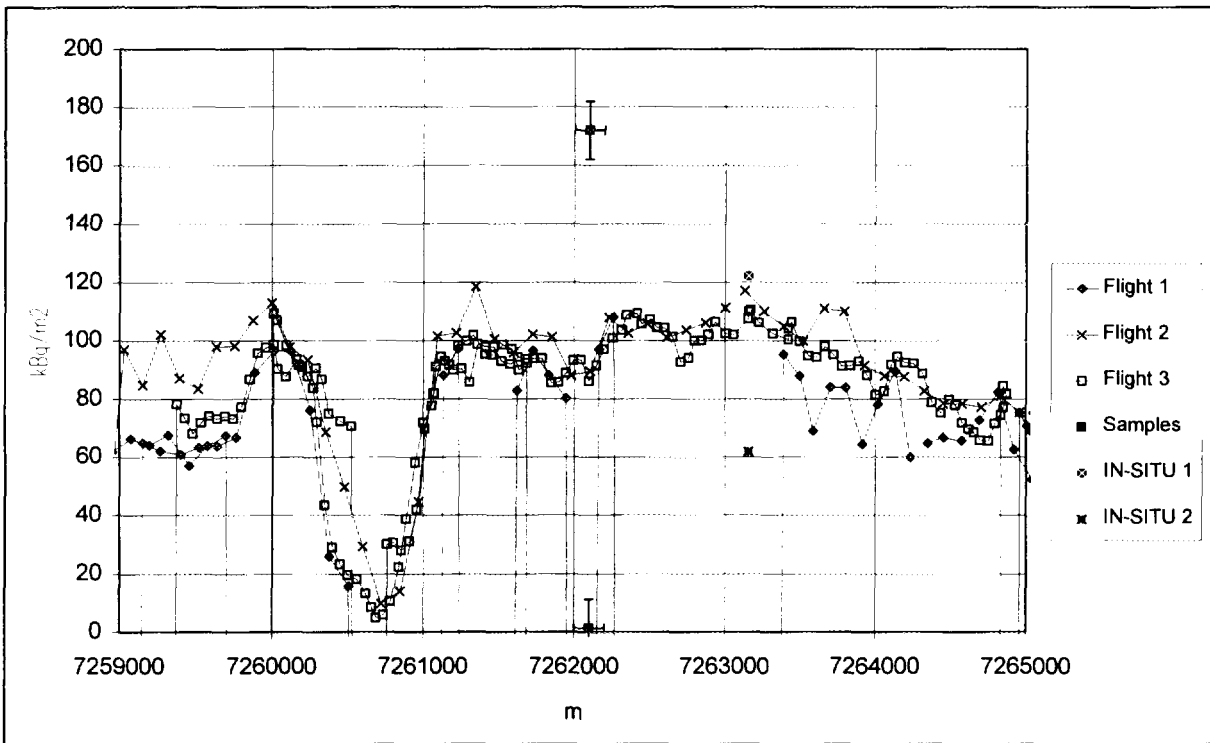


**Figure 1** Line data (profile) for three airborne data sets and nearby in-situ measurements and soil samples.

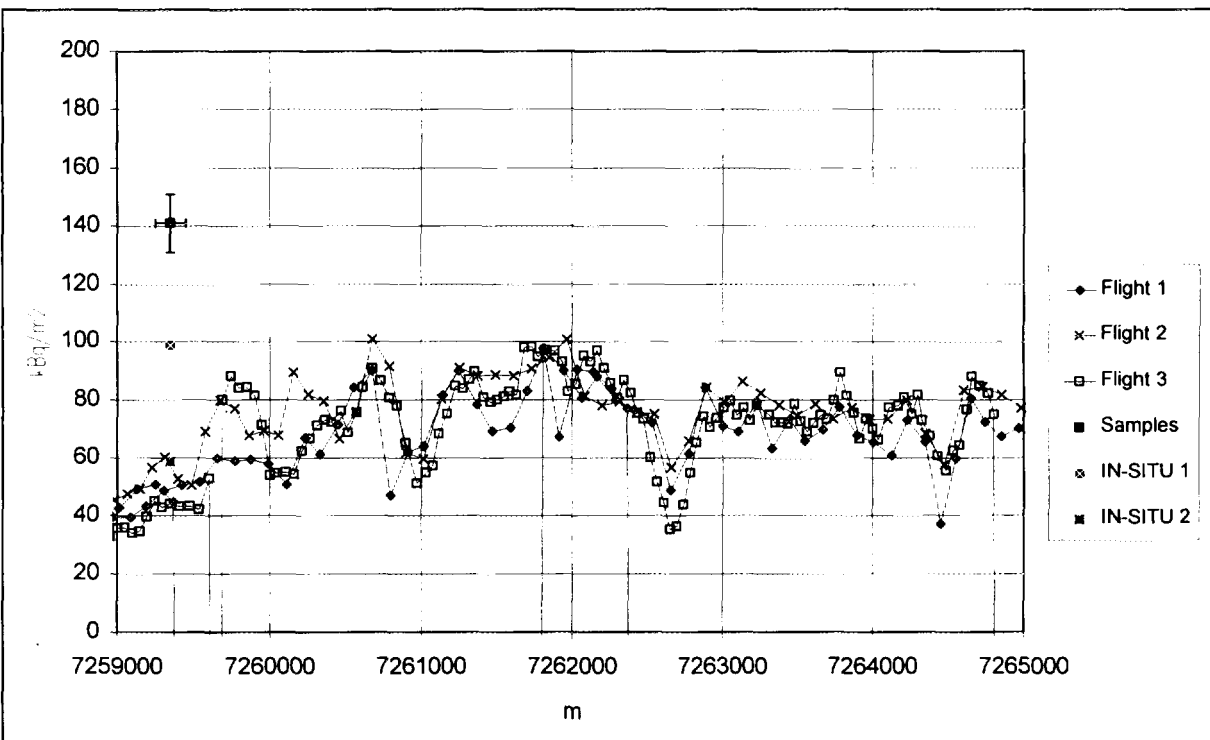


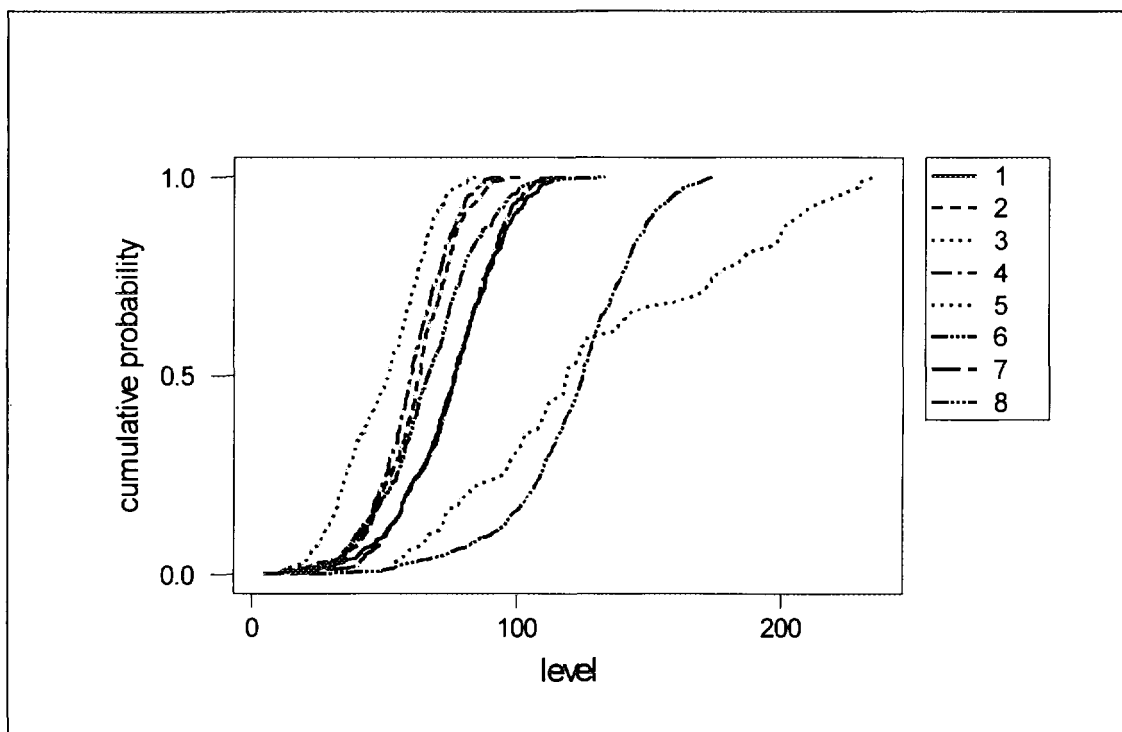
**Figure 2** Line data (profile) for three airborne data sets and nearby in-situ measurements and soil samples.

Due to some of the factors mentioned above, before beginning the analysis the eight data sets have been re-gridded to compensate for differences in sampling time as well as variations in flight tracks. In area II, the planned flight lines had a heading of  $22^\circ/202^\circ$  and were displaced 150m apart. A new rectangular grid was defined by first turning all observation points  $22^\circ$  counter clockwise and then arranging all observations in cells of size 150m perpendicular to the lines and 300 m along the lines. The resulting grid is 21 columns by 22 rows. The value for each grid cell for each data set has been taken as the mean value of all observations within that cell.

### Data analysis

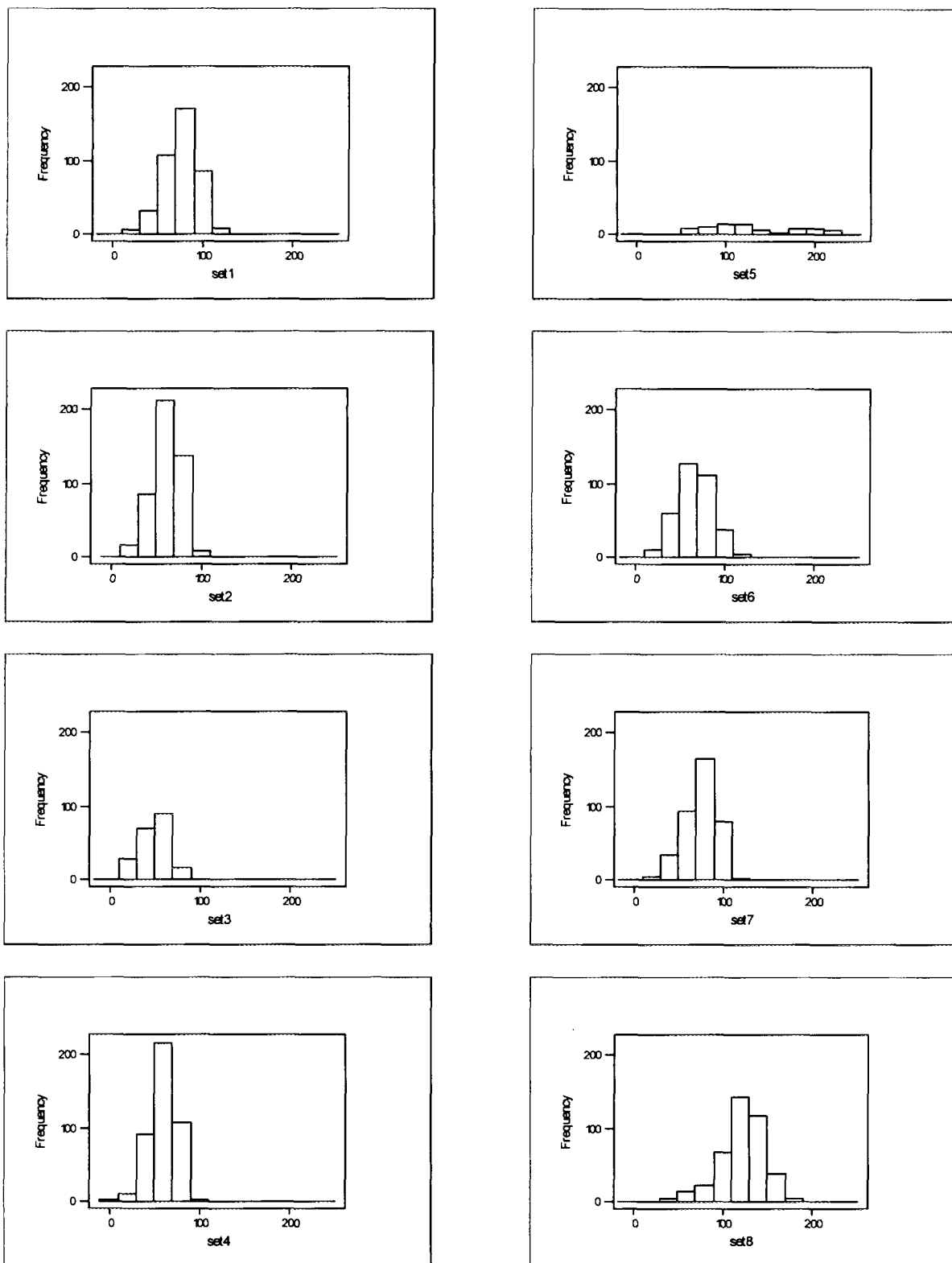
The analysis reported in this paper has two main objectives: the first to consider the general distributional properties of each data set and to explore their common features in particular the spatial distribution of results; the second to consider the scaling of the different sets.

Figure 3 shows the cumulative distribution plots for all 8 data sets, such plots show the level and distribution of results in terms of the percentiles of the distribution. From Figure 3, it is clear that two sets have significantly shifted distributions, these are sets 5 and 8 (given in different units), but that the remaining sets have similarly shaped distributions, (they are effectively parallel) but with small offsets.



**Figure 3** Cumulative distribution functions

The equivalent histograms are shown below. The histograms are normalised to the actual number of observations and show some interesting features.:



**Figure 4** Histograms for the 8 data sets. The histograms are normalised to the true number of observations.

It is observed that range of values are relative small for all sets, It is also seen that set 1, 2, 3, 4, 6 and 7 show similarly shaped distributions whereas there exist a noticeably different distribution for set 5 (remembering that there are only 79 observations in that set). All distributions show evidence of asymmetry, with a long tail at low values and this is particularly pronounced for set 8 (HPGe system given in cps).

Table 2 shows the summary statistics for each data set. The same features as observed in the cumulative distributions are also observed here, namely that with the exception of sets 5 and 8 which are given in different units (nGy/hr and Cps respectively), we see broadly similar distributions, but with differences in the mean levels. The coefficient of variation (st dev/mean \*100) give a measure of the relative variation in the sets and again we see strong similarities in the values with the exception of those for the car-borne systems.

**Table 2: Summary statistics**

Set	N	Number missing	Mean	Median	Stdev	Minimum	Maximum	Coeff of variation (%)	25% quartile	75% quartile
1	410	52	74.78	76.60	19.56	10.03	118.04	26.1	62.27	88.41
2	459	3	61.63	62.99	15.57	5.59	100.90	25.2	52.31	72.87
3	204	258	49.17	51.26	16.33	11.36	84.16	33.2	35.49	62.45
4	429	33	59.34	59.93	14.75	4.27	93.57	24.8	50.45	70.24
5	79	383	131.54	119.15	51.82	52.45	234.94	39.4	94.70	176.72
6	352	110	66.30	66.21	19.35	16.10	132.92	29.2	54.61	78.85
7	380	82	74.79	75.95	17.74	14.63	113.16	23.7	63.03	87.85
8	411	51	121.65	124.50	25.50	22.00	173.25	20.9	108.50	139.50

In addition to these basic summary statistics, a further exploration of the distributions of the results were explored and are shown in Figure 5 **Boxplots showing distribution of results for each team..**

Boxplots show the central 50% (box ) of the distribution, the median and the minimum and maximum. Starred values are considered to be extreme. Figure 5 shows that most of the distributions are not symmetrical, with extreme values identified and typically at low values and only observed among the airborne data sets. One possible reason for this is that area II included a number of small lakes and observations over lakes will be very low. The middle 50% (the central box in each boxplot) is similar in range for all sets with the exception of set 5 (a car-borne system and which has only few (79) observations in the grid) and is typically symmetrical. Some variation in the medians (the central line in each box) is apparent (even discounting sets 5 and 8) and again points to a problem in scaling.

### **Spatial distribution**

To investigate the spatial features of the distributions, we must first then be able to discount any possible scaling effects. To this end, we have chosen to study specific percentiles of the distributions and to compare the resulting spatial patterns.

The 10<sup>th</sup> , 50<sup>th</sup> , and 90<sup>th</sup> percentiles of the distributions for each set are shown in Table 3. The percentiles were used to identify locations in each data set where values exceeding a given percentile were found. Using percentiles effectively removes any influence of different scaling (calibration constants) and units. For a given percentile, the locations within each grid at which the percentile level was exceeded were coded as 1 and all other grid cells were

coded as 0. Grey scale maps were then constructed to show the degree to which the percentile areas overlap in each set.

**Table 3: Percentiles of the distributions**

Set	10 percentile	50 percentile	90 percentile	Unit
1	50.6	76.6	98.1	kBq/m <sup>2</sup>
2	42.3	62.9	79.6	kBq/m <sup>2</sup>
3	27.2	51.2	69.1	kBq/m <sup>2</sup>
4	40.1	59.9	77.7	kBq/m <sup>2</sup>
5	66.2	119.1	207	nGy/h
6	39.2	66	91	kBq/m <sup>2</sup>
7	49.8	75.9	96.1	kBq/m <sup>2</sup>
8	89	124.5	151	Cps

The grey scale maps are shown in Figures 6 to 8 and show the degree to which percentile areas overlap in each set. Only data from sets 1,2,4,6,7,8 have been used in the images. Sets 3 and 5 were rejected because being car-borne systems, they do not have the same spatial attributes as the other air-borne sets. Each grid cell for each set is given the value 1 if the cell exceeds a specific percentile and 0 if not, if no value is available for the grid cell the value "unknown" is used. For each cell the average of the observed zeroes or ones are formed, if less than 3 observations are available for a given cell, "X" is assigned to the cell. A grey value proportional to the average value is used to produce the images, black is equal to 0 and white is equal to 1. If there is complete agreement among the data sets the images would comprise only completely white and black cells. The observed patterns clearly show that for the 50 and 90 percentiles, all the data sets agree very well, for the 10 percentile the agreement is good, but poorer than for the other two. Some discrepancy in results is to be expected close to the contour curve following the percentiles caused by small positioning

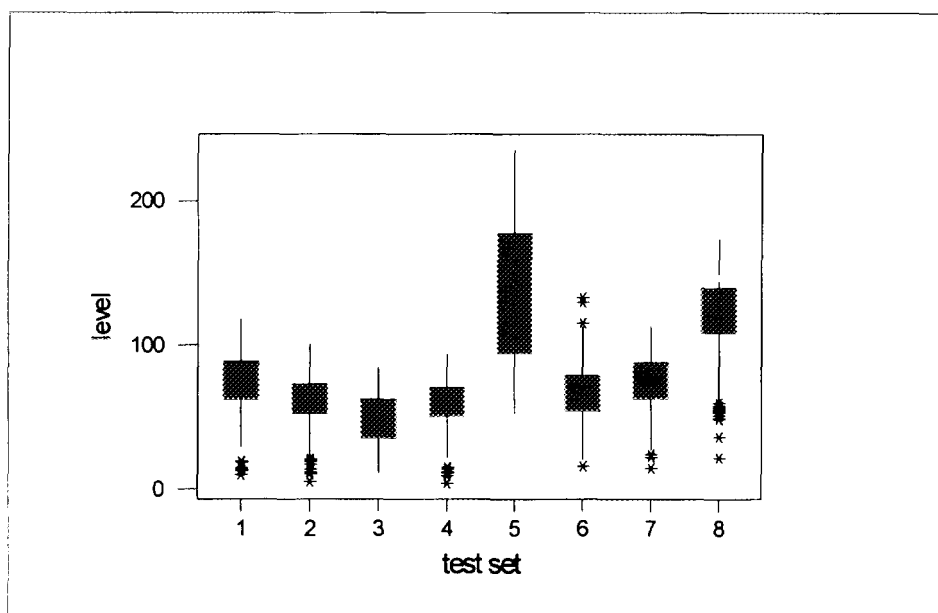


**Figure 5** Boxplots showing distribution of results for each team.

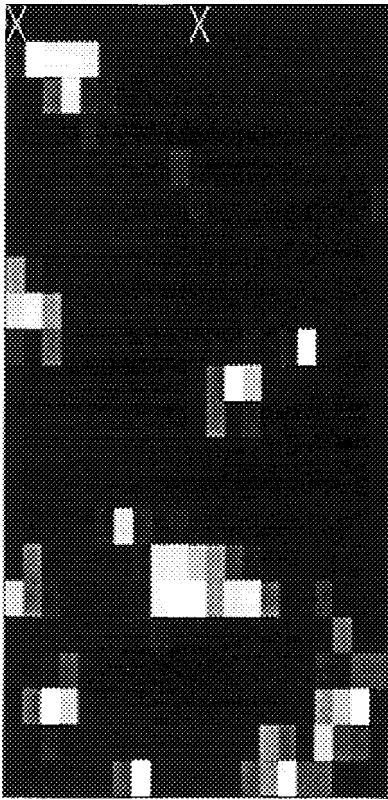


**Figure 6** 10 percentile

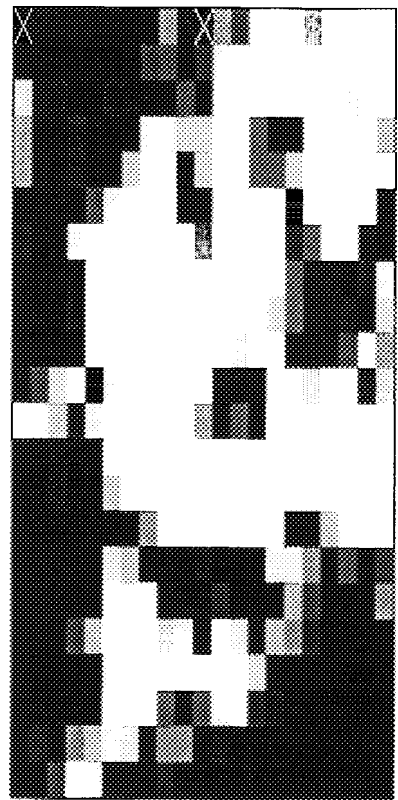


**Figure 7** 50 percentile

Figure 6 **10 percentile**-Figure 8 **90 percentile**  
 Grey scale encoded match of the 10th, 50th, and 90th percentile. Each grid cell for each set is given the value 1 if the cell belongs to a specific percentile and 0 if not, if no value is available for the grid cell it is given the value "unknown". For each cell the average of the observed zeroes or ones are formed, if less than 3 observations are available for a given cell the "X" values is given to the cell. A grey value proportional the average values is used for presenting image, black is equal to 0 and white is equal to 1.

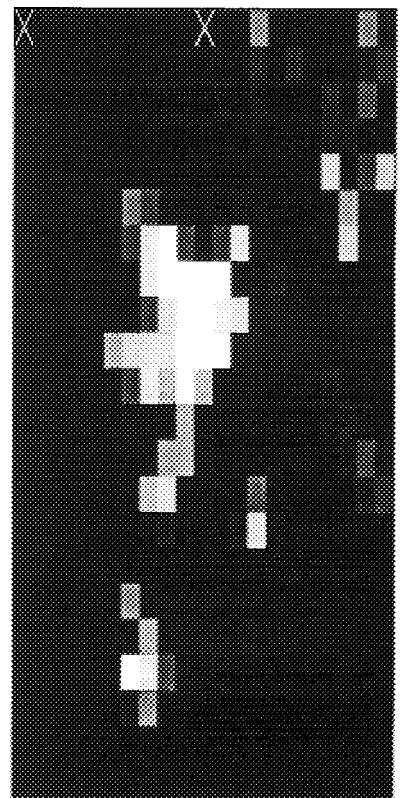


**Figure 8** 90 percentile

errors and statistical scattering in the results. On the images these effects are seen as a grey zone around white features. For the 90<sup>th</sup> percentile image, we see that there is one main area within the grid where levels exceed the 90<sup>th</sup> percentile and that all teams agree on this location, there is also a grey ‘halo’ around this location reflecting some differences in the spatial extent of the feature. There are also a number of other smaller features, where there is only limited agreement. For the 50<sup>th</sup> percentile image, it is clear that there is overwhelming agreement in the features, since the image is predominantly black and white. For the 10<sup>th</sup> percentile image, here are a few distinct white features which are spatially dispersed, but the image generally shows relative more dispersion in the grey scale. Further spatial analysis of the results is being undertaken.

The second objective of the preliminary analysis was to investigate the relationships between the different sets and to investigate any scaling issues.

### Investigation of the correlation in the results and exploration of the sources of variation

The correlations between all data sets based on all the data points in the grid were calculated and are shown in Table 4 below. It is clear that there are substantial correlations between a number of sets, with exceptions being notably sets 3,5 and 8 where correlations are low (with the exception of sets 3 and 5, both car-borne). Highest correlations are between sets 1, 2, 4 and 7 (all with similar detectors).

**Table 4: Correlation coefficients**

	set1	set2	set3	set4	set5	set6	set7
set2	0.863						
set3	0.456	0.493					
set4	0.838	0.941	0.472				
set5	0.648	0.560	0.946	0.534			
set6	0.603	0.633	0.293	0.625	0.495		
set7	0.827	0.930	0.512	0.935	0.569	0.660	
set8	0.231	0.280	0.305	0.227	0.175	0.211	0.259

It is seen that the correlation between the group of sets 1,2,4, and 7 (all airborne results) is good (exceeding 0.83). Correlations for set 6 with sets 1,2,4 and 7 are also high (typically greater than 0.6). Considering sets 3 and 5 (both car-borne systems) the correlation is also very good (0.946), but correlations between the air-borne and car-borne systems are generally low. The likely explanation is probably that the car-borne systems get a great deal of the measured signal from the road. The roads in area II were a mixture of asphalt and skit roads where the former presumably contains very little contamination. The cause for the poor correlation between set 8 and all others was investigated further. One possibility was a difference in the positioning, and as a result a different repositioning for data set 8 was tried and it was found that matching each position with the next but one measurement improved correlation with other sets. The correlations shown below are for set 8 after repositioning and show a marked increase.

set8	0.587	0.703	0.272	0.641	0.289	0.445	0.628
------	-------	-------	-------	-------	-------	-------	-------

We have also selected a number of scatterplots to illustrate the nature of the different relationships. Most plots show similar features, including more scatter in the results at lower

levels, and substantial linearity. Two contrasting examples are shown below in Figures 9 (sets 1 and 2) and 10 (sets 2 and 8).

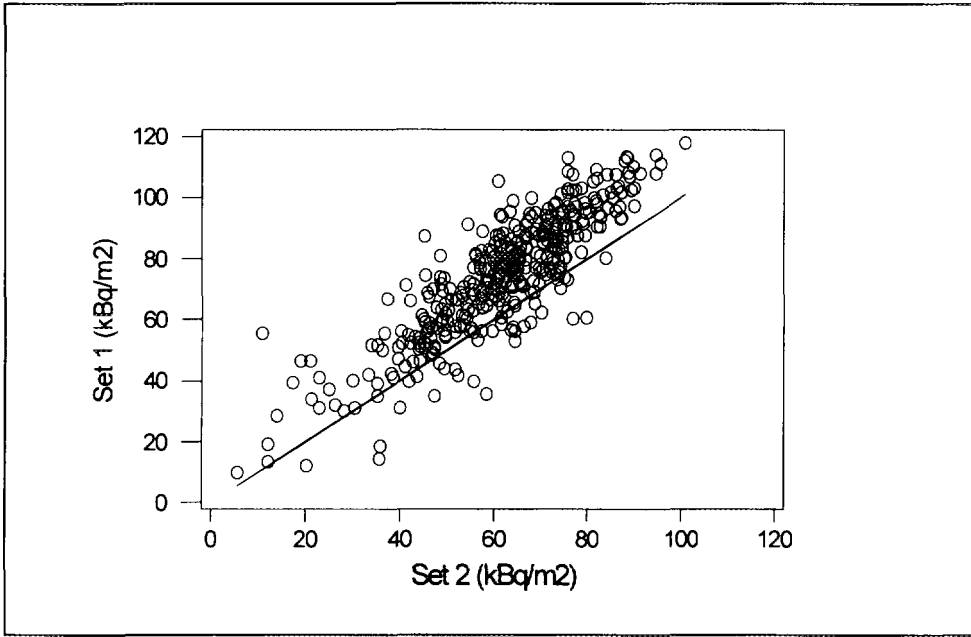


**Figure 9**

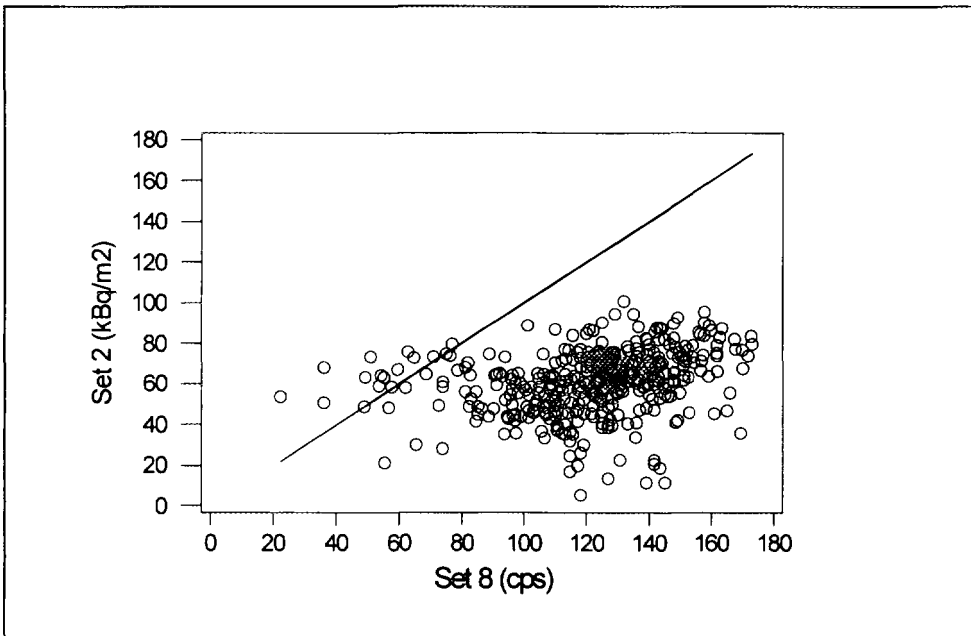


**Figure 10**

From the scatterplots we can see that sets 1 and 2 are clearly linearly related, but that sets 2 and 8 show no evidence of a linear relationship. In Figure 11, we show the relationship between the sets 2 and 8 after re-positioning of set 8.

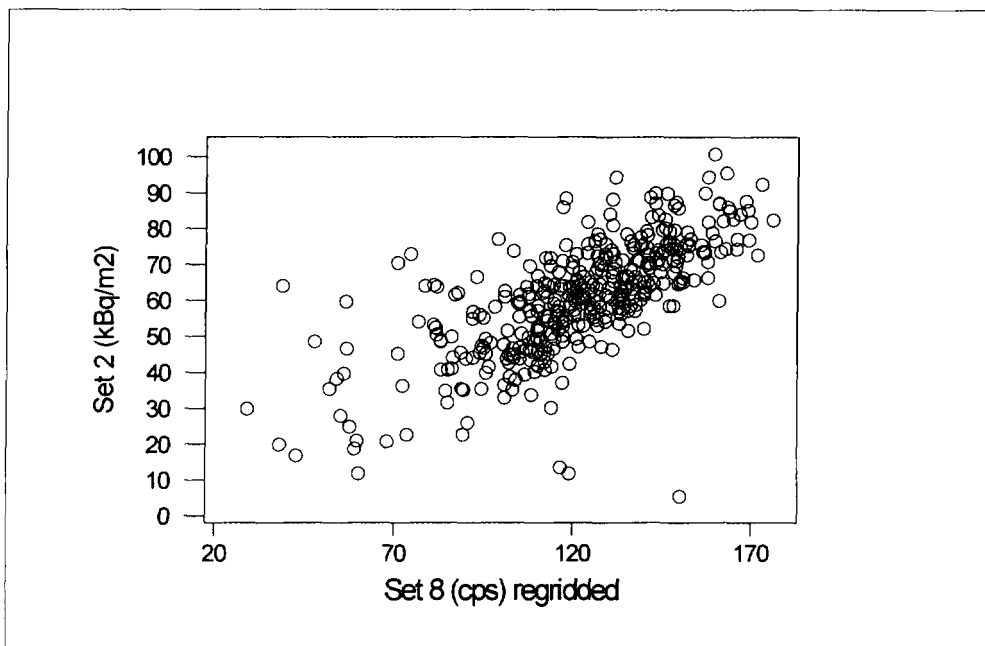


**Figure 11**

There has been a noticeable improvement in the relationship, and a clear linear relationship is evident. Existence of a linear relationship allows the possibility of the scaling the different sets and thus improving comparability in absolute terms. In the next section, we investigate the linear relationships.

### **Regression analysis**

For regression analysis, the data sets have been grouped into sets 1,2,4 and 7 (all air-borne NaI(Tl)), sets 3 and 5 (car-borne) and sets 6 and 8 (air-borne HPGe) and the results are discussed below.

#### **Case 1: Sets 1,2,4 and 7 (airborne NaI(Tl))**

All regressions involving these four sets gave highly significant results, with the percentage of variation explained ranging from 68.3 to 88.5%. Thus in conclusion, for these sets, there is evidence of a strong linear relationship. The linear models fit included an offset term and it is of interest to consider the estimated offsets, which if significantly different from zero, may indicate some small bias.

Significant offsets (i.e. different from zero) were found. The offsets ranged in value from 8 to 9 for (set 1 with 2, 4 and 7), 2 to 3 for (set 2 with 4 and 7) and 4 for sets 4 and 7. So for this group of 4 teams the offsets are all very small and statistically significant. Their practical significance of course depends on the lower limit of detection of the systems (which may be less than 2 kBq/m<sup>2</sup>).

**Case 2: Sets 3,5 (car-borne )**

The regression between the two car-borne teams is also extremely good with 89.3% of the variation explained using a simple linear regression allowing a calibration of nGy/hr to kBq/m<sup>2</sup>. A small offset (4) was found in the linear relationship.

**Case 3: Sets 6 and 8, (HPGe)**

No satisfactory relationships could be found between set 8 and any of the other sets (including set 6), until a re-positioning of that particular set had taken place. After re-positioning, the relationships did improve (in terms of % variation explained) but were still generally poorer than those seen in sets 1,2,4 and 7. It should however be remembered that both germanium detector data sets have used much longer integration times and this may explain the poorer correlations.

To conclude, there was strong evidence of significant linear relationships between at least some of the data sets (in particular 1,2,4 and 7 and 3,5). Where the relationship proved satisfactory (in terms of % variation explained), there were often significant though small offsets. Further investigation to explore the extent and reasons for the existence of such offsets is required, and this should be explored at finer spatial resolution than the level of re-gridded data currently under investigation.

In addition to considering the full spatial distribution, and the pointwise relationships between the different sets, we have also considered the comparability of results along flight lines. In this way, some of the effects of 'small scale' spatial variation have been removed.

**Summary of the flight lines**

Along each of the 21 flight lines, we have evaluated the distribution of the results and Figure 12 shows the mean level for each line for each of the teams. Table 5 summarises the statistics. It should be noted that some of the lines for a given data set have only few observations which will greatly influence the precision of the mean value and this is especially true for the two car-borne data sets.

**Table 5: Summary of flight lines**

	N	Mean	Median	St dev	Minimum	Maximum	Coeff of Variation (%)	25% quartile	75% quartile
set1	21	74.53	75.26	7.45	58.87	86.02	9.9	69.66	80.42
set2	21	61.64	63.24	6.48	49.02	71.40	10.5	59.11	65.35
set3	21	49.11	50.93	6.95	37.33	59.65	14.1	43.09	54.56
set4	21	59.03	60.13	6.45	46.16	69.46	10.9	56.35	62.53
set5	21	126.49	131.10	27.31	79.90	176.60	21.6	102.86	142.80
set6	21	65.97	66.18	7.06	52.05	74.77	10.7	60.49	72.33
set7	21	74.22	75.07	9.01	51.58	88.41	12.1	70.26	81.82
set8	21	122.07	123.07	8.82	104.72	138.01	7.2	115.64	129.60

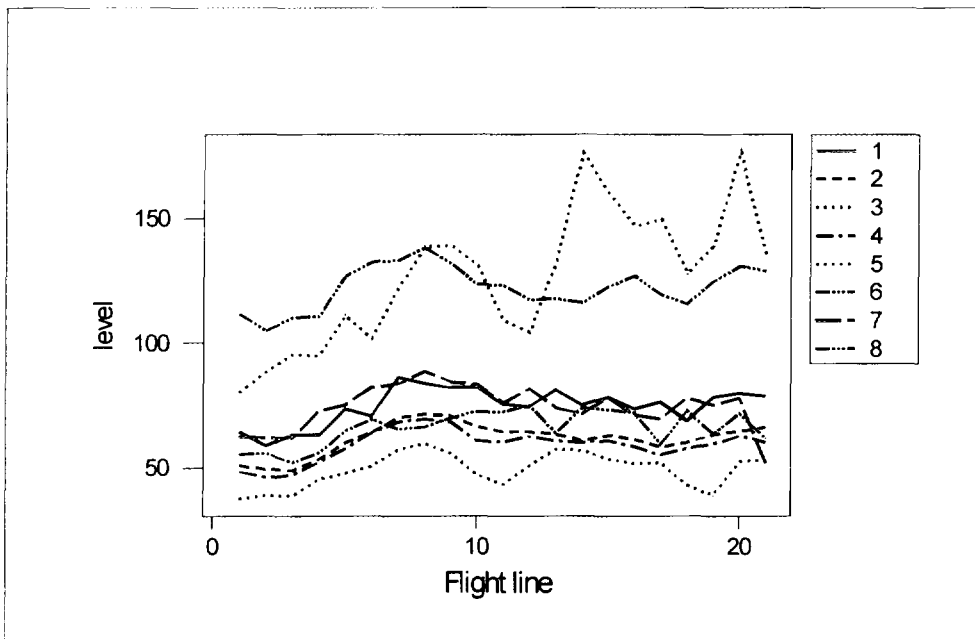


**Figure 12**

The coefficients of variation have been considerably reduced when compared to the equivalent figures in Table 2 with the exception of set 5.

The correlations between the different sets is shown in Table 6, with only few exceptions we see an improvement in the correlations compared to those in Table 4. The correlations for set 8 are substantially improved providing further evidence of positional difficulties in the original reporting of this set.

**Table 6**

	set1	set2	set3	set4	set5	set6	set7
set2	0.917						
set3	0.742	0.733					
set4	0.873	0.975	0.780				
set5	0.640	0.517	0.621	0.508			
set6	0.543	0.670	0.477	0.685	0.559		
set7	0.548	0.650	0.438	0.734	0.235	0.620	
set8	0.787	0.868	0.634	0.868	0.443	0.470	0.544

In addition to calculating correlations as above at lag 0, it is also possible to investigate the degree of shift to maximise these correlations (using the cross-correlation function). This has been done and in a few cases, the correlation is maximised at lags different from 0 (thus indicating again that there may be effects of small positional shifts in the data sets).

In addition, to the correlation it is possible to estimate the mean difference in level for those sets reporting results in  $\text{kBq/m}^2$ , this has been done using 95% confidence intervals and the results are reported in Table 7.

Table 7 : Mean difference(kBq/m<sup>2</sup>)

	set 1	set 2	set 3	set 4	set 6
set 2	12.9				
set 3	25.4	12.5			
set 4	15.5	2.6	-9.9		
set 6	8.6	-4.3*	-16.9	-6.9	
set 7	0.3*	-12.6	-25.1	-15.2	-8.3

\* indicates a non-significant result

It is clear from the table, that there are small, significant differences between the sets with the exception of sets 1 and 7 and sets 2 and 6.

### Conclusions and recommendations:

1. RESUME 95 has demonstrated conclusively that it is possible to integrate different mobile teams within the framework of emergency response. Over a period of a 1 and a half hours, each airborne team (3-8 hours for car-borne teams) was able to make a detailed survey of an area of roughly 3 km by 6 km. Contours maps were produced and presented at a seminar three days after the survey. Data delivered to the organisers however indicates that data processing can be carried out at the same rate or higher as the data collection. These are indeed very impressive results.
2. Analysis of the results has however indicated the existence of some general difficulties in comparing data sets with quite different spatial attributes, so that although the main features are identified by all the teams, there still remain some additional work to ensure full integration of different types of systems. Further analysis of data from the calibration area (area I) may help provide a better understanding of these difficulties and suggest some solutions.
3. These difficulties notwithstanding, it is clear that similar features have been identified as, seen in the grey scale plots. Thus on a relative scale there is good agreement between the air-borne systems.
4. The distributions of results (with the exception of set 5) all show a similar range but also some different features. It is noticeable that the distributions all show a long left tail, and more scatter at the lower end. There is however convincing evidence of comparability of results in relative terms.
5. Investigation of the relationships between team results has shown high degrees of linearity (correlations up to 0.95) but that there is a need for scaling of results, and interestingly estimated linear relationships in some cases have shown evidence of small, but systematic differences. It is clear that causes of these differences need to be further investigated (possible sources include calibration and assumptions about depth distributions).
6. Further investigation of the comparability, based only the flight line summaries has also shown the existence of offsets between team. Thus before we are able to claim complete comparability, it is important to improve our understanding of the spatial characteristics of the equipment and of the calibration procedures adopted.
7. The comparison and interpretation of results from air-borne, in-situ and soil sampling techniques also requires more detailed study to enhance our understanding of the relationship between in-situ, soil samples and aerial results. Further investigation of area I (calibration site) is underway.

RESUME-95 has indeed shown that the air- and car-borne measuring techniques tested are consistent, nevertheless some problems have been exposed which require to be resolved. These problems may be categorised into two groups; the first concerns the environmental radioactivity field and its spatial properties and hence its interaction with the sampling and positioning of the instruments; the second concerns the basic problem of measurement of radioactivity and includes aspects of calibration, background correction, spectral stripping etc.). The former is a problem which has implications not only for mobile techniques, but for all general means of mapping radioactivity and so is a general sampling problem. For mobile techniques, the problem presents itself due to the spatial averaging implicit in the techniques. The lessons learned from RESUME 95 indicate that there is a need for a further European operational exercise, and that in future exercises, both problems should be addressed through careful design of the exercise and choice of the areas to be surveyed. It is possible to make a number of recommendations for such exercises on the basis of our experience in RESUME 95.

1. Some aspects of the spatial problems could be examined by surveying the same line a number of times, to examine variations.
2. Difficulties with accurate and precise positioning could also be improved by introducing checkpoints (e.g. known radioactive sources at set locations).
3. To investigate the so-far unresolved question of systematic offsets, it might be possible to identify an area where the radioactivity field has homogeneous properties on the scale finest to coarsest spatial resolution of the monitoring systems in question.
4. For trials under operational conditions, it would be useful to identify areas with a wider range of activity concentrations than those seen in Area II and include nuclides other than Cs-137.
5. Technical questions including calibration, background corrections, effects of depth distribution and the uncertainties of the estimated distributions should also be addressed..

RESUME 95 has clearly shown the capabilities and comparabilities of the existing European mobile teams, but it has also highlighted the need within the development of a pan-European integrated mobile system for nuclear emergencies for further development of standardisation procedures, including calibration. It is important, that such exercises be continued to ensure that (as in any measurement technique), the results being produced are directly comparable and so can be used in off-site emergency management.

**NEXT PAGE(S)  
left BLANK**

# **APPENDIX 1: The Exercise Plan**

**NEXT PAGE(S)  
left BLANK**

EKO3

## EXERCISE RÉSUMÉ 95

### Rapid Environmental Surveying Using Mobile Equipment.

#### 1. PURPOSE OF THE EXERCISE

##### 1.1 The major purposes of exercise RÉSUMÉ 95 are

- to investigate the possibility of multilateral assistance by transferring equipment and operating staff in case of accidents involving dispersion of radioactive material,
- to test the ability of the existing measuring systems available in the Nordic countries with different airborne, carborne and in-situ instruments to map a radioactive contamination, in this case from the Chernobyl fallout, and
- to test exchange of data and to establish if comparable results can be obtained with the different systems.

##### 1.2 In order to obtain further standards of reference, measuring systems from Canada, France, Germany and Scotland, besides several Nordic teams, will participate in the exercise.

#### 2. ACCOMPLISHMENT OF THE MEASUREMENTS

##### 2.1 The measurements are planned to take place between 15 August and 17 August, the 18 August will be in reserve for measurements, otherwise it will be used for presentation of results.

##### 2.2 The measurements will take place in three different areas known as area I, II and III

###### Area I: see enclosed map 1

The area is a part of VESIVEHMAA airfield and is used for intercomparison and other controlled measurements. A number of soil samples have been taken in the area. The results of the analysis will be available for the participants just before the exercise. The contamination level at the airfield is about  $50 \text{ kBq/m}^2$   $^{137}\text{Cs}$ .

###### Area II: see enclosed map 1, details fig. 1a and area II

The 3 km by 6 km area was contaminated during the first few days after the release from Chernobyl. The original contamination was not established in detail at once, but a later survey established that a strong contamination had taken place and there is still a general

level of approximately 50 kBq/m<sup>2</sup> (<sup>137</sup>Cs) present. The contamination is not homogenous and may differ a great deal from place to place.

The landscape is mainly covered with forest (coniferous and birch trees) but the density of the trees changes very much. In some places there are bogs or swampy areas. In other places there are rocky ground or big boulders (Iso kivi). In many places there are steep gradients in the terrain even if the differences in height are seldom more than 50 m within each square kilometre.

There are some minor lakes and some of the slopes of the edges of the lakes are quite steep.

There are small cultivated areas in the neighbourhood of the villages AUTOINEN and VESIJAKO.

Only a minor part of the roads in the area have hard surface and the earth roads are often narrow, but two-wheel driven vehicles can drive on most of the earth roads.

**Area III: see enclosed map 1, details fig. 1b and area III**

The 1 km by 5 km area is probably contaminated to the same degree as area II, but besides this a number of radioactive sources have been hidden in the area.

### 2.3 Airborne measurements

The intention with the airborne measurements is to let the 11 participating measuring systems fly three different missions covering the areas, named I, II, and III.

The airborne measurements are to be carried out using standard technique that is known and practicable when a contamination is required to be mapped and when radioactive point sources are to be recovered.

Afterwards the measuring results will be compared with the purpose to establish whether the same picture of the contamination is obtained by the different systems.

#### **Mission over area I**

The area is used for crosscalibrating the airborne systems. Helicopters should measure at ground level and then hover for a few minutes at 10 m, 25 m, 50 m, and 75 m over a marked hexagonal grid. Fixed wing aircraft can fly a number of times over the same area at the same altitudes.

**Mission over area II**

The area is surveyed by each airborne team. Predefined parallel lines with a line spacing of 150 m are to be flown. A total of 21.6 km lines plus 20 turns adds up to a total of approximately 200 km flying distance. The flying height should be about 200 feet above ground level.

When this survey is completed the flying teams shall fly along a road to area III in order to find a hidden radioactive source placed somewhere near the route.

**Mission over area III**

All teams shall plan and conduct the search for the radioactive sources as they find adequate and report the position in co-ordinates to the DISTAFF, when they find a source.

For further details see appendix AIR.

**2.4 Carborne measurements****Mission in area I**

The area is used for calibrating the different systems.

**Mission in area II**

The measuring teams are expected to collect measuring data from all the roads that are marked on the special road map.

For further details see appendix CAR.

**2.5 In-situ measurements****Mission in area I**

The area is used for intercomparison of the different systems. A number of sites will be marked by poles. At each such site a reading is to be taken.

**Mission in area II**

The measuring teams are expected to measure at least in two fixed points. Besides these two points a number of sites might be specified for further measurements. Each team is then free to take as many measurements as they wish within area II.

For further details see appendix IN-SITU.

## 2.6 Reporting and presentation of results

All participating institutions are expected to give a presentation of their results at the end of the exercise. The figures of interest are  $^{137}\text{Cs}$  and  $^{134}\text{Cs}$  (preferably in  $\text{Bq/m}^2$ ), U, Th and  $^{40}\text{K}$  (preferably in  $\text{Bq/kg}$  and dose rate if possible). The official co-ordinate system used is Longitude, Latitude in WGS-84.

A simple X-Y-Z format has been defined for easy exchange and comparison of results. Raw data, including a full written description of the data format, can be delivered to a common data pool. Each team who delivers data to this pool will be given access to all data.

See appendix DATA for details about data exchange.

## 2.7 Detailed plan for the measurements

The airborne measurements are described in appendix AIR.

The carborne measurements are described in appendix CAR.

The In-situ measurements are described in appendix IN-SITU.

The exchange of data is described in appendix DATA.

In order to reach all the planned activities it is necessary to follow the time schedule as closely as possible

## 3. EXERCISE ARRANGEMENTS

### 3.1 Responsibilities

All participating institutions are responsible for insurance of their own personnel.

All participating institutions are responsible for shipping, operation, safety, security and insurance of their own equipment.

NKS can not be held responsible for any kind of injuries to personnel or damage to equipment or property caused by the participants during the exercise or in connection with the exercise.

### 3.2 Travelling expenses to and from Finland

Authorities and institutes, which send personnel to participate in or observe the exercise will pay all travelling expenses according to own existing rules.

### 3.3 Transport in the exercise area

It is desirable, that participants in the exercise to the greatest possible extent can be transported in own service cars or if that is not possible in rented cars in the exercise area. Four wheel driven cars can be suggested, especially for carborne measuring teams, when measuring in area II.

A minor number (2-3) of vehicles with drivers may be made available for the exercise direction from the Finnish authorities.

### 3.4 Accommodation and meals

Quarters and meals are to be paid for by every single person.

#### Quarters.

Hotel TALLUKKA in Vääksy, 20 km North of Lahti, is the only hotel in the area that can room the expected number people to the exercise. The distance to area I is less than 10 km. The distances to area II and III are about 35 km and 40 km.

Hotel TALLUKKA can offer rooms to reduced prices (140 FM per person in a double room/225 FM per person in a single room) to all participants in the exercise. It is suggested that institutions book hotel rooms for the people they send to the exercise.

Telephone to TALLUKKA is +358 18 68 611 or

+358 18 88 881

Telefax to TALLUKKA is

+358 187 661 529.

In the neighbourhood of the hotel there is a shopping centre.

#### Meals.

Breakfast is included in the price. The restaurant in hotel TALLUKKA can serve other meals.

## 4. DIRECTION OF THE EXERCISE

The exercise will as the main principle follow the detailed plan described in section 2 and in the appendices AIR, CAR and IN-SITU.

However, it is not possible to foresee the nature and the amount of problems, that may arise during the exercise. It is found necessary to establish a staff element that can see to that the plan is followed, ensure that the planned activities are carried out and intervene if something goes wrong.

#### 4.1 The Directing Staff

A directing staff (DISTAFF) with representatives from the Nordic countries will be established at Hotel TALLUKKA in Vääksy and it will be operational from about noon August 12.

The DISTAFF has functions in relation to

- the measuring teams,
- all other participants in the exercise and
- the public.

#### 4.2 Relations between DISTAFF and measuring teams.

The DISTAFF

- prepares checklists for all the activities, that are planned,
- keeps a log for all incoming information from the measuring teams,
- gives starting signals to the measuring teams, when they are ready to start their tasks,
- can delay a team if a previous team has not finished its task,
- calls for assistance from rescue service in case of accidents.
- rescue service and police are called for by dialling 112.

The MEASURING TEAMS from the different institutions shall report to the DISTAFF

- when they are ready to move from one area to another,
- when they are ready to take off on a measuring task,
- when a measuring task is finished,
- if a measuring task takes longer time than planned,
- if there are problems with the measuring platforms (aeroplane or vehicle) and the measuring instruments,
- in case of air or road accidents (injuries to persons and damage to equipment, place, time, whether rescue service is needed or already requested).

#### 4.3 Relations between DISTAFF and other participants in the exercise

The DISTAFF will inform teamleaders each day at 0645 verbally at a morning briefing in the conference room at TALLUKKA about

- the weather forecast for the day and the following day,
- changes in programme for the exercise,
- other information.

This information will also be distributed in writing and placed on a poster at the DISTAFF office.

The DISTAFF will distribute incoming mail and establish a mailbox for outgoing mail.

#### **4.4 Relations to the public**

The DISTAFF shall be able to inform the media (written press, radio and TV), visitors and observers to the exercise about the plan for and progress of the exercise. Information to the media is preferably given to groups at certain prearranged hours.

In case of accidents with injuries to personnel names are not released before relatives have been informed.

### **5. COMMUNICATIONS**

- 5.1 A telephone catalogue with all relevant numbers is given in appendix COM.
- 5.2 Communications between the DISTAFF and exercise participants will preferably take place via the switchboard in the TALLUKKA and mobile telephones.
- 5.3 Communications between exercise participants will take place via mobile telephones.
- 5.4 Telefax communication to and from the DISTAFF will be possible via the switchboard in TALLUKKA.
- 5.5 Communications between the airfield tower and aeroplanes will take place via VHF radio on channel 123.40 MHz.
- 5.6 Communications between the DISTAFF and the airfield tower is by telephone.

GEOLOGICAL SURVEY OF FINLAND  
Jukka Multala

KARAIR OY  
Niilo Erkinheimo

## Airborne measurements RÉSUMÉ 95

### 1. Cs fallout mapping

Place

Area II

Measurements

The teams should map the Cs fallout on area II using 150 meters flight line separation and the nominal flight altitude of 200 feet above any obstacle. The flight altitude is permitted in a letter from the Finnish Civil Aviation Administration:

#### **Finnish Aviation Administration/Flight Safety Authorities**

**Subject:** Permission to fly minimum flight altitude:

- in Area II and Area III the lowest altitude is 200 feet above any obstacles,
- the flight should be done so that no danger is caused to third parties or their property and without causing unnecessary noise,
- the aviation authority should be kept informed about any flight below minimum flight altitude including area, time and aircraft,
- any flight below flight altitude only the necessary personnel are permitted to be in the aircraft.

The flight lines are numbered from 101 to 121 and the co-ordinates of each flight line in WGS-84 co-ordinate system are given below. Airphotos (in the scale 1:10 000) will be available on which the flight lines are drawn.

Line	Latitude			Longitude		
no	DD	MM	SS.SSSS	DD	MM	SS.SSSS
101 SOU	61	18	16.0761	25	2	3.1168
101 NOR	61	21	13.1615	25	4	45.0686
102 SOU	61	18	14.132	25	2	12.324
102 NOR	61	21	11.2144	25	4	54.2874
103 SOU	61	18	12.1877	25	2	21.5309
103 NOR	61	21	9.267	25	5	3.5059
104 SOU	61	18	10.2427	25	2	30.8047
104 NOR	61	21	7.319	25	5	12.7914
105 SOU	61	18	8.2981	25	2	40.0109
105 NOR	61	21	5.3713	25	5	22.0092
106 SOU	61	18	6.3528	25	2	49.284
106 NOR	61	21	3.4229	25	5	31.294
107 SOU	61	18	4.4079	25	2	58.4896
107 NOR	61	21	1.4749	25	5	40.5112
108 SOU	61	18	2.4304	25	3	7.6939
108 NOR	61	20	59.4944	25	5	49.727
109 SOU	61	18	0.4851	25	3	16.8988
109 NOR	61	20	57.546	25	5	58.9435
110 SOU	61	17	58.5396	25	3	26.1035
110 NOR	61	20	55.5975	25	6	8.1598
111 SOU	61	17	56.5935	25	3	35.375
111 NOR	61	20	53.6482	25	6	17.443
112 SOU	61	17	54.6153	25	3	44.5779
112 NOR	61	20	51.667	25	6	26.6574
113 SOU	61	17	52.6688	25	3	53.8488
113 NOR	61	20	49.7174	25	6	35.94
114 SOU	61	17	50.7227	25	4	3.0522
114 NOR	61	20	47.7682	25	6	45.1549
115 SOU	61	17	48.7763	25	4	12.2553
115 NOR	61	20	45.8188	25	6	54.3696
116 SOU	61	17	46.8298	25	4	21.458
116 NOR	61	20	43.8692	25	7	3.5839
117 SOU	61	17	44.8831	25	4	30.6604
117 NOR	61	20	41.9194	25	7	12.7979
118 SOU	61	17	42.9357	25	4	39.9297
118 NOR	61	20	39.969	25	7	22.0788
119 SOU	61	17	40.9887	25	4	49.1315
119 NOR	61	20	38.0188	25	7	31.2922
120 SOU	61	17	39.0409	25	4	58.4001
120 NOR	61	20	36.068	25	7	40.5725
121 SOU	61	17	37.0935	25	5	7.6013
121 NOR	61	20	34.1176	25	7	49.7852

## 2. Location of point sources

Place Area III and the road from Area II to Area III

Measurements After mapping the Area II the flight should continue along the road 43-100 (see details in measurements using cars fig 1b). Each team can use a flight pattern/line spacing of their own choice on Area III in order to locate as many point sources as possible. The only restriction is that both the Area II and III should be flown during one flight. If some team will like to fly several flights that might be possible after every team has made their first flight.

The corner co-ordinates of Area III in WGS-84 system:

	DD MM SS.SSSS	DD MM SS.SSSS
South West	61 18 50.1585	24 58 2.3057
South East	61 18 49.6755	24 59 9.4940
North West	61 21 31.1806	24 59 14.5730
North East	61 21 31.6644	24 58 7.2886

## 3. Calibration of equipment

Place Area I (Vesivehmaa airfield)

Measurements Calibration of the instruments can be done at the Area I after the main measurement flight. The detailed description of area I is given in "measurements using cars".

## 4. Reporting

A) Immediately after the measurement flight the teams will report to the representative of the organising committee at the airfield, who will forward the information to the DISTAFF the number and the locations of the detected point sources.

B) Each team will have 24 hours to process their data to the extent that is possible for them. After that each team should present their results concerning Areas II and III in the DISTAFF. (Details and hints see "Measurements using cars/4. Reporting).

## 5. **Flight directive**

### 5.1 **General arrangements**

The aim of this flight directive is to help the teams/pilots to operate during the RÉSUMÉ 95 exercise. It should be understood that this flight directive does not in any respect minimise the responsibilities and obligations of the pilots. The pilots are fully responsible of the safety of the flights. The teams shall indemnify and hold harmless the organising committee against all claims and demands.

The Vesivehmaa airfield will be used as base. The length of the runway is 1100 metres and the width 30 metres. The airfield is located about 120 km North from Helsinki.

There will actually be three different areas where airborne measurements will be carried out:

- Area I is Vesivehmaa airfield.
- Area II is 3 x 6 km, which should be mapped using 150 metres line spacing.
- Area III is 1 x 5 km, where several artificial sources will be hidden and every team has to try to find as many of them as possible. The team can use a flight pattern/line spacing of their own choice.

Distance from Vesivehmaa airfield to area II is about 37 km, from area II to area III about 3 km, and from area III to airfield 43 km.

At least the following maps will be available in hotel TALLUKKA:

- Air photos in the scale 1:10 000
- Topographic maps in 1:20 000
- Road map in 1:200 000

Unfortunately we have to charge the costs of the maps from each team.

The routes to Area II and from Area III will be arranged so that background measurements over water (lake) are possible if needed.

## 5.2 General description of Vesivehmaa airfield

Vesivehmaa airport is unmanned and mainly used by general aviation. Airspace classification is G.

Airspace in operation area is uncontrolled up to 4 500 feet QNH. Above that level are airways which are controlled by ACC (127.100).

Radio frequency for the airfield is 123.40 MHz.

## 5.3 Measurement flights

The measurement flights will be made in according to the schedule below (local times, UTC + 3h). However it should be noted that before take off the prior team must report that they have left area II.

Tuesday August 15, 1995

Take off	Team/country	Landing
08:00	SURRC/UK	11:00
09:30	DEMA/DK	12:30
11:00	C.E.A.-D.A.M./F	14:00
12:30	SGU/S	15:30
14:00	NGU/N	17:00
15:30	SSI/S	18:30

Wednesday August 16, 1995

Take off	Team/country	Landing
08:00	BfS/GER	11:00
09:30	NILU/N	12:30
11:00	ARMY/FIN	14:00
12:30	STUK/FIN	15:30
14:00	GSF/N	17:00

The flight routes to and from the measurement areas as well as report points/sites are presented in visual navigation charts, that are available for the flight crews at the DISTAFF at latest the day before the flights. During the measurement flights pilot will report to the Ground Station when entering and leaving area II and when leaving area III.

**5.4 Platform arrangements**

Parking can take place on free sites/no special places reserved.

The only fuel type normally available is 100 LL petrol from a petrol gauge automate, operating with Neste company's credit card. For those teams who need 100 LL petrol and don't have Neste company's credit card GSF/Karair will organise such and will invoice the teams afterwards.

Jet A1 fuel will be arranged according to the need, at the price of 2.31 FIM/litre. Shell credit card is honoured as well as cash

**5.5 Weather information**

Weather information will be available by text television, telephone and fax.

**5.6 Flight plans**

Final flight plans will be prepared by the organisers the day before the flights.

FINNISH CENTRE FOR RADIATION AND NUCLEAR SAFETY  
Harri Toivonen

## Measurements using cars RÉSUMÉ-95

### 1 <sup>137</sup>Cs fallout measurement and location of a point source

*Place* Area II and a road from area II to area III

*Time* Tuesday and Wednesday, 15 - 16.8

*Measurements* The teams drive systematically along all the roads in area II and measure the <sup>137</sup>Cs deposition. A short sampling time should be used ( $\leq 10$  s) for comparing results. The roads are numbered and segmented in such a way that the results ( $y$ ) can later be presented as curves  $y = f(x)$ ;  $x$  refers to distance (km) from a certain fixed point. For the labels see Fig 1. The junctions or the end points of the roads are numbered from 1 to 100. The teams should drive as many of these roads as possible. For more detailed fallout mapping, <sup>137</sup>Cs deposition near other roads and paths can also be studied, particularly if the car is a four wheel drive. Minimum requirement is, however, the survey along the following roads:

<u>Name</u>	<u>Locations</u> (start - stop)
Road 1	43-100
Road 2	44-24
Road 3	29-39
Road 4	78-83
Road 5	46-85

The results of the scanning should be stored in separate files for later comparison.

One source is hidden near the road 1 from area II to area III (78 - 100). The survey of locating the source should take place on Tuesday or Wednesday afternoon (later than 15:00). The road 1 should be scanned twice: (1) from 43 to 100 with average velocity of  $50 \text{ km h}^{-1}$  and (2) from 100 to 43 with average

velocity of 30 km h<sup>-1</sup>. The teams are not allowed to stop during these two surveys.

Other measurements can be performed at any time chosen by the teams.

## 2 Crosscalibration of equipment

*Place* Area I (Vesivehmaa air field)

*Time* Thursday morning 17.8

*Measurements* The instruments in the vehicles are calibrated against the known <sup>137</sup>Cs distribution of the grass field (about 50 kBq m<sup>-2</sup>), i.e. calibration factors cps/(Bq m<sup>-2</sup>) are measured for NaI and HPGe detectors (Fig 2). Typical measuring time is 5 - 10 min.

Soil samples have been taken in advance from 31 locations (see Fig 3 and Table 1). The depth distribution of the activity is also available. The results of these studies are given to the measuring teams before the exercise.

## 3 Estimation of detection limits for point sources

*Place* Area I (Vesivehmaa air field)

*Time* Thursday morning 17.8

*Measurements* A <sup>137</sup>Cs point source of known activity (1.85 GBq, 50 mCi) is used to measure detector responses at the following distances (m): 10, 20, 40, 60, 100, 150, 200. At each distance two speeds are used (20 kmh<sup>-1</sup> and 50 kmh<sup>-1</sup>). A background measurement (5 min) is performed at the location where the distance between the source and the car is shortest (point C, Fig 4 and Table 2).

## 4 Reporting

(1) *A fallout map of area II.* Free style of presentation

(2) *A fallout map of area II.* Point presentation, i.e. each measurement refers to one coordinate point that is coloured using 8 different categories. This point should refer to the middle of the sampling interval. The lower border lines of the fallout categories are defined as

$$F_{\min} + (F_{\max} - F_{\min})n/8, \quad n = 0, 1, \dots, 7$$

where  $F_{\min}$  is the lowest value and  $F_{\max}$  the highest value for the measured quantity describing fallout (cps, kBq m<sup>-2</sup>,...).

The following colours should be used if possible:

<u>Category</u>	<u>Colour</u>
7	purple
6	red
5	light red
4	orange (red)
3	orange (yellow)
2	yellow
1	green
0	blue

This colour presentation can be prepared in the DISTAFF using facilities and software provided by STUK. Ms. Tarja Ilander and Mr. Arto Leppänen operate the desk top mapping system (MapInfo). However, the users have to supply their data in the X,Y,Z format described by Jens Hovgaard.

(3)  $y = f(x)$  presentation of the profiles for the roads 1 - 5.

(4) Location and identification of the source. Immediately after the detection of the source the coordinates and information about the source (nuclide and its activity) should be passed to the DISTAFF.

(5) Detection limits. This analysis is a home work. The results are given in conference that is organised later during autumn 1995.

**Table 1. Hexagonal sampling pattern in the Vesivehmaa air field in Finnish KKKJ-3 coordinate system (see Fig 3).**

```

ORIGIN 3429857.2 6782711.0
ORIGIN 3429857.9 6782708.7
ORIGIN 3429859.0 6782711.1
ORIGIN 3429858.5 6782709.8
3,1 3429882.2 6782687.1
3,2 3429852.4 6782677.7
3,3 3429826.9 6782701.5
3,4 3429832.4 6782731.5
3,5 3429865.2 6782741.2
3,6 3429888.8 6782718.0
4,1 3429953.1 6782624.4
4,2 3429833.8 6782584.3

```

4,3	3429733.7	6782678.0
4,4	3429761.4	6782794.1
4,5	3429889.4	6782831.9
4,6	3429978.7	6782747.6
5,1	3430048.4	6782538.9
5,2	3429803.8	6782457.9
5,3	3429606.1	6782647.0
5,4	3429666.7	6782879.8
5,5	3429920.6	6782959.9
5,6	3430104.4	6782783.6

5,i - 256 m circle

4,i - 128 m circle

3,i - 32 m circle

**Table 2. KKKJ coordinates for control points at the Vesivehmaa air field. These location are used in test 3.**

A	3429551.53	6782340.47
B	3429583.41	6782641.90
C	3429568.31	6782532.96

SWEDISH RADIATION PROTECTION INSTITUTE  
Division of Environmental Radiology  
Hans Mellander

## Measurements with in-situ gamma spectrometry systems RÉSUMÉ-95

### 1. General instructions

Each team brings all equipment necessary for the measurements. Maps will be supplied by the organizers. Each team arriving by car is expected to bring their own supply of liquid nitrogen. A limited quantity of liquid nitrogen will however be available. Soil sampling can be made anywhere but is especially encouraged in area II. The measurement strategy is decided by each team but directions and recommendations from the organizers should, if possible, be followed. The location of each point should, if possible, be reported in WGS-84 coordinates, alternatively in local Finnish coordinates (KKG3). Results may be reported in any format but using the format specified in appendix DATA is encouraged at least for the most essential information.

### 2. Measurements

#### 2.1 Measurements in area I

In area I which is a grass field at the Vesivehmaa air field detailed in-situ measurements will be made in a hexagonal grid where each gridpoint is marked with a wooden pole. A more detailed description of the area can be found in the CAR appendix.

Task 1: To measure at 19 specified grid points. All teams should measure at these points. The time needed to complete this task is 5-6 hours, using integration times around 1000 s. Soil samples may be taken but the organizers will provide soil data for the field. The field will be available for measurements Tuesday, Wednesday and Thursday afternoon. On Tuesday and Wednesday the airborne measurements will take place but the central parts of the grid can be measured before the first aircraft arrives around 11 am.

Task 2: To estimate the activity of a source lying on the ground. The time needed for this exercise is ½-1 hour. This exercise is planned for Thursday afternoon.

Task 3: To estimate the activity of a buried source and its depth below the soil surface. The time needed for this exercise is ½-1 hour. This exercise is planned for Thursday afternoon.

Task 4: To measure at 10 points or more selected by the team. The time needed for this task is 2-3 hours.

## 2.2

### Measurements in area II

The area is described in appendices AIR and CAR.

Task 1: To measure 2-3 points selected by the organizers all of them marked with a wooden pole. At these points the procedures of each team should be followed. This means that more than one detector position may be used but one of them should be at the wooden pole exactly. The total time for this task is 3-5 hours. The measurements can be performed at any time.

Task 2: To estimate and map the fallout in area II and to produce a fallout map over the area. The total time for this task depends on the ambition and the time available. The measurements can be performed at any time.

## 3.

### Calculation and reporting of results

A preliminary report containing a selection of the following results shall be delivered to the organizers on Friday (last day). The most important variables are Cs-137 assuming a plane distribution, natural nuclides assuming uniform distribution and dose rate. The format specified in the DATA appendix should be used for the preliminary report. Each team has the possibility to recalculate and adjust the results before 15th of October 1995. The final report shall include data on the measurement system, calibration method and if soil samples have been taken results from these as well. The uncertainty of each result should be calculated and reported as well. If separate dose rate measurements have been made these results should also be reported.

All teams are encouraged to report at each point:

- Cs-137 activity assuming plane, uniform and real source distribution
- Cs-134 activity assuming plane, uniform and real source distribution
- activity assuming uniform source distribution
- U-series activity assuming uniform source distribution
- Th-series activity assuming uniform source distribution

- Cs-137 dose rate assuming real source distribution
- Cs-134 dose rate assuming real source distribution
- dose rate assuming uniform source distribution
- U-series dose rate assuming uniform source distribution
- Th-series dose rate assuming uniform source distribution
- Dose rate sum
- Integrated dose from 1995-2045 (50 years) assuming real source distribution for whole period
- and for area II:
- Cs-137 average activity assuming plane, uniform and real source distribution
- Cs-134 average activity assuming plane, uniform and real source distribution
- average activity assuming uniform source distribution
- U-series average activity assuming uniform source distribution
- Th-series average activity assuming uniform source distribution
- Average dose rate from fallout and natural activity respectively
- A fallout map of the area

DANISH EMERGENCY MANAGEMENT AGENCY  
Nuclear Inspectorate  
Jens Hovgaard

## Data Exchange Format RÉSUMÉ-95

### 1. Reporting and presentation of results

All participating institutions are expected to give a presentation of their results at the end of the exercise. The figures of interest are primarily  $^{137}\text{Cs}$  and  $^{134}\text{Cs}$  (preferably in  $\text{Bq/m}^2$ ), and secondly U, Th and  $^{40}\text{K}$  (preferably in  $\text{Bq/kg}$ ). The official co-ordinate system used is Longitude, Latitude in WGS-84.

### 2. X-Y-Z format

A simple X-Y-Z format in clear text has been defined for easy exchange and comparison of results. Each text line is defined as all characters between consecutive line breaks. A line break is composed of the two ASCII characters 13 and 10 (or begin and end of file). Two types of lines exist data lines and comment lines. Data lines are defined as lines where three or more numbers in free format separated by space(s) (ASCII 32) can be read. It is recommended that comment lines begins with the “/” character. The first and second values (X and Y) are used in general as geographical co-ordinates, and the following Z values are measured figures. In case of missing values they should be represented as -9.99E+99.

In the following some examples of data and comment lines are given. The | symbol is used in the following to indicate beginning end ending of lines, symbols like <SPACE> or <ASCII(32)> indicates special characters:

|61.2<SPACE>25.1<SPACE>120| is thus a data line, whereas

|This is a text 1 2 3 4| is a comment line. The lines

|61<SPACE>25.1<SPACE>23.0E05|,

|61E03<SPACE>-0.3<SPACE><SPACE><SPACE>23.0E05<SPACE>111.1|,

|61<SPACE>25.1<SPACE>23.0E05<SPACE>123.01<SPACE>;comment line 1| are all data lines.

A file should look similar to this:

```
//COMMENTS This file contains surface concentrations of 137-Cs in Area II
//The X-Y co-ordinates are given in decimal degree longitude and latitude in
WGS-84
// The values are given in kBq/m2
//
61.103      25.01  35.1
```

```
61.110      25.02  41.3
61.119      25.05  39.0
// COMMENT end of file
```

**or**

```
//COMMENTS This file contains concentrations of various nuclides in Area II
//The X-Y co-ordinates are given in decimal degree longitude and latitude in
WGS-84
// The first value is given in 137-Cs kBq/m2
// The 2nd value is given in 40-K Bq
// The 3rd, 4th and 5th value are UTC time hour min sec
// N      E      Cs      K      hour  min  sec
61.103    25.01  35.1  11.3   8     31   0
61.110    25.02  41.3  12.0   8     32   0
61.119    25.05  39.0  13.1   8     33   0
// COMMENT end of file
```

### 3. **Raw data**

Raw data, including a full written description of the data format, can be delivered to a common data pool. Each team who delivers data to this pool will be given access to all data. Such an exchange of data can be very useful for special studies like spectral analysis. Any restriction on delivered data has to be given in writing. If a restriction is given then it enters into force both with respect to the delivered as well as any received data.

## List of Participants in RESUME95 and Contributors to the Publication

CANADA	Grasty, Bob	3924 Shirley Avenue Gloucester, K1V 1H4 Ontario
	Cox, John R.	Exploranium 264 Watline Avenue Mississauga, Ontario, Canada L4Z 1P4
DENMARK	Jensen, Johs	Jensen Consult Virumvej 108B DK-2830 Virum
	Lund, Birger Olsen, René	Kanal 2 Forsvarets TV Mileparken 20 A DK-2740 Skovlunde
	Benthin, Søren Hein, Vibeke Hovgaard, Jens Juil, Kirsten B.	Ministry of the Interior Danish Emergency Management Agency Datavej 16 DK-3460 Birkerød
	Andersen, Frank Bargholz, Kim Korsbech, Uffe Paulsen, Dorte Eide	Technical University of Denmark Department of Automation Bygn. 327 DK- 2800 Lyngby
FINLAND	Pulakka, M.	Finnish Air Force Depot FIN-33101 Tampere
	Honkamaa, Tapani Huotari, Tuija Illander, Tarja Karvinen, Ali Karvonen, Jari Lahtinen, Juhani Lemmelä, Heikki Markkanen, M. Niskala, P. Pöllänen, Roy Tiilikainen, Hannu Toivonen, Harri	Finnish Centre for Radiation and Nuclear Safety P.O. Box. 14 FIN-00881 Helsinki

	Heininen, Tapio Jappinen, Arto Keskitäio, Kari Kettunen, Markku Kortesoja, Kari Laine, Ilkka Puputti, Margit	Finnish Defence Force Research Centre P.O. Box 5 FIN-34111 Lakiala
	Hautaniemi, H. Multala, Jukka	Geological Survey of Finland P.O. Box 96 FIN-02151 Espoo
	Aarnio, Pertti Mäkinen, Susanna Nikkinen, Mika	Helsinki University of Technology FIN-02150 Espoo
	Koivukoski, Janne Peltola-Lampi, Tiina	Ministry of the Interior, Rescue Department P.O. Box 257 FIN-00171 Helsinki
	Lehtonen, Erik	RADOS Technology Oy P.O. Box 506 FIN-20101 Turku
FRANCE	Bourgeois, Christian Bresson, Jean Chiffot, Thierry Guillot, Ludovic Tresamini, Eric	Commissariat à L'Energie Atomique Direction des Applications Militaires Centre d'Etudes de Valduc F-21 120 Is/Tille
GERMANY	Barke, Holger Carloff, Gunter Mönch, Thomas Scharmacher, Volkmar Wetzlar, Peter Wilkendorf, Dieter	Federal Border Police Bundesgrenzschutzstrasse 100 D-53757 Sankt Augustin
	Brummer, Ch. Buchrüder, Helmut Thomas, Michael Winkelmann, Ingolf	Federal Office for Radiation Protection Köpenicker Allee 120-130 D-10318 Berlin
NORWAY	Håbrekke, Henrik Mogaard, John Olav	Geological Survey of Norway P.O. Box 3006 - Lade N-7002 Trondheim
	Willoch, Harald	NILU Instituttveien 18, Postpoks 100 N-2007 Kjeller

	Berg, Thor Ch. Henriksen, Ole Larsen, Sven	Norwegian Institute for Air Research Instituttveien 18, Postpoks 100 N-2007 Kjeller
	Larsen, Erlend	Norwegian Radiation Protection Authority N-9425 Svanvik
	Rønning, Stig Smethurst, Mark A	Geological Survey of Norway P.O. Box 3006 - Lade N-7002 Trondheim
	Flø, Lise Mikkelborg, O. Ugletveit, Finn	Norwegian Radiation Protection Authority P.O. Box 55 N-1345 Østerås
SWEDEN	Råäf, Christopher	Department of Radiation Physics, Malmö Lund University Malmö University Hospital S-205 02 Malmö
	Byström, Sören Lindén, Anders Lindgren, Jonas	Geological Survey of Sweden Dept. of Geophysics P.O. Box 670 S-751 28 Uppsala
	Almén, Anja Eberhardt, Jacob	Lund University Department of Radiation Physics S-221 85 Lund
	Samuelson, Christer	Lund University Radiation Physics Department S-221 85 Lund
	Arnising, Rune De Geer, Lars Erik	National Defence Research Establishment Nuclear Detection Group S-17290 Stockholm
	Lidström, Kenneth Ulvsand, Thomas Ågren, Göran	National Defence Research Establishment Division of Ionising Radiation and Fallout S-90182 Umeå
	Vintersved, Ingemar	National Defence Research Establishment Nuclear Detection Group S-17290 Stockholm

	<p>Finck, Robert Hagberg, Nils Mellander, Hans Samuelsson, Göran Åkerblom, Gustav</p>	<p>Swedish Radiation Protection Institute S-17116 Stockholm</p>
	<p>Vesanen, Raine Isaksson, Mats</p>	<p>University of Göteborg Department of Radiation Physics Sahlgrenske sjukhuset S-413 45 Göteborg</p>
SCOTLAND	<p>Scott, Marian</p>	<p>Department of Statistics University of Glasgow G12 8QW Scotland</p>
	<p>Allyson, David Heathcote, Paul McConville, Paul Murphy, Simon Sanderson, David</p>	<p>Scottish Universities Research &amp; Reactor Center NEL, Technology Park East Kilbride G75 0QU Scotland</p>
USA	<p>Hendriks, Thane</p>	<p>EG&amp;G/EM P.O. Box 1912 M/S RSL-20 Las Vegas Nevada 89125</p>

# COLOUR APPENDIX

Map of the Exercise Area.....	plate 1
<b>1. DENMARK</b>	
Danish Emergency Management Agency:	
"The Danish Airborne Gamma Ray Surveying Results"	
Fig. 4. <sup>137</sup> Cs deposition in Area II .....	plate 2
Fig. 5. Estimated cesium deposition depth in Area II.....	plate 2
Fig. 12. Maps showing the source search result from Area III.....	plate 3
<b>2. FINLAND</b>	
Finnish Defence Force Research Centre:	
"Airborne Fallout Mapping of <sup>137</sup> Cs"	
Fig. 2. Fallout map of area II measured with HPGe on 16 <sup>th</sup> August 1996 .....	plate 4
Geological Survey of Finland:	
"Exercise Results and Experience"	
Fig. 1. The Cs window kBq/m <sup>2</sup> and Co count rate maps showing the location of two hidden sources on Area III June 9 <sup>th</sup> 1995.....	plate 5
Fig. 2. Cs-137 map from Area II on 9 <sup>th</sup> of June 1995.....	plate 6
Finnish Centre for Radiation and Nuclear Safety / Helsinki University of Technology:	
"Airborne Fallout Mapping of <sup>137</sup> Cs"	
Fig. 2. Fallout map of area II measured with NaI on 16 <sup>th</sup> August 1996 .....	plate 7
"Carborne Fallout Mapping"	
Fig. 1. (a) Fallout map measured using HPGe. (b) Dose rate measured using PIC.....	plate 8
"Detecting Hidden Sources"	
Fig. 1. Maps of area III.....	plate 9
<b>3. FRANCE</b>	
Commissariat à L'Energie Atomique - Hélinuc:	
"RESUME95 Nordic Field Test of Mobile Equipment for Nuclear Fallout Monitoring"	
Map Area 2 - <sup>137</sup> Cs Activity .....	plate 10
Map Area 2 - <sup>40</sup> K Activity .....	plate 11
Map Area 3 - <sup>137</sup> Cs Activity .....	plate 12
<b>4. GERMANY</b>	
Bundesamt für Strahlenschutz:	
"Aerial Measurement in Finland"	
Fig. 1. <sup>137</sup> Cs soil contamination measured by NaI(Tl)-detector in the cesium window during the flight over area II.....	plate 13
Fig. 3. <sup>137</sup> Cs soil contamination measured by HPGe-detector during the flight over area II .....	plate 14
<b>5. NORWAY</b>	
Geological Survey of Norway:	
"Airborne Mapping of Radioactive Contamination"	
MAP 1 Cesium Ground Concentration .....	plate 15
MAP 2 Point Source Detection Area III.....	plate 16
Norwegian Institute for Air Research:	
"Exercise Résumé95. Report from NILU team"	
Fig. 1. Cesium Ground Concentration .....	plate 17

Norwegian Radiation Protection Authority:	
"Car-borne Survey Measurement with a 3x3" NaI Detector"	
	Fig. 3. Fallout maps area II and III ..... plate 18
6.	SCOTLAND
Scottish Universities Research & Reactor Centre:	
"Airborne Gamma Ray Measurements Conducted During an International Trial in Finland"	
	Fig. 4.2. <sup>137</sup> Cs deposition map ..... plate 19
	Fig. 4.4. Mapped data for four of the channels examined ..... plate 20
7.	SWEDEN
Department of Radiation Physics, Lund University, Lund:	
"Carborne Measurements in Area II by the Jubileum Institute"	
	Fig. 2. Gammadata GDM 40 RPS with Ortec $\mu$ ACE multichannel analyser card and NEC V25+ microprocessor ..... plate 21
	Fig. 3. The software for extracting and treatment of spectral- and GPS-data is written by Hans Mellander ..... plate 21
	Fig. 4. <sup>137</sup> Cs results from area II and the road between area II and III ..... plate 22
Geological Survey of Sweden:	
"REUMÉ95"	
	Cesium -137 AREA 2, Surface Activity ..... plate 23
	Area III, Final Map ..... plate 24

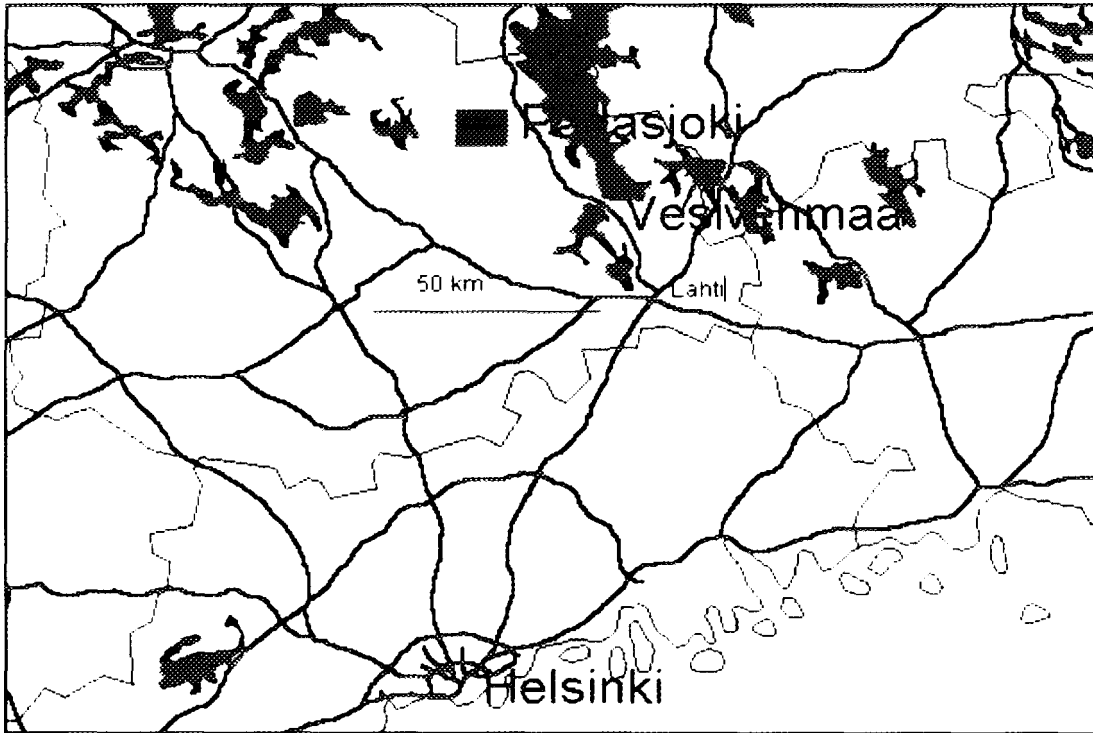


**Plate 1a** Key map of exercise area

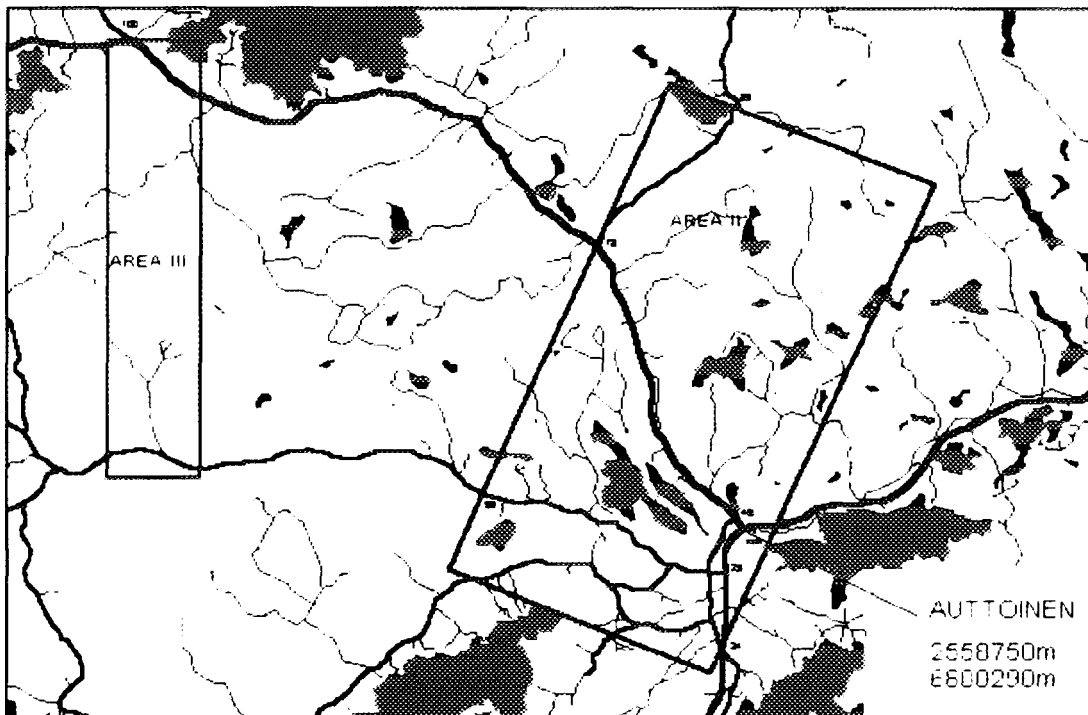


**Plate 1b** Exercise area II & III

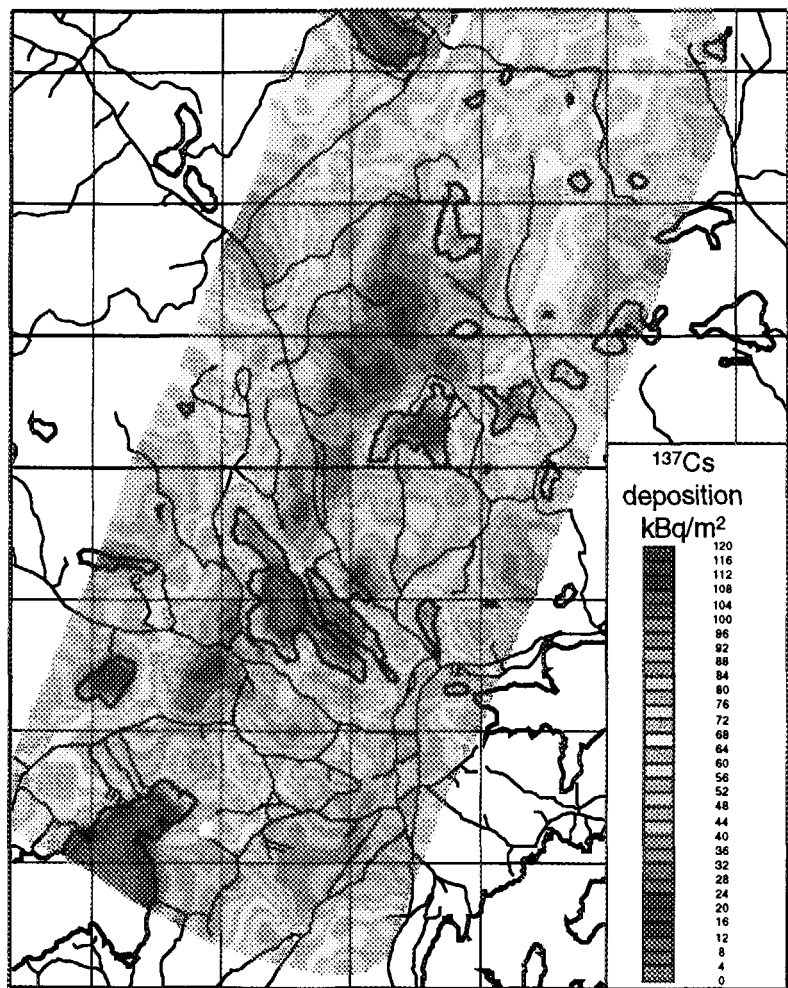


Figure 4  $^{137}\text{Cs}$  deposition in AREA II

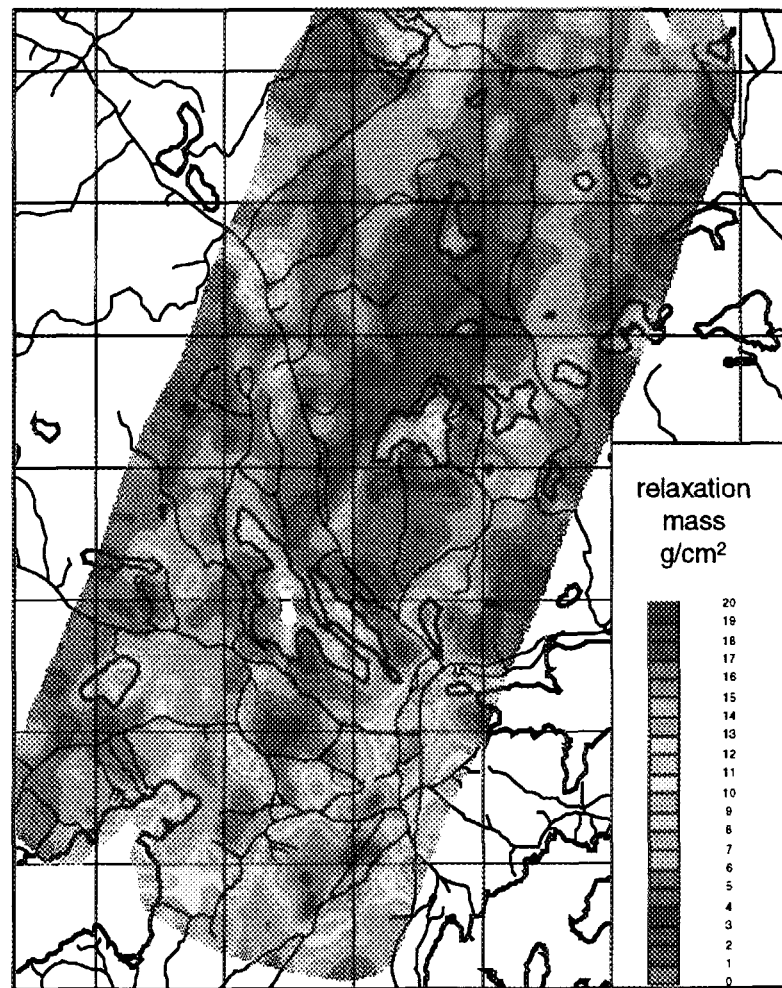
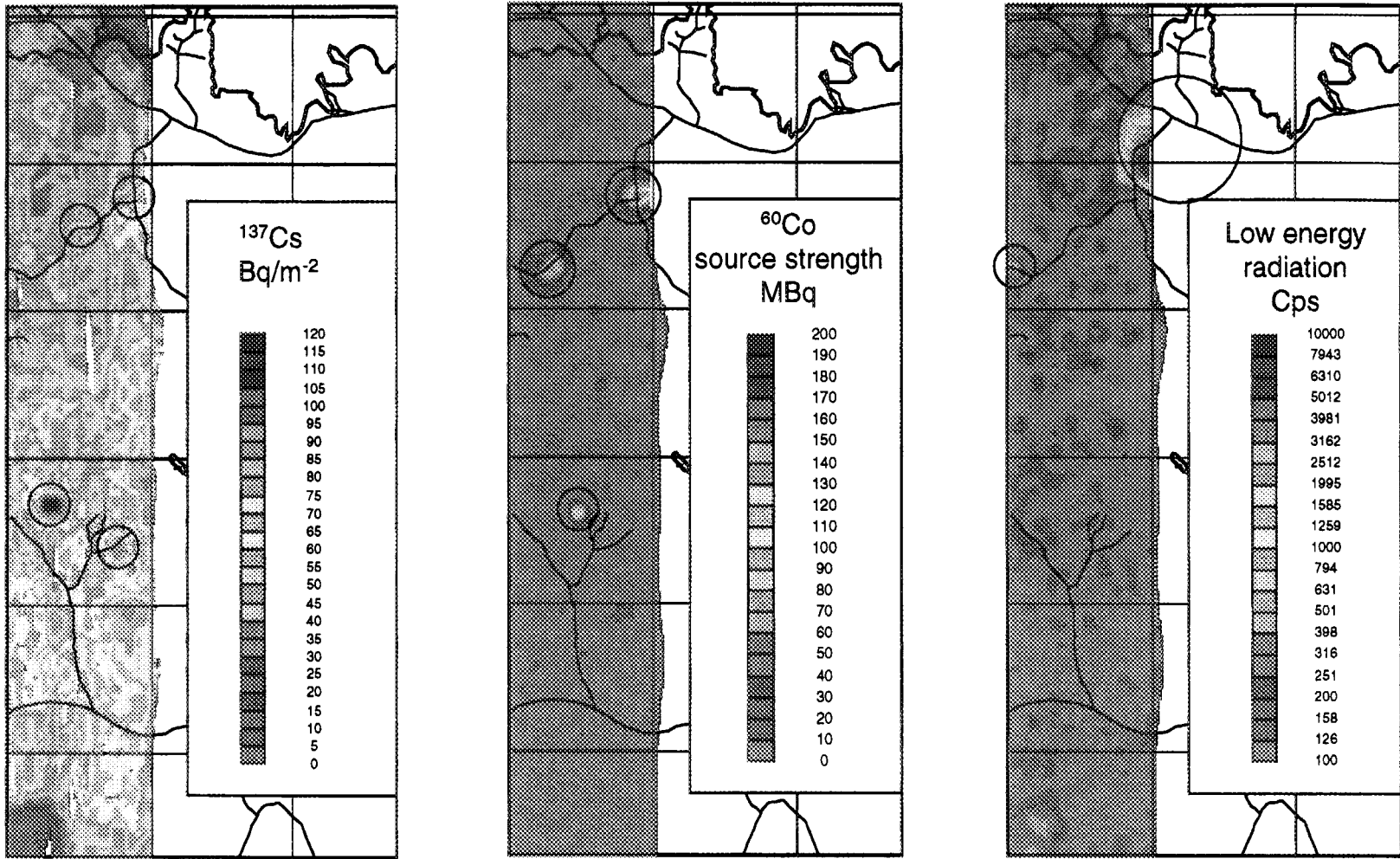


Figure 5 Estimated cesium deposition depth in AREA II



**Figure 12** Maps showing the source search result from AREA III, all sources present are marked with circles. a)  $^{137}\text{Cs}$  deposition map to identify  $^{137}\text{Cs}$  sources. b)  $^{60}\text{Co}$  map converted to equivalent source strength based on flight altitude. c) "Stripped" low energy radiation in cps.



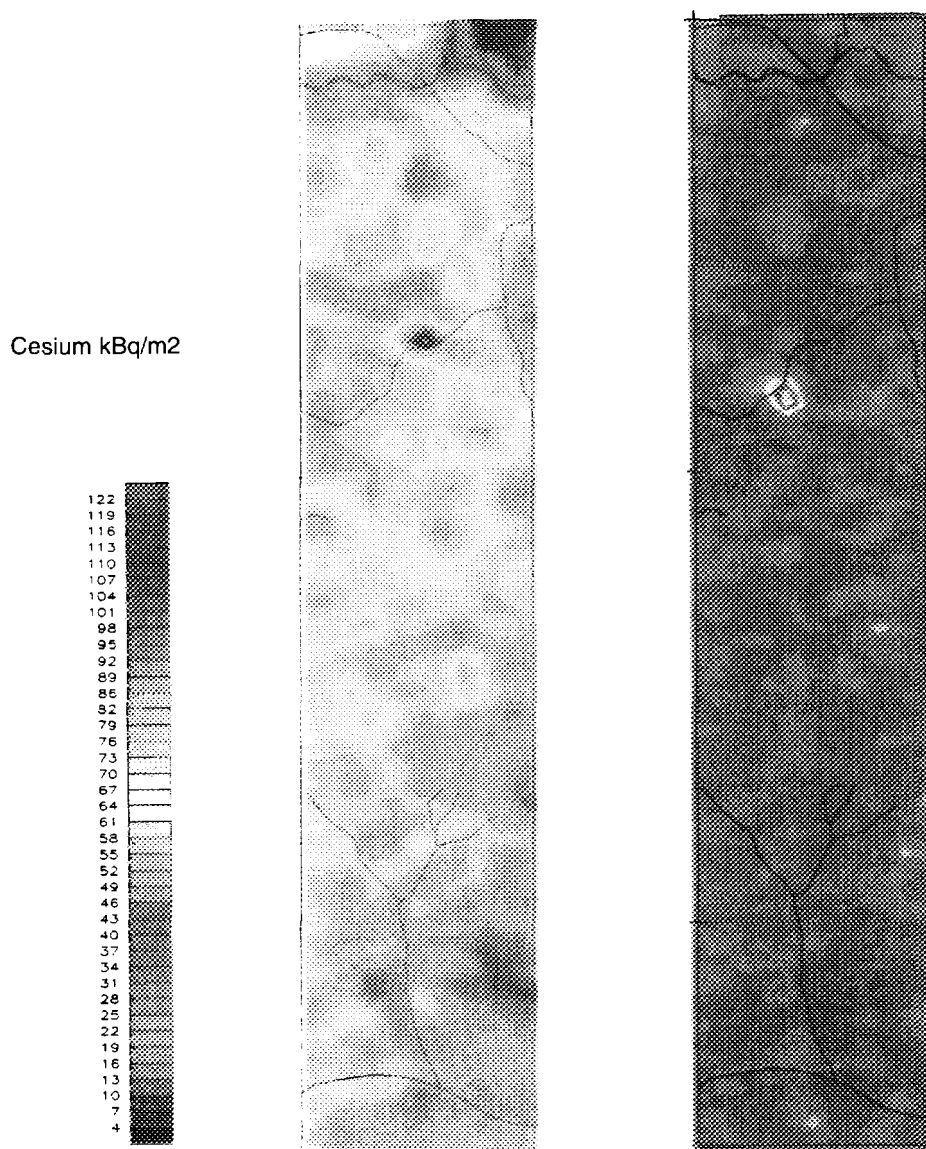


Figure 1. The Cs window kBq/m<sup>2</sup> (on left) and Co count rate (on right) maps showing the location of two hidden sources on Area III on June 9th 1995.

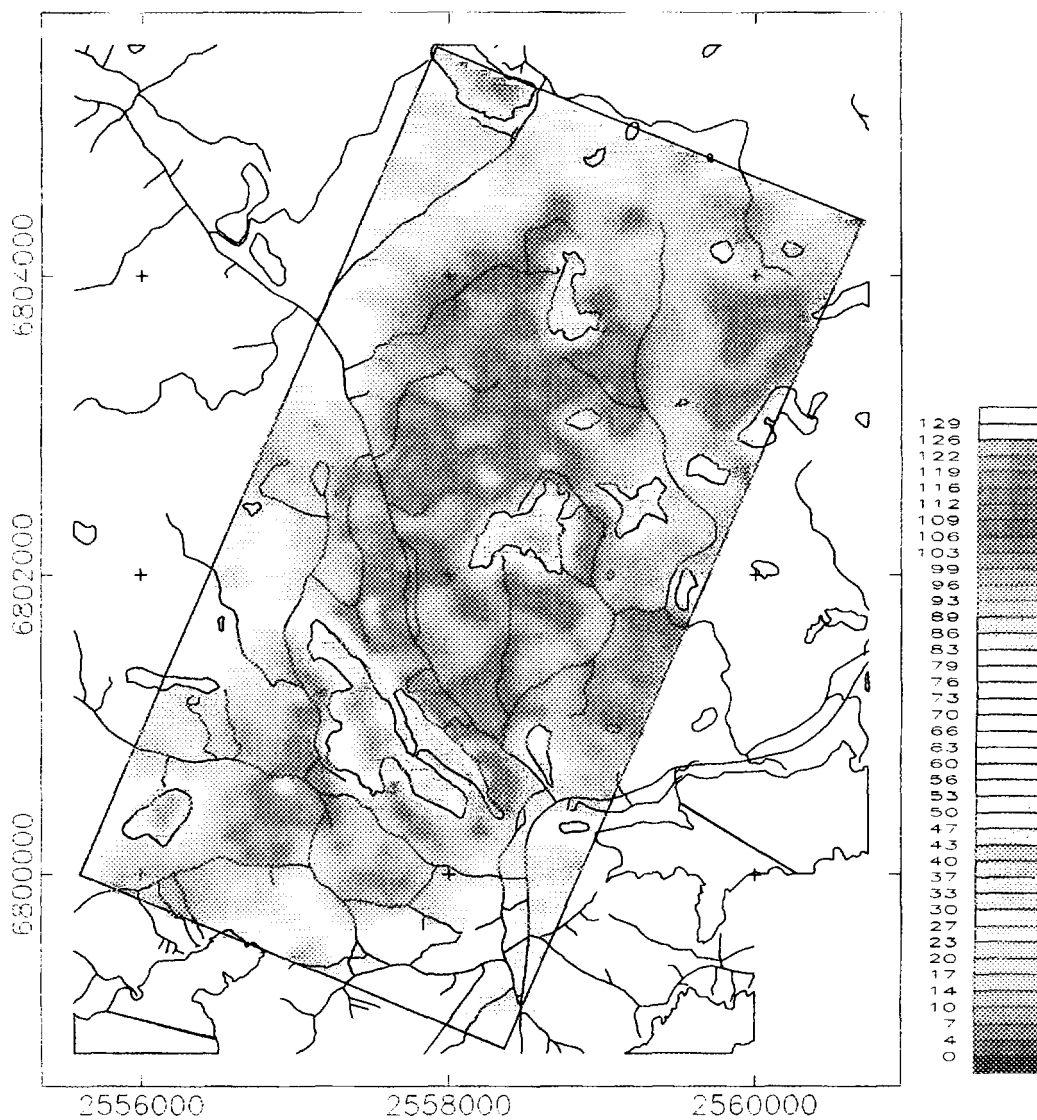


Figure 2. Cs-137 map from Area II on 9th of June 1995.

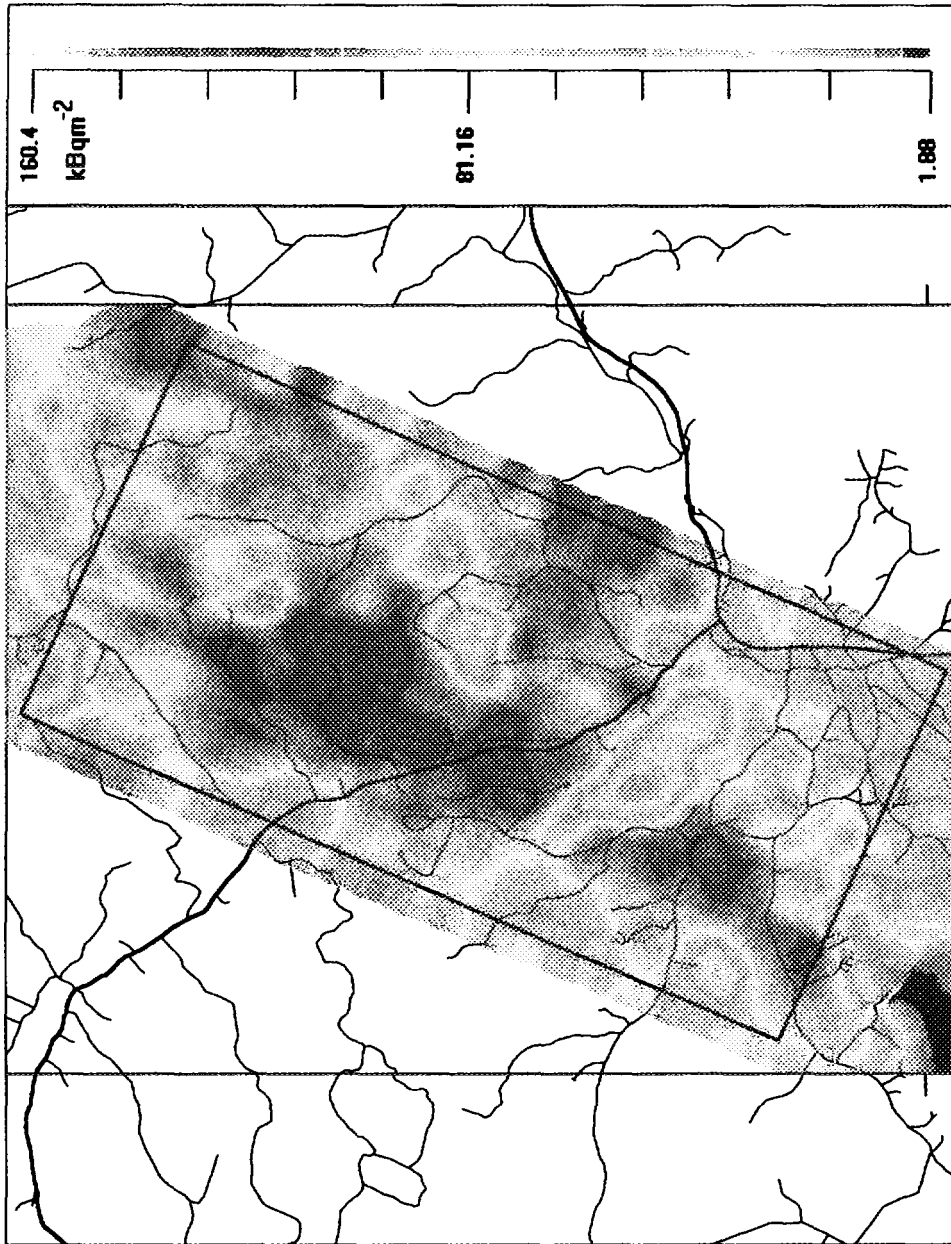
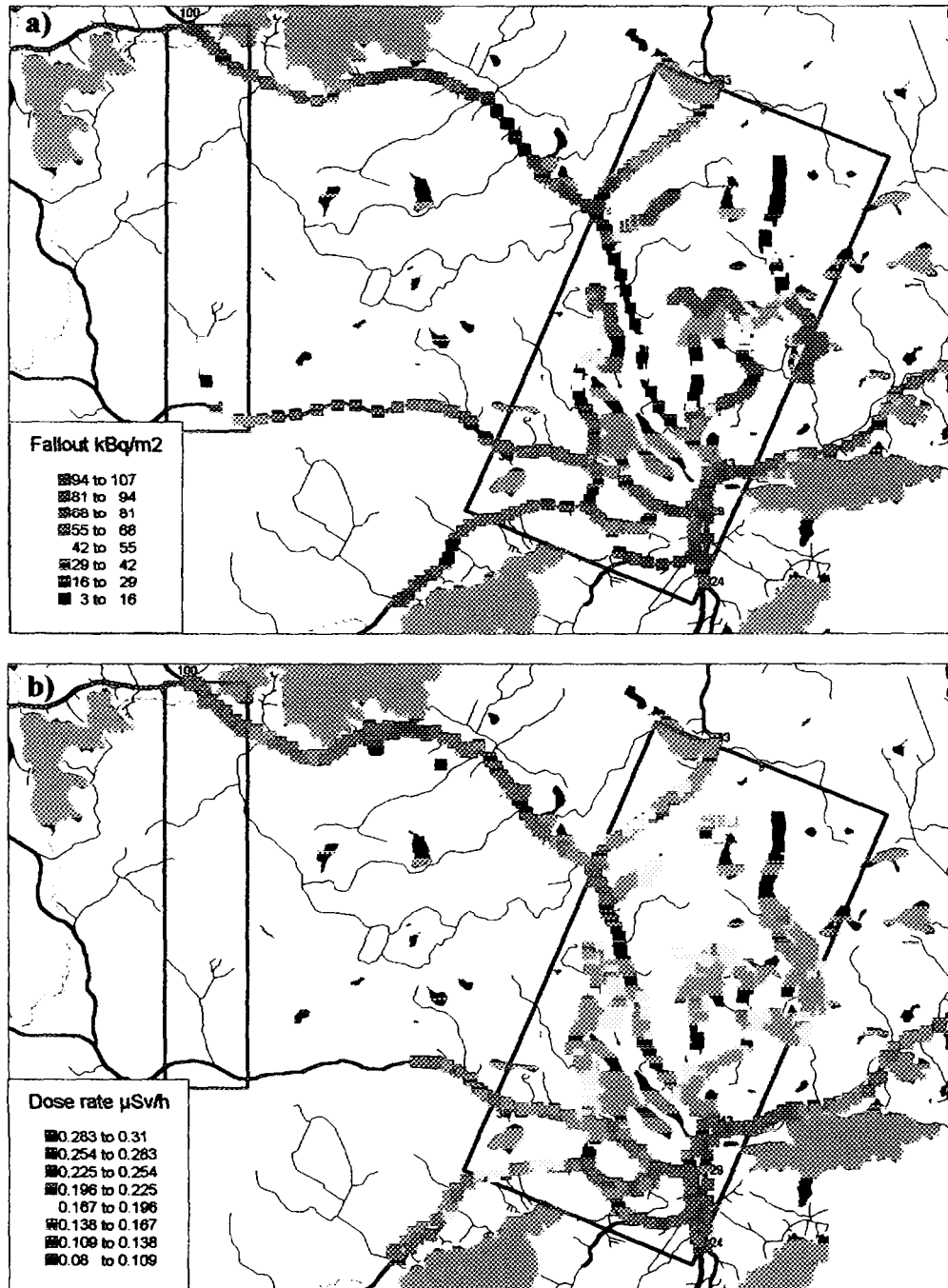


Figure 2. Fallout map of area II measured with NaI on 16th August 1995.



**Figure 1.** (a) *Fallout map measured using HPGe.* (b) *Dose rate map measured using PIC. 20th of June 1996.*

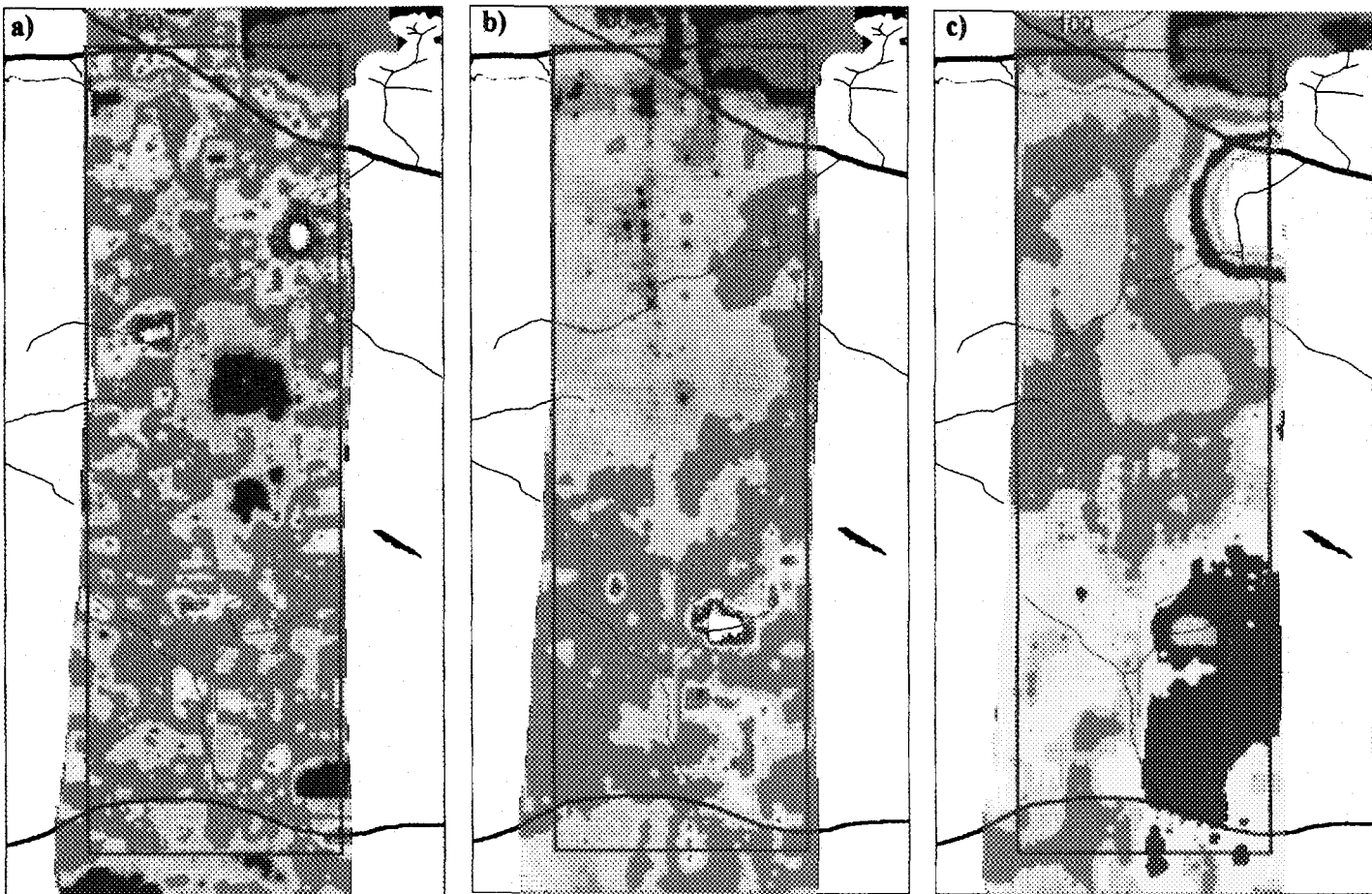
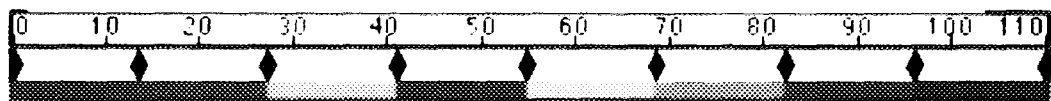
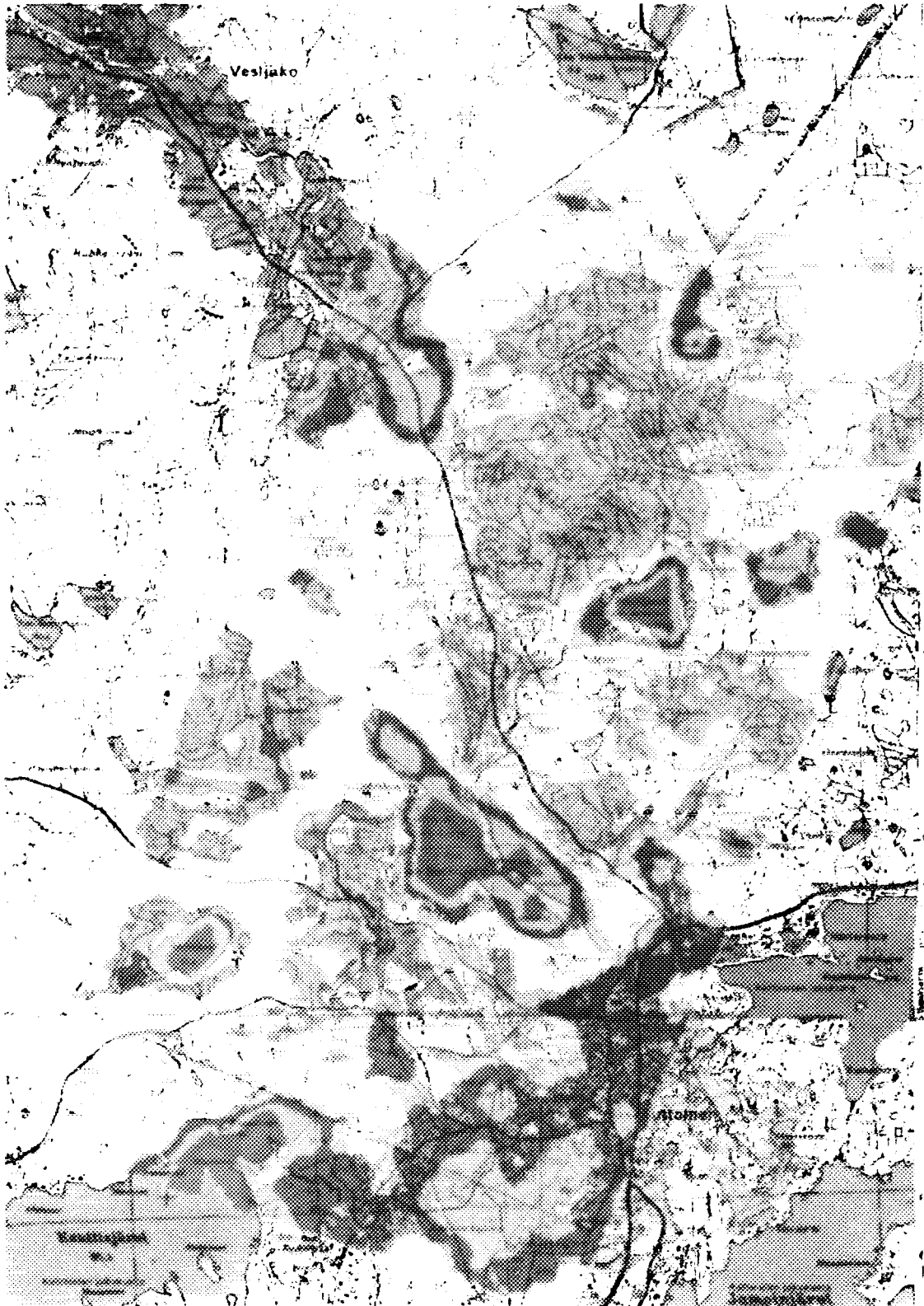


Figure 1. a) Co-60, b) Cs-137 and c)  $< 450\text{ keV}$  count rate maps on area III. The measurement is performed using a  $5'' \times 5''$  NaI detector.

# R.E.S.U.M.E. 95

## Area 2 - Cs137 Activity

Equipe Hélicoptère



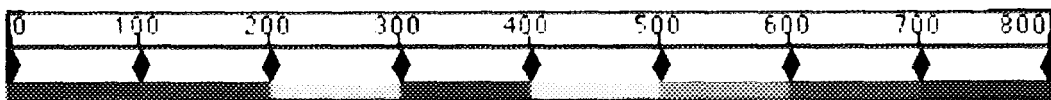
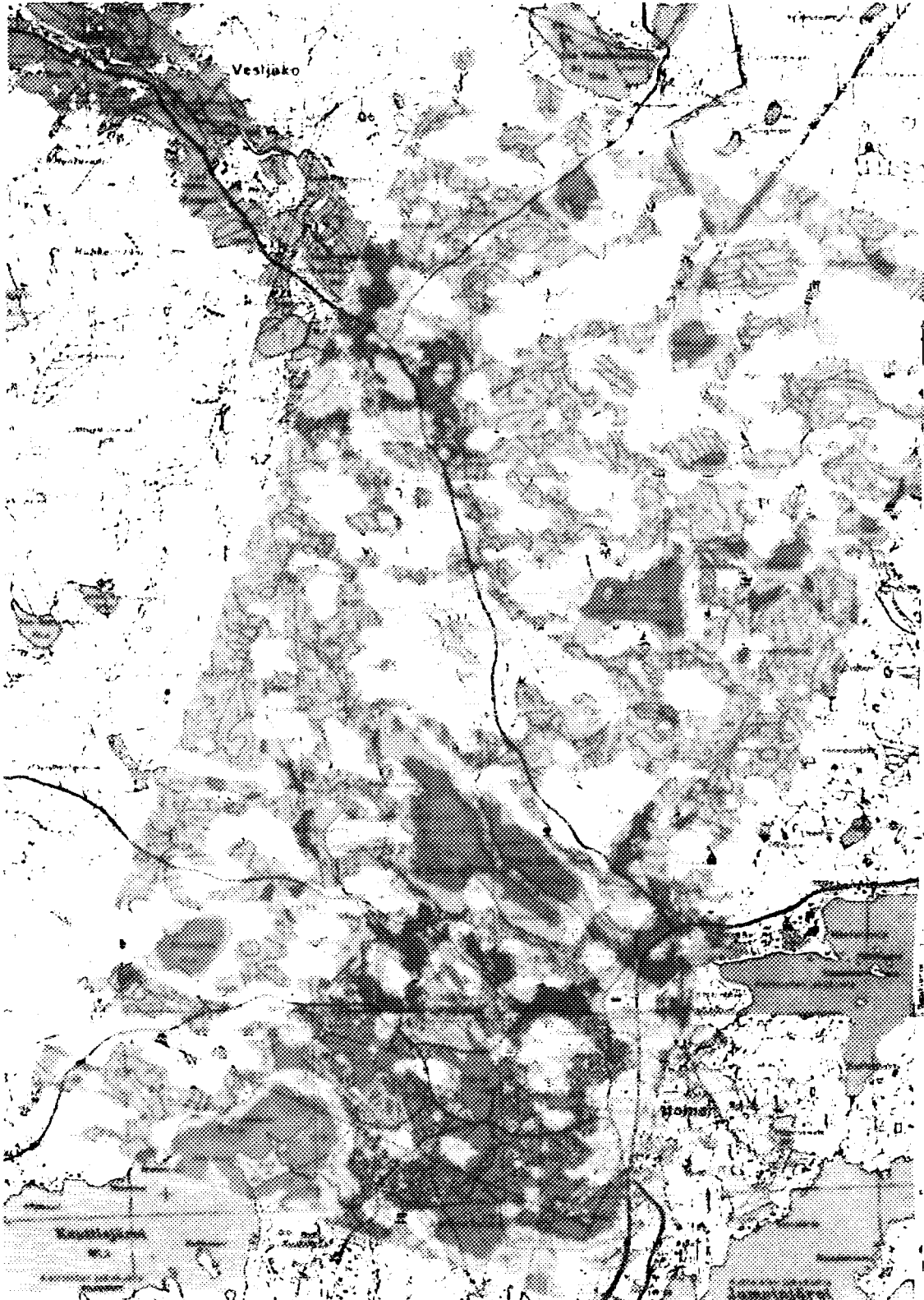
Scale : 1/32000e

kBq/m<sup>2</sup>



# R.E.S.U.M.E. 95

## Area 2 - K 40 Activity



Scale : 1/32000e

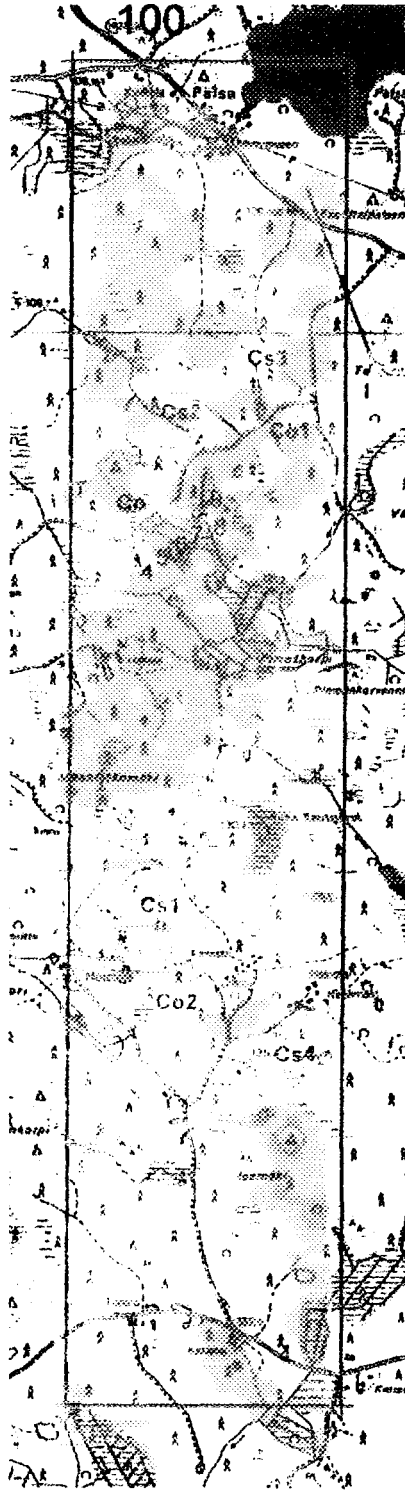
Bq/kg



# R.E.S.U.M.E. 95

## Area 3 - Cs137 Activity

Equipe Hélicoptère



Scale : 1/28000e

kBq/m<sup>2</sup>

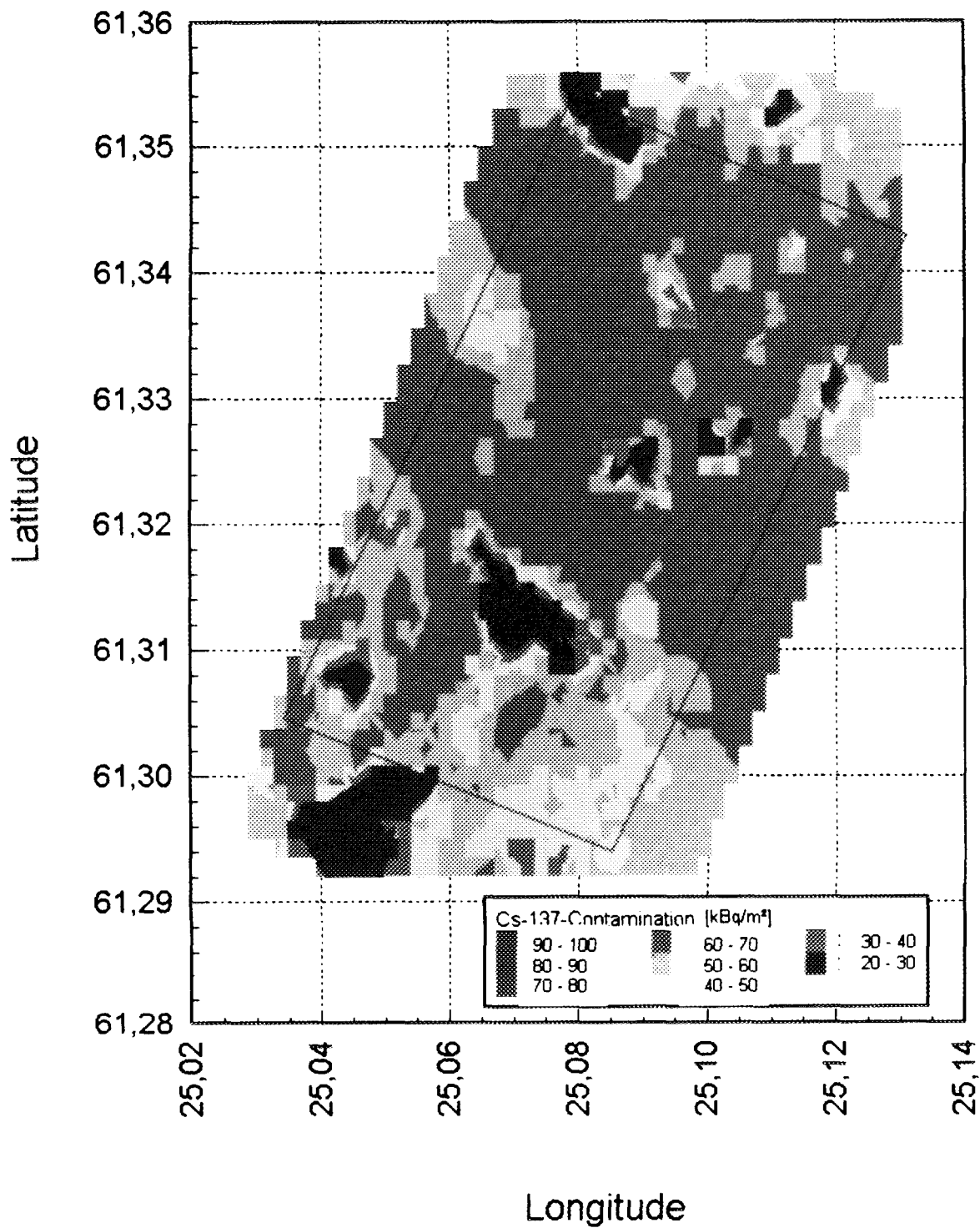


Figure 1. <sup>137</sup>Cs soil contamination measured by NaI(Tl)-detector in the cesium window during the flight over area II.

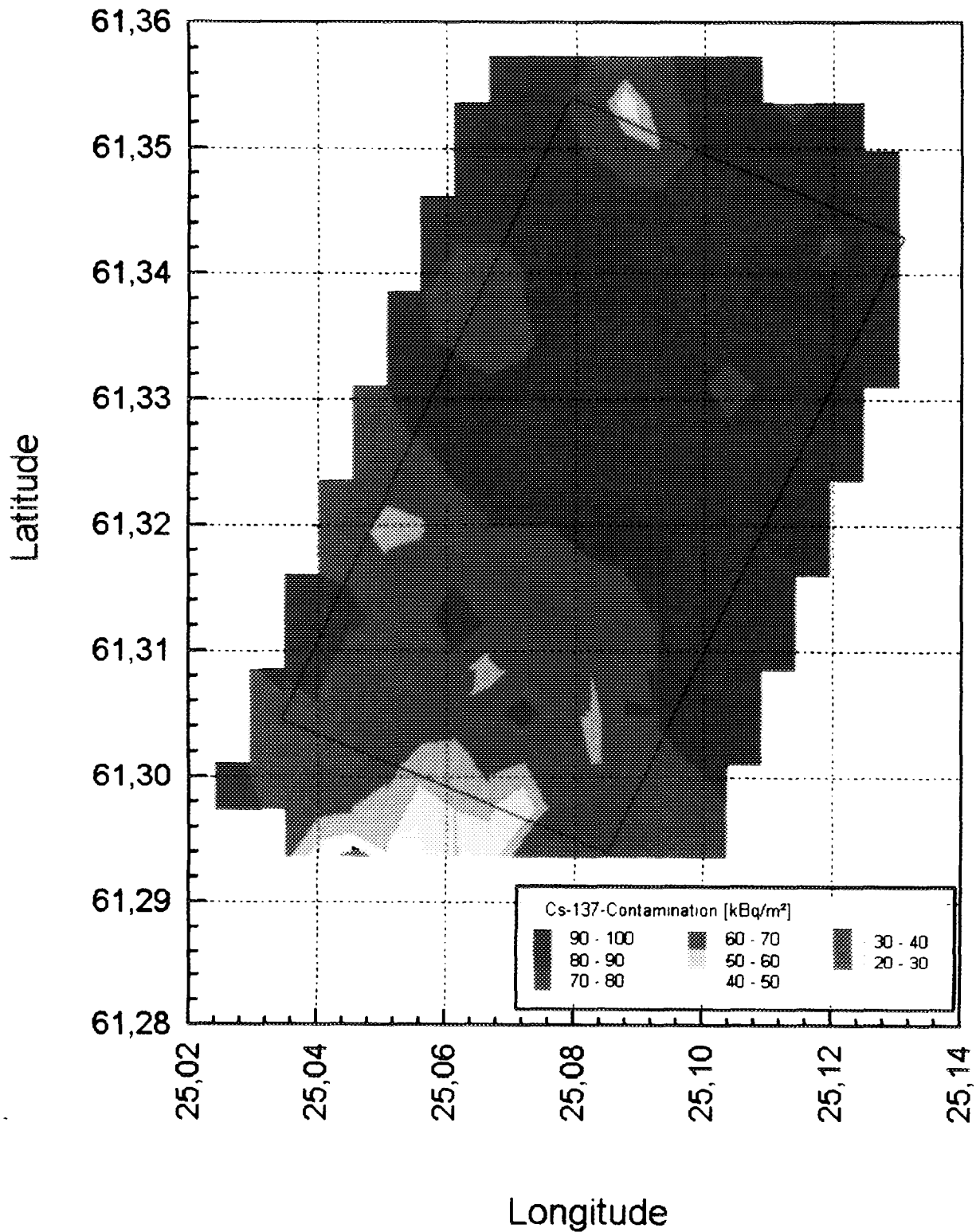
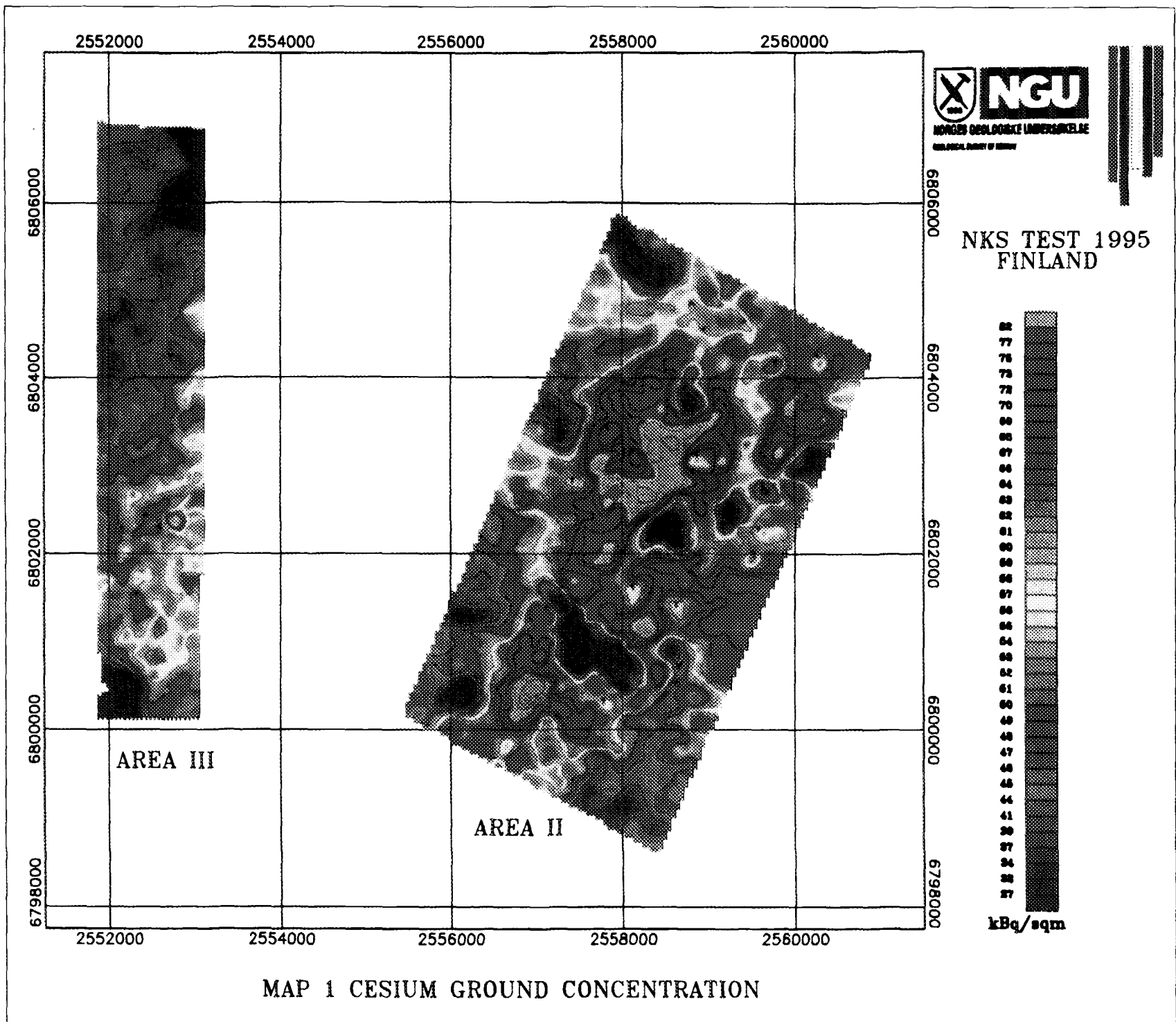
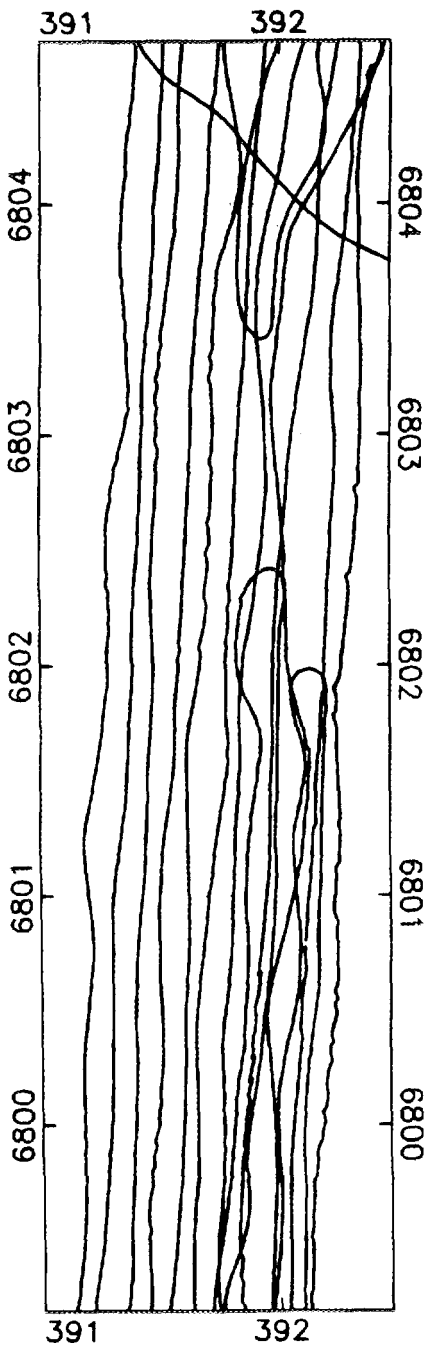


Figure 3. <sup>137</sup>Cs soil contamination measured by HPGe-detector during the flight over area II.

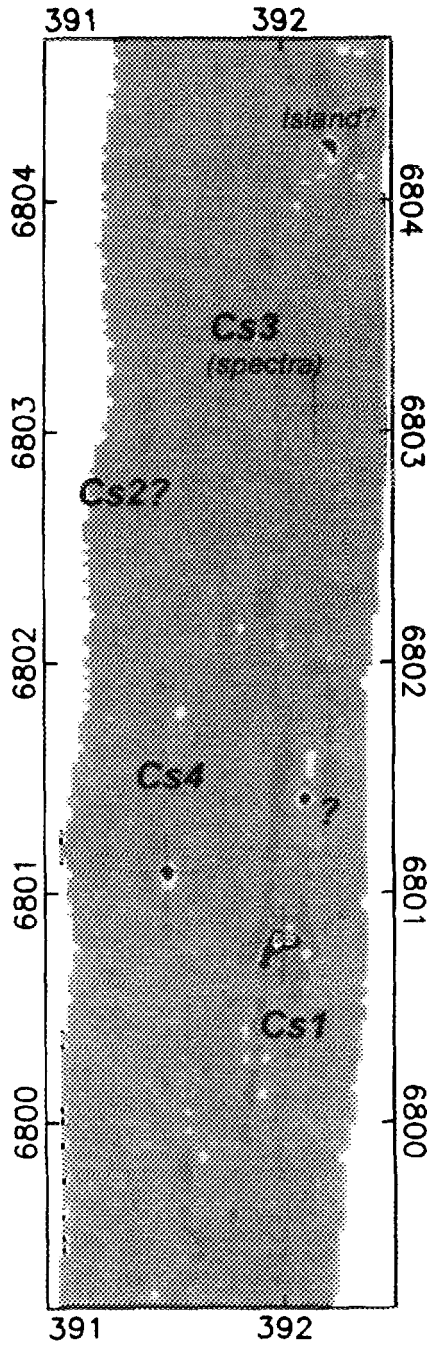


# Map 2 Point source detection area III

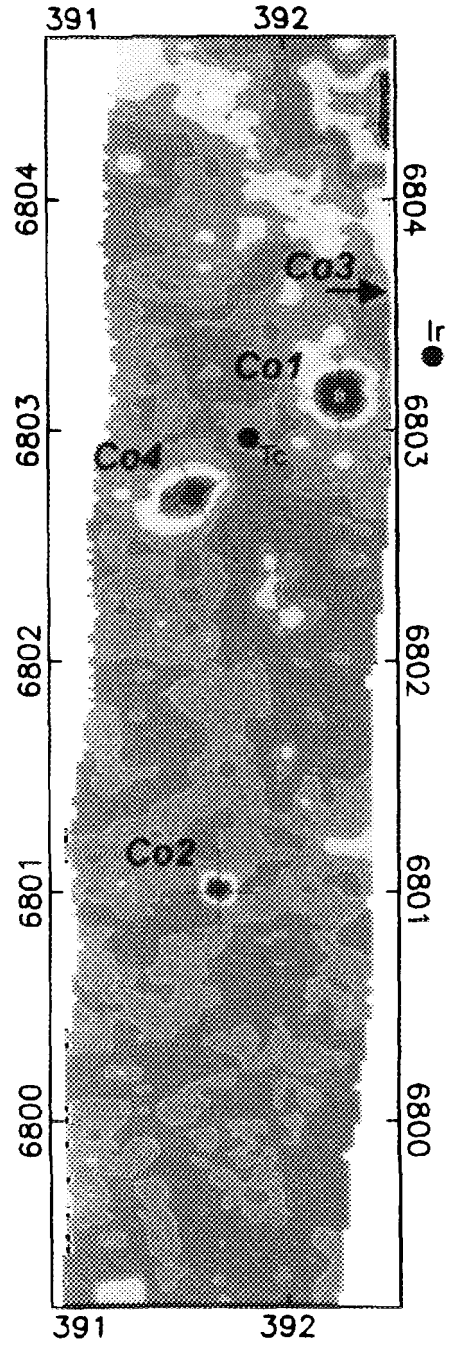
a) Flight pattern



b) Cesium-137 point source detection



c) Cobalt-60 point source detection



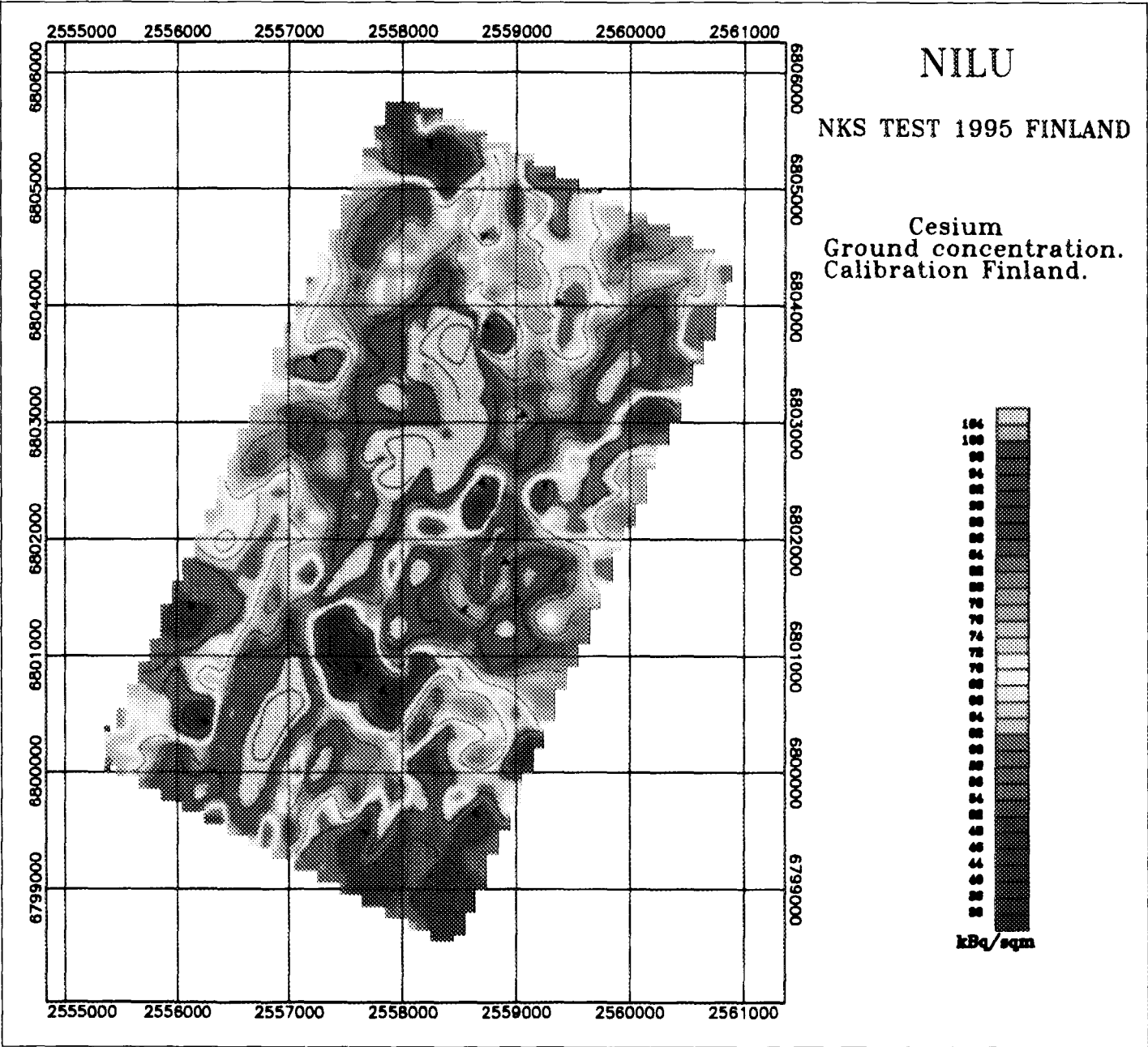
Counts per second



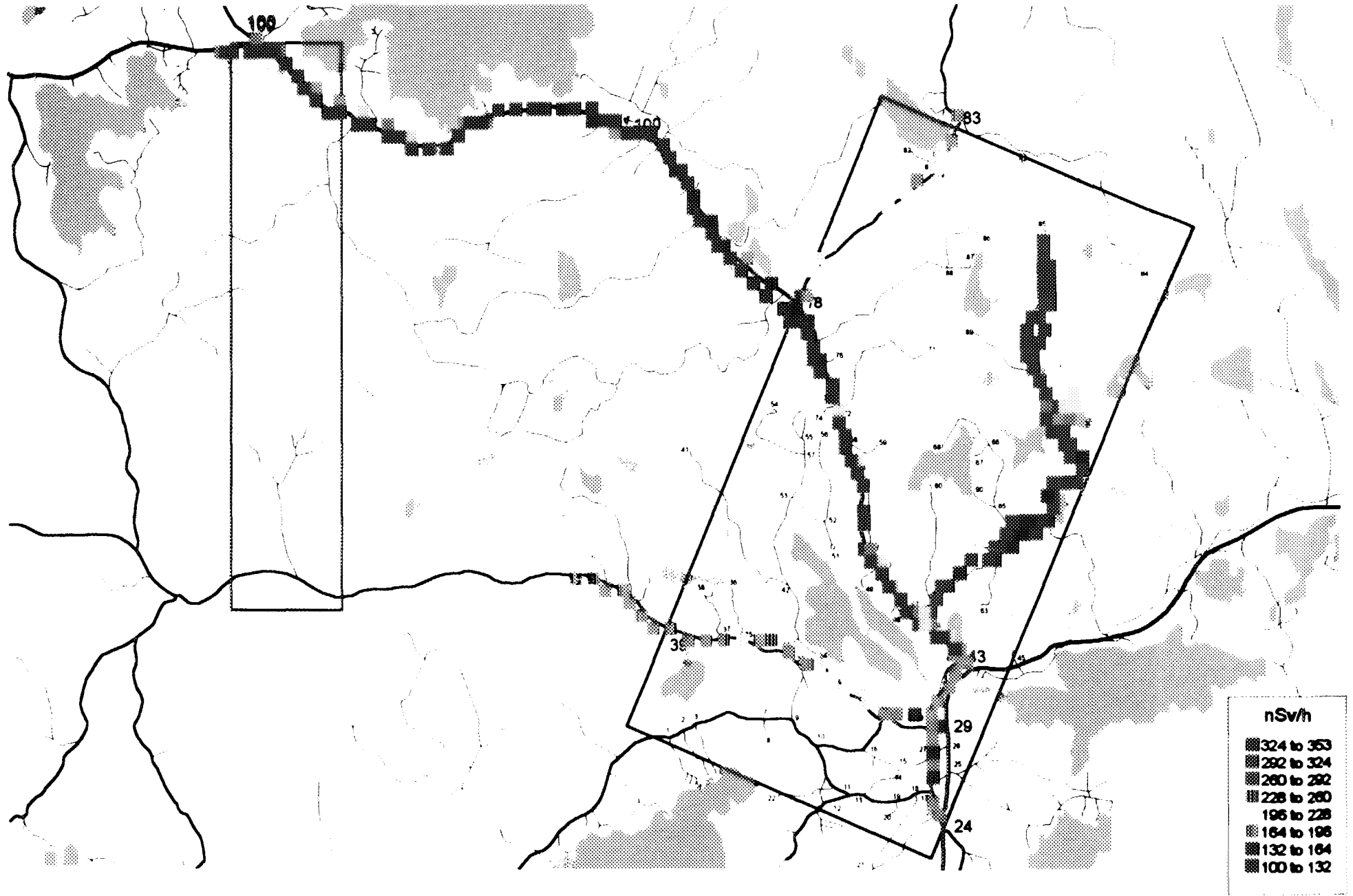
Low

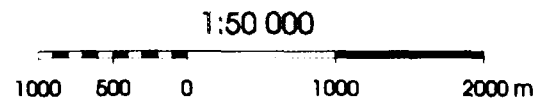
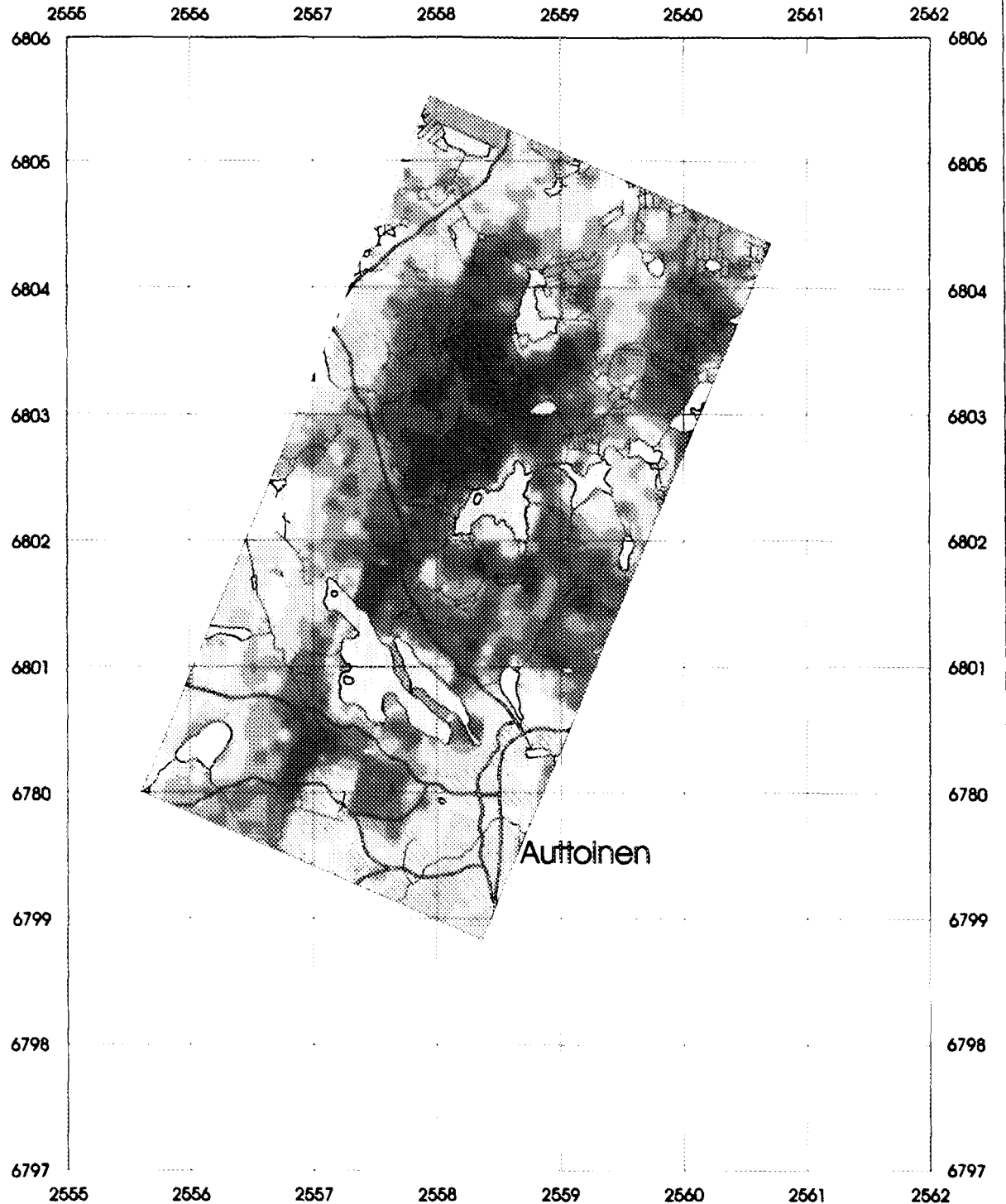
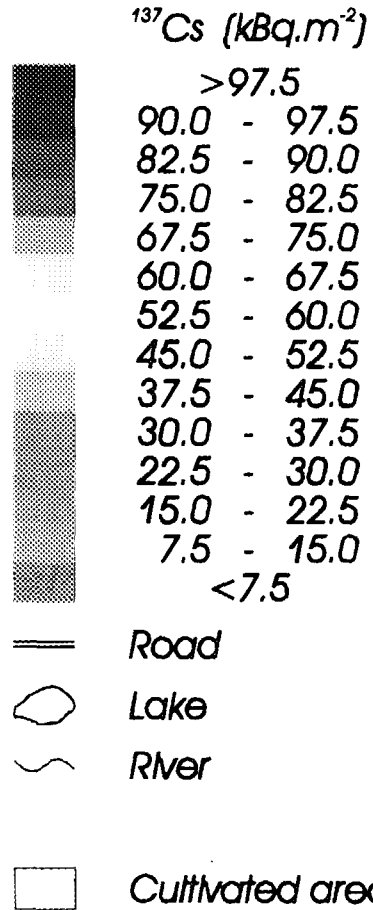
High





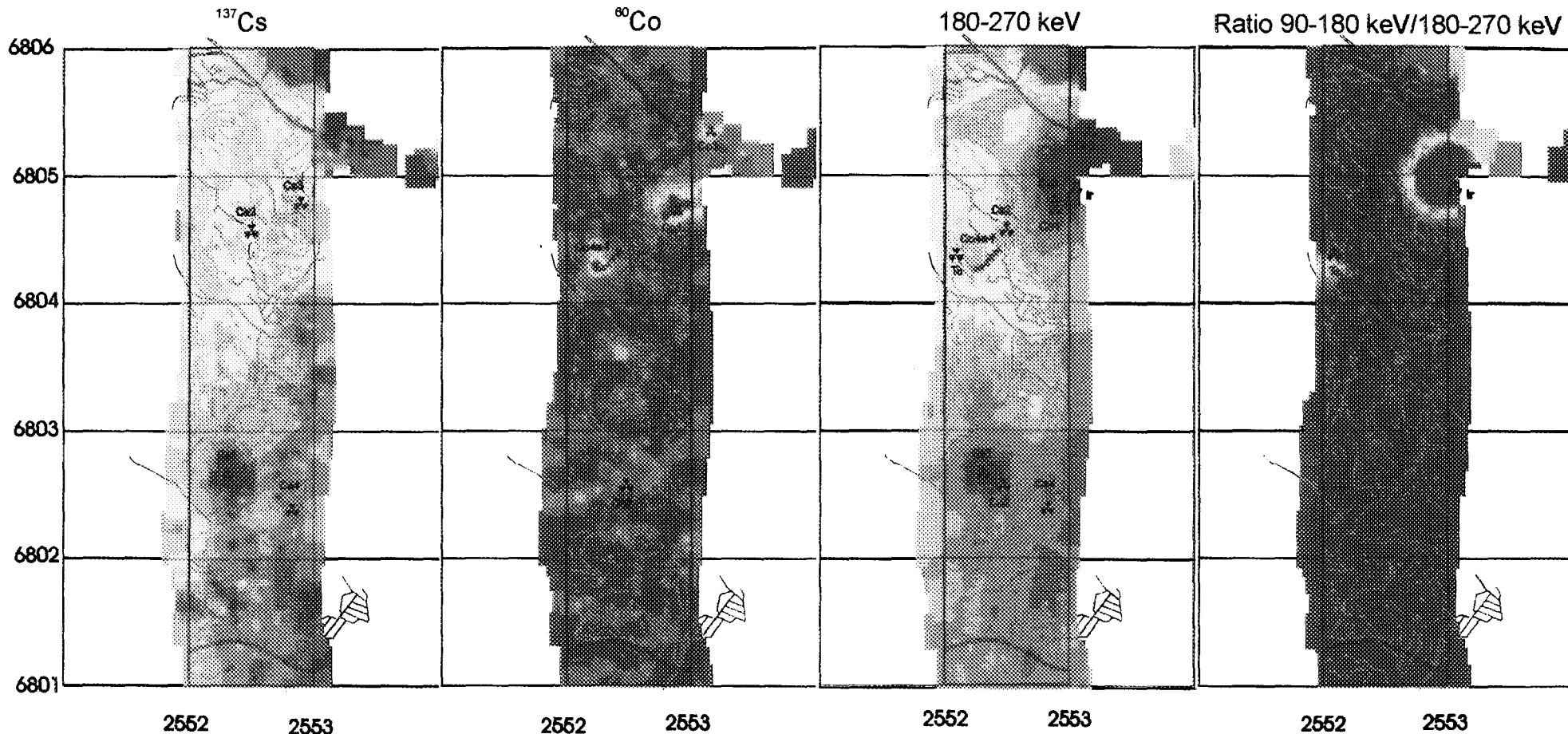
NRPA dose rate measurements, area II







Scottish Universities Research and Reactor Centre



1:50 000



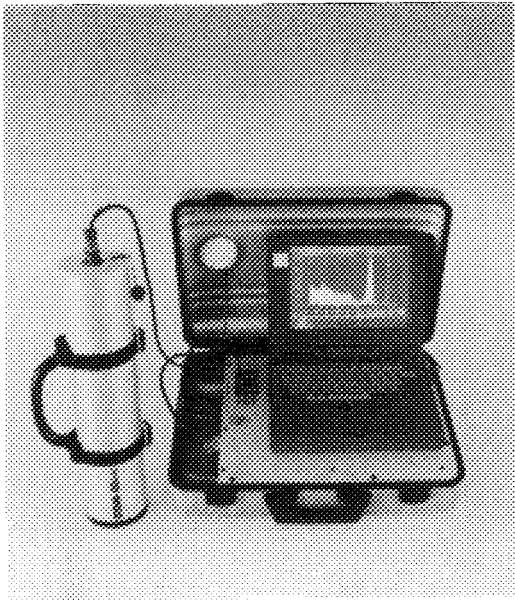


Fig 2. Gammadata GDM 40 RPS with Ortec  $\mu$ ACE multichannel analyzer card and NEC V25+ microprocessor. The detector is a 0.35 litre (3"x3") Teledyne NaI(Tl).

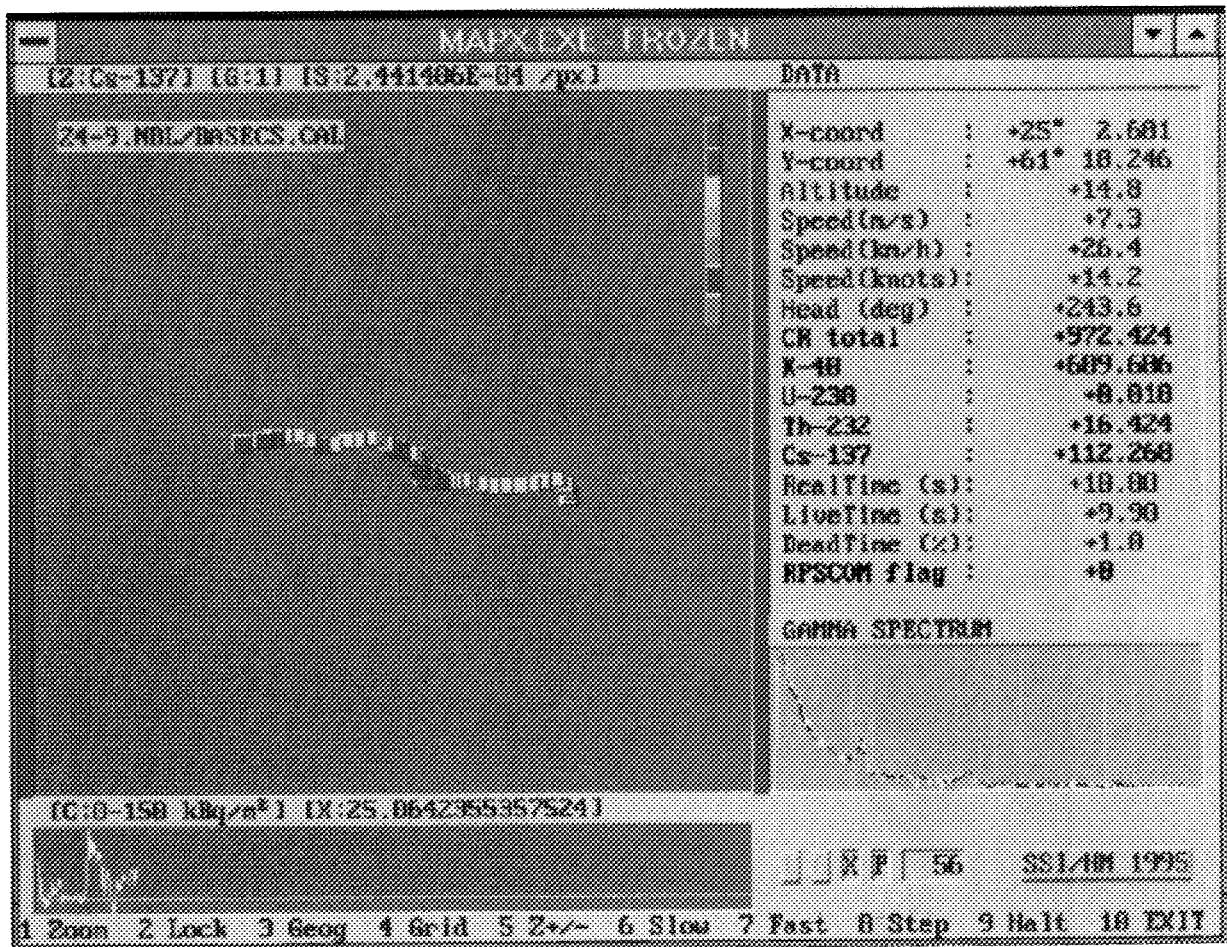
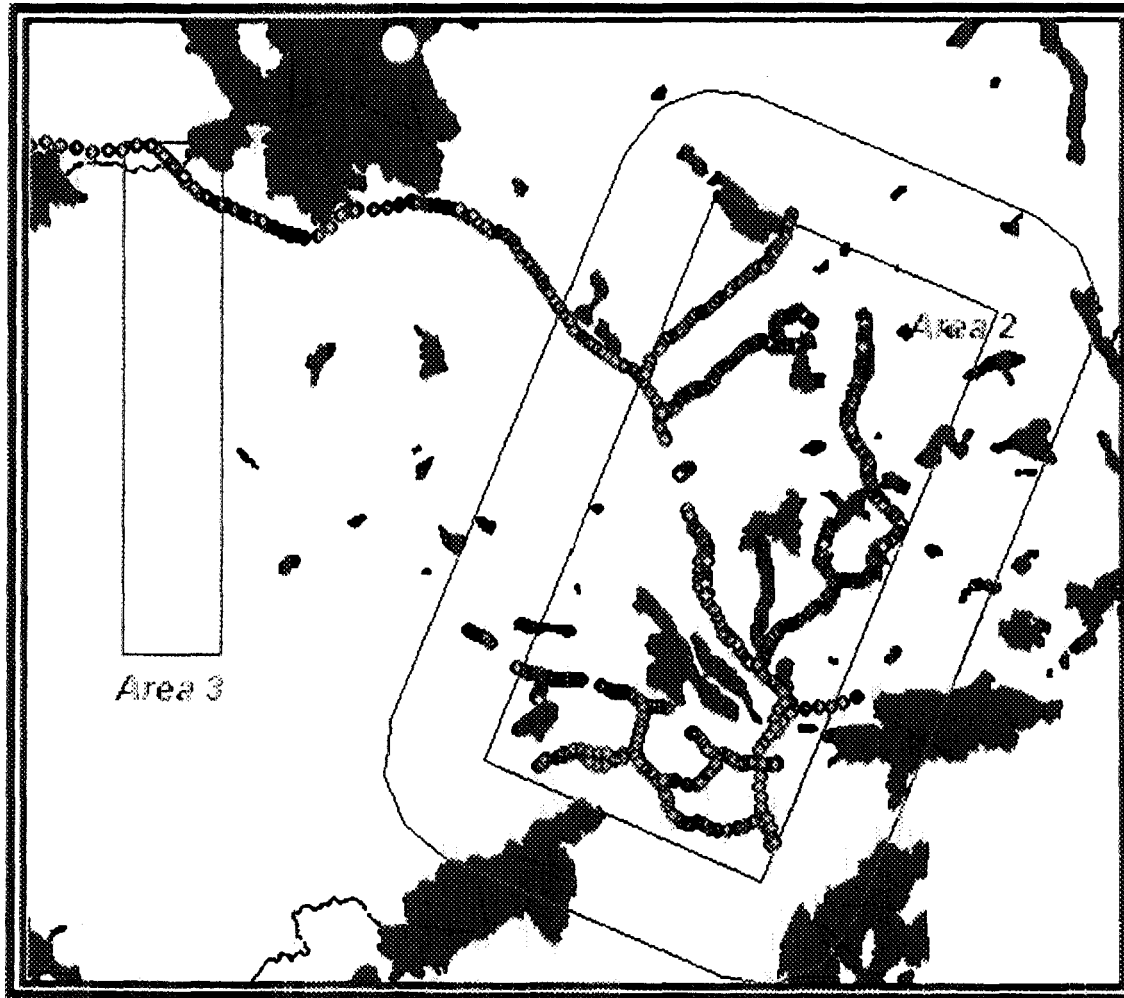


Fig 3. The software for extracting and treatment of spectral- and GPS-data is written by Hans Mellander, SSI. The PC used was a HP Omnibook 600C.

# TEAM LUND

Radiation Physics Department



Cs-137  
CAR measurements  
equipment: GDM 40 RPS  
3"X3" NaI  
10 s sampling time  
Preliminary results

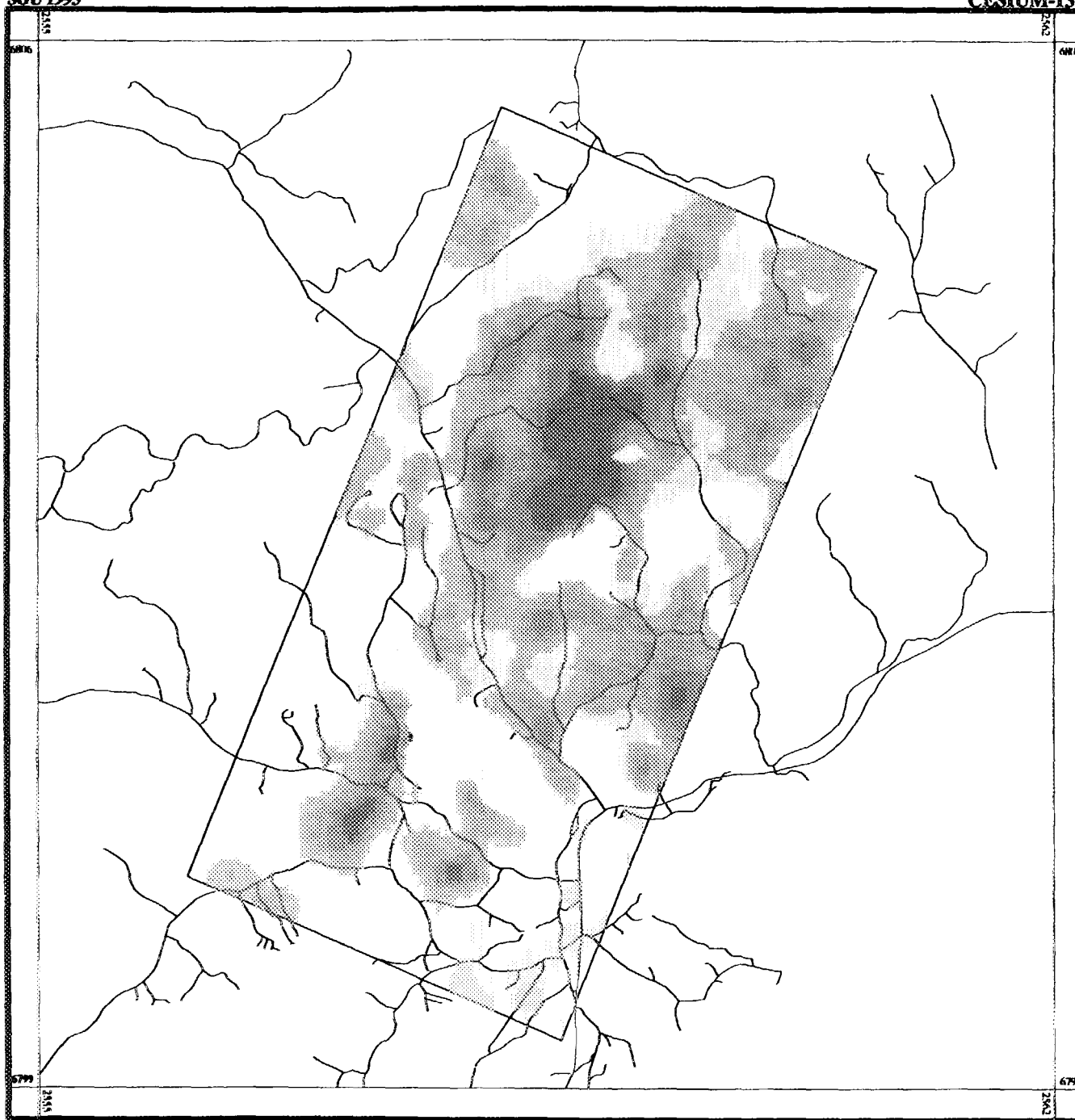
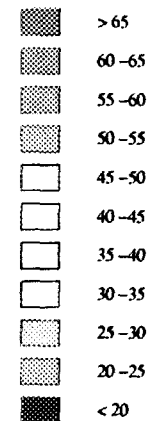
Cs137 window  
KBq/m<sup>2</sup>

- 225 to 252
- 200 to 225
- 175 to 200
- 150 to 175
- 125 to 150
- 100 to 125
- 75 to 100
- 50 to 75
- 25 to 50
- 0 to 25

Fig 4. Cs-137 results from area II  
and the road between area II and III.

# CESIUM-137 AREA #2

Surface Activity  
(kBq/m<sup>2</sup>)



[Return to document](#)

